Università degli Studi di Milano
Dipartimento di fisica

REPORT 2006

DIPARTIMENTO DI FISICA

Editing: Marco Lombardi, Giuseppe Bertin
Progetto grafico: Filippo Bolzonella
Impaginazione: BLZ comunicazione e immagine
Stampa: Arti Grafiche Pinelli Srl, Milano
Dicembre 2006

The Department of Physics* was founded in 1924 by Aldo Pontremoli (1896 – 1928), in response to the demand of science and technology from the social and industrial environment of Milan, the largest of the country. Pontremoli, who had lively interest in different fields of physics **, introduced to the Department the research topics of major interest in Europe, built the first experimental installations, and with the support of local institutions founded a radiology laboratory for studies on UV and X radiations, and radio-active materials. He prematurely died in a dramatic dirigible accident during a scientific expedition to the North Pole.

In the following pre-war period further instrumental installations were set on and studies on main classical physics subjects, such as electrodynamics and statistical physics, were developed. At the end of the 40's and the beginning of the 50's, after a period of reconstruction, the financial support and number of people were large enough to resume a well coordinated research activity.

The main research lines started in the Department at different times. First were the studies on nuclear and particle physics, based on the investigation of cosmic rays, given the lack in Europe of particle accelerators at that time. This activity was favored by the growing interest of the country towards the development of nuclear physics and its applications, which led in 1951 to the foundation of the National Institute of Nuclear Physics (INFN), with the scope of funding and coordinating the research in the field. From these first research lines the research in accelerator physics and related technologies, astrophysics, and medical physics later grew in the Department.

Although the electromagnetic properties of matter and gas discharges have been among the preferred topics since the beginning of the Department, well organized research in physics of matter began in the Department in the mid-50's, with studies in condensed matter. Quantum optics, plasma physics, and biophysics were introduced later, in the 60's and 70's. A national institution for the co-ordination and support of the research in the physics of matter (INFM) was founded in 1994. In this field nanotechnology is a more recent research line. From the very beginning theoretical studies in nuclear and particle physics, in physics of matter and in more speculative areas have received great attention. The most prominent scientists who contributed to the growth of research in the Department from its beginning to the 80's were Giovanni Polvani (1892-1970), Giuseppe (Beppo) Occhialini (1907-1993), and Pietro Caldirola (1914-1984).

In 2006 the Department staff is composed of 107 faculty members (30 professors, 37 associate professors, 40 assistant professors), 23 technicians, 11 administration officers, and 7 custodians. The number of professionals working in the Department is quite larger than that of the Department staff. In fact, the Department hosts in its buildings several research institutions, which participate in joint research projects with their own personnel and funds: the Interdisciplinary Center for Nano-structured Materials and Interfaces (CIMAINA), a "Center of Excellence" of our University; the Milan Division of the National Institute of Nuclear Physics (INFN); the Milan Division of the National Institute for the Physics of Matter (INFM). The personnel of the nearby Institute of Applied General Physics closely collaborates with the Department staff.

Most of the infra-structures and institutions of our University devoted to higher education in physics reside in the Department: a three year, first level, and a two year, second level, Physics Degree Course; a three year Doctorate School in Physics, Astrophysics, and Applied Physics; a four year Post-Graduate School in Health Physics, and one year topical Master Courses. A Specialization Course for physics teachers is also held every year in the Department.

A Computer Center, with Department and INFN personnel, maintains the computational facilities and gives support to research and computer science laboratories. Essential support to experiments and maintenance of laboratories is provided by the Department Workshop, where technicians can design and produce high-quality tools and components.

The members of the Department are organized in different Divisions, on the basis of their scientific interests. The research is mostly performed in the framework of

* The first name of the Department was "Institute of Complementary Physics". It was later changed in "Institute of Physics". In 1982 the Institute was split into the "Department of Physics" and the "Institute of Applied General Physics".
** Referring to the young physicist Pontremoli, who spent a period of study at the Cavendish Laboratory, Rutherford wrote that he shows "great fertility in speculation and suggestions for further experiment".

international collaborations, both on large scale installations and on university scale devices operating in the Department. Valuable support to research comes from graduate students and research fellows.

Small-group research environments are equally supported by the Department as larger groups; both can provide occasions for generating technological advances and new ideas. The main characteristics of the Department are: a balance between research in basic physics and applied physics and technological applications; a commitment to education in physics; and the diffusion of scientific issues in the community. In a recent evaluation of the quality of the research carried out during a three year period in Italian universities, by means of international peer review, our Department has been rated very close to the top level.

This Report refers to the scientific activity of the Department*** in the period 2005-2006; most of the material (updated and abridged) originates from the presentations made at the Department Congress in October 2005 (*Highlights in Physics 2005*), available online at the address http://www.fisica.unimi.it/highlights2005/

Milan, July 2006

Roberto Pozzoli
Head of the Department

*** Research by members of the Institute of General Applied Physics is also included. In particular, the contributions listed under the headings “Environmental Physics” and ”Physics, Arts, and Cultural Heritage” refer to research carried out primarily by scientists at the “Institute of Applied General Physics”.

Professors
Emilio Acerbi
Gianpaolo Bellini
Enrico Bellone
Marco Bersanelli
Giuseppe Bertin
Pier Francesco Bortignon
Ilario Boscolo
Angela Bracco
Ricardo Americo Broglia
Sergio Caracciolo
Graziano Cavallini
Paolo Cotta Ramusino
Ruggero Ferrari
Stefano Forte
Ettore Gadioli
Marzio Giglio
Ileana Iori
Lodovico Giovanni Lanz
Luciano Mandelli
Piergiuseppe Maranesi
Emanuela Meroni
Paolo Milani
Laura Perini
Marcello Pignanelli
Roberto Pozzoli
Giovanni Maria Prosperi
Francesco Ragusa
Luciano Reatto
Guido Vegni
Daniela Zanon
Alberto Pullia
Lucio Rossi
Enrico Spoletini
Giuliano Strini
Dario Teodoro
Alberto Vailati
Luisa Zetta

Associate Professors
Giovanni Bellomo
Daniela Bettega
Mauro Bonardi
Silvia Bonetti
Franco Camera
Daniel Victor Camin
Bruno Candoni
Marie Claire Cantone
Federico Casagrande
Gianluca Colò
Franca De Luca
Carlo De Martinis
Michelangelo Fazio
Franco Gallone
Grazia Gambarini
Anna Maria Grassi
Paolo Guazzoni
Dietmar Klemm
Silvia Leoni
Giulia Luisa Masserini
Luca Molinari
Evelina Mulazzi
Giovanni Onida
Carlo Pagani
Constantinos Paizis
Fernando Palombo
Guido Parravicini
Luciana Pirola
Pierre Massimo Pizzochero
Ivano Ettore Pollini

Assistant Professors
Maria Cristina Abbati
Attilio Andreazza
Bruno Franco Bassetti
Lanfranco Belloni
Nora Serafina Brambilla
Francesco Caravaglios
Leonardo Carminati
Fabrizio Castelli
Michela Cavinato
Anna Luisa Ciapi
Marcello Fanti
Davide Emilio Galli
Marco Alessandro Luigi Giliberti
Augusto Marco Giussani
Flavia Groppi Garlandini
Marco Lombardi
Giancarlo Lupieri
Davide Maino
Nicola Manini
Aniello Mennella
Lino Miramonti
Matteo Paris
Vittoria Petrillo
Davide Enrico Pini
Nicola Umberto Cesare Piovella
Paolo Giuseppe Carlo Piseri
Alessandro Podestà
Marco Alberto Carlo Potenza
Giovanni Puddu
Mario Raciti
Stefano Riboldi
Franco Riva
Marco Riva
Massimiliano Romé
Massimo Sorbi
Guido Tiana
Bassano Vacchini
Fausto Valz Gris
Alessandro Vicini
Antonio Zecca

Technicians
Alessandro Andreani
Augusto Adriano Bassi
Paola Calzolari
Marina Carpineti
Giancarlo Cartegni
Francesco Cavaliere
Carlo Cicardi
Maurizio Cignoli
Daniele Cipriani
Giuseppe Di Pietro
Matteo Faleschini
Francesca Fiorentini

Attilio Giuseppe Gandini
Ambra Dionigia Gianola
Luciano Grilli
Salvatore Incorvaia
Nicola Ludwig
Franco Leveraro
Giuliano Manassi
Giuliano Malvezzi
Claudio Piazzoni
Giancesare Rivoltella
Carlo Valentini

Administrative Staff
Tiziana Asperges
Tiziana Bussini
Franca Cordani
Eulalia Maria Gattullo
Fortunato Laface
Giuseppe Martelli
Maura Soler
Maria Stiffoni
Cesare Tondelli
Stefano Zanchi
Andrea Zanzani

Custodians
Virginia Duretto
Bruno Laurendi
Maria Mangiacasale
Maurizio Pezzano
Angela Pignataro
Angelo Rodolfi
Maria Giuseppina Vitarelli

Research Fellows and Associates
Antonio Vairo
Francesco Belgiorno
Federico Belloni
Giovanni Bettega
Gero Antonio Bongiorno
Marco Caldarelli
Benedetta Capellini
Roberto Cerbino
Francesco Cerutti
Mary Cola
Marco Cosentino
Marco Delmastro
Paola Donati
Davide Franco
Guido Fratesi
Katalin Gaal Nagy
Maria Vittoria Garzelli
Simona Gay
Valerio Grassi
Alfio Lazzaro
Cristina Losa
Alfredo Lulli
Marco Mauri
Stefano Olivares
Gregory Potel Aguilar
Davide Provasi
Andrea Quadri
Antonio Rago
Maurizio Rossi
Andrea Sportiello
Ivan Veronese
Ashish Warrier

Workshop

F. Cavaliere
G. Malvezzi
A. Gandini
S. Incorvaia

Since 1995 the Workshop supports research and teaching activity in the Department. It uses traditional and computer assisted machine-tools, welding machines based on electric gas metal and gas tungsten arc (TIG) processes, and advanced CAD/CAE design tools.

The Workshop can treat all metal alloys, steels, copper, thermoplastics and ceramics, and build high-vacuum and technical apparatuses for experiments in different fields, as nanotechnology, astrophysics, plasma physics, optics, medical physics.

Computer Center

F. Leveraro
M. Faleschini
G. Manassi

The Computer Center supports the computational needs of the administration and of the scientific and academic communities of the Department, provides hardware and software solutions, and manages the local area network. The computer room houses 171 computers: 112 are calculation farms, 52 run the main Department computing services, and 7 are single research groups dedicated servers. The local area network has 47 network switches and is distributed over 11 different buildings. Daily and weekly backups are executed. The data storage holds about 1200 Gigabytes and is always available.

The Center operates in collaboration with the Milan Division of INFN. In the frame of the Italian LHC Computing Grid a Tier-2 facility will be completed by 2010, with about 130 calculation nodes (dual processors), with a CPU total power of 1.6 MSI2k and about 800 TB of storage.

The Milan Division of the National Institute of Nuclear Physics (INFN)

INFN is one of the public research institutes in Italy. It is devoted to research in the fundamental area of nuclear and subnuclear physics and related applications. Almost all of the Italian basic research in these fields is financed and organized through INFN, which also has its own research and technical personnel.

INFN has been operating in collaboration with the Physics Department of the Università degli Studi di Milano since the birth of this institution, i.e. in the 50's.

The INFN division of Milan is currently engaged in many different and important activities, where both INFN and University scientists and technicians cooperate in national and international projects.

The activity of INFN is normally divided into five independent sectors:

- Experimental subnuclear physics at accelerators
- Experimental neutrino physics and subnuclear physics without accelerators
- Nuclear physics
- Theory
- Interdisciplinary activities and applications

Experimental subnuclear physics at accelerators

At present there are two strong INFN groups who participate in the ATLAS collaboration for the LHC proton-proton collider. ATLAS is a huge multipurpose detector, run by a large international collaboration, to be operated at the CERN European laboratory in Geneva starting in the fall of 2007. It has the purpose to investigate the mechanism of mass generation for Fermi particles and to explore the new scenarios, such as supersymmetry, which are expected beyond the so called "standard model" of fundamental particles. The two groups in Milan are involved in two different contributions to the detector: calorimetry with lead and liquid argon detectors and the tracking by means of silicon pixel detectors. After completing the construction, these groups will be deeply involved in the analysis of data.

Another group in Milan is active in particle physics at accelerators, participating in the BABAR international experiment at SLAC (USA), which investigates the violation of the CP symmetry in the decays of B mesons.

Experimental neutrino physics and subnuclear physics without accelerators

The main research project of this sector concerns the Borexino experiment at the Gran Sasso laboratory of INFN, which is designed for solar neutrinos, to be detected by means of a large volume of high purity liquid scintillator; it will start to operate in 2007. The Milan group has the leadership of the international collaboration which runs the experiment.

Another group in Milan is in turn involved in the ICARUS international project: a large volume detector based on the liquid argon technology to be operated at Gran Sasso for atmospheric and artificial (from a beam originated at CERN) neutrinos. This detector will also be used for other important topics such as the search for proton decay, as predicted by Grand Unification Theories.

A third group in Milan then participates in the international collaboration for the Auger project: a giant surface detector to investigate cosmic rays at the highest possible energies (10^{20} eV or more).

Nuclear physics

Traditionally this is one of the most important INFN sectors in Milan. At present there are nine groups that are active in different Italian and international collaborations investigating topics such as: nucleon strangeness, phase transitions in hadronic and nuclear matter, meson properties in nuclear matter, multi-fragmentation processes, nuclear structure and reaction dynamics, measurement of cross sections of interest for nuclear astrophysics and, more recently, a test of the equivalence principle for antimatter using anti-hydrogen atoms.

Theory

The theoretical group involves several scientists and is oriented along six main lines of activity: (i) field and string theory; (ii) phenomenology of particle physics (with main interest in the standard model, QCD, and new ideas); (iii) theoretical nuclear physics (mainly for multi-body systems), (iv) mathematical methods (with particular concern for a rigorous formulation of quantum mechanics, chaotic classic and quantum systems); (v) astro-particle physics (with emphasis on the study of star interiors); (vi) statistical physics and applied field theory (mainly dedicated to biological applications).

Interdisciplinary activities and applications

The activities in this sector are several and diversified (more than 25). These include the development of new particle detectors, electronics, with an important contribution to medical physics, from hadron-therapy to radiobiology and radiotherapy with radionuclides. Also to be mentioned is the theoretical study of Free Electron Laser acceleration techniques in quantum regimes and the development of simulation tools for particle transport and interactions.

Special projects

The Milan division of INFN is also involved in several projects of special interest, such as those of the NTA project, i.e. the development of new techniques for particle acceleration. Some of these are mostly carried out at the LASA site in Segrate (resonant cavities, fast pulsed magnets), with a strong connection with superconductive technologies. Other related activities concern the research and development in the framework of the Global Design Effort for a Linear Collider. The research in high brightness electron beams, coherent X-ray production, and plasma accelerations are covered in the SPARC, SPARX, and PLASMONX projects.

Of a totally different nature, i.e. information technologies, is the deep involvement of the division in the GRID project, aiming at the development of a global system of distributed computing.

Courses and Degrees

Bachelor of Science

The aim of the Bachelor of Science program is to give students a broad background in physics and related fields such as mathematics and computing. Students take a core sequence of courses in classical physics, quantum physics, mathematics, and computing. The program is designed to give students solid foundations to prepare them for work in the field or for a physics graduate program. We believe that a physics degree should represent a strong training for a broad range of careers. Our students develop strong mathematical and analytical skills, very good laboratory and programming proficiency, and a solid knowledge of the fundamental laws that govern nature.

Most of the students thus graduated in physics (Laurea Triennale) continue their studies with an additional 2 year course leading to a Master (Laurea Magistrale). However, 10 to 20% of them look for a job immediately and find good opportunities in a variety of fields: high-tech companies, electronics, information technologies, environmental research and protection, and consulting.

Master of Science

The aim of this degree program is to provide the student with an advanced knowledge of physics, as required to pursue a career in pure or applied physics, either in research or in industry. The courses leading to this degree will provide the student with a thorough knowledge of classical and modern physics, as well as the necessary knowledge of mathematical methods, modern experimental tools, data analysis, and computing techniques. The student will also receive advanced training leading to the forefront of research in at least one major subfield of physics, such as astrophysics, electronics, applied physics, optics, quantum optics, condensed matter physics, plasma physics, nuclear physics, particle physics, medical and health physics, biophysics, theoretical physics, geophysics, environmental physics, and archaeometry.

This degree program aims at developing the modeling skills which characterize the physical sciences and at learning how to apply them independently to problems in the fields of fundamental and applied science and technology. These skills are useful and prized for a variety of career choices, both in academia and in industry, including fundamental and applied research, teaching, science journalism, and a variety of management and technical jobs in industry, environment, health, and civil service.

Doctorate School in Physics, Astrophysics, and Applied Physics

The Doctorate School in Physics, Astrophysics, and Applied Physics is a joint initiative of the Department of Physics, the Department of Chemistry, Biochemistry, and Biotechnology, and the Institute of General Applied Physics of the Università degli Studi di Milano and of the Department of Mathematics and Physics of the Brescia University. The Department of Physics is the administrative seat of the School.

The School offers a three year long international training curriculum, with intensive courses, series of seminars, research stages in high-quality public and private laboratories for fundamental and applied physics. The students are involved in research projects at the Departments and Institutes of the Doctorate School, in practically all mainstream areas of physics such as: applied superconductivity (magnets and accelerators), astroparticle physics, astrophysics, biophysics, biotechnology, condensed matter, cosmology, electronics and microelectronics, earth physics, elementary particle physics at accelerators and underground, environmental science, medical and health physics, nanotechnologies, nuclear physics, optical methods, plasma physics, quantum optics, and theoretical physics.

Agreements have been signed with various European doctorate schools, with mutual recognition of the doctorate qualifications, and with European networks aimed at a joint organization of schools and exchanges of teachers and students. The number of the graduate students admitted to the School ranges from 20 to 30 per year, coming from various Italian universities and foreign countries also outside Europe. Each year, the students admitted to the School are selected out of a number of candidates typically larger than one hundred.

Post-Graduate School in Health Physics

The School of Health Physics of the Università degli Studi di Milano is a four year post-graduate School that leads to a diploma in Health Physics. A maximum of ten students are admitted per year. The School, with administrative seat at the Department of Physics, operates within the Faculty of Science in cooperation with the Faculty of Medicine. In addition, structures and personnel of the National Health Service, as well as national and international, private and public institutions, contribute to this program, within suitable cooperation agreements. The School serves a community that is not limited to the Milan urban area or to the Lombardy region, attracting students from universities scattered across Italy. In 2006 the Università degli Studi di Milano signed an inter-university cooperation agreement with the University of Pavia and the Insubria University for a joint management of the School.

With the aim of creating Health Physicists with the professional and the cultural expertise needed to manage the medical physics activities, each of the four years of the School is based on about 200 hours of classes and a mandatory practical experience, through residency traineeships in one of the more than thirty structures, among universities, research centers and hospitals, that are partners of the School. In particular, the student is asked to cooperate in specific professional actions related to: radiation therapy, nuclear medicine, diagnostic imaging, medical statistics, and informatics. There are approximately twenty well defined specific actions, some of which are listed here as an example: personalized treatment planning; metabolic therapy treatment planning; process for patient dosimetry; quality controls over computer tomography and magnetic resonance equipments; biomedical image processing.

The main scope of the professional education at this School can be described as follows:

- The area of General Introduction provides the student with specific knowledge about the interaction of radiation with matter, radiobiology, biophysics, statistics, informatics, and electronics applied to medicine. In addition, it provides fundamentals of physiology, biology, anatomy, and biochemistry, as well as the main principles of radiation protection and prevention, within the relevant national and international standards.
- The area of Oncological Therapies provides basic knowledge on dosimetry of external beam radiotherapy and brachytherapy, basic theoretical and practical know-how allowing the student to define and implement treatment planning for ionizing and non-ionizing radiation therapy, as well as the required expertise needed to instruct and implement therapeutic protocols and quality assurance programs for applications involving therapeutic use of radiations.
- The area of Diagnostic Imaging provides fundamentals of tracer theory, nuclear medicine, and clinical diagnostic systems (CT, NMR, gamma-camera, PET, IR radiometry, endoscopy equipment, optical and electronic microscopy, fluorescence and spectrophotometry), as well as the basis for quality assurance and control programs for diagnostic imaging, with particular attention to the protection of the patient.
- The area of Information Technology provides the basic knowledge for the treatment and processing of biomedical signals and for supporting the hospital management.

To obtain the Health Physics Diploma, the student is asked to prepare and to defend a thesis concerning one of the fields within the scope of the School, which is assigned at the beginning of the last year. The thesis is prepared under the guidance of a tutor and is subject to the independent evaluation of a referee.

Divisions and Current Research

Elementary Particle Physics

G. Bellini
L. Mandelli
E. Meroni
L. Perini
F. Ragusa
G. Vegni
S. Bonetti
D. Camin
F. Palombo
A. Andreazza
L. Carminati
M. Fanti
L. Miramonti
M. Delmastro
D. Franco
V. Grassi
A. Lazzaro

Research in Elementary Particle Physics aims at the understanding of the elementary constituents of our universe. This research is performed either at high energy accelerators or with apparatuses studying the cosmic ray radiation. Several groups of the Department are active in the following experiments:

ATLAS: A high energy frontier experiment at the Large Hadron Collider (LHC), the new accelerator currently near completion at the CERN laboratory near Geneva which will reach, by far, the highest collision energy in the world, giving access to physics at an energy scale about ten times higher than has been open to exploration so far. The main scientific targets are the confirmation of the Standard Model, with the discovery and study of the last missing piece of this model, the Higgs boson, providing a possible way to explain the masses of particles. Another top priority is the search for phenomena beyond the SM such as particles predicted by Supersymmetry. The lightest of these might be what makes the dark matter that no telescope can detect but which must exist to explain the structure of the Universe and the formation of sub-structures, like galaxies, within it. Other theories which postulate the existence of extra dimensions of space can also be investigated. This may allow LHC to enter the domain of quantum gravity, providing experimental data that will help to understand how to reconcile quantum mechanics and gravity. Three groups are present in Milan and working on the large Barrel Superconducting Toroid, the Liquid Argon electromagnetic calorimeter and the Pixels Vertex Detector. The detector is in an advanced assembly stage. First data are scheduled for 2007. Groups are also very active in preparing for the data analyses particularly in the search of the Higgs boson and of particles predicted by Supersymmetry models.

GRID: a new tool which in the frame of the LHC experiments aims at providing access to computer resources at a world scale.

BaBar: experiment performed at SLAC (Stanford) Laboratory is investigating with very high statistic the CP violation and the decays of particles with a Beauty quark. The understanding of CP violation is a critical point toward the understanding of the matter-antimatter asymmetry in the universe.

The group present in the Milan Department is actively involved in the data analysis and in particular has measured the time-dependent CP-violating parameters in B^0 decays to $\eta' K^0_S$. This is the first observation of CP violation in this channel. The group has also measured the branching fractions of B meson decays in final states involving η, η', and a_1 (1260) mesons, and also radiative B decays to $\eta' K \gamma$ and ηK^0_L.

ALEPH and DELPHI: these two experiments at the Large Electron Positron (LEP) collider at CERN, provided a very solid experimental foundation to the Standard Model. The accelerator has concluded the data acquisition in 2000 to allow the assembly of LHC. The collaboration is currently completing the publication of final measurements.

The experiments studying the cosmic radiation either in underground laboratories or with surface detectors are:

BOREXINO: this is an experiment located at the INFN Gran Sasso laboratory planning to study the Solar neutrinos below 1 MeV in real time. It also plans to study the Geo neutrinos, by taking advantage of the lowest background in the world (due to the absence of nuclear reactors in Italy), and neutrinos from possible Supernovae explosions. The detector resumed its activity after a long interruption due to upgrading of the safety and service plants of the laboratory. The final filling of the detector with scintillator will be completed by the end of April 2007. In the meantime the Counting Test Facility (the more sensitive detector in the world at ton level) continued its activity of checking the ultra low level radiopurity of the scintillator, and produced several important physics results such as: the world best limit on electron stability; the most stringent limit on neutrino magnetic moment obtained with low-energy neutrinos; the first limit at low energy of antineutrinos from the

Sun; the world best limit on nn and pp decay into invisible channels; limits on the Pauli Exclusion principle (improving up to three orders of magnitude the previous limits) and limits on heavy neutrino mixing stronger than those obtained in experiments using accelerators and reactors, in the energy range 4-10 MeV.

ICARUS: a Liquid Argon drift chamber also located at the Gran Sasso Laboratory to study neutrinos from cosmic radiation and from the CERN neutrino beam.

AUGER: this experiment which is dedicated to the study of very high energy cosmic rays (10^{18} eV) at two different sites, one in Argentina (presently collecting data) and one (planned) in USA. The research activity comprises both the contribution to the data taking with fluorescence detectors, and the hybrid reconstruction of the events, to improve strongly the data quality.

Nuclear Physics

P.F. Bortignon
A. Bracco
R. Broglia
E. Gadioli
I. Iori
M. Pignanelli
F. Camera
G. Colò
P. Guazzoni
S. Leoni
A. Pullia
L. Zetta
M. Cavinato
S. Riboldi
G. Tiana
F. Cerutti
M.V. Garzelli
C. Losa
G. Potel Aguilar
D. Provasi

The research activity of this Division is focused on the study (experimental and theoretical) of nuclear structure and nuclear reaction mechanisms induced by accelerators or present in astrophysical and medical environments.

Nuclear structure studies focus on the collective properties of nuclei, namely vibrations and rotations, through the measurement of the electromagnetic decay of the excited nuclei of heavy ions. In this way it is possible to study the shape and the deformation of the nucleus, the relaxation mechanism of the degrees of freedom and the order-chaos transitions that take place as the nuclear excitation energy increases, with special attention to exotic nuclei far from the stability valley. In addition to the reactions induced by heavy ions, the use of polarized protons makes it possible to analyze experimentally the predictions of the microscopic shell model.

The research program in nuclear reaction mechanisms is based on heavy ion reactions at intermediate and relativistic energy. In this energy range it is possible to study both multifragmentation and chiral symmetry at high temperature and baryon density.
In the field of experimental nuclear astrophysics activity we are measuring cross sections of the reactions involved in the stellar p-p chain and in the CNO and MgAl cycles (which enter in the hydrogen burning of stars). The ^{12}C induced reaction on nuclei of the biological tissues are measured and studied for the improvement in the therapy of cancer (adrotherapy) and to better understand the radiation damage in space environments. On the theoretical side, the group makes use of a Boltzmann Master Equation approach and collaborates in the development of the transport code FLUKA.

The experimental research activity for the development of detection arrays is carried out in collaboration with other European countries, in the framework of the Integrated Infrastructure Initiative of the European Community. Several projects focus on the construction of complex, new generation arrays for the measurement of gamma and charged particles. Analogical and Digital electronics, Detectors and Pulse Shape Analysis algorithms for the identification of the interaction particles and the gamma ray incident direction and trajectory are developed.

The theoretical research activity concerns the collective and single particle properties in exotic nuclei. The theoretical group performs systematic calculations on nuclear masses, charged exchange transitions, and nuclear compressibility. The origin of pair interaction is also studied.

The methods developed in the many-body approach to the description of nuclear matter are applied to the many-body theory which is the core in the description of the nuclear system and can be successfully applied to several other fields. In particular, it is possible to use the many-body approach to study the metal carbon clusters. Many-body theory is also used in the study of protein folding and protein building. These results are also relevant to the development of medical drugs.

Accelerators and Related Technologies

E. Acerbi
G. Bellomo
M. Bonardi
C. De Martinis
C. Pagani
L. Rossi
F. Groppi
M. Sorbi
M. Mauri

The research on accelerator physics and the development of related technologies are carried out at the LASA Laboratory and are mainly funded by INFN. Main research activities are on the future electron linear collider (ILC), high intensity proton beam accelerators (SPL at CERN and European project EUROTRANS), magnets for LHC detectors (ATLAS barrel toroid), proton therapy machine at CNAO (Pavia), RF compressors for electron beams, applied superconductivity and radiochemistry.

Significant contributions have been produced for TTF at DESY, the machine built as a test facility, in view of the future electron linear collider ILC: cryomodules and ancillaries engineering and construction, superconducting cavity production in collaboration with the Italian industry, and photocathode development and production. Superconducting cavity and cryomodule design and production for low beta high intensity proton beams, accelerator reliability studies, and lattice optimization are the main activities in the proton machine field.

The magnet group at the LASA laboratory has been active since the 80's in the field of superconductivity applied to magnets. A high field laboratory is active, where we currently perform measurements at liquid helium temperature on transport properties and mechanical characteristics of high-current superconductors. The facilities of the laboratory include the unique SOLEMI solenoid system, which allows for a magnetic field up to 18 Tesla. The group future plans include the development of high-performance dipoles for future particle accelerators, for the LHC upgrade at CERN and the FAIR facility at GSI (Darmstadt, Germany).

The radiochemistry group studies the optimisation of the cyclotron production and quality control of short and medium lived radionuclides to be used in environment and in nuclear medicine studies. In particular, alpha and beta emitting radionuclides for metabolic radiotherapy are under investigation. The radioanalytical quality control of radiopharmaceutical compounds labelled with beta, Auger and alpha emitters for metabolic radiotherapy are made in collaboration with Nuclear Medicine Departments. The determination and speciation of radionuclides, like actinoids, in biological and environmental samples by radiochemical and radioanalytical techniques,is also performed.

Electronics

P. Maranesi
E. Spoletini
M. Riva
F. Belloni

Work in progress: Development of CAD tools for the dynamic characterization and control optimization of power electronic circuits and realization of an apparatus for automatic tests and measurements. Innovation of circuit topologies and control techniques for DC to DC converters switching at high frequency. Radiation detectors using composite semiconductors (SiC, CdTe). Low noise preamplification of nuclear signals by digital filters and relevant front-end VLSI design. Techniques for optimal transmission of analog signals through optical fibers. Development of low temperature opto-devices. Realization of electronic subsystems for the AGATA Experiment.

Main results: HV generator for ionic motor drive. Theoretical and experimental characterization of lift converters. Experimental results on SiC and CdTe radiation detectors. Realization of low-noise digital filters. Characterization of criogenic optoelectronic devices.

Structure of Matter

P. Milani
L. Reatto
G. Masserini
E. Mulazzi
G. Onida
I. Pollini
D. Galli
N. Manini
D. Pini
P. Piseri

The research activity comprises theory and experiments on a number of topics in condensed matter physics.

Experimental activity
The molecular beams and nano-crystalline materials laboratory is active in the fields of gas phase nano-particle synthesis, nano-structured films and micro-pattern formation by Supersonic Cluster Beam Deposition (SCBD). The film properties are investigated by Raman spectroscopy, XPS, AFM and SEM. The electronic and structural properties of

A. Podestà
G.A. Bongiorno
G. Fratesi
K. Gaal Nagy
M. Rossi
A. Warrier

free particles are studied by Time of Flight Mass Spectrometry and X-ray Absorption Spectroscopy by synchrotron radiation (at the ELETTRA facility), with special emphasis on the study of growth processes and separation effects in gas-dynamics. The soft landing conditions typical of SCBD allow the formation of metastable structures in the form of thin filmsthat are reminiscent of the particle properties. The investigation of such correlations is one of the principal activities of the group. Other activities include the use and development of AFM techniques for the investigation of tribological properties at the nano-scale, for the study of protein, DNA and cell interaction with nano-structured surfaces, for the investigation and modification of electric transport properties and surface chemistry at the nano-scale. Other fields of experimental activity (performed in collaboration with European accelerator facilities) are: Photoemission spectroscopy of Mott compounds; Time-of-Flight Electron Spectroscopy on cathodic materials; Heterogeneous catalysis by gold nano-particles; Quantum conductance studies on carbon nanotubes. Recent achievements refer to: Gas phase NEXAFS on mass resolved transition metal particles, development of microarrays for reverse infection on cell cultures. Work in progress focuses on: Investigation of sp carbon formation and stability by gas phase light scattering experiments; Unraveling the ns-TiO2 interaction with protein functional groups through in situ XPS, XAS studies.

Theoretical activity

A) Solid state

Ab-initio study of the excited state properties of solids, including low-dimensional systems such as surfaces, nano-wires, and clusters. Most of the work is based on the Green's function approach, and/or on the Density Functional Theory methods. Our aim is to support the experimentalist in the physical understanding of electronic excitations of real systems, by calculating the relevant electronic and optical spectra. Applications to surfaces are presently mainly directed towards semiconductors and metals, with emphasis on silicon and silicon oxide. Other fields of theoretical activity are: Correlation effects in the dynamics of fermions, in particular of electrons in the molecular orbitals of C_{60} and in solid fullerides, and in droplets of ultra-cold alkali atoms; Electron-vibration effects in polyatomic molecules, with particular attention to Jahn-Teller systems and non-adiabatic effects; Anharmonic vibrational spectra of polyatomic molecules; Investigation of a model for lubricated nano-friction; Study of the optical absorption, photoluminescence, Raman scattering spectra of carbon nano-tube-PPV composite films.Since 2004, we are part of a NoE (Network of Excellence) named “Nanoquanta”, funded by the European Community under the 6th Framework program. Recent achievements are: Implementation of a numerical method for disentangling surface contributions to the optical spectra of solids; Study of the local-field effects in the optical spectra of oxidized silicon nanoclusters, including stoke shifts; Understanding of optical signatures related to oxygen adsorption on the Silicon (100) surface; Realization of a model chemical potential for interacting atomic fermions; Determination of the condensed fraction within the generalized BCS for interaction fermions; Quantitative explanation of the observed changes in the optical spectra of PPV and PPV-carbon nano-tube films as a function of the polymer conversion temperature. Work in progress focuses on: Study of the optical anisotropy of the low-index Silicon (113) surface; Study of the optical properties of the PPV film and PPV-SWNCT composite films as a function of the precursor dilution.

B) Quantum many body systems

Study of superfluids and of quantum solids based on microscopic theories and quantum simulations. We have extensively studied bulk superfluid ^{4}He as well as droplets and ^{4}He in nano-pore and in thin films on graphite. Great attention has been given also to the solid phases of ^{4}He, especially in connection with the recently observed supersolid phase. These studies have been performed by variational Monte Carlo and by exact projection methods. Another area of interest is that of trapped quantum Bose gases. In this case, the mean field approximation has been used to study problems such as the formation of solitons, dimensional crossover, and quantum tunneling and coherence. Recent achievements refer to: Development of the exact projection method Shadow Path Integral Ground State; Vacancy induced Bose Einstein condensation in solid ^{4}He; Layer by solidification of ^{4}He in nano-pores. Work in progress focuses on: Determination of presence of ground state vacancies in solid ^{4}He; Clarification of mechanism of supersolidity in ^{4}He; Phases of boson atoms in a toroidal trap.

C) Soft matter physics

Theory and simulation of models for complex fluids such as colloids, polymers and biopolymers in solution. Special attention is given to phase diagrams, to critical phenomena and to structural arrest in such systems. These problems are studied by our own renormalization group liquid state theory and by the replica theory for the glass transition. Another topic addressed in our research is the formation of micro-phase separation in the presence of competing forces over different length scales. Since 2004, we are part of a Marie Curie Network “Dynamical arrested state of soft matter and colloids”, funded by the European Community under the 6th Framework Program. Recent achievements refer to: Phase diagram of star polymers; Micro-phases of soft particles at an interface; Critical phenomena in soft matter fluids. Work in progress focuses on: Theory of fluids with very short range attraction; Micro-phases of soft particles in bulk and surface effects.

Quantum Optics, Coherent Phenomena, and Optoelectronics

I. Boscolo
F. Casagrande
A. Grassi
G. Strini
L. Belloni
F. Castelli
M. Paris
V. Petrillo
N. Piovella
M. Cola
A. Lulli
S. Olivares

The interaction between radiation and matter is investigated both theoretically and experimentally, with special focus on coherent phenomena and collective effects. Among the main lines of research: interaction of atoms and photons in a cavity; quantum regime of free electron laser dynamics and collective effects in the coherent interaction between laser and atomic condensates; new protocols to characterize and exploit nonclassical light in quantum information processing; Thomson scattering between high brilliance electron beams and laser radiation; photoemission, photocathodes and laser applications to particle acceleration; implementation of photonic crystal fibre systems; quantum computing and cryptography.

Recent results: Generation and decoherence of mesoscopic superposition states in a cavity field and atomic correlations; quantum purification of the free electron laser spectrum, and collective recoil lasing with atoms in an optical cavity; novel, experimentally realized schemes to obtain photon statistics without photocounters and realize telecloning in a noisy environment; evaluation of the spectra for incoherent Thomson scattering; generation of rectangular laser pulses for high brilliance electron guns and photoemission from diamond films; microphotographic system for spectral analysis of photonic crystal fibres; characterization and effects of errors in quantum computing and cryptography. Work in progress: Generation and manipulation of entanglement in atoms-photons systems; 3D description of the quantum free electron laser, and self-induced focussing forces in Bose-Einstein condensates; novel schemes to enhance entanglement and improve high-precision measurements; dynamics and radiation of particles in laser fields; spatial modulation of laser pulses and laser excitation of positronium for experiments on anti-matter; limits of single-mode behaviour in photonic crystal fibres; error-correcting codes under multiple-errors conditions in quantum computing.

Optics

M. Giglio
A. Vailati
M. Potenza
R. Cerbino

The research focuses on:
Non equilibrium fluctuations in stressed liquids, mainly within the ESA-NASA sponsored GRADFLEX experiment to be flown in 2007. Giant large scale fluctuations will be measured in a single component fluid and a mixture under a temperature gradient and in microgravity conditions. Convective instabilities in complex fluids, such as large molecular weight solutions where the Soret effect is very large and the primary source for buoyancy forces. A model for Earth mantle dynamics. Extension of speckle methods to X-Ray radiation, like synchrotron radiation. Development of innovative instrumentation, mainly for particle size determination.

Specific results obtained recently are:
The definition of the selection of the flight hardware for the GRADFLEX instrumentation and the beginning of the selection of tests and calibration procedures. A detailed study of scaling behaviour in the transient of a convective instability in a large molecular weight solution. The scaling of the equivalent of the Nusselt number is reported. Near Field

Scattering speckles are observed in the deep Fresnel region of the synchrotron scattered radiation from a statistical sample. This opens the possibility of performing static and dynamic scattering at extremely small wavevectors where no alternative instrumental methods are available. Innovative single particle scattering methods have been proposed, capable of performing well into the submicron regime. The ideas are covered by two international PCT procedures.

Plasma Physics and Astrophysics

M. Bersanelli
G. Bertin
R. Pozzoli
F. De Luca
C. Paizis
P. Pizzochero
A. Ciapi
M. Lombardi
D. Maino
A. Mennella
M. Romé
G. Bettega
B. Cappellini
P. Donati

The research focuses on the following topics: basic processes in plasma physics, dynamics of non-neutral plasmas, formation and evolution of non-linear coherent structures in electron plasmas, physics of thermonuclear plasmas, astrophysical plasmas, accretion disks, dynamics of galaxies and other stellar systems, clusters of galaxies, dark matter, gravitational lenses, cosmic rays, nuclear astrophysics of compact stellar objects, gravitational collapse and supernova explosions, pulsar glitches and superfluid vortices, observational and experimental cosmology, studies of the diffuse galactic microwave emission, measurements of the anisotropies and polarization of the Cosmic Microwave Background radiation. On the experimental side, two main projects are in progress: ELTRAP, a small experiment for the study of non-linear phenomena in non-neutral plasmas confined in a Malmberg-Penning trap; the design, construction and development of instrumentation within the PLANCK project, an international space mission that will be launched soon to measure the properties of the Cosmic Microwave Background with unprecedented precision, with related activity referring to the Background Anisotropy Scanning Telescope experiment and the development of corrugated feed horns, arrays, and other RF components. In addition, we actively participate in the ULYSSES mission, devoted to the study of the properties of the heliosphere outside the plane of the ecliptic, and in the COROT mission, devoted to the study of asteroseismology and to the search for extrasolar planets. Some observational projects address the study of distant galaxies and clusters of galaxies with observations at the major telescopes from the ground and from space. The research is carried out within national and international collaborations, in close contact with the Italian Research Organizations INAF, INFN, INFM, and CNR.

Theoretical Physics

S. Caracciolo
P. Cotta Ramusino
R. Ferrari
S. Forte
L. Lanz
G. Prosperi
D. Zanon
F. Gallone
D. Klemm
L. Molinari
G. Parravicini
M. Abbati
B. Bassetti
N. Brambilla

Theory of fundamental interactions, standard model and beyond: precision tests, perturbative QCD, heavy quarks, neutrinos, confinement, supergravity and superstrings, M-theory. General problems in field theory: gauge theories renormalization, renormalization group and effective theories, geometric aspects of gauge theories, two-dimensional problems, field theories for confined systems out-of-equilibrium. Statistical mechanics: stochastic processes and dissipative systems, quantum Hall effect, mesoscopic systems, phase transitions in polymer physics, quantum model for biological systems, Berry phase in quantum computing. Foundations of Quantum Mechanics. Mathematical Physics methods for Geophysics.

Recent results refer to: heavy-quarks effective-field theory, renormalization of the non-linear sigma model in D = 4, formulation of the Electroweak model with an explicit mass a la Stueckelberg; unitarity in Landau gauge and non-abelian gauge-theories with an explicit mass a la Stueckelberg; study of partonic structure of the nucleons, superpotential in supersymmetric gauge theories with N = 1, microsystem dynamics both at equilibrium and out-of-equilibrium, decoherence; relativistic field equations for spin 1 massive particles in curved space-time; 1/N expansion for field theories with strong nonlinear interactions; O(N)-invariant models at negative N; counting Feynman diagrams in fermionic systems.

Work in progress: supersymmetry N = 3 in D = 4 and relation with QCD, AdS/CFT correspondence. Field-theoretic approach to decoherence; application to the statistical operator formalism out-of-equilibrium; study of the logical-chemical structure of networks for cell regulation of transcription. Heavy-quarks effective-field theory on a lattice, effective theory for adronic states over the threshold; quarkonium suppression in heavy-ion collisions; realization of a Monte Carlo event-generator for a phenomenological study of Drell-Yan processes at adronic colliders; analytical study of the next-to-leading order correction to the process of the Higgs boson production via gluon fusion; quantization of

non-renormalizable gauge-invariant theories; algebraic approach to the Slavnov-Taylor identities for multi-loop amplitudes in the standard model; physics beyond the standard model.

Medical and Health Physics

F. Caravaglios
G. Lupieri
G. Puddu
M. Raciti
F. Riva
B. Vacchini
F. Valz Gris
A. Vicini
A. Zecca
A. Vairo
F. Belgiorno
M. Caldarelli
M. Cosentino
A. Quadri
A. Rago
A. Sportiello

The scientific activities of this Division are directed to studies of interest for radiotherapy and radioprotection. Main topics are: Radiobiological properties of heavy ions relevant to space radiation protection. One of the risks of prolonged manned space flight is the exposure to high energy heavy ions. The biological impact of these particles is poorly known, especially for the induction of delayed effects. Cultured human cells are exposed to accelerated heavy ion-beams with energies up to 1 Gev/nucleon to determine survival of the irradiated cells and of their progeny as a function of dose, particle type, and beam energy.

Some research projects are focused on novel techniques for radiotherapy and on the related dosimetry. The main interest concerns Boron Neutron Capture Therapy (BNCT), a new kind of radiotherapy that seems to be promising for diffuseand radioresistant tumours. The Division is developing innovative dosimetry methods for BNCT and conformal radiotherapies, aimed at achieving experimental imaging of the spatial distribution of absorbed doses during treatments, and improved analytical methods for calculating dose distributions.

Biokinetics of incorporated radionuclides in humans are studied by using stable (non-radioactive) tracers. Nuclear analytical techniques, such as activation analysis and mass spectrometry, are employed to measure the tracer concentration in biological samples. The experimental studies are aimed at developing biokinetic models to provide a more realistic estimation of the internal dose after incorporation of radioactive material (e.g., after a nuclear accident and in relation to diagnostic or therapeutic medical use).

History of Science and Physics Education

D. Bettega
B. Candoni
M.C. Cantone
G. Gambarini
L. Pirola
A. Giussani
S. Gay
I. Veronese
E. Bellone
G. Cavallini
M. Fazio
D. Teodoro
M. Giliberti

History of Science: analysis of the development of science in Italy; development of an evolutionary model for science and culture; analysis of the evolution of scientific theories. Physics Education: preparation of lectures and selected experiments for training the teachers of secondary schools; realization of a theatrical play where the basic properties of matter and light are presented to elementary school children; study of the relationship between psychology and physics.

Elementary Particle Physics

23

Elementary particle physics: from matter-antimatter asimmetry to the origin of masses

1 Dipartimento di Fisica, Università degli Studi di Milano & INFN

A. Andreazza[1], for the BaBar, FOCUS, and ATLAS Milano groups

Two of the main lines of research in elementary particle physics concern the quest for answers to fundamental questions:

• According to quantum mechanics and to experimental evidence, particles and antiparticles are almost identical: they have exactly the same mass, exactly the same lifetime, and their charges are exactly opposite. Nevertheless, they are different, as we can infer from the fact our universe contains almost exclusively matter particles and no anti-matter. The search of an asymmetry between matter and antimatter, a phenomenon usually referred to as CP violation, is therefore fundamental in describing our universe.

• The most successful theories in particle physics, the so-called gauge theories, describe the fundamental interactions as mediated by the exchange of spin-1 massless "force" particles between spin-1/2 massless "matter" particles. Nevertheless we know particles are not massless! It is therefore of paramount importance to explain how particles get their masses.

A guideline in this quest is the so-called Standard Model [1], which till now has been able to quantitatively describe all known fundamental processes. In this model there are 12 fundamental spin-1/2 "matter" particles, 6 quarks and 6 leptons, grouped in three families. Quarks can be found only in composed particles, like protons and neutrons, while lepton can exist in unbound states. Ordinary matter is composed from first generation fermions. Interactions among quarks and leptons are mediated by 12 spin-1 particles, named "vector bosons" (Fig. 1).

Fig. 1
The particles in the Standard Model.

Matter Particles				Forces			Higgs boson
				electro-magnetic	weak	strong	
quarks	u	c	t	γ	Z	8 gluons	H
	d	s	b		W^+ W^-		
leptons	ν_e	ν_μ	ν_τ				
	e^-	μ^-	τ^-				

In the Standard Model a difference between particles and anti-particles may appear in the transition processes mediated by the weak interaction, when a quark transform into a quark of another type by emitting or absorbing a $W^{\pm}$ vector boson. The relative strengths of these transitions form a matrix, named Cabibbo-Kobayashi-Maskawa matrix.

The first evidence of CP violation was obtained in 1964 in the quantum mechanical process in which one particle (in that case the K^0) transforms into its anti-particle and vice-versa. The discovery of the heavy quarks c, and b in 70's and the t in 1995 [2], opened a wide range of processes involving quark transitions and finally succeeded in confirming the CKM picture by observing CP violation in many b-quark decays. The groups of the Department of Physics of the Università degli Studi di Milano and of the Milano Section of Istituto Nazionale di Fisica Nucleare, are involved in leading experiments in the study of c and b quarks: FOCUS and BaBar.

The way of generating masses in the Standard Model is through spontaneous symmetry breaking, the so-called Higgs mechanism. In this framework masses are not an intrinsic property of particles, but are due to a new interaction mediated by a particle which, differently from the other "force" particles, has spin-0. The experimental validation of this theoretical picture requires the observation of such a particle, called Higgs boson.

Elementary particle physics groups of Milano have taken part in the search of the Higgs boson at the LEP (Large Electron-Positron collider) at CERN in Geneva, which has explored the mass range up to 114 GeV/c^2 [3]. After the end of the LEP physics program in 2000, a new

REFERENCES
1. For a general overview and history of particle physics, see Cahn R. and Goldhaber G., *The experimental foundations of particle physics*, Cambridge: Cambridge University Press (1989).
2. Abe F. et al., "Evidence for top quark production in $p\bar{p}$ collisions at $\sqrt{s}$ =1.8 TeV," *Physical Review*. D50 2966 (1994).
3. Barate R. et al., "Search for the Standar Model Higgs boson at LEP," *Physics Letters* B 565 61 (2003).

accelerator, the LHC (Large Hadron Collider) is being built at CERN, using the same LEP tunnel. In this accelerator protons accelerated to 7 TeV energy, more than 7000 times their rest mass, will collide providing 14 TeV energy in the center of mass frame of the collision. At such high energy it will be possible to produce the Higgs boson in all the range of possible masses. Milano groups are giving a big contribution to the ATLAS experiment, one of the two biggest apparatuses foreseen to operate at the LHC.

Besides the above mentioned research topics, it is generally accepted the Standard Model is only an effective theory that describes well the fundamental interactions up to the energy scale of 100 GeV. It is therefore interesting to investigate how nature behaves at the energy scales above its validity range. LHC will be the perfect tool for such exploration and to see which (if any) of the many theoretical speculations about the physics at high energy will survive the experimental tests.

The FOCUS and BaBar experiments: heavy quark physics

The FOCUS experiment (Fig. 2) is a fixed target charm photoproduction experiment, i.e. an experiment in which charm quarks are produced by the interaction of a beam of high energy photons on a target.

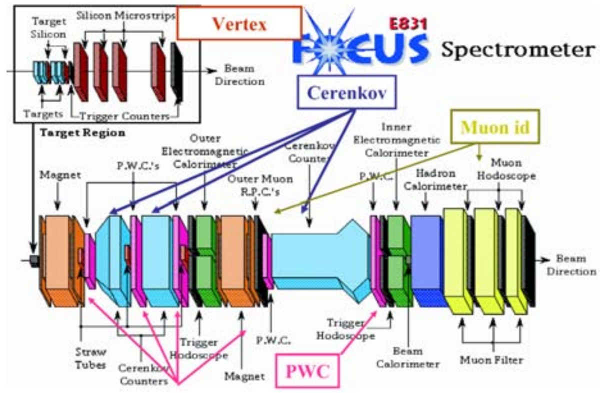

Fig. 2
Layout of the FOCUS apparatus.

This experiment is mainly an USA-Italy collaboration, with participation also of Brazilian, Mexican and Korean institutes. It involves approximately 110 physicists. Data taken was performed in 1996 and 1997, and data analysis is still on going, having reconstructed more than one million charmed particles.

Detailed information on the dynamics involved in charmed quark decays were gathered and the strong interaction effects involved in these reactions are investigated, with the idea to apply the same methods to the analysis of b-quark decays [4].

Decays of b-quarks are the main object of study of the BaBar experiment, which is located at the Stanford Linear Accelerator Center. It uses colliding electron and positron beam with the energy tuned to produce with high rate the $\Upsilon(4s)$ particle: a bound state of b quarks. It is a collaboration consisting of about 660 physicists from 10 countries. It started collecting data in 1999 and will continue until 2008. Till now more than 250 million b quark pairs have been produced.

BaBar is the first experiment to have observed CP violation in a system different from the K^0 [5], measuring a difference in the time behaviour of the processes in which a B^0 and an anti-B^0 decay into the same state of two particles J/ψ and K^0_S (Fig. 3).

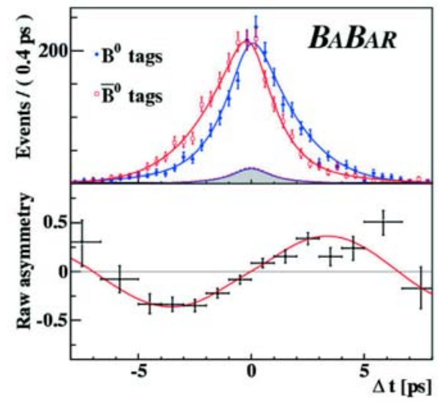

Fig. 3
Different time distribution for the decay $B^0 \to J/\psi K^0_S$ and the one for its anti-particle: a clear sign of CP violation.

REFERENCES
4. Link J.M. et al., "Study of the D^0_$K^+K^-\pi^+\pi^-$ decay" *Physics Letters* B610 225 (2005).
5. Aubert B. et al., "Measurement of CP-Violating Asymmetries in B^0 Decays to CP Eigenstates," *Physical Review Letters* 86, 2515 (2001).

To have a complete description both of the strong interaction dynamics and of the CKM matrix this asymmetry must be tested in as many reactions as possible. The BaBar Milano group is working on rare B^0 decays containing the η and η' particles [6], which is a channel very sensitive to CP violation effects due to sources different from the CKM matrix and therefore is a probe for the search of new physics.

Besides the data analysis, the FOCUS and BaBar Milano groups both contributed to the vertex detector of these experiments. These are silicon detectors with a very fine segmentation into strips. They are able to reconstruct charged particle trajectories with few micrometers resolution. Highly technological, they are a fundamental tool for detecting b and c quarks, by observing the separation between the production and decay point of these short-lived particles.

The ATLAS experiment: Higgs search at the LHC

A Toroidal Lhc ApparatuS (ATLAS) is likely to be the most ambitious project for a detector at the LHC. The apparatus size is 45 m length and 22 m diameter, as big as a seven storeys building. To reflect the complexity of the system, it also requires a strong collaboration of more than 2000 physicists from 150 institutions and 34 countries. It is currently under construction at CERN and it is expected to become operational at the end of 2007.

Milano groups are strongly involved in the construction of some key parts of the detector (Fig. 4). As a benchmark for discussing these components I will use the Higgs boson search for different ranges of masses, but physics topics at the LHC are much richer and a small review can be found in a separate article in this report [7].

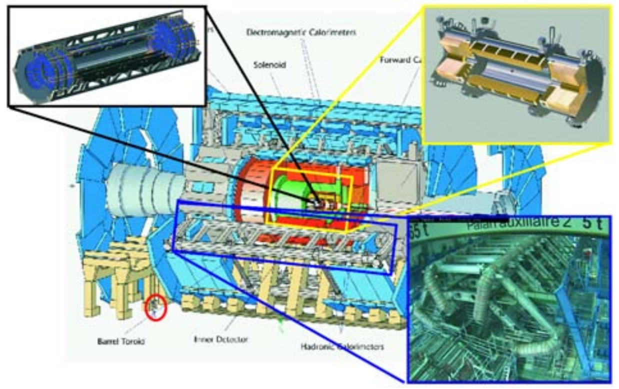

Fig. 4
Layout of the ATLAS Experiment. In evidence are, clockwise, the Pixel Detector, the Liquid Argon Calorimeter and the coils of the toroidal magnets.

Starting from the center of the apparatus, the ATLAS Pixel Detector is the vertex detector for the ATLAS experiment [8,9]. It is a silicon detector with the active area segmented into 80 million pixels of 50 μm x 400 μm size. It uses a new technology requiring very fast custom made electronics able to sustain both the high instantaneous rate of particles at the LHC and the very harsh radiation environment. It provides reconstruction of charged particle trajectories with a precision better than 10 μm. This is essential to identify the Higgs boson in the low mass region, where the predominant decay is in b-quark pairs.

Fig. 5
Invariant mass peak for $H \to \gamma\gamma$ decay superimposed to prompt photons from the LHC interactions.

The Liquid Argon electromagnetic calorimeter [10] extends between a radius of 1.4 m and 2 m from the interaction point. It is an instrument devoted to measure with high resolution the energy of electrons and photons. It also allows the distinction between electrons and other charged particles. There is an intermediate range of Higgs masses, around 130 GeV, where a promising channel for its discovery is via the rare decay $H \to \gamma\gamma$. The LAr calorimeter allows reconstructing the mass of the Higgs boson from the two photons with a precision of about 1.5%, making possible the identification of its presence over the background (Fig. 5).

REFERENCES
6. Aubert B. et al., "Measurements of branching fractions and time-dependent CP-violating asymmetries in $B \to \eta' K$ decays," *Physical Review Letters* 94, 191802 (2005).
7. Alimonti G. et al., "Discovery potential for Higgs bosons and supersymmetric particles with the ATLAS detector at the LHC", this report.
8. Andreazza A. for the ATLAS Pixel Collaboration, "Developements of the ATLAS pixel detector," *Nuclear Instruments and Methods* A540 259 (2005).
9. Alimonti G. et al., "The ATLAS Pixel detector," this report.
10. Tartarelli G.F. et al., "The ATLAS liquid argon electromagnetic calorimeter," this report.
11. Michelato P., "LASA activity on accelerators," this report.

The outermost detector is the muon detection system which uses a toroidal magnet built by the LASA laboratory of Segrate [11]. The muon system and the LAr calorimeter are the key detectors for Higgs search in the mass region above 130 GeV, where the easiest process to observe is the decay of the Higgs boson in a pair of Z vector bosons which both decay to $\mu^+\mu^-$ or e^+e^- pairs (Fig. 6).

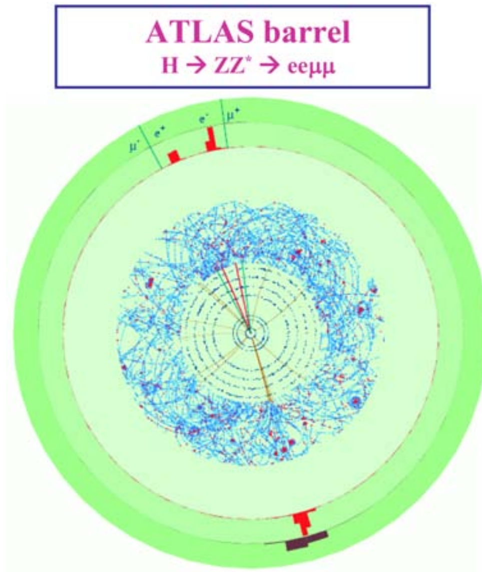

Fig. 6
How a Higgs boson decay into a Z pair will appear in the ATLAS detector.

From Fig. 4 you can see ATLAS is fully in the construction phases and this ambitious project will become operational in 2007, when, together with the other LHC detectors, ALICE, CMS and LHC-b will be the focus of the world of particle physics for a decade of LHC operation.

Conclusions

After this review of the activities of the Università degli Studi di Milano and of the Milano Section of Istituto Nazionale di Fisica Nucleare in particle physics at accelerators, it is clear how research in this field is driven by the need to find answers to fundamental questions about why the universe is the way it is.

Doing that requires a continuous interplay between experimental findings and theoretical developments and also the design and construction of complex and technological state of art apparatus, involving big international collaborations. Milano groups are in the forefront of this intense field of research.

Aknowledgements

I must thank all the colleagues of Università degli Studi di Milano and of the Milano Section of Istituto Nazionale di Fisica Nucleare, which share with me the interesting activity of particle physics at accelerators. A special thanks to T. Lari, A. Lazzaro, S. Malvezzi, F. Palombo, D. Pedrini and F. Tartarelli, which actively contributed to this report.

REFERENCES
11. Michelato P., "LASA activity on accelerators," this report.

Non-accelerator astroparticle physics: Borexino, CTF, and ICARUS detectors

1 Dipartimento di Fisica, Università degli Studi di Milano & INFN

L. Miramonti[1] (on behalf of the Borexino and ICARUS groups)

Borexino and ICARUS are two experiments both located at the Gran Sasso Underground Laboratory in central Italy. Borexino is under commissioning in hall C; its main goal will be the real time measurement of the low energy component of the solar neutrino flux. ICARUS T600 is now in hall B and will be operating starting from the end of next year. It combines the characteristics of a bubble chamber with the advantages of electronic read-out and represents a multipurpose detector for non-accelerator astroparticle physics. In addition, the Borexino prototype, the Counting Test Facility (CTF) is also presented. Thanks to the CTF, it was possible to measure very low contamination levels (~10-16 g/g U/Th equivalent) of radionuclides. Furthermore the very peculiar characteristics of this detector enable the search for rare and forbidden processes with high sensitivity in the low energy region (i.e. below 1 MeV).

Introduction

Non-accelerator astroparticle physics encompasses a large number of areas including cosmic ray physics, solar neutrino physics, dark matter, neutrino properties, nucleon stability, supernovae, gamma ray and neutrino astronomy, astrophysics, cosmology and particle physics. I will focus the attention on three experiments located in the Gran Sasso Underground Laboratory (LNGS) in central Italy: Borexino, its Counting Test Facility (CTF) and ICARUS.

Borexino is a scintillator detector designed for sub-MeV solar neutrino detection. Other topics can be investigated such as supernovae neutrinos and neutrinos coming from the earth (geo-neutrinos). A Borexino prototype, called Counting Test Facility (CTF), was built in order to measure ultra-low level of radio contamination (radiopurities of the order of 10^{-16} g/g of ^{238}U equivalent) on the several-ton scale.

ICARUS is a liquid argon time projection chamber (TPC) detector able to provide a three dimensional imaging and calorimetry of ionizing particles. A 600 tons module is now in hall B and will be operating starting from the end of next year. With a detector of several kton active mass, it would be possible to act as an observatory for astroparticle and neutrino physics and a second-generation nucleon decay experiment.

Borexino

The main goal of the Borexino detector is the direct observation and measurement, in real time, of the low energy component (< 1 MeV) of the neutrinos coming from our star; in particular the neutrino monochromatic line at 862 keV due to the electron capture of ^{7}Be. Up to now, less than 0.1% of the solar neutrino spectrum has been measured in real time. The long standing solar neutrino problem (i.e. deficit in solar neutrino flux) is explained in term of the neutrino oscillations in the frame of the so-called MSW-LMA solution; this model still need to be confirmed with low energy solar neutrinos. Furthermore a real time measurement below 1 MeV region will allow the possibility to test at the level of few % the Solar Standard Model. Borexino (for more information see for instance [1]) is a large unsegmented calorimeter featuring 300 tons of liquid scintillator, contained in a 8.5 meter nylon vessel with a thickness of 125 µm. The scintillator is surrounded by a pseudocumene (PC) buffer fluid for shielding external radiation. The buffer fluid is contained within a 13.7 m diameter stainless steel sphere (SSS) which also serves as a support structure of the 2200 8-inches diameter photomultiplier tubes (PMTs). An external tank contains high-purity water as a final shield against gamma rays and neutrons from the LNGS rock. Thanks to the Cerenkov light the water also serves as a muon veto (see Fig. 1 and Fig. 2).

The achievement of a high radiopurity level and the definition of the fiducial volume allows a sensitivity as low as 0.1 events per day per ton via the $\nu + e^- \rightarrow \nu + e^-$ electroweak scattering reaction. In order to allow the direct observation of the neutrino low energy component, the uranium and thorium content for the scintillator must be in the range of 10^{-16} g/g (values obtained were $3.0 \pm 0.3 \times 10^{-16}$ g/g and $\leq 4.8 \times 10^{-16}$ g/g at 95% C.L. for ^{238}U and ^{232}Th daughters, respectively).

REFERENCES
1. Borexino Collaboration. Astroparticle Physics 16 (2002) 205-234.

The amount of $^{14}C/^{12}C$ must be around 10^{-18} in order to reach the desired 250 keV threshold (measured values of $1.85 \pm 0.13 \times 10^{-18}$ for the isotopic abundance of ^{14}C relative to ^{12}C were obtained). Furthermore, radioactive noble gases content as low as $1.12^{+0.42}_{-0.37} \times 10^{-7}$ Bq/kg for ^{85}Kr and 2.20 ± 0.29 Bq/kg for ^{39}Ar have been obtained. The Borexino detector can investigate a wide range of open questions in particle physics, astrophysics and geophysics; in fact besides solar neutrinos, Borexino will be able to detect neutrinos coming from Supernovae and from the Earth (geo-neutrinos). For what concerns the antineutrino detection (actually geo-neutrinos are antineutrino and they can be detected by the β-inverse reaction), Borexino has the advantage to be located far away from nuclear plants which represent the most important background to electron antineutrino detection.

Fig. 1

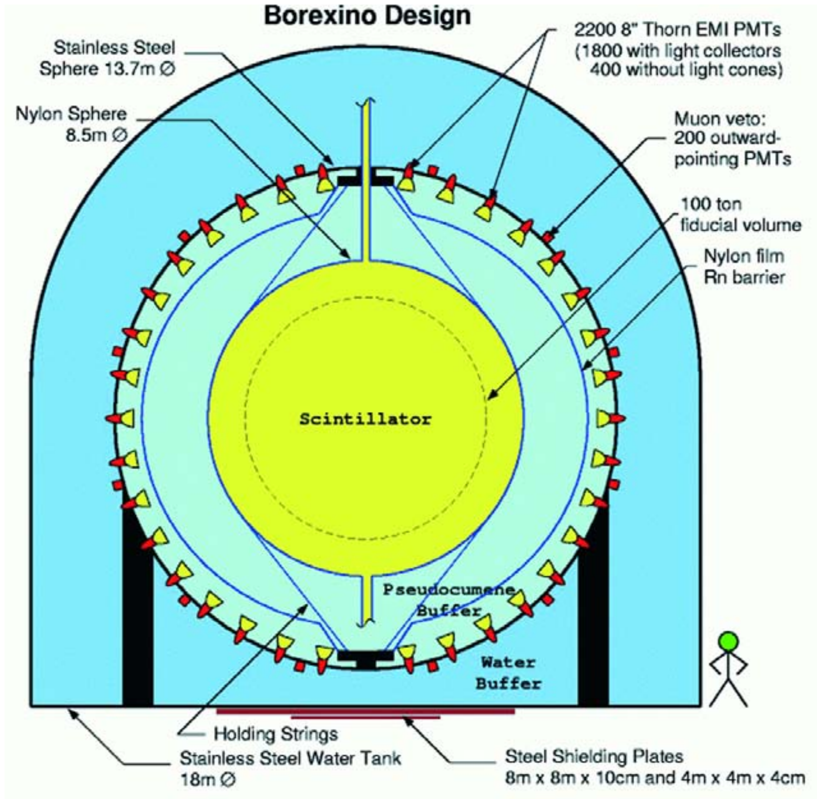

Fig. 2

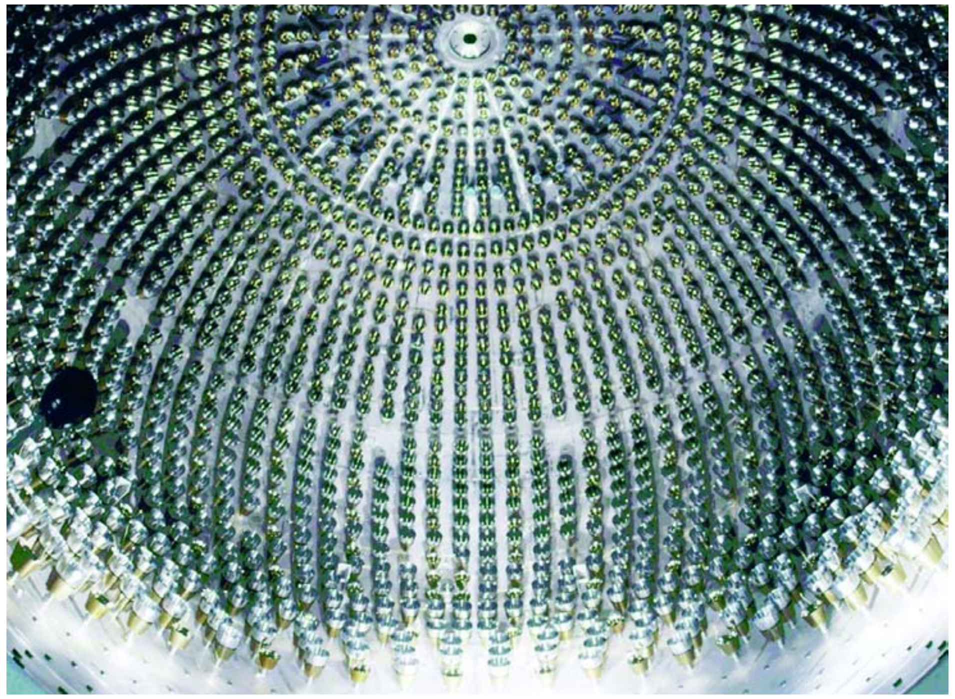

CTF

In order to test the feasibility of the Borexino detector and to measure concentration smaller than 10^{-16} g/g U/Th equivalent, a prototype was built: the Counting Test Facility (CTF). It consists of about 4 tons of ultra high-purity liquid scintillator contained in a 1 meter nylon vessel (500 μm thick), viewed by 100 PMTs (see Fig. 3). This detector is unique for its size and low contamination levels. These characteristics enable the searching for rare and forbidden processes with high sensitivity in the low energy region (i.e. MeV region). Since mid 90's, data collected with this detector have contributed in a significant way to the world best limits on quantities such as electron stability, neutrino magnetic moment, nucleon decay into invisible channels, violation of the Pauli exclusion principle and production of heavy neutrinos in the Sun [2].

Fig. 3

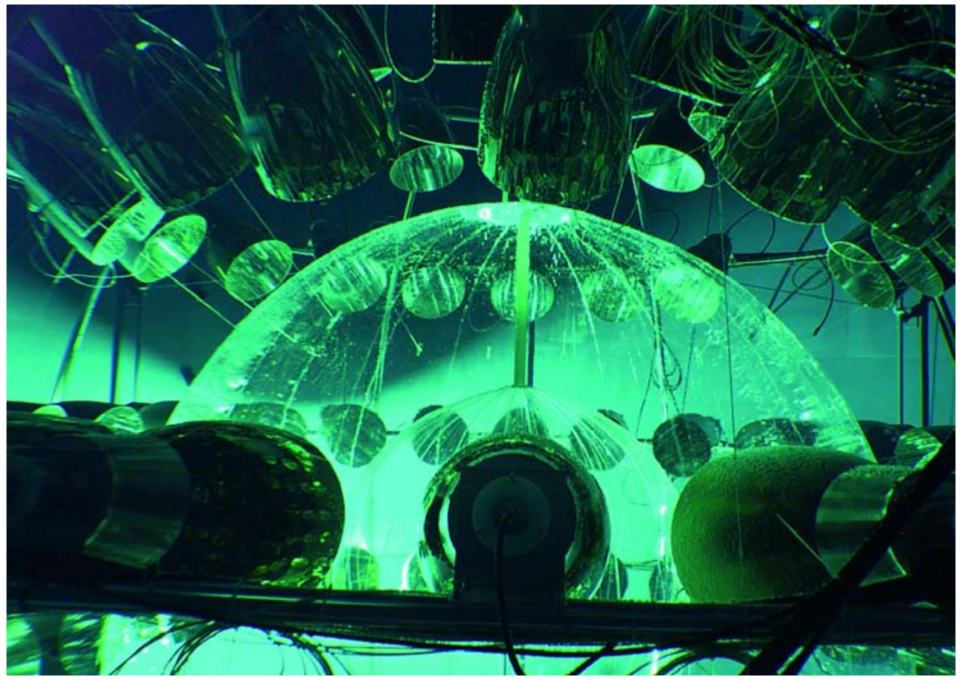

ICARUS

The ICARUS technology combines the characteristics of a bubble chamber with the advantages of electronic read-out. It was proposed in 1977 [3] and represents an ideal device in order to study particle interactions. This technology enables a very precise three dimension reconstruction of the event. It is continuously sensitive, self-triggering and is also an excellent calorimeter. Besides it is simple to build in modular form and sufficiently safe to be installed in underground laboratories. The physics goals are studies of neutrino physics: solar, atmospheric, supernova and from accelerator, and the study of nucleon stability. The ICARUS T600 detector is a large cryostat divided in two identical, adjacent half-modules. The internal dimensions are 3.6 x 3.9 m and 19.9 m long, each cryostat containing more than 300 tons of liquid argon [4]. Each half-module contains an internal detector and is externally surrounded by a set of thermal insulation layers. This detector is composed by two Time Projection Chambers (TPC), purity monitors, probes and photomultipliers. Each TPC is composed by three parallel planes of wires, 3 mm apart, oriented at 0° ± 60° angles, of 3 mm pitch parallel wires, (see Fig. 4). The drift (maximum drift length: 1.5 m) of the ionization electrons is obtained by a high voltage system (75 kV) that produces a uniform electric field perpendicular to the wire planes. The ICARUS detector measures the total ionization loss of a track with very high sampling, comparable to a bubble chamber. The number of ionization electrons, produced by charged particles traversing the liquid argon sensitive volume, is proportional to the energy transferred from the particle to the liquid argon. Thanks to the electric field, ionization electrons drift perpendicularly to the wire planes, inducing a signal (hit) on the neighbor wires while approaching the different wire planes. It is possible to reconstruct a three dimensional spatial and calorimetric picture of the event knowing the energy deposited by the different particles and the point where such a deposition has occurred. Each wire plane constrains two spatial degrees of freedom of the hits, the first common to all the wire planes (the drift time) and the second specific for each plane (the wire coordinate). The identification and association of hits in the wire output signal of the different wire planes gives the possibility to reconstruct the event in three dimensions.

For a given medium, the energy released per unit length (dE/dx) by the ionizing particles depends of the particle type and its momentum. In the ICARUS detector particle momentum is measured from the range (for stopping particles) or multiple scattering meas-

REFERENCES
2. Borexino Collaboration. Physics Letters B 525 (2002) pp 29. Physics Letters B 563 (2003) pp 35-47. Physics Letters B 563 (2003) pp 23-34. Eur. Phys. J. C37, 421-431 (2004). JEPT Letters Pis'ma v ZhETF, vol 78, iss. 5 pp. 707-712.
3. C. Rubbia. CERN-EP/77-08 (1977).
4. ICARUS Collaboration. NIM A527, 329 (2004).

urement; the dE/dx measurement is performed for a large number of points along a given track. Thanks to the simultaneous measurement of range and dE/dx then it is possible to perform the particle identification (see Fig. 5). Another appealing feature of this technology is the very good π^0/e discrimination capability. This is interesting for the investigation of $\nu_\mu \rightarrow \nu_e$ oscillation.

Fig. 4

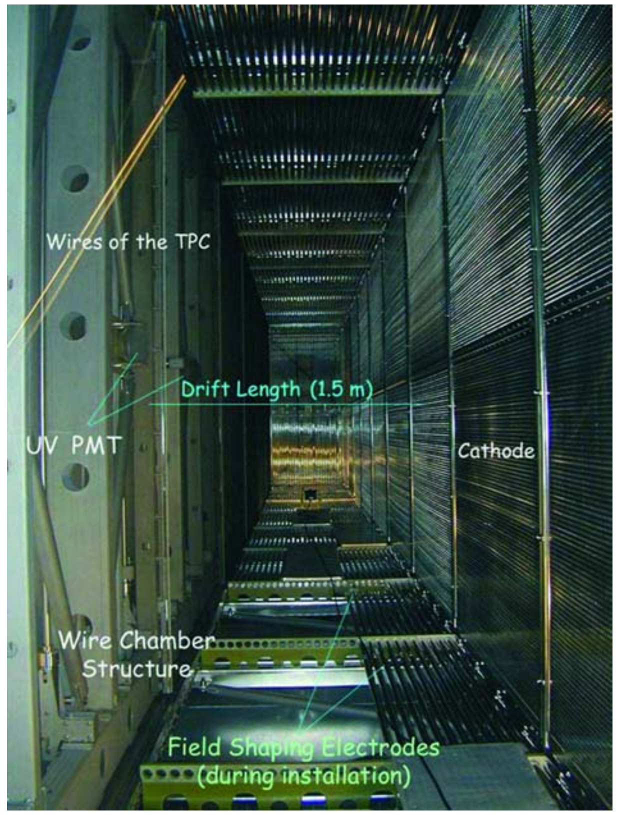

Fig. 5

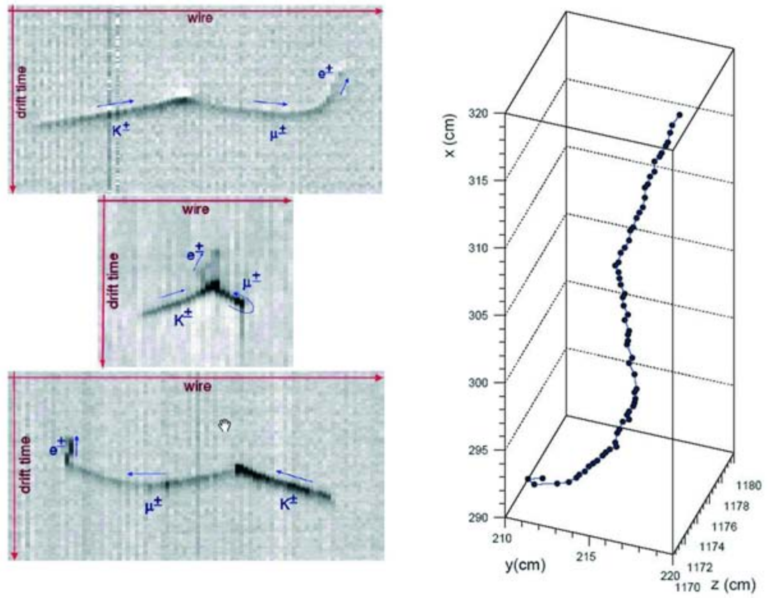

The Pierre Auger Observatory for the Ultra High Energy Cosmic Rays

1 Dipartimento di Fisica, Università degli Studi di Milano and INFN

F. Sanchez[1], C. De Donato[1], D. Camin[1], and V. Grassi[1]

Introduction: what is a cosmic ray?

Since its discovery in 1912 by the Austrian physicist Victor Hess, the cosmic rays field has been a long story of technology and experimental developments, mixed with many theoretical successes and some unavoidable wrong speculations. In fact, it was R. A. Millikan in 1926 who coined the name of cosmic rays reflecting the early belief that this extraterrestrial radiation was made of gamma rays. Nowadays, we know that most of that cosmic rays detected by Hess at altitudes close to 5300 m were subatomic particles, ranging from hydrogen to uranium, with only a small fraction of gammas. Nevertheless, we still preserve the tradition of calling rays every kind of unknown radiation arriving at the Earth from the outer space. This is the case of the most energetic cosmic radiation we are able to measure with the modern detectors and which is in the range of 10^{18}-10^{20} eV (an energy scale much higher than the one achievable with any kind of modern accelerator).

The fact that a single particle, most probably an atomic nucleus, can be accelerated to nearly 16 J is one of the reasons why cosmic ray field has regained so much interest in the physics community in the recent years. In the early days around the beginning of the 20^{th} century, astroparticle physics and fundamental particle physics shared common roots: observing cosmic rays in a cloud chamber, in 1932, Carl Anderson discovered antimatter (the positron) and only five years later, together with Neddermeyer, he discovered the moun. During the 1930s the dominant motivation for investigating cosmic rays was by the particle's physic field. It was not until 1938, when the energy scale known to the science was extended beyond 10^{15} eV thanks to the discovery by Pierre Auger of what was denominated as extensive air showers (EAS), that the astrophysical interested revived.

Some of the crucial questions which play a major role in the cosmic rays puzzle are: What is the nature of the particles which we observe as cosmic rays? What its chemical composition and its energy spectrum? How can they acquire such macroscopic energy? What and where are their sources? Does the distribution of cosmic rays in the sky follow the distribution of matter within our galaxy or the distribution of nearby extragalactic matter? Or, is there no relation with any distribution of known matter? Are there point sources or very tight clusters? How do they propagate through interstellar and intergalactic space to reach the Earth? Today there is a clearly great hope that the present and operating experiments, as the Pierre Auger Observatory (PAO), will solve some of the still open question in astrophysics and even cosmology and, at the same time, contribute to our knowledge of fundamental particle interactions at the highest energies.

First results of the Pierre Auger Observatory

The existence of cosmic particles with energy 5 x 10^{19} eV is beyond any doubt [1]. Indeed, it is probable that the cosmic ray spectrum extends to at least 3 x 10^{20} eV and there is no clear evidence that this should be its end. One of the most striking facts is that the spectrum spans over roughly 11 decades of energy with a flux that falls down from 10^{4} particles per m^2 per second at 1 GeV to 10^{-2} particles per km^2 per year at the highest energies. This is the reason why a direct measurement of the end of the cosmic ray spectrum is unfeasible. Fortunately, when an ultra high energy cosmic particle enters the atmosphere does not penetrate but collides with air molecules to initiate shower cascades ending up with billions of sub-particles before reaching the ground. These secondary particles can be sampled and the properties of the primary cosmic ray inferred. Arrays of ground detectors supply the low event statistic with large apertures. On the other hand, the air itself is a good calorimeter and the fluorescence light produced by the de-excitation of nitrogen air molecules along the shower axis is another way to detect the cosmic particles of extremely high energy. The Pierre Auger Observatory combines in the same experiment these two detection techniques allowing an energy estimation that does not rely on detailed numerical simulations (of the shower and the detector) or any assumption about the primary chemical composition [2]. The events recorded by both the surface (SD) and the fluorescence (FD) detectors are called the "hybrid data". The distribution of the impact points of the hybrid events observed so far is shown in Fig. 1. The PAO has

REFERENCES
1. M. Nagano and Watson A, Rev. Mod. Phys. 72, 689 (2000)
2. Abraham J. et al., Nucl. Instr. Meth., A523, 50 (2004)

recorded 3525 events of energies above 3 x 10^{18} eV. The highest energy event observed by the SD has 86 x 10^{18} eV and is shown in the top panel of Fig. 2. At the left of the figure are the triggered stations where the arrow shows the fitted direction (the spacing of the stations is 1,5 km). At the right, the measured lateral distribution of particle density with its best fit is shown. In the bottom panel of Fig. 2 is the second highest energy SD event with 79 x 10^{18} eV. The longitudinal profile, as observed by the FD is shown in Fig. 3. The profile is shown as the number of charged particles (which are proportional to the amount of fluorescence light in the detector) versus the traversed depth in the atmosphere.

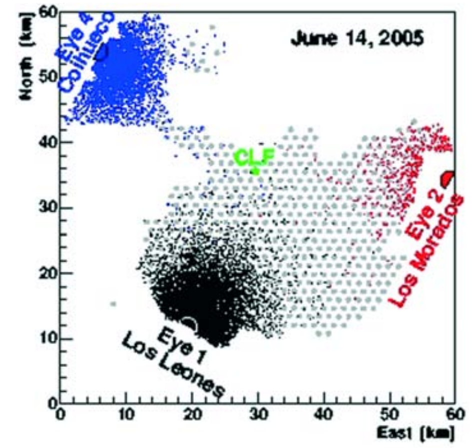

Fig. 1
Status of the Pierre Auger Observatory on June 14, 2005. Each grey full circle represents a surface station while each dot is the core location of a reconstructed air shower in the hybrid mode.

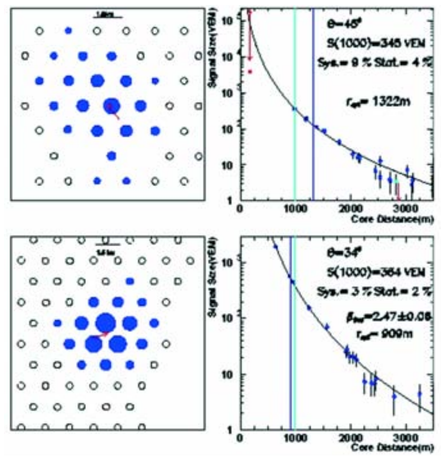

Fig. 2
The highest (top) and the second highest (bottom) energy event recorded by the surface detector. At left, triggered stations, at right lateral distribution function.

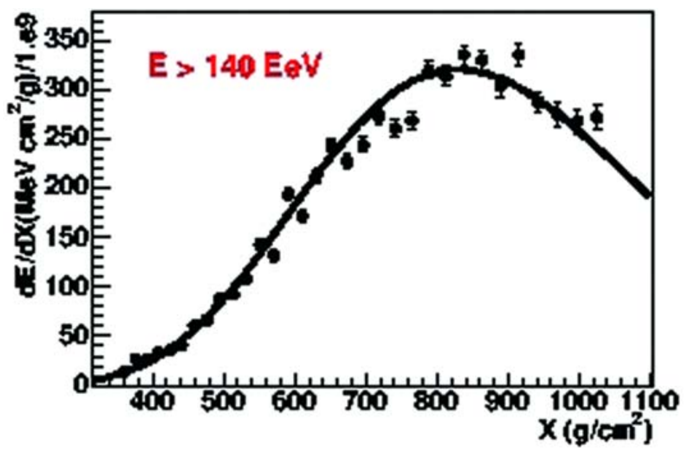

Fig. 3
The highest energy event recorded by the fluorescence detector with energy E >140 x 10^{18} eV.

When using hybrid data to calibrate in energy the ground detector, the major source of uncertainty comes from the fluorescence yield (15%) and the absolute calibration of the FD telescopes (12%). Together with other smaller FD uncertainties, the total systematic energy uncertainty is presently estimated to be 25%. Actually, because the limited available statistics, the total systematic energy uncertainty grows from 30% at 3 x 10^{18} eV to 50% at 100 x 10^{18} eV [3].

The observed differential energy spectrum is shown in Fig. 4. As can be noted in the figure, the low statistics does not yet allow to solve the discrepancy between the previous results

REFERENCES
3. Sommers P.. by the Pierre Auger Collaboration, 29th ICRC, Pune (2005)

of AGASA (which is a surface experiment) and HiRes (which uses the fluorescence technique) experiments. The former claims the existence of events above the GZK cutoff while the latter shows results that are consistent with the cutoff. If the primary particle is of extragalactic origin, it must traverse the medium of the region where it was created, then traverse the intergalactic space between the source and our galaxy, and finally, traverse the interstellar medium to reach the Earth. But at 5×10^{19} eV the universe is opaque to cosmic rays (of any kind, with the exception of neutrinos) due to their interaction with the ubiquitous cosmic microwave background radiation (CMB). Therefore, the spectrum should have a cutoff around 10^{20} eV or the sources should be within tens of Mpc. But in the latter case, the arrival direction distribution of the highest energy events should have the signature of their origin, i.e., a strong correlation with nearby astrophysical objects. This is because at such energies the magnetic fields are not strong enough to bent the particle trajectories and make their propagation diffusive. Therefore cosmic rays should keep the "memory" of their birth place. Astrophysical objects considered as accelerator candidates are active galactic nuclei (AGN), shocks in the AGN jets, shocks in the cluster of galaxies or ultra-relativistic shocks (gamma-ray bursters). Also large electric potentials, due to unipolar induction, could be the accelerators in accretion disc around massive black holes.

The long period of stable data acquisition, started on the beginning of 2004, allowed a systematic data analysis in the search of significant deviations from isotropy in the arrival direction distribution of the cosmic rays. Forerunner experiments as AGASA [4] and SUGAR [5], have reported excesses in directions close to the galactic center within a limited energy range. Nevertheless blind source searches with Auger data did not reveal any remarkable excess in any of the energy bands 1×10^{18} eV $\leq E \leq 5 \times 10^{18}$ eV and $E \geq 5 \times 10^{18}$ eV [6].

Fig. 4
First Auger estimated energy spectrum (blue) with previous results from AGASA (red) and HiRes (cyan).

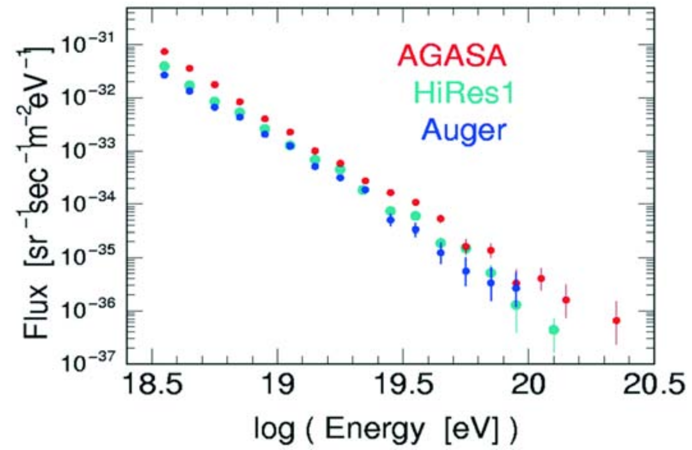

Conclusions

The Pierre Auger Observatory is still under construction and growing rapidly. Its construction will finish by the end of 2006. By the following 2 years its cumulative exposure will be approximately 7 times greater. The statistical errors will shrink accordingly, permitting a search in the southern hemisphere skyes for energy spectral features (including the predicted GZK suppression), excesses or deviations from isotropy of arrival direction distribution and finally composition studies of the primary cosmic rays of the highest energies. Many of the still open questions in this fascinating field will finally find a satisfactory answer.

REFERENCES
4. Hayashida N. et al., Astropart. Phys. 10, 303 (1999)
5. Bellido J.A., et al, Astropart. Phys. 15, 167 (2001)
6. Revenu B., by the Pierre Auger Collaboration, 29th ICRC, Pune (2005)

Limits on electron and nucleon stability, neutrino magnetic moment, antineutrinos in the solar flux; recent measurements at Gran Sasso

B. Caccianiga[1], G. Bellini[2], S. Bonetti[2], D. Franco[2], M. Giammarchi[1], P. Lombardi[1], E. Meroni[2], L. Miramonti[2], M.E. Monzani[1], L. Perasso[1], and G. Ranucci[1],

1 INFN, Sezione di Milano
2 Dipartimento di Fisica, Università degli Studi di Milano

CTF (Counting Test Facility) is a prototype built to test the feasibility of the Borexino experiment. It consists of 4 tons of liquid scintillator contained in a 1-meter-radius nylon vessel and surrounded by 100 photomultiplier tubes pointing towards the center (see Fig.1).

Fig. 1

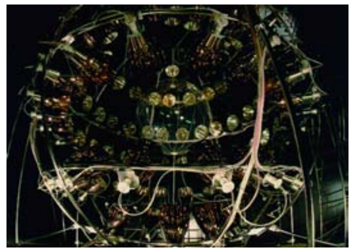

CTF is a unique detector, whose size and low contamination levels make it capable of searching for rare and forbidden processes in the low energy region (~ 1MeV) with high sensitivity. In particular, the data collected with CTF have contributed significantly to the world best limits on quantities such as neutrino magnetic moment, electron lifetime, nucleon decays in invisible channels, violation of the Pauli Esclusion Principle, production of heavy-neutrinos in the sun, flux of anti-neutrinos from the sun. As for the electron stability, the data have been analyzed to search for the 256 keV line of the γ emitted in the decay channel $e^- \rightarrow \gamma + \nu$. No signal was found and this enabled us to set a limit on the electron lifetime of $\tau > 4.6 \times 10^{26}$ y (90% C.L.) which was published in 2002 and is still the best limit in the world for the electron decay in this channel [1].

The analysis of the CTF data has also addressed the neutrino magnetic moment question: a non-zero neutrino magnetic moment would increase the cross-section of neutrino-electron elastic scattering by a term that depends on μ_ν. This effect becomes dominant at low energy (< 400 keV) which makes CTF particularly sensitive to μ_ν. In a paper published in 2003, we were able of setting the limit $\mu_\nu < 5 \times 10^{-10}\ \mu_{\nu B}$ [2] which is still a very competitive result and in any case the only one obtained with low-energy neutrinos (MUNU uses low-energy anti-neutrinos).

The possibility of heavy neutrinos ($M > 2m_e$) being emitted in the ^8B reaction in the sun has been investigated with CTF: heavy neutrinos would decay to light neutrinos via the reaction $\nu_H \rightarrow \nu_L + e^+ + e^-$. The study of CTF energy spectrum above 4.5 MeV has allowed us to enlarge the excluded region of the parameter space ($|U_{eH}|^2$–$M_{\nu H}$) with respect to previous experiments, especially for $M_{\nu H}$ in the interval (4-10) MeV [3].

The stability of nucleons bounded in nuclei has been studied in CTF searching for the decays of single nucleon or pair of nucleons into invisible channels: if one of such decays occurs inside the ^{12}C, ^{13}C nuclei of the scintillator or in the ^{16}O nuclei of the shielding water, daughter nuclei would be produced such as ^{11}C, ^{10}C, ^{12}B, ^{11}Be, ^{14}O which in turn would decay radioactively. The limits obtained with CTF are comparable to or improve the previously set world limits [4].

The last article on CTF data was published in 2004 and concerns the search for non-Paulian transitions of nucleons from 1P shell to a filled $1S_{1/2}$ shell to put limits on the Pauli Esclusion Principle. The analysis consists in searching for α, p, n, γ emitted in non-Paulian decays of ^{12}C and ^{16}O nuclei present in the scintillator and in the shielding water. The obtained limits significantly improve (up to 3 orders of magnitude) the previously set limits [5].

Several analyses are still ongoing on the last CTF data-taking campaign. For example, an article is being prepared concerning the anti-neutrino flux from the sun: we know that in case of non-zero neutrino magnetic moment, the transition nu $\rightarrow$ anti-nu would be possible, allowing us to see a small component of anti-neutrinos in the solar flux (which otherwise would be absent). The anti-neutrinos are detected via the inverse beta reaction anti-$\nu + p \rightarrow e^+ + n$ whose strong signature makes the analysis virtually free of random background. Furthermore, the Gran Sasso location is particularly favorable for this search, since it is almost free of background from nuclear reactors.

Only one candidate event has been selected analyzing 687 days of data-taking, which allowed us to set an upper limit on the solar anti-neutrino flux of $1.3 \times 10^5\ cm^2\ s^{-1}$. This is the first result obtained at low energy (< 5 MeV).

REFERENCES
1. Borexino coll., Phys.Lett. B 525 (2002)29
2. Borexino coll., Phys. Lett. B 563 (2003)
3. Borexino coll., JETP Lett. 78 (2003)
4. Borexino coll., Phys. Lett. B 563 (2003)
5. Borexino coll., Eur.Phys.Jour C37 (2004)

Discovery Potential for Higgs bosons and Supersymmetric particles with the ATLAS detector at the LHC

1 Dipartimento di Fisica, Università degli Studi di Milano and INFN

G. Alimonti, A. Andreazza, D. Banfi, L. Carminati, D. Cavalli, M. Citterio, G.C. Costa, M. Delmastro, M. Fanti, T. Lari, L. Mandelli, M. Mazzanti, C.Meroni, L. Perini, F. Ragusa, S. Resconi, G.F. Tartarelli, C. Troncon, G.Vegni

The Standard Model of Particle Physics successfully describes most of the experimental data of high-energy physics, but the Higgs sector of the theory, which predicts the existence of a new vector boson, is still untested. The Standard Model is also known to be incomplete. Its most popular extension is Supersymmetry, which predicts the existence of at least five Higgs bosons and a still unobserved partner for each of the Standard Model particles. Both the Higgs bosons and the Supersymmetric particles are expected to be accessible at the Large Hadron Collider energy scale. The two Milano ATLAS groups of the Department, the ATLAS Liquid Argon and the ATLAS Pixel group, are working to prepare the physics analysis of the LHC data.
In particular, the Milano groups are involved in three analysis:

1) The reconstruction of the decay of the Higgs boson of the Standard Model (SM) in two photons. This decay is expected to be a promising discovery channel in the low Higgs mass scenario (110 < MH < 140 GeV) which is presently favoured by SM. It is a rare decay mode which places severe requirements on the electromagnetic calorimeter performance in terms of photons energy and position reconstruction accuracy as well as identification capabilities. The Higgs search in this channel is not straightforward: it has been estimated [1] that in a leading order inclusive analysis the Higgs boson could be discovered in ATLAS with at least 100 fb-1 (= one year in the high luminosity phase).

2) The reconstruction of the decay of the neutral heavy Higgs bosons of the Minimal Supersymmetric Standard Model (MSSM), that is an extension of SM including SUSY particles. In MSSM 5 Higgs are foreseen: h (neutral lighter scalar), H (neutral heavier scalar), A (neutral pseudoscalar) and the charged Higgs H+ and H-. ATLAS will be able to discover the MSSM Higgs bosons in many different decay channels for almost the entire region of the allowed parameter space (Fig. 1). One of the most promising channels is the H/A to tau-tau [1]. The excellent capability of ATLAS in identifying tau-jets and the excellent transverse missing energy measurement allow the reconstruction of the invariant tau-tau mass, that should appear as a peak over the large background for certain values of the MSSM parameters.

Fig. 1
MSSM Higgs discovery potential in ATLAS after 3 years of data at low luminosity.

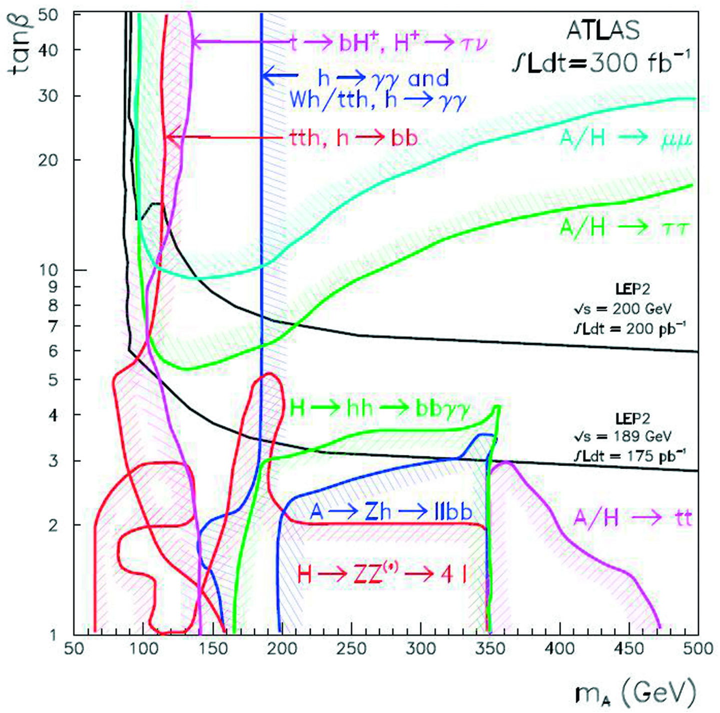

REFERENCES
1. The ATLAS Collaboration: The ATLAS Detector Physics and Performance TDR CERN/LHCC/99-14/15
2. T. Lari, AIP Conf. Proc. 794, 131 (2004)

3)The reconstruction of the cascade decays of the Supersymmetric partners of Standard Model particles [2]. The production of strongly interacting Supersymmetric particles (gluinos and scalar quarks) which decay into energetic jets and a pair of undetected LSP particles should be observed as an excess of events with energetic jets and transverse missing energy. The properties of Supersymmetric particles (masses, branching ratios…) will be studied using the kinematical distributions of their decay products, such as the invariant mass of lepton pairs from the decay of an heavy neutralino into a lighter neutralino and two leptons (Fig. 2).

Fig. 2
Invariant mass of lepton pairs (3 years of data at high luminosity).

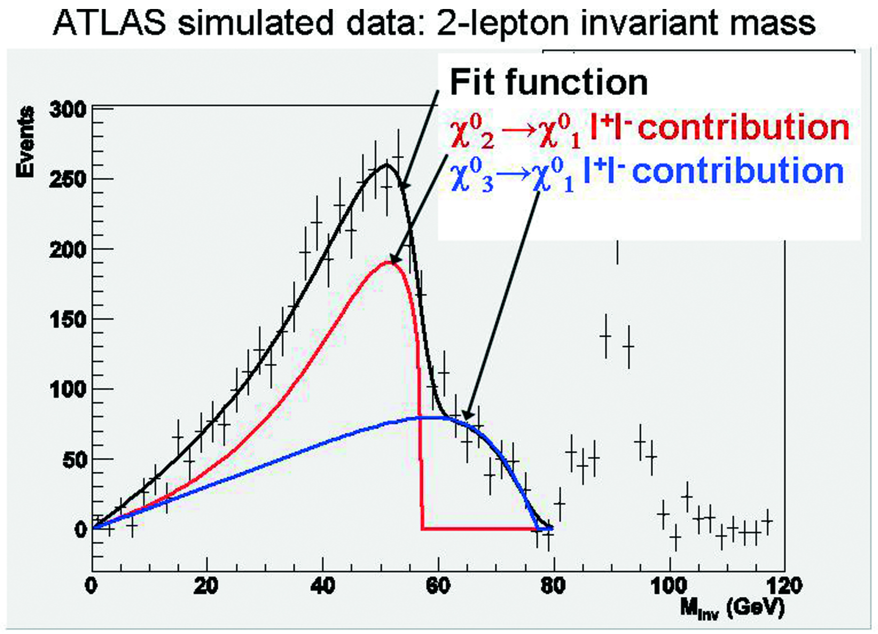

The ATLAS Pixel Detector

G. Alimonti, A. Andreazza, M. Citterio, S. Coelli, D. Giugni, T. Lari, C.Meroni, F. Ragusa, C. Troncon, G. Vegni

1 Dipartimento di Fisica, Università degli Studi di Milano and INFN

ATLAS is a general purpose high energy particle detector presently under construction at the Large Hadron Collider. ATLAS is expected to start taking data in 2007 and to provide an answer to some of the most outstanding questions in Particle Physics today, such as the origin of particle masses, and how to extend the Standard model to incorporate gravity, neutrino masses, a Dark Matter candidate and the required but unknown sources of matter-antimatter asymmetry.

The reconstruction of charged particles produced in the pp collisions will be performed by three concentric detectors inside a magnetic field sustained by a superconducting solenoid. The innermost detector is the Pixel Detector, which will enhance the pattern recognition to separate tracks in a high multiplicity environment and will provide high-precision reconstruction of decay vertices allowing the identification of particle jets containing B-mesons.

The pixel detector [1,2] will consist of three concentric cylindrical layers (barrel) and three disks on each side. The silicon tiles (modules) will contain a total of 100 milion pixel cells, each one connected to a dedicated readout electronic chain. The detector will provide three measurement for each track, with a spatial resolution of about 10 mm and an efficiency larger than 97%. The signal must be associated to a unique LHC bunch crossing, whose frequency is 40 MHz. These performances must be provided in an harsh radiation environment, with an integrated particle flux of the order of 1015 charged hadrons per square centimeter and an integrated dose of 500 kGy. No previous solid state detector was able to meet these specifications.

The basic unit is the module [2,3], which is a complex object. Charged particle produce an electric signal in the sensor [4], segmented into 50 x 400 mm2 pixel cells, each one connected to a matching cell in the front-end readout chips by a solder or indium bump [5]. The module signals are processed by the Module Controller Chip and sent off-module via an optic link.

The group of Milano contributed in particular to

The design of the sensor [4], in particular the isolation between pixel cells

The test of bare modules (sensor and electronic chips) during production [5], the development of power supplies and regulator electronics board, and the tools to assemble the layer modules, survey the module placement precision, and insert the detector into ATLAS

The analysis of test beam data [2,6,7,8,9,10], measuring the spatial resolution, the detection efficiency, the high-rate data acquisition capabilities and the active thickness of the detector after irradiation.

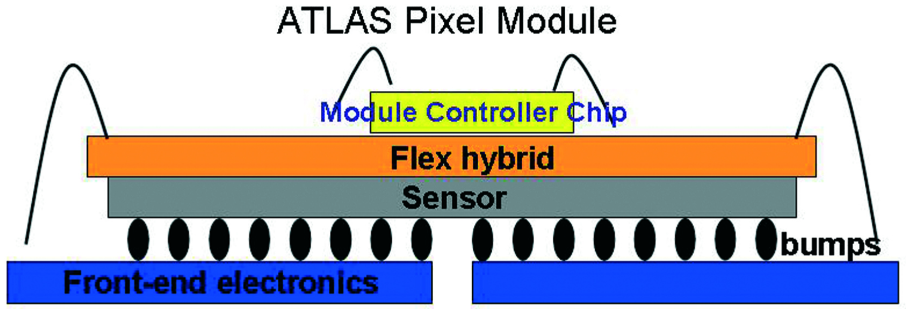

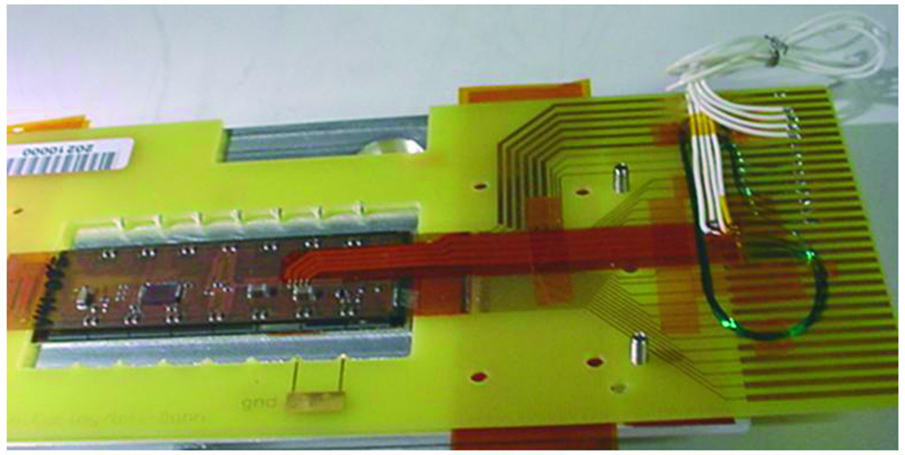

REFERENCES
1. A. Andreazza, Nucl. Instr. Meth. A461,168 (2001)
2. A. Andreazza, Nucl.Instr. Meth. A513, 103 (2003)
3. A. Andreazza, Nucl. Instr. Meth. A535, 357 (2004)
4. I. Gorelov et al. Nucl. Instr. Meth. A489, 202 (2002)
5. A. Airoldi et al., Nucl. Instr. Meth. A540, 259 (2005)
6. F. Ragusa, Nucl. Instr. and Meth. A447, 184 (2000)
7. C. Troncon, IEEE Trans. on Nucl. Sci. 47, 737 (2000)
8. T. Lari, Nucl. Instr. Meth. A465, 112 (2000)
9. I. Gorelov et al., Nucl.Instr. Meth. A481,204 (2002)
10. T. Lari, Nucl. Instr. Meth. A518,349 (2004)

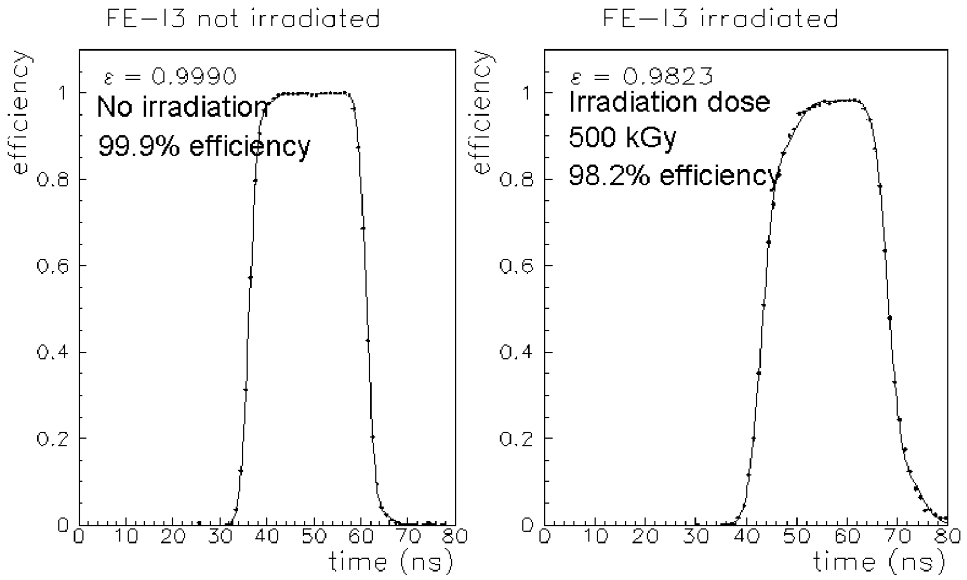

Pixel detection efficiency, before (left) and after (right) irradiation, as a function of the data acquisition timing, which will be tuned for best efficiency at the LHC.

The Pierre Auger Observatory: a hybrid detector looking for the Ultra High Energy Cosmic Rays

C. De Donato[1,2], F. Sanchez[1,2], D.V. Camin[1,2], and V. Grassi[1,2]

1 *Dipartimento di Fisica, Università degli Studi di Milano*
2 *INFN – Milano*

The Ultra High Energy Cosmic Rays (UHECR) form the tail of the cosmic ray spectrum, which extends from 1 GeV to beyond 10^{20} eV. To solve the enigma of the origin of such energetic particles, the Pierre Auger Observatory (PAO) has been conceived to measure the flux, the arrival direction and mass composition of UHECRs of $E > 10^{18}$ eV with unprecedented statistical precision and full sky coverage. To obtain these goals the project foresees two sites, one in each hemisphere, each one with an aperture of 7850 Km^2 sr above 10^{19} eV. Actually only the Southern site is under construction in Argentina (Malargue, Mendoza) and will be completed within the end of 2006, while the Northern site in Colorado (USA) is in the first phase of design. The Southern observatory comprises the Surface Detector (SD), a ground array of 1600 water-Cherenkov detectors spaced each other by 1.5 km over an area of 3000 km^2, and the Fluorescence Detector (FD), consisting of 24 fluorescence telescopes (grouped in 4 optical stations) overlooking the SD array. Optical systems for atmospheric monitoring and calibration and LIDARs, complete the Observatory [1]. The SD provides the lateral density distribution of the shower particles at the ground level. On the other side, the FD detects the fluorescence light generated in Earth atmosphere by extensive air showers (EAS), from which the longitudinal profile of the EAS can be obtained. From the lateral density distribution and the longitudinal profile, information about the EAS can be inferred independently from complementary set of parameters. These two traditional techniques are combined for the first time in a unique hybrid detector to achieve high resolution in the reconstruction of the parameters of the EAS with full efficiency above 10^{19} eV. The detection in coincidence of an EAS with the two techniques, possible for the 10% of the events, allows the cross-calibration of the two detectors with a consequent reduction of the systematic errors. The Observatory began to acquire data regularly in January 2004. The data collected up to June 2005, when the construction reached the 75% for the FD and ~ 50% for the SD, allowed preliminary analysis and results for the PAO [2,3]. With 180000 SD events and 18000 hybrid events recorded, the cumulative exposure reached ~ 1750 km^2 sr yr, ~ 7% more than AGASA. The current rate of hybrid events (1800 events/month) increases as the construction proceeds. Despite the actual hybrid energy resolution is limited by the available statistics and by the systematic uncertainties in the FD and SD reconstruction, the data acquired provided a first estimate of the primary cosmic ray energy spectrum above 3 EeV.

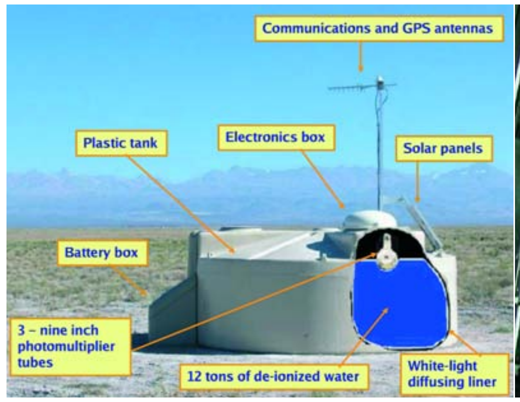

Fig. 1
SD water-Cherenkov detector: the main elements of the detector are shown.

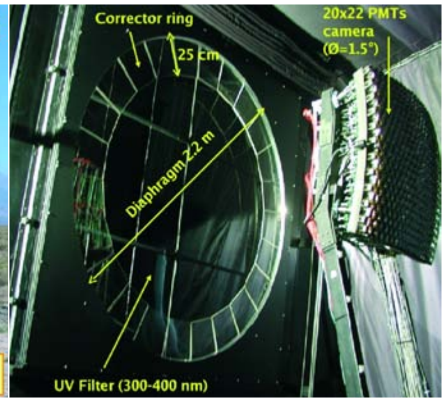

Fig. 2
FD telescope: the main elements of the aperture and the camera, composed of 20 x 22 photomultiplier tubes (PMTs), are shown.

REFERENCES
1. Abraham J. et al., "Properties and performance of the prototype instrument for the Pierre Auger Observatory", Nuclear Instruments and Methods A523, pp.50-95 (2004).
2. Pierre Auger Collaboration, "Performance of the Pierre Auger Observatory Surface Array", 29th ICRC, Pune (2005).
3. Pierre Auger Collaboration, "Performance of the Fluorescence Detectors of the Pierre Auger Observatory", 29th ICRC, Pune (2005).

Borexino: a real time solar neutrino detector below 1 MeV

P. Lombardi[1], G.P. Bellini[2], S. Bonetti[2], B. Caccianiga[1], D. Franco[2], M. Giammarchi[1], E. Meroni[2], L. Miramonti[2], M.E. Monzani[1], L. Perasso[1], and G. Ranucci[1]

1 *INFN - Sezione di Milano*
2 *Dipartimento di Fisica, Università degli Studi di Milano*

The BOREXINO experiment aims to measure low energy solar neutrinos in real time by elastic neutrino-electron scattering. The experiment's goal is the direct measurement of the flux of ^{7}Be solar neutrinos of all flavors in an ultra-pure scintillation liquid. The experiment, located near L'Aquila in Italy in the underground laboratory LNGS (Laboratori Nazionali del Gran Sasso) will use 300 t of liquid scintillator (fiducial volume 100 t) to detect the scattered electrons. The energy window in which the ^{7}Be neutrino induced events will be observed is in the range of 250 keV to 800 keV, at an expected rate of a few tens of events per day. Since these very rare events are practically indistinguishable from other ionizing events produced by natural radioactivity at the same energy, extremely high radiopurity standards must be met by the experiment. Muon induced background events are strongly suppressed (6 orders of magnitude) by the overburden (~ 3500 meter water equivalent, m.w.e.) and by the aid of an additional muon veto shield. The shell type structure of the detector will reduce the environmental γ-ray and neutron fluxes to an insignificant level at the central fiducial volume. The total shield thickness of ~ 5 m.w.e. consists of ~ 2.1 m pure water, ~ 2.6 m Pseudocumene (1,2,4-trimethylbenzene, PC, p = 0.89 g/cm^3) and the outer ~ 1.2 m of the liquid scintillator. The latter is contained in a thin nylon wall inner vessel. The scintillation light is viewed by 2200 photomultiplier tubes (PMT) mounted on the stainless steel sphere (SSS). A muon veto is formed by 200 outward looking PMTs detecting the čerenkov light of through-going muons in the water buffer. The outer shell of the detector is a stainless steel tank of 18 m diameter. The inner part of the PC buffer is protected against radon (^{222}Rn) emanated from the PMTs and the SSS by another nylon film (outer vessel). An elaborate system handles and purifies some 300 tons of PC based scintillator and ~1040 tons of PC buffer liquid. Further ancillary plants are a water purification system and a nitrogen plant to supply the experiment with high purity water and nitrogen.

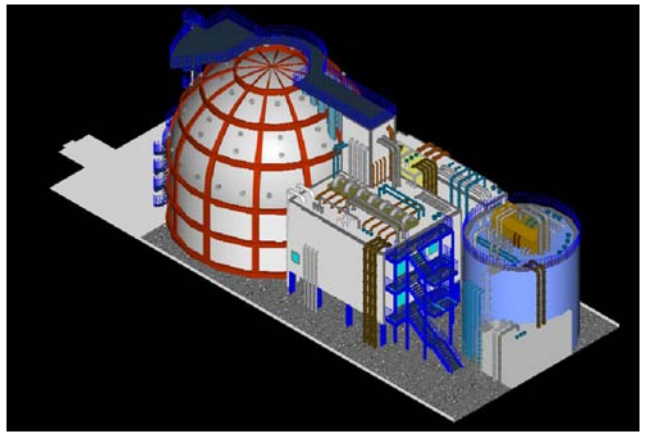

Fig. 1
Sketch of the Borexino apparatus with auxiliary plants.

Fig. 2
View of the internal apparatus; inner vessel and photomultipiers are shown.

REFERENCES
1. Borexino collaboration, *"Light propagation in a large volume liquid scintillator"*, N.I.M. A 440, 360 (2000)
2. Borexino collaboration, *"Science and Technology of BOREXINO: a real time Detector for Low Energy Solar Neutrinos"*, Astroparticle Physics16, 205 (2002)

The Counting Test Facility: a world record in low radioactivity measurements

1 INFN, Sezione di Milano
2 Dipartimento di Fisica, Università degli Studi di Milano

M.E. Monzani[1], B. Caccianiga[1], G. Bellini[2], S. Bonetti[2], D. Franco[2], M. Giammarchi[1], P. Lombardi[1], E. Meroni[2], L. Miramonti[2], L. Perasso[1], and G. Ranucci[1],

The Counting Test Facility (CTF) is a prototype built to test the feasibility of the Borexino experiment[1], realized for the detection of low energy Solar neutrinos (E_ν < 1MeV). The CTF detector consists of 4 tons of liquid scintillator contained in a 1-meter-radius nylon vessel and surrounded by 100 photomultiplier tubes pointing towards the center. The detector is placed inside a cylindrical tank, 10 m of height and 11 m of diameter, filled with purified water (^{232}Th and ^{238}U at the level of 10^{-14} g/g_{water}), which shields neutrons and gammas from the rocks. All the materials have been selected to assure low radioactivity, while during the construction special working procedures have been adopted to minimize the risk of dust contamination. The location of the detector under the Gran Sasso mountain at a water-equivalent depth of 3800 m provides shielding from cosmic rays.

The experimental quantities measured in CTF are essentially the number of photons collected at the PMTs and their arrival times, from which it is possible to extract the energy and position of each event occurring in the scintillator on a real-time basis. The energy resolution is 8% at 1 MeV (and scales with,$\sqrt{N}$ being the number of collected photoelectrons), while position resolution is approximately 12 cm (at 1 MeV).

Different methods for scintillator purification were tested (N_2 stripping, water extraction, distillation) with good performances in reducing radioactive isotopes present in the scintillator. The optical properties of a large volume of liquid scintillator and the propagation mechanism of the optical photon inside it were studied carefully for the first time.

The use of subsequent layers of increasingly pure materials to shield the innermost part of the detector creates an environment almost free of background coming from outside: thanks to these extremely clean conditions, the sensitivity of the CTF has reached records never achieved until now with classic methods of measurements. The low half-life of ^{212}Po and ^{214}Po (see fig. 1) allowed tagging of the Bi-Po delayed coincidences in the ^{232}Th and ^{238}U chain: this made it possible to measure U and Th contamination down to the level of 10^{-16}g/g (assuming secular equilibrium of the chain) [2]. It was also possible to measure ^{14}C content in the organic scintillator to the unprecedented level of about 1 nucleus of ^{14}C every 10^{18} nuclei of ^{12}C[3].

Fig. 1

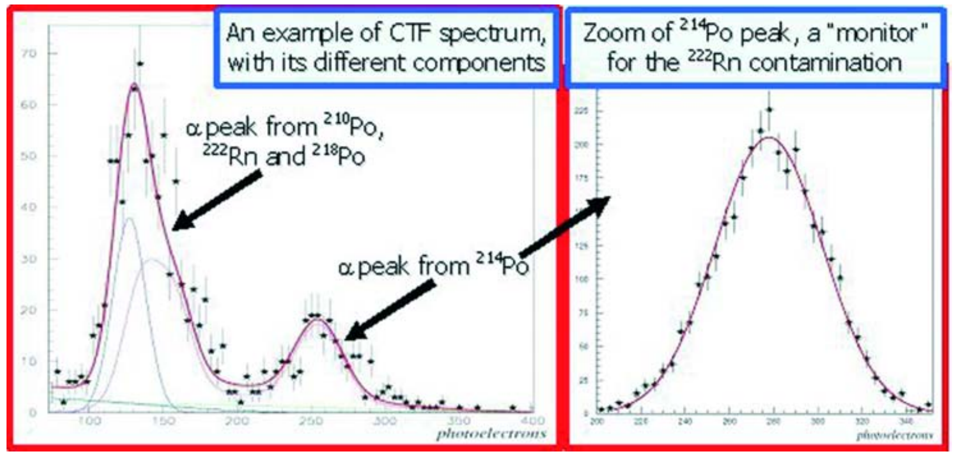

REFERENCES
1. Borexino Collaboration, *A large scale low background liquid scintillator detector: the counting test facility at Gran Sasso*, NIM A406(1998) 411.
2. Borexino Collaboration, *Ultra-low background measurements in a large volume underground detector*, Astr.Phys. 8(1998) 141.
3. Borexino Collaboration, *Measurement of the C-14 abundance in a low-background liquid scintillator*, Phys.Lett. B(1999) 349.

The LHC Computing Grid and the ATLAS experiment

1 Dipartimento di Fisica, Università degli Studi di Milano and Sezione INFN
2 INFN.
3 Progetto EGEE.
4 CNAF, INFN Bologna.

L. Perini[1], T. Lari[2], G. Negri[3], F. Prelz[2], D. Rebatto[2,4], S. Resconi[2,4], and L.Vaccarossa[2,4]

The four experiments at the LHC collide located at CERN are now preparing for the first collisions (pp at 14 TeV) scheduled in the second half of 2007. They are designed for getting new results in many fields of particle physics, but the handling of their data is also an informatics challenge that is being addressed with the new technology of GRID computing, developed in close contact with the experiments themselves.

The LHC experiments involve 5000 physicists located in more than 400 institutions spread in the five continents and the amount of data collected in each year of running is over 10 PB. This amount of data needs to be processed for getting the physics results, giving to each physicist the possibility of acceding the data from his/her home institute, selecting and analysing them with the algorithm of his/her choice together with the ones embodied in the experiment software.

The LCG (LHC Computing Grid project) has the mission of building up the hardware and software infrastructure needed, in collaboration with the GRID projects funded in the major regions of the world, and has just completed its prototyping phase.

In Europe the major GRID project developing the middleware and infrastructure in collaboration with LCG is EGEE (Enabling GRID for E-science in Europe), a two year project, started in April 2004, funded by EU with 32 M Euro, and expected to continue for 2 further year into EGEE2, with similar funding.

The four experiments and LCG[1] have completed in June 2005 their Computing Technical Design Report, describing the status and planning of their software and computing, and all of them adopt the GRID technology as basis of their computing model.

To validate the computing and data model, test the complete software suite and its reliability, ATLAS went through a series of Data Challenges. A data challenge consists in the full simulation and reprocessing of data coming from the detector, carried out with the same software and computing infrastructure expected to be employed during data taking.

Up to now, ATLAS ran two data challenges, DC1 in 2002-2003 and DC2 in the second half of 2004, followed by a large scale production to provide data for physics studies for the ATLAS Rome Workshop in June 2005.

Fig. 1

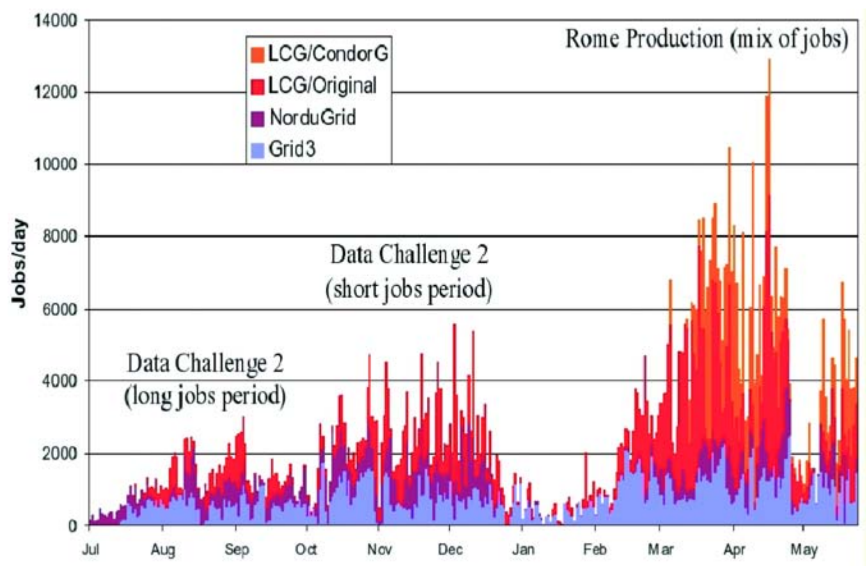

REFERENCES
1. The LCG Editorial Board " LHC Computing Grid Technical Design Report", LCG--TDR--001, CERN-LHCC-2005-024, 20 June 2005.
2. ATLAS Computing Group, "Technical Design Report" ATLAS--TDR--017, CERN-LHCC-2005-022, June 2005.

The production for the Rome workshop consisted of a total of 380k jobs submitted to the LCG GRID infrastructure, out of which 109k simulation jobs (typical duration 20 hours each), 106k digitization jobs, 125k reconstruction jobs and 40k pile-up jobs (the reconstruction has been performed on digitized events and only partially on piled-up events). In total, 1.4M files have been stored in LCG, both on disk-only and Mass Storage Systems corresponding to an amount of data of about 45 TB.

Milan was the first Italian site to enter LCG for ATLAS computing resources (Tier2 prototype) and is giving important contributions to the Grid (responsibility of 1 of the 4 middleware activity of EGEE by F. Prelz, and of the ATLAS-LCG-EGEE task force by L:Perini, 8 people funded by EGEE): the successful ATLAS Rome production on LCG was for > 50% in charge of the Milan group.

Fig. 2

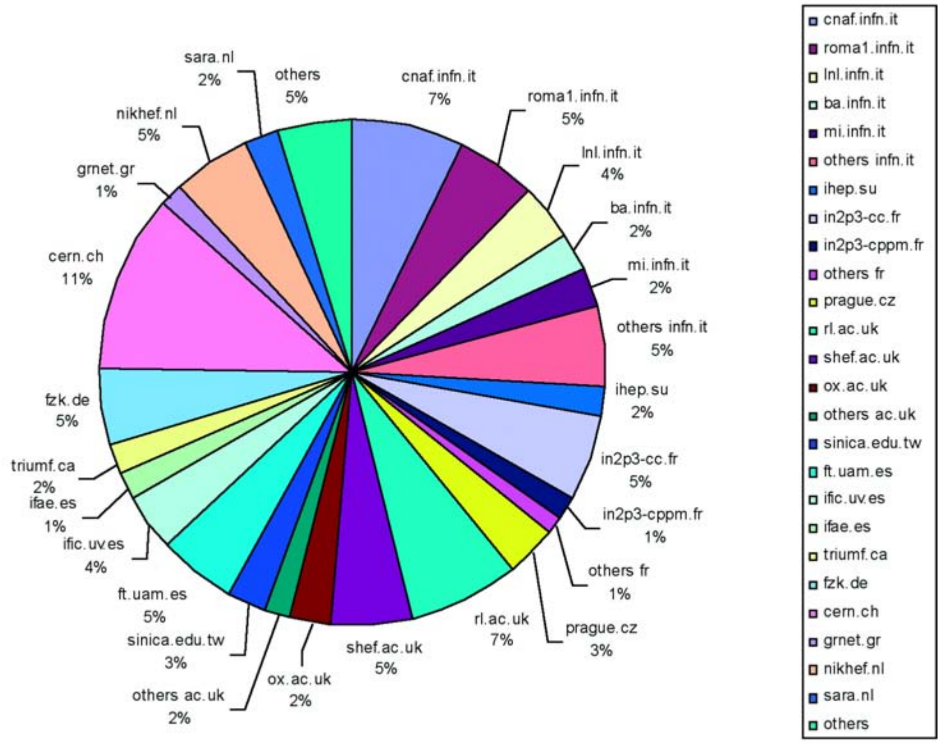

The ATLAS liquid argon electromagnetic calorimeter

1 Dipartimento di Fisica, Università degli Studi di Milano & INFN

G.F. Tartarelli[1], D. Banfi[1], L. Carminati[1], D. Cavalli[1], M. Citterio[1], G.C. Costa[1], M. Delmastro[1], M. Fanti[1], L. Mandelli[1], M. Mazzanti[1], L. Perini[1], and S. Resconi[1]

The electromagnetic calorimeter of the ATLAS experiment is a lead-liquid argon sampling calorimeter with accordion geometry that is expected to play a key role in the Higgs search (in particular in the decay channels $H \to \gamma\gamma$ and $H \to 4e$).

Intoduction

The ATLAS experiment is a general purpose detector designed to exploit the discovery potential of the proton-proton Large Hadron Collider (LHC) at CERN. The ATLAS electromagnetic calorimeter is a lead-liquid Argon (LAr) sampling calorimeter with an accordion geometry. It is composed by a Barrel and two End-Caps (see Fig. 1). The signal in the detector is generated by the drift of ionization electrons between lead absorbers and read-out electrodes.

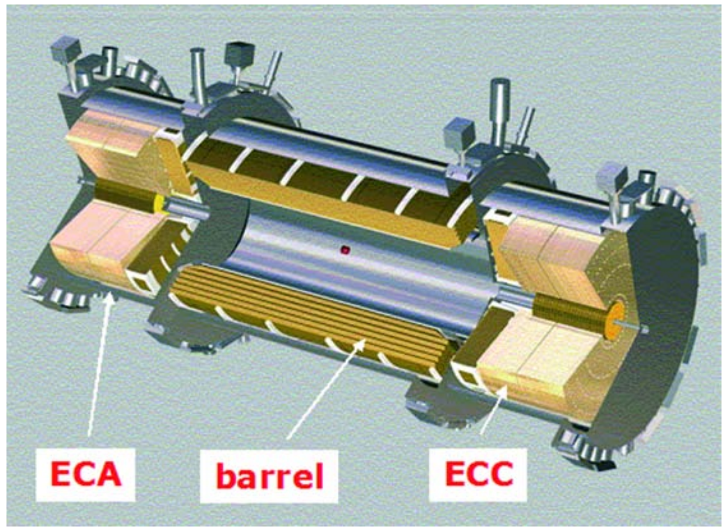

Fig. 1
The ATLAS Liquid Argon Calorimeter.

The read-out electrodes

The read-out electrodes are custom-made three-layer copper-Kapton® electrodes. Their production, carried out in a specialized company, was very challenging due to the large size of the electrodes (about 1 – 2 m^2). Our group has been a key player in designing and testing the electrodes.

The preamplifiers

The analog signal generated in the LAr gap is preamplified by custom-made current amplifiers. About half of the ~ 200,000 preamps needed by the LAr calorimeter were produced by an Italian electronic company under our supervision and testing.

The signal reconstruction

The peak and the arrival time of the calorimeter signal are reconstructed using an Optimal Filtering technique. The calculation of the optimal filtering coefficients requires the knowledge of the normalized shape of the signal, and of the noise autocorrelation function. In the method developed by the Milano group, the parameters needed to perform the ionization signal prediction can be directly retrieved from the calibration pulses.

Test-beam

Prototypes first and production modules of the calorimeters later were exposed to test beams to assess the calorimeter performance. These studies included a cell-by-cell position scan of an entire module at fixed electron energy to assess the uniformity of the response. The good uniformity obtained (at the level of 0.6%) reflects the homogeneity of construction of the detector and the effectiveness of our calibration strategy.

The HV system

In the LAr calorimeter the Detector Control System (DCS) controls high voltage, liquid Argon purity and temperature and so on. The high-voltage system alone consists of ~ 50,000 channels. A commercial Supervisory Control And Data Acquisition (SCADA) package, PVSS-II®, has been chosen to control the system. Milano is responsible of the HV control software for the entire LAr calorimeter system.

Conclusions

The calorimeters construction has successfully finished. The barrel is already in the ATLAS pit at the interaction point (see Fig. 2). With the instrumented detectors in the pit ready to take cosmic data, the year 2006 will be an exciting one for the ATLAS Collaboration. Summer 2007, when the first LHC beam is expected, is just around the corner. It will be the beginning of a new era of discoveries that will lead us toward a deeper understanding of the forces and the particles that govern the universe.

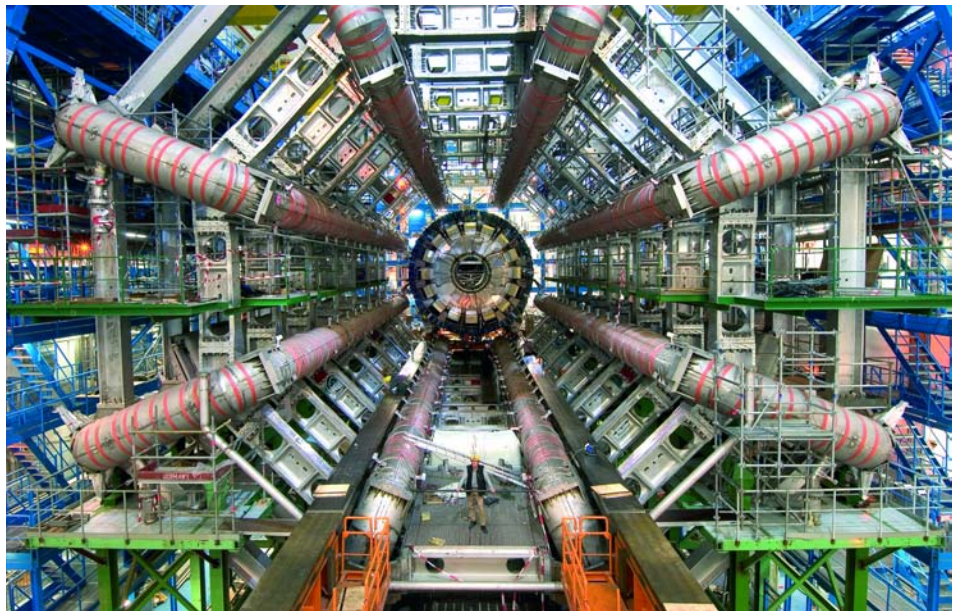

Fig. 2
The barrel calorimeter (shown inside the muon toroids) being moved towards the ATLAS interaction point.

Nuclear Physics

From nuclei to proteins: interdisciplinary research in finite many-body physics

1 Dipartimento di Fisica, Università degli Studi di Milano
2 INFN
3 The Niels Bohr Institute, University of Copenhagen

R.A. Broglia[1,2,3], G. Tiana[1,2], P.F. Bortignon[1,2], G. Colò[1,2], D. Provasi[1,2], F. Marini[1], and E. Vigezzi[1,2]

(The complete manuscript can be found at ***http://merlino.mi.infn.it/papers/broglia_ea_060509.ps)***

Concepts developed to describe the nuclear structure have been found to be rather universal and particularly powerful to describe the properties of the finite many-body systems. In fact, it will be shown that these concepts (like e.g., interwearing of single-particle and collective motion, medium (surface) polarization induced interactions, hot orbitals and phase transitions, etc.) can be used at profit to discuss the physics which is at the basis of neutron stars, atomic clusters and fullerenes, nanomaterials, as well as protein folding.

Independent particle model

In classical mechanics, a system of particles of mass *m* which interact through a two-body force (particle-particle potential) will find the lowest state at zero temperature, by minimizing, for each particle, its potential energy with respect to all its neighbours. Such static, localized particles, provide the basic design for the ground state of molecules and crystals. This phenomenon, known as *spontaneous symmetry breaking*, is at the basis of the *emergent properties* of systems of many particles. In fact, a piece of condensed matter will display localization and rigidity, *properties not contained in each individual particle, nor in the Hamiltonian describing their interaction* [1].

In quantum mechanics, momentum and coordinate are conjugate variables fullfilling Heisenberg's relation. From this relation one can calculate the (zero point) energy associated with the localization of a particle. In the nuclear case, this quantity is of the order of the local-potential energy. It is thus expected that nucleons, inside the nucleus, are delocalized. This is an example of the fact that while *potential energy always prefers special arrangements, fluctuations, quantum or classical, favour symmetry*.

Further examples of spontaneous symmetry breaking and its restoration are provided by the atomic nucleus. These systems can deform in 3D- and in gauge- space. The fingerprints of these phenomena is the presence of rotational bands excited through e.g. Coulomb excitation, and of pairing rotational bands which can be excited in two-particle transfer reactions induced by scattering of two superfluid nuclei [2,3].

Mean field and beyond

Mean field theory, where nucleons move independently of each other in an average potential produced by the effect of all the other nucleons, is applicable to the description of the nuclear structure. A powerful scheme to calculate the mean field potential is provided by Hartree-Fock (HF) theory, and by HF-Bogoliubov (HFB) theory in the case in which pairing is considered. Within this context it is important to mention that a (non-constrained) solution of HFB equations will, in general, display a lower symmetry than the original Hamiltonian. That is, the lowest energy state will identify privileged direction in 3D- as well as in gauge space (deformed, superfluid).

In fact, with the exception of very few doubly closed shell systems, the overwhelming majority of all nuclei are described by states which are deformed in 3D- or in gauge spaces or in both (rotational and/or superfluid nuclei), as well as localized in space. Not surprisingly, there is a term in the residual interaction, neglected in HF as well as in HFB, which leads to zero-point fluctuations in the orientation of the deformed nucleus in 3D-space and in gauge space [2], as well as center of mass translation . Taking these fluctuations into account leads to symmetry restoration [2,4,5].

The importance of the interweaving of single-particle and of collective motion, does not reduce only to the case of static deformations, but it is also valid in the case of the dynamical breaking of the symmetry (vibrations), as observed for example in the case of closed shell nuclei plus (minus) one nucleon (e.g. septuplet of states in ^{209}Bi, as well as effective charge

REFERENCES
1. P. W. Anderson, Science 177 (1972) 393
2. D. M. Brink and R. A. Broglia, *"Nuclear Superfluidity: pairing in finite systems"*, Cambridge University Press, Cambridge (2005)
3. R. A. Broglia and A. Winther, *"Heavy Ion Reactions"*, 2nd Edition, Westview Press, Boulder (2004)
4. A. Bohr and B. R. Mottelson, *"Nuclear Structure"*, Vol. II, Benjamin, New York (1975)
5. P. Ring and P. Schuck, *"The Nuclear Many-Body Problem"*, Springer, Heidelberg (1980)

and mass phenomena). It also plays an important role in closed shell nuclei plus or minus two nucleons, where it gives rise to a pairing induced interaction. The associated zero point fluctuations give important contributions to, among other things, the nuclear masses (see S. Baroni et al, this Volume). All these effects can be systematically treated within the framework of the Nuclear Field Theory (NFT), see [6-8].

Because collective vibrations (see the contribution of G. Colò et al. this Volume) are displayed not only by spherical, normal nuclei but also by deformed, superfluid nuclei (β-, γ- and pairing- vibrations), medium polarization effects and the corresponding dressing of single-particle motion are expected to play a central role in the description of the nuclear structure, in particular in the case of highly polarizable systems like halo nuclei (^{11}Li, ^{12}Be). This is true not only close to the ground state, but also in nuclei at finite temperature (see the contribution of S. Leoni, this Volume and ref. [9]).

Pairing in finite (atomic nuclei, metal clusters) and compact (neutron stars) systems

The bare nucleon-nucleon interaction is essential for the production of pair correlations in nuclei, but the induced interaction due to phonon exchange also contributes. As already mentioned, polarization effects are also important in the calculation of nuclear masses (S. Baroni et al. in this Volume, see also [10,11]) as well as of superfluidity in the inner crust of neutron stars (see also Fig. 1 and 2).

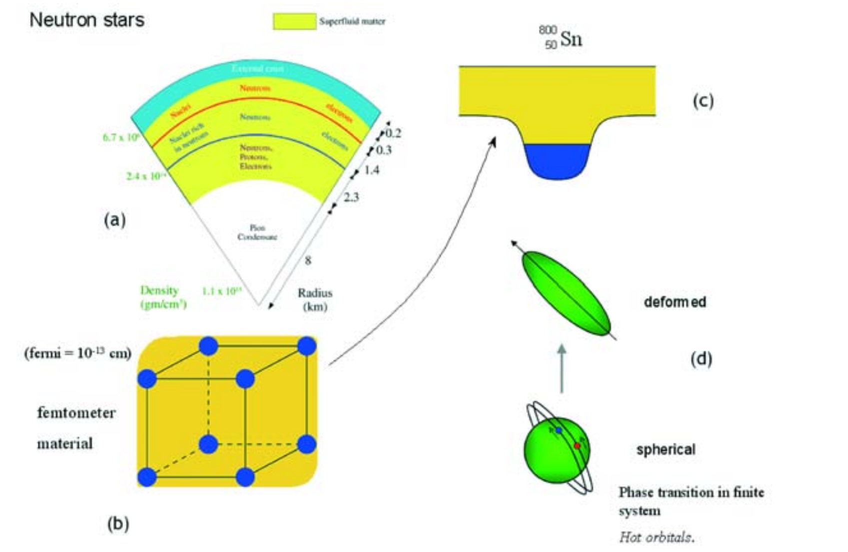

Fig. 1
(a) Cross section of a neutron star, (b) and (c) schematic representation of a Wigner cell in the inner crust of a neutron star, (d) phase transition (e.g. between spherical and deformed nuclei) is controlled by (few) hot orbitals.

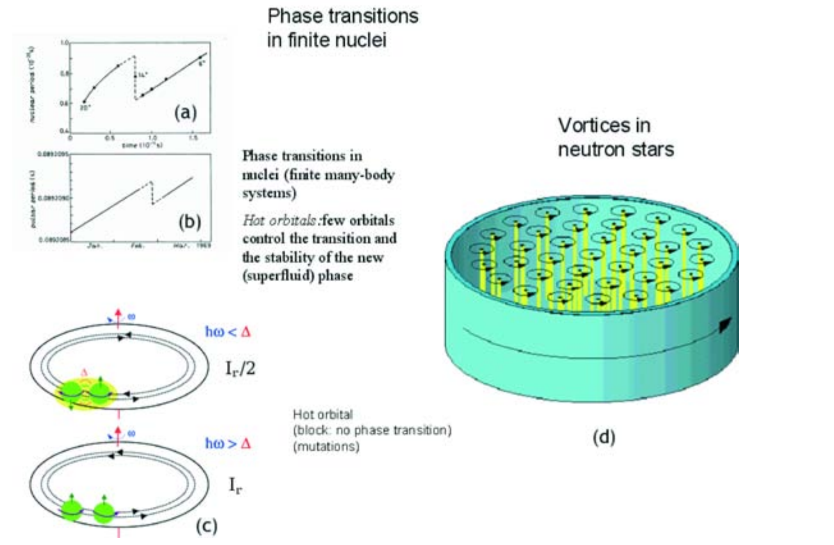

Fig. 2
(a) Backbending phenomenon associated with the breaking of Cooper pairs in nuclei (high-l, hot orbitals) as a function of the rotational frequency (c). (b) Similar phenomena seem to be associated with the rotation frequency changes displayed by pulsars (neutron stars) and related with vortices in these systems (d). I_r is the rigid moment of inertia of the deformed system.

Rotation in a Fermi superfluid polarizes and eventually breaks Cooper pairs leading to a phase transition between superfluid and normal systems. In the description of such a phase transition one does not need the use of singular functions as in the case of infinite systems. In fact, the phase transition is controlled by hot orbitals (e.g., $i_{3/2}(\nu)$, $h_{11/2}(\pi)$) and can be fol-

REFERENCES
6. P.F. Bortignon, R.A. Broglia, D.R. Bes and R. Liotta, Phys. Rep. **30C** (1977) 305-360
7. D.R. Bes and J. Kurchan, *"The treatment of Collective Coordinates in Many-Body Systems"*, World Scientific, Singapore (1990)
8. B.R. Mottelson, *"Elementary Modes of Excitation in Nuclei"*, Le Prix Nobel en 1975, Norstedts Tryckeri, Stockholm (1976) 102
9. P.F. Bortignon, A. Bracco and R.A. Broglia, *"Giant Resonances: nuclear structure at finite temperature"*, Harwood Academic Press, Amsterdam (1998)

lowed in terms of the breaking of Cooper pairs associated with these orbitals [4].

A compact superfluid system, like the inner crust of a neutron star, rotates by generating vortices. The study of the interaction of these vortices with the atomic nuclei immersed in the sea of free neutrons is of central importance to understand the phenomenon of *glitches* observed in these systems [12,13]. HFB theory has been used to determine the properties of these femtometer materials. Also in this case, the role of induced pairing correlations is a central issue in the question of obtaining a quantitative description of these systems.

Making use of the ideas and techniques which are at the basis of the study of femtometer compact systems, one can approach the question of designing nanometer materials with customer tailored properties. In fact, with the help of mean field theory plus correlation effects within the framework of density functional theory (DFT), new superconducting nanometer materials are being designed, using as building blocks metallic clusters. In particular Au_8 clusters (see contribution, M. Bonomi et al, this Volume). Such materials are different from bulk gold, displaying (calculated) properties quite different from this system.

Summing up, the treatment of finite many-body (complex) systems within the "mean field" framework is very useful but lacks essential physics. This physics can be explained as realization of a single dynamical concept: *spontaneous symmetry breaking*. In the case of nuclear physics and neutron stars the corresponding emergent properties are: (a) *generalized rigidity* in 3D- as well as in gauge space; (b) *new dynamics* i.e. long-wavelength collective motions (rotations and GDR) which are Goldstone and Higgs modes of the system; (c) *order parameter singularities*, leading for example to breaking of high-l Cooper pairs (hot orbitals) as seen in the backbending phenomenon in atomic nuclei; (d) arguably, unpinnning of vortices in the phenomenon of glitches associated with neutron stars. All the above are subjects which lie at the forefront of today's research.

One may argue that the "mean field"/continuum/linear way of thinking is what conserved the classical sciences as independent subcultures. Indeed, the great conceptual jumps separating the various sciences and the accompanying paradoxes connected to the nature of life, intelligence, culture arise exactly from the failure of these assumptions. The study of the emergence of new collective properties qualitatively different from the properties of the elementary components of the system breaks the traditional boundary between sciences: concepts developed in the study of one finite many-body (complex) system, like the atomic nucleus (the fact that the normal-superfluid phase transition is controlled by few hot orbitals), can be used at profit (see next section) to describe the folding of proteins.

Protein folding and non-conventional drug design

Proteins are chains made out of 20 different types of amino acids (primary structure) which, starting from a denaturated (random) elongated conformation fold in short times (1 ms - 1 s) on the native, biological active, conformation. How does a linear sequence determine the 3D-structure is not known. This is the protein folding problem.

Because a protein, like an atomic nucleus is a finite many-body system, both undergoing phase transitions, e.g. superfluid-normal (atomic nucleus), random - good folder sequences (proteins), one expects this last process to be controlled by few, hot amino acids. This in keeping with the fact that few, hot (high-*l*) orbitals control nuclear phase transitions of finite systems [14].

Making use of these concepts and of a simple model of proteins, where the 20 different types of amino acids are represented by beads of equal size, forced to move on the vertices of a lattice and interacting through a 20 x 20 contact matrix, one finds that good folders are those sequences which, in the native conformation display a particular low energy [15,16].

With the help of Monte-Carlo simulations it is found that all proteins folding to a selected native conformation display the same set of amino acids on few hot sites. At the very beginning of the folding process local elementary structures (LES) are built stabilized by these hot, highly conserved amino acids (Fig. 3b). LES, and not single amino acids, control from now on the whole folding process. In this way the system reduces in an important way the degrees of freedom of the chain and overcomes the highest barrier of the free energy associated with the folding process, docking the LES in their native conformation (folding nucleus, Fig. 3c). Shortly after, the remaining amino acids reach their native positions (Fig. 3d).

REFERENCES
10. S. Baroni, F. Barranco, P.F. Bortignon, R.A. Broglia, G. Colò and E. Vigezzi, Phys. Rev. C (in press)
11. S. Baroni, M. Armati, F. Barranco, R.A. Broglia, G. Colò, G. Gori and E. Vigezzi, J. Phys. G : Nucl. Part. Phys. **30** (2004) 1353
12. M. A. Alpar, H. F. Chan, K. S. Cheng and D. Pines, Ap. J. **459** (1996) 706
13. P. Avogadro, F. Barranco, R.A. Broglia and E. Vigezzi, (to be published)
14. R.A. Broglia, Rivista del Nuovo Cimento, **28**, no. 1, (2005) 1-25
15. R.A. Broglia, E. I. Shakhnovich and G. Tiana, eds., *Protein Folding, Evolution and Design*, Proceedings of the International School of Physics "Enrico Fermi", Course CXLV, IOS Press, Amsterdam (2001)
16. R.A. Broglia, G. Tiana, *"The physics of protein folding: design of non-conventional drugs"*, Cambridge University Press, Cambridge (to be published)

Viruses and bacteria depend, for their reproduction, on specific enzymes, central for their vital cycle. Drugs are molecules blocking their activity. These drugs, aimed at the active site of the protein, develop, as a rule, resistance (think about antibiotics (bacteria) and about the flu virus, let alone HIV).

If one would like to permanently inhibit the folding of a protein, one could use peptides displaying identical sequence as that of a LES (called p-LES). Because LES are specific of each protein, such peptides would be highly specific and effective, as they would attach to the complementary LES with the strength associated with the corresponding LES, not allowing the protein to fold, and thus blocking its biological activity. Furthermore, the virus or bacteria expressing the protein should, to avoid its action, mutate some of the hot amino acids of the protein, leading in this way to its denaturation. Note that if one blocks one or two of the hot orbitals of a superfluid nucleus, this nucleus would not display any normal-superfluid phase transition.

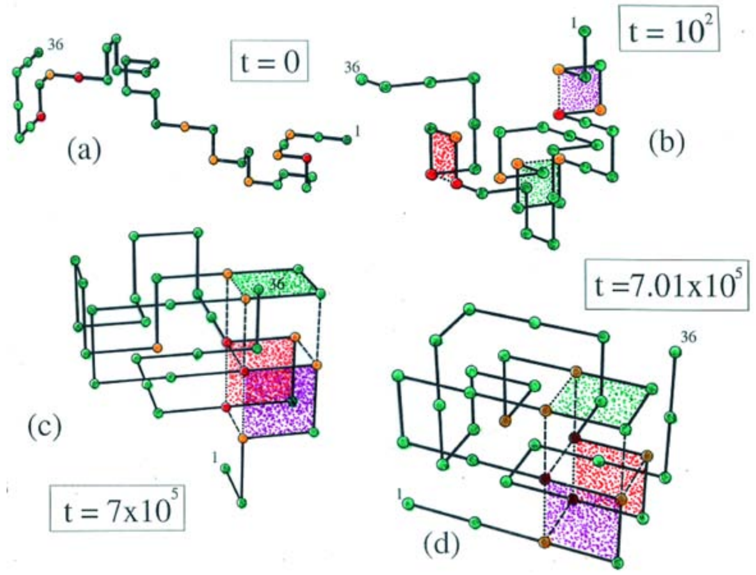

Fig. 3
Snapshots of a Monte Carlo simulation trajectory of a lattice model protein which folds into the native structure shown in (d). Hot, warm and cold amino acids correspond to red, yellow and green beads. The coloured surfaces are the LES.

This strategy has been applied to an enzyme important for the maturation of the HIV. Simulations as well as experiments in vitro [17,18], indicate the inhibitor properties of the corresponding p-LES (see the contribution of Tiana et al, this Volume).

Summing up, one of the most ambitious challenges posed by the present understanding of finite many-body (complex) systems like the atomic nucleus, is prospecting, mapping, colonizing and developing the "interdisciplinary" territory. To do so, bringing people from the different disciplines together is not enough. These fields (nuclear physics, astrophysics, cluster physics, proteomics, brain research, etc) have very different "cultures": different objectives, criteria of success, techniques and languages. A deep shift in their way of thinking is necessary.

To realize it requires "growing" a new generation of "bilingual" young scientists (including medical doctors) that will produce the necessary synthesis in their own minds.

Finite many-body (complex) systems induce also a new relation between theoretical and applied science. In fact, the generality of concepts developed to treat "inanimate" objects (like e.g. the atomic nucleus or fullerenes) are so general that they carry onto real proteins, providing brand new glasses to look at these systems, building blocks of life on earth.

REFERENCES
17. R.A. Broglia, G. Tiana, L. Sutto, D. Provasi and F. Simona, Protein Science **14** (2005) 2668
18. R.A. Broglia, D. Provasi, F. Vasile, G. Ottolina, R. Longhi and G. Tiana, Proteins **62** (2006) 928

Heavy ion interactions relevant to hadrontherapy

F. Cerutti[1,2], E. Gadioli[1,2], E. Gadioli Erba[1,2], M. Cavinato[1,2], P. Colleoni[1], A. Mairani[3], and A. Pepe[1]

1 Dipartimento di Fisica, Università degli Studi di Milano
2 INFN
3 Dipartimento di Fisica Nucleare e Teorica, Università di Pavia and INFN, Sezione di Pavia

There is an ever growing belief of the need of inclusive information on the nuclear reactions induced by light ions for their relevance in interdisciplinary and applicative fields such as hadrontherapy and space radiation protection. To these reactions a large variety of different mechanisms contribute even at low energies, originating both by their fusion and their fragmentation. We will show the results of a case study of the interaction between carbon and aluminium ions which show that the contemporary investigation of a reaction ($^{12}C + {}^{27}Al$) and its inverse, at the same channel energy, greatly helps in identifying the contributing mechanisms and estimating the probability of their occurrence.

1. Introduction

The interactions of two light nuclei are of great interest not only for understanding the underlying reaction mechanisms but also for their applications in fields such as hadrontherapy and radiation protection of the crew and the equipment in space missions. In a recent experiment performed at iThemba LABS [1] the interaction of ^{12}C with ^{27}Al was studied at an incident energy of 13 MeV/n. This study suggested that the same mechanisms which were found to dominate in the interaction of light nuclei (^{12}C and ^{16}O) with heavier targets (complete fusion (CF) and break-up-fusion (BU-F) reactions) [2-6] could still account for most of the reactions observed in the interaction of two light nuclei at energies of few tens of MeV/n – corresponding also to the Bragg peak region (BPR) of higher energy ions interacting with thick materials. Section 2 summarizes the experimental and theoretical background which led our group to identify the main interaction mechanisms of the light nuclei ^{12}C and ^{16}O with matter. In Sect. 3 we present the main results of the study of the interaction between carbon and aluminium. Section 4 is devoted to a discussion of the perspectives of these investigations.

2. Leading reaction mechanisms in the interaction of light nuclei with matter

The analysis of the ejectile spectra in heavy ion CF reactions leads one to recognize the need of describing the nuclear thermalization of the nucleus which the two nuclei form when they interact, i.e., the process through which the initial energy distribution of the projectile and target nucleons transforms into the thermal equilibrium distribution. This mechanism is assumed to consist of a cascade of nucleon-nucleon interactions simulated by a set of coupled Boltzmann Master Equations (BMEs) [7,8]. Their solution gives the time evolution of the occupation probability of predefined bins of nucleon states as a result of nucleon interactions which redistribute the nucleons within different bins and emission of particles into the continuum. The theory considers the possibility of emission not only of single nucleons but also of clusters (including intermediate mass fragments, IMFs) which may be formed by coalescence of nucleons, and evaluates their double differential spectra. Coupled with a Monte Carlo calculation and a statistical evaporation code it allows to evaluate the probability of particular sequences of events and thus of exclusive processes providing a comprehensive description of all possible reactions. These calculations allow to reproduce accurately a large number of ejectile spectra.

With increasing interacting ion energy, CF contributes increasingly less to the reaction cross section and one must consider the possibility of different processes. The most probable of these alternative mechanisms are, in the case of ^{12}C and ^{16}O, BU-F reactions, i.e., binary fragmentation of the projectile followed by the fusion of one of the fragments with the target nucleus, and inelastic scattering. The analysis of the IMF spectra, which (see Fig. 1) show two distinct contributions due to fragmentation at high energy and nucleon coalescence at energies slightly above the Coulomb barrier, suggests that before fragmentation the projectile may suffer a quite considerable loss of energy [2-6].

A systematic study of ^{12}C and ^{16}O reactions allowed us to estimate the relevant parameters for the theoretical calculations: the cross sections for fragmentation, CF and inelastic scattering, the average energy loss before fragmentation and so on. Figure 2 shows, in the

REFERENCES
1. S.V. Förtsch et al., Proc. International Conference on Nuclear Data for Science and Technology, Santa Fe, 2004, Edts. R.C. Haight, M.B. Chadwick, T. Kawano and P. Talou, AIP Volume 769 (2005) Part 2, 1642
2. E. Gadioli et al., Eur. Phys. J. A8 (2000) 373; A11 (2001) 161
3. E. Gadioli et al., Nucl. Phys. A708 (2002) 391
4. E. Gadioli et al., Eur. Phys. J. A17 (2003) 195
5. B. Becker et al., Eur. Phys. J. A18 (2003) 639
6. L.J. Mudau et al., Nucl. Phys. A761 (2005) 190
7. M. Cavinato et al., Nucl. Phys. A643 (1998) 15
8. M. Cavinato et al., Nucl. Phys. A679 (2001) 753

case of ^{12}C reactions on ^{103}Rh, the cross sections for the mechanisms which are found to contribute to the reaction cross section [9]. These results indicate that the fragmentation process is considerably more complex than thought before, not only for the presence of the quite significant energy exchange before fragmentation, but also because ^{12}C and ^{16}O may fragmentate in many possible ways and not exclusively into α-type fragments as previously assumed.

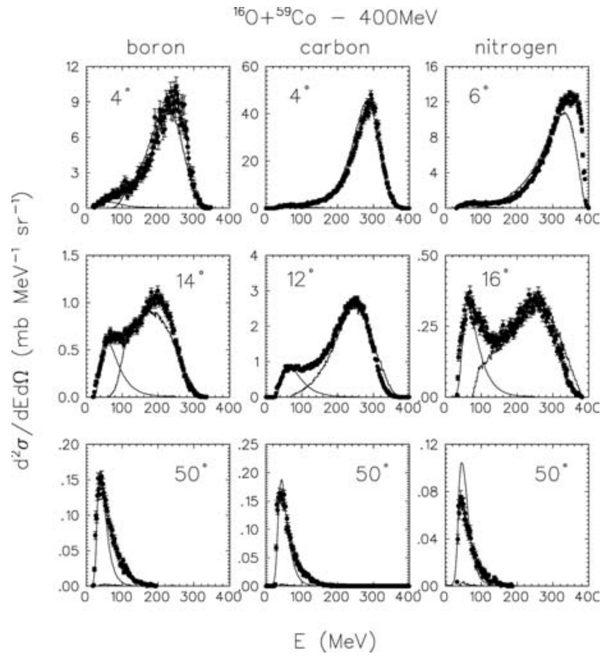

Fig. 1
Spectra of boron, carbon and nitrogen fragments produced in the interaction of ^{16}O with ^{59}Co at an incident energy of 400 MeV [3,4]. The experimental values are given by the solid dots. The theoretical prediction of the spectra of fragments produced by ^{16}O break-up is given by the solid line histograms extending up the highest emission energies. The expected contribution of fragments produced by nucleon coalescence is given by the solid lines peaking slightly above the emitted fragment's Coulomb barrier.

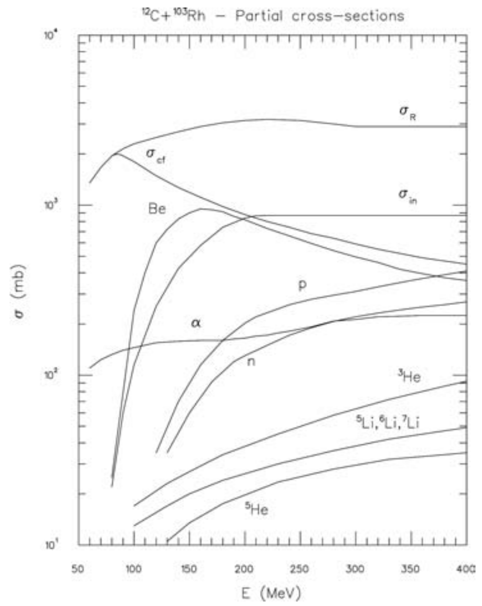

Fig. 2
Reaction cross section and cross sections of the contributing reaction mechanisms in the interaction of ^{12}C with ^{103}Rh up to an incident energy of 400 MeV (*cf* = complete fusion, *in* = inelastic scattering, *Be* = incomplete fusion of a beryllium isotope, α = incomplete fusion of one α particle, *p*, *n* = transfer of a proton or a neutron from the projectile to the target, $^{5,6,7}Li$ = incomplete fusion of one of these lithium isotopes, $^{3,5}He$ = incomplete fusion of a ^{3}He or a ^{5}He).

3. The interaction of ^{12}C and ^{27}Al at 13 MeV/n

In the low energy interaction of two light nuclei it is not possible to separate the IMFs produced in the fast stage of the reaction (both by projectile and target fragmentation and nucleon coalescence) from the evaporation residues, whose masses, in the interaction of a light projectile with a much heavier target nucleus, are considerably different. This complication may be alleviated by studying (i) the interaction of nuclei with somewhat different masses such as ^{12}C and ^{27}Al because their fragments are more easily distinguished, and (ii) both the direct and the inverse reaction exchanging the roles of the projectile and the target. In fact, for kinematical effects, in the laboratory system fragments originating from the projectile are mostly emitted at very forward angles with considerable energy, while those originating from the target are emitted at larger angles with greatly reduced energy so that their spectra display quite different features [1].

In spite of the enormous variety of processes which might occur, most of the measured spectra are very reasonably reproduced simply considering the CF of the two ions as well as BU-F reactions. These processes create with quite significant cross sections a large number

REFERENCES
9. E.Z. Buthelezi et al., Nucl. Phys. A753 (2005) 29

of ejectiles, ranging from fragments with mass smaller than the mass of the lighter interacting ion to residues with mass exceeding that of the heavier interacting ion. To the lightest ejectile spectra, break-up fragments from both interacting ions and fragments produced by nucleon coalescence in CF reactions mainly contribute. Nuclei with mass intermediate between those of the interacting ions may be produced by the heavier ion fragmentation, by the nucleon coalescence in CF reactions, and as evaporation residues in CF and BU-F reactions. As an example, the spectra of fluorine isotopes are shown in Figs. 3 and 4. Evaporation residues heavier than ^{27}Al are also observed with sizeable cross sections and their spectra are reasonably well reproduced by our calculations.

Many different isotopes may be produced by coalescence or as evaporation residues. In evaluating nuclear fragmentation, for sake of simplicity, we considered only the break-up modes requiring the lowest fragmentation energies, and the spectator fragments are assumed to be in their ground state.

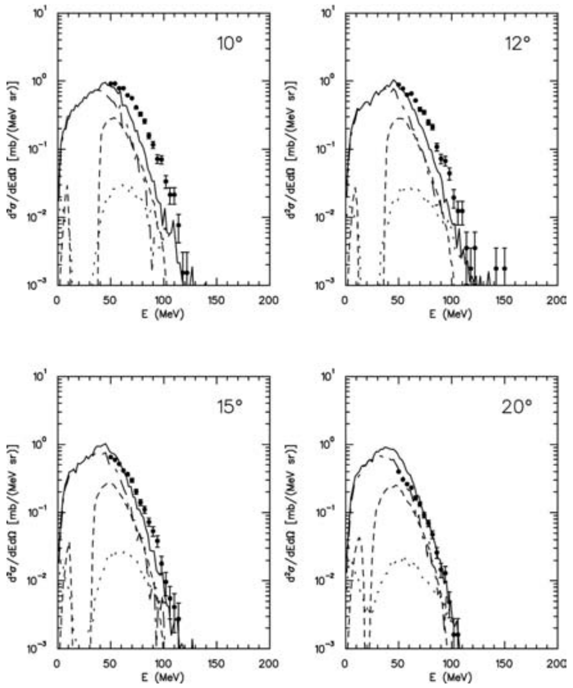

Fig. 3
Double differential spectra of F in the ^{12}C+^{27}Al reaction at E_{Lab}=156 MeV. Experimental data (full circles with error bars) are compared with the theoretical prediction (solid line) which is the sum of three contributions: fragments from ^{27}Al break-up (dashed line), from nucleon coalescence in complete fusion reactions (dotted line), and produced as evaporation residues in complete fusion and break-up-fusion reactions (dashed dotted line).

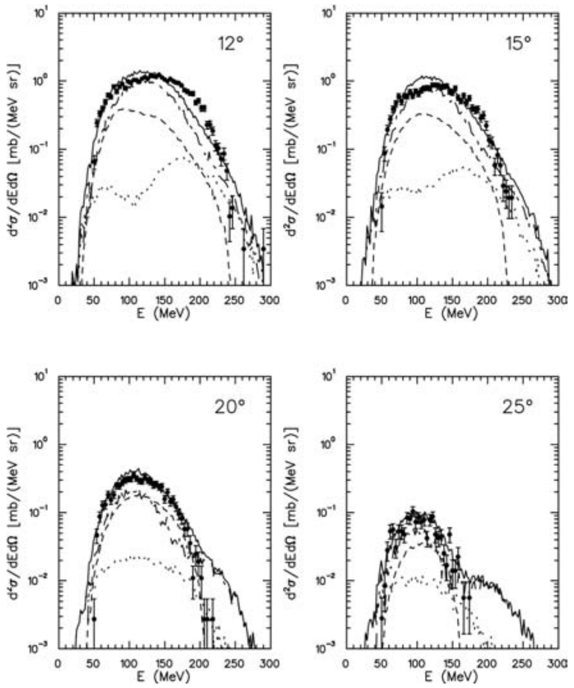

Fig. 4
Double differential spectra of F in the ^{27}Al + ^{12}C reaction at E_{Lab} = 348 MeV. Experimental data (full circles with error bars) are compared with the theoretical prediction (solid line) which is the sum of three contributions: fragments from ^{27}Al break-up (dashed line), from nucleon coalescence in complete fusion reactions (dotted line), and produced as evaporation residues in complete fusion and break-up-fusion reactions (dashed dotted line).

The total cross section obtained by adding up the contributions of all the considered mechanisms and the cross section for inelastic scattering, pick-up as well as stripping reactions amounts to about 80% of the reaction cross section estimated to be 1700 mb [10]. The results of this analysis are encouraging because the qualitative features of all observed spectra are satisfactorily reproduced and the theory seems to be able to provide also a reasonable quantitative account of them in spite of the simplifying assumptions which are made. Some results were rather unexpected such as the sizeable production of evaporation residues with mass exceeding the interacting ion masses, as a consequence of the leading role of complete and incomplete fusion reactions.

4. Perspectives

Extension of this study to the interaction of even lighter systems (^{12}C + ^{12}C and ^{16}O + ^{12}C) is of the uttermost importance for hadrontherapy for the following two reasons: (i) firstly and more importantly in order to obtain information about the production of positron emitters used for visualizing the beam during irradiation through PET techniques, and consequently allow a better conformation of actual dose delivering to the tumour volume, (ii) secondly in order to evaluate the amount of fragments with mass greater than those of the interacting ions which are mainly produced as evaporation residues with relatively low energies and may thus considerably increase the relative biological effectiveness of the beam in the Bragg peak region, which otherwise might be noticeably reduced due to reactions occurring along its passage through the healthy tissue before reaching the tumour.

REFERENCES
10. F. Cerutti et al., Eur. Phys. J. A25 (2005) 413

The physics of nuclear collective states: old questions and new trends

1 Dipartimento di Fisica, Università degli Studi di Milano and INFN

G. Colò[1], P.F. Bortignon[1], R.A. Broglia[1], and E. Vigezzi[1]

It has been known for many decades that atomic nuclei display collective vibrational modes. These modes carry different quantum numbers and a major goal of the nuclear structure community has been, and still is, to try to obtain information about the nature of the correlations associated with those quantum numbers, and about a proper nuclear effective Hamiltonian, from the analysis of the vibrations which are experimentally observed. These issues have been studied by the Nuclear Theory Group of our Department for quite a long time, in the context of various international collaborations. In the present contribution, emphasis will be put on (a) the monopole vibration and the extraction of the nuclear compression modulus, and on (b) the dipole vibration and its properties in neutron-rich nuclei. This latter theme is quite important as the physics of neutron-rich, unstable isotopes lies at the forefront of nuclear research. This study allows exploring nuclear matter in novel and unprecedented conditions of large N-Z.

Introduction

Our understanding of the structure of atomic nuclei is limited by our incomplete knowledge of the effective nuclear Hamiltonian. The bare interaction between two nucleons in the vacuum has not yet been derived from first principles, that is, from low-energy QCD. There exist, however, phenomenological forces, which have been fitted to the nucleon-nucleon (NN) scattering data with remarkable accuracy. These forces can be employed in calculations of light nuclei (up to mass number $A \approx 12$: cf., e.g., [1]). Not only the large amount of mutual correlations among nucleons prevents from applying these "ab-initio" methods in medium-heavy nuclei: we can say that the bare force is so strongly renormalized that, repeating the words of Ben Mottelson (Nobel prize winner of physics), "we are simply forced to simplify the force". In fact, aside from the bare NN force, there exist correlations which have long-range character and that have their origin in the polarization of the nuclear medium as a whole [2].

For all these reasons, there exists some consensus nowadays among nuclear theorists that, to explore the nuclear isotope chart, the most "microscopic" method which is feasible is density functional theory (DFT) based on an effective interaction V_{eff} [3]. In this scheme, one can start from an effective interaction which already contains a number of important correlations and eventually improve on it. In practice, V_{eff} contains a small number of parameters (less than ten) and is used to build the energy functional $E[\rho]$, where ρ is the density, as the expectation value of $H = T + V_{eff}$ on a given model wavefunction (T denotes the kinetic energy). The simplest choice is that of a Slater determinant. Since in this case the one-body density matrix ρ (with $\rho^2 = \rho$) is the single physical quantity which determines the properties of the system, we have indeed defined a density functional. The condition that the energy is minimum with respect to density variations defines the nuclear ground state. In practice, different kinds of densities must be introduced (spin and isospin densities, kinetic energy densities, abnormal densities). The minimum condition corresponds to the Hartree-Fock (HF) equations, which generalize into the Hartree-Fock-Bogoliubov (HFB) equations - also known in literature as de Gennes equations - in the case of open-shell isotopes where the nuclear "pairing" force gives rise to nuclear superfluidity. Relativistic covariant density functionals (based on the description of nucleons as Dirac particles, and of their mutual interactions as mediated by the exchange of effective mesons) have been studied in recent years [4]. The parameters of non-relativistic or relativistic functionals are fitted to reproduce basic properties of nuclear matter and selected observables of a small set of magic nuclei, and then used to predict a variety of properties displayed by nuclei throughout the mass table. In the non-relativistic framework, the most widely used parametrizations of the two-body effective forces are of the so-called Skyrme type (zero-range) or Gogny type (finite-range) [5].

The global aim of this approach is to find a "universal" functional - which can account for the large variety of phenomena displayed by the nuclear species throughout the isotope chart (Fig. 1). It would be desirable to reproduce the behaviour of the nuclear masses, also in the regions far from stable nuclei, of the different nuclear shapes (i.e., for static quadrupole and octupole deformations), as well as for the vibrations and rotations of all these systems.

REFERENCES
1. See: Pieper S.C., Wiringa R.B., Carlson J., "Quantum Monte Carlo calculations of excited states in A=6-8 nuclei", *Physical Review* C 70, 54325 (2004), and references therein.
2. Cf. Broglia, R.A., in this volume.
3. Bender M., Heenen P.-H., Reinhard P.-G., "Self-consistent mean field models for nuclear structure", *Reviews of Modern Physics* 75, 121 (2003).
4. Ring P., "Relativistic mean field theory in finite nuclei", *Progress in particle and Nuclear Physics* 37, 193 (1996).
5. Vautherin D., Brink D.M., "Hartree-Fock calculations with Skyrme's interaction. I Spherical nuclei", *Physical Review* C 5, 626 (1972); Dechargé J., Gogny D., "Hartree-Fock-Bogoliubov calculations with the D1 effective interaction on spherical nuclei", *Physical Review C* 21, 1568 (1980).

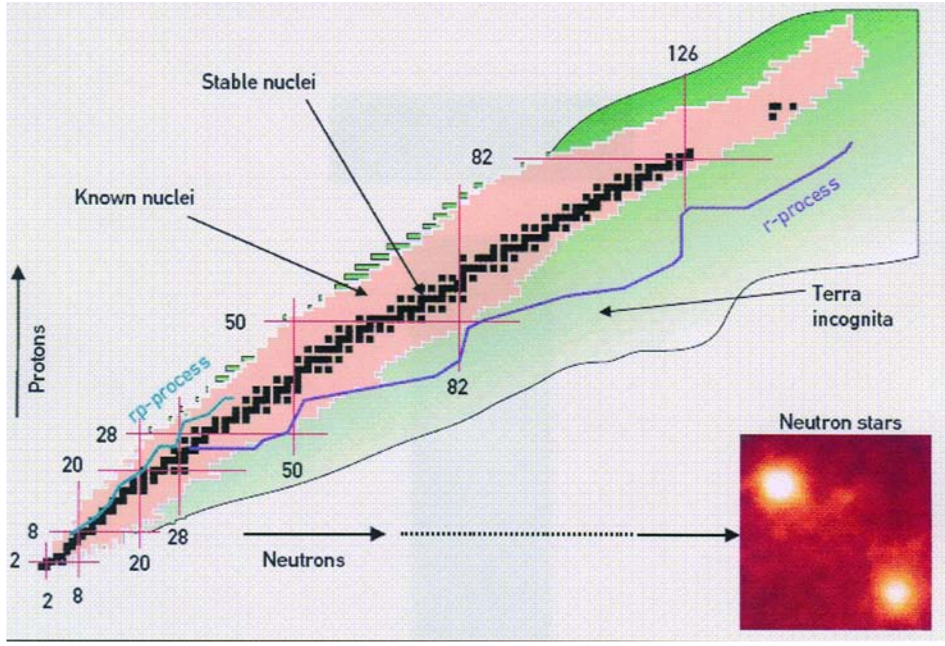

Fig. 1
The isotope chart (Z vs. N plane).
The location of stable (black) and known (pink) nuclei is indicated, together with the regions in which unstable or unbound nuclei have still to be identified (green).
The link with nuclear astrophysics (properties of infinite matter in stars, and location of the nucleosynthesis paths) is evident.

However, as emerged from the results of this work, as well as of large amount of work appeared in the literature under the main title of particle-vibration coupling (PVC) [6], the practical implementations of DFT, in which the effective interactions are trated at the mean field (HF or HFB) level, cannot be considered as a complete theory. Correlations effects are taken into account only in an average, energy-independent fashion, and this approximation is bound to fail in case in which particular orbitals close to the Fermi energy play a relevant role, or in other cases like in the description of the damping phenomena (see below). Coming back to the main subject of the present contribution, the small oscillations around the ground state, that is, the nuclear vibrations, can be studied within DFT as well. These oscillations are produced if an external field induces an initial displacement of the density: as the system is moved from equilibrium, the second derivative of the total energy with respect to ρ provides the restoring force for the vibrational mode. The self-consistent theory of small nuclear vibrations is called Random Phase Approximation (RPA) and generalizes to quasi-particle RPA (QRPA) when the pairing force is taken into account.

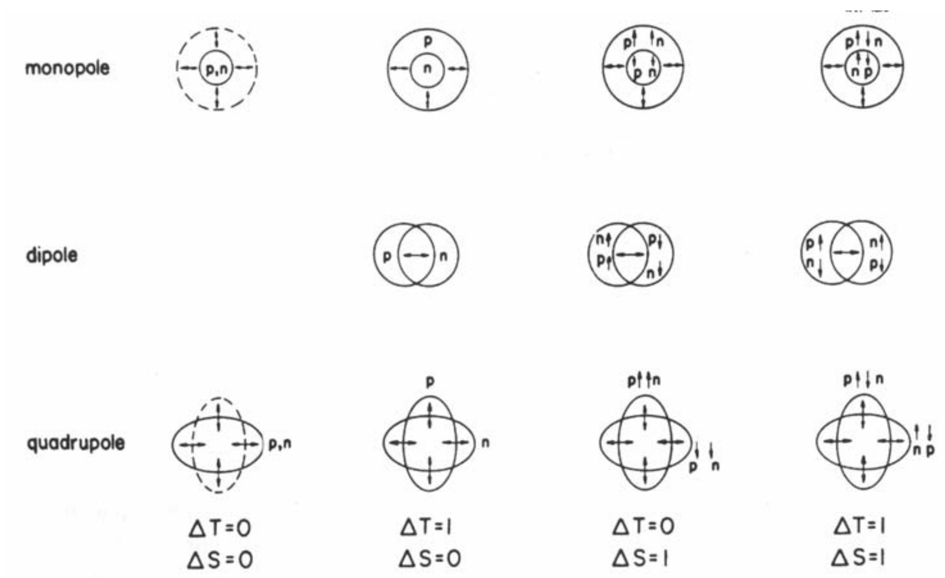

Fig. 2
See the discussion in the text.

Vibrational modes of nuclei are characterized by different quantum numbers: angular momentum ΔL, spin ΔS and isospin ΔT (Fig. 2). In particular, states with isospin equal to zero (isoscalar) correspond to neutrons and protons which oscillate in phase, whereas states with isospin equal to one (isovector) are characterized by neutrons and protons which oscillate in opposition of phase. For each set of quantum numbers, normally there exist few states which are associated with large collectivity, i.e., which involve a large fraction of nucleons and have large probabilities to be excited. These are called giant resonances and have energies of the order of 10-20 MeV [7]. Their width (of few MeV) is associated with the fact that the energy of the ordered collective motion can be transferred to more complicated degrees of freedom

REFERENCES
6. Bohr A., Mottelson B.R., Nuclear Structure (vol. II), New York: W.A. Benjamin (1975).

or to a particle which leaves the nucleus, being emitted in the continuum. These resonances are usually excited by means of different reactions (mainly inelastic hadron scattering). In this contribution, we will discuss the giant monopole (GMR) and dipole resonances (GDR). Charge-exchange resonances are considered in [8].

The monopole resonance and the nuclear incompressibility

The simplest part of the nuclear energy functional is the one which describes the uniform nuclear matter (that is, a system with equal number of neutrons and protons without the Coulomb interaction) close to the saturation point. The curvature of the energy per particle *E*/*A* as a function of the density defines the compression modulus, or the "incompressibility" of nuclear matter: the precise definition of this quantity is $K_\infty = 9\rho^2\ (d^2E[\rho]/d\rho^2)$.

There have been many attempts to extract K_∞ from different kinds of empirical data: the most natural are the data concerning the GMR, that is, the isotropic compression of finite nuclei, which are quite selectively excited by α-particle scattering at small angles. However, the relationship between the compressibility of a finite system and of infinite matter is not at all straightforward. Self-consistent RPA calculations using an effective force provide a link between these two quantities which is physically sound: if a parametrization of V_{eff} is able to reproduce the experimental value of the monopole energy in a set of nuclei, the associated value of K_∞ should be the proper one. Of course, in such a framework a critical assessment of the approximations involved in developing a concrete scheme for solving the HF-RPA equations must be made.

For some time, predictions coming from relativistic and non-relativistic models seemed to predict values of K_∞ which were very different. Recent work seem to have solved this problem [9], leading to the conclusion that $K_\infty = 240 \pm 20$ MeV. The remaining uncertainty is mainly due to the fact that measuring the monopole in finite nuclei brings the asymmetry part of the energy functional into play (see below).

The dipole states and the nuclear symmetry energy

A poorly known part of the nuclear energy functional is the one which describes the neutron-proton asymmetry. In fact, having simplified for the above discussion, we have not said explicitly so far that the dependence of *E* on the density is actually on the proton and neutron densities ρ_n and ρ_p, or on the total density $\rho = \rho_n + \rho_p$ and on the isovector density $\rho_- = \rho_n - \rho_p$. The part of the microscopic functional which depends on the isovector density is the so-called symmetry energy - which gives rise to the symmetry term in the nuclear mass formula. There is an intense effort to determine the features of the density dependence of the symmetry energy: this behavior determines at the same time both the limits of the nuclear existence and the properties of exotic objects like the neutron stars. The new radioactive beam (RIB) facilities aim at studying this problem, together with the many other prominent features displayed by neutron-rich (and proton-rich) isotopes.

Fig. 3
Photoabsorbtion cross section, associated with the dipole excitation, in ^{132}Sn.
The experimental data (crosses) are compared with the theoretical calculation of [11].

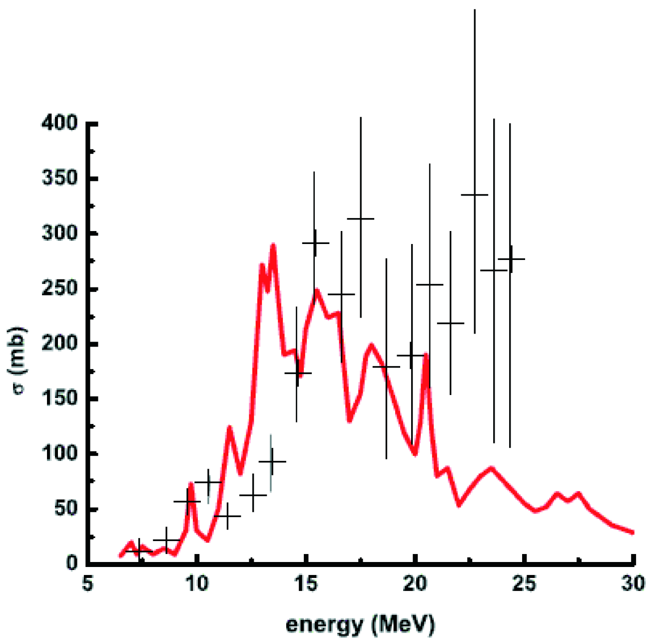

REFERENCES
7. Bortignon P.F., Bracco A, Broglia R.A., *Giant Resonances*, New York: Harwood Academic (1998); Harakeh M.N., Van Der Woude, A., *Giant Resonances*, Oxford: Oxford University Press (2001).
8. Cf. Fracasso, S., in this volume.
9. Agrawal, B.K., Shlomo, S., "Nuclear matter incompressibility coefficient in relativistic and nonrelativistic models", *Physical Review C* 68, 031304 (2003); Colò G., Nguyen Van Giai, Meyer J., Bennaceur K., Bonche P., "Microscopic determination of the nuclear incompressibility within the nonrelativistic framework", *Physical Review C* 70, 024307 (2004).

In fact in light nuclei with large values of (N-Z)/A the phenomena of neutron "skins" or "haloes" have been observed. These are caused by loosely bound neutrons whose wavefunction extends much further outside the nucleus (compared with the standard cases in which the radius is well described by the usual formula $R = R_0 A^{1/3}$). In these systems, the dipole response at low energy is characterized by a marked "threshold" effect, that is, it is enhanced because of the optimal matching of the initial wavefunction with that of a scattering state in the continuum. However, in these systems the neutrons which form the halo are one or two (in cases like ^{11}Be, ^{11}Li) and, by definition, the dipole state cannot be highly "collective". A case in which more "valence" neutrons are decoupled from a "core" with $N \approx Z$, and can vibrate independently, would be ideal for the study of the evolution of the symmetry energy when the ratio $(N - Z)/A$ increases. The recently discovered isotope ^{132}Sn could have been a candidate. However, both the experiment [10] and the theoretical study [11] have suggested that the excess neutrons are relatively tightly bound and do not give rise to an independent, well developed collective state. The comparison between experiment and theory is shown in Fig. 3. There are differences in the predictions of relativistic and nonrelativistic theories [12]. In the case of [9], the coupling between different vibrational modes calculated in RPA, that is, the anharmonicities of the system, have been taken into account [13]. In this sense, we have extended the usual implementation of DFT.

We conclude by mentioning that the low-lying dipole is also important for astrophysics, since the cross sections for the neutron capture process and its inverse, that is, (n,γ) and (γ,n), affect the nucleosynthesis r-process ("rapid" process).

REFERENCES
10. Adrich P. et al., "Evidence for Pygmy and Giant Dipole Resonances in ^{130}Sn and ^{132}Sn", *Physical Review Letters* 95, 132501 (2005).
11. Sarchi D., Bortignon P.F., Colò G., "Dipole states in stable and unstable nuclei", *Physics Letters B* 601, 27 (2004).
12. Vretenar D., Paar N., Ring P., Lalazissis G.A., "Collectivity of the low-lying dipole strength in relativistic random phase approximation", *Nuclear Physics A* 692, 496 (2001).
13. Bertsch, G.F., Bortignon P.F., Broglia R.A., "Damping of nuclear excitations", *Reviews of Modern Physics* 55, 287 (1983).

Measurement of cross sections of nuclear reactions of astrophysical interest (LUNA experiment)

1 Istituto di Fisica Generale Applicata,
Università degli Studi di Milano
and INFN

A. Guglielmetti[1] and R. Bonetti[1] for the LUNA collaboration

It is well known [1] that stars generate energy and produce elements by means of thermonuclear fusion reactions which start from the most abundant and lightest element, Hydrogen, and gradually synthesize heavier elements. All fusion reactions occur in stars in a very well defined energy range, the so called *Gamow peak*, which is the result of the overlapping between the energetic distribution of nuclei in stars at a given temperature and the energetic dependence of the reaction cross section. The first, given by the Maxwell-Boltzmann distribution, has a maximum for $E = kT$ (where T is the star temperature) and then decreases exponentially for increasing energy while the second, given by the tunneling probability through a Coulomb barrier, decreases exponentially for decreasing energy. In particular the reaction cross section for charged particles can be written as:

$$\sigma(E) = (S(E)/E)\exp(-2\pi\eta)$$

where $S(E)$ is the *astrophysical factor* which contains the pure nuclear behavior of the cross section and η is the *Sommerfeld parameter* given by:

$$\eta = (31.29/2\pi)\, Z_1\, Z_2\, (\mu/E)^{1/2}$$

being Z_1 and Z_2 the charges of the interacting nuclei, μ the reduced mass and E the interaction energy in keV. As an example, in our Sun whose temperature is 1.5×10^7 °K the maximum of the Maxwell Boltzmann distribution occurs at about 1 keV, the Coulomb barrier for the ^{3}He + ^{3}He reaction (one of the most important reactions in the p-p cycle, which converts 4 protons in Helium with a net energy release of about 27 MeV) is 1500 keV and the Gamow peak (21 ± 5) keV: the cross section at the minimum energy of 16 keV is 20 femtobarn. Such low value of the cross section at the Gamow peak has always prevented a direct measurement in a laboratory at the earth surface where the signal to background ratio would have been too small due to cosmic ray interactions. Instead, the observed energy dependence of $\sigma(E)$ at high energies is extrapolated to the low energy region, leading to substantial uncertainties. In particular, a possible resonance in the unmeasured region is not accounted for by the extrapolation, but it could completely dominate the reaction rate at the Gamow peak. Therefore the search for narrow resonances demands the direct measurements of the nucleosynthesis cross section in the low energy range of few tens of keV.

To fulfill such goal, the LUNA (Laboratory for Underground Nuclear Astrophyisics) collaboration installed two small accelerators underground in the INFN Gran Sasso National Laboratory. Here the mountain provides a natural shielding of 1400 m of rock equivalent to at least 3800 m of water which reduces the muon and neutron fluxes by a factor 10^6 and 10^3, respectively. The two installed accelerators with maximum terminal voltage of 50 kV and 400 kV respectively, produce very intense and stable beams (current of the order of 250 µA) with very low energy spread (0.1 keV), these features being very important for measuring low cross sections strongly energy dependant.

With the first 50 kV machine the LUNA collaboration studied two key reactions of the p-p cycle: ^{3}He + ^{3}He and p + d at the relevant Gamow peak energies by using gas targets and very efficient particle or gamma detectors. The first reaction plays a big role in the proton-proton chain strongly affecting the calculated solar neutrino luminosity. A resonance at the thermal energy of the Sun was suggested long ago [2] to explain the observed ^{8}B solar neutrino flux: it would have possibly decreased the relative contribution of the alternative reaction ^{3}He + ^{4}He which generates the branch responsible for ^{7}Be and ^{8}B neutrino production in the Sun. The LUNA result [3] shown in Fig. 1 inferred the absence of resonances up to the lower limit of the Solar Gamow peak thus excluding the old possible explanation of the solar neutrino puzzle now ruled out by the recent discovery of neutrino oscillations [4]. At the lowest energy the count rate was of 2 events/month, rather low even for the "silent" experiments of underground physics.

REFERENCES
1. C. Rolfs and W. Rodney, Cauldrons in the Cosmos, University of Chicago Press, Chicago (1988)
2. W. A. Fowler, Nature (London) 238, 24 (1972)
3. R. Bonetti et al., Phys. Rev. Lett. 82, 5205(1999)
4. Q. R. Ahmad et al., Phys. Rev. Lett. 89, 11301 (2002)

The p+d reaction is fundamental for regulating the life of a proto star before the main sequence is reached. This reaction allows the burning of primordial deuterium by conversion into ^{3}He with a net energy release : in such way the gravitational contraction of the protostar is slowed down and its life made longer. The measured astrophysical factor [5] is shown in Fig. 2 together with older results. Also in this case the Gamow peak was reached.

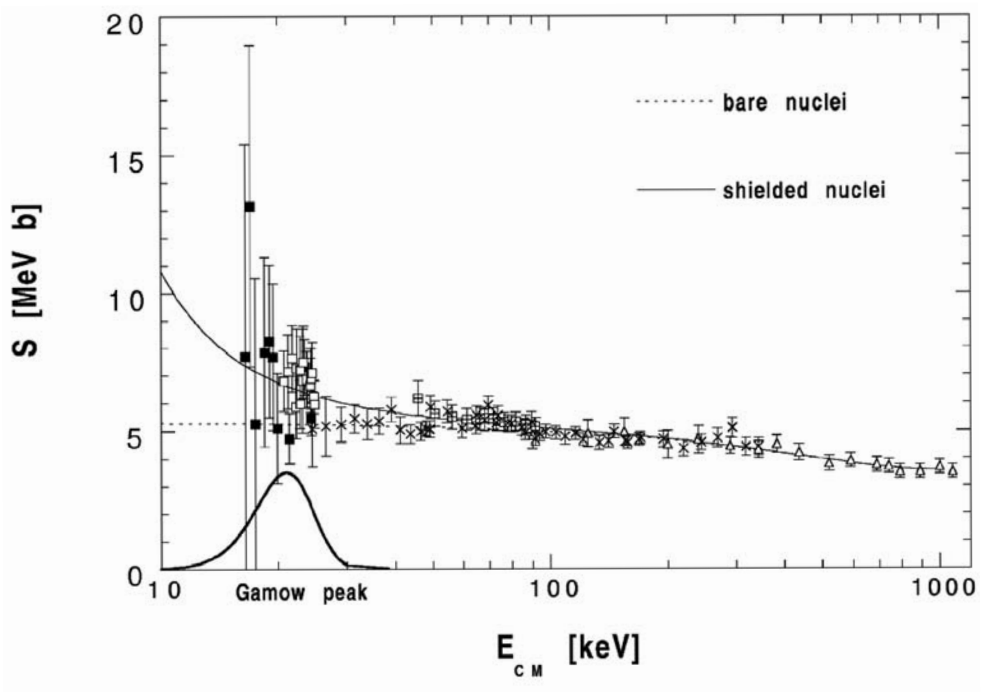

Fig. 1
Astrophysical factor for the ^{3}He + ^{3}He reaction measured by the LUNA Collaboration at the Gamow peak energy. No resonance was found in the Sun energetically interesting region.

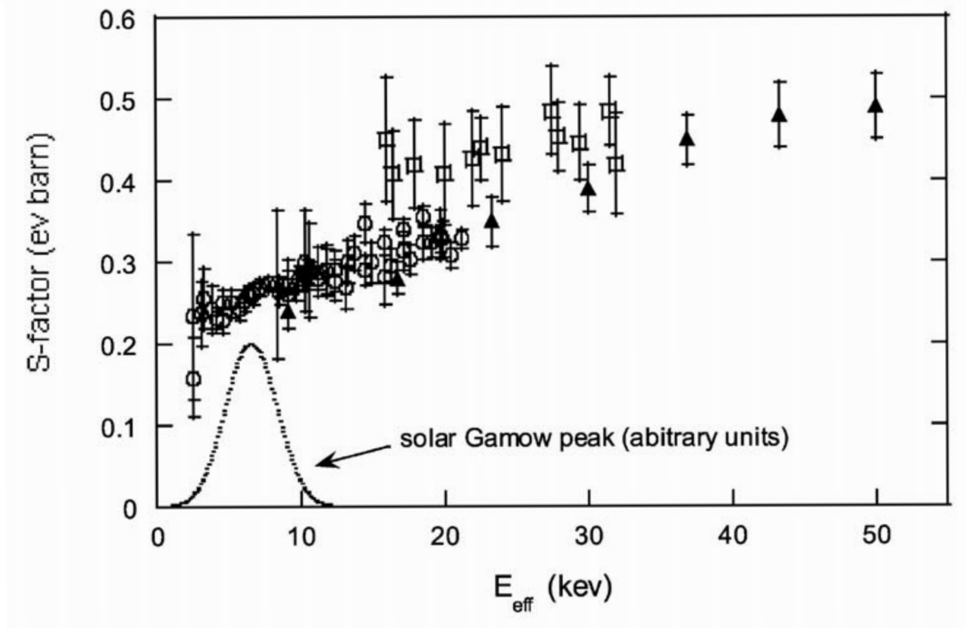

Fig. 2
Astrophysical factor for the p + d reaction: The LUNA collaboration results are shown as open circles.

The 400 kV accelerator was up to now mainly used for measuring the p + ^{14}N reaction, the bottleneck of the CNO cycle which, as the p-p cycle, converts 4 protons into Helium with a net energy release of about 27 MeV. This cycle becomes important for massive ($M > 1.1\, M_{sun}$) and quite "hot" stars ($T > 1.6 \times 10^7$ K). The p + ^{14}N reaction is the slowest reaction of the CNO cycle, the key one to determine the age of globular clusters, the oldest systems in the Galaxy as well as to predict the CNO neutrino flux from the Sun. As a matter of fact, during most of its life, a low mass star burns hydrogen in the center via the p-p chain. However, when the central H mass fraction reduces down to 0.1, the nuclear energy produced by the H-burning becomes not sufficient and the stellar core must contract to extract some energy from its gravitational field. Then, the central temperature (and the density) increases and the H-burning switches from the p-p chain to the more efficient CNO burning. Thus the escape from the main sequence is powered by the onset of the CNO burning whose bottleneck is the p + ^{14}N reaction. In particular, a rate modification of this reaction changes the luminosity of the turn-off point in the Hertzprung-Russell diagram of a globular cluster. The luminosity of this point gives then the age of the cluster: the higher the cross section is, the youn-

REFERENCES
5. C. Casella et al., Nucl. Phys. A 706, 203 (2002)
6. A. Formicola et al., Phys. Lett. B 591, 61 (2004)
7. A. Lemut et al., Phys. Lett B, in press
8. C. Angulo et al. (NACRE collaboration), Nucl. Phys. A 656, 3 (1999)
9. G. Imbriani et al., Astronomy and Astrophysics 420, 625 (2004)

ger is the age, for a given turn-off luminosity. In the center of the sun the CNO cycle is also partially active. Then a fraction of the total neutrino flux comes from the β-decay belonging to the cycle. The total amount of CNO solar neutrinos directly depends on the value of the p + ^{14}N cross section. CNO neutrinos from the Sun play important role in the solar neutrino experiment detecting neutrinos at about 1 MeV energy, e.g. BOREXINO, where the CNO neutrino flux was calculated to account for about 20% of the expected neutrino signal.

Two different apparata were used to study this reaction: a solid target coupled with HPGe detector in the energy region from 140 to 400 keV [6] to measure single gamma transition and angular distribution and a gas target with very efficient BGO detector down to 70 keV [7] to obtain the total astrophysical factor at the lowest measurable energy. The two results (the first of which in shown is Fig. 3), in very nice agreement in the overlapping energy region, determine a value of the astrophysical factor lower by a factor 2 with respect to that given in most recent compilations [8]. The astrophysical consequences are significant: the CNO neutrino yield in the Sun is decreased by about a factor 2 and the age of the Globular Clusters is increased by 0.7-1 Gyr [9] with respect to current estimates. This last result reflects in an increase of the lower limit on the age of the Universe.

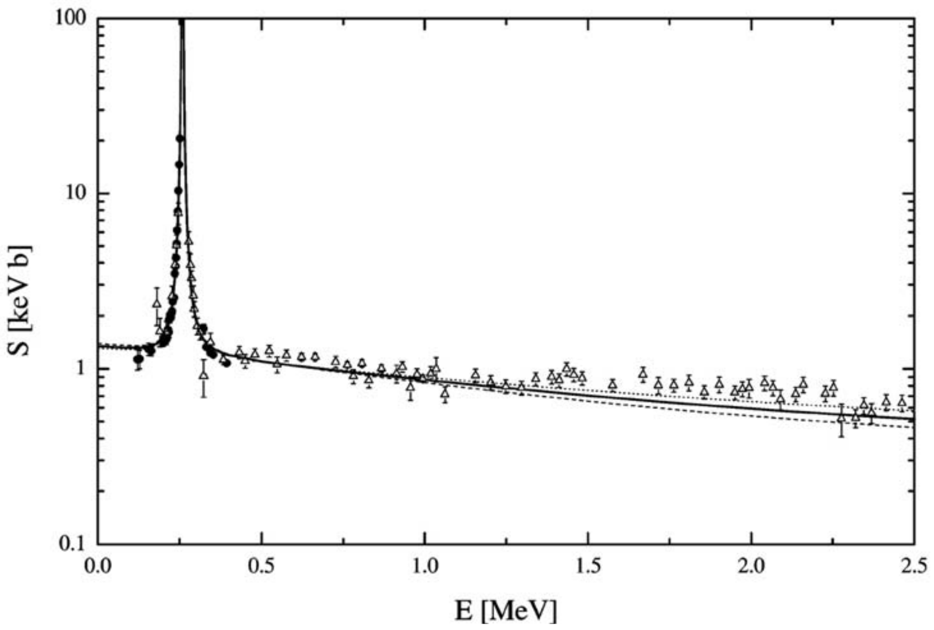

Fig. 3
Astrophysical factor for the p + ^{14}N reaction: The filled points refer to LUNA measurement with solid target and HPGe detector while the open triangles are previous measurements done in laboratories at the earth surface.

The LUNA collaboration is now measuring with the 400 kV machine another very important reaction of the p-p chain, namely the ^{3}He + ^{4}He. This reaction, as reported by J. Bahcall [10] "is the largest nuclear physics contributor to the uncertainties in the solar model predictions of the neutrino fluxes in the p-p chain". The uncertainty on its astrophysical factor reflects almost linearly in an uncertainty on the ^{8}B neutrino flux from the Sun. Previous measurements have been performed using two different techniques: the detection of prompt gamma or the measurement of ^{7}Be produced activity. The values obtained with the first method are systematically lower than those obtained with the latter giving an overall uncertainty of about 10%. The LUNA measurement will use both techniques at the same time and will try to diminish at the lowest possible value all systematical sources of errors giving an overall uncertainty of about 5%. The investigated energy region will be lower than the one of all previous measurements due to the possibility of measuring underground with very well shielded gamma detectors.

REFERENCES
10. J. Bahcall et al., astro-ph/0402114v1 (2004)

Nuclear structure at extreme conditions through γ spectroscopy measurements

S. Leoni [1,2], G. Benzoni [2], A. Bracco [1,2], N. Blasi [2], F. Camera [1,2], F. Crespi [1,2], B. Million [2], and O. Wieland [2]

1 Dipartimento di Fisica, Università degli Studi di Milano
2 INFN

The atomic nucleus is a unique laboratory for studying different fundamental physics phenomena. Being made of a finite number of strongly interacting fermions (protons and neutrons), it allows to study the interplay between single particle and collective degrees of freedom, under the influence of electromagnetic, weak and strong interactions. Most of our current understanding of nuclear structure results from the study of reactions between stable nuclei, which until now have allowed to produce ~ 3000 radioactive nuclides, at quite low values of excitation energy and angular momentum (spin). The availability of beams of unstable ions (see Wieland et al.) has recently opened up the possibility to explore the properties of the atomic nucleus far away from the stability line, gaining access to a much wider region of exotic, loosely bound nuclear systems, at the limit of the proton and neutron binding. The study of nuclei far away from stability and under extreme conditions of excitation energy and angular momentum is important not only for a full comprehension of the nuclear many-body system, but also for their astrophysical implications, not least the nucleosynthesis of the heavy elements in the stellar environment.

In this contribution we will present selected studies of the collective response of the atomic nucleus under extreme conditions of temperature and angular momentum [1], so far experimentally investigated through the γ-decay of excited nuclei formed by nuclear reactions between stable ions only. In particular, the temperature degree of freedom allows one to study the order-to-chaos transition and the persistence of collectivity and damping mechanisms, while the angular momentum induces changes in pairing correlations and in the nuclear shape. As schematically shown in figure 1, fast rotating nuclei can be formed at the highest values of angular momentum and excitation energies by fusion reactions between heavy ions, with typical beam energies of 5 MeV/nucleon. After rapid evaporation of light particles (mainly neutrons), the warm nucleus de-excites emitting long sequences of γ transitions, ending up in discrete regular rotational bands when the nuclear temperature T of the system is almost zero. Therefore, by detecting the largest number of γ-rays emitted by the excited nucleus, nuclear structure properties can be investigated as a function of angular momentum and excitation energy. This can be achieved by the use of high-efficiency Ge-array spectrometers (such as EUROBALL [2] or AGATA [3], see Crespi et al.) consisting of more than 100 Ge crystals in 4π geometry around the reaction center usually combined with other types of detectors.

A statistical analysis of the nuclear level distribution has shown, both experimentally and theoretically, that the atomic nucleus displays properties typical of an ordered system at T = 0, as shown by the corresponding Poisson level spacing distribution (see Fig. 1a) [4], and of a chaotic systems at the compound nucleus level, as shown by the Gaussian Orthogonal Ensemble (GOE) distribution of energy levels of p and n-resonance states (see Fig. 1c) [5]. Therefore, the γ-decay of the nucleus at high spins and moderate excitation energy (represented by the yellow area labelled WARM in Fig. 1) offers a unique possibility to study the transition between order and chaos in a finite quantum system.

The WARM region above ≈ 1 MeV internal excitation energy is where the nuclear rotation becomes damped and the rotational decay is fragmented over a large number of states with an energy spread Γ_{rot} ≈ 200 keV, as a consequence of the rapidly increasing level density and of the presence of a residual two-body interaction mixing the nuclear states (see Fig. 1b) [1]. A powerful experimental way to study the warm rotational decay consists in constructing γ-γ spectra from the measured energies of high-fold γ cascades, such as the one shown in Fig. 2a In fact, from the spectrum landscape one can distinguish between the contribution from the COLD region of regular decay ("ridges") and the one from the WARM region of damped rotation ("valley"), as a consequence of the constant spacing between consecutive transitions emitted by a perfect-rotor [1,6]. As shown in Fig. 2b, the analysis of the valley region corresponding to different nuclear configurations, namely characterized by different values of the K-quantum number (being K the projection of the angular momentum on

REFERENCES
1. A. Bracco and S. Leoni, Rep. Prog. Phys. 65(2002)299 and references therein.
2. J. Simpson Z. Phys. A358 (1997)139.
3. AGATA: Technical Proposal for and Advance Gamma Tracking Array for the European Gamma Spectroscopy Community, edited by J. Gerl and W. Korten, September 2001, see also http://www-w2k.gsi.de/agata/Agata_pub-proposal.pdf
4. J.D. Garrett et al, Phys. Lett. B392 (1997)24.
5. R.U. Haq, A. Pandy and O. Bohigas, Phys. Rev. Lett. 48 (1982)1086.
6. T. Døssing et al., Phys. Rep. 268(1996)1.

the symmetry axis, as sketched in Fig. 2b) has revealed a marked difference in the number of states populated in the warm rotation up to $E_\gamma \approx 1.1$ MeV, corresponding to spin $I \approx 40\hbar$ and internal excitation energy $U \approx 1.2$ MeV, while a convergence is observed at higher energies. This points to a vanishing of selection rules on K and to the onset of a chaotic regime, in which quantum numbers and selection rules loose their meaning [7,8].

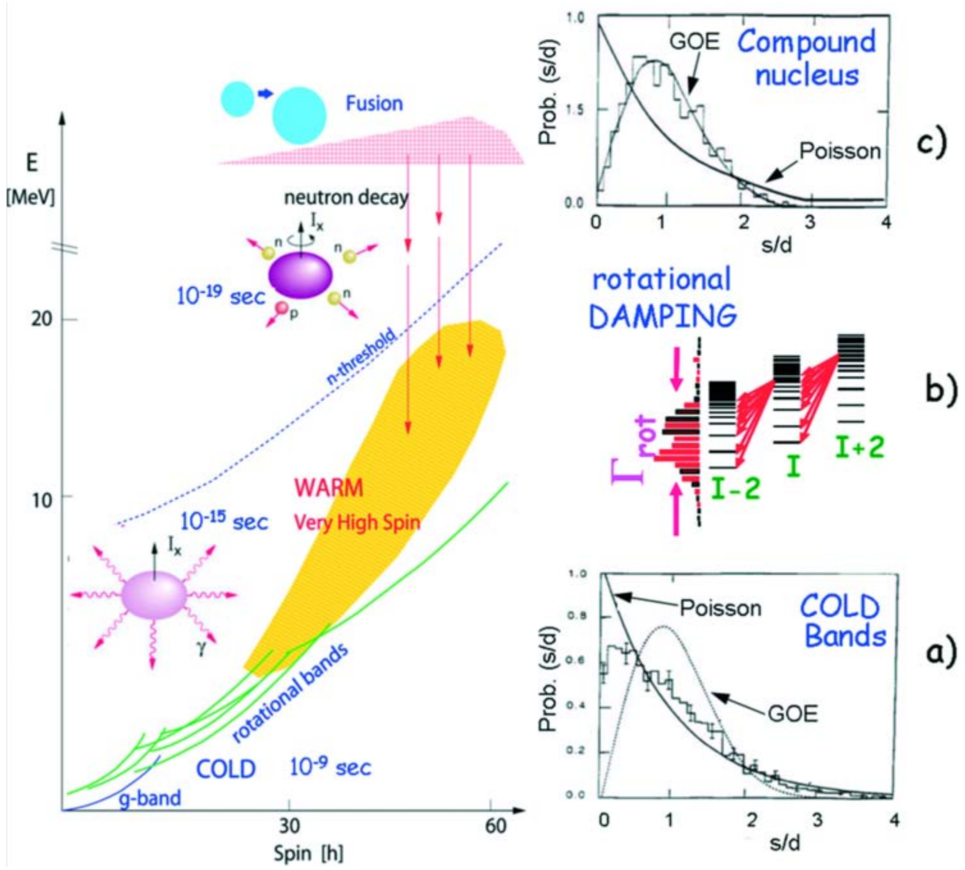

Fig. 1
Left panel: schematic representation in the excitation energy versus spin plane of the formation and decay of a compound nucleus by heavy ion fusion reaction: after light particles emission the major part of the decay proceeds through γ-ray cascades which rapidly cool the nucleus from the WARM region at the highest spins and excitation energies down to the COLD region of regular rotational bands. The energy and spin values refer to a typical nucleus of mass A = 160. The time scale of the various steps in the process is also given. The right column shows the experimental level spacing distributions of energy levels, for COLD states (panel a)) and compound nucleus states (panel c)), revealing the typical properties of an ordered and chaotic system, respectively. On the x-axis s/d is the ratio between the level spacing s and the average spacing d among levels. Panel b) shows the highly fragmented rotational decay, characteristic of the damped rotation in the WARM region.

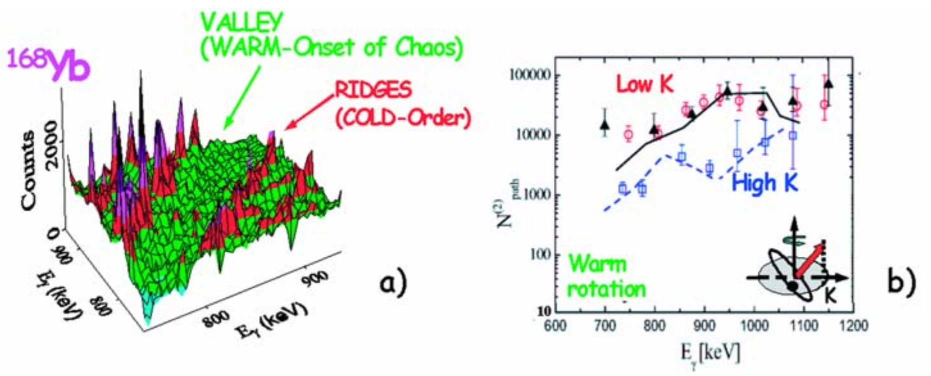

Fig. 2
Left panel: region of a γ-γ spectrum showing the different contributions from the COLD regular decay at zero temperature (ridges) and from the WARM region of rotational damping (valley), where the transition between order and chaos is expected to take place. Right panel: number of strongly interacting bands (indicated by $N^{(2)}_{path}$), obtained from the analysis of the valley region of γ-γ spectra corresponding to different values of the K-quantum number (shown in the inset), pointing to an onset of chaos at internal excitation energies higher them 1.2 MeV (corresponding to $E_\gamma \approx 1.1$ MeV) .

The study of the properties of the COLD atomic nucleus as a function of angular momentum also offers unique opportunities to learn about the interplay between collective and single particle degrees of freedom, particularly in connection with the phase transition between a superfluid and a normal system [9]. In the atomic nucleus, pairs of protons and neutrons tend to bind together with angular momentum zero, forming Cooper pairs similarly to electrons in a superconducting metal. This is revealed by a number of properties of the nuclear system, not least the fact that in nuclei with stable deformation (such as the rare earth nuclei with A ≈ 160) the moment of inertia at low rotational frequencies is intermediate between the limiting values corresponding to rigid rotation and the ones corresponding to the hydrodynamical picture of irrotational flow, as illustrated in Fig. 3a [10]. This is because the superfluid state is the natural state for nuclei in their ground-state configurations. In fact, as illustrated in the inset of Fig. 3a, the spherical superfluid core of the nucleus does not rotate, resulting in a large reduction of the moment of inertia. The easiest way to induce in a nucleus a phase transition from superfluid to normal is to spin the nucleus to high rotational frequencies. The Coriolis force acts in fact in opposite ways on states in time

reversal orbits, as shown in the inset of Fig. 3b, with a strength proportional to the rotational frequency ω_{rot}. For values of the Coriolis force of the order of the pairing strength, the Cooper pairs will be broken, and the atomic nucleus will cease to be in a superfluid phase. This results in a discontinuity in the smooth increase of the moment of inertia $\Im$ with rotational frequency, known as *backbending.* As an example, in the case of the nucleus ^{158}Er, shown in figure 3.b, the first abrupt change in the moment of inertia, occurring at spin I = $14\hbar$ ($\hbar\omega_{rot} \approx 0.25$ MeV), corresponds to the break of a pair of neutrons in $i_{13/2}$ orbitals, which suddenly decouple from the superfluid core and start participating to the nuclear rotation contributing 10 units of angular momentum, thus inducing a sudden increase in the nuclear moment of inertia. At frequencies of the order of $\hbar\omega_{rot} \approx 0.4$ MeV (corresponding to spin $I = 28\hbar$) a pair of protons in $h_{11/2}$ orbitals break, producing a further sudden increase in $\Im$ [11].

Pairing correlations also play a central role in the understanding of exotic phenomena, such as the sudden disappearance of intensity of rotational bands associated to the rotation of nuclei with largely elongated rugby-ball shapes (with a 2:1 ratio between the major and the minor radius), usually named superdeformed (SD) [9]. As shown in the inset of Fig. 4a, superdeformed nuclei manifest themselves with amazing long sequences of γ transitions with almost constant spacing, implying a constant moment of inertia consistent with a rigid body rotation. The observation of such weakly populated structures (at the level of ≈ 1% intensity) is confined at rather high spins, where changes of the nuclear shells favour the existence of nuclei in such elongated shapes. The study of superdeformation has therefore became a key issue in recent nuclear physics research, not only because the existence of largely deformed nuclei in different regions of mass is a test bench for modern shell model calculations, but also because their population and decay require a deep understanding of the evolution of the collective response of the atomic nucleus with both angular momentum and temperature [12,13].

Figure 3:
Panel a): at low rotational frequencies nuclei with stable deformation show moment of inertia with values intermediate between a rigid rotor and an irrotational fluid, as a consequence of the strong pairing correlations giving rise to a superfluid system in the ground state (Adapted from ref. [10]). Panel b): by setting the nucleus into rotation the Coriolis force can break the Copper pairs inducing a transition from a superfluid to a normal system (Adapted from ref. [11]).

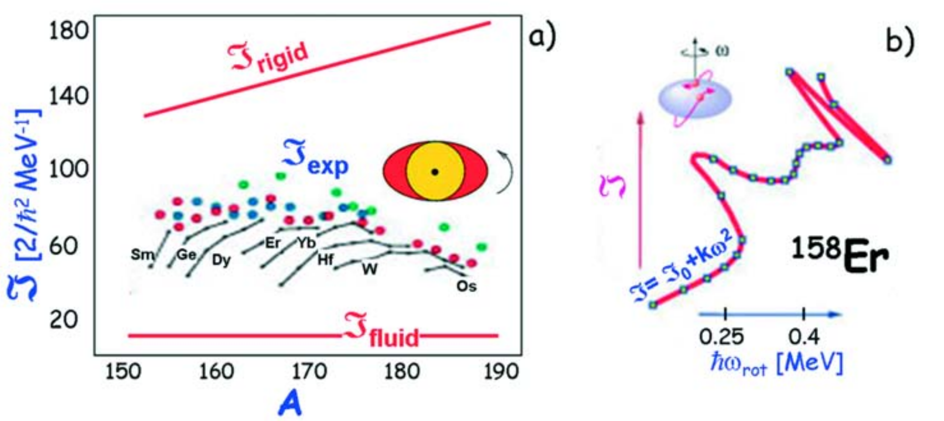

REFERENCES
7. G. Benzoni et al. Phys. Lett. B615(2005)10.
8. S. Leoni et al., Phys. Rev. C72(2005)034307.
9. A. Bracco et al., Cont. Phys. 37(1996)183 and references therein.
10. A. Bohr and B. Mottelson, Nuclear Structure, Volume II, World Scientific (1998).
11. J. Burde et al, Phys. Rev. Lett. 48(1982)530.
12. S. Leoni et al., Phys. Lett. B498(2001)137.
13. G. Benzoni et al., Phys. Lett. B540(2002)199.
14. D.M. Brink and R.A. Broglia, Nuclear Superfluidity: Pairing in Finite Systems, Cambridge University Press.

As an example, in the case of ^{152}Dy, shown in figure 4a, after the SD band has been populated at the highest spins (above 60 $\hbar$), the nucleus remains in it through a sequence of 19 γ transitions and suddenly, at spin 24 $\hbar$, it terminates abruptly, decaying into a large number of states of much lower deformation. Such an observation has been interpreted as a tunnelling through a potential barrier separating the superdeformed and the normal deformed minima, as depicted in Fig. 4b, resulting in a phase transition between a normal and a superfluid phase in the nucleus (namely the superdeformed configuration and the one with low deformation). In fact, a superfluid system will find it much easier to tunnel through a barrier than a normal fluid, implying that the sudden depopulation of the SD band is associated with a condensation into the superfluid states at low angular momenta [9]. Such a mechanisms has also been found to apply to excited superdeformed bands. This is shown in Fig. 4c, where the number of excited SD bands in the nucleus ^{143}Eu is found to gradually decrease with spin, as a consequence of their decay-out into the low deformation minimum [12]. Therefore, the study of the evolution of pairing correlations with angular momentum and temperature in the atomic nucleus is one of the central topics in modern nuclear structure studies, being also connected to similar phenomena in other physics research fields [14].

In conclusion, the study of nuclear structure properties of excited nuclei at extreme conditions of temperature and angular momentum makes it possible to investigate the interplay between single particle and collective degrees of freedom in a many-body finite system. Such studies, carried out so far in nuclei close to the stability line, become particularly important in weekly bound systems far away from stability, not least for their astrophysical implications. Therefore, one of the main tasks of the present research projects is to produce in laboratory nuclei that are only present in stellar environment, and to study their properties at extreme conditions.

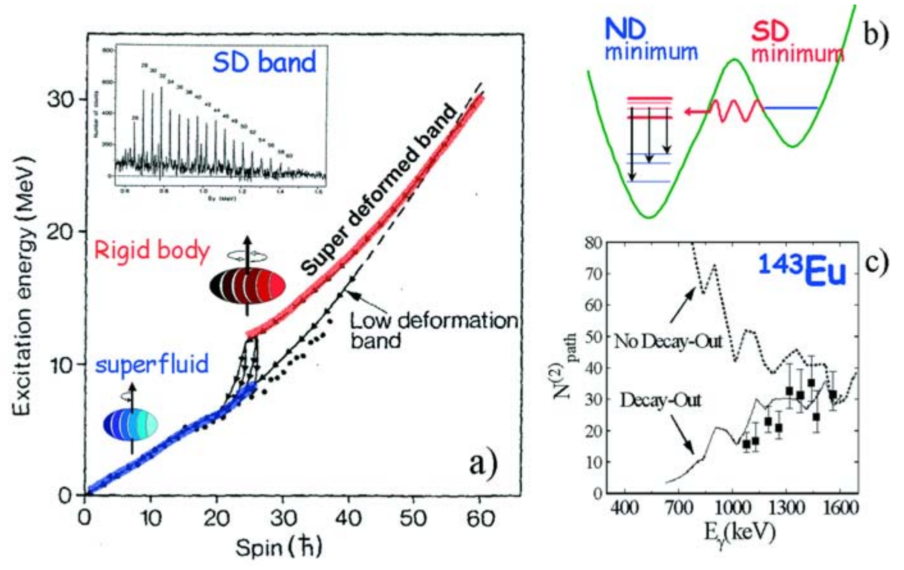

Fig. 4
Panel a): Schematic illustration in the excitation energy versus spin plane of the depopulation of a superdeformed band into lower deformation states. The inset shows the long sequence of equally spaced γ transitions of the SD band of ^{152}Dy. The decay-out process has been interpreted as a tunnelling through a potential barrier separating the SD and the ND (low deformation) minima, as shown in panel b). This mechanism is also responsible for the gradual decrease in the number of excited SD bands as a function of γ-energy (spin), as shown in panel c) in the case of the superdeformed nucleus ^{143}Eu.

Study of exotic nuclei with radioactive beams

O. Wieland[2], G. Benzoni[2], N. Blasi[2], A. Bracco[1,2], S. Brambilla[2], F. Camera[1,2], F. Crespi[1,2], S. Leoni[1,2], B. Million[2], and M. Pignanelli[1,2]

1 Dipartimento di Fisica, Università degli Studi di Milano
2 INFN

The nucleus is a finite many body system of strongly interacting particles described by quantum mechanics. It consists of an ensemble of protons and neutrons and its structure combines macroscopic features like collective vibrations or rotations and microscopic properties associated to the motion of very few nucleons in a potential well (see also A. Bracco et al. and S. Leoni et al.).

The nuclear chart of isotopes, shown in Fig. 1, organizes all nuclei as a function of number of proton (Z) and neutron (N), the vertical and horizontal axis respectively. Theoretical predictions indicate that there could be up to 10000 nuclei, however, only 280 of them are stable and lie in the so called “valley of stability”, while 68 are naturally radioactive. Using stable ion accelerators it has been possible so far to access to not more than 3000 nuclei, the yellow region in figure 1. The rest of the nuclides are still completely unknown and lie in a territory represented in green in the figure. In fact, in any nuclear reaction performed with a stable beam accelerator facility, both the beam and the target species must be in the ensemble of the 280 stable + 68 naturally radioactive nuclei, thus limiting the number of nuclei possibly created. Nuclei away from the valley of stability are commonly referred to as “exotic” or “radioactive” nuclei.

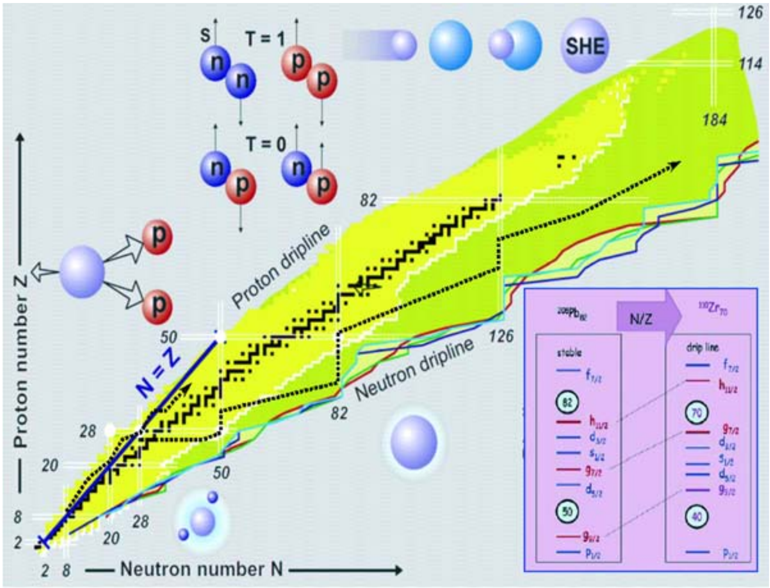

Fig. 1
The nuclear landscape. Stable nuclei, as found on earth, are marked by black squares, while the yellow area covers unstable (radioactive) nuclei already produced in the laboratory. Many more unstable nuclei are predicted to exist (green area), up to the limits for binding of protons or neutrons (the so-called proton or neutron driplines). The different neutron driplines shown in the figure illustrate the uncertainty of theoretical predictions. Also shown are: the magic proton and neutron numbers (2,8,20…), the observed unstable doubly magic nuclei (full white dots), the N = Z line, where proton and neutron numbers of a nucleus are equal, and the superheavy elements (SHE) synthesized so far. A major goal of future rare isotope beam facilities is the exploration of the limits of nuclear stability when approaching either of the borderlines. Some examples of specific questions are illustrated in the figure: two-proton decay; isospin T = 1 and T = 0 pairing, production of superheavy elements, formation of neutron skins and halos, disappearance of shell gaps (50, 82, 126) or modification of shell structure with increasing neutron number [2].

The importance of studying exotic nuclei, which constitute the majority of the unknown isotopes, lies in the fact that for these systems particular aspects of the nuclear interaction and dynamics are expected to be amplified, therefore favouring the occurrence of new symmetries and phenomena [1]. In particular, the structure and dynamics of loosely bound nuclei is very different from that of stable nuclei, giving rise to rather diffuse surface zones (the so-called halos and skins, observed so far mainly in light neutron-rich unstable isotopes), novel types of shell structures, new collective modes, new kind of pairing phases (due to the proton-neutron interaction) and possibly new decay modes (double proton emission), as schematically illustrated in Fig. 1. In addition, since the majority of the nuclei have not yet been studied, one of the fundamental open questions is the location of the “drip lines” which define the limits of the nuclear stability. They mark, in fact, the region outside which the nuclear binding forces are no longer strong enough to hold the nuclei together, leading to prompt decays by emission of protons and neutrons. This is particular important for its astrophysical implications, not least the nucleosynthesis of the heavy elements in the stellar environment which follows the r-process line, as indicated in Fig. 1.

The most straightforward way to study exotic nuclei is to overcome the limitation that both beam and target must be stable. Therefore, accelerator facilities which are able to produce and accelerate not only stable beams, but also radioactive beams are currently under development in

REFERENCES
1. GSI physics case, see also http://www.gsi.de/
2. NUPECC Long Range Plan 2004: Perspectives for Nuclear Physics Research in Europe in the coming Decade and Beyond, see also http://www.nupecc.org/pub/

Europe, North America and Japan. Such facilities, called “Radioactive Ion Beam” (RIB) facilities will offer unique research opportunities in nuclear physics and nuclear astrophysics [2].

Two basic techniques to produce radioactive beams are mainly used: the ISOL (Isotope Separation On Line) method and the “in-flight” method [3]. The basic steps of the two different processes that lead to the production and acceleration of radioactive nuclei are sketched in figure 2. The two techniques are complementary in terms of production methods and lifetime ranges.

The ISOL method, which was developed first, uses either ions beams from a primary accelerator or neutrons from a nuclear reactor [3]. The primary beam is impinging on a very thick target or catcher arrangement which stops the recoils and reaction products. The produced activity is transported from there into an ion-source via physical and chemical diffusion, by jet transport or similar techniques. Chemical selectivity in the transfer process to the ion-source can be obtained by a suitable choice of the target material, of its operating temperature and of the “connection” to the source. A broad variety of ion sources and production techniques is available today, offering additional selectivity. After the extraction, the radioactive nuclei can be used for experiments at low energy or can be re-accelerated by a secondary accelerator system. Due to the nature of the extraction processes this method is suitable to produce radioactive species with a relative long half life (of the order of 100 ms of longer) and the corresponding accelerated beams have good optical qualities.

Several European laboratories currently use the ISOL technique to produce radioactive beams: among them there are GANIL in France, the REX-ISOLDE facility at CERN and EXCYT at the South Italian National Laboratory (LNS) of the Italian Institute of Nuclear Physics (INFN). Two new generation facilities based on the ISOL technique are presently under development, namely SPIRAL2 at GANIL and SPES at the Legnaro National Laboratories (LNL) of INFN [4,5]. SPES will produce neutron rich isotopes in the mass region A ~ 80-160, via the fission process induced by neutrons in a thick uranium target. In the post accelerating process the radioactive beams extracted from the target-source system will achieve a maximum final energy of 20 MeV/u.

The second technique, the so called “in-flight” method [3], is well suited for the production of secondary beams of energy typically around a few hundreds of MeV/u. The “in-flight” method uses fragmentation of intense energetic heavy-ion beams on a thin light target (few gr/cm^2). The fragmentation process creates simultaneously a large number of different nuclear species ranging from the beam down to the lightest nuclei, the so-called “cocktail beam”. The reaction’s products are forward focused and usually identified and separated in a 0-degree spectrometer. The properties of these nuclei, such as their masses and lifetimes, can then be studied or they can be used to make secondary reactions. These beams are independent of chemistry and allow the study of short living isotopes (<1µs). As a drawback they do not have good optical qualities, and need carefully designed mass separators with high acceptance. The intensity of such beams varies a lot and depends strongly on the nature of the produced nucle-

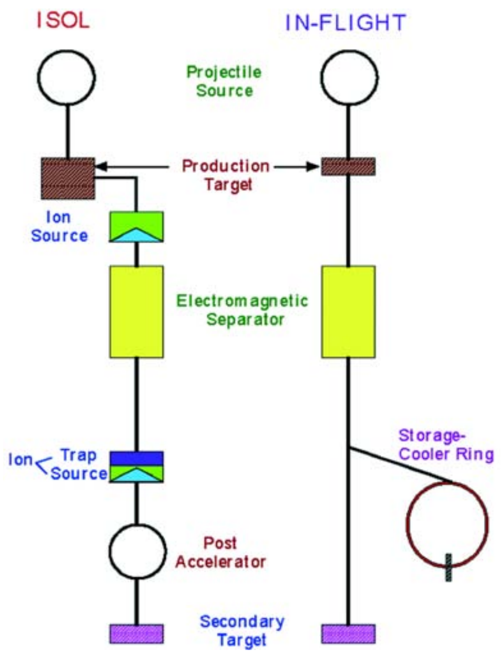

Fig. 2
Schematic illustration of the ISOL (left) and in-flight (right) methods. Future planned ISOL and fragmentation facilities will also make use of storage rings and/or high intensity linear accelerators to expand the types of research and application that can be done with the rare isotopes.

REFERENCES
3. Radioactive Nuclear Beam Facilities, NUPECC 2000, see also http://www.nupecc.org/pub/
4. The SPIRAL2 project APD Report, January 2005, see also http://www.ganil.fr/research/developments/spiral2/
5. SPES: Technical Design for an Advanced Exotic Ion Beam Facility at LNL, editord A. Bracco and A. Pisent, June 2002, see also http://www.lnl.infn.it/~spes/

us. At variance from the ISOL method many more nuclear species are accessible by the in-flight technique. One advanced facility based on this technique is currently in operation at the GSI laboratory in Germany.

The intensities of the first generation Radioactive Beam Facilities are typically 4 to 5 orders of magnitude smaller than the ones commonly achieved with stable beams (≈ 10^{10} particles per second). In addition, the radioactive nature and the production process of the secondary beams generate a background that cannot in many cases be disentangled from the real signals. New and more powerful detection devices are therefore under development, in order to maximize the efficiency and to suppress as much as possible the background radiation. As an example, the European project AGATA is a 4π Ge array for γ-detection studies, which will substitute the traditional Compton suppressed germanium spectrometers [6]. It will be constituted by 180 high purity segmented germanium detectors and will be based on γ-ray tracking techniques, as discussed in F. Crespi et al.

One of the first experimental setup for γ spectroscopy with radioactive beams is the “Rare Isotope Investigation” (RISING) setup placed at the GSI laboratory in Germany [7]. This setup consists of an in-beam spectroscopy detector system for relativistic exotic beams, and it is located at the “Fragment Separator” (FRS), a large angle acceptance magnetic separator for fragments [8]. The RISING spectrometer, shown in Fig. 3, is a combination of different γ-ray and particle-tracking detectors. The exotic beam, produced by fragmentation in a primary target, is selected and transported by the FRS system. In the focal plane of the spectrometer a secondary target is placed allowing to perform Coulomb excitations or secondary fragmentation. After the secondary reaction, the final products are stopped and identified using a ΔE-E telescope.

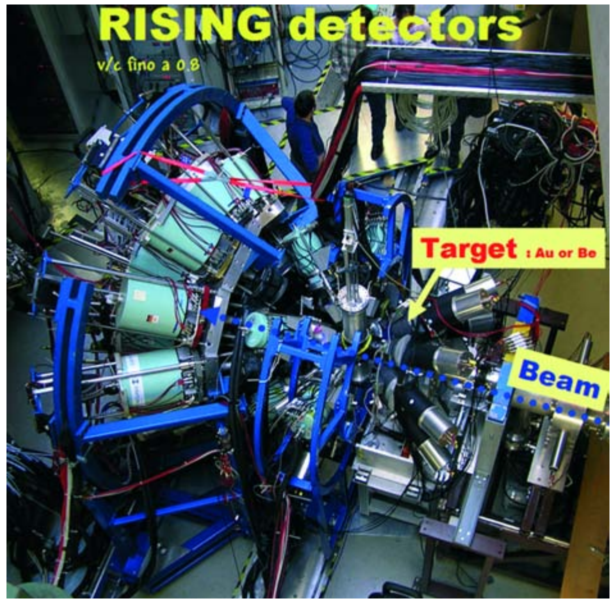

Fig. 3
Picture of the Rising γ-detection system. The exotic beam coming from the right hand side is produced by fragmentation on a primary target and is then transported by the FRS magnetic system before impinging on the secondary reaction target.
The outgoing products after the target are tracked and identified inside calorimetric and position sensitive detectors. The emitted γ-rays are measured with Ge and BaF_2 detectors placed at different angles (see text).

Due to the relativistic Lorentz boost of the excited fragments moving at a high velocity (typically $v/c > 0.4$ for fragment energies $E > 100$ MeV/u), the γ-rays emitted after the secondary reaction are mainly forward focused. Therefore the γ-detection array has been placed at forward angles as close as possible to the beam line, in order to increase the detection efficiency. In particular, 15 high purity Ge detectors of composite type (clusters) are mounted at forward angles, while at 90 degree around the target area 8 segmented Ge are positioned. In the backward direction 8 large volume BaF_2 scintillators have been placed for high energy γ-ray detection and fast timing measurements. The typical full energy peak efficiency achieved with such a set up is ≈ 3% for 1.3 MeV γ-rays emitted in flight ($v/c > 0.4$).

The array is employed for high-resolution γ-spectroscopy experiments on exotic nuclei. Several nuclear structure research topics are addressed, as (i) changes in the shell structure and appearance of new shapes, (ii) isospin symmetry in mirror nuclei and (iii) evolution of the collective response of the nucleus as a function of N/Z (as for example the strength distribution of the giant dipole resonance (GDR)).

One of the recent results obtained in an experiment with the RISING array is the evidence for a change in the shell structure of very neutron-rich nuclei along the N = 20 and 28 isoton-

REFERENCES
6. AGATA: Technical Proposal for and Advance Gamma Tracking Array for the European Gamma Spectroscopy Community, edited by J. Gerl and W. Korten, September 2001, see also http://www-w2k.gsi.de/agata/Agata_pub-proposal.pdf
7. H.J. Wollersheim et al. Nuc. Inst. Met. A537, Issue 3, (2005) 637
8. H. Geissel et al., Nucl. Instrum. Meth. B70 (1992) 286

ic sequence (Fig. 4). Modifications of the shell structure have far reaching consequences for nuclear properties and also for the understanding off rapid neutron capture process (r-process) of stellar nucleosynthesis and the resulting isotopic abundance of the elements in the universe.

In the experiment the first excited 2^+ states in ^{54,56,58}Cr were populated by Coulomb excitation at relativistic energies. As shown in figure 4, the Cr isotopes have first been identified among the different fragments and their γ-decay have been measured in the RISING Ge detectors. The obtained results are consistent with a newly discovered subshell closure at neutron number $N = 32$ [9].

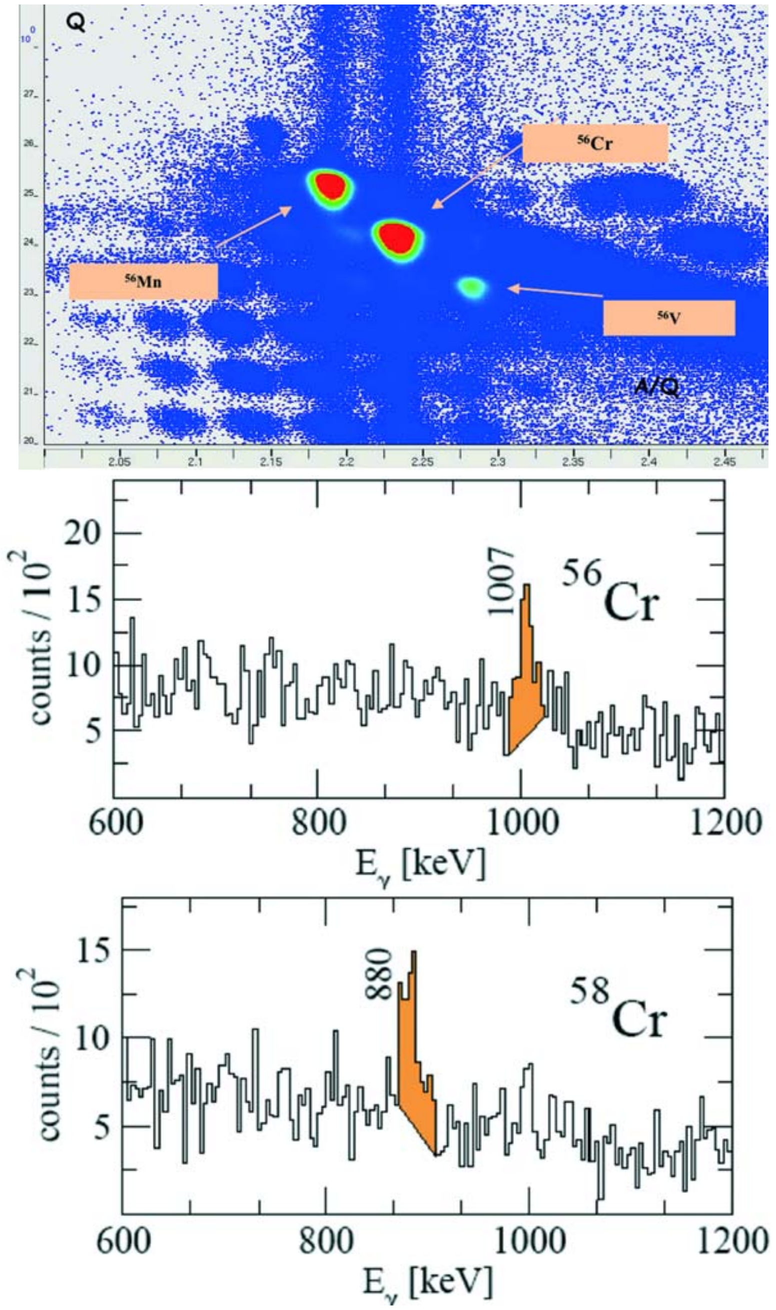

Fig. 4
The top panel shows the measured distribution of fragments with different charge and mass/charge ratio. In this way one can identifify and select specific isotopes and their respective γ-ray spectra. The bottom panels show examples of Doppler- and efficiency-corrected γ-ray spectra of ^{56}Cr and ^{58}Cr, in which the $2_1^+ \rightarrow 0^+$ transition is highlighted. It is found that the intensities of these peaks are consistent with a sub shell closure in the exotic system with $N = 32$ [9].

We can conclude pointing out that the next generation of exotic radioactive beam facilities together with the new detection systems, such as γ detectors arrays like AGATA, will give a more deep insight into the problem of nuclear structure far from stability, which is a fundamental question in nuclear physics. In particular, the study of the properties of exotic nuclei will allow to learn much more about the origin of the elements in the cosmos and the limits of nuclear stability. Theoretical predictions on such limits are extremely challenging since they require accurate solutions of the many-body quantum problem for strongly interacting particles. Finally, it is worth noticing that the intensive technological research and development in the field of production and measurement of exotic nuclei, especially in connection with γ detection techniques, have given rise to new important applications in medicine, human science, industry and applied research.

REFERENCES
9. A. Buerger et al. Phys. Lett. B 622 (2005) 29

Contribution to nuclear binding energies arising from surface and pairing vibrations

S. Baroni[1,2], F. Barranco[3], P.F. Bortignon[1,2], R.A. Broglia[1,2,4]
G. Colò[1,2], and E. Vigezzi[2]

1 Dipartimento di Fisica, Università degli Studi di Milano
2 INFN
3 Departamento de Fisica Aplicada III, Escuela Superior de Ingenieros, c Camino de los Descubrimientos s/n, 41029 Sevilla, Spain.
4 The Niels Bohr Institute, University of Copenhagen, Blegdamsvej 17, 2100 Copenhagen, Denmark.

During the last years, much effort has been made to develop a microscopic description of the nuclear masses based on mean field theory [1]. The accuracy achieved, when phenomenological parameters are added to take specific effects into account (Wigner term, cutoff in pairing space, etc.) leads to a rms of 0.6-0.7 MeV [2]. Important steps to provide a solid basis to this development, steps which follow the LDA philosophy of developing an accurate exchange-correlation term, have been also carried out during the last years (see e.g. [3]).

The agreement between theory and experiment is achieved in refs. [1,2] by means of effective interactions whose parameters are fitted to force mean field predictions to reproduce experimental masses. However, mean field theory does not include the contribution of the collective modes to the nuclear binding energy, which cannot be ignored in a consistent treatment. It is as if one wanted to cover a large table with a short and quite elastic tablecloth: one would probably manage to cover the table, but the result will appear quite unnatural with respect to the coverage obtained with a larger tablecloth, which fits better the board and doesn't need to be stretched so much. In the same way it seems quite unnatural to force mean field theory to account for experimental binding energies all over the table of nuclei, because this approximation lacks important ingredients able to describe collective modes of the nucleus.

The aim of the present contribution follows these lines, providing detailed results to assess the importance correlation effects have on nuclear ground state energies (see also [4]). For this purpose, we perform a mean field calculation for the ground state of 121 stable spherical even-even nuclei and evaluate the zero point fluctuation energies arising from two well-known nuclear collective modes: surface and pairing vibrations [5,6].

The main goal is to expand the theoretical framework beyond mean field and only in a second step to fit the force parameters to better reproduce experimental masses. We compute the correlation energies in the (Q)RPA approximation, built on top of a HF + BCS treatment of the nuclear system, making use of a Skyrme-type interaction supplemented by a contact pairing force. Concerning surface vibrations, the most collective quadrupole and octupole (Q)RPA phonons up to 10 and 7 MeV respectively have been taken into account, while, for pairing addition and removal modes, contributions of the lowest monopole pairing vibration phonon have been considered for neutron and/or proton closed shell nuclei [7].

Although the absolute value of these corrections represents a small fraction (from 0.3% to 1.5%) of the total binding energies, their contribution is large enough so as to modify conspicuously the mass dependence of specific isotopic chains improving the overall agreement between theory and experiment by a small but finite amount (reduction of the rms by about 8%).

REFERENCES
1. F. Tondeur et al., Phys. Rev. 62, 024308 (2000).
2. S. Goriely et al., At. Data Nucl. Data Tables 77, 311 (2001).
3. S.A. Fayans et al., Nucl. Phys. A676, 49 (2000).
4. M. Bender et al., Phys. Rev. Lett. 94, 102503 (2005).
5. R.A. Broglia et al., Adv. Nucl. Phys. 6, 287 (1973).
6. D.M. Brink and R.A. Broglia, *Nuclear Superfluidity: pairing in finite systems*, Cambridge University Press, Cambridge (2005).
7. S. Baroni et al., J.Phys.G:Nucl.Part.Phys. 30, 1353 (2004).

Design and characterization of nanostructured solids assembled from metallic clusters

1 Dipartimento di Fisica, Università degli Studi di Milano
2 INFN
3 INFM
4 The Niels Bohr Institute, University of Copenhagen, Denmark

M. Bonomi[1,2,3], D. Provasi[1,2], R.A. Broglia[1,2,4], and G. Onida[1,3]

This research is aimed to the study of nanostructurated solids assembled from metallic cluster of non-alkaline elements, starting from the impossibility of building stable periodic solids using clusters of alkaline elements in which the binding electron lies in a spherical-symmetrical orbital.

In fact, previous works have brought to light that the only stable solid which can be built using a cluster of eight atoms of sodium is the common (bulk) metallic sodium and that this result depends essentially on the elevated symmetry of the cluster's orbitals. Therefore, in order to produce metallic nanostructurated crystals, is necessary to take into consideration clusters whose electronic structure has directional orbitals. Gold clusters of 8 and 20 atoms are, for the large stability coming from the elevated homo-lumo gap (larger than C_{60}), the two ideal candidates.

Using *ab-initio* tecniques, we have studied periodic solids assembled using a cluster of eight atoms as building-block, exploring face-centered, body centered and simple cubic cells: for all these symmetries we have discovered an equilibrium structure. Here we focus on the simple cubic solid, for which we obtained the electronic structure, vibrational properties, stability studies and electron-phonon coupling.

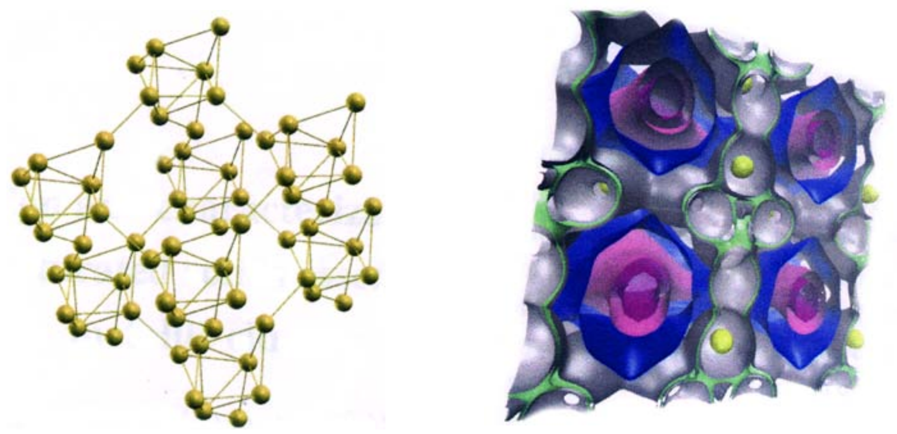

Fig. 1
Ionic structure of the stable simple cubic super lattice (left). Valence electronic density isosurfaces (right).

The crystal assembled with Au_8 cluster is a metal: the density of state at Fermi energy is 2.4 states/(eV spin). The binding energy per atom for this structure is b_{SC} = 3.46 eV/atom, slightly less than the bulk gold one (recall that b_{bulk} = 3.81 eV/atom), while the density of this crystal is d_{SC} = 8.23 g/cm³, much smaller of the bulk one (d_{bulk} = 19.28 g/cm³). Also phonon dispersion has been calculated in density-functional perturbation theory; we have found very flat bands, which suggests a weak interaction between different clusters in the crystal. In this case, we can estimate the value for the electron-phonon coupling λ from a calculation made only at Γ point. This estimation gives $\lambda_{SC} = 0.5 \pm 0.1$ (again, compare to bulk $\lambda_{SC} \approx 0.15$).

In conclusion, we have found a new nanometer material assembled from Au_8 clusters in a simple cubic symmetry, stable and with different properties with respect to the common bulk gold.

Quantum methods in protein science

1 Dipartimento di Fisica, Università degli Studi di Milano
2 INFN
3 Niels Bohr Institute, Copenhagen, Denmark

C. Camilloni[1,2], P. Cerri[1,2], D. Provasi[1,2], G. Tiana[1,2], and R.A. Broglia[1,2,3]

The study of phenomena taking place in proteins which can only be described by quantum mechanics is particularly complicated, due to the large size of the system and the lack of symmetries. In these cases, a possible approach is to describe quantum-mechanically only a part of the whole protein, accounting for the rest of it in an approximated way.

One example is the calculation of the binding free energy of small ligands to the Carbonic Anhydrase (HCAII) [1], a protein involved in the glaucoma disorder. Due to the presence of a zinc atom, standard methods based on classical empirical potentials fail to predict correctly the binding free energy. The use of density functional theory, together with a novel conformational sampling algorithm, allows for a description of the interaction consistent with the experimental data. Metadynamics [2] approach to quantum molecular dynamics allows the exploration of the free energy surface as a function of a selected set of collective variables (CV). A fictitious time-dependent potential acting on the CVs is added to the Lagrangian in order to escape free energy minima. In an ideal (infinite time) metadynamics simulation, after filling free energy wells, collective variables evolve in time with brownian motion. Keeping track of the hills allows the reconstruction of the free energy surface. Results for HCAII with trifluoromethane-sulfonamide: ΔF_0 ~ 21.1 kcal/mol $T\Delta S$ ~ 15.5 kcal/mol, *at room temperature (300K)* ΔF ~ 5.5 kcal/mol. Experimental values of ΔF are on the order of 5 kcal/mol [1].

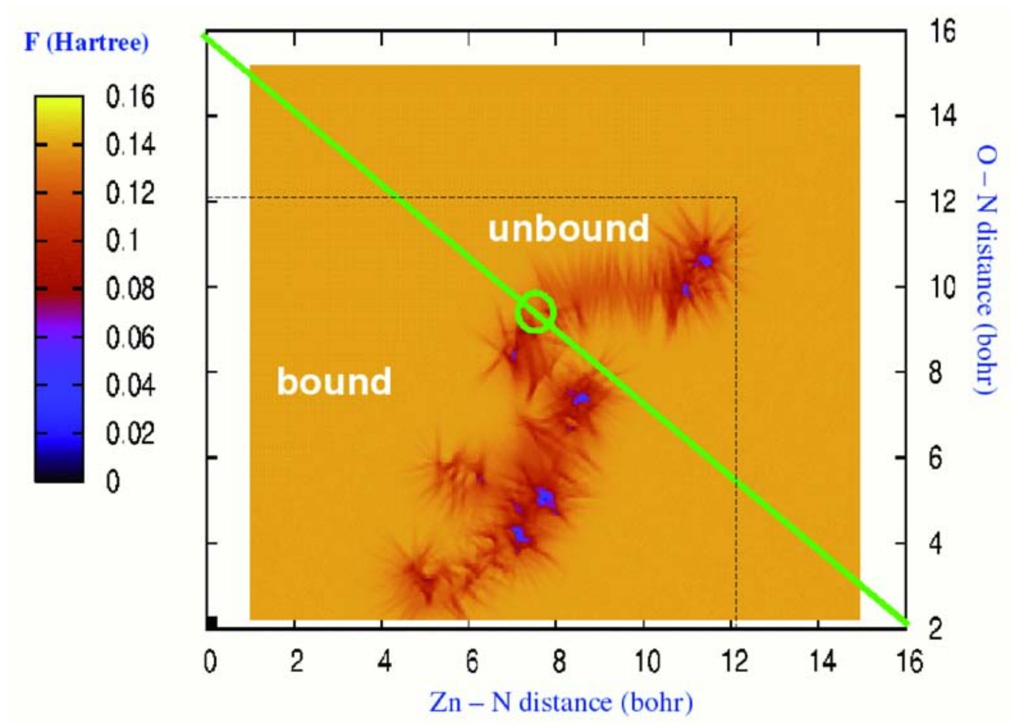

Fig. 1
The free energy of carbonic ANYDRASE

Another example of this procedure is the description of the fluorescence properties of the Green Fluorescent Protein [3], a protein widely used in biology to detect the expression of genes. Time dependent density functional calculations highlight the mechanism which allows to switch on and off the fluorescence by means of beams of different wavelengths. The protein can be in a fluorescent (BRIGHT) and non fluorescent (DARK) conformations, which can be switched by appropriate wavelength. The dark state corresponds to an absorption peak at 3.5 eV [4]. To compute absorption we use the Time Dependent Density Functional Theory. Studying the chromophore alone we have observed the absorption peak at 3.5 eV and identified the dark state of the protein with the trans conformation of the chromophore.

We have then improved the degree of approximation, considering: Fig. 1 the amino acids close to the chromophore, in particular the hydrogens bond network, Fig. 2 the chromophore

REFERENCES
1. A.V. Ishchenko, and E. Shakhnovich, *J. Med. Chem.*, 45:2770
2. A. Laio and M. Parrinello, *PNAS*, 99:12562
3. R.Y. Tsien, *Annu. Rev. Biochem.* 67, 509
4. R. Nifosi, A. Ferrari, C. Arcangeli, V. Tozzini, V. Pellegrini, F. Beltram, *J. Phys. Chem.* B, 107, 1679

and the Coulombian field of the whole protein, showing that the two effects are complementary on the absorption spectrum prediction and must be accounted in a realistic description of the optical properties of the system.

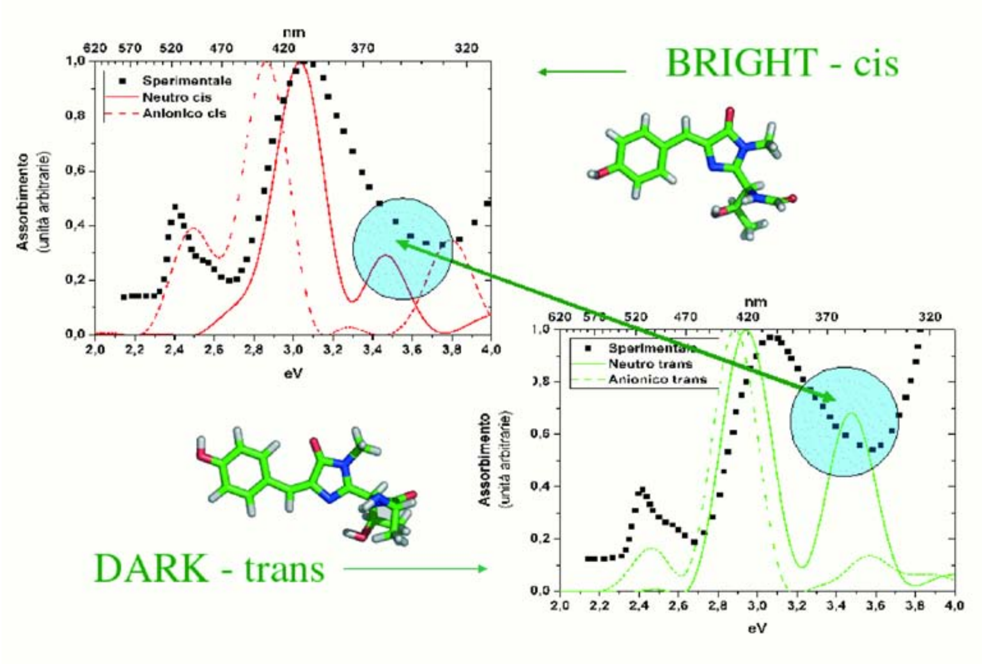

Fig. 2
The experimental and predicted spectra of two conformers of GFP.

Future developments in γ-ray spectroscopy: the European project AGATA

A. Bracco[1], F. Camera[1], F. Crespi[1], S. Leoni[1], M. Pignanelli[1], G. Benzoni[2], N. Blasi[2], Brambilla[2], B. Million[2], and O. Wieland[2]

1 Dipartimento di Fisica, Università degli Studi di Milano
2 INFN

The study of nuclei far from stability in extreme conditions of temperature and angular momentum has a very bright future due to the developments in the production of second generation radioactive beams leading, in the next future, to new facilities worldwide. However, experiments with radioactive beams need detector technologies which are very different from those typically used with stable beams. Besides, the experiments are particularly difficult for the measurement of γ-rays because very often the nucleus to be studied is characterized by very high levels of background and very high velocity (up to relativistic energy) and require very accurate Doppler Broadening corrections. A completely new technology for γ-rays detection, based on digital electronic and electrically segmented HPGe detectors, which is capable to reconstruct the path of the γ-ray , needs to be developed.

The AGATA project (Advanced GAmma Tracking Array) is a collaboration between 12 European countries and more than 30 institutions which has been established for the construction of a detector array based on tracking-digital technologies. AGATA is also a Joint Research Activity in the EURONS Integrated Infrastructure Initiative of the European Community. The AGATA array in its final configuration will consist of 180 HPGe detectors (see Fig. 1).

Fig. 1
The picture in the left panel displays an AGATA capsule containing the segmented HPGe detector. In the middle panel a picture of the single cryostat used for the acceptance tests is shown. In the right panel the triple cryostat, which is the basic module of the AGATA array, is displayed.

The reconstruction of the γ-ray track inside a HPGe detector could be schematized, in a simplified way, with five steps: i) the pre-amplification, ii) the digitization of the electrical signal, iii) the Pulse Shape Analysis (PSA) process for the identification of the coordinates of the interaction points and the energy there deposited, iv) the clusterization and tracking procedure and the v) acquisition and storage of the data [1]. In the AGATA collaboration, the nuclear structure group of Milano is active in the design of the pre-amplifier (see the contribution of A. Pullia), in the Pulse Shape Analysis and Tracking procedures. A new PSA procedure which is able to extract the number of γ-ray hits and their radial coordinates has been developed. The new PSA procedure has produced encouraging results in term of efficiency and CPU requirement [2]. Different tracking γ-ray techniques have been tested and particular effort has been dedicated in the analysis of the consequences that incorrect PSA results could introduce in tracking efficiency [3]. The first short term objective in the AGATA project is the construction of the “Demonstrator” which consists on 5 clusters (15 capsules) fully coupled to the new developed AGATA digital electronics. This AGATA sub-array is scheduled to be ready for tests in 2008.

The development of a γ-ray tracking technology is of extreme interests also in fields different than nuclear physics. For example, satellites for the measurement of γ-ray sources in the universe could benefit from this technology as well as medical diagnostic or industrial non destructive assessments applications.

REFERENCES
1. AGATA technical paper available at agata.pd.infn.it/info.html.
2. F. Crespi et al submitted to Nucl. Instr. dnd Meth. A.
3. O.Wieland et al. IEEE trans. on Nucl. Phys. 48(2001)296 and Nucl. Inst. and Meth. A487(2002)44.

Microscopic theory of charge-exchange nuclear excitations

S. Fracasso[1,2] and G. Colò[1,2]

1 Dipartimento di Fisica, Università degli Studi di Milano
2 INFN

Charge-exchange nuclear transitions from the ground state of the (N,Z) nucleus excite states in the near isobaric nuclei (Z $\pm$ 1, N $\mp$ 1) (Fig. 1a) and are in general difficult to be experimentally investigated. In fact, reactions like (p,n) and (n,p) populate states with different angular momentum ΔL and spins ΔS, in presence of a strong continuum background. Since the isospin degrees of freedom ΔT_z and ΔT are involved, these are isovector excitations, eventually with a collective character. Their study is so expected to improve the understanding of the role played by fundamental symmetries in nuclei, such as the isospin symmetry, and of the isospin dependence of the N-N effective interaction. These excitations occur also in weak processes mediated by charged-currents; in particular they can be the final states of β- or ββ-decays. Therefore, their investigation is also aimed to solve open questions for particle physics (Majorana neutrinos, unitarity of CKM matrix, ...) and astrophysics (weak processes governing stellar evolution: neutrino-nucleus interactions, electron capture).

We have developed a model [1] to microscopically describe the charge-exchange excitations in the standard framework of the linear response theory (that is, the non-relativistic random-phase approximation), including both the isovector and isoscalar pairing correlations, built on a Hartree-Fock-Bardeen-Cooper-Schrieffer (HF-BCS) ground state. Our model is fully self-consistent, which means that the residual interaction, which acts as restoring force against the small oscillations around the ground-state solution, is derived from the same mean-field employed in the HF-BCS equations, without neglecting terms. The consequent restoration of the symmetries spontaneously broken at the ground-state level provides the removal from the calculations of the (not negligible) spurious contributions.

The model have been tested on the Fermi transitions (Fig. 1b), which excite the isobaric analog state (IAS), in the even-even $^{104-120}$Sn isotopes (Fig. 2). The IAS is a serious benchmark because of its strict relation with the isospin symmetry: it would be degenerate with the parent ground state in absence of the explicit breaking due to the Coulomb interaction and the electromagnetic corrections to the strong N-N effective force (mass difference between neutral and charged mesons, the ρ-ω mixing, etc). We have discussed how these isospin non-conserving terms in the nuclear Hamiltonian affect the IAS energy and the isospin admixture in the parent ground-state [2]. Our results reproduce well the presently available experimental data [3], making us confident to extend the investigation to the unstable isotopes which may be produced in the next future by means of the new radioactive beams facilities.

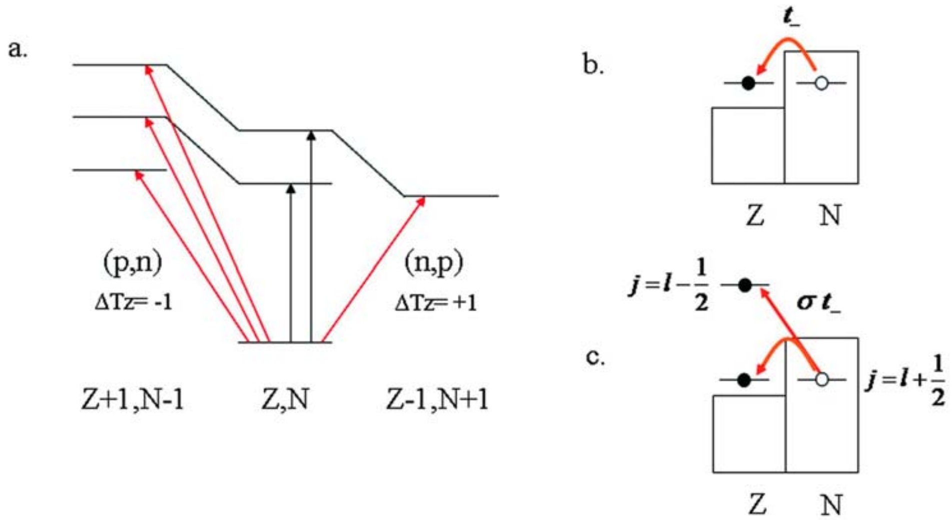

Fig. 1
Schematic representation of charge-exchange transitions (red line in Fig. 1a) induced between a generic (Z, N) target ground state and states in the neighbouring isobaric nuclei. In particular, the case of zero orbital momentum transfer in the ΔT_z = -1 channel: Fermi (b) and Gamow-Teller (c) modes.

REFERENCES
1. Fracasso S. and Colò G., "Fully self-consistent charge-exchange quasiparticle random-phase approximation and its application to isobaric analog resonances", *Physical Review C 72*, 064310 (2005)
2. Fracasso S. and Colò G., "Microscopic calculations of charge-exchange excitations in stable and unstable nuclei", in AIP Conference Proceedings series for the International Conference on "Frontiers in Nuclear Structure, Astrophysics and Reaction", Vol. 831, pag. 240.
3. Pham K., Jänecke J., Roberts D.A. et al., "Fragmentation and splitting of Gamow-Teller resonances in Sn(^{3}He,t) charge-exchange reactions, A=112-124", *Physical Review C* 51, 526 (1995).

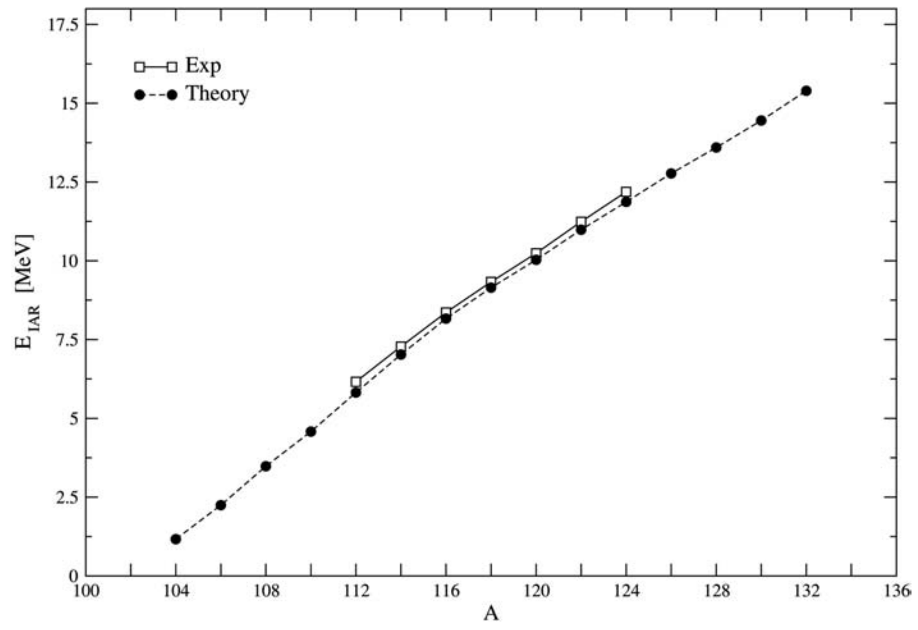

Fig. 2
Energy trend of the isobaric analog state (IAS) in Sn isotopers.
Predictions (2) and the comparison with the presently available experimental data (3) are shown.

Calculations of the Gamow-Teller resonance (Fig. 1c), and, for the first time in this frame work, of the states with ΔL = 1 are presently under investigation. The comparison with new experimental data [4] will be discussed also by properly matching the description of the nuclear response with the reaction dynamics. This will allow to overcome the lack of systematic microscopic calculations of hadronic charge-exchange cross-section, providing more realistic comparisons between theoretical predictions and data, and the estimate of the errors often introduced by many approximations done while extracting the information about the nuclear structure from the measured observables.

REFERENCES
4. Zegers, R.G.T., for the "RCNP E219 Collaboration", private communication.

Digital pulse shape acquisition from the telescopes of CHIMERA AZ-4 detector

P. Guazzoni[1], S. Russo[1], M. Sassi[1], and L. Zetta[1]

1 Dipartimento di Fisica, Università degli Studi di Milano and INFN

Aim of the present contribution is to present the preliminary tests done with the Superconducting Cyclotron beam at LNS in Catania for time measurements using digital pulse shape acquisition technique for CHIMERA multidetector [1] large area detection cells, made of silicon detector (300 μm x 5 cm x 5 cm) and CsI(Tl) scintillator up to 12 cm thick, read by a photodiode. From this kind of telescopes, different physical information can be extracted. In our previous work [2], matching properly the acquired information, we have verified the feasibility via digital pulse shape acquisition of: a) charge identification for product crossing the silicon (ΔE_{Si}-E_{C1I} technique), and stopping in silicon detector (E_{Si}-RT technique); b) light charged product isotopic identification for products leaving an under threshold energy in silicon, by means of the charge comparison method (Fast-Slow technique). In view of measuring also the time of flight of the reaction products, to obtain mass identification (measurement allowed by CHIMERA and to date analogically done) and the silicon rise time with a better accuracy, we have used two different sampling analog to digital converters, SIS3301 and CAENV1729. SIS3301 is an 8-channel digitizer/transient recorder with a sampling rate of up to 105 MHz for the individual channel, 14-bit resolution, 80 MHz of analog bandwidth and 5V dynamical range. CAENV1729 is a module suited for sampling acquisition of fast analog signals based on a circular buffer. The board performs the coding of 4 analog channels of bandwidth up to 300MHz over 12 bits at a sampling frequency reaching up to 2GHz with a 1V dynamical range. The on beam tests have been done at the LNS Superconducting Cyclotron in Catania, with a 21.1 AMeV ^{20}Ne beam on ^{12}C target. The time difference between the rising edge (Start) of the silicon pulse and one of the bumps of the radio-frequency (Stop) is assumed as a time of flight measurement.

To perform time of flight computation we use algorithms based on polynomial fitting and Fast Fourier Transform (FFT). The Start time is calculated for SIS3301 and CAEN V1729 in the same way. A 3rd degree fitting algorithm and a bisection method are used to calculate the point on the leading edge of the input pulse where the input pulse has risen to 30% of its maximum amplitude. For the Stop Time calculation different algorithms are used. For SIS3301 the radio-frequencies wave is reconstructed with MATLAB, using standard FFT algorithms, to allow for a better interpolation of the sampled signal. For CAEN V1729 it is used the same algorithms as for Start Time. As previously said, to obtain Start Time, the silicon rising edge is reconstructed. In this way it is easy to obtain the silicon rise time too. Consequently, (E_{Si}-RT) and (E_{Si}-ToF) scatter plots for the three different set-ups have been collected at the same time. In Fig.1 the (ESi-ToF) mixed scatter plot for a ^{27}Al target, obtained with the SIS3301 (14-bit, 100M Sample/s) for pulse height reconstruction and CAENV1729 (12-bit, 2GSample/s) for ToF measuring is shown. We have to note that

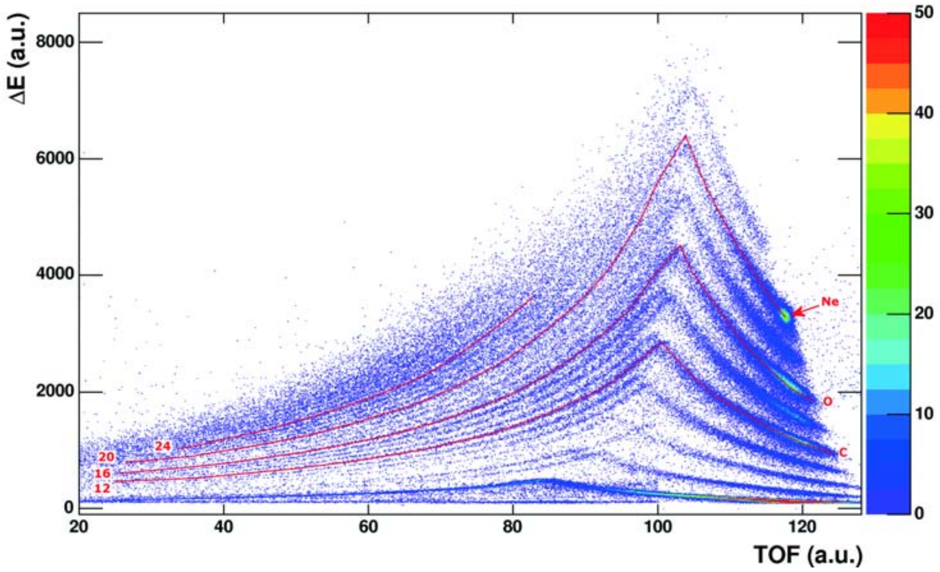

Fig.1
(E_{Si}-ToF) scatter plot. Mass identification up to A = 20, at least, is clearly possible.

REFERENCES
1. Pagano A. et al., "Physics with the CHIMERA detector at LNS in Catania: the Reverse experiment," *Nucl. Phys.* 681,331c (2001)
2. Alderighi M et al., "CHIMERA data acquisition via digital sampling technique," *IEEE Trans. Nucl. Sci.* 51, 1475 (2004)

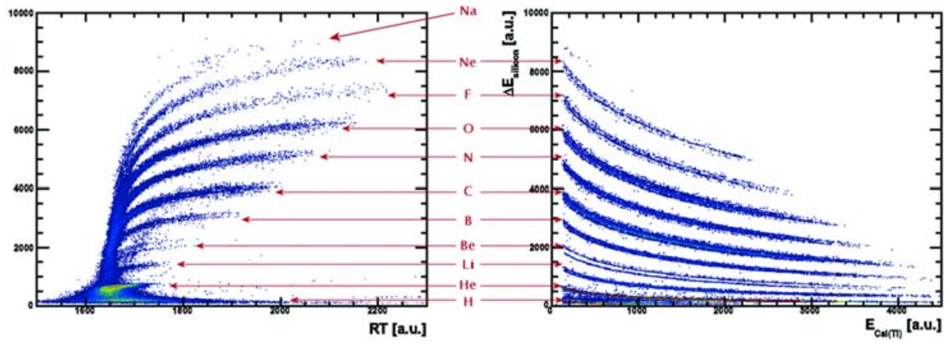

Fig. 2
(E_{Si}-RT) scatter plot for products stopping in silicon (left), compared with the corresponding (ΔE_{Si}-E_{CSI}) scatter plot for reaction products punching through silicon (right).

it is the first time the time of flight is computed with data collected on beam via digital pulse shape technique and that a high quality mass identification (up to ^{16}O at least) is performed with this method. In Fig. 2 the (E_{Si}-RT) scatter plot for products stopping in silicon is compared with the corresponding (ΔE_{Si}-E_{CSI}) scatter plot for reaction products punching through silicon. Good charge identification up to Z = 10 is possible for the stopping products. For punching through products a good isotopic identification is also possible.

Spectroscopy of ^{120}Sn homologous levels via the high resolution ^{123}Sb($\vec{p}$,α) ^{120}Sn reaction

P. Guazzoni[1], L. Zetta[1], A. Covello[2], A. Gargano[2], G. Graw[3], R. Hertenberger[3], H.F. Wirth[3], B. Bayman[4], and M. Jaskola[5]

1 Dipartimento di Fisica, Università degli Studi di Milano and INFN
2 Dipartimento di Scienze Fisiche, Università di Napoli and INFN
3 Section Physik der Universität München, Germany
4 School of Physics and Astronomy, University of Minnesota, USA
5 Soltan Institute for Nuclear Studies, Warsaw, Poland

The (p,α) reactions on nuclei around closed or semi-closed shells display several properties that make it a useful spectroscopic tool for supplementing level structure information obtained by other charged-particle reactions. In our previous work concerning Z = 40 and Z = 82 regions [1-3] we have shown that an interesting behavior can be observed for a number of transitions induced by (p,α) reactions on near magic target nuclei having one nucleon outside a completely filled magic shell. In this case the unpaired nucleon, slightly bound, may act as spectator in the process. In this framework, in order to complete spectroscopic study of ^{120}Sn, a high resolution experiment was carried out with the 24 MeV polarized proton beam of the Munich MP Tandem accelerator, using the new Stern-Gerlach source, the Q3D magnetic spectrograph and the new light ion focal plane detector to study ^{123}Sb(p,α)^{120}Sn, to be compared with ^{122}Sn(p,α)^{119}In. This has allowed a remarkable increase of the knowledge of ^{120}Sn nucleus, because 19 new levels have been identified, with the attribution of energy, spin and parity. To 16 levels spin and parity have been attributed, while the only parity has been attributed to 11 levels. For the attribution of spin and/or parity the methodology introduced by our group for homologous states has been applied. In such a way multiplets of states of ^{120}Sn homologous to the low-lying states of ^{119}In have been identified. In case of weak coupling the cross section of a homologous state with spin J_i in a given multiplet can be related to that of the corresponding parent state by the following expression: $\sigma(J_i)_{120Sn} = [(2J_i+1)\sigma_{119In}]/\Sigma_i (2J_i+1)$. In Fig. 1 the quantities $[\sigma(J_i)_{120Sn}/\sigma_{119In}]/\Sigma_i (2J_i+1)$ are reported for each member of the multiplet vs. J_i, together with the straight $(2J_i+1)$ line. The good agreement between the experimental data and the prediction of the weak coupling model supports the spin and/or parity assignment of ^{120}Sn homologous levels.

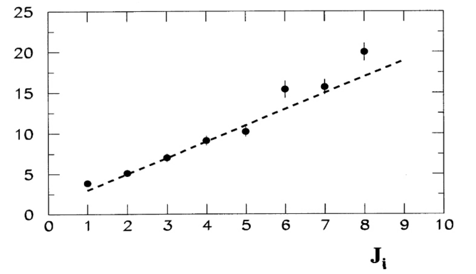

Fig.1
Plot of the quantities $[\sigma(J_i)_{120Sn}/\sigma_{119In}]\ \Sigma_i\ (2J_i + 1)$ for each member of the multiplet of parent ^{119}In G.S. vs. J_i (dots), together with the straight $(2J_i + l)$ line.

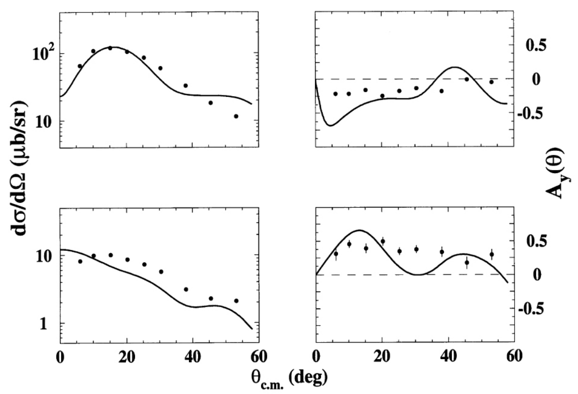

Fig.2
Comparison between experimental and microscopically calculated angular distributions of cross section and asymmetry for the transition to ^{120}Sn 0^+ G.S. (bottom) together with the comparison for cumulative angular distributions of the ^{119}In G.S. homologous multiplet (top), obtained in finite range approximation (dots represent experimental values, solid lines microscopic calculations).

In order to analyze the transitions populating the homologous levels for both differential cross sections and asymmetries, microscopic DWBA calculations have been performed using spectroscopic amplitudes obtained from a shell model study of the 22- and 20-neutron systems outside the N = 50 major neutron shell, in ^{123}Sb target nucleus and ^{120}Sn residual nucleus, respectively. Fig. 2 shows the comparison between experimental and microscopically calculated angular distributions of cross section and asymmetry for the transition to ^{120}Sn 0^+G.S. together with the cumulative angular distributions for the ^{119}In G.S. homologous multiplet. The calculations were done in finite range approximation, with the previously described microscopic configurations. The overall multiplicative factor, used to give a reasonable fit to the experimental data, is the same for the cumulative and G.S. cross sections.

REFERENCES
1. Guazzoni P. et al., “Spectroscopy of ^{88}Y homologous levels,” *Z. Phys.* A 356, 381 (1997)
2. Guazzoni P. et al., “^{206}Pb states homologous to the 1.484 MeV, 11/2- state of ^{207}Tl,”*Phys. Rev.* C 49, 2784 (1994)
3. Gu J.N. et al., “Homologous states and the structure of nuclei in the lead region,” *Phys. Rev. C 55*, 2395 (1997)

Recent results of HADES and future upgrading of the spectrometer

I. Iori[1,2], M. Cavinato[1,2], S. Riboldi[1,2], D. Maiocchi[1,2], R. Bassini[2], C. Boiano[2], S. Brambilla[2], and A. Bortolotti[1]

1 Dipartimento di Fisica, Università degli Studi di Milano
2 INFN

HADES (High Acceptance DiElecton Spectrometer) [1] is designed for a systematic study of e^+e^- pair production in hadron and heavy ion induced collisions : it is installed at the heavy ion syncrotron SIS at GSI. The aim of the activity with HADES is to study the hadron properties in nuclear matter in extreme conditions of high density and/or temperature: in these conditions , theoretical models predict a partial restoration of the QCD chiral symmetry and a modification of hadron properties as effective mass and decay width.The energy regime available at SIS allows to access densities up to 3 times the normal density of hadronic matter and temperatures of up to 80 MeV: this gives the possibility to investigate precursor effects of chiral symmetry restoration.

HADES is composed of different detectors forming a hexagonal structure (Fig.1) It covers polar angles 18° < θ < 85° and has 2π azimuthal acceptance. Starting from the target, there is a hadron blind RICH, two layers of MDC (Mini Drift Chambers) with six wire planes each, a superconducting toroidal magnet with B_{max} = 0.7 T and bending power 0.34 Tm, two more layers of MDC, a time of fight detector, TOF [2,3] and a SHOWER detector for small polar angles (18°-45°). The TOF, with all the front end electronics, has been built in our physics department: it is used for particle identification as well as first and second level trigger based on the multiplicity of charged particles and particles identification. It consists of ~ 400 plastic scintillators oriented perpendicular to the beam axis: each of them is read by two photomultipliers.

The magnet with the two modules of MDC in front and two planes of MDC behind the magnet, measure the momenta of charged particles. The lepton identification is made with RICH+TOF+SHOWER. The total number of detector channel in HADES is about 100.000. The second level trigger is functioning [4]. The start and veto detectors are CVD (polycrystaline chemical vapor deposition diamond) placed in front and behind the target. The position resolution is provided by the segmentation of the start and veto diamond into 8 strips.

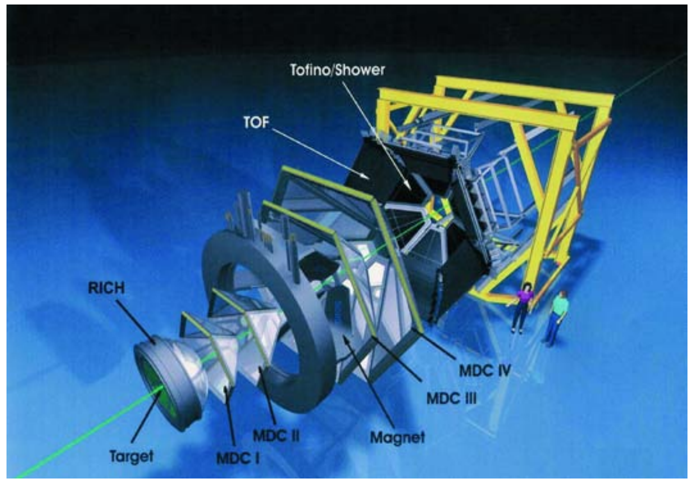

Fig. 1
HADES.

To quantitatively understand and interpret the measured e^+e^- spectra, elementary reactions (pp,π p), hadron induced reactions (pA) and heavy ion collisions (A,A) are investigated. The reaction ^{12}C + ^{12}C at 1 and 2 A GeV, the p + p at 2.2 GeV and Ca + Ca at 2 AGeV have been studied.

The p + p reaction (with a liquid Hidrogen target) has permitted to verify the reconstruction efficiency and to optimize the alghorithm of analysis. The cross section for the production of the η both in the hadronic ($\eta \rightarrow \pi^+\pi^-\pi^0$) and in the leptonic ($\eta \rightarrow e^+e^-\gamma$) channels have been investigated with the missing mass approach. The η peak is well visible at the expected mass value; the angular distribution has been evaluated.These mesurements will be extended from 1 to 5 GeV and to the (pn) reaction.

REFERENCES
1. Salabura P. et al, *HADES a high acceptence di electron spectrometer*: Nuclear Physics B 44,701 (1995)
2. Agodi C.et al, *The HADES time of flight,* Nuclear Instrument and Method A492,14 (2002)
3. Bassini R. et al , *A 32 channel ADC(TDC)on VME board:* IEEE Nuclear Science (1997)
4. A. Toia et al: *The HADES second level trigger: from the concept to the first results with C+C reactions.* Ricerca Sc & Educazione P vol 120 pag 35, (2003)

The analysis of C + C at 2AGeV has been completed. In Fig. 2 the invariant mass spectrum toghether with a simulation is reported. The region of small masses is dominated by the π_0 Dalitz decay; at intermediate masses an excess of masses is visible: it could be due to the reaction dynamics or to effects of the nuclear medium. Calculations based on different theoretical models (HSD,RQMD,URQMD) are in progress. The analysis of the reaction C + C at 1AGeV is almost completed and Ca + Ca is in progress.

To extend the study to nuclei heavier than Ca the forward part of the TOF, now TOFINO with low granularity, will be substituted with glass RPC: a sector prototype made of 180 cells, 2x60 cm^2 each, has been tested. The time resolution, the efficiency as a function of the counting rate, have been measured. The position resolution obtained is less than 6 mm and the time resolution 50-75 ps, the crosstalk is less than 0.4%. The proposed design is made with 180 cell/sector that is 360 channels/sector for a total of 2160 channels.

Fig. 2
e^+e^- invariant mass distribution in $^{12}C + ^{12}C$ at 2AGeV.

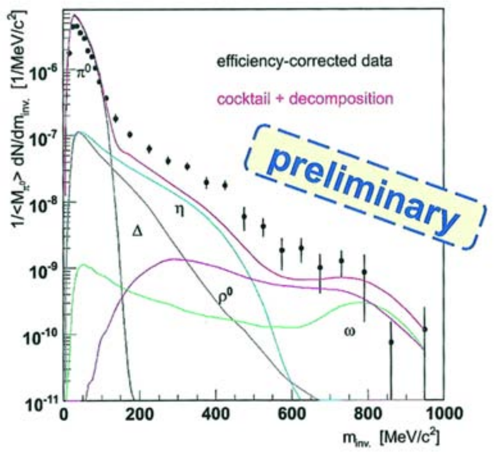

Physics of protein folding and drug design

1 Dipartimento di Fisica, Università degli Studi di Milano & INFN
2 Niels Bohr Institute, Copenhagen, Danmark

G. Tiana[1], D. Provasi[1], L. Sutto[1], A. Amatori[1], and R.A. Broglia[1,2]

Each protein is characterized by a one-dimensional sequence which determines completely its unique three-dimensional conformation. The underlying mechanism is an intriguing problem of biological physics. Studying simplified models of the protein chain and comparing the results with the experimental data, it was found that a hierarchical mechanism, involving a few local elementary structures (LES, folding units stabilized by strongly interacting and highly conserved amino acids), can explain the fast and efficient folding of protein chains. But the protein folding problem is not only of academical interest. Exploiting the associated hierarchical mechanism, it is possible to design non-conventional drugs which inhibit a selected target protein by destabilizing its active conformation. This is particularly useful in the case of viral proteins, like HIV protease [1] (see Fig. 1). For this protein it has been possible to design a folding-inhibitor which is as efficient as traditional drugs but which likely does not suffer the uprising of resistance [2] (see Fig. 2).

Fig.1
The HIV-1-Protease homodimer in its native conformation.

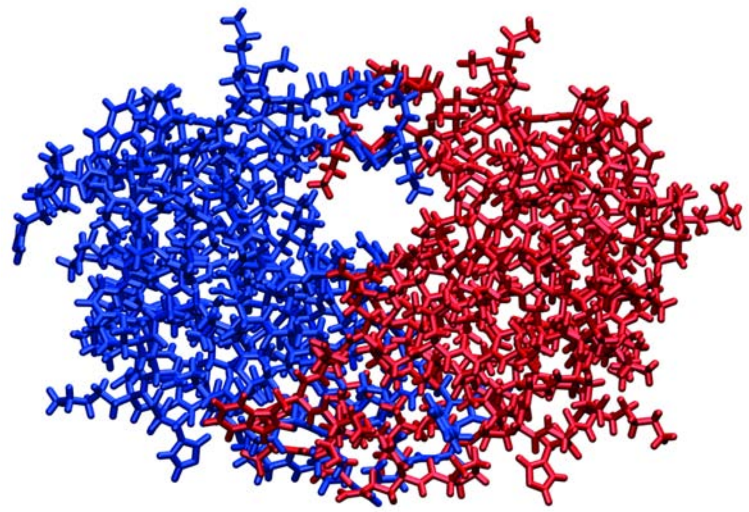

Fig. 2
The inhibitory effect of small peptides with the same sequence of one of the LES: by competing with the corresponding LES in binding the rest of the protein, they destabilize the native state of the protein (above) blocking its biological activity. Spectrophotometric experiments can be used to quantify the inhibitory ability of such peptides (below).

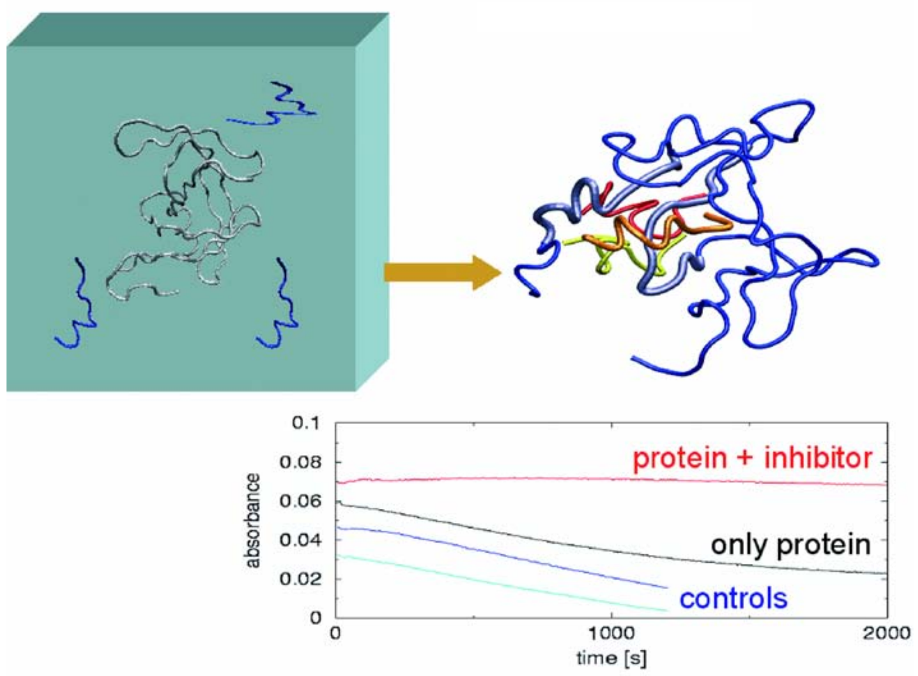

REFERENCES
1. R.A. Broglia, G. Tiana, L. Sutto, D. Provasi and F. Simona, “Design of HIV-1-PR inhibitors which do not create resistance: blocking the folding of single monomers”, *Protein Science* 14, 2668 (2005)
2. R.A. Broglia, D. Provasi, F. Vasile, G. Ottolina, R. Longhi and G. Tiana, “A folding inhibitor of the HIV-1 Protease”, *Proteins* 62, 928 (2006)

Nuclear structure at finite temperature probed by the Giant Dipole Resonance

1 Dipartimento di Fisica, Università degli Studi di Milano
2 Istituto Nazionale di Fisica Nucleare

A. Bracco[1], F. Camera[1], F. Crespi[1], S. Leoni[1], M. Pignanelli[1], G. Benzoni[2], N. Blasi[2], Brambilla[2], B. Million[2], and O. Wieland[2]

The Giant Dipole Resonance (GDR) is the simplest nuclear collective excitation mode. Macroscopically, it is described as an oscillation of protons against neutrons while, microscopically, a GDR state is a coherent superposition of many particles-holes (p-h) states. Experimentally, the GDR can be observed as an increase in the photo-absorption/photo-emission cross section between 10-20 MeV. The strength function of a GDR state built on ground state nuclei can be parametrized as a superposition of three Lorentians associated to the vibrations along the three principal axes. The centroid of each component is inversely proportional to the length of the oscillation axis, consequently, the more the nucleus is deformed, the more splitted will be the components of the GDR strength function. At zero temperature, the width of each component (damping width) is between 3-5 MeV and reflects the damping of such collective and ordered state to more complicated np-nh states. As the coupling of the GDR to the quadrupole deformation is a property independent on spin and temperature, the GDR is an unique tool to study nuclear structure in hot rotating nuclei. The major difference between the GDR properties in hot and ground-state nuclei concerns its width. In fact, it has been experimentally observed that the GDR width in exited nuclei is larger than the width measured in ground states (generally indicated as G0) [1].

The group of nuclear structure of Milano has a well established tradition in the study of the γ-decay of the GDR in hot rotating nuclei. To perform a systematic measurement of the GDR properties as a function of temperature, angular momentum and isospin the group has constructed a system of BaF2 detectors which has been coupled to large detectors arrays for the measurement of coincidence with particles, residues or low energy γ-rays. Some of the latest results of the Milano group experiments concern the study of the damping properties at high temperature, T > 2 MeV. In that region, the few existing studies did not give a clear picture of the evolution of the width as some data indicated a saturation of the width temperature while others indicate a continuous increase. The data shown in Figs. 1 and 2 refers to an experiment performed at the Legnaro Laboratories of INFN with the detector system GARFIELD-HECTOR using heavy ions beams from the Tandem and LINAC accelerators [2].

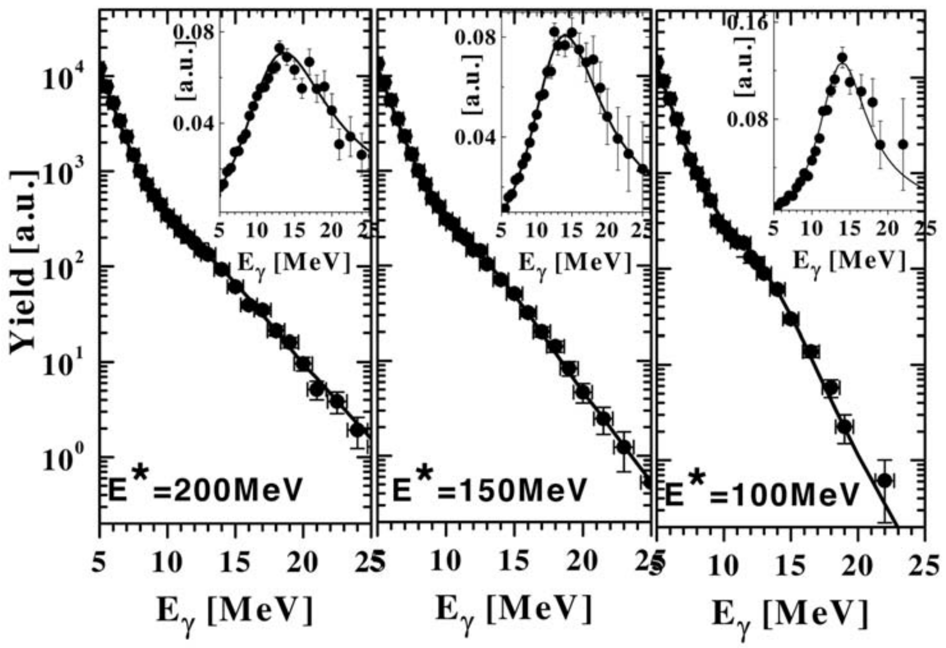

Fig. 1
The high energy γ-ray spectra measured in the reactions 64Ni+ 68Zn at beam energies 300, 400 and 500 MeV are displayed. In the inset the extracted GDR line-shapes are shown [2].

REFERENCES
1. Giant Resonances: Nuclear Structure at Finite Temperature, P.F.Bortignon, A.Bracco and R.A.Broglia Harwood Academic Publishers, Amsterdam
2. O.Wieland et al. submitted to Phys. Rev. Lett.

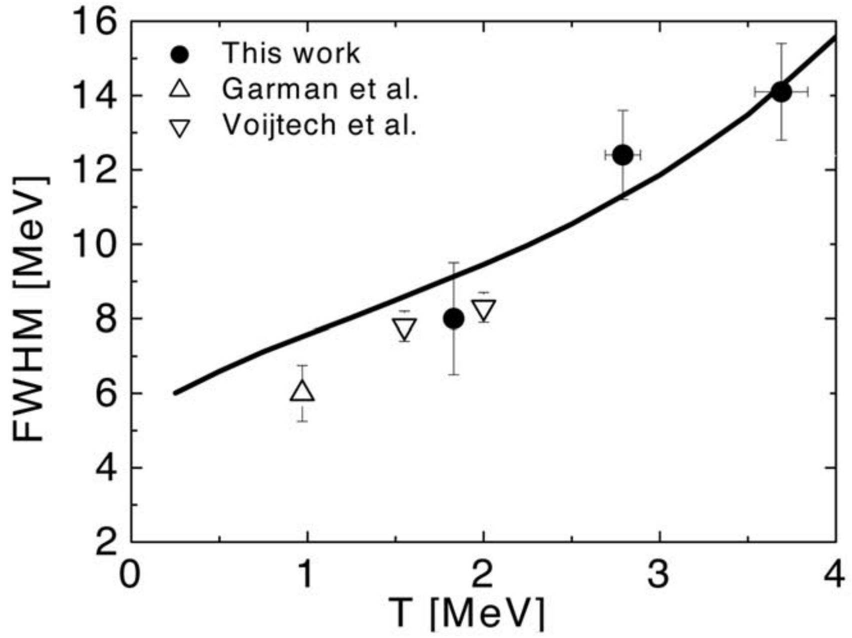

Fig. 2
The dependence of the GDR width on the average nuclear temperature in medium mass nuclei A ~ 130 is shown. The thick continuous line indicates the results of theoretical TFM calculations including the compound nucleus width.

The experimental data are well described in the framework of the thermal fluctuations model (TFM) first developed by the group of theoretical nuclear physics of Milano. In particular, it has been found that the observed increase of the width with temperature is not an additional GDR damping mechanism but an effect only due to the 'hot and rotating' environment in which the collective state happens to be [3]. In fact, the hot rotating nucleus does not have a fixed shape and orientation but feels a whole distribution of shapes with a probability proportional to the Boltzmann term exp(-F/T) where F is the free energy and T the nuclear temperature. The measured GDR is consequently a weighted average of the GDR built on this ensemble of shapes.

REFERENCES
3. F.Camera et al Phys. Lett. B560 155 (2003)

Accelerators and Related Technologies

LASA activity on accelerators

1 INFN

P. Michelato[1] for the LASA Laboratory

Introduction

The accelerator physics and the development of the related technologies are the main fields in which the "Laboratorio Acceleratori e Superconduttività Applicata" (LASA) is involved. LASA researchers are involved in different projects, ranging from the future electron linear collider (ILC, in the past TESLA) to the high intensity proton beam accelerators (as SPL), from magnets for LHC detectors (as the ATLAS barrel toroid) to proton therapy machine as CNAO, from RF compressors for electron beams to applied superconductivity and radiochemistry.

LASA activities

LASA, the acronym for Laboratorio Acceleratori Superconduttività Applicata, is located in the neighborhood of Milano (Segrate) and its activity, mainly funded by the INFN Sezione di Milano, is dedicated to the development of superconducting particle accelerator physics and technology, in strong cooperation with the industry. LASA counts a staff of 30 peoples (from Università degli Studi di Milano-UNIMI and INFN) plus temporary positions as PhD, graduate and diploma students.

Fig. 1
View of the LASA building.

Founded in the 80's, the laboratory was first dedicated to the K800 superconducting cyclotron (CS) project, whose construction started under the direction of Francesco Resmini. After the first magnet and RF system tests, the accelerator moved to Catania, at INFN Laboratori Nazionali del Sud (LNS), where it is still in operation.

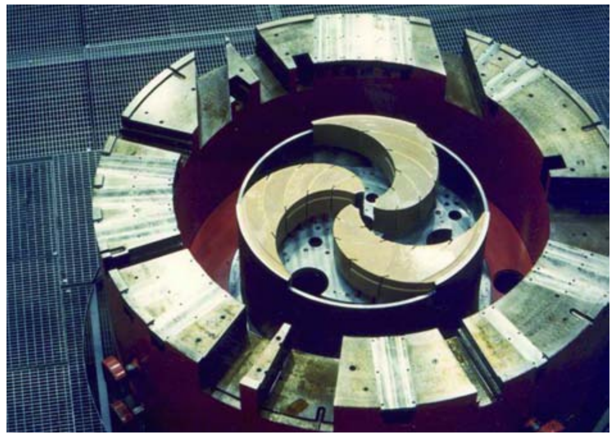

Fig. 2
The K800 superconducting cyclotron iron yoke.

After the CS project, LASA concentrated its activity in the design, development and test of accelerator components and ancillaries like superconductive cables and magnets, RF superconducting cavities, cryomodules, photoemissive films for high brightness electron sources, etc. The laboratory infrastructures includes Liquid Helium (LHe) plants with an He liquefier, a high magnetic field solenoid system (SOLEMI) up to 18 Tesla, a class 10 clean room, an ultra pure water plant, and an X ray shielded cryostat for cavity test. A 1000 m^3/h pumping system, for LHe sub cooling, gives the possibility to test components in superfluid helium.

At LASA, as a matter of fact, both test of RF superconductive (SC) cavities and SC cables are possible. Moreover, using the class 10 clean room, with the ultra pure water high pressure rinsing (HPR) system, the final cleaning treatment of SC cavities is also possible.

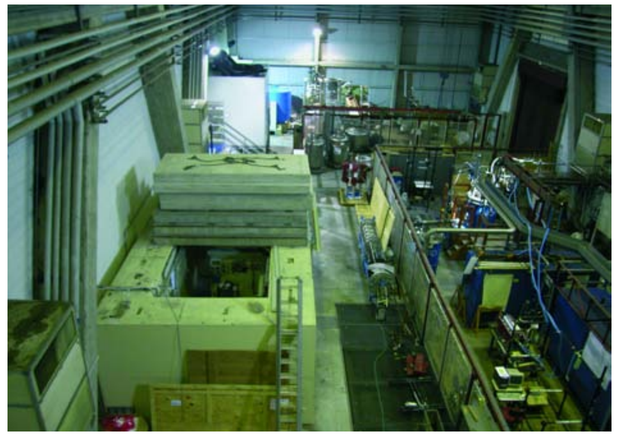

Fig. 3
View of the LASA experimental hall: on the left the SC cavity area, on the right the SOLEMI facility and the SC magnet activity area.

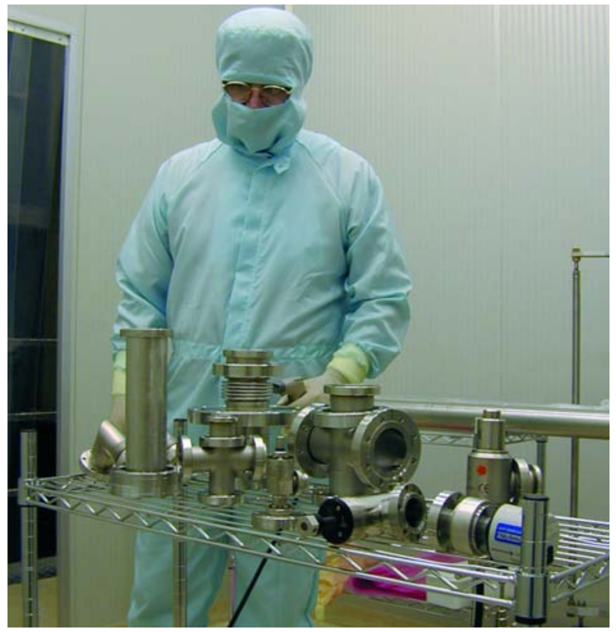

Fig. 4
LASA class 10 clean room operation: components for SC cavity are cleaned before the assembly.

In the last 10 years, the most meaningful contributions in the accelerator technology and physics field are relative to SC magnets, SC cavities and ancillaries, photoemissive films for high brightness electron guns and medical accelerators.

Superconductive magnets

The magnet group at LASA has been active since the 80's in the field of superconductivity applied to magnets, and works in strong collaboration with the Italian industry. The group has had major responsibilities in the design, manufacture and servicing of a number of world-rank superconducting magnets for research applications, as the first long prototypes of the LHC accelerator (CERN) main dipole and many NbTi and Nb3Sn solenoids for laboratory use. In the last years the activity concerning magnets was concentrated on the ATLAS detector magnet system (LHC, CERN), the largest superconducting magnet ever realized. The construction and test of the prototype B0, the construction and delivery of SC cables, coils, thermal shields of the BT (Barrel Toroid), together with the participation to the cryostat integration and test, was responsibility of LASA magnet group. It worked in strong collaboration with industrial partners as ETH and Zanon. The high magnetic field laboratory group at LASA currently performs measurements, at liquid helium temperature, on transport properties and mechanical characteristics of high-current superconductors using the SOLEMI solenoid system.

The magnet group future plans include the development of high-performance dipoles for next particle accelerators, among which LHC upgrade at CERN and the FAIR facility at GSI (Darmstadt, Germany).

Cryomodules, SC cavities and ancillaries for electron and proton superconductive cavities

SC cavities development at LASA started in the 80's, with the collaboration with Ansaldo, for the production of copper niobium sputtered and bulk niobium SC cavities, both for the LEP upgrade at CERN (350 MHz) and the ARES INFN project (500 MHz). Afterwards, LASA joined the TESLA collaboration, whose mission was the design of the TeV- Energy Superconducting Linear Accelerator (TESLA) and the development of the related R&D activities. Core fields of the TESLA collaboration were the SC cavities, the cryomodules and the SC cavities ancillaries. The experimental demonstration activity was carried out mostly at DESY (Hamburg), with the construction of the TESLA Test Facility (TTF), a machine build to provide a test bed for the TESLA linear collider project. TTF was especially dedicated to the superconducting niobium cavities. In this framework LASA, with its experience in SC components and cryostat design, has produced significance impact in different fields. Production of high quality niobium bulk SC cavities is now routinely performed by the Italian firm Zanon at Schio, thanks to the LASA collaboration. More than 1/3 of the cavity produced for TTF comes from this firm.

Fig. 5
ATLAS detector magnet system (BT) during the installation at CERN.

Fig. 6
TTF SC 9-cell niobium cavity before the integration in the helium tank

The experience acquired with the contribution to the TESLA Collaboration, gave the possibility for an active involvement of LASA also in the field of SC cavities for high intense proton beam with the TRASCO/ADS project. An ADS, (Accelerator Driven System), consists of a sub-critical nuclear reactor maintained critical by the intense neutron flux produced by the interaction of the high power proton beam (MW) with a liquid metal target. TRASCO/ADS was dedicated both to the project of an accelerator for an ADS (lattice and optics, reliability analysis, etc.) and to the design and construction of low beta proton SC accelerating structures (from mechanical and electromagnetic to the industrial production). Two 5-cells SC cavities have been produced and successfully tested, with high level results. In the field of SC high power low beta cavities, LASA has active collaboration for the design and development of pulsed proton accelerator structures, as the one used for the SNS (Spallation Neutron Source) at Oak Ridge.

Cryomodule design

Cryomodule design, development and production, in collaboration with the Italian industry, was one of the most successful activities worked out at LASA in the framework of the TESLA collaboration. Three cryomodule generations, with increased reliability and performances, have been designed and produced. The last generation, the third one, is characterized by extremely low static cryogenic losses for a 12 m long cryostat (as low as 2 W at 2 K), reduced production cost and simplified assembly and alignment procedure. They represent at the moment the state of the art in this field. They are characterized by original fixtures as finger welded thermal contact on the shields, braided thermal connections, sliding system for the mechanical decoupling of the cold mass, etc. Seven cryomodules have been produced and used in the TTF facility. Two more are under construction, while the generation four, the one foreseen for the ILC, the acronym of the International Linear Collider (TESLA in the past) is under development with a strong involvement and responsibility of LASA.

Fig. 7
The TRASCO/ADS low beta SC cavity for high power proton beams.

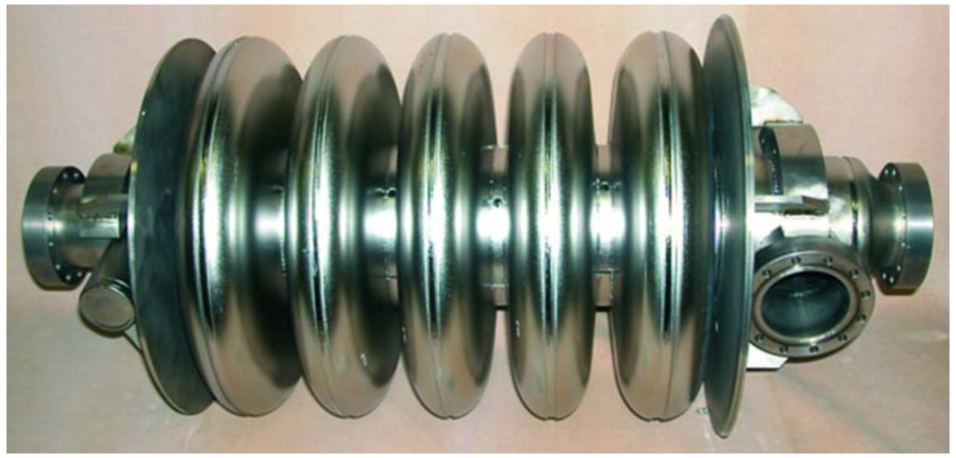

Fig. 8
Cryomodules at the TESLA Test facility (DESY Hamburg).

Ancillaries for SC cavities

The monitoring of the cold mass position, movement and vibration is a crucial problematic in "cold" accelerator structures. LASA has developed a special device, called WPM (Wire Position Monitor), that gives the possibility to acquire, monitor and analyze the cold mass position and vibration. WPM diagnostics have been installed and are routinely used to monitor cold mass position in all cryomodules used at TTF.

The control of the correct tuning condition of the SC cavity is another crucial argument in a SC accelerator. The high quality factor (Q) of the cavities implies that their bandwidth is quite small. So a low speed device (tuner) acts on the cavity to maintain it tuned with the RF generators. Moreover a fast tuning system, counteracting for the deformations produced by the electromagnetic field (Lorentz force detuning) and vibrations, have to be implemented. LASA has designed and built a special high stiff tuner (blade tuner): it is based on the deformation of titanium blades and will be able to make both slow and fast corrections. A stepper motors acts on the blade structure for the large cavity frequency compensation while two piezoelectric actuators compensate the fast perturbing components.

Photocathode for high brilliance electron gun

Besides cryomodule, SC cavities and ancillaries, LASA has done in these years strong activity on high brilliant electron sources. TTF operates using a RF gun, where a thin (30 nm) high quantum efficiency (QE) semiconductor photocathode (Cs2Te) is placed in a RF accelerating structure. Photoemitted electrons are then immediately accelerated, preserving the quality of the electron bunch and reducing the negative effects of space charge and other phenomena. LASA is responsible for photocathode production for DESY. They are used daily for the operation of the TTF, now known as the FLASH FEL facility.

Photocathode are currently produced at LASA and transported in UHV (ultra high vacuum) to DESY Hamburg and DESY Zeuthen. Moreover, a dedicated preparation system was designed and built for Fermilab and is in operation in the A0 facility. The photocathode system at FNAL will be soon integrated in the cryomodule test stand SMTF (superconducting module test facility).

Photoemissive film quality (lifetime, QE, uniformity, etc), thanks to a strong activity of R&D applying surface analysis techniques and developing dedicated instrumentation, like a low energy time of flight spectrometer, was greatly increased. For instance the photocathode mean operative lifetime is longer then 4 months of continuous operation and usually do not represent a serious limit factor in the RF gun operation.

The SC RF group future plants foreseen a strong participation and involvement in the International Linear Collider (ILC) collaboration and in the possible developments of the high power proton machine (neutrino factory, neutron spallation source, ADS).

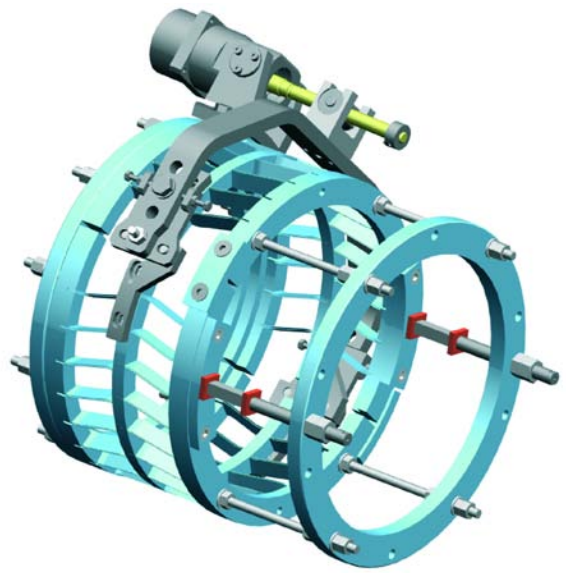

Fig. 9
Blade tuner design using CAD and FEA (finite element analysis) at LASA.

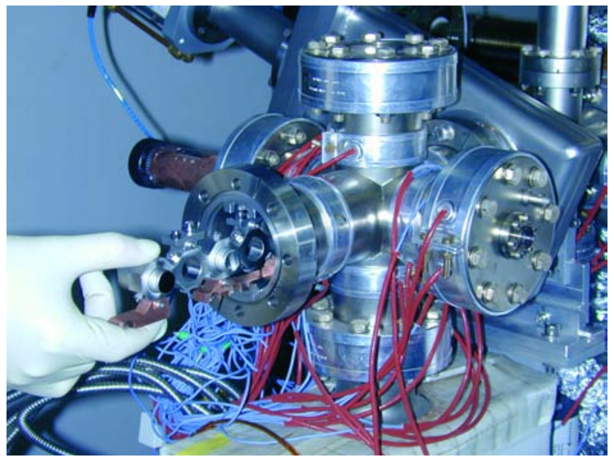

Fig. 10
Photocathode transfer system: cathodes are prepared at LASA and transported to DESY

Other activities at LASA

LASA is active in other high impact accelerator activities as the TERA-CNAO (Centro Nazionale di Adroterapia Oncologica) hadron therapy facility under construction at Pavia, the LIBO compact booster accelerator for adroterapy and the radioisotope preparation and characterization in the class 2 radiochemistry lab.

REFERENCES AND LINKS

Information about activities can be easily found on the web. Here are some useful links.

LASA:
http://wwwlasa.mi.infn.it/
LASA SC RF group:
http://wwwsrf.mi.infn.it/
ILC:
http://www.linearcollider.org/cms/
DESY TTF:
http://tesla.desy.de/TTF_intro.html
DESY FLASH:
http://flash.desy.de/
SNS:
http://www.sns.gov/
CNAO/TERA:
http://www.tera.it/

Applied superconductivity for particle accelerators and detectors: the Milan role

L. Rossi [1]

1 Dipartimento di Fisica, Università degli Studi di Milano
CERN - Accelerator Technology Department Geneva

Superconductivity has become an enabling technology for particle accelerators and detectors. The possibility to generate dissipationless high magnetic fields – from 2 to 10 tesla – has greatly improved the momentum precision and particle recognition in detectors and has given access to unprecedented energy range to particle accelerators. With the LHC, the new circular superconducting collider, 27 km long, under construction at CERN, superconductivity will allow us to reach 14 TeV energy and to explore matter in conditions that took place only 1 picosecond after the big bang! And for the next decade we hope to build a new linear collider 30 km long based on superconducting radiofrequency cavities, to explore with more precision the energy range open by the LHC. Milan has had a seminal role in the R&D for superconductors, magnets, cavities and photocathodes and a key role in the industrialization phase of such a complex apparata. Milano has been at the crossroad of the international collaborations supporting these projects and, with a proper organized program, can play an even more decisive role for future application in researches and applications.

Particle accelerators

Accelerators concentrate energy into beams of electrically charged particles. The main components of an accelerators are the following:

- The vacuum chamber: ultra-high vacuum is extremely important to allow colliding beams circulating for hours without significant losses, and has to reach level around 10^{-10} torr.
- The accelerating structures, constituted by cavities where an e.m. standing wave resonates. The electric field component of the e.m. field transfers energy to the particles. Therefore the cavity has a shape that maximizes the integrated electric field along the particle trajectory and that minimizes it on the cavity walls, in order to avoid power losses as much as possible.
- Quadrupole magnets (and magnets of higher order: sextupoles, octupoles, etc.) which focalize the beam and correct the aberrations. Light beams need lenses and other optical devices in order to avoid excessive divergence and increase of the size; similarly, a charged particle beam (which has also internal repulsive electrostatic forces, although weakened by the internal magnetostatic ones) need magnetic lenses to stay focussed along the whole trajectory.
- Dipole magnets which are needed to bend the beam, keeping it in circular trajectory. Through beam re-circulation, the very expensive accelerating structure is used by the particles many times to increase the energy up to desired level.

In circular accelerators the dipole magnets are the backbone of the machine and determine the final beam energy which is approximately given by $E \cong 0.3\ BR$ (TeV, T, km) for relativistic protons. From this formula it is evident the interest in increasing the magnetic field well above the 1.8 T attainable by mean of ferromagnetic alloys. Actually, thanks to the development of superconductors and associated technologies, the LHC dipoles, which fill 18 of the 27 km of the tunnel length, will operate at 8.3 tesla, with possibilities of reaching 9 T in a second phase. In Fig. 1 an artistic sketch of the LHC dipoles is shown, while in Fig. 2 the first

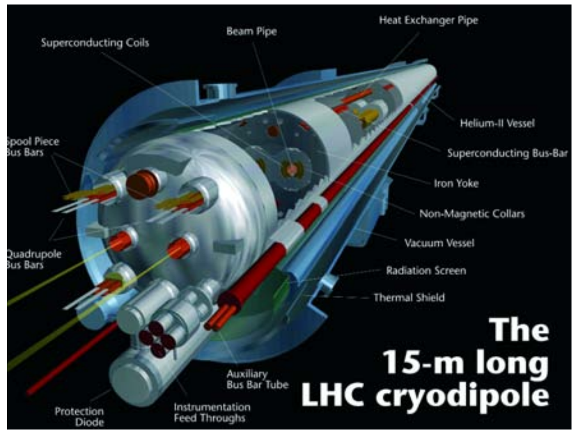

Fig. 1
Artistic view of the LHC dipoles, showing all main components.

LHC dipole prototype CERN-INFN 1 (manufactured in Italy under INFN and university of Milan supervision) is shown during first cold test at CERN.

Linear accelerators are the only machines that can accelerate electrons beyond 100 GeV, because of the synchrotron radiation limit for light particles, and they features accelerating cavities as backbone. The maximum energy is indeed given by the total voltage: E = E L (GeV, MV/m, km). In order to maintain the accelerator within acceptable size and cost – let's say 2 x 15 km – we need electric field of at least 35 MV/m. Again, this would be impossible to be reached, with accelerators working in a continuous mode or with high duty cycles, without the use of superconductivity. In Fig. 3 a superconducting accelerating structure designed for the Tesla project.

Fig. 2
The LHC dipoles, manufactured under supervision of the LASA Milan group, during the first cold test at 1.9 K in the CERN cryogenic station.

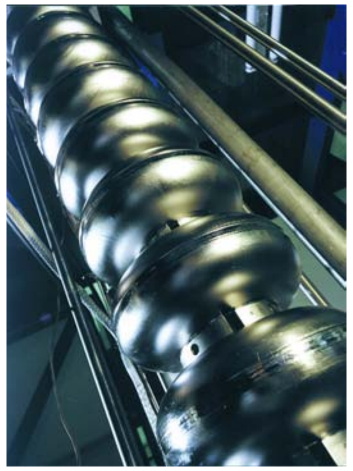

Fig. 3
Accelerating structure in pure niobium at 1.3 GHz developed for the Tesla project.

The contribution of Milan

The group of Milan, LASA laboratory (which is formed by a university component and an INFN one) has been in the year 1990-2005 strongly engaged in International collaborations for LHC and Tesla. Let's review in the following the main action taken by LASA in these collaboration.

LHC, ATLAS and CERN collaboration

For the LHC, LASA was responsible of the industrialization and construction of the first three superconducting dipoles, entirely manufactured by Italian industry, included the 13 kA superconducting cable based on 250,000 fine filaments (6 to 7 mm in diameters) of Nb-Ti alloy embedded in a pure copper matrix. This prototype work has launched the Italian industry in a privileged position in many high-tech works in the LHC construction.

In more recent years the LASA team has developed the superconductor for the toroidal magnet of the ATLAS experiment (the largest detector on the LHC machine). The conductor is constituted by a superconducting cable in Nb-Ti/Cu, somehow similar to the one employed LHC dipoles except that filaments have standard 30-40 mm size, however with current of 60 kA and with a super-stabilization obtained by adding a large very pure aluminum matrix. Just in 2005 the group is finishing the engineering, construction and test of the magnet itself, the world largest coil with its 25 m of length. The LASA group has designed the conductor and the coils, which generate 3.8 T of peak field, as well as the thermal shield and the protection unit (dumper). In Fig. 4 the giant ATLAS coil is shown in an intermediate phase of assembly in the 100 m underground gallery. One of the reasons for the huge size is the fact that momentum resolution scales as: $Ap/p \propto B L^2$: therefore large volumes pays off better than high fields. The detector works indeed at "moderate" field, 4 T against the 9 T of the machine magnets, in exchange of getting considerable dimensions.

An important role in all these developments and constructions, was played by apparata for evaluating the critical surface of superconductor, with field up to 15 T , test currents up to 30 kA and temperatures as low as 2 K. Also important have been the apparata for cryogenic characterization of materials and the development of an original numerical code for evaluation of the quench behaviour (quench is the sudden lost of the superconductive state, with consequent need of protection of the magnet).

Future collaborations in this sector aim to the upgrade of the luminosity of the LHC, by means of 12-15 T magnets, and to the project of the pulsed magnets for the FAIR project at GSI (Darmstasdt, De).

Fig. 4
The ATLAS barrel toroid during assembly in the CERN cavern.

TRASCO, Tesla and ILC collaboration

Concerning the superconducting RF structures, LASA has played an important role for the design and e.m. optimization of the cavity, with development of original codes in which the e.m. design is coupled to the beam dynamics. This allowed the evolution of two research lines. One is constituted by the development of cavity for electrons, pursued in the frame of the Tesla (now ILC, International Linear Collider) collaboration. Of great importance are the studies of the LASA group on the cryostat and on the cavity integration in the cryomodules. A variety of developments stemmed out from these studies, like the special RF sensors for precise alignment, as well as a strong push for industrialization of the Tesla project. All this is complemented by a number of studies on materials and cryogenic test of cavities, that make the group a key component of the ILC collaboration. In Fig. 5 a cryomodule, the accelerating structure complete of all power and cryogenic services, is shown during installation in TTF (Tesla Test Facility) at Desy, Hamburg.

Fig. 5
One of the first cryomodules completed under INFN-LASA supervision, in Desy during installation in the test facilitiy.

A slightly different accelerating structure has been developed for TRASCO, a linear accelerator for proton at medium energy (1-2 GeV) and high intensity, developed in the frame of an European collaboration for new techniques of radioactive waste incineration. The group is responsible of the e.m. design and of the cryomodule. These superconductivity studies are completed by a very advanced R&D on high quality electron sources based on photo-cathodes, which require vacuum of 10^{-11} torr and are ideal to be coupled to superconducting accelerators.

The group will continue the development of cavity for proton linacs (for incineration or as injector for synchrotrons, like the SPL at CERN) and will participate to the industrialization of the electron cavities for the X-FEL of Desy and, primarily, for the ILC project that will be based in a site to be established around 2009.

Electronics

Power electronics CAD: from space applications to industrial applications

P.G. Maranesi and M. Riva[1]

1 Dipartimento di Fisica, Università degli Studi di Milano

Electronic devices era either employed to process the information associated to electric signals or to process the electric power. The latter role is that of Power Electronics. Its applications span over several areas: power semiconductor devices, power supply, control of power networks, HV dc systems, automotive, aircraft electric power systems, spacecraft power systems, biomedical instrumentation, etc. Constraints and critical aspects are related to each specific application. Space applications are most demanding in terms of reliability, efficiency and radiation hardness for the apparatus. The electronic section of the Department of Physics in the University of Milan has been involved in the last years in electronic power applications for space: the design of power converters and distribution apparatus aboard satellites and the International Space Station and also of HV supplies for ionic propulsion.
In the figure 1a) a DC-DC converter payload supply circuit, proposed by the power electronics laboratory of the Department of Physics and installed aboard the International Space Station, (ISS) is shown; in 1b) the schematic of a HV generator for Radiofrequency Ion Thruster (RIT), developed in the same lab, is given.

Another field of the activities of the lab is the development of automatic CAD tools for the analysis and the design optimization of electronic power systems. The main product of this activity is an innovative CAD tool (FREDOMSIM) for the characterization in the frequency domain of the dynamic behaviors of the switched converters. Starting from the schematic entry according to the SPICE simulator of the circuit considered (in fig. 2 an example is represented), FREDOMSIM provides forecasts of the frequency responses of the transfer functions, characterizing the circuit with the feedback loops open. The high degree of compliance with real life can be evaluated in the fig. 3, where the plots are relevant to the boost converter in the fig. 2. The application of FREDOMSIM is user friendly (its visual interface is shown in the fig. 4) and it supports the designer in the optimization of the inner and external feedback loops. Even though the automatic tool was devoted to space applications, it demonstrated validity for the design of electronic circuits for terrestrial application too. The fig. 5 shows the block scheme of a distributed power assembly developed for industrial applications in cooperation with a semiconductor manufacturer. The high efficiency reached at 500kHz of switching frequency has been made possible by the technologies and the automatic tool originally developed for the design aid of space power circuits.

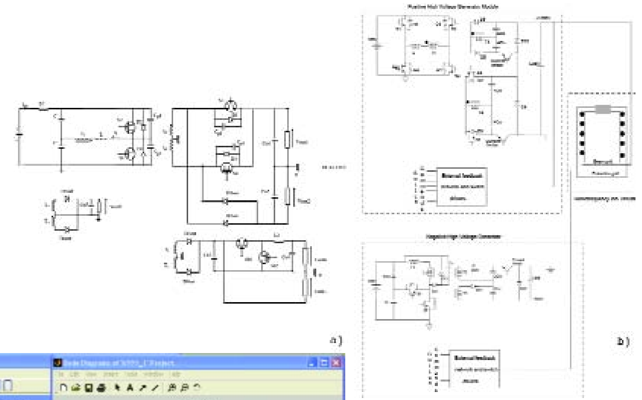

Fig. 1
Examples of power electronics converter;
a) a phase-shifted full-bridge applied aboard the ISS and b) HV generators for ion thruster drive.

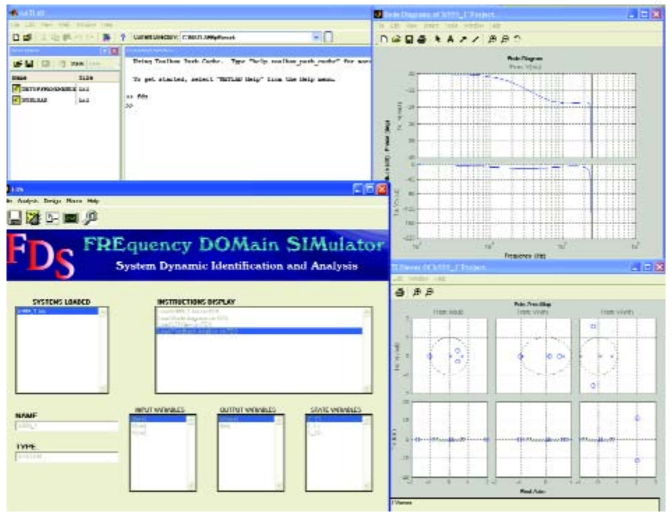

Fig. 2
Some of the FREDOMSIM features.

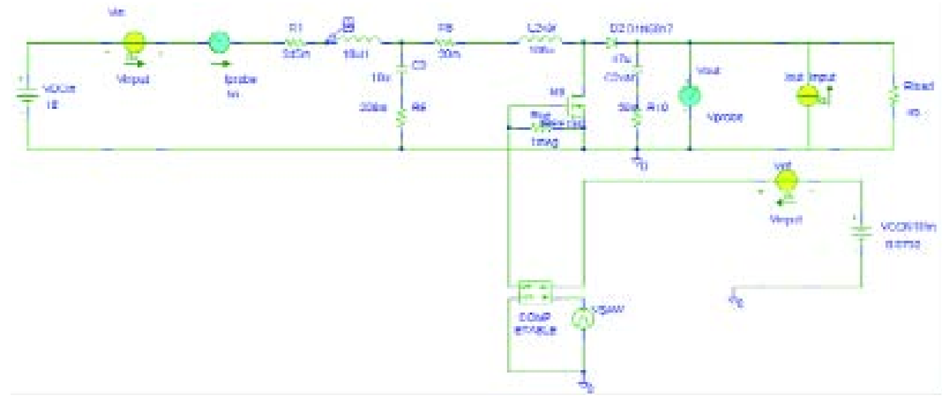

Fig.3
Globalstar boost pre-regulator schematic.

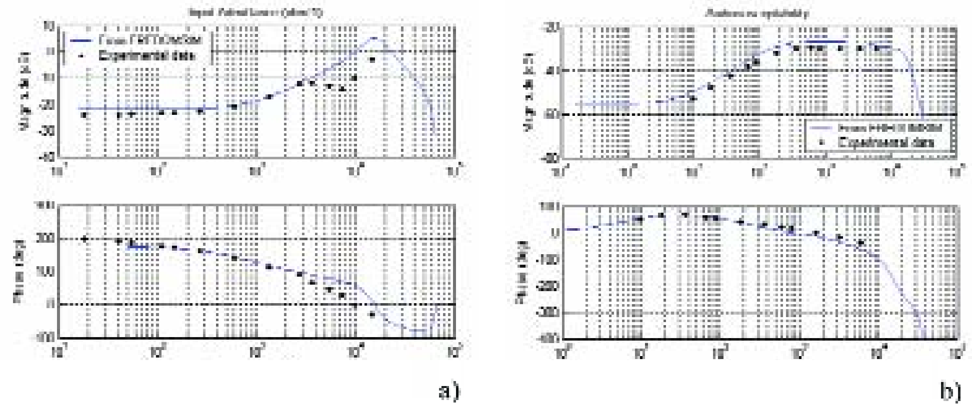

Fig. 4
FREDOMSIM forecasts vs experimental data of the frequency responses of input admittance a) and audio-susceptibility b) transfer functions.

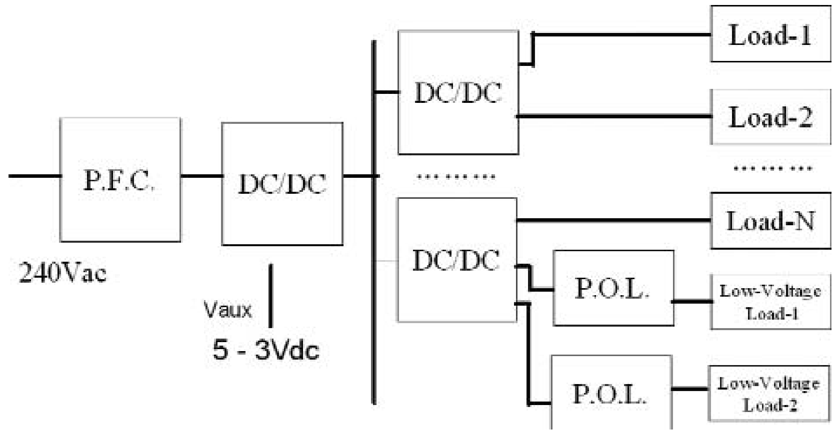

Fig. 5
Typical scheme of a distributed power assembly.

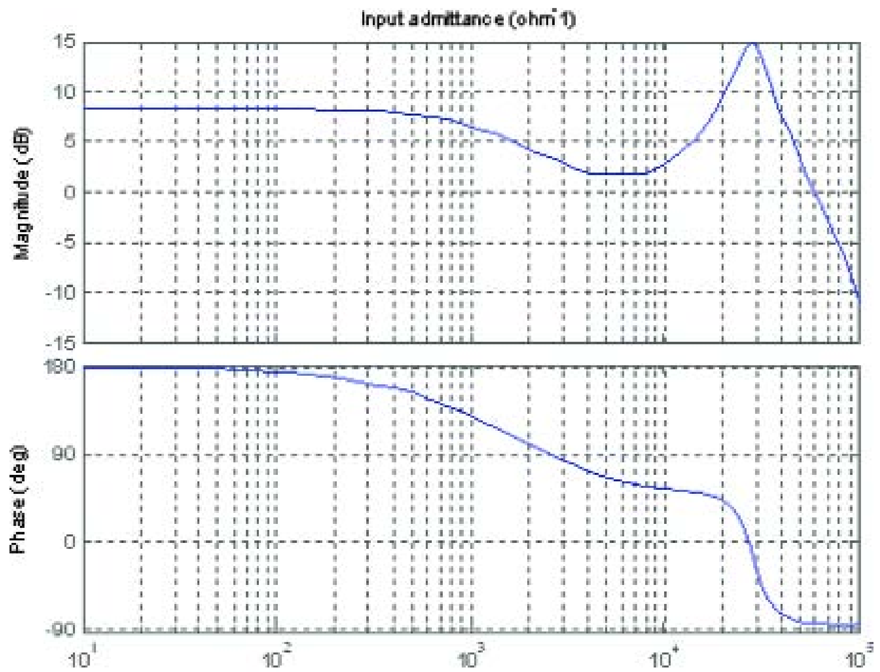

Fig. 6
Example of the input admittance frequency responses of a closed-loop buck converter.

High dynamic range low-noise preamplification of nuclear signals

1 Dipartimento di Fisica, Università degli Studi di Milano
2 INFN

A. Pullia[1,2], F. Zocca[1,2], C. Boiano[2], R. Bassini[2], S. Riboldi[1,2], and D. Maiocchi[1,2]

We have developed and realized a new mixed continuous-pulsed reset preamplifier purposely conceived for advanced multi-channel gamma-ray sensors. The continuous-reset mode is used for typical signal amplitudes within the ADC input range, or from a few keV to a few MeV. The pulsed-reset mode works on larger signal amplitudes, up to 100 MeV caused by either individual events or by bursts of piled-up events. Such operation mode maximizes the live time in the typical energy range and minimizes the dead time caused by ADC saturation on large individual signals or at high count rates. The amplitude of large individual signals can also be estimated from the reset time still achieving a high resolution. Using this technique and a bulky HPGe detector we got a "continuous-reset" range of 2 MeV with a resolution of 2.02 keV fwhm at 1.408 MeV, and an extended "pulsed-reset" range of 27 MeV, with a typical resolution of 0.3% at 27 MeV.

1. Introduction

The development of advanced segmented detectors for the new generation of nuclear physics experiments with exotic beams (AGATA, GRETA) [1,2] poses challenging requirements to the front-end electronics, including an extremely high dynamic range and an ultra low noise over the whole range. The typical energy range of a digitized preamplifier for γ-ray spectroscopy is from a few keV to a few MeV. Individual highly energetic events which exceed this range or bursts of piled-up events at high count rates can easily cause ADC saturation and introduce a significant system dead time. We suggest that a mixed reset technique for the preamplifier can address these issues. The idea consists of using a simple continuous reset in the typical amplitude range and a fast pulsed reset for larger signals. When the amplitude of the preamplifier output signal is within the ADC input range, the circuit works in the classic continuous-reset mode, i.e. with the typical resistive continuous discharge of the feedback capacitance. But when the preamplifier output signal exceeds the ADC voltage range, the pulsed-reset mode intervenes which yields a fast recovery (in a few μs) of the output voltage to its floor level. The amplitude of a large individual signal can be indirectly estimated from the reset time, when the ADC overflow condition would give no possibility to make a direct measurement of the pulse height. Using this technique, we were able to measure highly energetic signals up to 30 MeV, still achieving a high resolution. As a result the dynamic range of a digitized preamplifier is substantially increased, as given by a "continuous-reset" range of a few MeV and a "pulsed-reset" range which can reach 30 MeV or more. Such a large energy range is of interest for the last generation of nuclear physics experiments with bulky 4π germanium detectors. In fact, Montecarlo simulations show that a 9 cm germanium layer still has a detection efficiency of 9 to 14% for γ-rays photons of 20 to 30 MeV. This large dynamic range is required for a class of experiments where giant-dipole resonances can produce γ photons of energies up to 30 MeV.

2. Architecture of the time-variant charge preamplifier

The architecture of the proposed time-variant preamplifier is shown in Fig. 1. Continuous reset is ensured through the feedback resistance R_F, while pulsed reset is realized through an add-on switchable device we called Large-Signal Manager (LSM). It consists of an inverting Schmitt-trigger comparator and a temperature stabilized switchable current sink. The LSM senses the amplitude of the preamplifier output signals. On small-amplitude signals the current sink is in the off condition. In this case the circuit behaves like a classic charge preamplifier, with resistive continuous reset of the detector charge stored on the feedback capacitance. But when a large signal arrives, which exceeds the comparator threshold, the LSM switches the current sink on and puts the preamplifier into a pulsed-reset mode, so as to swiftly desaturate the ADC. As shown in Fig.1, in this phase the current sink continuously absorbs charge from capacitance C of the P/Z stage until the preamplifier output voltage is brought back to its DC level. At this point the comparator automatically turns over and switches the current sink off so completing the fast reset procedure.

REFERENCES
1."Technical Proposal for an Advanced Gamma Tracking Array for the European Gamma spectroscopy Community", *http://agata.pd.infn.it/documents/Agata-proposal.pdf*
2. I. Y. Lee, "Gamma-ray tracking detectors," Nucl. Instrum. and Meth., vol. A422, pp. 195-200, 1999

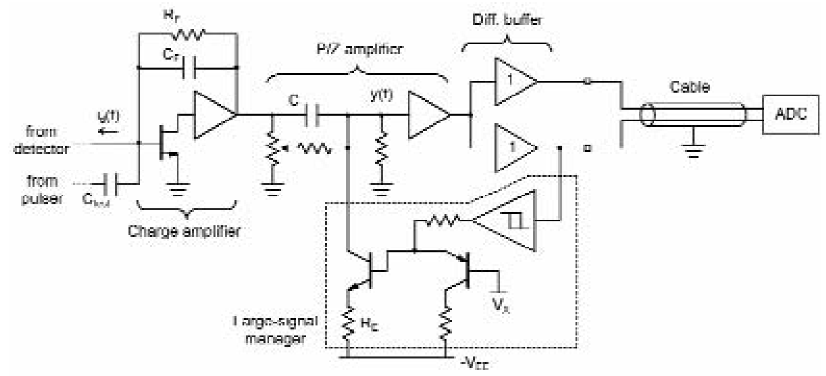

Fig. 1
Architecture of the time-variant preamplifier. The connection cable and the ADC are also shown.

3. Large signal measurement technique

In Fig. 2a we show the typical reset transient seen at the P/Z amplifier output, when a large individual signal (*H*) occurs upon a tail of a regular signal (*h*). Figure 2b shows the corresponding waveform seen at the Schmitt-trigger comparator output, which delivers a rectangular pulse of width *T*, corresponding to the pulsed-reset time. The regular signal which provides the tail h does not exceed the threshold corresponding to ADC saturation and has the typical exponential decay time of about 50 μs. The large signal *H* is instead over threshold and puts the preamplifer into the pulsed reset mode. In the figure the ADC saturation at a voltage level of about 1V is not shown, as the signal has been acquired through a digital oscilloscope. But in the real acquisition chain, the preamplifier output is directly sampled by the ADC module and so it would not be possible to directly estimate the amplitude of the over-threshold signal. However, the energy information can be indirectly obtained. By accurately calculating the expression of the reset transient at the P/Z stage output, we can derive the exponential relation between the reset time *T* and the sum of the energy E_S of the large event and the energy E_C of the tail:

$$E_S + E_C = A\,(\exp\,(T/\tau) - 1), \qquad (1)$$

where *A* and τ are coefficients depending on circuit parameters. As the reset time *T* results substantially shorter than the time constant τ, the relation can be linearized by expanding the exponential term with no loss of accuracy. We can then express the large signal energy E_S as a function of the reset time T and the energy of the tail E_C, obtaining

$$E_S = b_1\,T + b_2\,T^2 - E_C, \qquad (2)$$

where b_1 and b_2 are the first and second order coefficients. The reset time *T* can be obtained through a time over threshold measurement performed on the waveform acquired at the comparator output (see Fig. 2b), while the tail energy E_C can be obtained from the difference of the pre and post large event voltage levels evaluated on the output signal of the preamplifier. So Eq. (2) can be written as

$$E_S = b_1\,T + b_2\,T^2 - (V_1 - V_2)\,/G + E_0, \qquad (3)$$

where $(V_1 - V_2)$ is the voltage amplitude of the tail, G is the energy-to-voltage gain of the preamplifier and E_0 is an offset term. We can conclude that (3) permits to indirectly derive the large signal energy E_S. In this relation T, V_1, and V_2 must be evaluated any time an over-threshold signal occurs, while b_1, b_2, G, and E_0 are parameters which must be obtained through preliminary calibrations.

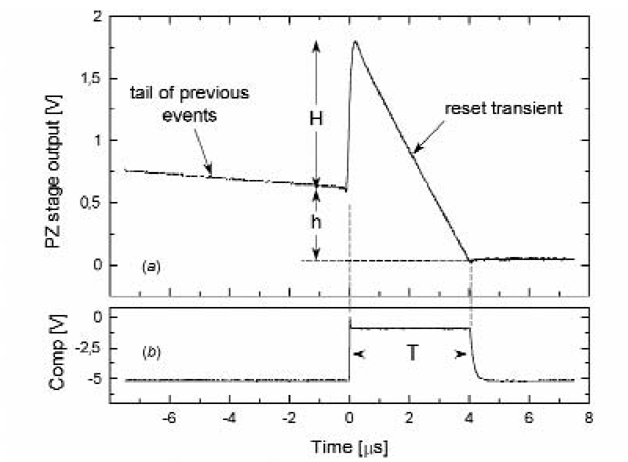

Fig. 2
(a) Large signal (H) upon a tail (h) at the PZ stage output. (b) Schmitt-trigger comparator signal.

4. Gamma spectroscopy with mixed continuous and pulsed reset: experimental results

We tested the mixed-reset technique by using a custom-made preamplifier equipped with the add-on LSM device sketched in Fig. 1, connected to a state-of-the-art closed-end cylindrical HPGe detector. We used ^{152}Eu and ^{60}Co calibration sources placed at different distances from the detector, obtaining overall counting rates in the range 1 kHz to 32 kHz. We could also artificially simulate energetic events in the range 5 MeV to 27 MeV by providing large signals at the preamplifier input with a spectroscopy-grade pulser and a calibrated test capacitance. The pulser signals were large enough to trigger the LSM device. The fast-reset transients were superposed to the tails caused by the distribution of γ photons delivered by the mentioned radioactive sources.

In Fig. 3 we show the result of the algorithm for the estimation of a ~ 10 MeV signal injected at the preamplifier input, when a background of 32 kcounts/s of ^{60}Co signals is present. As evident, if we try to reconstruct the large signal energy only by evaluating the reset time with no tail correction, the line completely disappears, as the stochastic distribution of tails due to ^{60}Co signals scrambles it out. When the tail correction from (3) is made, the line gets nicely reconstructed showing a relative fwhm of 0.56 % @ ~ 10 MeV. As shown in Fig. 4, the resolution improves if the counting rate of the ^{60}Co regular signals is reduced, which diminishes the disturbing effect of the tails. In Fig. 5 the obtained resolution is shown in an energy range of 5 to 27 MeV.

Fig. 3
Large pulser line. A background of 32 kcounts/s of ^{60}Co signals is present which destroys the large signal resolution if no correction is made.

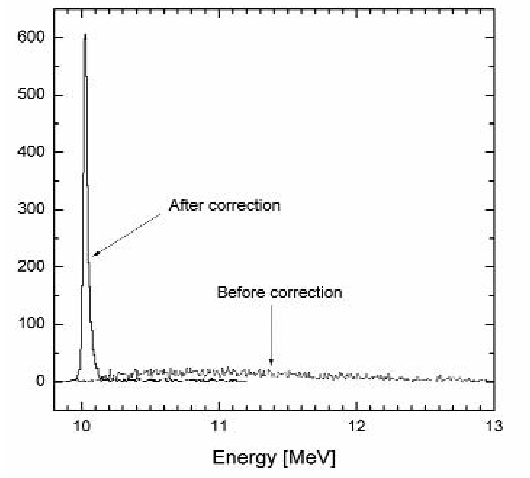

Fig. 4
Obtained energy resolution at 10 MeV for increasing counting rates of the ^{60}Co regular signals.

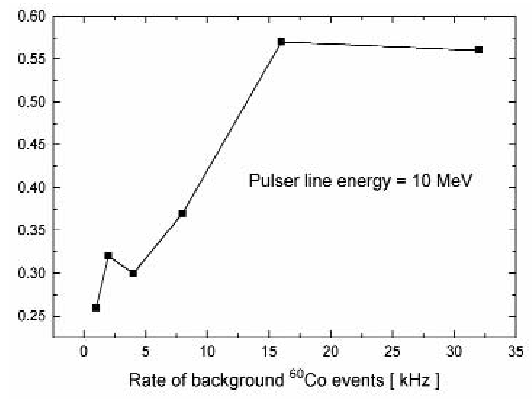

Fig. 5
Obtained energy resolution at high energy for two different values of background event rate.

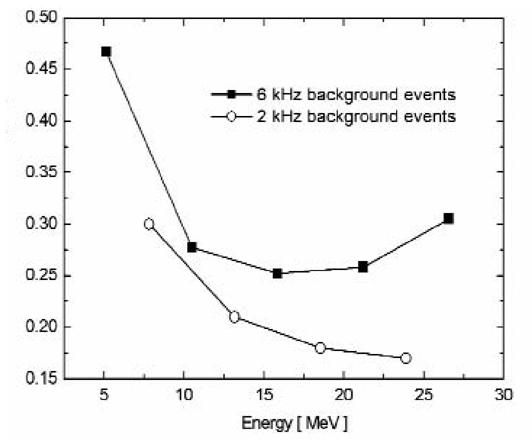

We then irradiated the detector with a ^{152}Eu source placed in such a way to get an event rate of 6 kHz, and injected large pulser signals in the energy range from 5 to 27 MeV. All signals from the ^{152}Eu source were “under threshold” and have been acquired in the continuous-reset mode, while the pulser signals were “over threshold”, and have been acquired through the pulsed-reset technique, as explained before. As a result we got the overall spectrum shown in Fig. 6 in the extremely wide range from 10 keV to 27 MeV. All ^{152}Eu lines are well resolved, the 1.408 MeV line having a fwhm of 2.02 keV. The high-energy pulser lines are also finely resolved, having a relative fwhm of the order of 3 perthousand.

Fig. 6
Spectrum of ^{152}Eu with high-energy pulser lines. The average event rate is 6 kHz.

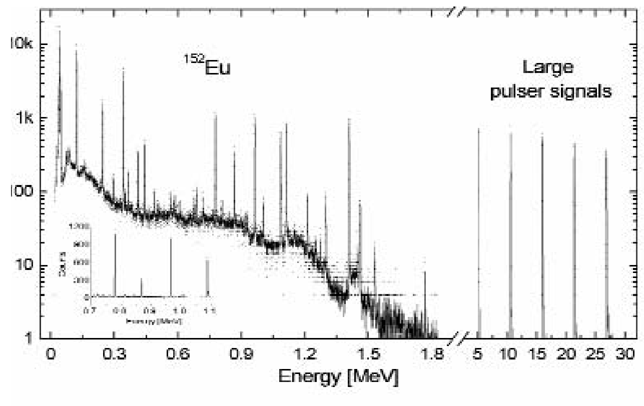

Ion thruster high voltage drive

1 Dipartimento di Fisica, Università degli Studi di Milano

F. Belloni[1], P.G. Maranesi[1], and M. Riva[1]

Electrostatic Radiofrequency Ion Thrusters (RIT) have been introduced in the last years for propulsion, orbit control, and orientation of space vehicles. This type of engines is characterized by the generation of a heavy ion plasma which is accelerated by the electric field of the high voltage supplies before ejection from the spacecraft. Accelerating forces in the order of several tens of millinewtons, as required by interplanetary missions, can be obtained by RITs of a few Kilowatts. The propellant is an inert gas, such as Argon, Krypton or most commonly Xenon that is ionized by a radiofrequency (RF generator) and then accelerated by two high voltage grids. The first (beam grid) is maintained at a positive voltage (Positive High Voltage Generator - PHVG) and the second one (extraction grid) at a negative level (Negative High Voltage Generator - NHVG). The schematic of the RIT, with HV and RF generators is shown in Fig. 1.

Short circuit between the positive and the negative voltage grids happens not rarely and the capacity of withstanding such occurrence is mandatory as well as of removing the short circuit. Due to the threshold effect of the positive grid, the beam current decreases by increasing the voltage generating a negative resistance behavior. Moreover, the plasma accelerated from the PHVG, constitutes a non-linear load. It's advisable that the high voltage cell consists of a transconductance power stage supplying current to the load and to the output capacitance with a single pole behavior. The proposed solution for a module PHVG module is a phase-shift PWM controlled converter switching at the frequency = 65.5 kHz, rated power of 1.5kW and V_{out} = 1500V. The input DC voltage is 100V, the output is obtained by the connection in series of two 750V transformer coupled half bridges. The former is active and it uses MOS switches, the latter employs rectifying diodes. Zero voltage switch-on and voltage clamping characterize the switching transients. The IGBTs, in series to the output, avoid to overcome the load current limit in cases of short circuit or overcurrents and provide prompt switch-off of the output currents. The NHVG consists in a flyback topology, operating in discontinuous conduction mode, modified to achieve zero voltage transitions. The switching frequency is 65.5 kHz, the rated power is 300W at maximum load and the output voltage can vary between -150V and -800V. The output voltage rectification is made by two passive single-ended rectifiers, in order to reduce the voltage stress on each diode. Schematics of both the PHVG and the NHVG are represented in Fig. 2.

Short circuits between the two grids can happen due to impacts of positive ions on the grids and material settling. The protection implies current limitation and switch off. This inconvenience is removed by a dedicated operating procedure of the PHVG that aims to sublimate the short circuit material by Joule effect. The delay time is fixed at and the control of the current injected to the short circuit is done by varying the switching frequency.

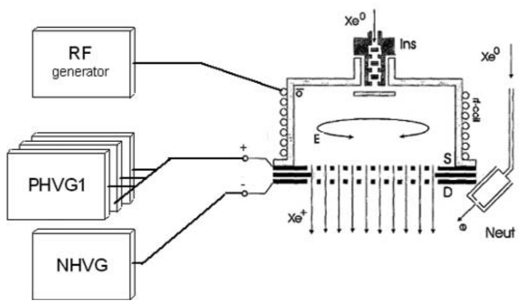

Fig. 1
RIT and voltage generators schemes

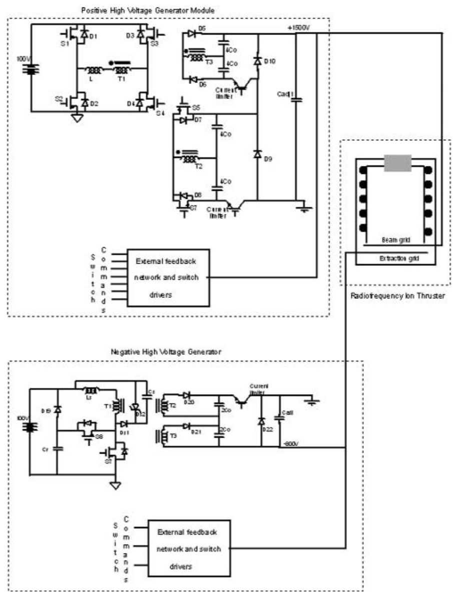

Fig. 2
Electrical schemes of the PHVG and the NHVG

Structure of Matter

Bose Einstein condensation in solid ^{4}He

1 Dipartimento di Fisica, Università degli Studi di Milano

D.E. Galli [1], M. Rossi [1], and L. Reatto [1]

We have found the first microscopic evidence for Bose-Einstein condensation in crystalline ^{4}He based on a quantitative variational theory of solid ^{4}He: the Shadow Wave Function technique. With this technique we have computed the one–body density matrix ρ_1 in solid ^{4}He at T = 0 K. We find that off-diagonal long range order is present in ρ_1 for a perfect solid ^{4}He for a range of densities above the melting one, and the condensate fraction decreases by increasing the density. This is the first microscopic indication that Bose Einstein condensation could be present in perfect solid ^{4}He. The key process giving rise to Bose Einstein condensation is the formation of vacancy–interstitial pairs. Such processes have a finite probability to be present in the ground state of the system; we have verified this also with an exact Quantum Monte Carlo projector method. Due to exchange processes these vacancy–interstitial pairs are unbound; however they are not permanent excitations but simply fluctuations of the perfect crystal induced by the large zero-point motion.

Since the first pioneering papers in the sixties, the prospect that a solid could have superfluid-like properties has fascinated and attracted a great number of physicists and the topic of such super-solid has received a considerable theoretical and experimental attention [1]. The experimental search of the supersolid gave no results [1] until 2004, when Kim and Chan [2] claimed to have observed a NCRI effect for solid ^{4}He adsorbed in Vycor during a torsional oscillator experiment. In such a confinement solid ^{4}He will be surely rich of defects, especially vacancies near the pore wall, and these defects were considered responsible for the observed NCRI effect. But later on, NCRI effects were also observed for the bulk solid ^{4}He [3]. These observations have given a new life to the interest on the supersolid state, whose existence is still an open problem. In fact, up today there is no experimental evidence for the zero-point vacancies in bulk solid ^{4}He and arguments against bulk superfluidity have appeared in literature [4, 5].

Leggett showed that BEC, at least at $T = 0$ K, is a sufficient condition for the observation of NCRI effects [6]. So a central quantity to compute is the one-body density matrix $\rho_1(\boldsymbol{r},\boldsymbol{r}')$, whose Fourier transform represents the momentum distribution. A non-zero limit at large distance of ρ_1 (off-diagonal long-range order, ODLRO) implies BEC and then NCRI. In ref. [7] we discuss the results for ρ_1 in a perfect ^{4}He crystal, computed with a variational Monte Carlo which uses as trial function a shadow wave function (SWF). By perfect solid, we mean a solid where the number of maxima in the local density $\rho(\boldsymbol{r}) = \rho_1(\boldsymbol{r},\boldsymbol{r})$ is equal to the number of ^{4}He atoms. The use of SWF, whose accuracy is well documented [8] is specially useful in the present context because the crystalline order is an effect of the spontaneously broken symmetry so that local disorder processes like exchange of two or more particles or more complex processes are in principle allowed. The major finding of our computation is the presence of a small but finite condensate for a range of densities above melting [7]. For example at ρ = 0.031 Å^{-3}, which corresponds to a pressure of about 54 bars, we find a condensate fraction of $n_c = (2.0 \pm 0.4) \times 10^{-6}$. These results constitute the first microscopic indication that BEC can be present in commensurate solid ^{4}He.

The variational theory is very useful to describe strongly interacting systems like liquid or solid ^{4}He but it is always open to debate how much the results depend on the ansatz on the wave function, specially for quantities other than the energy. To this purpose we have tested the accuracy of the SWF with an exact projector method that we have recently introduced, the shadow path integral Ground State (SPIGS) [9, 10]. By comparing the static structure factor $S(\boldsymbol{k})$ and the local density $\rho(\boldsymbol{r})$ with the exact ones, we have found that within the SWF description the ^{4}He atoms are more localized. This stronger localization of the atoms given by SWF compared to the exact results suggests that the present SWF might underestimate the condensate. Very recently we have improved our variational description [11] obtaining a better agreement with the exact results for $S(\boldsymbol{k})$ and $\rho(\boldsymbol{r})$. With this improved SWF, we have computed ρ_1 in a perfect *hcp* solid ^{4}He, which is plotted in Fig. 1. The lower degree of order in the structure of the crystal is observable in the oscillations of the plateau which reflect the crystalline order in the system; they are still present but very much damped. The value of the condensate fraction obtained with the new SWF at ρ = 0.031Å^{-3} increases up to $n_c = (1.1 \pm 0.3) \times 10^{-4}$. So the improved description of the crystalline structure has a very relevant effect on ρ_1 and on the value of n_c.

REFERENCES

1. For a review see Meisel M.W., *"Supersolid ^{4}He: an overview of past searches and future possibilities", Physica B* **178**, 121 (1992).
2. Kim E. and Chan M.H.W., *"Probable observation of a supersolid helium phase", Nature (London)* **427**, 225 (2004).
3. Kim E. and Chan M.H.W., *"Observation of superflow in solid helium", Science* **305**, 1941 (2004).
4. Ceperley D.M. and Bernu B., *"Ring exchanges and the supersolid phase of ^{4}He", Phys. Rev. Lett.* **93**, 155303 (2004).
5. Prokof'ev N. and Svistunov B, *"Supersolid state of matter", Phys. Rev. Lett.* **94**, 155302 (2005).
6. Leggett A.J, *"Topics in the theory of helium" Physica Fennica* **8**, 125 (1973).
7. Galli D.E., Rossi M. and Reatto L., *"Bose-Einstein condensation in solid ^{4}He", Phys. Rev.* B **71**, 140506 (2005).
8. Vitiello S.A., Runge K. and Kalos M.H., *"Variational calculations for solid and liquid ^{4}He with a shadow wave function", Phys. Rev. Lett.* **60**, 1970 (1988); Pederiva F., Ferrante A., Fantoni S. and Reatto L., *"Quantum theory of solid-liquid coexistence and interface in ^{4}He", Phys. Rev. Lett.* **72**, 2589 (1994); Pederiva F., Chester G.V., Fantoni S. and Reatto L., *"Variational study of vacancies in solid ^{4}He with shadow wave functions", Phys. Rev. B* **56** 5909, (1997); Galli D.E. and Reatto L., *"Disorder phenomena in quantum solids with vacancies", J. Low Temp. Phys.* **134**, 121 (2004);
9. Galli D.E. and Reatto L.,*"Recent progress in simulation of the ground state of many Boson systems", Mol. Phys.* **101**, 1697 (2003).
10. Galli D.E. and Reatto L., *"The Shadow Path Integral Ground State Method: Study of Confined Solid ^{4}He", J. Low Temp. Phys.* **136**, 343 (2004).
11. Galli D.E., Rossi M. and Reatto L., *"Off-Diagonal long-range order in solid ^{4}He", Phys. Rev. B* **71**, 14056 (2005).

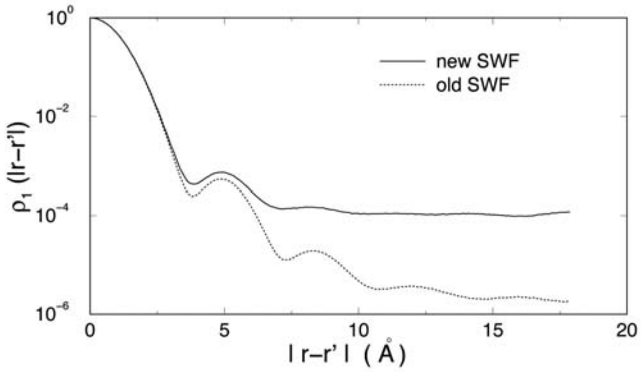

Fig. 1
One-body density matrix computed in a perfect *hcp* solid ^{4}He at a density of 0.031 Å^{-3} with the old SWF [7] and with the new SWF [11].

As shown in ref. [7], from the behavior of the oscillations in the plateau of ρ_1, it is possible to gain informations on the microscopic mechanism at the basis of ODLRO in the solid. By analyzing the particle configurations which contribute to the plateau of ρ_1, we found that at least one of the coordinates ***r*** and ***r'*** refers to an interstitial position, i.e., a vacancy-interstitial pair (VIP) is present in the system [7]. The presence of VIP is the key process that gives rise to BEC in solid ^{4}He. Due to the fact that VIPs can appear with a small, but finite, probability at any lattice points in the perfect solid, one can destroy a particle in any lattice position and create it at any far distance with a nonzero probability due to the presence of holes in the crystal. Since the concentration of VIPs is finite the destruction-reconstruction process at arbitrary large distance is a zero energy cost process due to the indistinguishability of the atoms. Differently from the defected solid case, the microscopic processes that give rise to a finite probability to find an unoccupied (distorted) lattice position are part of the zero-point motion and are not excitations of the system. The exchange of atoms and VIPs are evident not only in ρ_1 but also in $|\Psi|^2$ as seen in the configurations generated with SWF and with the exact SPIGS method [7] (see Fig. 2). It is worthy to stress that the name "pairs" is given to the vacancy-interstitial fluctuation of the crystal only to underline the origin of this microscopic process. Due to the exchange between atoms or other zero-point processes, in fact, these VIPs are unbound and interstitials can annihilate far away from the original partners, with vacancies coming from other VIPs.

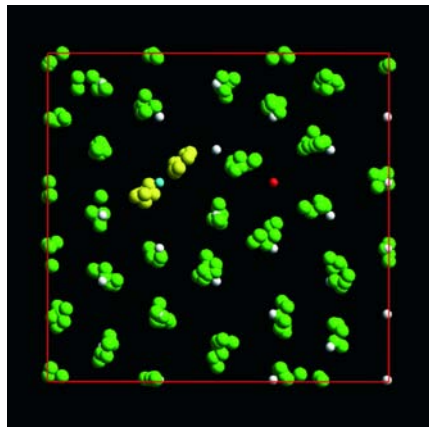

Fig. 2
Snapshot of a VIP during a SPIGS simulation run. The discrete path integral representation of the imaginary time projection maps the quantum system into a classical system of special interacting open polymers [7]. In the plot only the internal atoms of the open polymers (those which represent the true ground state) are shown (green). The white spots represent the lattice positions of a basal plane of an hcp crystal, the red one indicates the vacant lattice site while the blue one the doubly occupied lattice site (the associated polymers are shown in yellow).

The success of SWF in describing diagonal properties like the energy or the structure of solid ^{4}He does not strictly ensure that the off-diagonal properties of ρ_1 are accurately reproduced. However, since BEC implies NCRI, our results, if confirmed by an exact calculation, are very relevant, in that they could provide the basic explanation of effects recently measured [3]. Moreover these NCRI effects can only be increased by the presence of disorder, if the experimental bulk sample contains some defects. Then, even if the bulk sample would be a perfect solid, the observed NCRI effects should be present in any case, perhaps at a different transition temperature and with a different superfluid fraction than the ones measured in ref. [3]. This indicates the relevance of computing ρ_1 also by an exact Quantum Monte Carlo method. The computation of ρ_1 by means of an exact projector method, such as SPIGS, is in progress.

Theory and computation of electronic excitations in condensed matter systems: the ETSF project

1 Dipartimento di Fisica and INFM, Università degli Studi di Milano
2 LSI-SESI, Ecole Polytechnique, Palaiseau, France

G. Onida[1], N. Manini[1], E. Mulazzi[1], A. Bordoni[1], K. Gaál-Nagy[1], A. Incze[1], L. Caramella[1], M. Cazzaniga[1], E. Ponzio[1], A. Miglio[1], and M. Gatti[2]

Excited states and electronic excitations are a key for the understanding of condensed matter properties, and for the design of novel materials, systems, and solid-state devices. In fact, many properties of solids depend on their excitation spectrum: from the external aspect (colors), to electrical or thermal conductivity, to the way an LCD screen operates, up to the exotic behaviour of nano-machines such as molecular engines (see, e.g., [1]).

From the physicist's point of view, electronic excitations are at the base of many modern spectroscopic techniques: electrons, photons, or atoms can be sent as probes which, impinging on a sample, induce some kind of excitation. By measuring, e.g., the excitation energies, one can obtain useful compositional and/or structural informations about the sample itself. Typical examples are optical spectroscopy and photoelectron spectroscopy, two of the most widely used characterization techniques in condensed matter laboratories.

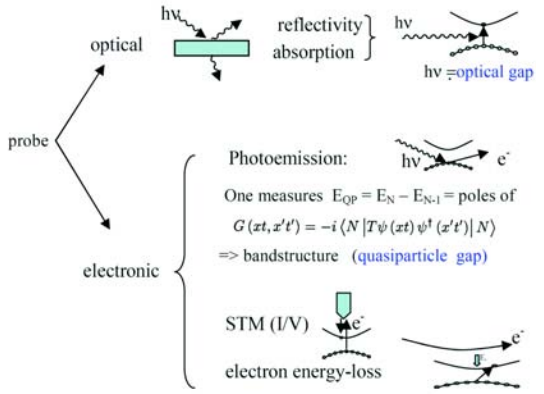

Fig.1
Different experimental techniques, and the related different types of electronic excitations which must be considered in the theoretical description.

Experiments, of course, are most useful if they can be interpreted in the light of a theoretical model, and theoretical models can be useful in order to suggest how to perform new experiments. For this reason, large efforts are being done in order to deepen and to extend our theoretical understanding of electronic excitations in condensed matter. The task is not an easy one, being the many-body problem very hard to solve for the ground state of a system of interacting electrons.

Among the state-of-the-art theoretical methods and tools, a prominent role is today played by the so-called *ab-initio* approaches. These are characterized by a complete absence of free (adjustable) parameters in the theory: everything is directly derived from the fundamental equations of quantum mechanics (since only Coulomb forces and interactions are relevant in our case, the ingredients from which to start are exactly known). The scope of the calculations is not, however, simply to reproduce the experimental results, which will be of little interest: aim of the theoretician should be to derive from his results some new information about the system, namely informations which are not accessible through experiment. In practice, a theoretical calculation should be thought as an additional "microscope" that can be used, besides the "experimental" one, to look inside the sample in order to understand its behaviour.

Ab-initio methods for the many-electrons system have been developed since many years, starting from the pioneering works of Hartree [2] and Fock [3]. However, in the last 20-25 years the use of ab-initio methods in the study of real systems has become more and more frequent, not only because of the availability of powerful computers, but also thanks to the introduction, between the sixties and the eighties, of novel theoretical approaches which have allowed us to simplify substantially the required numerical calculations. The main progress has been done with the Density Functional Theory (DFT), introduced by W. Kohn and Hohenberg in 1964 [4]. Through suitable theorems, DFT allows one to shift the attention from the many-body wavefunction (a "monster" quantity for a system of many interacting particles

REFERENCES
1. J. D. Badjic, V. Balzani, A. Credi, S. Silvi, and J. F. Stoddart, Science 303, 1845 (2004).
2. D. R. Hartree, Proc. Cambridge Philos. Soc. 24, 89 (1928).
3. V. Fock, Z. Phys. 61, 126 (1930).
4. P. Hohenberg, and W. Kohn, "Inhomogeneous Electron Gas", Phys. Rev. 136, B864 (1964).
5. W. Kohn, "Nobel Lecture: Electronic structure of matter-wave functions and density functionals", Rev. Mod. Phys. 71, 1253 (1999).

[5]) to the much simpler *electronic density*, i.e. essentially to the squared modulus of the *N*-body wavefunction integrated over (*N*-1) of its variables.

In its original formulation, DFT only applies to the system's ground state: it can be found as the minimum of a suitable functional, with respect to the variation of the sole density. Only in 1984 DFT has been generalized by E.K.U. Gross to Time-Dependent DFT (TDDFT) [6], allowing one to study also the excited states. Hence, the available excited state theoretical and numerical tools, being about twenty years younger, are still much more primitive than those dedicated to the ground state, and much work remains to be done in their development.

Another important aspect which explains why the excited-state ab-initio methods are still in their early stage is related to the fact that excitations of many different types are possible, and different excitations often are better studied with different theoretical tools. As shown in Fig. 1, light absorption or electron energy-loss spectroscopy involve an excitation which does not change the number of electrons in the sample, while photoemission (PES), inverse photoemission (IPES), and scanning tunneling microscopy (STM) involve excited states with *N*-1 or *N* + 1 electrons, being hence directly related to the poles of the one-particle Green's function. Different methods, such as the GW method, the Bethe-Salpeter Equation (BSE) method, and the previously mentioned TDDFT, should be selected and used to study these different kind of excitations [7].

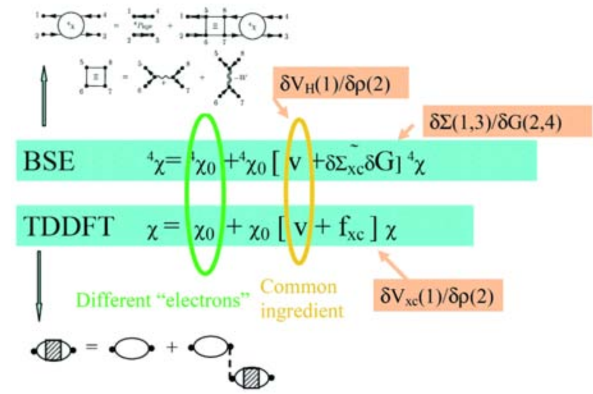

Fig.2
Schemes for computing the dynamical polarizability from an ab-initio point of view: Bethe-Salpeter Equation (top), or Time Dependent Density Functional Theory (bottom). See Ref. 7 for details.

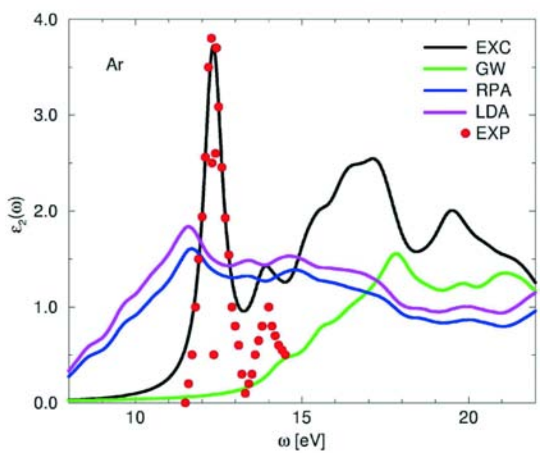

Fig.3
Optical Absorption spectrum of solid Argon (imaginary part of the dielectric function), computed at different levels of the theory: Independent particle (LDA bandstructure); Independent Quasiparticles with self-energy effects (GW); LDA plus Local Fields (RPA); Full calculation with excitonic effects (EXC). The last curve can be obtained either within the BSE scheme, or using TDDFT. Red dots are the experimental data.

Nowadays most of these ab-initio approaches can be applied to realistic and complex systems, such as surfaces [8] and nanostructures [9]. However, different degrees of approximation can be considered in order to be able to evaluate numerically the resulting equations and formulas. To this aim, it has revealed particularly useful to make an effort to compare efficiently different approaches, bringing them on similar grounds, and singling out the common ingredients and formulas. For example, this has been done by some of us in the case of TDDFT and BSE approaches in [7]. An example is shown in Fig. 2, where differences and similarities between the BSE and TDDFT equations for the system's polarizability are displayed.

Several successful applications of the ab-initio BSE and TDDFT approaches can be found in the recent literature (see, e.g., [10-12]). Between the most striking results, those concerning optical properties of solids and solid surfaces should be mentioned. In Fig. 3 we reproduce the absorption spectrum of solid Argon, which is very well described both within BSE and

REFERENCES
6. E.K.U. Gross, and W. Kohn, Phys. Rev. Lett. 55, 2850 (1985); 57, 923 (E) (1985).
7. G. Onida, L. Reining, and A. Rubio, "Electronic Excitations: Density-Functional versus Many-Body Green's Functions Approaches", Reviews of Modern Physics 74, 601 (2002).
8. K. Gaál-Nagy and G. Onida, "Ab-initio calculations of the optical properties of the Si(113)(3x2) ADI surface", in preparation.
9. M. Gatti and G. Onida, "Effects of oxidation on the optical properties of small silicon nanocrystals: the role of Local Fields", Phys. Rev. B 72, 045442 (2005).
10. M. Rohlfing, M. Palummo, G. Onida, and R. Del Sole, "Structural and Optical Properties of the Ge(111)-(2x1) Surface", Phys. Rev. Lett. 85, 5440 (2000).
11. E. K. Chang, M. Rohlfing, and S. G. Louie, "Excitons and Optical Properties of α-Quartz", Phys. Rev. Lett. 85, 2613 (2000).

TDDFT, while standard bandstructure calculation (RPA or independent quasiparticles approaches), neglecting the excitonic effects, fail to describe the absorption peaks, even qualitatively.

Other applications, between the most recent ones, are those realized by some of the authors in the case of semiconductor surfaces, namely silicon and oxidized silicon reconstructed surfaces. Fig. 4 shows surface optical anisotropic reflectivity spectra for the Si(100) surface, decomposed in its contributions coming from different layers below the surface [13]. This technique allows one to associate some of the spectral features to specific bonds or structures, like silicon dimers at the surface.

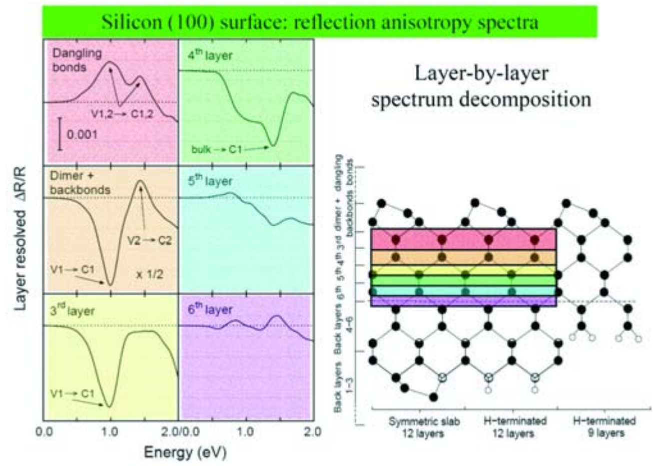

Fig. 4
Optical anisotropy spectra calculated for Si(100), an important surface of Silicon since it is used in microchips and semiconductor device technology. The possibility to look at contributions coming from different atomic layers is a nice example of the use of calculations as a "theoretical microscope" (see text).

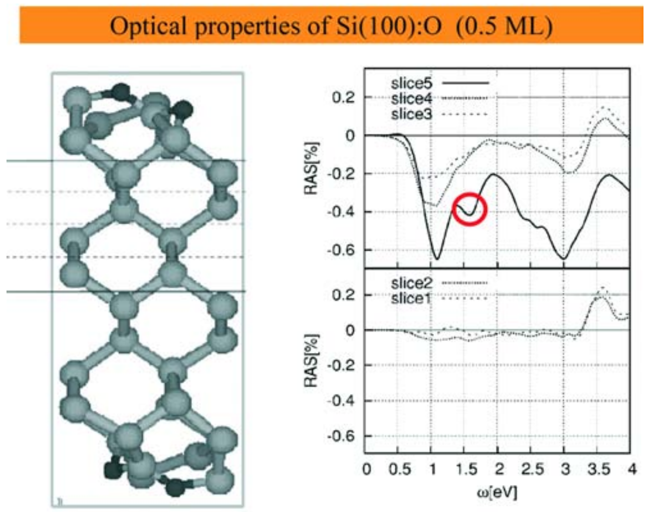

Fig. 5
Same as Fig. 4, but for a half-monolayer oxidized surface: the red circle shows a spectral feature which is associated to the presence of oxygen on surface dimers and backbonds.

Surface optical spectra are very sensitive to compositional and structural details. Si(100) has hence also been studied in presence of oxygen, in connection with its interest for semiconductor technology. In fact, thin oxide layers can be grown on Si(100) as insulating layers for building MOS devices. Fig. 5 shows a spectral feature which can be associated to the presence of oxygen atoms on specific adsorption sites, namely surface dimers and surface backbonds in a 0.5 ML oxygen-covered surface [14].

As shown by the examples above, the development and the numerical implementation of reliable ab-initio theoretical tools for computing the spectra of real systems is an important issue in today's condensed matter and solid state physics. In many cases, expertises from different research groups must be put together in order to realize and apply such tools in the most effective way. In fact, the demand for collaborations using state-of-the-art software -and for support- is rapidly growing, amongst both the theoretician and experimentalist communities. Starting from this observation, the idea of creating a dedicated collaborative structure was born, building on an existing 15-years ongoing and expanding collaboration between a number of condensed-matter theory groups in Europe.

In 2004, a NoE (network of excellence) named "Nanoquanta", funded by the European Community under the 6th Framework program, has been set up with the major aim to find a long-term answer to this challenge. Nanoquanta is a substantial undertaking, involving many

REFERENCES
12. L. Reining, V. Olevano, A. Rubio, and G. Onida, "Excitonic Effects in Solids Described by Time Dependent Density-Functional Theory", Phys. Rev. Lett. 88, 066404 (2002); A. Marini, R. Del Sole, and A. Rubio, "Bound Excitons in Time-Dependent Density-Functional Theory: Optical and Energy-Loss Spectra", Phys. Rev. Lett. 91, 256402 (2003).
13. C. Hogan, R. Del Sole, and G. Onida, PRB 68, 035405 (2003).
14. A. Incze, G. Onida, and R. Del Sole, "Ab initio study of reflectance anisotropy spectra of a sub-monolayer oxidized Si(100) surface", Phys. Rev. B 71, 035350 (2005).

research groups and interested users across Europe. Today, the ten nodes constituting the network are in charge of building up the so called "European Theoretical Spectroscopy Facility" (ETSF).

The ETSF, inspired to the large experimental facilities, will be a "knowledge center" in which expertise, theory, and the associated software for excited-state calculations will be developed and used in different ways, according to the interests and background of the users. Its aim will be to make available the "integrated resources" developed within Nanoquanta to a wide scientific community, after the end of the EU-funded period. These "integrated resources" consist in the theoretical tools, computer codes, and scientific know-how, which is strongly complementary between the groups forming our network. ETSF will be a distributed structure, with offices in different countries, and will be open to the insertion of new research groups which can contribute with their expertises, specially if it is complementary to the already present ones.

One of the primary objectives of ETSF will also be that of fostering the scientific and cultural interchange with researchers from other scientific disciplines, like chemists and biologists who could be interested in the use of theoretical tools and computational codes available within the ETSF.

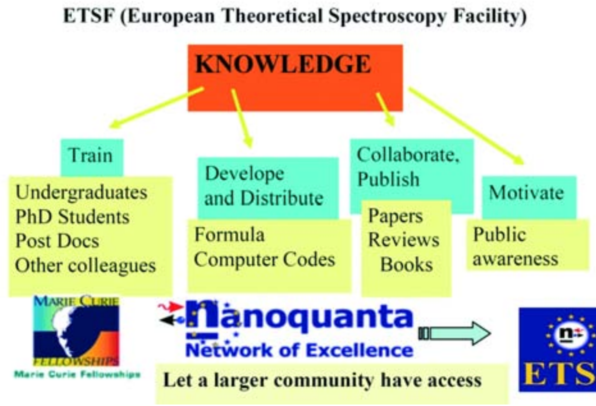

Fig. 6
The European Theoretical Spectroscopy Facility (ETSF), an initiative of the "Nanoquanta" Network of Excellence, has been devised to ease and encourage the sharing of theoretical tools and computer codes for the calculation of electronic excitations and related spectra. Significant progress has already been made, and the ETS Facility is planned to become a lasting structure after the end of the Nanoquanta NoE in 2008, independent of support from the EU.

The Nanoquanta groups will constitute the core of ETSF, which will also build a broad and federal community of research groups working on similar topics. Besides those groups directly involved in the theory and software development, users of the facility will be a larger and varied group, composed of researchers from the public and private sector wishing to benefit from the developments in the field of electronic excitations (see Fig. 6). The ETSF concept is hence introducing an important novelty with respect to the past, when EU and national organisations were supporting scientific collaborations for fundamental developments of theory and computational approaches by funding self-contained, fixed-term research projects and networks, with no permanent opportunity for other researchers to benefit from the "products".

Clusters in supersonic beams: from fundamental studies to applications, and the way back

P. Piseri[1,2,3], M. Amati[1,2,3], D. Bandiera[4], E. Barborini[4], M. Blomqvist[1], G. Bongiorno[1,3], F. Fiorentini[1], E. Gualandris[1], T. Mazza[1,3], A. Podestà[1,2,3], L. Ravagnan[1,2,3], S. Vinati[3], C. Lenardi[1,2,3], and P. Milani[1,2,3].

1 Dipartimento di Fisica, Università degli Studi di Milano.
2 CIMAINA, Università degli Studi di Milano.
3 CNR-INFM
4 Tethis s.r.l.
.

Free clusters are a system of choice for the investigation of the complex evolution of electronic and structural properties of condensed matter from those typical of molecular systems to bulk-like behaviour. Molecular beam techniques allow to prepare and manipulate such systems and to perform a variety of experiments but, with a major disadvantage; i.e. the sample is continuously destroyed shortly after being produced as the particles are only available before they hit the walls of the vacuum system. This characteristic implies that any in depth study on cluster beams is possible provided that a sufficiently intense and stable cluster source is on hand. The Molecular Beams an Nanocrystalline Materials Laboratory of our Department has a more than ten years history in the development of nanoparticle beams techniques; this paper will review the activity of the Lab in this field giving an example of the close connection that is often present between basic research and the development of new applications.

In the last decade, for the needs of basic research experiments on free aggregates, we developed a novel type of cluster source, the PMCS (Pulsed Microplasma Cluster Source), that performs very high intensity and stability for the production of refractory metal, metal oxide, and carbon clusters. A number of aerodynamic techniques taken from the aerosol science have been applied in the subsonic part of the flow inside the PMCS allowing a size selection of the particles and a further increase of the particle beam intensity by particle concentration on the beam axis. Present level of development of the cluster beam technique allowed us recently to perform for the first time a core-level absorption spectroscopy investigation on free refractory metal clusters. Besides of fundamental studies, this development proved also to be an enabling technology for more applicative studies on a new class of materials; the high intensity of the PMCS source made indeed viable the synthesis of cluster assembled materials. As a matter of fact, a possible approach to the controlled synthesis of nanostructured systems is the direct assembly of clusters onto a substrate, with the nanoparticles acting as building blocks for the growing material. Aerodynamically accelerated clusters have typical impact energies of few hundreds meV/atom, which is low enough to ensure a memory effect of their structure in the assembling of the material. The high directionality of molecular beams allows to fabricate microscopic patterns of nanostructued material by the simple use of stencil masks. This technique, the so called SCBD (Supersonic Cluster Beam Deposition), has a large potential for applications and has mostly been limited to date due to a lack of availability of suitable cluster sources on the market.

Introduction

Since the first observations of atomic like shell structures on sodium clusters depending on their size [1], the understanding of the size dependence of the electronic, optical and magnetic properties of clusters, i.e. finite aggregates up to tens of thousands of atoms, is a fascinating challenge for a vast community of researchers and is presently a key target in nanotechnology [2-4]. An important step for the attainment of this objective is the ability to investigate the nano-systems free from perturbations. The investigation of the "intrinsic" properties of clusters is very difficult: clusters are highly reactive and the interaction with solid or liquid matrices substantially affects their properties [5, 6]; deposited clusters may suffer from aggregation, coalescence, chemical contamination, or structure distortions, and a large uncertainty in their size determination affects their investigation [7]. Particles produced in the gas phase and, in particular, in supersonic expansions, represent the ideal "isolated" system where the nanoparticle mass and physical status can be precisely selected [8, 9], however the high degree of dilution makes the use of spectroscopic techniques based on electron or photon scattering and absorption a formidable challenge and mostly only the tools based on intense laser sources have been successfully applied [8].

REFERENCES
1. W.D. Knight, K. Clemenger, W.A. de Heer, W.A. Saunders, M.Y. Chou, M.L. Cohen, *Phys. Rev. Lett.* **52**, 2141-3 (1984).
2. J. Bansmann et al. *Surf. Sci. Rep*. **56**, 189–275 (2005)
3. B.von Issendorf, O. Cheshnovsky, *Annu. Rev. Phys. Chem.* **56**, 549-80 (2005)
4. T.P. Martin, (ed.) *Large clusters of atoms and molecules.* NATO ASI Series vol. 313 Kluwer, Dordrecht 1996
5. Z.V. Saponjic, et al. *Adv. Mater*. **17**, 965-971 (2005)
6. M.G. Mason, *Phys. Rev. B* 27, 748-762 (1983)
7. P. Milani, & S. Iannotta, *Cluster beam synthesis of nanostructured materials.* Springer Berlin 1999
8. E. Ruehl, I*nt. J. Mass Spectrom.* **229**, 117-142 (2003)
9. S.N. Khanna, A.W. Castleman, *Quantum phenomena in clusters and nanostructures.* Springer, Berlin 2003

From cluster beams to nanostructured materials:

In the last decade our group significantly contributed to the progress of the supersonic cluster beams technique [10], and owing to its success in the development of high intensity cluster sources, brought the SCBD (Supersonic Cluster Beam Deposition) technique to an industrial pre-competitive level [11]. SCBD is essentially the process of assembling aerodynamically accelerated clusters into a nanostructured film by particle deposition under high vacuum. A key factor for this success has been the introduction of a novel type of cluster source, the PMCS (Pulsed Microplasma Cluster Source) [12], that performs very high intensity and stability for the production of refractory metal, metal oxide, and carbon clusters. The working principle of the PMCS [12, 13] consists in the ablation of a target electrode by means of a spatially confined plasma discharge. The vaporized species are then quenched by a pulsed helium beam and condense into clusters. The relative high pressure in front of the cathode surface that can be seen in the simulation reported in the left side of figure 1 produces a localization of the discharge to a small region inside the source located at the surface of the eroded material. These conditions are favorable for a high degree of condensation and limited contamination from other source material.

One peculiarity of pulsed vaporization sources is that, unlike other supersonic cluster sources, condensation occurs mainly inside the source and not during the expansion. In this respect PMCS, like the laser vaporization sources for supersonic cluster beams developed in the eighties [14], is a sort of gas-aggregation device. This behavior makes the understanding of particle motion inside the source volume very important with regard to the maximization of beam intensity and the control of the particle size distribution. As a matter of fact, a number of aerodynamic techniques taken from the aerosol science can be successfully applied in the subsonic part of the flow inside this class of sources allowing a size selection of the particles and a further increase of the particle beam intensity by particle concentration on the beam axis [15]. A cluster density in the range of $10^{13}/cm^3$, as typically obtained by the PMCS, and the high stability of this source over many hours operation make this technology a candidate of choice for the industrial application of SCBD.

Supersonic cluster beams are characterized by high directionality, collimation, and intensity and thus are well suited for patterned deposition of films through stencil masks that are placed into the beam in front of the substrate [16, 17]. A remarkably high step sharpness (a width of 450 nm) could be obtained using a mask placed at 0.33 mm from the substrate [17]. The profile of the mask was reproduced even in its sub-micrometer features. By the use of micromachined masks patterns with micrometric pitch can be reproduced in the deposited material (see Fig. 1).

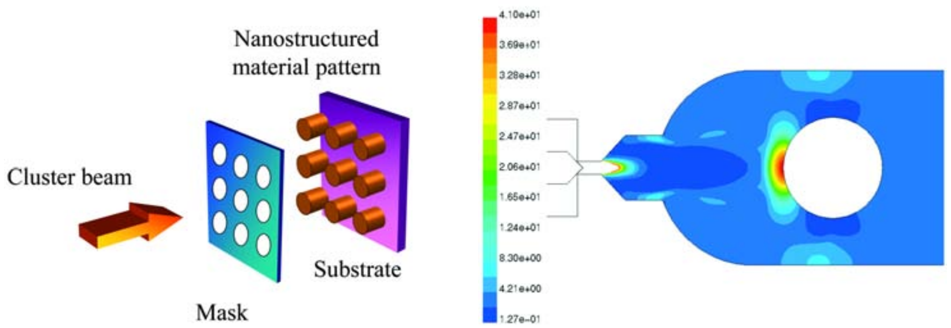

Fig. 1
a) Schematic representation of the Supersonic Cluster Beam Deposition method. The use of a stencil mask for the production of micropatterns of nanostructured material through the exploitation of the high directionality of the beam and the reduced diffusion of deposited aggregates is also illustrated. b) contour map of the gas pressure inside the PMCS source as obtained form numerical simulation with the FLUENT® code.

Supersonic expansions have a higher collimation compared to effusive beams, however, clusters in supersonic beams can still have a non negligible thermal divergence and a broad mass distribution [13]. In order to study the effect of the transverse cluster velocities on the step sharpness, films were deposited at different supersonic conditions by masking part of the substrate with a straight edge mask. Assuming the film thickness as a measure for the beam flux, integrated over the deposition time, the profile of the step obtained with the mask is affected by the distribution of cluster transverse velocities. With a standard supersonic beam the step is very noisy and not well defined. In order to increase the step sharpness one should increase the mach number of the beam but this will require a huge pumping system [13]. The use of particle focusing techniques can circumvent this problem by concentrating the clusters on the centre beam thus producing sharper steps still keeping intact the other expansion parameters. This has clear effects on the application of cluster beams to the deposition of nanostructured materials and systems as discussed in next section; nevertheless this has important consequences also on more fundamental studies on free clusters.

REFERENCES
10. K. Wegner, P. Piseri, H. Vahedi Tafreshi, P. Milani, *J. Phys* (in press, 2006).
11. Tethis srl is a spin-off company from the University of Milan founded in 2004, headquarters are in Milano, Piazzetta Bossi, 4 I-20121. contact: info@tethis-lab.com
12. E. Barborini, P. Piseri, and P. Milani, *J. Phys. D (Appl. Phys.)* **32**, 105 (1999).
13. P.Piseri, A.Podestà, E. Barborini, and P.Milani, *Rev. Sci. Instrum.* **72**, 2261 (2001).
14. R.W .Siegel, *Mater. Sci. Eng. B* **19**, 37 (1993).
15. P. Piseri, H. Vahedi Tafreshi, P. Milani. *Curr. Op. Solid State Mat. Sci.* **8** , 195 (2004).
16. T. Mazza, E. Barborini, I.N. Kholmanov, P. Piseri, G. Bongiorno, S. Vinati, P. Milani, C. Ducati, D. Cattaneo, A. Li Bassi, C.E. Bottani, A.M. Taurino, P. Siciliano, *Appl. Phys. Lett.* **87** 103108 (2005).
17. E. Barborini, P. Piseri, A. Podestà, P. Milani, *Appl. Phys. Lett.* **77** 1059 (2000).

Applications

Nanostructured carbon systems have been proposed as promising materials for electron field emission applications such as for the production of stable and inexpensive cold flat cathodes, as they might be superior to conventional materials in terms of extraction fields, current densities and site emission densities [19]. Using supersonic cluster beam deposition, we produced such carbon films on double polished *n*-doped monocrystalline silicon substrates [19]. The samples (heated during deposition) showed a stable and reproducible emission, a threshold field as low as 4 V/μm and a saturation current density of the order of 0.5 mA/cm^2. It was found that the presence of graphitic particles in the films substantially enhances the field emission performance. Working on patterned films (arrays of micrometric dots made by deposition through hard masks) in the ball-tip anode configuration, a localized effective conditioning could be obtained which led to an emission site density of 5 x 10^4 cm^{-2}.

Nanostructured carbon films made by supersonic cluster beam deposition over large areas were also applied for energy storage in supercapacitors [20, 21]. The carbon film electrodes showed high power density of 500 kW/kg and can be deposited at room temperature on thin foils, thus ensuring compatibility with actual manufacturing processes for supercapacitors.

Cluster beam deposition was then employed to fabricate 1-10 mm nanostructured carbon films for humidity sensing [21, 22]. The capacitive-type sensors were tested at relative humidity of 10-70 % and favourably compared to commercial devices. Using a titanium cathode in the PMCS we produced titania films deposited by SCBD on microfabricated substrates using stencil masks. The substrates were prepared with interdigitated gold electrodes in order to be used as gas sensors for volatile organic compounds [16]. A total of 210 sensors was made in one-step on an alumina wafer with a 14 x 15 array of contacts. Gradients in the anatase/rutile phase composition across the sensor array resulted in individual sensing elements with different performance. By using a combinatorial approach, such an array can give more reliable information then a single sensor.

The biocompatibility of nanostructured TiO_2 films produced by the deposition of a supersonic beam of TiOx clusters was characterized in the framework of a collaboration with the IEO (Istituto Europeo di Oncologia, in Milano) [23]. The cluster-assembled film supported normal growth and adhesion of primary and cancer cells with no need for coating with

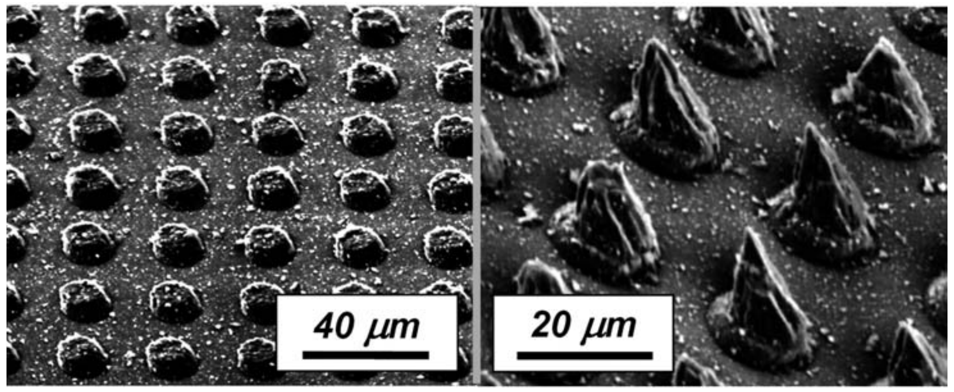

Fig. 2
Array of micron sized dots of SCBD nanostructured carbon. The field emission properties of a similar system have been investigated as a possible candidate for the chathode element in field emission display devices.

extracellular matrix proteins. Physical analysis showed that the films possess a nanoscale granularity and porosity mimicking that of typical extracellular matrix structures and adsorption properties that could allow surface functionalization with different macromolecules such as DNA, proteins, and peptides. Films of nanostructured titania are proposed as an optimal substrate for different applications in cell-based assays, biosensors, bioactive orthopedic, dental and vascular implants or microfabricated medical devices.

Free clusters

This paper was introduced with the citation of the beautiful fundamental results on free sodium clusters by Knight et al. in 1981 [1]; still, the study on free clusters is important on the application side for the comprehension of cluster assembling processes occurring in SCBD; exploring the correlation between the properties of free clusters and those of cluster – assembled materials is of paramount importance for the engineering of nanostructures.

One of the most powerful tools for the characterization of the local electronic structure, electronic density of states and correlation effects in the solid state is X-ray absorption spec-

REFERENCES
19. C. Ducati, E. Barborini, P. Piseri, P. Milani, J. Robertson, *J. Appl. Phys.* **92** 5482 (2002).
20. L. Diederich, E. Barborini, P. Piseri, A. Podestà, P. Milani, A. Schneuwly, R. Gallay, *Appl. Phys. Lett.* **75** 2662 (1999).
21. G. Bongiorno, A. Podestà, L. Ravagnan, P. Piseri, P. Milani, C. Lenardi, S. Miglio, M. Bruzzi, C. Ducati, *J. Mater. Sci.: Mater. Electron.* **17** 427 (2006).
22. M. Bruzzi, S. Miglio, M. Scaringella, G. Bongiorno, P. Piseri, A. Podestà, P. Milani *Sensors Actuators B* **100** 173 (2004).
23. R. Carbone, I. Marangi, A. Zanardi, L. Giorgetti, E. Chierici, G. Berlanda, A. Podestà, F. Fiorentini, G. Bongiorno, P. Piseri, P.G. Pelicci, P. Milani *Biomaterials* **27**, 3221 (2006).

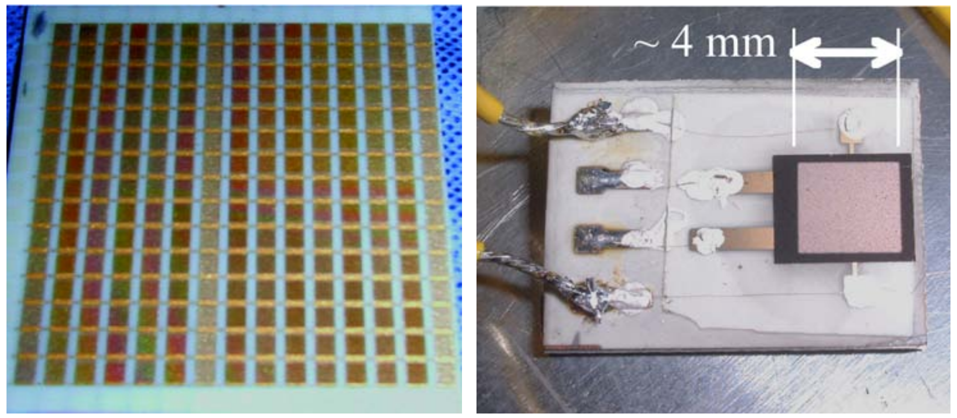

Fig. 3
a) a ns-C based capacitive type humidity sensor; b) batch deposited array of ns-TiO2 sensors. The sensing elements have been deposited by SCBD using aerodynamic separation for the production of a gradient in the phase composition across the array.

troscopy (XAS) using synchrotron radiation [24]. This technique is based on the excitation of electrons from deeply bound core levels to unoccupied levels. The core levels selected are element-specific and the spectrum is determined by the local surroundings of the excited atom [24]. The availability of high-brilliance, synchrotron radiation facilities has made possible the study of core-level excitation of free van der Waals and molecular clusters produced in supersonic beams [8, 25, 26]. Rare gases and volatile molecules condense into clusters very efficiently during a supersonic expansion [27], thus producing a particle density suitable for third generation synchrotron light sources [8, 28]. However despite widespread interest in free transition metal clusters, no results have been published to date on their core-level spectroscopy; this is due to the fact that available cluster sources cannot provide adequate cluster densities even for third generation synchrotron light sources. In this case, the difficulties related to free clusters' dilution are increased by the low absorption cross section for transition metal clusters (typically in the Mbarn range or below) [24]. To overcome these limitations the possible solutions are to increase the photon flux, or to develop high intensity cluster sources.

Owing to the high cluster beam intensity achieved by the use of the PMCS and aerodynamic focusing techniques our group recently obtained the first XAS characterization of free titanium clusters. The experiment was performed at the high flux beamline "GasPhase photoemission", a third generation light source of the Elettra synchrotron radiation facility in Trieste, Italy) [28, 29]. In Fig. 4 we show a schematic representation of the experimental set-up.
The most prominent features observed by a size resolved analysis of the XAS data (a study of the White Line intensity [30]) correspond to the highest cluster mass abundances in our mass spectra and fit with the second and third geometric shell closings of icosahedral or cuboctahedral systems (at 55 and 147 atoms/cluster) [31]; a distinct change in the behaviour is observed instead around 540 atoms/cluster, corresponding to the region of the closing of the fifth atomic shell at 561 atoms/cluster (see Fig. 5). To summarize, the X-ray absorption spectroscopy indicates that free titanium clusters, in mass range between 15 up to 1000 atoms per cluster, have a core-level electronic structure where atomic-like and bulk-like features coexist. The geometric structure of the clusters reflect on the electronic structure showing regularities compatible with icosahedral or cuboctahedral structure up to the fifth shell closing, where possibly a structural transition takes place.

REFERENCES
24. J. Stöhr, *NEXAFS Spectroscopy*, Springer Series in Surface Sciences, Berlin, 2003.
25. F. Federmann, O. Bjoerneholm, A. Beutler, T. Möller, *Phys. Rev. Lett.*, **73,** 1549-1552 (1994).
26. M. Tchaplyguine, et al. *J. Chem. Phys.*, **120**, 345 (2004).
27.O.F. Hagena,; W. Obert, *J. Chem. Phys.*, **56,** 1793 (1974).
28. R. Karnbach, M. Joppien, J. Stapelfeldt, J. Woermer, T.Möller, *Rev. Sci. Instrum.*, **64**, 2838 (1993).
29. R.R. Blyth, et al. *J. Electron Spectrosc. Relat. Phenomena*, **101/103,** 959 (1999).
30. P.Piseri et al, *New J. Phys* (in press 2006).
31. T. P. Martin, T.Bergmann,; H. Goehlich, T. Lange, *J. Phys. Chem.*, **95,** 6421 (1991).

FURTHER AFFILIATIONS
a. Department of Material Science and Metallurgy, University of Cambridge, Cambridge CB2 3QZ, UK
b. Montena SA, Switzerland now Maxwell Technologies, USA
c. Univ. di Firenze, Dipartimento di Energetica, Via S. Marta 3, 50139 - Firenze
d. IEO, Milano; present address Tethis srl, Via Russoli 3, 20151 - Milano
e. ETH, Zuerich & Tethis srl, Milano
f. NCRC, North Carolina State University, 2401 Research Dr., Raleigh, NC 27695-8301, USA
g. CESNEF, Politecnico di Milano
h. CNR IMIP & GasPhase Beamline, Sincrotrone Trieste

Conclusion

In this paper a selected number of examples from the recent history of the Molecular Beams and Nanocrystalline Materials Laboratory has been presented; the strong correlation and interdependence of technological advance and progress in fundamental science issues clearly appears in the background of the presented picture.

Acknowledgments

The work reviewed in the present paper could not be produced without the help of a vast number of collaborators among whom we like to cite C. Ducati [a], R. Gallay [b], M.Bruzzi [c], R. Carbone [d], K.Wegner [e], H. Vahedi Tafreshi [f], F. Di Fonzo [g], M. Coreno [h].

Fig. 4
Schematic representation of the experimetal setup for mass resolved XAS studies of free clusters in a molecular beam. The mass of Ti clusters is determined after core photo-ionization by time of flight mass spectrometry (TOF/MS) in a Photo-Electron – Photo-Ion Coincidence scheme (PEPICO).

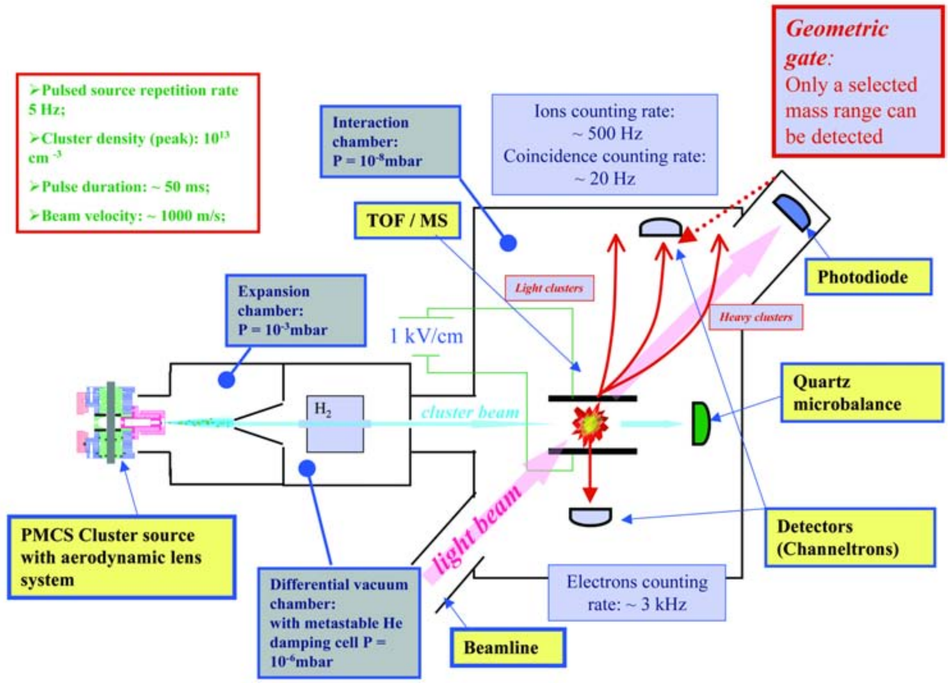

Fig. 5
Evolution of the White-Lines intensity with cluster size (Intensity of the L23 X-ray absorption resonances compared to the absorption in the continuum region see ref. 30 for a detailed discussion).

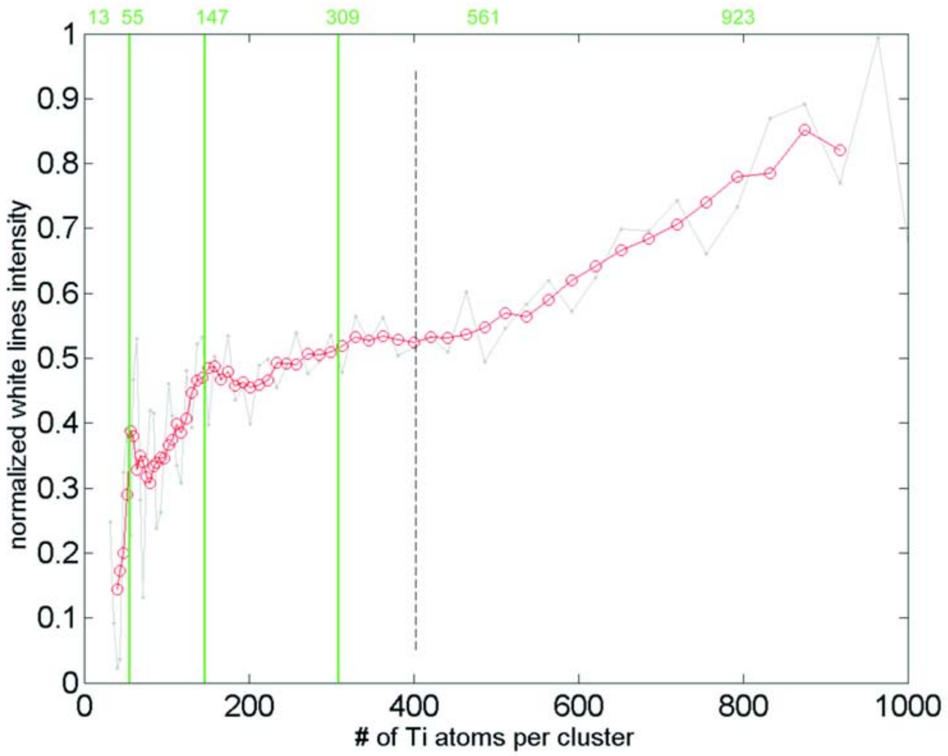

Quantum transport in carbon nanotubes

M. Baxendale[1], M. Melli[2], and I. Pollini[2]

1 University of London, Queen Mary and Department of Physics, London, UK
2 Dipartimento di Fisica, Università degli Studi di Milano

Electronic transport in nanometer structures has novel characteristics. In an ideal mesoscopic conductor the resistance is not proportional to the ratio between its length and section (Ohm's Law), but it is independent of the length and quantized in the universal unit $R_0 = h/2e^2 = 1/G_0$. This is due to the electron transversal confinement and the ballistic nature of the transport. In fact, the electron free mean path is longer than the conductor itself. To study real systems the Landauer formalism is used: the electrical current is expressed as a function of the probability that an electron can transmit through the conductor. The possibility of manufacturing nanometer circuits with advanced lithographic techniques allows proving this theory experimentally. However, there are objects which are intrinsically mesoscopic due to their dimensions, as carbon nanotubes (CNTs), which are cylindrical macromolecules formed by periodic hexagonal structures of carbon atoms. They can be made by one single wall nanotube (SWNT) or more coaxial multiwall nanotubes (MWNTs), whose length is of the order of micron and diameter of nanometer.

In the literature SWNTs are classified as mono-dimensional, ballistic conductors with conductance $G = 2G_0$, while MWNTs, which are still mono-dimensional ballistic conductors, may present an anomalous quantization (as for instance $G = 0.5\ G_0$) not well understood. As a contribution to this research, we have performed measurements on the conductance of both SWNT and MWNT samples at room temperature. As for the MWNTs we have studied the simplest of them, the double wall nanotubes (DWNTs), and we have modified a technique used for the study of the atomic wires which are formed between two separating metallic surfaces. By sampling with an appropriate frequency the voltage time evolution between two parting contacts through which the electric current flows, it is possible to observe the system just before their opening. In our set-up some powder of CNT bundles has been glued on the contacts, and images from the high-resolution electronic microscope have revealed that long single nanotubes can protrude from the bundles. Therefore, by changing the sample time, we can measure the conductance of the single nanotubes. Besides, this technique allows to collect the data automatically and to obtain a good statistics. Our results, where the conductance is analyzed by the histogram technique, are shown in Figs. 1 and 2.

In conclusion, we have observed the electronic transport in CTNs at room temperature, which is found to be ballistic. For single SWNTs the histograms show peaks at integer values of the conductance quantum G_0, and in particular the lowest observed value $2\ G_0$ shows that there are two channels crossing the Fermi energy. As for the DWNTs we have found two types of ballistic pathways, whose conductance is $1\ G_0$ and is also between 2 and $5\ G_0$. The anomalous conductance value $1\ G_0$ (or even $0.5\ G_0$) can arise from interwall interactions and is due to the metallic sub-bands. Instead, the higher values of the conductance between $2\ G_0$ and $5\ G_0$ may be due to excitations of semi-conducting sub-bands of the band structure diagram. From our results we can also conclude that the total conductance in MWNTs is not simply due to the sum of each sub-band conductance. Further theoretical and experimental investigations at high voltages are in order to better understand this important aspect of the CNTs.

Fig. 1
SWNT conductance histogram corrected with a serial resistance of 720 ohm.

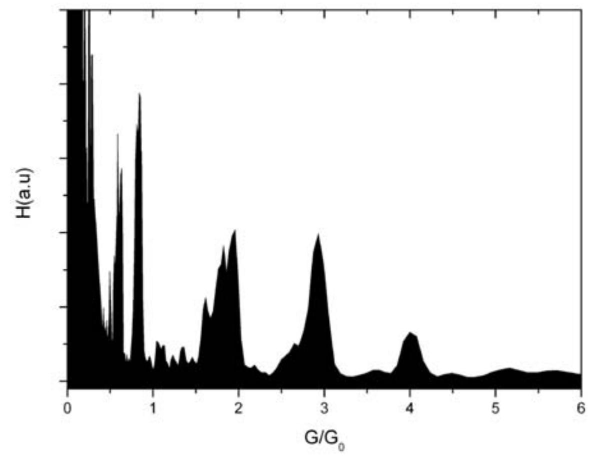

Fig. 2
DWNT conductance histograms:
a) 0.37; b) 0.76; c) 1.15 and d) 1.35 V.

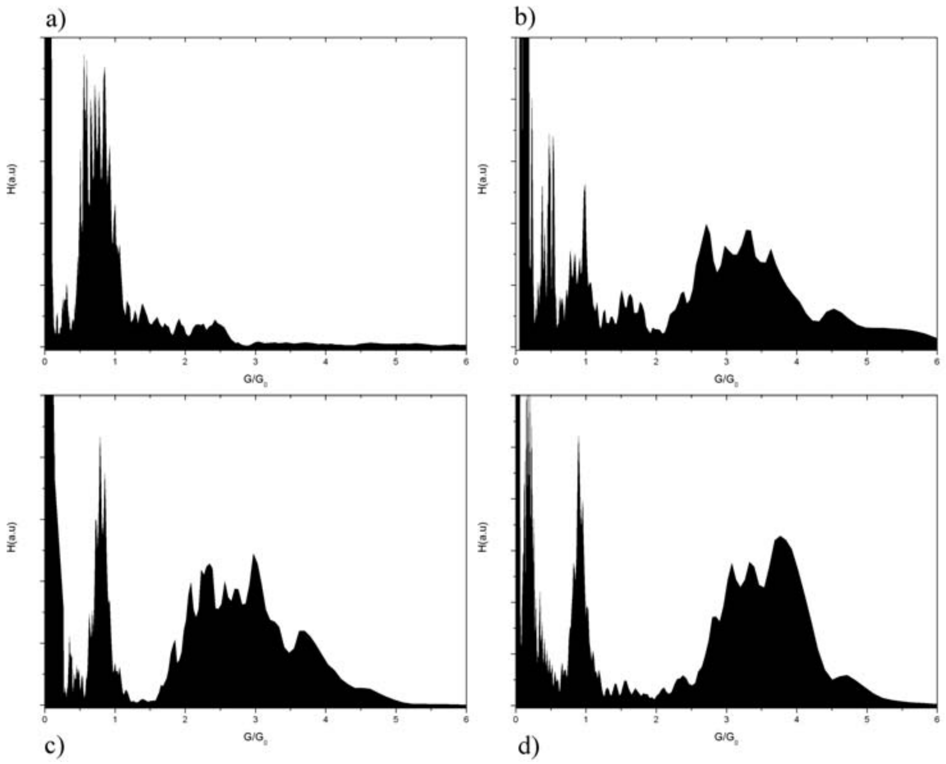

Fluctuations and pattern formation in fluids with competing interactions

A. Imperio[1], A. Parola[2], D. Pini[3], and L. Reatto[3]

1 CNISM, Università degli Studi di Milano
2 Dipartimento di Scienze Fisiche, Università dell'Insubria
3 Dipartimento di Fisica, Università degli Studi di Milano

The soft-matter realm encompasses systems as diverse as colloidal dispersions, biopolymer solutions, dendrimers, and liquid crystals. One of the most interesting phenomena in this field consists in the spontaneous formation of super-molecular structures. A simple mechanism responsible for this self-organization is based on the competition between attractive and repulsive forces with different characteristic lengths in the microscopic potential, typically, a short-range attractive interaction against a longer-range, repulsive one.

We have analyzed this problem by simulation in bidimensional fluids [1], which are relevant for modeling Langmuir monolayers and ferrofluids. We find that, as the temperature is lowered, liquid-vapor phase separation is inhibited by the competition between repulsion and attraction, and replaced by a transition to non-homogeneous phases. At low average density, we observe the formation of a fluid-like phase of disordered droplet-shaped clusters. As the density increases, the droplets become larger and tend to arrange into a triangular lattice. However, above a certain density the morphology changes and stripes are formed. Close to the transition from the microphases to the homogeneous fluid, the specific heat exhibits a peak which is due to the breaking up of clusters. This peak appears to be quite insensitive to the system size, thereby ruling out a first-order transition or a critical point, and suggesting instead the possibility of a Kosterlitz-Thouless transition. The structure of the fluid shows well defined signatures of the presence of both intra- and inter-cluster correlations. The latter appear as sharp peaks at small wave vector k in the structure factor $S(k)$, whose symmetry is related to the possible occurrence of a cluster superlattice.

Even when the competition between attraction and repulsion is not so strong as to cause microphase formation, it still induces large density fluctuations in a wide region of the temperature-density plane [2]. In this large-fluctuation regime, pattern formation can be triggered by a weak external modulating field [1].

REFERENCES
1. Imperio A. and Reatto L., "A bidimensional fluid system with competing interactions: spontaneous and induced pattern formation" J. Phys.: Condens. Matter 16, S3769 (2004).
2. Pini D., Jialin G., Parola A., and Reatto L., "Enhanced density fluctuations in fluid systems with competing interactions", Chem. Phys. Lett. 327, 209 (2000).

Optical properties of PPV and PPV-carbon nanotube thin films

E. Mulazzi[1], R. Perego[1], H. Aarab[2], F. Massuyeau[2], S. Lefrant[2],
E. Faulques[2], and J. Wéry[2]

We present experimental and calculated optical absorption, photoluminescence (PL) and Raman scattering spectra of PPV thin films and of PPV-carbon nanotube (SWCNT) composite films. In particular we study the changes of PL spectra of PPV films as function of sample thickness and of PPV-SWCNT compounds at different SWCNT concentration (x = 0%-64%) and as function of precursor conversion temperature. Dramatic changes are observed in all these spectra with respect to the ones reported for standard PPV films [1]. By the analysis of the PL spectra it is found that the modifications induced in the band shapes due to low conversion temperature are similar to those due to the increase of the SWCNT concentration x in the samples and to the decrease of the film thickness. In fact in all these conditions the PL spectra peaks which are determined by the short segment transitions become more intense with respect to those due the longer segment contributions. This trend is also observed in optical absorption and Raman scattering spectra recorded in the same conditions. A theoretical model based on the distributions of PPV conjugated segments of different lengths and on their electronic and vibrational properties is able to reproduce all these spectra in very good agreement with the experimental data, taking into account all the band shape changes recorded [1-3]. In addition, from the modifications of the band relative intensities in the PL spectra, taken at 300K and 77K, we can prove, by using the same model as proposed in [2,3], that the temperature dependent charge migration process between segments is the most important mechanism for the energy transfer from short to long conjugated segments. In fact in standard PPV samples at 300K, the peak which is determined by the emission transitions occurring on long segments, constitutes the most intense feature of the spectra. On the contrary, at 77K, due to the hindered charge migration, all the peaks which are due to the radiative recombinations on the short segments become more intense with respect to all the other features in the spectra.

Solitons in attractive Bose-Einstein condensates

L. Salasnich[1], A. Parola[2], and L. Reatto[1]

1 Dipartimento di Fisica and CNISM, Università degli Studi di Milano
2 Dipartimento di Fisica e Matematica, Universita dell'Insubria

Over one hundred and fifty years ago, while conducting experiments to determine the most efficient design for canal boats, a young Scottish engineer named John Scott Russell (1808-1882) made a remarkable scientific discovery: a solitary wave travelling in a narrow channel for chilometers without deformations and diminution of speed [1]. Such waves, now called solitons, are shape-invariant due to the interplay between the dispersive term and the nonlinear term of the equations of motion. It is now clear that solitons can be found in many fields of research: hydrodynamics, light pulses in optical fibers, plasma physics, elementary particles of matter, and many others [2].

In 2002, for the first time, single and multiple bright solitons have been produced with Bose-Einstein condensates made of 7Li atoms [3]. A Bose-Einstein condensate (BEC) is a macroscopic quantum matter wave. A BEC is made of large number of bosons, which are all in the same quantum state. The complex macroscopic wave function of the BEC is described by the time-dependent Gross-Pitaevskii equation (GPE). In the GPE the kinetic term is dispersive but its effect can be balanced by a self-focusing attractive nonlinear term giving rise to bright solitons [4]. This is the case of 7Li atoms where the inter-atomic scattering length is negative. The atom wave solitons may be useful as the atom laser input to an atom interferometer.

Recently we have investigated static and dynamical properties of an attractive BEC in a quasi-1D ring. By using the GPE we have proved that the system has a transition from a uniform state to a localized solitonic state, which collapses at a critical interaction strength. In addition, we have found that the Bose condensate supports also multi-peak solitons. Finally, we have shown that the phase diagram of the system strongly changes if the trap is set into rotation [5]. We are now studying quantum depletion and finite-temperature effects on such a system.

REFERENCES
1. Scott Russell J., XIV meeting of the British Association for the Advancement of Science, York, September 1844 (London 1845), pp 311-390, Plates XLVII-LVII
2. Drazin P.G. and Johnson R.S., Solitons: an Introduction (Cambridge University Press, Cambridge, 1989)
3. K.E. Strecker et al, Nature 417, 150 (2002); Khaykovich L. et al., Science 296, 1290 (2002)
4. Salasnich L., Parola A., and Reatto L., Physical Review A 66, 043603 (2002); Salasnich L., Parola A., and Reatto L., Physical Review Letters 91, 080405 (2003)
5. Salasnich L., Parola A., and Reatto L., Physical Review A 72, 063612 (2005)

Quantum Optics, Coherent Phenomena, and Optoelectronics

Photon statistics without photon counting

A.R. Rossi [1], S. Olivares [1], and M.G.A. Paris [1]

1 Dipartimento di Fisica, Università degli Studi di Milano

Abstract

An indirect method to obtain the photon distribution of a single-mode field using only on/off avalanche photodetectors is suggested. The method is based on measuring the field at different quantum efficiencies and then inferring the photon distribution by maximum-likelihood estimation. It works with a limited range of quantum efficiency values and even when these values are not precisely known. The method has been successfully applied experimentally to the reconstruction of photon number distributions of continuous-wave and pulsed light beams, both semiclassical and quantum states of light, single-mode as well as for multimode beams.

The statistical distribution of the number of photons provides fundamental information on the nature of any optical field. The choice of a detector suitable for the measurement is not trivial when the flux of the photons to be counted is such that more than one photon is detected in the time-window of the measurement, which is set by the detector pulse-response, or by an electronic gate on the detector output, or by the duration of the light pulse. In this case, we need a congruous linearity in the internal current amplification process: each of the single electron produced by the different photons either by ionization or by promotion to a conduction band must experience the same average gain and this gain must have sufficiently low spread. The fulfillment of both requisites is necessary for the charge integral of the output current pulse be proportional to the number of detected photons. Photon detectors that can operate as photon counters are rather rare. Among these, PhotoMultiplier Tubes (PMT's) [1] and hybrid photodetectors [2] have the drawback of a low quantum efficiency, since the detection starts with the emission of an electron from the photocathode. Solid state detectors with internal gain, in which the nature of the primary detection process ensures higher efficiency, are still under development. Highly efficient thermal detectors have also been used as photon counters, though their operating conditions are still extreme (cryogenic conditions) to allow common use [3,4]. The advent of quantum tomography provided an alternative method to measure photon number distributions. However, the tomography of a state, which has been applied to several quantum states [5] needs the implementation of homodyne detection, which in turn requires the appropriate mode matching of the signal with a suitable local oscillator at a beam splitter. Such mode matching is a particularly challenging task in the case of pulsed optical fields.

Photodetectors that are usually employed in quantum optics such as Avalanche PhotoDiodes (APD's) operating in the Geiger mode [4,6] seem to be by definition useless as photon counters. They are the solid state photodetectors with the highest quantum efficiency but they have the obvious drawback that the breakdown current is independent of the number of detected photons, which in turn cannot be determined. The outcome of these APD's is either "off" (no photons detected) or "on" *i.e.* a "click", indicating the detection of one or more photons. Actually, such an outcome can be provided by any photodetector (PMT, hybrid photodetector, cryogenic thermal detector) for which the charge contained in dark pulses is definitely below that of the output current pulses corresponding to the detection of at least one photon. Note that for most high-gain PMT's the anodic pulses corresponding to no photons detected can be easily discriminated by a threshold from those corresponding to the detection of one or more photons.

The statistics of the "no-click" and "click" events from an on/off detector, assuming no dark counts, is given by

$$p_0(\eta) = \sum_n (1-\eta)^n \rho_n\,, \qquad p_{>0}(\eta) = 1 - p_0(\eta)\,, \tag{1}$$

where ρ_n is the photon distribution of the quantum state ρ and η is the quantum efficiency of the detector, *i.e.* the probability of a single photon to be revealed. At first sight the statistics of an on/off detector appears to provide quite a scarce piece of information about the state under investigation. However, if the statistics about $\rho_0\ (\eta)$ is collected for a suitably large set of efficiency values then the information is enough to reconstruct the whole photon distribution ρ_n of the signal, upon a suitable truncation at $\underline{n}$ of the Hilbert space. The reconstruction of photon distribution through on/off detection at different efficiencies has been analyzed [7] and its statistical reliability investigated in details [8]. In addition, the case of few and small values of η [9] has been addressed. These theoretical studies found an application to realize a multichannel fiber loop detector [10,11] and, most importantly, for reconstructing the photon distribution of a free-propagating field [12]. In view of the relevance of photon distribution for applications in quantum information and foundations of quantum mechanics, our purpose is to show that a reconstruction of the photon distribution by using this technique can be effectively realized gathering results obtained from measurement at different quantum efficiencies. As we will see this method leads to excellent results both for free-propagating continuous-wave (cw) and pulsed light beams, for both single-mode semiclassical and quantum states, as well as for multimode states.

The procedure consists in measuring a given signal by on/off detection using different values η_ν (ν = 1,...,K) of the quantum efficiency. The information provided by experimental data is contained in the collection of frequencies $f_\nu = f_0(\eta_\nu) = n_{0\nu}/n_\nu$ where $n_{0\nu}$ is the number of "no-click" events and n_ν the total number of runs with quantum efficiency η_ν. Then we consider expression (1) as a statistical model for the parameters ρ_n to be solved by maximum-likelihood (ML) estimation. Upon defining $p_\nu = p_0(\eta)$ and $A_{\nu n} = (1-\eta_\nu)^n$ we rewrite expression (1) as $p_\nu = \Sigma_n A_{\nu n}\, \rho_n$. Since the model is linear and the parameters to be estimated are positive (LINPOS problem), then the solution can be well approximaed by using the Expectation-Maximization algorithm (EM) [13]. By imposing the restriction $\Sigma_n\, \rho_n = 1$ we obtain the iterative solution

$$\rho_n^{(i+1)} = \rho_n^{(i)} \sum_{\nu=1}^{K} \frac{A_{\nu n}}{\sum_\lambda A_{\lambda n}} \frac{f_\nu}{p_\nu[\{\rho_n^{(i)}\}]} \tag{2}$$

where $p_\nu\,[\{\rho_n(i)\}]$ are the probabilities as calculated by using the reconstructed distribution at the *i*-th iteration.

Before briefly describing the experimental results we report on the accuracy and reliability of the method. Since the solution of the ML estimation is obtained iteratively, the most important aspect to keep under control is its convergence. A suitable parameter to evaluate the degree of convergence at a given step is the total absolute error at the *i*-th iteration *i.e.*

$$\varepsilon^{(i)} = \sum_{\nu=1}^{K} \left| f_\nu - p_\nu[\{\rho_n^{(i)}\}] \right| \tag{3}$$

Indeed, the total error measures the distance of the probabilities calculated at the *i*-th iteration, from the actual experimental frequencies and thus, besides convergence, it quantifies how the estimated distribution reproduces the experimental data. The total distance is a decreasing function of the number of iterations. Its stationary value is proportional to the accuracy of the experimental frequencies. For finite data sample this value is of order $1/n_\nu^{1/2}$ for each value of the quantum efficiency giving us a rough estimate of $\underline{n}/n_\nu^{1/2}$ for the total error. If the stationary value of $\varepsilon^{(i)}$ is of this order, we have double checked the convergence of the whole method. Notice that these properties are not shared by the log-likelihood: its stationarity certainly reveals convergence, but the stationary value depends on the statistics to be retrieved and so can not even be estimated by *a priori* considerations. In order to check the convergence of the iterations in (2), we run simulated experiments to reconstruct some of the states subsequently investigated experimentally. The results show that the total error has a transient behaviour and then quickly converges to its stationary value. The rate of convergence depends on the signal under investigation. Our results show that the iterative algorithm always converges and the asymptotic value of $\varepsilon^{(i)}$ is of the expected order of magnitude. An estimate of the confidence interval on the determination of the element ρ_n can be given in terms of the variance $\sigma_n = N\, F^{-1/2}$, N being the total number of measurements, and F the Fisher's information [14]. Notice that the algorithm provides a solution once an initial distribution $\rho_n^{(0)}$ is chosen. A convenient setting is the uniform distribution $\rho_n^{(0)} = (1+\underline{n})^{-1}$ in $[0,\underline{n}]$. Other choices however, the only constraint being $\rho_n^{(0)}$ different from zero, do not influence the convergence properties of the algorithm. Finally, in order to check robustness, simulated experiments have been performed where, during the run, the quantum efficiency may fluctuate. The reconstructions are not dramatically affected by fluctuations, though errors bars are sli-

REFERENCES
1. G. Zambra, M. Bondani, A. S. Spinelli, A. Andreoni, Rev. Sci. Instrum. **75**, 2762 (2004).
2. E. Hergert, Single Photon Detector Workshop, Gaithersburg, NIST (2003).
3. J. Kim, S. Takeuchi, Y. Yamamoto, and H.H. Hogue, Appl. Phys. Lett. **74,** 902 (1999); A. Peacock, P. Verhoeve, N. Rando, A. van Dordrecht, B. G. Taylor, C. Erd, M. A. C. Perryman, R. Venn, J. Howlett, D. J. Goldie, J. Lumley, and M. Wallis, Nature **381**, 135 (1996).
4. G. Di Giuseppe, A. V. Sergienko, B. E. A. Saleh, and M. C. Teich in *Quantum Information and Computation*, E. Donkor, A. R. Pirich, and H. E. Brandt Eds., Proceedings of the SPIE **5105**, 39 (2003).
5. M. Raymer, M. Beck in *Quantum states estimation*, M. G .A Paris and J. Rehacek Eds., Lect. Not. Phys. **649** (Springer, Berlin-Heidelberg, 2004).
6. F. Zappa, A. L. Lacaita, S. D. Cova, and P. Lovati, Opt. Eng. **35**, 938 (1996); D. Achilles, C. Silberhorn, C. Sliwa, K. Banaszek, and I. A. Walmsley, Opt. Lett. **28**, 2387 (2003).
7. D. Mogilevtsev, Opt. Comm **156**, 307 (1998).
8. A. R. Rossi, S. Olivares, and M. G. A. Paris, Phys. Rev. A **70**, 055801 (2004).
9. A. R. Rossi and M. G. A. Paris, Eur. Phys. J. D **32**, 223 (2005).
10. J. Rehacek, Z. Hradil, O. Haderka, J. Perina, Jr., and M. Hamar, Phys. Rev. A **67**, 061801(R) (2003).
11. K. Banaszek, I. A. Walmsley, Opt. Lett. **28**, 52 (2003).
12. M. Bondani et al, Phys. Rev. Lett. **95**, 063602 (2005).
13. A.P. Dempster, N.M. Laird, D.B. Rubin, J. R. Statist. Soc. B **39**, 1 (1977); Y. Vardi and D. Lee, J. R. Statist. Soc. B 55, 569 (1993).
14. H. Cramer, *Mathematical Methods of Statistics*, Princeton University Press, Princeton, NJ, 1946.

ghtly larger.

The method has been successfully applied experimentally to the reconstruction of photon number distributions of continuous-wave and pulsed light beams, both semiclassical and quantum states of light, single-mode as well as for multimode beams. In Fig. 1 we report the reconstruction of a continouos-wave single photon state that have been generated by producing Parametric Down Conversion (PDC) heralded photons and of a pulsed multithermal state obtained from the blue portion of the down conversion fluorescence produced by a type I BBO crystal.

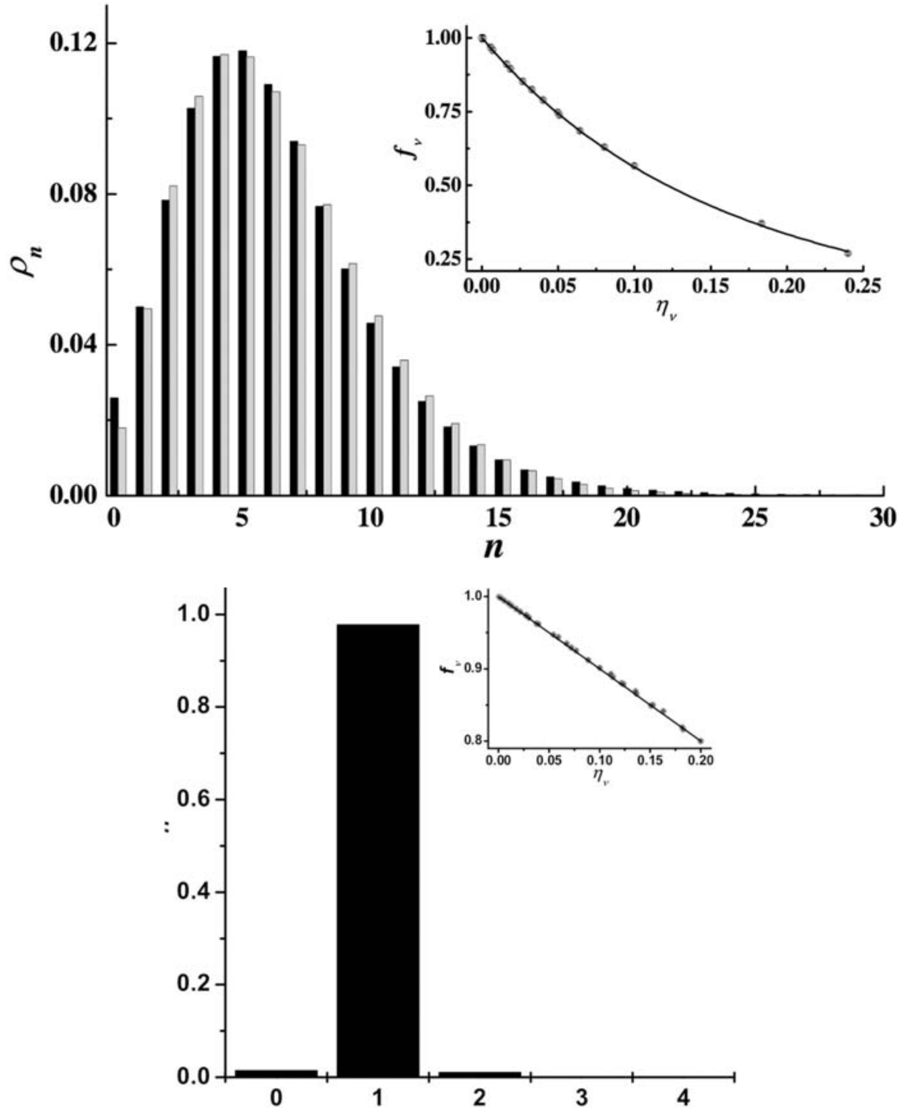

Fig. 1
Top: reconstruction of the photon distribution for a heralded single-photon state produced in type II PDC; inset: experimental frequencies f_ν of no-click events as a function of the quantum efficiency compared with the theoretical curve. Bottom: reconstructed photon distribution and best theoretical fit (grey bars) for a multimode thermal state produced in type I PDC; insets: experimental data frequencies f_ν as a function of the quantum efficiency compared with the theoretical curve.

Concerning the cw beam: a pair of correlated photons has been generated by pumping a type II β–Barium-Borate (BBO) crystal with a cw Argon ion laser beam (351 nm) in collinear geometry. After splitting the photons by a polarizing beam splitter, the detection of one of the two by an avalanche photodiode detector (SPCM-AQR-15, Perkin Elmer) is used as trigger for the presence of the second photon in the other channel, namely a window of 4.9 ns was opened for detection in arm 2 in correspondence to the detection of a photon in arm 1. This “heralded photon” was then measured by a silicon avalanche photodiode detector (SPCM-AQR-15, Perkin Elmer) preceded by an iris and an interference filter (IF) at 702 nm, 4 nm FWHM, inserted with the purpose of reducing the stray light. The quantum efficiency of the detection apparatus (including IF and iris) was measured to be 20% by using the PDC calibration scheme (see [15]) Lower quantum efficiencies were simulated by inserting calibrated neutral optical filters on the optical path. A comparison of the observed frequencies with the theoretical curve is presented in the inset of Fig. 1 (left). The photon distribution has been reconstructed using K = 34 different values of the quantum efficiency from zero to 20% with $n_\nu = 10^6$ runs for each η_ν. Results at iteration $i = 10^6$ are shown in Fig. 1. As expected, the PDC heralded photon state largely agrees with a single photon Fock state. The small ρ_2 contribution is expected, by estimating the probability that a second photon randomly

REFERENCES
15. G. Brida, M. Genovese, and C. Novero, J. Mod. Opt. **47**, 2099 (2000).

enters the detection window, to be 1.85% of ρ_1, in agreement with what observed. A non zero ρ_0 is also expected due to background. Also this estimate is in good agreement with the reconstructed ρ_0.

As concern the pulsed regime: the measurement was performed on the blue portion (420 nm) of the down conversion fluorescence produced by a type I BBO crystal (10 mm depth, cut at 34 deg) pumped by the laser pulse. The pump, incident orthogonally to the crystal face, had an intensity about 60 GW/cm^2. In this experimental condition we expect a coherence time of the generated field of about 1 ps, that corresponds to measuring a convolution of 4-5 temporal modes. The photon number distribution is expected to be a multithermal one. The photon distribution reconstructed at the $i = 1.5 \times 10^4$ iteration, is shown in Fig. 1 (top) along with the expected result. In the inset of the figure we show the experimental frequency f_ν data (K = 18 values of η, 10^4 runs for each η) and their theoretical values.

As to the comparison of the present technique with other schemes to reconstruct the photon distribution we have to distinguish between CW and pulsed regime. For CW field an alternative technique is represented by quantum homodyne tomography (QHT), which has indeed been applied to the reconstruction of single-photon and single-photon added states of light [16]. The advantage of our technique compared to QHT is twofold. On one hand qht requires, for the same task, a more complex apparatus and high-efficiency photodetectors. On the other hand, QHT is more noisy. In fact, homodyne data contains the whole information about the state under investigation (not only the photon distribution) and, in turn, this results in a more noisy determination when only part of the information is of interest [17]. In order to obtain results such those of Fig. 1 QHT requires a by far larger set of data. In the pulsed regime, where realization of QHT is still challenging, the direct measurement of the photon statistics can be conveniently done by PMT’S or hybrid photodetectors [1,2]. However, owing to limitations of the values of the maximum detection efficiency, results at number of photons as low as those in Fig. 1 cannot be obtained by PMT’S and are at limit of feasibility for hybrid photodetectors. While our method is particularly suited to measure the photon distributions of low-intensity field, where the above detectors are not effective, it can be always applied to higher intensity fields.

In conclusion, we reviewed the theoretical analysis [8] and the experimental implementation [12] of a reconstruction method for the photon distribution based on on/off detection at different quantum efficiency followed by a ML iterative algorithm. Our results demonstrate that the technique can be applied to both CW and pulsed regimes, and for a wide range of signal energy (from single-photon states to mesoscopic signals), a feature that makes it preferable to other methods till now devised for reconstructing photon number distribution.

REFERENCES
16. A. Zavatta, S. Viciani, M. Bellini, Science 306, 660 (2004).
17. G. M. D’Ariano, M. G. A. Paris, Phys. Lett. A 233, 49 (1997).

Quantum recoil effects in BECs and FELs

N. Piovella[1,2], M.M. Cola[1], L. Volpe[1], and R. Bonifacio[2,3]

1 Dipartimento di Fisica, Università degli Studi di Milano
2 INFN
3 Departamento de Fisica, Universidade Federal Alagoas, Maceiò, Brazil

Free electron lasers (FELs) and collective atomic recoil lasers (CARLs) are examples of collective recoil lasing, where exponential amplification of the radiation occurs simultaneously with the formation of a density grating ('bunching'). The dimensionless classical model (describing both FEL and CARL) have been recently extended to the quantum domain, where it predicts new lasing regimes. In particular, recent experiments using a Bose-Einstein Condensate (BEC) have demonstrated the superradiant quantum CARL regime. On the FEL side, the quantum regime is particularly attractive for x-ray operation in the Self-Amplified-Spontaneous Emission (SASE) regime, since here the coherence of the emitted radiation is largely enhanced, with a strong narrowing of the spectrum, otherwise broad and chaotic in the classical SASE.

Collective recoil lasing (CRL) is a new method to generate coherent radiation by collective scattering of photons from a cold sample of particles. An example of CRL is the Free Electron Laser (FEL) [1], in which a relativistic electron beam passing trough a magnet (undulator) emits coherent radiation at a wavelength $\lambda \sim \lambda_w/\gamma^2$, where λ_w is the periodicity of the undulator and $\hbar$ is the electron energy in mc^2 units. The initial radiation (from an external seed or starting from noise) is exponentially amplified along the undulator and the electrons bunch on a radiation wavelength scale, to emit coherently [2]. FELs, conceived in the 70's, are now often user's facilities in many laboratories in the world, offering an high quality light source for many experiments in solid-state physics, biology etc., at wavelength regions not covered by standard laser sources, from the far infrared to the vacuum UV [3]. Most of the efforts in the FEL's research are presently aimed to realize an x-ray source in the Ångstrom region, in the Self-Amplified-Spontaneous Emission (SASE) regime, i.e. starting from noise [4]. The main drawback of SASE-FELs is that they require high-energy linacs (GeV) and very long undulator magnets (~100 m). Also, the output radiation contains many random spikes and has a broad and chaotic spectrum [5] (see Fig.1a and c). These advantages could be avoided operating an FEL in the new quantum SASE regime that we have recently proposed for a future experimental test [6,7]. This regime has two main important advantages: 1) it produces a much more coherent X-ray signal, with a narrow spectrum; 2) it uses a laser undulator instead of the usual static undulator magnet, reducing by orders of magnitude the dimensions and the cost of the future X-ray FEL sources.

An other example of CRL is the Collective Atomic Recoil Laser (CARL), the atomic analog of the FEL [8]. In CARL, a cold sample of neutral two-level atoms back-scatters the photons of a laser of frequency near the atomic transition. The atoms recoil by $2\hbar k$ and the scattered field combines with the incident laser field to form a pendulum potential which bunch the atoms. As in FELs, the scattered field grows exponentially in time with the formation of a density grating spaced by the radiation wavelength.

The dynamics of CARLs and FELs are described by the same set of equations, in which dimensionless variables have a different meaning, depending if they refer to FEL or CARL [9,10]. The original model assumes that the particle motion (either relativistic electron or atoms) and the radiation field are classical. However, CARL has been observed experimentally in the 1999 using a Bose-Einstein Condensate (BEC) [11], in a regime where the atomic motion must be necessarily treated quantum-mechanically. This results have motivated us [12,13] and other researchers [14] to extend the CARL, and a successively also the FEL [9], to a quantum domain where the particle dynamics is described by a Schröedinger equation for a macroscopic wave function, coupled to the equation for the radiation field. The model has been able to interpret successfully an experiment on the superradiant regime of CARL, realized BECs of Rubidium atoms [15]. Furthermore, on the theoretical side, we have demonstrated atom-atom and atom-photon entanglement in CARL [16,17], together with other effects on coherent interaction between radiation and BECs [18,19,20]. More recently, CARL has been observed also, in the classical regime, with atoms trapped in a ring cavity and in the presence of a friction force [21].

The main interest of our research relies presently on the feasibility of building an X-ray FEL source based on the quantum SASE regime [6] (research funded by INFN), which should have important and widespread experimental applications. For these reasons, the following description on the quantum regime refers to FELs only. However, analog considerations may be done also for CARL.

REFERENCES
1. See for instance: C.A. Brau, "Free-Electron Lasers" (Academic Press, Boston 1990).
2. R. Bonifacio, C. Pellegrini and L. Narducci, Opt. Commun. 50 (1984) 373.
3. See for instance the web site: *http://sbfel3.ucsb.edu/www/vl_fel.html.*
4. S.V. Milton et al., Science 292 (2001) 2037; A. Murokh et al., Phys. Rev. E 67 (2003) 066501; J. Andruszkow et al., Phys. Rev. Lett. 85 (2000) 3825.
5. R. Bonifacio, L. De Salvo, P. Pierini, N. Piovella, and C. Pellegrini, Phys. Rev. Lett. 73 (1994) 70.
6. R. Bonifacio, N. Piovella and G.R.M. Robb, Nucl. Instrum. Meth. A 543 (2005) 645.
7. R. Bonifacio, Nucl. Instrum. Meth. A 546 (2005) 634.
8. R. Bonifacio, L. De Salvo Souza, Nucl. Instrum. and Meth. in Phys. Res. A 341 (1994) 360; R. Bonifacio, L. De Salvo Souza, L. Narducci and E.J. D'Angelo, Phys. Rev.A 50 (1994) 1716.
9. R. Bonifacio, M.M. Cola, N. Piovella, and G.R.M. Robb, Europhys. Lett. 69 (2005) 55.
10. R. Bonifacio, N. Piovella, G.R.M. Robb, and M.M. Cola, Opt. Commun. 252 (2005) 381.
11. S. Inouye et al., Science 285 (1999) 571; S. Inouye et al., Nature 40 (1999) 641.
12. N. Piovella, R. Bonifacio, B.W.J. McNeil, G.R.M. Robb, Optics Comm. 187 (2001) 165.
13. N. Piovella, M. Gatelli and R. Bonifacio, Optics Comm. 194 (2001) 167.
14. M.G. Moore, and P. Meystre, Phys. Rev.A 58 (1998) 3248.; M.G. Moore, O. Zobay and P. Meystre, Phys. Rev.A 60 (1999) 1491.
15. L. Fallani, C. Fort, N. Piovella, M. Cola, F.S. Cataliotti, M. Inguscio, and R. Bonifacio, Phys. Rev. A 71, 033612 (2005).
16. N. Piovella, M. Cola, R. Bonifacio, Phys. Rev.A 67 (2003) 013817.
17. M.M. Cola, M.G.A. Paris and N. Piovella, Phys. Rev. A 70 (2004) 045601.
18. M.G.A. Paris, M.M. Cola, N. Piovella, and R. Bonifacio, Opt. Comm. 227 (2003) 349.
19. N. Piovella, V. Beretta, G.R.M. Robb and R. Bonifacio, Phys. Rev. A 68 (2003) 021801(R).
20. M.M. Cola and N. Piovella, Phys. Rev. 0A 70 (2004) 043809.
21. D. Kruse, C. von Cube, C. Zimmermann, and P.W. Courteille, Phys. Rev. Lett. 91 (2003) 183601; C. von Cube et al., Phys. Rev. Lett. 93 (2004) 083601.

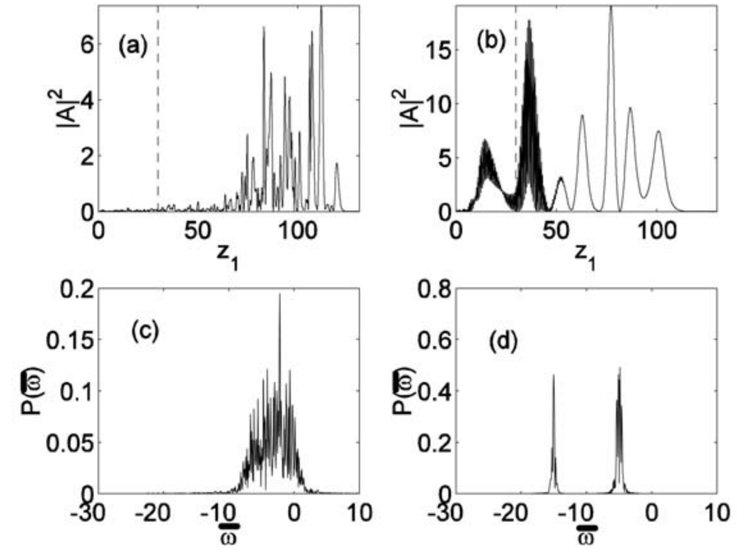

Fig. 1
SASE radiation in the classical (a and c) and quantum (b and d) regimes. Top: temporal profile as a function of $z_1 = (z-vt)/l_c$; Bottom: power spectrum as a function of $(\omega-\omega_s)/\rho\omega_s$.

The quantum regime in FELs occurs when the electron momentum spread $mc\delta\gamma$ (both the initial one and the one induced by the interaction with the radiation) is less than the momentum $\hbar k$ of the emitted photon. It has been shown [9,13] that in this limit the probability of emission of a photon is much larger than those of absorbtion, and each electron emits coherently a single photon, recoiling by $\hbar k$. The particle ensemble behaves as a two-state system with only two possible average momenta, $p = mc\gamma_0$ and $p = mc\gamma_0-\hbar k$. In this sense, an FEL in the quantum regime is more similar to a laser where (instead of the electronic transitions between internal energy levels, as it occurs in a laser) the electrons back-scatter the photons of the pump field (i.e. the static or laser wiggler) into the forward radiation mode, making recoil transitions between discrete momentum levels, separated by $\hbar k$. For these reasons, the intensity profile (Fig.1b) of the SASE radiation is almost coherent and the power spectrum, shown in fig.1d, is composed by narrow lines separated by $\hbar k$, corresponding to a sequential scattering of single photons. On the contrary, in a classical FEL the electron has comparable probabilities to emit or absorb a photon, so that the net gain is given by the difference between the emission and absorbtion probabilities. It has been shown [9] that in the classical regime each electron emits in average many photons, with a decrement of the coherence of the produced radiation. As a consequence the intensity profile of the classical SASE radiation is very spiky (see Fig.1a) and the power spectrum, shown in Fig.1c, is much more broad. The quantum limit set a severe condition on the quality of the electron beam, *i.e.* $\delta\gamma < \lambda_c/\lambda$ (where $\lambda_c = 0.024$Å is the Compton wavelength). This condition suggests the use of a laser wiggler with a wavelength of about $\lambda_w \sim 1$ µm, and a low energy beam (~ MeV), to generate x-rays in Ångstrom region. On the other hand, the same quantum condition set also a limit of the coupling strength between beam and radiation. In fact, in the classical regime the maximum induced energy spread is $\delta\gamma/\gamma_0 \sim \rho$ (where ρ is the collective FEL parameter [2], proportional to $J^{1/3}B_w^{2/3}\gamma_0^{-1}$, where J the density current and B_w is the wiggler strength). Hence, the condition $mc\delta\gamma \leq \hbar k$ implies that the parameter $\rho' = (mc\gamma_0/\hbar k)\,\rho$ must be less than unity, whereas an FEL behaves classically when $\rho' >> 1$. This condition has been proved analytically and numerically [9,10]. Similar results have been demonstrated for CARL [13] and in the experiments of superradiant Rayleigh scattering [15].

In conclusion, we have investigated a new quantum regime of operation for Collective Recoil Lasing, in which each particle scatters a single photon of the incident pump field into the forward radiation field. In FELs the frequency of the forward photon is Doppler shifted by a relativistic factor γ^2, which makes an FEL in SASE regime a tunable source for coherent high-power X-rays. The very attractive feature of the quantum regime is that the generated radiation has a coherence much larger than those of the classical SASE regime. Furthermore, it can be realized with a laser undulator instead of the much longer static undulator, presently used in the current classical SASE-FEL experiments. However, a better understanding of the 3D effects (optical guiding and influence of beam emittance on the radiation emission) is needed before saying that an FEL in the quantum SASE regime can be realized with the present (or in a near future) beam and laser technologies.

Decoherence of mesoscopic superposition states in a strongly driven micromaser

1 Dipartimento di Fisica, Università
degli Studi di Milano
CNR-INFM - Sezione di Milano

F. Casagrande[1] and A. Lulli[1]

One of the most intriguing problems in modern physics is to explain the emergence from the quantum mechanical laws of the classical appearance of the macroscopic world. The fundamental features of quantum mechanics, such as linearity and entanglement, imply the occurrence of interference effects and nonlocal correlations, hence of seemingly paradoxical behaviours that we do not see in the world around us. As early as in 1935 Schrödinger pointed out these problems by a caricatural metaphor, in which he described a cat in a closed box containing a diabolic apparatus correlating his life or death to the excited or unexcited state of an atom, so that the cat was in a sense alive *and* dead. The absence of quantum coherence effects in macroscopic systems originates from their unavoidable interaction with the environment, that induces a *decoherence* that is practically instantaneous. However, the investigation of systems of *mesoscopic* size allowed the first observation of decoherence in progress [1] for superpositions of two coherent cavity field states with the same amplitude but different phases, called *cat states*. Besides its deep fundamental importance, the study of decoherence plays a central role in quantum information and communication.

We suggest an alternative scheme [2] for the generation and the decoherence of mesoscopic cavity field superposition states, based on a strongly driven micromaser. In this system a beam of two-level atoms crosses a superconductive microwave cavity where the atomic transition is resonant with one cavity mode. The atoms cross the cavity one at a time and during the passage they are strongly driven by a classical field.

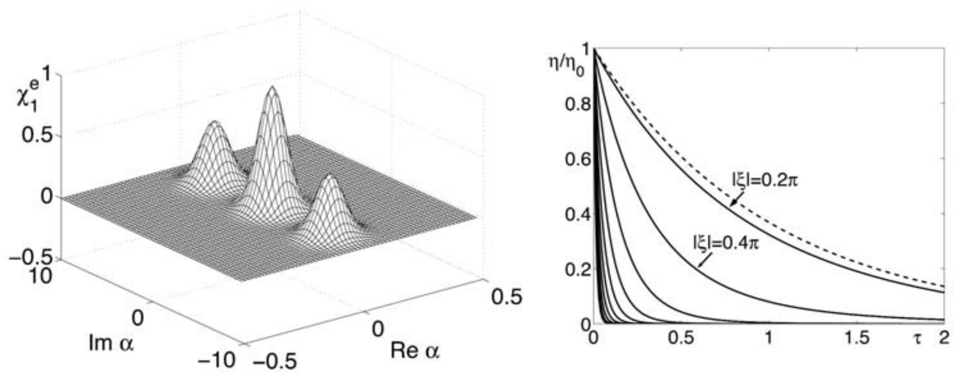

The dynamics of this quantum open system was analytically solved [3] in spite of the presence of pumping, driving, dissipative, and thermal effects, showing remarkable atom-atom correlations at steady-state. Furthermore [2], in atomic correlation measurements, the detection of the first probe atom prepares a mesoscopic superposition field state, as shown in phase space in Fig. 1, whose decoherence can be described by conditional probabilities for the detection of the second probe atom after a time τ. From these probabilities one can derive a decoherence signal $\eta(\tau)$, shown in Fig. 2 for different dimensionless interaction times $|\xi|$. The decoherence rate is proportional to the squared interaction time, that rules the separation in phase space between the superposition components, whereas it is independent of the atomic pumping rate. When the cavity is not pumped and the temperature is negligible, the superpositions are just *cat states*, whose decoherence can be thus monitored by a scheme that may offer some advantages in comparison with [1]. In particular, the atom-photon interaction is resonant rather than dispersive; there is one coherent field driving the atoms in the cavity, instead of two fields acting on the atoms in auxiliary cavities; the cat states are maximally rather than partially separated, i.e., the coherent states have opposite phases.

REFERENCES
1. Brune M. et al, *Phys. Rev. Lett.* 77, 4887 (1996)
2. Casagrande F. and Lulli A., *Eur. Phys. J. D* 36, 123 (2005); *J. Opt. B: Quantum Semiclass. Opt.* 7, S437 (2005)
3. Lougovski P. et al, *Phys. Rev. A* 69, 023812 (2004); Casagrande F. et al, *Opt. Spectrosc.* 99, 301 (2005)

SFERA, a laboratory of laser physics: realization of a laser pulse shaping system

1 Dipartimento di Fisica, Università
degli Studi di Milano & INFN

S. Cialdi[1], F. Castelli[1], I. Boscolo[1], and D. Cipriani[1]

The laboratory SFERA, located in the Department of Physics of the Milan University, is actively involved in studies on fundamental physics and on technological applications of the sources of coherent radiation usually known as lasers. Here we present a recent achievement: a system providing a suitable self consistent control of the temporal shape of a laser pulse, whose practical realization is shown in the picture in Fig. 1.

Laser pulses of proper temporal profiles and different spectral bands are required by high brilliance electron gun of UV-X FEL machines and by new laser-plasma particle sources. In particular rectangular laser pulses are required, and their length and amplitude must be manageable: the beam quality depend on temporal and spatial profile of the exciting laser pulse.
A pulse with a rectangular profile is produced by using a shaping system to manipulate the Gaussian-like pulses given by common lasers. Our research group developed a pulse shaping system based on a *liquid crystal programmable spatial light modulator mask* (LCP-SLM) [1], that is an array of 640 pixels made of nematic liquid crystal, whose refraction index, controlled by an electric potential can modulate the phase of the optical signal.

The shaping apparatus, depicted on the top of the Fig. 2, consists of a mode-locked Nd:YAG laser followed by a long optical fiber. The control of the pulse shape is obtained by modifying the phase of the spectral components with the LCP-SLM, inserted in an optical configuration called 4f-system, as schematized in Fig. 3. This shaper and the diagnostic tools, consisting in a spectrum analyzer and an autocorrelator, are interconnected to a computer in a feed-back loop for self consistent operation for providing target pulses [2].

Fig. 1
A picture of the laser pulse shaping system developed in the Sfera laboratory.

The Nd:YAG oscillator generates Gaussian pulses with a temporal length of about 90 ps. The spectrum of the pulse is than extended from 0.02 nm up to 3 nm by propagation in the fiber, as required for the pulse manipulation by the 4f-system. This device is composed by gratings and lenses placed at focal distance, with the LCP-SLM at the center focus plane. The physical operations done by the 4f-system are: a) spatial dispersion of the spectral components of the pulse and focalization over the mask; b) phase modulation of the spectral components given by the pixels of the LCP-SLM; c) recombination of the spectral components. The phase modulation performed by mask pixels is determined via an adaptive algorithm, matching a selected target profile with the actual pulse profile which is measured with an

REFERENCES
1. Cialdi S., and Boscolo I., “A shaper for providing long laser target waveforms” *Nuclear Instruments & Methods in Physics Research A538*, 1 (2005)
2. Cialdi S., Castelli F., and Boscolo I. “Rectangular pulse formation in a laser harmonic generation”, *Applied Physics B82*, 383 (2006)

autocorrelator combining the pulse with a time delayed copy of itself. The original laser pulse can be transformed in pulses of any profile with duration in the range 3-100 ps.

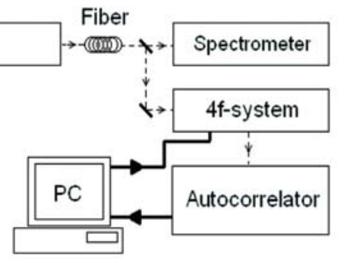

Fig. 2
Schematic of the laser system, with the shaping device and the fundamental diagnostics.

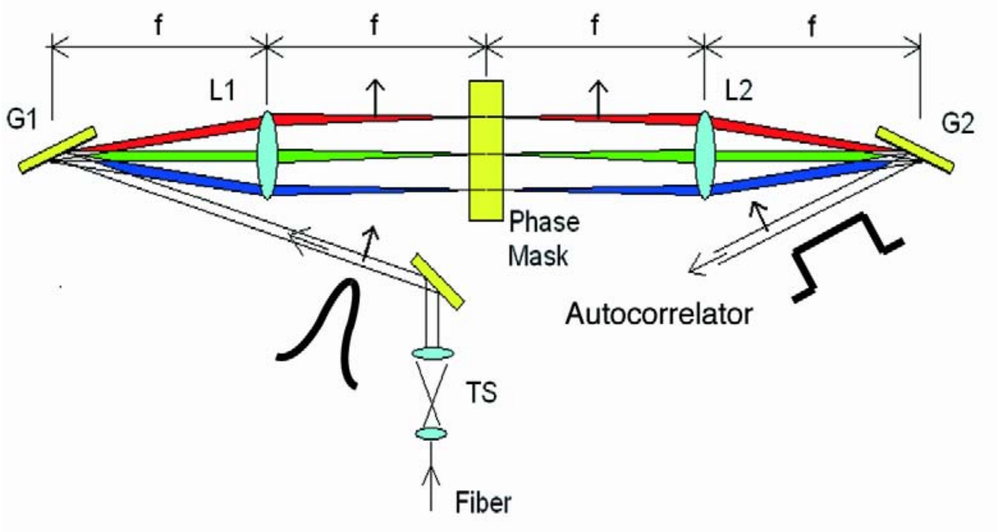

Fig. 3
A scheme of the 4f-system. The Gaussian input pulse is changed in a rectangular output pulse.

Experimental study of photonic crystal fibers

A.M. Grassi[1] and M. D'Alessandro[1]

1 Dipartimento di Fisica, Università degli Studi di Milano

Photonic crystal fibers (PCFs) are a novel type of optical fiber with a microstructured cladding, consisting of a matrix of air channels, running along the fiber, which approximates a 2D photonic crystal (see Fig. 1). Their optical properties (*e.g.* nonlinearity, dispersion, birefringence) are customizable by modeling the geometrical parameters of the periodic cladding and the refractive indices of the glass and of the inclusion channels, which may be filled with gases or fluids. Endlessly Single Mode (ESM) regime, supercontinuum radiation, and visible optical solitons are few examples of what PCFs make possible. The details of the microstructure may be of the order of few μm, so the experimental study of PCFs requires a powerful microphotographic system, able to resolve the features of the cladding. No commercial devices were found to be suitable for our purposes, nor to be sufficiently versatile, so we developed an *ad-hoc* system capable of making color digital pictures of PCFs' cross section, with high resolution and continuously varying magnification. We mounted it on the optical bench, since the optical train must be horizontal in order to avoid fiber bends. Filters or diaphragms may be easily inserted in the optical path with minimal influence on image quality and focus. Multimode fiber probes send the output fields to Visible and NIR Optical Spectrum Analyzers. A digital camera is connected to a computer from which images can be shot and analyzed. With a calibrated grid, drawn by software, we can estimate the mode field diameter and other features of the fibers. Figure 1 is taken using our microphotographic system.

Fig. 1

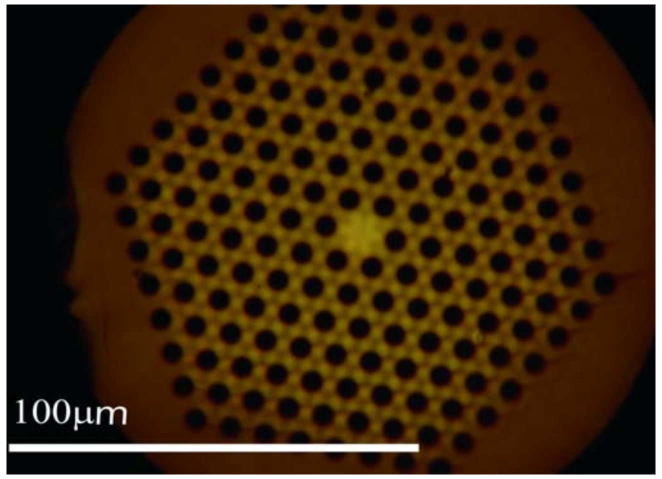

Fig. 2

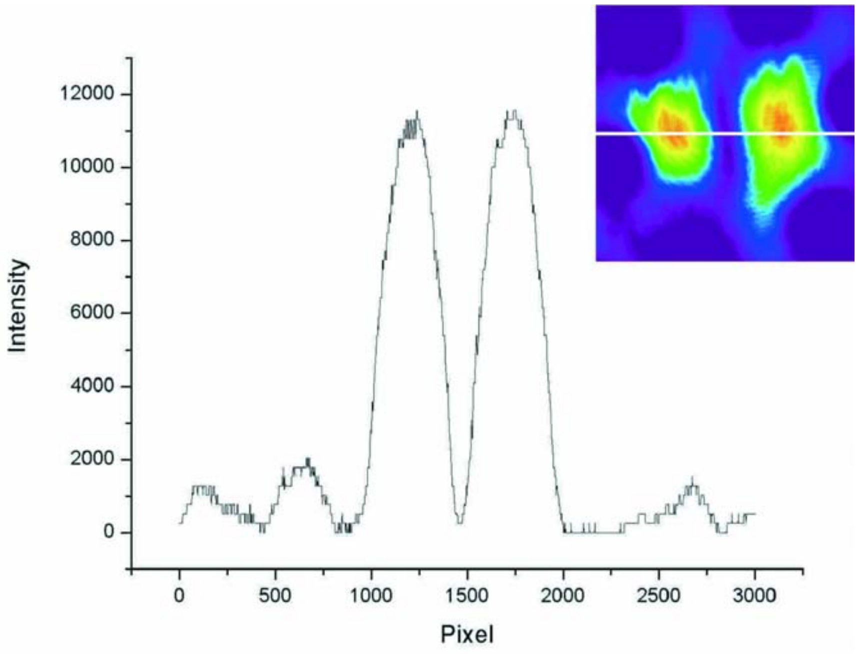

Our research is currently focused on modal behavior of PCFs. Modes and modal behavior of PCFs is a delicate theoretical issue. Since all modes supported by these fibers are leaky, it's impossible to draw a definite border between single and multimode operation, and even to clearly define PCFs' modes. This argument is currently object of many theoretical works, but to our knowledge there's not plenty of analogue experimental studies.
Since it is expected that an ESM PCF may in some cases guide more than one mode, we are experimentally investigating the limits of single-modeness of such a fiber.

We are approaching different methods to reveal the presence of higher order modes, such as mode profile analysis (Fig. 2), spectral analysis and polarization measures, collecting the first interesting results. We have also conducted a preliminary experimental study on the use of a PCF as an optical absorption sensor with minimal waste of sample. In these sensors, the field interacts with a fluid or a gas filling the capillaries of the cladding, mainly through evanescent waves. We are at the very beginning of this work.

Optics

Nanoparticles in a thermal gradient

A.Vailati[1], R. Cerbino[1], S. Mazzoni[1], F. Croccolo[1], D. Brogioli[1], F. Giavazzi[1], G. Donzelli[1], A. Zelioli[1] and M. Giglio[1]

1 Dipartimento di Fisica, Università degli Studi di Milano and CNR-Istituto Nazionale per la Fisica della Materia

Due to their small size nanoparticles are sensitive to the thermal agitation of the molecules in the solvent, which makes them move erratically in a Brownian motion. The fact that nanoparticles are sensitive to the thermal energy makes them very suitable to investigate phase transitions on the mesoscopic scale, thus mimicking the phase transitions observed at the atomic scale [1]. Moreover, the interactions between nanoparticles can be tuned at will by the addition of ions into the suspension. In this way one can control the height of the repulsive potential barrier between the particles and make them aggregate. Due to their random motion, the aggregation of nanoparticles gives rise to aggregates with a peculiar fractal morphology [2]. When the concentration of particles is high enough, the fractal grows up to form a gel invading the container [3]. In the following we will report on the investigation of the behavior of nanoparticles under the action of a thermal gradient and we will show that under appropriate condition the gradient promotes the self-organization of nanoparticles into macroscopic structures.

Beyond the action of the thermal energy, the nanoparticles feel the action of external fields. The gravitational field makes the particle sediment. However, due to their small size, the thermal agitation counteracts the sedimention process and, unless the vertical size h of the vessel containing the particles is very large (some centimeters), the sedimentation is not apparent. The rule here is that for small h the thermal energy kT is much larger than the energy gain due to the sedimentation of the particle mgh. By constrast, whenever particles get accumulated in a region of fluid the thermal energy might not be large enough to counteract the gravitational energy, and this could give rise to the sinking of the region. The other external field of interest here is a vertical temperature gradient applied to a horizontal layer of a suspension of nanoparticles, The gradient induces a flow of particles proportional to the gradient by means of the Soret effect. The flow promotes the development of a concentration profile of particles. The origin of this flow is still not well understood. The associated density profile can either be stable or unstable, depending on whether particles get accumulated at the top or at the bottom of the layer.

In the *stable configuration* nothing peculiar is predicted to happen: the flow induced by the thermal gradient is balanced by the back-diffusion of particles. Quite unexpectedly, large fluctuations in the concentration of particles are observed in this configuration [4]. These are due to the correlated motion of groups of particles induced by spontaneous velocity fluctuations in the suspension. The amplitude of the fluctuation diverges as the fourth power of their size. On Earth the divergence is partially prevented, as large fluctuations are stabilized by gravity. To fully exploit the divergence we will perform experiments under micro-gravity conditions within the GRADFLEX Project of the European Space Agency, in collaboration with the University of California at Santa Barbara and NASA. Figure 1 shows simulated images, represented in false colors, of the non equilibrium fluctuations. Figure 1a simulates fluctuations under the action of gravity.

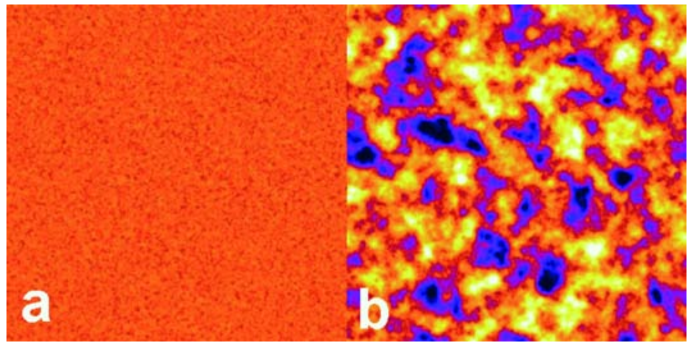

Fig. 1
Simulated images of nonequilibium fluctuations in a polymer suspension. Panel (a) corresponds to fluctuations in the presence of gravity, while panel (b) shows the divergence of the size and amplitude of the fluctuations in a microgravity environment. The side of each panel corresponds to 13mmx13mm in real space.

Figure 1b shows a simulation of the fluctuations in the absence of gravity. The size of each image is 13mm x 13mm in real space. One can immediately appreciate the increase in the contrast of the fluctuations due to the divergence of the amplitude of the fluctuations under microgravity. Another striking feature is that under microgravity the size of the fluctuations grows up to that of the container.

REFERENCES
1. A. M. Alsayed et al., Science 309, 1207 (2005); P. N. Pusey, Science 309,1198 (2005).
2. D. A. Weitz and M. Oliveria, Phys. Rev. Lett. 52, 1433 (1984).
3. M. Carpineti and M. Giglio, Phys. Rev Lett. 68, 3327 (1992); M. Carpineti and M. Giglio, Phys. Rev Lett. 70, 3828 (1993)
4. A.Vailati and M. Giglio, Phys. Rev Lett. 77, 1484 (1996); A. Vailati and M. Giglio, Nature 390, 262 (1997); D. Brogioli et al., Phys. Rev. E 61, R1 (2000).

The GRADFLEX experiment will fly onboard the Foton M3 satellite. Three months before the launch experiments will be tested and integrated inside a spherical capsule with a diameter of 2.2 m in Samara (RU). The capsule is shown in Fig. 2a. The capsule will then be sent to the Baikonur Cosmodrome in Kazakhstan, where two days before the launch it will be enclosed into the nose cone of the Soyuz Rocket (Fig. 2b). The rocket will then be launched in september 2007 (Fig. 2c shows the launch of the Foton M2 mission) and the satellite will remain into orbit for about two weeks. After that period the Foton capsule will return to Earth, where the scientific payload will be recovered.

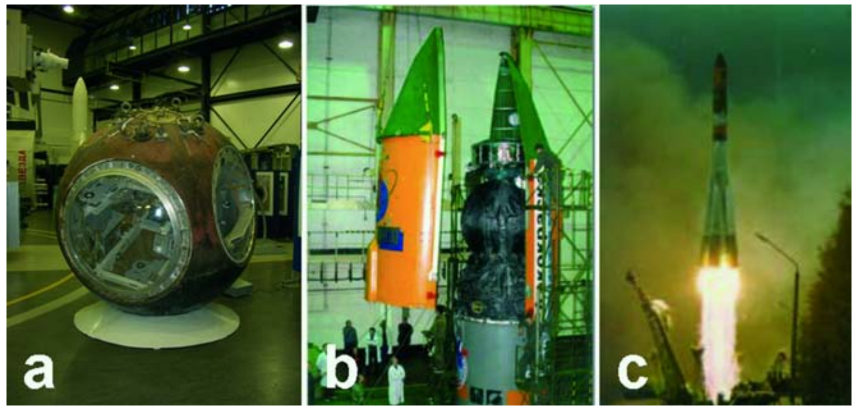

Fig. 2
Overview of the phases of the Foton M2 space mission. Panel (a) shows the Foton capsule which will host the GRADFLEX experiment. (b) shows the Foton M2 capsule being enclosed the nose cone of a Soyuz rocket. (c) shows the launch of the Soyuz rocket during the Foton M2 mission.

Let us go back on Earth and consider the *unstable configuration* where the density profile generated by means of the Soret effect is heavier at the top. In this configuration, and provided that the temperature gradient is large enough, two thin horizontal boundary layers are created inside the sample, particles being accumulated at the top of it and solvent at the bottom. The boundary layers are destabilized by gravity, which enhances spontaneous velocity fluctuations, and convection sets in. Quite interestingly, the convective planform of the instability is made up by two superimposed wire meshes making up a spoke pattern. A picture of the spoke pattern obtained by using the Shadowgraph technique is shown in Fig. 3.

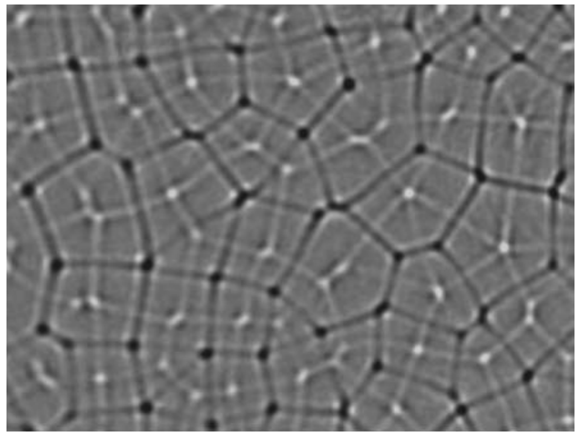

Fig. 3
Spoke pattern obtained during the convection of a water suspension of silica nanoparticles (looking from above). The pattern is made up by a white mesh staggered with a black mesh. The nodes of the meshes represent vertical plumes connecting the boundary layers. The plumes act as conduits for nanoparticles and water.

From the picture one can appreciate that the meshes are staggered so that the node of the black mesh falls at the center of a cell made up by white sides, and viceversa. Moreover, each white side crosses orthogonally with a black one. Further analysis [5] reveals that the two meshes are localized inside the two boundary layers. The particles and the solvent self-organize into vertical channels, the nodes of the meshes, which transfer mass from one boundary layer to the other. The sides of the meshes of one color represent ridges of the boundary layers, delimiting the zone of influence of a channel with the opposite color. This system mimics the conditions found on a larger scale for the circulation of heat in the Earth mantle. The high viscosity of the Earth's mantle and its large thickness involve that the convective transfer of heat occurs in time whose order of magnitude is measured in billions of years. To mimick such a slow dynamics in the laboratory we use a flow of nanoparticles to emulate a heat flow. Nanoparticles, notwithstanding their small size, move very slowly with respect to the solvent molecules surrounding them, which are about 100 times smaller.

Figure 4 shows a 3-dimensional simulation of the heat transfer in the Earth mantle [6]. Here the vertical columns connecting the two boundary layers are apparent, together with the ridges localized at the boundary layers. By looking at the results of this simulation from above one obtains images like that shown in Fig. 5a, which is shown back-

REFERENCES
5. R. Cerbino, A. Vailati and M. Giglio, Phys. Rev. E Rapid Communications 66, 055301 (2002)
6. F. Dubuffet, D. A. Yuen, Geophys. Res. Lett., 27, 17 (2000).

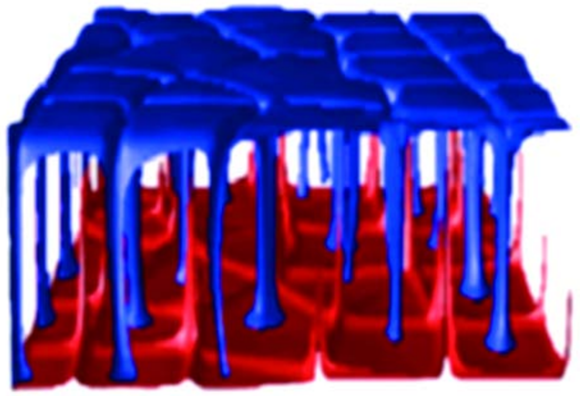

Fig. 4
Simulation of heat convection in the Earth's mantle.The image shows the hot boundary layer in red (located near the nucleus) and the cold boundary layer in blue (located under the crust). The boundary layers are connected by ascending and descending thermal plumes. Image courtesy of D. A. Yuen, University of Minnesota.

to-back to an image of spoke pattern convection obtained by using silica nanoparticles (Fig. 5b) [7]. From the images it is apparent how the two patterns exhibit common topological features. The investigation of the topological properties of the spoke patterns shows that the underlying structure of the pattern is that of a degenerate Voronoi diagram. The properties of such diagram differ much from those encountered in other natural systems, such as froths. The spoke patterns presents a higher degree of order than the usual cellular patterns, as the degenerate encounter of more than three sides into a vertex is allowed, and this gives rise to a tessellation made up by faces with four sides on average [8].

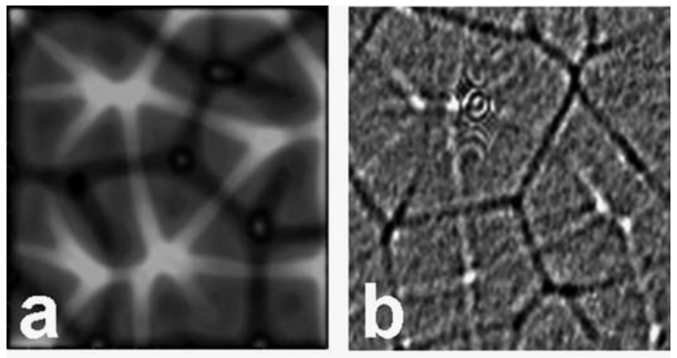

Fig. 5
Comparison of the spoke patterns obtained in simulations of heat convection in the Earth's mantle, (a), and in experiments on convection of silica nanoparticles, (b).

Another interesting application of nanoparticles is that they allow to tackle the problem of scaling in the convective heat and mass transfer [9] simply by looking at the very early stages preceding the onset of the instability [10]. Due to the slow dynamics of the nanoparticle suspension it is fairly easy to investigate the very early stages of the instability. During this stages the boundary layers are formed by diffusion, until they are destabilized by convection. The time when this destabilization occurs provides an indirect measurement of the thickness of the boundary layers at the onset of the instability. Quite interestingly, the heat/mass transfer in a convective process is entirely determined by the respective boundary layer thickness. Therefore, by looking at the onset of the instability one can yield information about the scaling properties of the convective heat or mass transfer. Roughly speaking, once that the applied temperature difference and the heat or mass transferred are expressed by appropriate dimensionless numbers, the transferred heat (mass) diverges algebraically with the applied temperature difference.

REFERENCES
7. R. Cerbino, PhD Thesis, University of Milan (2004).
8. S. Mazzoni, PhD Thesis, University of Milan (2005).
9. J. Niemela et al. Turbulent convection at very high Rayleigh numbers, Nature 404, 837 (2000).
10. R. Cerbino, S. Mazzoni, A. Vailati, and M. Giglio, Phys. Rev. Lett. 94, 064501 (2005).

Heterodyne ray speckles

R. Cerbino[1], L. Peverini[2], M.A.C. Potenza[1], and M. Giglio[1]

1 Dipartimento di Fisica and CNR - Istituto Nazionale per la Fisica della Materia, Università degli Studi di Milano
2 ESRF - European Synchrotron Radiation Facility, Grenoble

Scattering of coherent radiation from matter gives rise to speckles. While speckles are known from long time in visible optics, they entered the ray community only after the appearance of high brilliance third generation synchrotron sources. With these sources speckles are observed when a single coherence area of the electromagnetic field is selected. This is usually done by spatially filtering the beam with pinhole arrangements but leads to obvious limitations in terms of available photon flux. We will present evidence that high quality, low contrast speckles can be observed by simply placing a high resolution CCD sensor immediately behind a static sample. Measurements have been performed at the BM05 beamline of the European Synchrotron Radiation Facility (ESRF) in Grenoble and the experimental setup is schematically presented in Fig. 1. Radiation coming from a horizontally elongated incoherent source passes trough a double crystal monochromator and impinges on the scattering sample which is a microporous cellulose acetate (μPCA) filter. The diffracted intensity has the typical speckle distribution observed with optical coherent sources as is visible in Fig. 2. It is argued that the speckles are due to a self-referencing scheme where both the scattered radiation and the heterodyne local oscillator originate from the same rapidly changing, local coherent beam patch. It is suggested that these X-Ray speckles are of the same type of those obtained with the newly reported optical "Near Field Scattering" method [1,2] that has been shown to be equivalent to static light scattering. Therefore, the simple lensless arrangement described above could be used as a new ultra low-angle scattering method operative at very small angles where conventional X-Ray scattering methods fail. Speckle generated X-Ray scattering data are reported for the μPCA filters that exhibit a quasi spinodal structure. An anti-correlation peak at finite wavevectors is also reported, in agreement with optical measurement (obtained with partial index matching). In addition, we show that speckle patterns can also be profitably used to monitor the synchrotron beam angular stability with sub-arcsecond resolution, opening the way to immediate metrological applications.

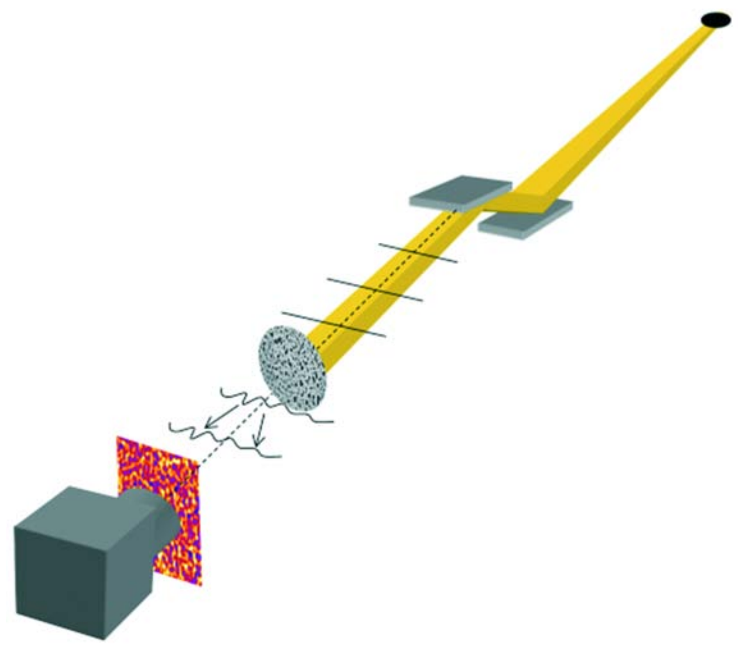

Fig. 1
Schematic drawing of the experimental setup used for the study of X-ray speckles. The light emerging from the source passes through a monochromator and impinges on the sample. A CCD camera collects the speckles produced by the sample.

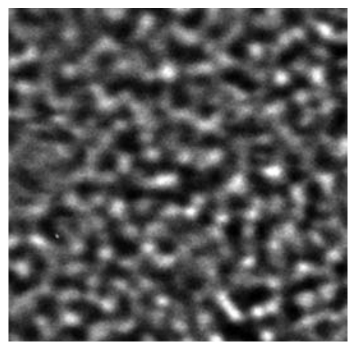

Fig. 2
Example of speckle pattern measured by the CCD camera.

REFERENCES
1. Giglio M., Carpineti M., and Vailati A., "Space Intensity Correlations in the Near Field of the Scattered Light: A Direct Measurement of the Density Correlation Function g(r)", Physical Review Letters **85**, 1416 (2000)
2. Brogioli D.,Vailati A., and Giglio M., "Heterodyne near-field scattering", Applied Physics Letters **81**, 4109 (2002)

An application of the Optical Theorem to the sizing of sub-wavelength particles

1 Dipartimento di Fisica, Università degli Studi di Milano

M.A.C. Potenza[1] and M. Giglio[1]

We present a novel technique based on the Optical Theorem (OT) for the determination of the size of scattering particles in the sub-wavelength range. When a plane wave impinges on a particle, a scattered spherical wave is generated. The scattered amplitude is in general made up by both in phase and in quadrature components. The OT states that the scattering cross section that describes the integral of the scattered intensity at any angle is proportional to the amplitude of the quadrature component at zero scattering angle. This remarkable result is the consequence of conservation arguments that require that the interference between the scattered wave and the incoming wave should exactly account for the power loss of the incoming beam due to scattering of power in different directions.

We will show an application of the method in the realistic case where an assembly of particles is present under the incoming beam. The scattered radiation in the far field is then a speckle field, with the intensity that fluctuates as a consequence of the stochastic interference between individual scattered waves. If the scattered intensity is collected fairly close to the scattering sample, and the incoming beam is wide enough, then low visibility speckle field is generated due to the interference between the weak scattered fields and the powerful transmitted beam. The method relies on the statistical analysis of these low visibility fringes due to the heterodyning between scattered field and the transmitted beam that acts as a self referencing local oscillator. The statistical processing of the instantaneous speckle distribution consists of the evaluation of the two dimensional power spectrum of the intensity distribution. It will be shown that the spectrum exhibits a multiple zero structure, from which an accurate estimate of the amplitude of the quadrature term can be performed. Spherical, calibrated polystyrene colloidal particles have been used. The results have been compared with the theoretical predictions based on Mie scattering functions and the OT. The data show a continuous variation of the phase of the scattered amplitude from zero to $\pi/2$ as the particle diameter is changed from well subwavelength values to many microns sizes, as expected from the OT as one moves from the Rayleigh scattering regime to the diffraction regime. Excellent accuracy for the subwavelength diameters determination is reported.

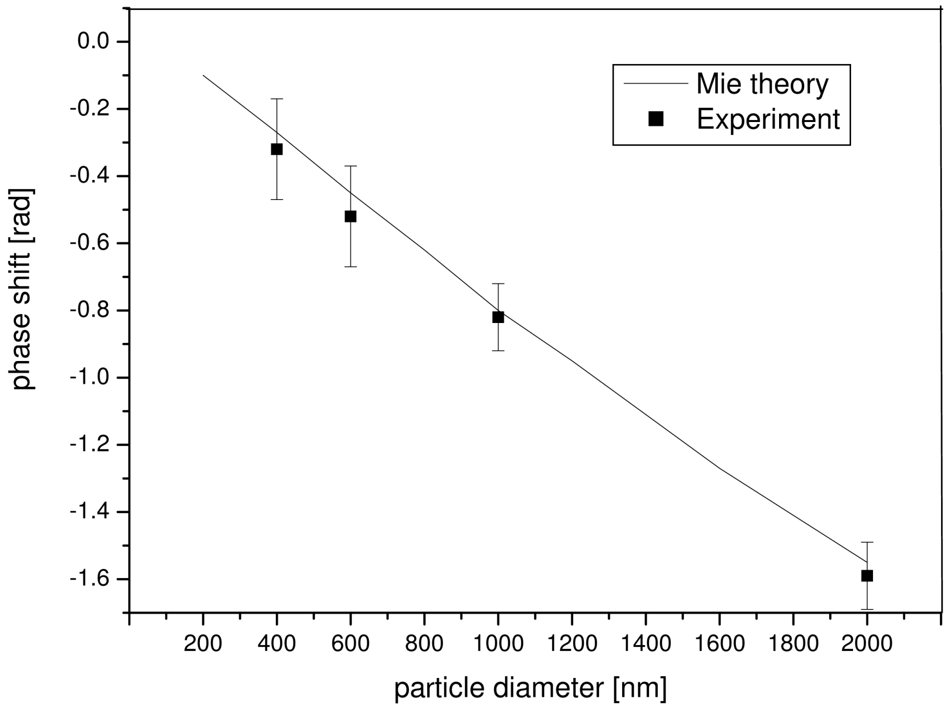

Fig 1.
Phase shift measured for water suspended particles of diameters 400 nm, 600 nm, 1000 nm, 2000 nm. The comparison with the Mie theory (solid line) is shown.

REFERENCES
1. H.C. van de Hulst, *Light scattering by small particles*, New York: Dover (1953)
2. J.S. Batchelder, M.A. Taubenblatt, Appl. Phys. Lett. 55, 215 (1989)
3. A. Bassini, *et. al.*, Appl. Opt. 36, 8121 (1997)

Plasma Physics and Astrophysics

Observations of the cosmic microwave background with the Planck space mission

M. Bersanelli[1,2], P. Battaglia[3], B. Cappellini[1], F. Cavaliere[1], O. D'Arcangelo[4], L. Figini[4], C. Franceschet[3], S. Garavaglia[4], P. Leutenegger[3], D. Maino[1,2], G. Mari[1], A. Mennella[1,2], S. Pezzati[1], P. Platania[4], A. Simonetto[4], C. Sozzi[4], and M. Tomasi[1,2]

1 Dipartimento di Fisica,Università degli Studi di Milano
2 INAF, Istituto G. Occhialini, Milano
3 Laben - Alcatel Alenia Space, Milano
4 Istituto di Fisica del Plasma, CNR, Milano

The cosmic microwave background (CMB) provides a direct view of the early universe and precise observations of its properties are a powerful tool to investigate cosmic evolution and composition. The angular power spectra of temperature and polarisation fluctuations encode information on fundamental cosmological parameters and on the physics of the early universe. After the COBE-DMR and WMAP space observations, the Planck satellite is the third-generation satellite devoted to CMB studies. Planck is expected to extract the full cosmological information from temperature anisotropies and to open up new frontiers in the CMB field. The two complementary instruments at the Planck focal plane are designed to achieve unprecedented combination of frequency coverage, angular resolution, sensitivity and sky coverage. In addition to the main cosmological goals, the nine full-sky maps expected from Planck in the range 30-850 GHz will represent a vast data base for galactic and extragalactic astrophysics.

Introduction

The cosmic microwave background (CMB) radiation is a relic of the universe at an early stage of evolution characterised by a hot and highly homogeneous plasma. The CMB photons provide us with a direct image of the universe at the time of matter-radiation decoupling at temperatures ~ 3000 K, the so-called last scattering surface. Cosmic expansion redshifted the photons by a factor $z \sim 10^3$, and they are now observed at millimeter wavelengths. A blackbody frequency spectrum is expected for the CMB, due to the high thermal equilibrium of the primordial plasma. This prediction has been beautifully confirmed over a large frequency range, and measured with high-precision in the peak region by COBE-FIRAS [1,2] with a temperature $T_0 = 2.725 \pm 0.004$ K. The absence of observable distortions from a Planckian shape demonstrates a smooth early expansion and places upper limits to possible energy releases at epochs as early as $z \sim 10^6$.

Following the CMB discovery in 1965 until the early 1990's, increasingly sensitive observations revealed an extremely isotropic distribution of the CMB intensity at all angular scales. However, it was soon realised that the hierarchy of structures observed in the present universe requires CMB anisotropy at some level, since structure formation theory predicts density perturbations at the epoch of last scattering capable of affecting the photon field. In 1992 the first detection of CMB temperature anisotropies was obtained by COBE-DMR on scales > 7° with fluctuations from uniformity of order $\Delta T/T_0 \sim 10^{-5}$ [3], opening up the road to new major advancements.

To quantify the level of CMB anisotropies and their statistical pattern, it is usual to represent the temperature distribution on the celestial sphere by spherical harmonics expansion. The amplitude of the fluctuations is then expressed in terms of coefficients $C_l = \langle |a_{mm}|^2 \rangle$ where the a_{lm} are the multipole moments and $l \approx 180°/\theta$ identifies the angular scale. The distribution C_l is called the angular power spectrum of the CMB anisotropies. Theory predicts a specific pattern for the C_l function, characterised by a series of peaks and throats (see [6] and references therein), generated by acoustic oscillations of density perturbations in the primordial plasma. The scale and amplitude of these features depend sensitively on the values taken by fundamental cosmological parameters such as the Hubble constant H_0; the total energy density Ω_{tot} and its components such as the cold dark matter and barion density, Ω_{CDM} and Ω_B, and the contribution from a cosmological constant, Ω_Λ; the spectral index of primordial fluctuations, n_S. Accurate high-resolution imaging of the CMB over large portions of the sky represents therefore a powerful method to derive the value of such key parameters. For example, a first peak at $l \sim 200$ (corresponding to an angular scale of about 1 degree) is expected for a flat $\Omega_{tot} = 1$ geometry. The limited resolution of DMR allowed to cover the spectum only up to $l < 20$.

REFERENCES
1. Mather, J.C., et al., *The Astrophysical Journal*, **420**, 439 (1994).
2. Bersanelli, M., et al., *The Astrophysical Journal*, **424**, 517 (1994)
3. Smoot, G.F. et al., *The Astrophysical Journal*, **396**, L1 (1982).

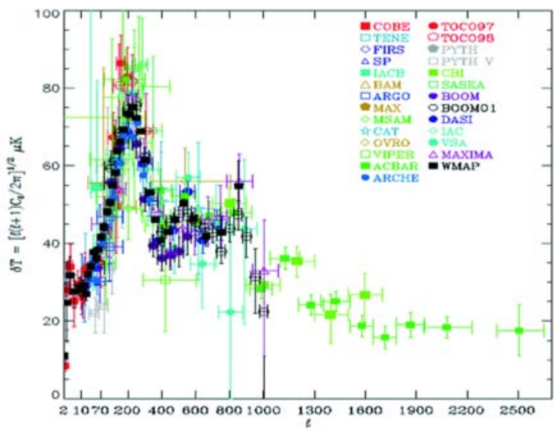

Fig. 1
Present status of observations of CMB anisotropy in terms of the angular power spectrum. The observation of a first peak at $l \sim 200$ (corresponding to an angular scale of about 1 degree) provides strong evidence for a flat $\Omega_{tot} \approx 1$ geometry.

Today, many experiments have been carried out (see Fig. 1) and the presence of acoustic peaks has been superbly confermed. In addition, the most recent data allow us to derive precise evaluations of some key cosmological parameters.

From COBE to WMAP

The COBE discovery of temperature fluctuations at a measurable level $\Delta T/T_0 \sim 10^{-5}$ started the race to unveil new features in the angular power spectrum. Increasingly ambitious sub-orbital programs were carried out mostly aiming at sub-degree scale detections in limited sky regions, such as the Boomerang experiment [5]. The next observational breakthrough came in 2003 with the results of the first-year WMAP data (see Fig. 1), which mark the current state of the art in the field [6]. The WMAP instrument is an array of differential radiometers, passively cooled to about 100K. The power spectrum extracted by WMAP is cosmic variance limited up to $l \sim 350$ (Fig. 1) and the sensitivity is expected to improve by a factor of 2 at the end of the mission. WMAP has also provided the first evidence of temperature-polarization cross power spectrum which shows the expected acoustic features and suggest reionization at $z \sim 20$. The WMAP data have enhanced precision and robustness to the evaluation of cosmological parameters leading, together with data from Ia-type Supernovae, to a critical density universe ($\Omega_{tot} = 1.02 \pm 0.02$) dominated by a Λ term.

Fig. 2
Picture of the Planck satellite (Qualification Model), showing the primary reflector, the baffle and the three thermal shields ("V-grooves") used to thermally decouple the cold (~50 K) telescope enclosure from the warm (~300 K) service module (lower black structure). The payload design was largely driven by thermal and radiation (stray-light) requirements. Courtesy of Alcatel Alenia Space.

Planck: precision cosmology

After NASA's COBE and WMAP missions, Planck is the third-generation space project devoted to CMB observations, to be implemented as part of the European Space Agency's (ESA) Cosmic Vision science program (Fig. 2). Planck is designed to image the CMB anisotropies with an unprecedented combination of sensitivity ($\Delta T/T_0 \sim 10^{-6}$ per sky pixel), angular resolution (5 to 30 arcmin depending on frequency), sky coverage (100%), and spectral coverage (30-857 GHz). Figure 3 shows a comparison between the expected reconstruction of the power spectrum by WMAP a Planck. The Planck detectors are also sensitive to polarisation in all the CMB channels. Control of systematic effects has been a driver of the instrument design, orbit choice and scanning strategy [7,8]. A 1.5m off-axis Gregorian telescope provides the required angular resolution and rejection of unwanted straylight effects. Two complementary instruments cover the spectral range 30-850 GHz, thus allowing accurate removal of astrophysical foregrounds whose spectral shape differs substantially from the CMB blackbody spectrum.

REFERENCES
4. Bersanelli M., Maino D., and Mennella A., *La Rivista del Nuovo Cimento* vol.25, n. 9, 1 (2002)
5. De Bernardis, P., et al., *Nature*, **404**, 995 (2000).
6. Bennett, C.L, et al., *The Astrophysical Journal Supplement Series*, **148**, 1 (2003)
7. Mennella A., et al., *Astronomy and Astrophysics* **384**, 736 (2002)
8. Maino, D., et al., *Astronomy and Astrophysics Suppl*. **140**, 383 (1999)

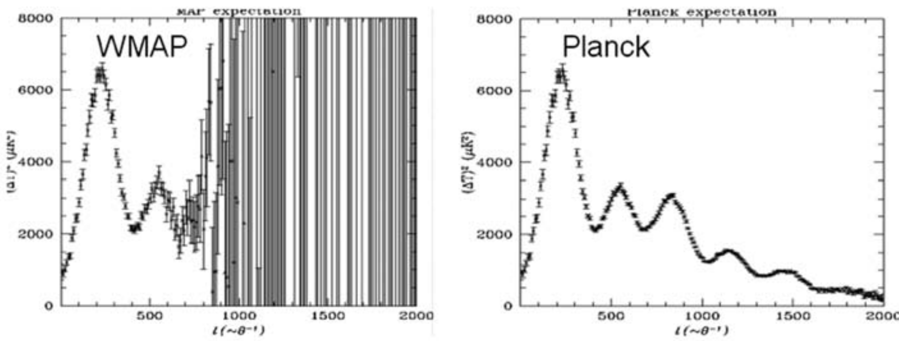

Fig. 3
Comparison of the power spectrum reconstructed by WMAP (left) and Planck (right).

The Low Frequency Instrument (LFI) covers the 27-77 GHz range with an array of pseudo-correlation cryogenic receivers [9]. The High Frequency Instrument (HFI) is an array of bolometers cooled at 0.1K covering the range 100-850 GHz. The instruments are now in an advanced stage of development: they have completed the qualification test campaign and the first flight units are being tested. The front-ends of the LFI and HFI receiver arrays are cooled to 20 K and 0.1 K, respectively. LFI, based on InP MMIC amplifiers, will have channels centered at 30, 44, and 70 GHz, with arrays of 4, 6, and 12 receivers at each frequency, all of which sensitive to polarization. Each corrugated horn on the focal surface will be followed by an orthomode transducer (OMT) to separate the two polarisations. HFI, based on bolometer technology, will have channels at six bands in the 100-857 GHz range.

The Planck LFI has been designed and developed by an International Consortium lead by an Italian team, with a strong contribution from our group at the Physics Department, University of Milano, together with collaborators in the Milano area (INAF, IFP-CNR, industrial partnership of Laben AAS). The demanding scientific performances and the complexity of the system called for early development of radiometer models and an accurate on-ground testing and calibration plan. Early in the project, we developed prototype radiometer chains to verify the receiver design, confirm feasibility of critical units and understand residual receiver systematics. As a second step, qualification models ("QM") of the radiometers have been produced with characteristics nearly identical to the flight models ("FM"), though not requiring full flight performances.

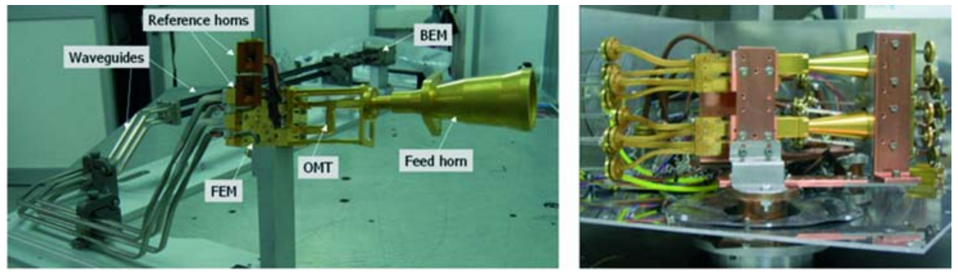

Fig. 4
The basic LFI unit is the radiometer chain assembly (RCA) comprising feed-horn, OMT, front-end module (FEM) connected to a back-end module (BEM) via a set of four waveguides. Left: 30 GHz RCA at Laben, Milano. Right: Front-end portion of the 70 GHz RCAs in cryo facility tested at Elektrobit in Helsinki, Finland.

In the QM and FM, the main radiometer calibration, RF tuning and performance characterisation is carried out at radiometer chain level (Fig. 4) and then verified at instument integrated level. The RCAs are integrated from components extensively tested at single unit level (i.e., feeds, OMTs, FEM, waveguides, BEM). A complete set of tests and calibration procedures has been defined and performend on each RCA in order to properly tune the amplifiers and phase switches and to measure the main radiometer characteristics such as noise temperature, gain, bandwidth, band shape, offset, isolation, linearity. Calibration is performed in cryo-facilities capable of reproducing nearly the thermal conditions expected in flight, i.e., 20K front-end temperature, V-groves temperatures at waveguides interfaces, 4K reference loads. Low return-loss "sky targets" were coupled to the feed horns, with temperature adjustable in the range ~ 7 to ~ 35K. High stability (sub-mK level) is required by the sky targets as well as reference loads to measure the noise spectrum of differenced data.

REFERENCES
9 Bersanelli M. and Mandolesi N., *Astroph. Letters and Comm.* 37, 171 (2000)

Gravitational lensing by high-redshift galaxy clusters

1 Dipartimento di Fisica, Università degli Studi di Milano
2 European Southern Observatory, Garching, Germany

M. Lombardi[1], G. Bertin[1], C. Grillo[1], and P. Rosati[2]

In the last decade we have witnessed a spectacular series of developments in cosmological studies, which have lead the large majority of astronomers to consider high-precision cosmological measurements as more than a simple possibility. At the same time, a widely accepted "standard cosmological model" has emerged. In this framework, the expanding Universe is well described by a Friedmann-Lemaître model, with cosmological parameters close to $\Omega_m = 0.3$ and $\Omega_\Lambda = 0.7$, and the structure formation follows the predictions of Cold Dark Matter (CDM) models; in addition, there some (less convincing) evidence that in the past the Universe has undergone an *inflationary* phase.

Still, these impressive progresses are closely linked to a number of uncertainties that plague our understanding of the physical processes observed in the Universe. For example, over the last 70 years we have postulated the existence of dark matter to explain some apparently contradictory astronomical observations, but since then we have failed to identify its nature and, to a large extent, its spatial distribution. Similarly, we are now measuring with exquisite accuracy the anisotropies of the Cosmic Microwave Background (CMB), which are identified as the seeds for the formation of large scale structures, but structure formation remains a largely unknown process (interestingly, things do not improve significantly on much smaller scales: since almost a century we know that stars form in dark molecular clouds, but star formation is still a mystery).

It has been long recognized that the study of the mass distribution of galaxy clusters conveys precious information on the relationship between dark and luminous matter and can be used to test cosmological models. Indeed, clusters of galaxies lie at the extreme of the mass spectrum of gravitationally bound structures, and therefore their physical properties are thought to be mainly driven by gravitational processes. Over the last decade, gravitational lensing has proved to be a powerful method for determining the mass and mass distribution of galaxy clusters (see [1] for a review). Compared to "standard" method, such as X-ray or dynamical analyses, gravitational lensing is particularly robust, because relies on simple, well-verified assumptions and is sensitive to the *total* mass of a cluster, regardless of the latter's physical state and spatial distribution. In particular, the weak-lensing technique, derived from a statistical analysis of small distortions of faint background sources, is a particularly valuable tool to investigate the matter distribution on the periphery of massive clusters, while the strong-lensing analysis, based on the observation of several arcs (which are highly-distorted images of distant galaxies, see Fig. 1) is able to pin down the small-scale mass density in the cluster cores.

Fig. 1
An image of the lensing cluster Abell 1689 observed with the Advanced Camera for Surveys on board of the Hubble Space Telescope (N. Benitez et al.). Note the impressive number of giant arcs and arclets present here.

REFERENCES
1. Bartelmann M., Schneider P., Physics Reports 340, 291 (2001)

Weak lensing

Weak lensing studies are based on the measurements of the elliptical shapes (ellipticities) of several thousands background galaxies. Unlensed galaxies are expected to be randomly oriented, but because of the lens tidal field, galaxies observed through a galaxy cluster will be preferentially oriented tangentially to the cluster center. As a result, statistical analysis of the local distribution of galaxy ellipticities will provide an estimate of the cluster mass (and distribution).

Following the early work of Tyson et al. [2], many massive clusters have been the subject of weak-lensing analyses (e.g., [3,4]). In most cases, these studies focused on clusters at low to medium redshifts ($0.1 < z < 0.5$), for which moderately deep imaging is sufficient to successfully apply this technique. After several fails, the first clear detection of a weak-lensing signal from a distant cluster, MS 1054.4-0321 at $z = 0.83$, was reported by Luppino & Kaiser [5]. Weak-lensing analysis of very luminous X-ray clusters at $z \sim 0.8$ is by now relatively straightforward (e.g., Clowe et al. [6] studied MS 1137.5 + 6625 at $z = 0.783$ and RX J1716.4+6708 at $z = 0.809$). Weak-lensing studies of clusters at $z \sim 1$ are, in contrast, particularly challenging and essentially impossible with ground-based observations. Most of the galaxies observed even in the deepest ground-based observations have redshifts smaller than unity, and thus are foreground with respect to high-redshift clusters, or are only weakly lensed. To avoid a severe dilution of the lensing signal, one needs to accurately select background galaxies, typically using photometric redshifts. In addition, galaxies at redshifts larger than unity are faint and small, so that measurements of their ellipticities, which are necessary for weak-lensing analysis, are difficult because of photometric uncertainties and the smearing effect of the PSF (in addition to the seeing in ground-based images). Finally, because of the redshift dependence of the lensing signal, weak-lensing masses of distant clusters are strongly sensitive to the redshift distribution of the background galaxies. For example, it is relatively easy to show that a systematic relative error of 5% on $(1 + z)$ of the background galaxies produces a systematic error of 15% on the lensing mass estimate of a $z = 1$ galaxy cluster.

The Advanced Camera for Surveys (ACS) on board the Hubble Space Telescope (HST) provides a unique opportunity to overcome many of the challenges posed by distant clusters. We made use of a deep ACS imaging to detect and measure a weak-lensing signal on the galaxy cluster RDCS 1252.9-2927 (hereafter RDCS 1252, see Fig. 2) at redshift $z = 1.237$, the first of this kind at $z > 1$ [7]. On the reduced images we measured the ellipticities for all galaxies detected with high signal-to-noise ratio; moreover, we tried to reduce the contamination by foreground galaxies (which do not contribute to the lensing signal, but increase the measurement noise) using appropriate selections in color and luminosity of the galaxies. Finally, we were left with approximately 4000 galaxies available for lensing measurements. After correcting these data for several observational and instrumental effects, we were able to obtain the cluster mass map. Overall, the cluster shows a clear East-West elongation (also visible on the cluster light distribution), and signs of substructure (see Fig. 3). The quality of the lensing signal is also evident from Fig. 4, where we plot the average tangential shear of the

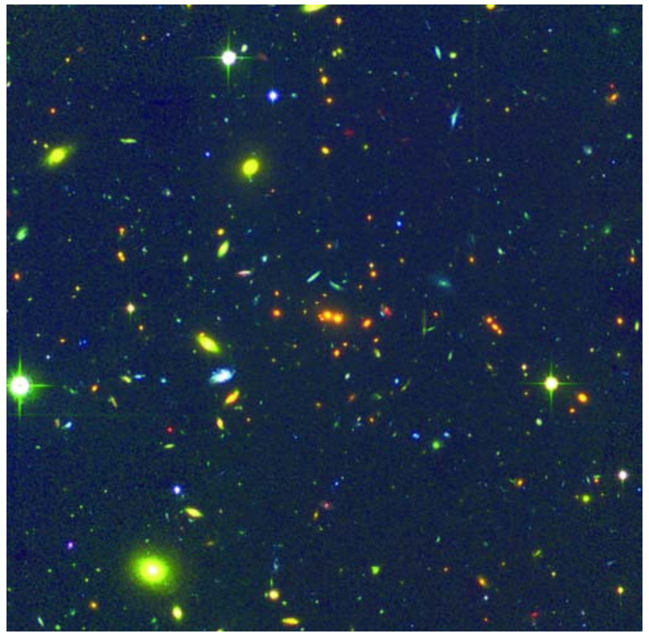

Fig. 2
An image of the galaxy cluster RDCS 1252.9-2927 observed by the ACS/HST. Cluster galaxies are easily identified as orange ellipticals in this image.

REFERENCES
2. Tyson J. A., Wenk R. A., Valdes F., The Astrophysical Journal 349, 1 (1990)
3. Seitz C., Kneib J.-P., Schneider, P., Seitz, S. Astronomy & Astrophysics 314, 707 (1996)
4. Lombardi M., Rosati P., Nonino M., Girardi M., Borgani S., Squires G. Astronomy & Astrophysics 363, 401 (2000)
5. Luppino G. A., Kaiser Nick, The Astrophysical Journal 475, 20 (1997)
6. Clowe D., Luppino G. A., Kaiser N., Henry J. P., Gioia I. M., The Astrophysical Journal 497, 61 (1998)
7. Lombardi, M.; Rosati, P.; Blakeslee, J. P. et al., The Astrophysical Journal 623, 42 (2005)

cluster (i.e. the amount of tangential elongation observed on the ellipticities of background galaxies) together with two simple models (solid lines). As expected, the shear is strong close to the center of the cluster, where the mass density is large, and decreases in the outskirts of the cluster.

This analysis, together with similar ones, can help us to understand the formation of galaxy clusters and the properties and fraction of dark matter in these objects. Overall, our results show that light traces with good accuracy the matter distribution (as frequently observed in galaxy clusters).

Fig. 3
Reconstructed weak lensing mass distribution of RDCS 1252. Green contours represent high-density regions, and red contours low density ones. The main peak is well centered at the location of the observed cluster galaxies.

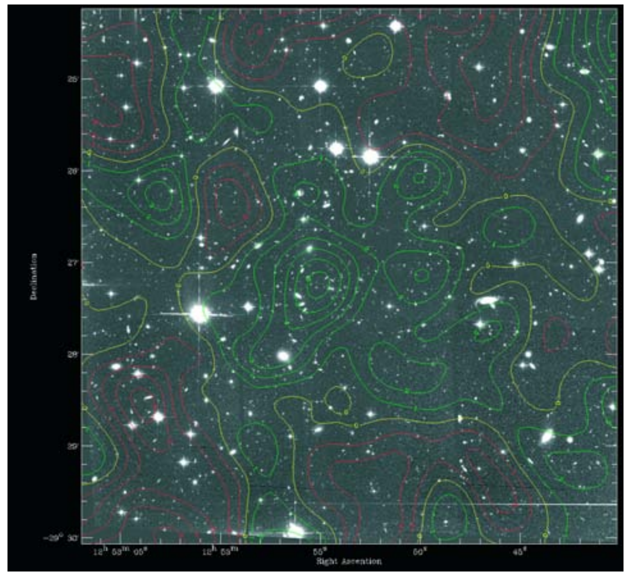

Fig. 4
A plot of the measured average tangential shear of background galaxies (diamonds). Note that the data are in agreement with simple mass models (red and yellow lines).

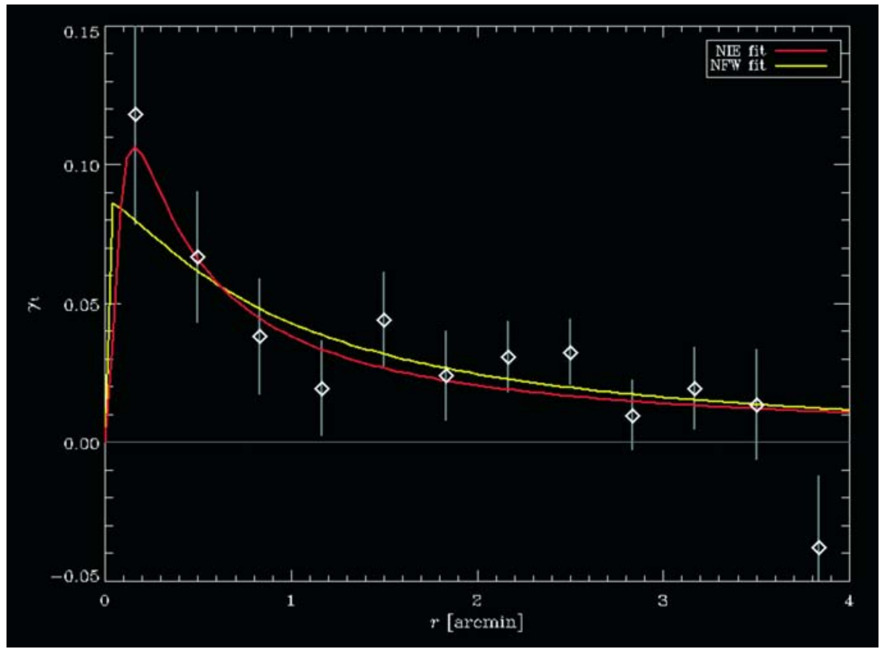

Strong lensing

Strong lensing studies are based on the reconstruction of the cluster mass distribution from the observation of several multiple images (usually arcs) of background galaxies. In its standard formulation, the analysis starts from the identification of images produced from the same source; then a mass distribution able to reproduce the observed configuration is looked for. Hence, a strong lensing analysis usually follows three steps: (i) *possible* multiple images are identified on the field; (ii) the candidates are further investigated by taking their spectra (which must coincide if the images are produced from the same source); (iii) a model (which includes the lens mass distribution and the source position and shape) is obtained. Clearly, the last step is an *inverse problem*, and is usually computationally intensive; moreover, often the three steps mentioned above are iterated (a good lensing model can help significantly in the search for new multiple images, which in turns can be used to refine the model).

Since gravitational lensing preserves the surface brightness, extended sources are particularly valuable for strong lensing studies, as they force the fiducial mass model to reproduce the observed distortions on the sources. Hence, in this respect the sub-arcsecond resolution offered by the HST is critical for the success of strong lensing studies. At the same time, deep ground-based spectroscopic observations are also crucial for the identification of sources and the calibration of the lens model. Still, these efforts are justified because strong lensing provides important complementary information with respect to weak lensing. Recently, we performed follow-up spectroscopic observations on both RDCS 1252 and CL J0152-1357 at z = 0.84 (see Fig. 5), and were able to confirm several arc candidates; the strong lensing analysis is currently carried out..

Fig. 5
An ACS/HST color image of the lensing cluster CL J0152-1357. Several complex arc systems are visible in this image as blue objects around the yellow cluster galaxies.

Future prospects

To large extent, the development of gravitational lensing is technology limited. As an example, although this phenomenon was predicted back in the 30s, the first lens was discovered only in 1979 because of the high requirements needed to observe two angularly close faint images (multiple images of gravitational lensing have typically a separation of a few arcseconds); similarly, microlensing was first proposed by the Polish astronomer Bohdan Paczynski in 1986 [8], and in 1991 he proposed to use it for extrasolar planet searches, but the first planet has been detected only very recently.

Thus, future telescopes will give further momentum to gravitational lensing studies. The development of 30m class telescopes will open several fundamental new opportunities, including spectroscopy of extremely fain source galaxies, and (with the help of adaptive optics) the imaging of small (< 0.1 arcsec) background galaxies. In addition, the spatial resolution and collecting power of these new instruments will allow us to measure ellipticities on extremely faint objects or, in other words, to dramatically increase the number of sources useful for weak lensing analysis and thus the resolution and sensitivity of the mass maps obtained.

The successor of HST, the James Webb Space Telescope (JWST), will be a large (~ 6.5 in diameter) infrared optimized telescope. It will be located at the L2 Lagrangian Sun-Earth libration point, and will be passively cooled using a sunshield as large as a tennis court. This spectacular instrument, scheduled for launch in 2013, will push weak lensing studies to mass concentrations at $z \sim 3$ (to be compared with the $z \sim 1.2$ current limit on ACS/HST data).
Future developments of lensing studies are not limited to standard imaging capabilities or to known lensing phenomena. For example, the GAIA astrometric mission will accurately measure parallaxes of one billion stars (approximately 1% of the total number of stars in our Galaxy), and will not only identify one million asteroids, 30,000 new extrasolar planets, and 100,000 new supernovae, but in its 5-year lifetime it will also measure ~ 4000 *astrometric* microlensing events with multiple images separated only a few microarcseconds.

Ulysses' odyssey

C. Paizis[1,2] and G. Sarri[2]

1 Dipartimento di Fisica, Università degli Studi di Milano
2 INAF/IASF sezione di Milano

The heliosphere, the vast zone over which the Sun extends its influence, is the only astrophysical environment directly accessible. It is a unique plasma laboratory in which we can carry out in situ observations and perform measurements of the relevant physical parameters necessary to understand and describe phenomena non reproducible in the laboratory. This environment has been studied for almost fifty years by Earth satellites as well as by interplanetary probes up to the borders of the heliosphere. Nevertheless, until 1990, the measurements were limited to a few degrees out of the Ecliptic. The heliosphere is not spherically symmetric and extrapolation to higher heliolatitudes would be tempting, yet inaccurate. A decisive step, with measurements above the solar poles, is made by the ULYSSES mission: the first and, for years to come, the only mission that studies the heliosphere in three dimensions and explores uncharted regions of our solar system. Ulysses, launched in 1990, will remain active up to 2008 doing six polar passages. In this talk some results of the cosmic ray experiments, onboard the spacecraft, will be discussed with emphasis on the latitudinal gradient of the cosmic rays in the heliosphere and on their time variation. It will be shown that thanks to the direct high latitude Ulysses measurements, our knowledge about the cosmic ray propagation in the heliosphere is greatly improved.

Full text (in Italian) can be found at *http://www.fisica.unimi.it/highlights2005/*

Coherent structures in electron plasmas: the ELTRAP experiment

M. Romé[1,2], G. Bettega[1,2], F. Cavaliere[1], M. Cavenago[3], F. De Luca[1], A. Illiberi[1,2], I. Kotelnikov[4], R. Pozzoli[1,2], L. Serafini[2], and Yu. Tsidulko[4]

1 *Dipartimento di Fisica, Università degli Studi di Milano*
2 *INFN*
3 *INFN - Laboratori Nazionali di Legnaro*
4 *Budker Institute of Nuclear Physics, Novosibirsk, Russia*

The formation and development of coherent structures in an electron plasma is investigated in the Malmberg-Penning trap ELTRAP [1], shown in Fig. 1, in operation at the Physics Department, and aimed to the study of the nonlinear dynamics of confined electron plasmas and low-energy electron beams. In this device a set of cylindrical electrodes, controlled by a suitable waveform generator and an axial magnetic field B (up to 0.2 T) with a high degree of uniformity are used to contain the electron plasma. An example of well developed coherent structures in the ELTRAP plasma is shown in Fig. 2: it represents, at a given time, the axially integrated electron density distribution, obtained by dumping the electrons on a phosphor screen and recording the images with a CCD camera. The occurrence of (almost) two-dimensional (2D) coherent structures is a clear signature of collective nonlinear processes, and is generally associated to rotation in a continuous medium. This feature occurs in various phenomena investigated in different fields as, e.g., fluid dynamics, atmospheric science, plasma physics and astrophysics.

Fig. 1
Overview of the Malmberg-Penning trap ELTRAP.

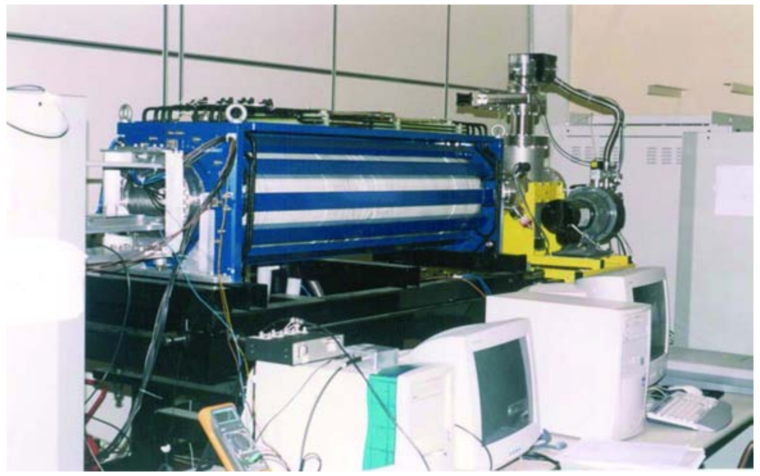

Fig. 2
Observed coherent structures in ELTRAP.

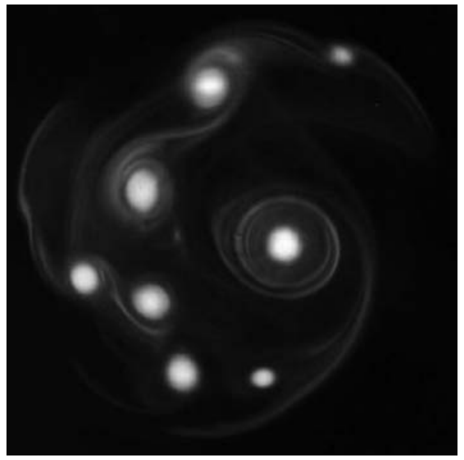

In the trapped plasma case, when the period of the axial electron bounce motion is much shorter than that of the drift rotation, the bounce averaged equations of motion describe a 2D dynamics of the electron columns, identical to the motion of a 2D uniform, incompressible, inviscid fluid, spatially limited by a circular free slip boundary. In this limit, the electric potential is proportional to the stream function, and the plasma vorticity is proportional to n/B, being n the (bounce averaged) plasma density and B the magnetic field strength. The formation and evolution of coherent structures in such conditions, including filamentation, merger, relaxation of turbulence, has been extensively studied using the inject-hold-dump technique, and good agreement with 2D numerical investigations has been found. On a long time scale

REFERENCES
1. Amoretti M., Bettega G., Cavaliere F., Cavenago M., De Luca F., Pozzoli R., and Romé M., "Cylindrical Penning trap for the study of electron plasmas," *Review of Scientific Instruments* 74, 3991 (2003).

(hundreds of rotation periods) the electron plasma can approach an equilibrium state evolving directly towards a stable density profile with cylindrical symmetry or passing through a series of long lived states characterized by regular patterns of localized vortices (vortex crystals), as shown in Fig. 3. A stable equilibrium is eventually reached through dissipative processes.

In the beam regime, all cylindrical electrodes are grounded and a low-energy electron plasma continuously flows from the emitting thermionic cathode to the charge collector (phosphor screen), held at a fixed potential (few kV). In these conditions, the images on the phosphor screen are detected continuously and correspond to almost stationary states of the three-dimensional (3D) structure of the beam. A rapid development of the structures is observed when, by increasing the emission current of the cathode, a sharp transition from a laminar to a space charge dominated regime occurs: the images (Fig. 4) show an annular beam shape, indicating the appearance around the axis of the electron column of a region inaccessible to beam electrons [2].

Fig. 3
Examples of vortex crystals observed in ELTRAP.

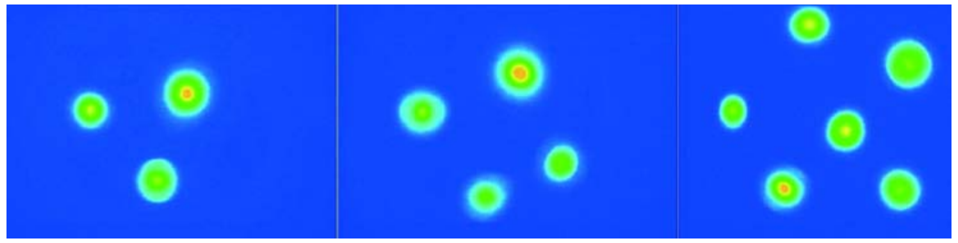

Fig. 4
CCD images showing the transition to a space charge dominated regime in the beam configuration.

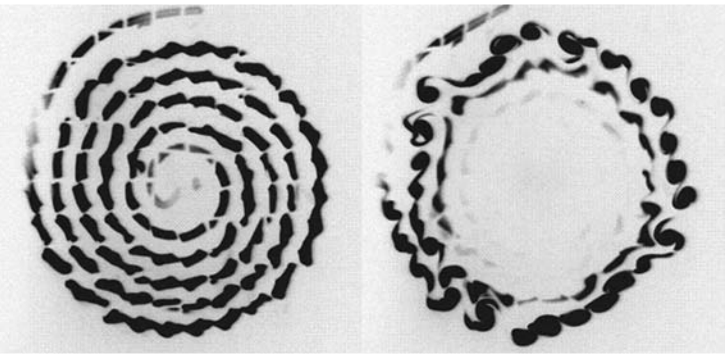

In the beam case the axial dependence can not be cancelled by bounce averaging, and to interpret the experimental results a 3D time dependent problem has to be solved: this can only be approached numerically. To this aim, the 3D PIC code MEP (Milan Electron Plasma) has been developed [3] which solves the 3D drift-Poisson system, both for trapped plasma and beam configurations. An example of the solution is shown in Fig. 5. The electrons are generated from a cathode with an Archimedean spiral shape. The effect of the presence of an accelerating grid is simulated by suitably "cutting" the spiral along rows and columns of a given width. The drift tube is equipotential (grounded), but the exit section is maintained at a (strongly) positive potential, simulating the voltage used to accelerate the electrons against a phosphor screen, for their imaging. Fig. 5 represents the plasma density distribution at a given time (when stationary conditions have been already reached) in different slices transverse to the drift tube: the first close to the source, the last close to the collector. From the analysis of the time evolution of the emitted electrons in the axial phase space, the formation of a "virtual cathode" close to the injection boundary is evidenced. The central part of the beam is reflected back to the cathode by the space-charge of the beam itself, and only the outer part of the beam reaches the opposite end of the trap, held at positive potential. The "annular" beam which travels to the collector shows a quasi-2D evolution of vortex structures. Thus, in almost stationary conditions, three regions can be distinguished: a reflection region close to the injection boundary, a central part with almost constant parallel velocity, and an acceleration region close to the exit boundary.

To account for the fast development (on the time scale of electron transit) of coherent structures observed in the space charge regime it is to be noted that, along most of the beam length L, close to the edge of the shadow region a sharp radial density variation is present and the radial part of the Laplacian in the Poisson equation becomes dominant with respect to lon-

REFERENCES
2. Bettega G., Cavaliere F., Illiberi A., Pozzoli R., Romé M., Cavenago M., and Tsidulko Yu., "Experimental investigation of coherent structures in a low-energy electron beam", *Applied Physics Letters* 84, 3807 (2004)
3. Tsidulko Yu., Pozzoli R., and Romé M., "MEP: a 3D PIC Code for the Simulation of the Dynamics of a Non-Neutral Plasma", *Journal of Computational Physics* 209, 406 (2005)

gitudinal: then, the plasma vorticity becomes proportional to plasma density, and the dynamics becomes again 2D Eulerian. Thus, following the mechanism of diocotron instability coherent tructures can easily develop. To study experimentally the transport of the structures along the beam, it can observed that in this 2D Eulerian limit the effective evolution time of the system is proportional to *L*/*B*. Since *L* is fixed, the evolution along the beam can be investigated by measuring the electron density on the phosphor screen at different *B* values (the variation of the emission flow due to change of the magnetic field must be balanced). A real time evolution can be then obtained by slowly decreasing (with respect to the rotation time scale) the magnetic field. The observed processes are described by a purely 2D dynamics as far as the mentioned approximations are valid. Three images representing the density distribution of a beam on the phosphor screen at different times, obtained by decreasing *B*, are shown in Fig. 6.

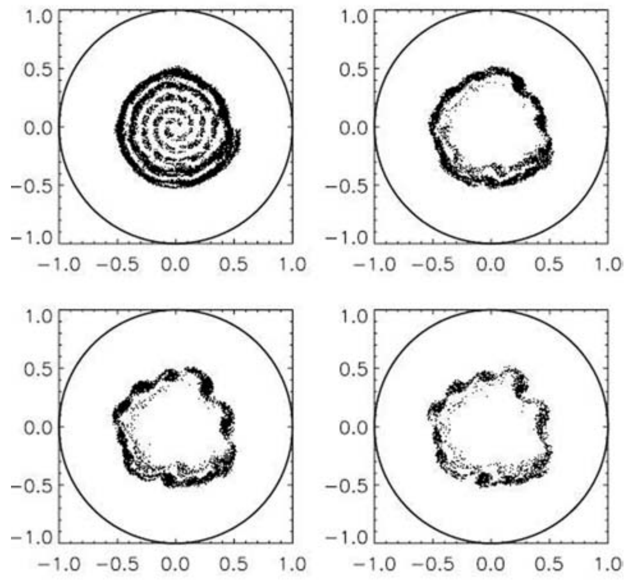

Fig. 5
PIC code results showing the plasma density distribution in different transverse slices of the electron column, at a given time.

Fig. 6
CCD images of the electron beam on the phosphor screen, for decreasing values of the magnetic field.

In conclusion, the formation and evolution of coherent structures in an electron plasma, of relevance for generic rotating systems, have been investigated experimentally in a Malmberg-Penning trap, both for a trapped plasma and an electron beam. The behavior of the system, in the considered range of parameters, is in good agreement with a cold fluid, drift-Poisson description. In particular, in the case of a low-energy electron beam, the main control parameters are the spatial distributions, at the source, of the electron density, energy and current, and the magnetic field. The behavior of the system has been investigated by varying the electron energy and emission current, and sharp or gradual transitions to the space charge dominated regime have been found. The longitudinal structure of the beam has been studied by varying the magnetic field and/or the emission current. In addition, it has been found that the observed behavior of the system, in the considered range of parameters, is in good agreement with the results obtained with a PIC code which solves the Vlasov-Poisson system in the lowest order drift approximation.

Structure, formation, and dynamical evolution of elliptical galaxies

S.E. Arena [1], G. Bertin [1], L. Ciotti [2], T.V. Liseikina [3,4], F. Pegoraro [5], M. Trenti [6], and T.S. van Albada [7]

1 Dipartimento di Fisica, Università degli Studi di Milano
2 Dipartimento di Astronomia, Università di Bologna
3 Institute of Computational Technologies, Novosibirsk, Russia
4 Ruhr-Universitaet, Bochum, Germania
5 Dipartimento di Fisica, Università di Pisa
6 Scuola Normale Superiore di Pisa
7 Kapteyn Astronomical Institute,Groningen, Olanda

Elliptical galaxies may be formed from collisionless collapse of an initially cold cloud of stars, reaching dynamical equilibrium by incomplete violent relaxation. We have tested this picture by means of analytical models and N-body simulations. The theoretical distribution function, called $f^{(\nu)}$, is derived by extremizing the Boltzmann entropy at fixed values of the total mass, of the total energy, and of a third global quantity, argued to incorporate the effects of the incompleteness of the process of violent relaxation. The resulting two-parameter (ν,Ψ) family of models is then constructed by solving the Poisson equation. The dependence on ν is weak, while Ψ is a concentration parameter describing the central depth of the galaxy potential well. The simulations are performed with a mean field code from a variety of initial conditions. We found that the analytical models not only match the basic structure of many elliptical galaxies (for a constant mass-to-light ratio), but are also able to fit the density profiles (over nine orders of magnitude; with relative error within 10%) and the phase space properties (predicting the pressure anisotropy profile with mean error of 5%) of the end products of the collisionless collapse simulations (Fig. 1) [1].

Fig. 1
Comparison between the results of a simulation of galaxy formation by collisionless collapse (error bars) and the best-fit $f^{(\nu)}$ model (Ψ = 4.2, ν = 1.0): density profile (left), pressure anisotropy profile (right). The local anisotropy is defined as $\alpha(r) = 2 - (\langle w_\theta^2\rangle + \langle w_\phi^2\rangle)/\langle w_r^2\rangle$, in terms of the relevant velocity dispersions.

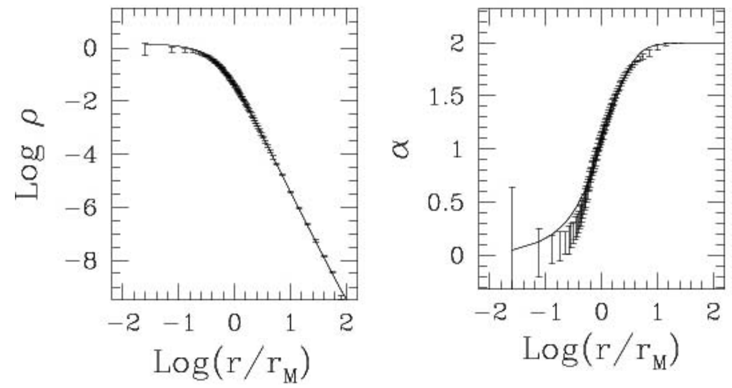

We have then addressed the issue of the dynamical evolution of such stellar systems, focusing on the slow evolution induced by dynamical friction of a host galaxy on a minority component of "satellites". The basic mechanisms of dynamical friction have been modeled long ago by Chandrasekhar (1943), but are not understood under realistic conditions. To study this problem and its consequent effects on the galaxy, we used the code mentioned above with the addition of finite-size satellites interacting directly with the simulation particles of the galaxy. The initial conditions represent a spherical galaxy in dynamical equilibrium in the presence of a quasi-spherical system of 20-100 satellites on circular orbits (see [2], [3]). We find, in general, that the role of collective effects and inhomogeneities is important, the density distribution of the host galaxy tends to relax to a broader profile, in contrast with the expectations of adiabatic models (Fig. 2), and that satellites spiraling in on quasi-circular orbits tend to heat the stellar system preferentially in the tangential directions.

Fig. 2
Comparison between final (solid) and initial (dotted) density profiles, illustrating the galaxy evolution induced by the infall of matter in the dynamical friction case (left) and in the adiabatic case (right).

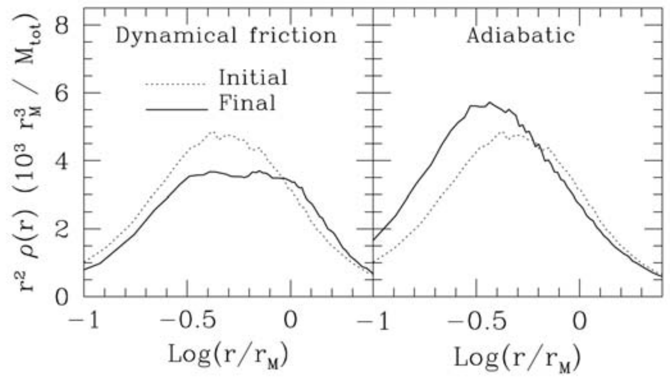

Finally, we have devised a systematic procedure for the construction of models characterized by a significantly non-spherical geometry [4].

REFERENCES
1. Trenti, M., Bertin, G., and van Albada, T.S., *Astronomy and Astrophysics*, 433, 57 (2005)
2. Bertin, G., Liseikina, T.V., and Pegoraro, F., *Astronomy and Astrophysics*, 405, 73 (2003)
3. Arena, S.E., Bertin, G., Liseikina, T.V., and Pegoraro, F. *Astronomy and Astrophysics*, 453, 9 (2006)
4. Ciotti, L. and Bertin, G., *Astronomy and Astrophysics*, 437, 419 (2005)

Structure and dynamics of nearby spiral galaxies

C.V. Barbieri [1,2], G. Bertin [1], D. Bettoni [3], R. Boomsma [4], A. Cava [1,3], F. Fraternali [5], T. Oosterloo [6], and R. Sancisi [2,4]

1 Dipartimento di Fisica, Università degli Studi di Milano
2 INAF - Osservatorio di Bologna
3 INAF - Osservatorio di Padova
4 Kapteyn Astronomical Institute,Groningen, Olanda
5 University of Oxford, Oxford, UK
6 ASTRON - Dwingeloo

Recently, the in-depth study of nearby galaxies has led to the surprising discovery that the HI distribution is not confined, as previously thought, to the thin equatorial plane of the disk, but may extend well out of plane, forming a slower-rotating halo-like structure (see the rotation curves in Fig. 1). Most likely this anomalous gas does not coexist with the normal gas in the region close to the equatorial plane. This finding has important consequences on our picture of how spiral galaxies form and evolve. More specifically, such extra-planar gas may be the result of a *galactic fountain* circulation or be indicative of ongoing accretion from the external environment; similar scenarios had been invoked to interpret the phenomenon of the high velocity clouds in our Galaxy. By a deep 21cm investigation of NGC 4559, we have found [1] one more example of this phenomenon, which adds to the very small number of firm cases of extra-planar gas identified so far. The extra-planar gas of NGC 4559 is similar to that found in NGC 891, UGC 7321, and NGC 2403. This suggests that the *anomalous* gas may be a common feature in spiral galaxies, missed earlier because of insufficient sensitivity of the previous observations.

From the dynamical point of view, finding new properties in the structure of galaxies raises new problems of equilibrium and stability. On a related theme, we have recently addressed the question of the stability of disks characterized by the presence of two components in relative motion [2]. We showed that the small relative motion between the two components associated with the so-called asymmetric drift can be the origin of instability for suitable non-axisymmetric perturbations [3]. The result is obtained by examining the properties of a local, linear dispersion relation for tightly wound density waves in such a two-component fluid model which extends the case analyzed in previous investigations.

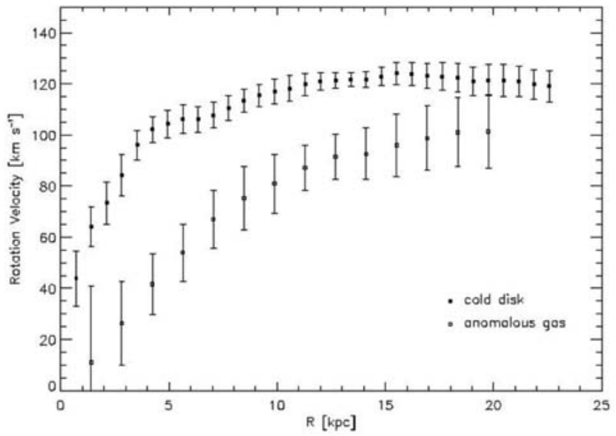

Fig.1
Rotation curves for the cold disk and for the anomalous gas in NGC 4559 (from [1]).

To get a statistically significant picture of the properties of galaxies, the deep study of individual galaxies should be accompanied by dedicated extensive surveys. One project which may bring important information on the dynamics of normal galaxies is WINGS (Wide-field Imaging Nearby Galaxy-cluster Survey; [4]), a wide-field spectro-photometric survey of a complete all-sky X-ray selected sample of 78 clusters in the redshift range z = 0.04-0.07. WINGS is the deepest ($M_V \leq$ - 14), best resolution (1'') survey of a complete sample of nearby cluster galaxies to date. A natural follow up of the photometric survey is the long term spectroscopic program that we are carrying out using spectra taken with the WHT-WYFFOS and AAT-2dF multifiber spectrographs which is fundamental to address the study of the dynamics of the clusters. Redshifts, line indices and equivalent widths of the main absorption and emission features are measured and provide cluster membership, star formation rates and histories, and metallicity estimates. An extensive observational program is planned to complete the spectral range from the NIR to the UV.

REFERENCES
1. Barbieri, C.V., Fraternali, F., Oosterloo, T., Bertin, G., Boomsma, R., Sancisi, R. *Astronomy and Astrophysics*, 439, 947 (2005)
2. Cava, A. Tesi di Laurea, Università degli Studi di Milano (2004)
3. Bertin G., Cava, A. *Astronomy and Astrophysics*, 459, 333 (2006)
4. Fasano, G., Marmo, C., Varela, J. et al. *Astronomy and Astrophysics*, 445, 805 (2006)

Structure and dynamics of clusters of galaxies

G. Bertin [1], S. Caffi [1,2], C. Grillo [1], A. Leccardi [1,2], M. Lombardi [1], S. Molendi [2], and M. Rossetti [1,2]

1 Dipartimento di Fisica, Università degli Studi di Milano
2 INAF - IASF di Milano

Associations of galaxies range from groups of tens to clusters of thousands of galaxies. Clusters of galaxies are the most massive ($M \sim 10^{14}$ M_{Sun}) gravitationally bound systems in the Universe. *Chandra* and *XMM-Newton* can perform high-resolution imaging of the X-ray emitting Intra-Cluster Medium (ICM), which is responsible for about 20% of the total mass. The ICM is a tenuous, hot (several keV), highly ionized and metal-rich plasma. In many clusters, the Hubble Space Telescope shows spectacular strong lensing patterns, in the form of giant luminous arcs, distorted arclets, and multiple images of background galaxies.

We measured the mean temperature profile [1] for a sample of 21 clusters selected from the *XMM-Newton* archive (high temperature kT > 4 keV, intermediate redshift 0.09 < z < 0.23, high galactic latitudes), to resolve the conflicting results of previous studies. The clear temperature decline (Fig. 1) found in the outer regions ($r > 0.2\, r_{180}$), with a common behavior for relaxed and non-relaxed clusters, confirms the picture proposed by De Grandi & Molendi [2]. This new measurement suggests the existence of a universal temperature profile for hot clusters. We have also performed a joint *Chandra* and *XMM-Newton* structural analysis of two clusters. In the cluster A3558, a cold front is detected and studied [3] with a metallicity profile continuous across the surface brightness discontinuity. Interestingly, a tail of gas with low entropy, high density, and low temperature is found behind the cold front. In the cluster A2199, an X-ray cavity filled with radio emission provides evidence for interaction between the central active galaxy and the ICM plasma [4]. Through the application of the standard synchrotron model, we found a magnetic field of a few tens of μG inside the radio bubble. A detailed modeling of another structure in the ICM, characterized by high density and metallicity and low temperature and entropy, suggests that we are witnessing the formation of the cool core in A2199.

Determining an accurate model for the mass distribution in distant clusters has important consequences on the currently developed cosmological scenarios. Since these clusters may be far from symmetry and equilibrium, gravitational lensing studies are especially valuable. We present a strong lensing study of RDCS 1252.9-2927, one of the most distant (z = 1.24), massive, and X-ray luminous clusters known to date. The images (i and z, *ACS*) from *HST* and others (B, V, and R, *FORS; J* and K, *ISAAC*) from *VLT* show the existence of several tangential arcs. The position and shape of two of them (Fig. 2), with measured redshift z = 3.3, lead to a measurement of the total mass inside the Einstein radius: $M(R < 130$ kpc$) = (1.2 \pm 0.1) \times 10^{14}$ M_{Sun}, in the current cosmological concordance model [5]. This lens model has then been used to discover two high-redshift galaxy candidates ($z_1 \sim 2.5$, $z_2 \sim 4$) magnified by lensing. The strong lensing mass measurement agrees well with the weak lensing [6] and the X-ray analyses.

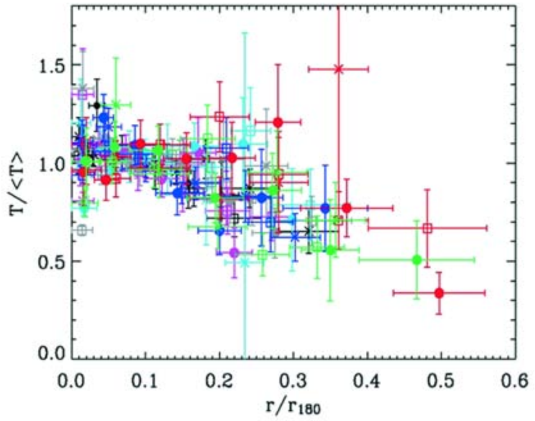

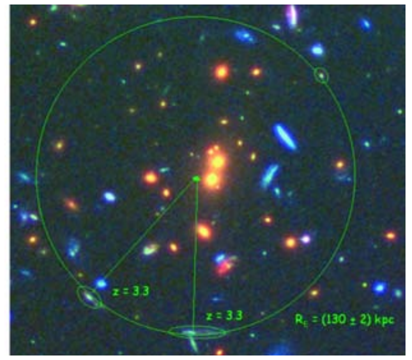

Fig. 1
Temperature profiles for a sample of 21 clusters of galaxies observed by *XMM-Newton*

Fig. 2
RDCS 1252.9-2927 in *B*, *V*, *z*, and *K* bands. Tangential arcs and the Einstein ring around the red massive cluster galaxies.

REFERENCES
1. Leccardi A., Tesi di Laurea, Università degli Studi di Milano (2005)
2. De Grandi S., and Molendi S., *Astrophysical Journal*, 567, 163 (2002)
3. Rossetti M. *et al., Astronomy and Astrophysics*, in press (2006)
4. Caffi S. *et al., Astronomy and Astrophysics* submitted (2005)
5. Grillo C., Tesi di Laurea, Università degli Studi di Milano (2004)
6. Lombardi M. *et al., Astrophysical Journal*, 623, 42 (2005)

Accretion and proto-stellar disks

G. Bertin[1], B. Coppi[2], A. Isella[1,3], G. Lodato[4], A. Natta[3], and L. Testi[3]

1 Dipartimento di Fisica, Università degli Studi di Milano
2 Massachusetts Institute of Technology, Cambridge, MA, USA
3 INAF – Osservatorio di Arcetri
4 Institute of Astronomy, Cambridge, UK

The paradigm of accretion has had a major impact on a variety of phenomena in astrophysics; in particular, it has often been applied to the context of proto-stellar disks. We have studied the role of the disk self-gravity on the properties of accretion disks and found that this role may help explain a number of observational properties of young proto-stellar objects, especially of FU Orionis stars [1]. The theory of such self-gravitating disks recognizes that disks in their outer parts cannot be too cold, otherwise they would be Jeans unstable; Jeans related instabilities, combined with dissipation, are thus bound to enforce a sort of "thermostat" (self-regulation), with properties that can be calculated analytically or studied by numerical simulations (see Fig. 1). In particular, self-gravity results to be very effective in (i) redistributing angular momentum in the disk and (ii) heating the disk up, so that a self-regulated equilibrium is rapidly established, where the stability parameter Q is maintained close to its marginal value $Q \approx 1$. Simple models of the self-regulated disks show that these disks are likely to be hotter in their outer parts than the corresponding non-self-gravitating disks and that they may show deviations from Keplerian rotation. These concepts might be extended to the case in which electric currents and magnetic fields are also dynamically important; work is in progress to find a consistent model for the transition region from a warm, plasma-dominated, magnetized inner disk [2] to a cool, neutral, self-gravitating outer disk.

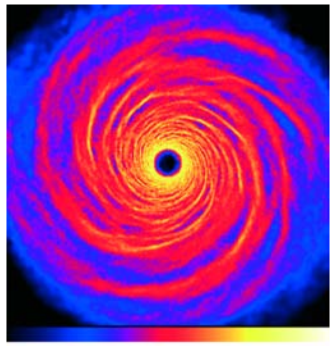

Fig. 1
Smoothed Particle Hydrodynamics simulation of a self-gravitating proto-stellar disk. The disk develops spiral structure which redistributes angular momentum and brings the disk to a quasi-stationary state, where cooling is balanced by the heating associated with spiral instabilities. The image shows the disk density when such self-regulated state is reached. In the case shown here, the disk mass is relatively light ($M_{disk} = 0.1M_*$; after Lodato & Rice 2004, MNRAS, 351, 630).

To explain the observations of young stellar objects, some models do not rely on the accretion paradigm but rather on the role of irradiation of the disk by the central star under a suitable geometry. The predictions of a new hydrostatic, axisymmetric, radiative equilibrium model for the innermost region of passive irradiated dusty disks [3] have been compared with the present near infrared interferometric observations of some intermediate-mass young stellar objects. The model incorporates the variation of the dust grain evaporation temperature with the gas density. The resulting dust evaporation distance depends on the grain composition and size; it increases with the height above the disk mid-plane, describing a curved surface (see Fig. 2). The calculated radius of the inner rim of the dusty disks is generally consistent with the interferometric observations of Herbig Ae stars. In four out of six analysed circumstellar disks, dust grains larger than 1 µm, much larger than typical grains in the interstellar medium, are either required by or consistent with the data, confirming that grain growth has taken place in the innermost disk regions [4].

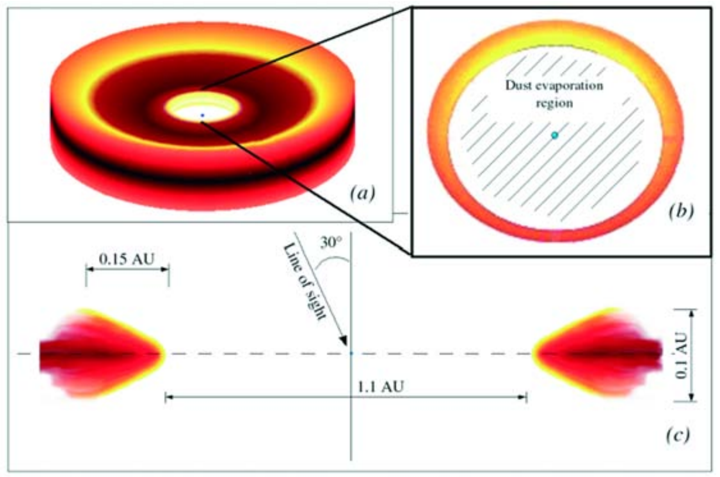

Fig. 2
Sketch of the structure of the inner disk (after [3]) for a star with temperature of 10000K, luminosity of 50 and mass of 2.5 in solar units. (a) The circumstellar disk is truncated internally at about 0.5AU from the star by dust evaporation, which produces a dust depleted inner hole and a "puffed-up" inner rim. (b) The inner rim appears as a bright ring in the sky. (c) The rim surface is curved.

REFERENCES
1. Lodato, G. and Bertin, G., *Astronomy and Astrophysics*, 408, 1015 (2003)
2. Bertin, G., Coppi, B., and Rousseau, F., American Physical Society, 47th Annual Meeting of the Division of Plasma Physics, Denver, CO, LP1.070 (2005)
3. Isella, A. and Natta, A., *Astronomy and Astrophysics*, 438, 899 (2005)
4. Isella, A., Testi L., and Natta, A., *Astronomy and Astrophysics*, 451, 951 (2006)

Diocotron instability in an electron plasma

G. Bettega[1,2], F. Cavaliere[1], M. Cavenago[3], A. Illiberi[1,2], R. Pozzoli[1,2], and M. Romé[1,2]

1 Dipartimento di Fisica, Università degli Studi di Milano
2 INFN - Sezione di Milano
3 INFN - Laboratori Nazionali di Legnaro

In a wide range of experimental conditions an electron plasma column trapped in a Malmberg-Penning device behaves like a 2D fluid [1]: diocotron modes (i.e. flute density perturbations analogous to Kelvin waves on an extended vortex patch) propagate on the plasma surface, and become unstable when the plasma density profile is hollow [2]. For the fundamental $l = 1$ diocotron mode, i.e. the propagation of a wave with spatial dependence $\exp(i\vartheta)$, which corresponds to an off-axis rotation of the plasma, the theory predicts marginal stability (the column orbits with a fixed radial displacement).

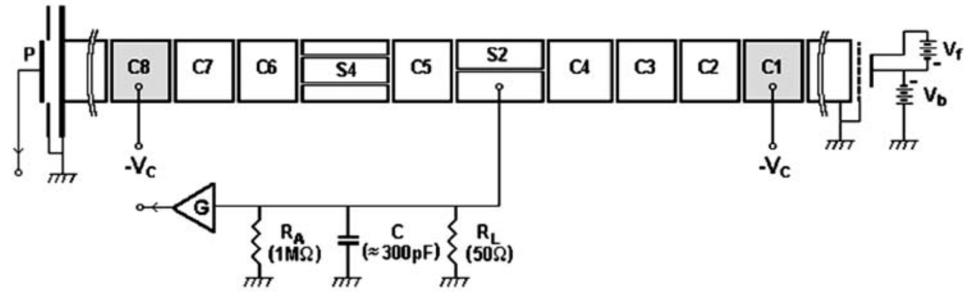

Fig. 1
Schematic of the Malmberg-Penning trap ELTRAP and its diagnostic system. The azimuthally sectored cylinders S2 and S4 allow to detect the plasma rotation. The source connections, the amplification circuitry and the phosphor screen for the optical diagnostic are shown. The aluminum polarization layer on the phosphor screen can also be used as a charge collector.

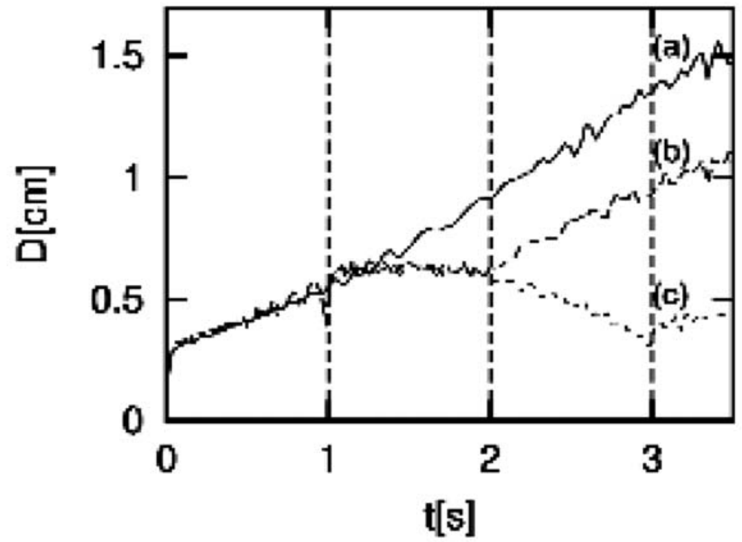

Fig. 2
Effect of the ion removing fields on the amplitude D of the diocotron mode. The constant voltages $V_{C3} = -4$ V, $V_{C4} = -2$ V, $V_{S2} = 0$ V are applied on the cylinders C3, C4 and S2, respectively. The ion removing fields are applied from 1 to 2 s (curve (b)), or from 1 s to 3 s (curve (c)). Curve (a) refers to a standard configuration, with the inner electrodes grounded.

The experiments performed on the ELTRAP device [3] show that the fundamental diocotron mode is destabilized by the presence of a small population of ions, produced by energetic electron-neutral collisions, occurring also in UHV conditions [4]. The schematic of the experimental set up is shown in Fig. 1. It is found that direct plasma heating with radio-frequency bursts increases the ionization rate, and triggers the instability. Similar results have been obtained adding a potential well for the ions, which causes their accumulation inside the trap.

The radial offset of the plasma linearly increases in time, moreover maximum growth rates have been measured when the system parameters (plasma radius, electron density, confining magnetic field) satisfy a resonance condition [5]. In practice this destabilization mechanism acts in all the experiments on magnetized plasma column and is likely to be at the basis of the particle loss also in toroidal devices [6]. According to the experimental results on the instability trigger an effective method of control has been developed, consisting of a continuous ions removal by low (1÷3 V) electrostatic potentials applied to the inner electrodes of the trap, which are usually grounded. The application of such an *ion removing field* stabilizes the plasma rotation and increases the plasma mean life. This effect is shown in Fig. 2. Time varying configurations of the ion removing field, which limit the plasma radial bulk expansion due to the cylindrical symmetry breaking, have been successfully tested.

REFERENCES
1. Durkin D., and Fajans, "Experiments on two-dimensional vortex patterns," *Physics of Fluids* 12, 289 (2000)
2. Davidson R. C., *An Introduction to the Physics of Nonneutral Plasmas* (Addison Wesley, Redwood City, U.S.A., 1990)
3. Amoretti M., Bettega G., Cavaliere F., Cavenago M., De Luca F., Pozzoli R., and Romé M., "Cylindrical Penning trap for the study of electron plasmas," *Review of Scientific Instruments* 74, 3991 (2003)
4. Bettega G., Cavaliere F., Cavenago M., Illiberi A., Pozzoli R., and Romé M., "Experimental investigation of the ion resonance instability in a trapped electron plasma," *Plasma Physics and Controlled Fusion* 47, 1 (2005)
5. Fajans J., "Transient ion resonance instability", *Physics of Fluids B* 5, 3127 (1997)
6. Clark W., Korn P., Mondelli P., and Rostoker N., "Experiments on electron injection into a toroidal magnetic field," *Physical Review Letters* 37, 592 (1976)

Towards an optimized scanning strategy for the Planck satellite

B. Cappellini[1], D. Maino[1], M. Bersanelli[1], A. Mennella[1], P. Platania[2], C. Burigana[3], M. Maris[4], and X. Dupac[4]

1 Dipartimento di Fisica, Università degli Studi di Milano
2 Istituto di Fisica dei plasmi CNR - Milano
3 INAF - IASF Bologna
4 INAF - Osservatorio di Trieste

Planck is an ESA mission planned to map the Cosmic Microwave Background (CMB) anisotropy in the frequency range 30-857 GHz, with 30'-5' angular resolution and sensitivity $\Delta T/T \sim 10^{-6}$ per resolution element. A key mission aspect is the choice of the satellite orbit and scanning strategy (SS). Their main features are now well established but details are not frozen yet. Accurate studies are in progress to identify the best choice for the scientific data exploitation [1, 2]. The SS must satisfy established attitude limits for the payload. Thermal and telemetry constraints require the spin axis to point within 10° with respect to the Sun and 15° with respect to the Earth.

Planck traces a Lissajous orbit about the Earth-Sun Lagrangian point L2, at ~ 1.5 x 10^6 Km from the Earth. The "Nominal" SS (NSS, spin axis always on the Ecliptic) is the simplest SS which satisfies the requirements, but also suffers from limitations. A displacement of the spin axis can solve them but can also induce thermal and stray-light contamination. The SS has to be chosen as the best trade-off among these factors. The choice is going towards a cycloidal pattern of the spin axis.

Telemetry limits the initial position (defined by a "phase" parameter) of the spin axis. We compute the telemetry angle during the observations, as a function of cycloidal amplitude, phase, spin axis period and motion direction, to settle the best configuration (Fig. 1). As expected, the best period is ~ 6 months, synchronized to the orbit around L2, for each amplitude. Higher is the amplitude and stronger is the limitation on the allowed periods and phases.

The SS geometry directly impacts the accuracy of the in-flight calibration [3] based on the dipole pattern. We propose an objective criterion to choose the phase, optimizing the calibration on time scales ~ 3-6 months. Figure 2 shows the minimum value of the dipole signal available for calibration vs phase, for two surveys. The maximum of each curve fixes the best phase. This optimization suggests a re-adjustment of the phase at the end of each survey.

In the NSS no full coverage of the sky is achieved and deep fields (DFs) are not-connected regions. This is not optimal, since DFs are promising for CMB polarization anisotropy imaging. A cycloidal pattern fills the polar holes and redistributes the sensitivity in the sky. Only an amplitude > 7.4° allows full-sky coverage for each detector. The phase fixes the orientation of the DF in the sky. Its value can be chosen to minimize the Galactic foregrounds in the DFs and to optimize the global sensitivity in the presence of sky masks.
A cycloidal pattern slightly reduces Earth and Moon stray-light contamination but substantially worsens the Solar one. The latter is largely below the CMB signal and noise levels only provided that the beam response in the relevant pattern region never exceeds well-defined values.

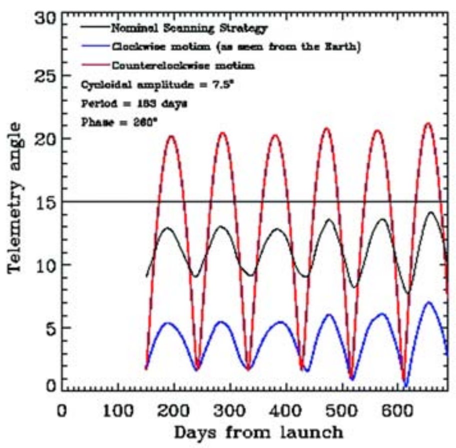

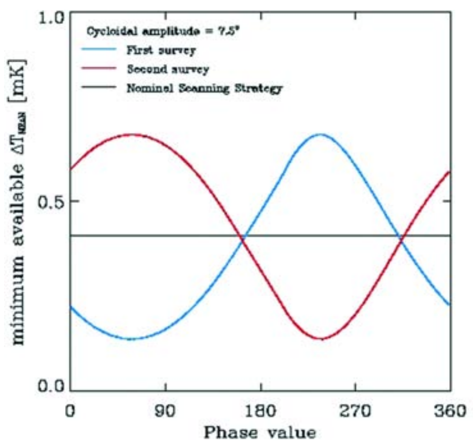

REFERENCES
1. Dupac X. & Tauber J., "Scanning strategy for mapping the Cosmic Microwave Background anisotropies with Planck", *Astronomy and Astrophysics* 430, 363 (2005)
2. Bernard J.-P., Burigana C., Tauber J. et al., "Definition of the Planck baseline scanning strategy", *Technical Note PL-WG9-TN-001* (2006)
3. Cappellini B., Maino D., Albetti G. et al., "Optimized in-flight absolute calibration for extended CMB surveys", *Astronomy and Astrophysics* 409, 375 (2003)

Catalogue of Apparent Diameters and Absolute Radii of Stars (CADARS) – 4th edition

A.L. Ciapi[1], S. Motta[2], and L.E. Pasinetti[1]

1 Dipartimento di Fisica, Università degli Studi di Milano
2 MIUR

Databases are an essential tool for the modern Astrophysical research. The need for archiving astronomical data was stressed also by the resolution A3 at the 23rd International Astronomical Union (IAU) General Assembly (KYOTO,1997) (Fig. 1).

Fig. 1
Resolution A3 from IAU General Assembly, Kyoto 1997

IAU RESOLUTION A3
ON THE NEED FOR ARCHIVING ASTRONOMICAL DATA
Proposed by Commission 5
The XXIIIrd International Astronomical Union General Assembly,
Considering
the continuing important role of astronomical data from the past, including bibliographical information,
Considering
the phenomenal increase in these data,
Considering
the importance of their safeguarding and of their accessibility to the entire astronomical community,
recommends
that the archiving of these data be an integral part of all major research projects and be taken into account by the editors of journals. The IAU recommends that astronomy archives be coded in the FITS format,
supports
supports the continued maintenance of the Data Centers whose role in the distribution of information is of prime importance for astronomy, and supports their collaboration.

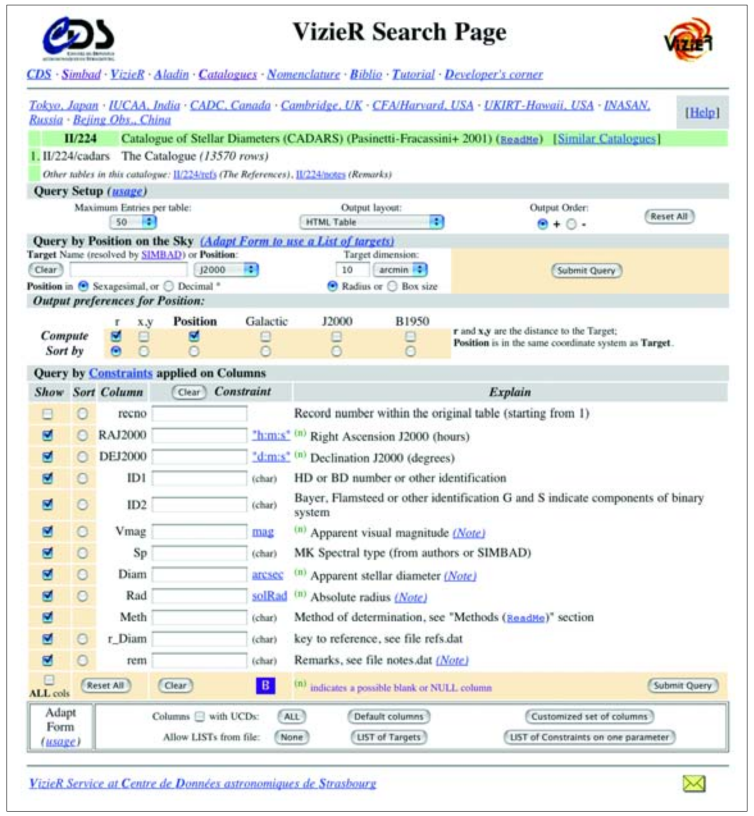

Fig. 2
Query page to retrieve the CADARS data

The first world-wide astronomical data centre was the "Centre des Données Astronomiques de Strasbourg" (CDS) which collaborates also with IAU Commission 5 "Documentation and Astronomical Data" and with CODATA (Committee on Data for Science and Technology of the International Council of Scientific Unions).

The archives of CDS and other astronomical data centres are available on line to the whole scientific community and give catalogues, elaborated by the authors, of the objects and their fundamental parameters, derived from ground based and space observations. Moreover it is possible to obtain bibliographical information, cross identifications, images, plots, field charts, links to external archives and so on.

On invitation of CDS and IAU Comm.5, a “Catalogue of Apparent Diameters and Absolute Radii of Stars (CADARS)” determined by different methods and technologies was planned in 1979 and published in 1981 [1,2]: CDS Catalogue II/61. The second edition (CDS Catalogue II/155) [3,4] is included in the CD ROM of the NASA [5], reporting the most frequently requested catalogues. CADARS is used by the scientific community both for studies on stellar structure and evolution, and for calibrations of astronomical instruments. The authors were encouraged to assemble a 3rd edition (CDS Cat II/224) updating the catalogue with the large amount of high precision data from the long baseline interferometers [6]. The data listed in the catalogue are reported in Fig. 2.

At present we are implementing and updating the 4th edition of the CADARS. Statistical researches are in progress on the catalogue, as well as comparisons and calibrations of the different methods used for the determination of the parameters. We note that most of the new data are derived from direct measures rather than from indirect methods as in the previous editions.

REFERENCES
1. Fracassini M, Pasinetti L.E., and Manzolini F., “Catalogue of apparent diameters and absolute radii of stars (CADARS)” Astronomy and Astrophysics. Supplement Series 45, 145 (1981)
2. Fracassini M., Manzolini F. and Pasinetti L.E., “Preliminary Comments on the Catalogue of Apparent Diameters and Absolute Radii of Stars (CADARS)” Astronomy and Astrophysics Supplement Series 44, 55 (1981)
3. Fracassini M., Pasinetti Fracassini L.E., and Pastori L., Bull. Inf. CDS, 35, 121 (1988)
4. Pastori L., Pasinetti L.E., and Pironi R.,Bull. Inf. CDS, 35, 69 (1988)
5. Schneider G.L., “Selected Astronomical Catalogs, Volume 2”, ADC Electronic News Vol.5, Issue 1, NASA GSFC (1996)
6. Pasinetti Fracassini L.E., Pastori L., Covino S., and Pozzi A., “ Catalogue of Apparent Diameters and Absolute Radii of Stars (CADARS)- Third edition- Comments and Statistics”Astronomy and Astrophysics.367, 521 (2001)

Dynamics, heating, and transport problems in fusion plasmas

F. De Luca[1], D. Farina[2], A. Jacchia[2], H. Maaßberg[3], R. Pozzoli[1], M. Romé[1], and F. Ryter[4]

1 Dipartimento di Fisica, Università degli Studi di Milano
2 CNR - Istituto di Fisica del Plasma, EURATOM-ENEA-CNR Association, Milano
3 Max-Planck-Institut für Plasmaphysik, Greifswald, Germany
4 Max-Planck-Institut für Plasmaphysik, Garching, Germany

Collective phenomena play a dominant role in the behavior of high temperature plasmas. Their occurrence in magnetic confinement configurations may enhance thermal energy and particle transport up to intolerable levels, a major obstacle to nuclear fusion. On the other hand, collective processes may be efficiently exploited in different methods used to heat the plasma and/or to modify the electric current distribution, and contrast the rising of instabilities. Three examples are presented, where investigations of such types of processes are performed in different plasma systems, and with different methods.

In the first problem the self-consistent dynamics of a beam-plasma system is considered, as paradigmatic case of plasma-wave interaction, where energy and momentum transfer occurs through plasma waves. The analysis is performed in the framework of a kinetic approach using a Hamiltonian technique, and leads to a N degrees of freedom Hamiltonian with generic characteristics. The connection between the behavior of nonlinear perturbations and stochasticity of the system (measured through the time-dependent maximum Lyapunov exponent) is investigated. It is found that the development of self-consistent large amplitude oscillations occurs in correspondence with the onset of chaos, and is related to a well defined change of topology of the phase space of the system. It is also shown that in a (Hamiltonian) linearly stable regime the development of large amplitude oscillations can occur when weakly dissipative processes are introduced [1].

The second problem refers to the production of electron current, by injection of electromagnetic waves, to sustain plasma confinement and stability. The electron cyclotron current drive (ECCD) with extraordinary mode at the second cyclotron harmonic launched from the high-field-side (HFS) has been investigated in W7-AS stellarator at the Max-Planck-Institute für Plasmaphysik in Garching (Germany). Trapped particle effects and quasi-linear effects are taken into account in linear ray-tracing and quasi-linear bounce-averaged Fokker-Planck computations of the driven current. The results for both low-field-side (LFS) and HFS injection in W7-AS have been compared with the experimental results. A slightly lower current drive efficiency has been obtained, both theoretically and experimentally, in the case of HFS injection, confirming the LFS launch as the preferred mode of operation for ECCD [2].

The third topic is a crucial issue for reactor extrapolation, and refers to the electron heat transport in high temperature plasmas. Steady state and perturbative heat transport studies allow a quite good theory-experiment comparison. In particular, the ETG model has been experimentally verified by analyzing and comparing data of Cold Pulses (LBO of silicon) and of MECH induced temperature perturbation in FTU (Frascati Tokamak Upgrade) and Asdex Upgrade tokamak. The model predicts that the heat transport is determined by the presence of instabilities due to critical values of the characteristic length of the electron temperature gradient. In FTU experiments [3] the measured critical value turns out to be related to the parameter s/q (where s is the shear, and q the security factor) determined by the plasma current profile. Additional confirmations of the model come from the analysis of experiments in ASDEX Upgrade [4]: steady ECH power induces a transition from low to high electron heat transport at the sides of the injection radius; close to the transition, temperature perturbations show a non-linear behaviour consistent with a critical gradient length concept.

REFERENCES
1. Farina D. and Pozzoli R., “Large-amplitude oscillations and chaos in a Hamiltonian plasma system with many degrees of freedom,” *Physical Review E* 70, 036407 (2004)
2. Romé M., Erckmann V, Laqua H. P., Maassberg H., and Marushchenko N. B., “Comparison of high field-side and low-field-side launch ECCD in the W7-AS Stellarator,” *Plasma Physics and Controlled Fusion* 45, 783 (2003)
3. Cirant S., Bracco G., Bruschi A., Buratti P., De Luca F., Esposito B., Gandini F., Giovannozzi E., Granucci G., Jacchia A., Lazzaro E., Minardi E., Nowak S., Ramponi G., Sozzi C., Tudisco O. and FTU Team and ECRH Group, “Transport studies with the ECH system on FTU tokamak”, *Nuclear Fusion* 43, 1384 (2003)
4. Jacchia A., De Luca F., Ryter F., Bruschi A., Leuterer F., Neu G., Pereverzev G., Suttrop W., Wagner D. and ASDEX Upgrade Team, “Nonlinear perturbative electron heat transport in the ASDEX Upgrade tokamak”, *Nuclear Fusion* 45, 40 (2005)

The Planck satellite: getting ready for data analysis

1 Dipartimento di Fisica, Università degli Studi di Milano
2 INAF – Osservatorio di Trieste
3 SISSA-ISAS, Trieste

D. Maino[1], M. Bersanelli[1], B. Cappellini[1], A. Mennella[1], F. Pasian[2], A. Zacchei[2], C. Baccigalupi[3], and F. Perrotta[3]

Planck is the third generation of CMB anisotropy space mission planned to fully map the sky emission with an un-precedented combination of frequency coverage (30-857/Hz), angular resolution (30' to 5') and sensitivity ($\Delta T/T \sim 10^{-6}$ per resolution element). It is an ESA mission scheduled for launch in 2007.

In order to fully exploit the wealth of cosmological and astrophysical information encoded into Planck frequency maps, a key issue is the control and removal of all possible instrumental systematic effects down to the μK level. This could be achieved by a detailed design of the instrument (see Mennella et al. this report). However it would be possible not to control systematic effects at the desired level only in hardware, so that suitable data processing techniques have to be "invented" in order to reduce unwanted effects [1].

After systematic effects have been reduced and clean sky maps are obtained, it is necessary to "separate" the individual different emissions contributing the observed signal in order to obtain genuine CMB signal. In this respect several approaches both blind and non-blind have been proposed [2].

A key theoretical prediction is the actual angular power spectrum of the CMB anisotropies. This could be extracted from a CMB map although a brute-force approach is unfeasible and proper approximation or Monte Carlo (MC) methods are usually considered. Figure 1 shows the reconstruction of the CMB temperature angular power spectrum using the MASTER approach for a simulated case of one of the Planck channels [3]. After noise bias have been estimated via noise-only simulations and data-processing effects evaluated by means of signal only MC simulations, the true angular power spectrum is extracted with high fidelity. From a CMB spectrum it is possible to extract the values of the principal cosmological parameters which will allow a better understanding of our Universe.

The pipeline so far described is handled by a software called Process Coordinator (ProC) developed within the Planck consortia by Max-Planck Institute in Garching. This software allows the final user to create his own pipelines. One has to provide a proper description of each software modules via an XML file in which all I/O interfaces as well as usual parameters are specified. Once this is done modules can be graphically connected. Figure 2 shows an example of such a pipeline including calibration and map-making processing steps.

Fig. 1

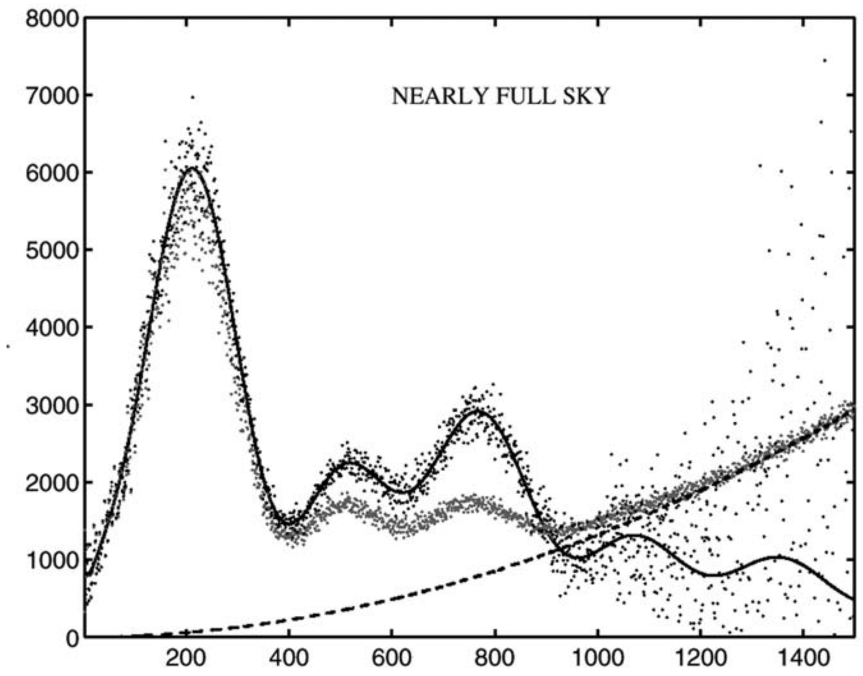

REFERENCES
1. Maino D., Burigana C., Gorski K.M., Mandolesi N., Bersanlli M., "Removing 1/f noise stripes from cosmic microwave background anisotropy observations", A&A, 387, 356 (2002)
2. Maino D., Banday A.J., Baccigalupi C., Perrotta F., Gorski K.M., "Astrophysical component separation from the COBE-DMR 4yr data with FastICA", MNRAS, 344, 544 (2003)
3. Poutanen T., Maino D., Kurkio-Suonio H, Keihanen E., Hivon E., "Cosmic microwave background power spectrum estimation with the destriping technique", MNRAS, 353, 43 (2004)

Fig. 2

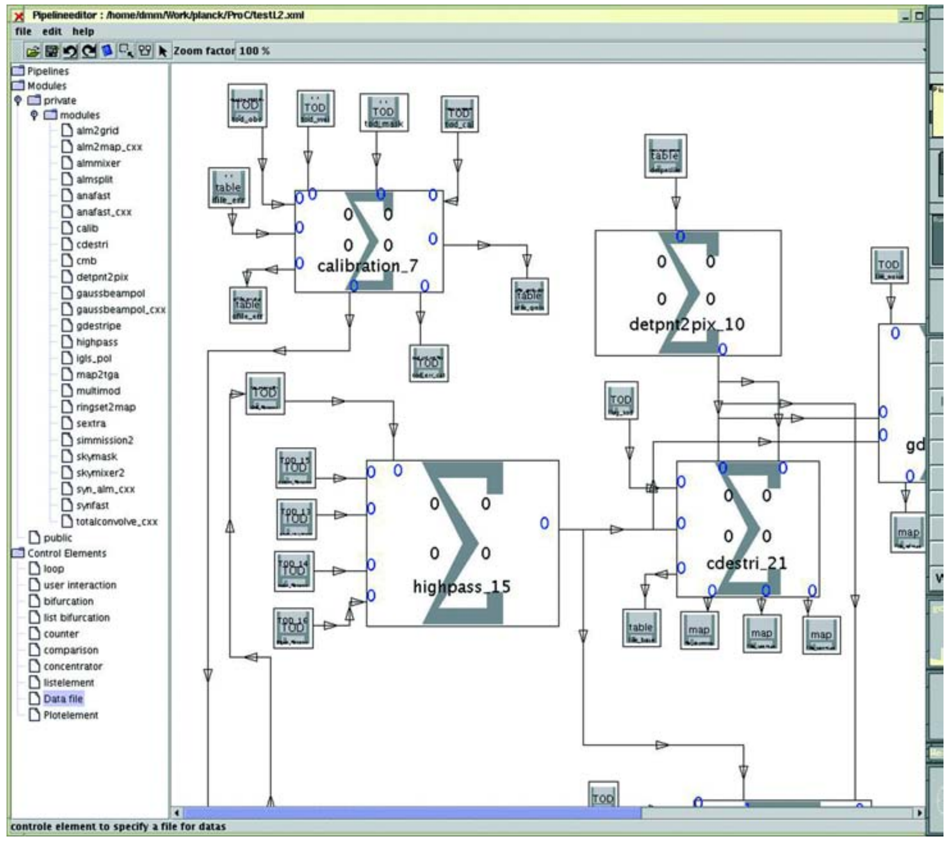

Calibration and testing of the Planck-LFI instrument

1 Dipartimento di Fisica, Università degli Studi di Milano
2 INAF-IASF sezione di Milano
3 CNR-IFP, Milano
4 Alcatel Alenia Space, Vimodrone, Milano

A. Mennella[1], M. Bersanelli[1], D. Maino[1], M. Tomasi[1,2], B. Cappellini[1], S. Pezzati[1], O. D'Arcangelo[3], L. Figini[3], S. Garavaglia[3], P. Platania[3], A. Simonetto[3], C. Sozzi[3], P. Battaglia[4], C. Franceschet[4], M. Lapolla[4], and P. Leutenegger[4]

This paper focuses on the Planck-LFI Qualification Model (QM) testing. In particular we describe the test setup and the performed radiometric tests.

Introduction

Planck, an ESA mission scheduled for launch in 2007, is the third generation space mission planned to fully map the CMB anisotropy with an unprecedented combination of frequency coverage (30-857 GHz), angular resolution (30' to 5') and sensitivity (few µK per pixel). Two instruments will be present in the focal plane of a 1.5 metre off-axis aplanatic telescope: the High Frequency Instrument (HFI), a bolometric array in the range 100-857 GHz, and the Low Frequency Instrument, an array of 11 pseudo-correlation radiometric receivers [1,2] in three frequency bands centred at 30, 44 and 70 GHz. LFI testing and calibration is carried out in three steps: (i) unit level testing, (ii) calibration of each radiometric chain (RCA) and (iii) testing and verification of the integrated instrument (RAA).

Test setup

The individual RCAs at 30 and 44 GHz and the complete RAA have been tested in Alcatel Alenia Space labs (Vimodrone - Milano). Each radiometer is tested under vacuum with flight-representative thermal conditions (see Fig. 1). The RCA is cooled at ~ 20 K at the front end and kept at ~ 300 K at the back end. Connecting waveguides are thermally linked to three interfaces at ~ 50 K, ~ 100 K and ~ 150 K, respectively. The receiver input loads are cooled at ~ 4K.

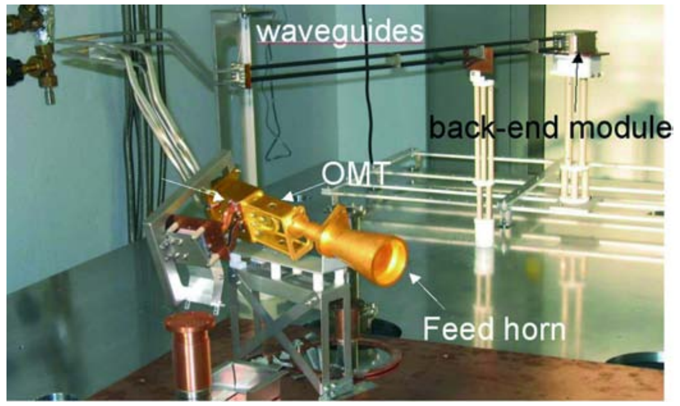

Fig. 1
The 44 GHz RCA integrated in the "small" facility

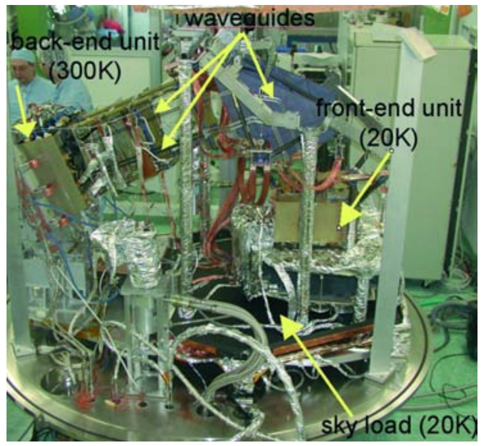

Fig. 2
The LFI QM ready for testing in the "big" chamber

The integrated LFI is tested in a second cryo-facility with flight representative thermal interfaces and ~ 20 K input loads (see Fig. 2).

REFERENCES
1. Seiffert, M., Mennella, A., Burigana, C., Mandolesi, N., Bersanelli, M., Meinhold, P., and Lubin, P., "1/f noise and other systematic effects in the Planck-LFI radiometers," Astronomy and Astrophysics, 391, 1185 (2002)
2. Mennella, A., Bersanelli, M., Seiffert, M., Kettle, D., Roddis, N., Wilkinson, A., and Meinhold, P., "Offset balancing in pseudo-correlation radiometers for CMB measurements," Astronomy and Astrophysics, 410, 1089 (2003)

Calibration test

Table 1 lists the main radiometric tests performed on the LFI QM.

Table 1 - List of radiometric calibration tests

TUNING	SKY LOAD
Dynamic range optimisation Phase switch balance Amplifier bias tuning	The input signal is optimised to To the ADC dynamic range and best bias conditions are found
BASIC PERFORMANCES	
Noise temp., calibration const., input offset, linearity	Data acquired during a ramp in the input load temperature
Bandwidth	Monochromatic wave swept through the receiver bandpass (RCA only)
NOISE	
White and 1/f noise, noise effective bandwidth	Data acquired in stable conditions
SUSCEPTIBILITY	
To temperature variations To bias variations	Test performed by changing boundary temperatures or bias input voltages

Data have been analysed with a software (LIFE, Lfi Integrated perFormance Evaluator) specifically developed by the LFI team. Current plans foresee its application to LFI flight model ground testing as well to performance evaluation during flight.

.

Glitches and vortex pinning in superfluid pulsars

1 Dipartimento di Fisica, Università
degli Studi di Milano & INFN

P. Pizzochero[1] and P. Donati[1]

The observed sudden spin-ups of magnetized rotating neutron stars (pulsar glitches) could be direct evidence of macroscopic superfluidity of the neutrons in their interior. A superfluid cannot sustain rigid rotations, but instead it develops an array of vortices to carry the angular momentum. If the neutron vortices are pinned to the nuclei present in the crust and are subject to drag forces, they can be unpinned catastrophically and deliver their angular momentum to the surface of the star, thus causing a glitch.

The crucial microscopic quantity is the vortex-nucleus interaction energy and the associated pinning force. We present the first realistic and fully consistent model to calculate unambiguously, within the framework of the Local Density Approximation, the structure and radius of the vortex core along the crust; the model takes into account all energy contributions to evaluate the vortex-nucleus configuration with lowest energy. The results show that pinning of vortices on nuclei occurs only in the deepest layers of the crust with average pinning forces that are quite weak, almost one order of magnitude smaller than in existing calculations.

REFERENCES
P. Donati and P. Pizzochero,
Phys. Rev. Lett. **90** (2003) 211101
Nucl. Phys. **A742** (2004) 363
Phys. Lett. **B640** (2006) 74

Asteroseismology and search for extrasolar planets with COROT

1 Dipartimento di Fisica, Università
degli Studi di Milano
2 INAF - Osservatorio Astronomico di Brera

M. Rainer[1], E. Poretti[2], L. Mantegazza[2], E. Antonello[2], M. Bossi[2], and L.E. Pasinetti[1]

The photometric satellite COROT (COnvection, ROtation and planetary Transits; see *http://corot.oamp.fr/*) was launched at the end of 2006. It carries on two main scientific programs: asteroseismological measurements (e.g. detection and analysis of the oscillation eigen modes of the stars) and detection of extrasolar planets with the transit method (e.g. the luminosity variation due to the crossing of the planet on the stellar disk). Its scientific outcome will be very high: for the first time it will be possible not only to test the diagnostic power of asteroseismology on the internal structure of solar-like stars, but also to detect the presence of telluric planets around main-sequence stars. Moreover, a large number of additional programs has been proposed in order to complete the observational program of the satellite and exploit its capabilities (high-precision photometry, long time-baseline and so on).

During the preparatory work for the space mission COROT, a huge program of ground-based spectroscopic and photometric observations has been performed, in order to choose and characterize the asteroseismological targets of the mission. This work, in which the Brera Observatory has been deeply involved, led to the creation of the GAUDI (Ground-based Asteroseismology Uniform Database Interface) database [1], where the high-resolution spectra and the photometric and fundamental parameters of the observed stars are available to the whole scientific community (http://sdc.laeff.esa.es/gaudi/). We used the GAUDI data to study stellar activity and differential rotation. Using the infrared doublet of CaII, we defined a new activity index to be used with the FEROS (Fiber-fed Extended Range Optical Spectrograph) spectra of the archive, for which it is very difficult to derive the classical activity indices [2]. Then we exploited the possibility to work on a large number of stars with different peculiarities in order to study the presence of differential rotation. Our technique requires mean line profiles dominated by rotational broadening, so we focused on the A- and F-type stars of the database. We found an interesting feature in the A-type stars: there seems to be an excess of anti-solar differential rotation in the stars with no outer convective zone [3].

REFERENCES
1. Solano E., Catala C., Garrido R., Poretti E., Janot-Pacheco E., Gutièrrez R., Gonzàlez R., Mantegazza L., Neiner C., Fremat Y., Charpinet S., Weiss W., Amado P.J., Rainer M., Tsymbal V., Lyashko D., Ballereau D., Bouret J.C., Hua T., Katz D., Lignières F., Lüftinger T., Mittermayer P., Nesvacil N., Soubiran C., Van't Veer-Menneret C., Goupil M.J., Costa V., Rolland A., Antonello E., Bossi M., Buzzoni A., Rodrigo C., Aerts C., Butler C.J., Günther E., Hatzes A., "GAUDI: a Preparatory Archive for the COROT Mission, " *Astronomical Journal* 129, 547 (2005)
2. Rainer M., Bossi M., Mantegazza L., "An Activity Index for the FEROS Spectra, "*ASP Conference Series* Vol. 349, 319 (2006)
3. Rainer M., Mantegazza L., "Search for Differential Rotation in the A- and F-type Stars of the GAUDI Database, "*ASP Conference Series* Vol. 349, 397 (2006)

Theoretical Physics

Neural networks and the structure of the proton

A. Piccione[1], L. Del Debbio[2], S. Forte[3], J. I. Latorre[4], and J. Rojo[4]

1 Dipartimento di Fisica Teorica, Università di Torino
2 Particle Physics Theory Group, University of Edinburgh
3 Dipartimento di Fisica, Università degli Studi di Milano
4 Departament d'Estructura i Consituents de la Materia, Universitat de Barcelona

Over the last few years, our knowledge of the structure of the nucleon and the techniques used to obtain it have progressed rapidly. This knowledge is essential in order to understand the data which will come from the future collider LHC, where the structure of fundamental interactions will be explored in proton-proton collisions. In principle, we should be able to determine the structure of a proton from QCD, the theory we use for strong interactions. In practice, however, we do not know how to solve QCD in the non-perturbative regime, and therefore the structure of the proton has to be determined experimentally. This is possible thanks to factorization, which states that a wide class of "hard" physical processes can be computed by folding parton distributions, which describe the structure of the proton in terms of its constituents – quarks and gluons – with a perturbative computation of the interaction between these constituents. These parton distributions are a property of the proton, i.e. they do not depend on the specific physical process in which the proton is involved. Therefore, we can extract the parton distributions from, say, an electron-proton scattering process (such as Deep Inelastic Scattering), and use this information to describe a proton-proton collision. Recent studies have shown that when computing cross sections for processes relevant for the LHC – in particular the production of the Higgs boson, the hitherto undiscovered particle which is responsible for the mass of all other particles - the uncertainty related to our incomplete knowledge of parton distributions may play an important role.

The parton distributions depends on two kinematic variables: x, which is essentially the fraction of the proton mass carried by the given parton, and the scale Q^2, which roughly corresponds to the resolution with which the nucleon is probed (high Q^2 means higher resolution). The dependence of a parton distribution on scale is governed by perturbatively known QCD evolution equations, so only the dependence on x must be extracted from experiment. Different pieces of data determine the parton distributions in different regions of x and Q^2, which can then be brought to the same scale by perturbative evolution, thereby determining a set of parton distributions (one for each species of quark and antiquark and one for the gluon) as functions of x at a given reference scale. The aim of a parton determination is to produce such a set of functions from all the available information, together with the associate experimental and theoretical uncertainties.

To extract a function from data is a mathematically ill-posed problem: a function is an infinite dimensional object, while only a finite set of data is necessarily available. Determining the uncertainty on a function is even harder. The standard approach to the problem is to choose a functional form with a fixed number of parameters and to determine these parameters by fitting to the data. This method has two main shortcomings. The first is the difficulty in propagating the error from data to the parametrization, and then from the parametrization to any observable that it is evaluated with it: this is easy to do only in a linearized approximation, which is not always adequate. The second is the difficulty in assessing the bias associated to the choice of functional form, which is done on the basis of theoretical prejudice. The latter is especially delicate, because a functional form parametrized by a small number of parameters must be chosen in order for the fits to converge, but this is then inevitably a source of bias: a bias free fit would never converge.

We have proposed [1-3] a new approach to this problem, which is based on the use of neural networks combined with the so-called Monte Carlo method. The Monte Carlo approach addresses the first difficulty of the standard approach. Instead of propagating the experimental error on the parameters of the parton distributions, we generate replicas of the true experimental data, which flucutate about the central experimental values in a way that reproduces the data uncertainty. If the number of replicas is sufficiently large, averaging over the replicas we can reconstruct the data we started from with their errors and correlations. Instead of producing a single set of parton distributions, we then produce as many replicas of the parton distributions as we generated replicas of the original data. The fluctuation of these replicas then automatically propagates the fluctuations of the data we started from, and averaging over them we can reconstruct the value and

REFERENCES
1. Forte S., Garrido L., Latorre J. I., Piccione A., *Neural network parametrization of deep inelastic structure functions*, JHEP 0205:062,2002, e-Print Archive: hep-ph/0204232
2. NNPDF Collaboration (Del Debbio L. et al.), *Unbiased determination of the proton structure function F(2)**P with faithful uncertainty estimation*, JHEP 0503:080,2005, e-Print Archive: hep-ph/0501067
3. NNPDF Collaboration (Rojo J. et al.), *The neural network approach to parton fitting*, Presented at 13[th] International Workshop on Deep Inelastic Scattering (DIS 05), Madison, Wisconsin, 27 Apr – 1 May 2005. e-Print Archive: hep-ph/0505044

uncertainty on the parton distributions, and indeed of any physical obsrevable which depends on them.

The second difficulty is addressed by using neural networks, instead of a functional form, to parametrize parton distributions. Neural networks are a class of algorithms designed in order to extract information from noisy or incomplete data, without having to make assumptions on the underlying law which is obeyed by the data. The only assumption is a certain degree of smoothness of the function which describes the data. Neural networks are made of nodes which receive inputs from others nodes, and give an output, if the weighted sum of the inputs is larger than a given threshold. The connection between two nodes is given by a non linear function. The parameters are the weights and the thresholds. In our case we use a multilayer feed forward neural network where each layer communicates only with its next neighbors. The neural networks can be fitted to the data by using a wide class of minimization techniques, which include standard steepest descent, but also methods which exploit the structure of the network themselves (back-propagation) or which are advantageous due to the neural network's flexibility (genetic algorithms) [2]. The general structure of our approach is graphically summarized in Fig. 1.

Fig. 1

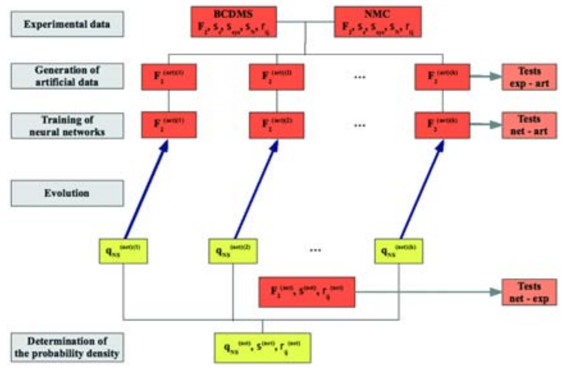

The first result that we discuss is the fit of the proton structure function from data. This case is very simple since it does not involve expressing the structure of the proton in terms of its constituents. Rather, the proton sctructure is parametrized directly. This much simpler problem is not so useful because ultimately it is the parton distributions that we are interested in, but it is interesting because it shows some general features of a fit done with neural networks. In Fig. 2 our fit is compared to data and also to a previous fit by the SMC experimental collaboration. The comparison is interesting since the SMC collaboration used a kind of polynomial parametrization, and its behaviour in the extrapolation region is the same of the standard parton sets. In the data region the two fits give the same description, but when extrapolating outside the data the SMC error band has the same width it has in the data region, while the neural network error band grows. This growth extrapolates the degree of smoothness displayed by the curve as reproduced by neural network in the data region. This is a more physically motivated way of estimating the uncertainty in the extrapolation than arbitrarily assuming a functional form. The adequacy of the fit in the data region (in particular the assumed smoothness) can be assessed by means of various statistical estimators. In particular, we checked that results do not depend on the architecture, of the neural networks and on various aspects of the way they are fitted to the data.

Fig. 2

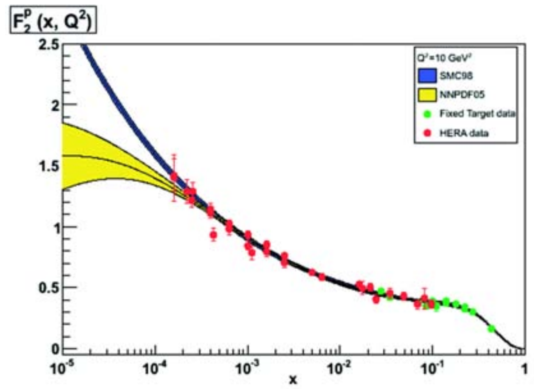

A fit of parton distributions is more complicated than that of a structure function, since the observable quantities have to be expressed in terms of a set of parton distributions. In the following we will show our result for the simplest parton distribution, i. e. the so-called non-singlet, essentially the difference between the proton and neutron quark content. In Fig. 3, we compare the non-singlet structure function data with the structure function evaluated starting from two standard parton sets, CTEQ and MRST (from the names of the respective collaborations) and from our fit. We see that the central values of all the fits coincides within their error bands, but the errors are rather different, especially in the small *x* region where they are significantly larger. This is interesting, because even though we expect the CTEQ and MRST fits to have a smaller error band, since they include a larger number of data, this is not the case at small *x*, where the experimental constraints are essentially the same in our fit and in those of MRST and CTEQ. Hence, we conclude that this wider uncertainty reflects the larger flexibility of the neural network approach, and it is likely to provide a more faithful assessment of the true experimental uncertainty.

Fig. 3

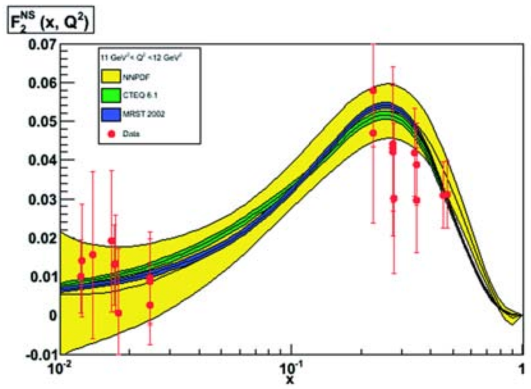

We have shown how neural networks can be successfully used to extract in an unbiased way the structure of the proton. The main perspective of our project is a global fit of all the parton distributions by fitting all the available experimental data, and its application to estimate the uncertainty of the relevant observables for the LHC.

Local functional equation of the nonlinear sigma model. Geometry and renormalization in $D = 4$

A. Quadri [1] and R. Ferrari [1]

1 Dipartimento di Fisica, Università degli Studi di Milano & INFN

The renormalization of the nonlinear sigma model in $D = 4$ is performed by enforcing the functional equation associated with the invariance of the Haar measure under local left multiplication. Pion fields are embedded into a flat connection F_μ, coupled to the external source J^μ. The recursive subtraction procedure of the poles in the D-dimensional amplitudes is carried out in a way compatible with the functional equation. This means that only local functionals invariant under the linearized functional operator have to be subtracted. We provide the complete classification of these invariants and show that their coefficients are uniquely fixed by the polar part of amplitudes only involving the external sources associated to the flat connection and the composite field ϕ_0 (the constraint of the nonlinear sigma model). The polar part of the amplitudes involving at least one pion field is then completely determined by the invariants themselves. Moreover the defining functional equation encodes a hierarchy among amplitudes allowing to obtain by functional differentiation all amplitudes involving at least one pion field once those only containing insertions of the flat connection F_μ and ϕ_0 (ancestor amplitudes) are known. The fact that the subtraction procedure is symmetric (i.e. fulfills the defining functional equation) has been checked by Quantum Action Principle arguments up to two loop level (but the recursive method can be applied to all orders).

The problem of the quantization of the nonlinear sigma model is strictly related to the program of giving a consistent structure to chiral perturbation theory. Since a long time people realized that the nonlinear sigma model cannot be renormalized in a symmetric way (chiral symmetry) already at one loop. Some of the unwanted (chirally breaking) terms can be disposed of by redefinition of the fields (quartic divergences). However some divergent terms of the one-loop off-shell pion-pion scattering amplitude still violate chiral symmetry and can be reabsorbed by redefinition of the pion field only if derivatives are allowed. This strategy of removing the divergences never turned to a consistent program both for technical difficulty and for the impossibility of fixing the necessary finite subtractions. From these previous experiences it is clear that the renormalization of the nonlinear sigma model cannot be achieved by using chiral-invariant counterterms only.

In [1,2] it is proposed to quantize the nonlinear sigma model in $D = 4$ by embedding the pion fields in a flat connection in order to solve the long-standing problem of a symmetric removal of the divergences. The theory is defined by the functional equation expressing the invariance of the Haar measure in the path-integral under local left multiplication. This is a local functional equation which allows to classify the whole structure of the divergences of the nonlinear sigma model in $D = 4$.

We show that standard perturbation theory in D-dimensions gives amplitudes that satisfy the equation without any subtractions. The limit to $D = 4$ of the properly normalized 1-PI amplitudes is divergent and needs subtraction of the poles of the Laurent expansion in D-4. The recursive subtraction procedure of the poles in the D-dimensional amplitudes order by order in the loop expansion is carried out in a way compatible with the functional equation. This means that only local functionals invariant under the linearized functional operator have to be subtracted.

We provide the complete classification of these invariants by cohomological methods and show that their coefficients are uniquely fixed by the polar part of amplitudes only involving the external sources associated to the flat connection and the composite field ϕ_0 (ancestor amplitudes). At any given order in the loop expansion only a finite number of divergent ancestor amplitudes exists. This establishes a weak power-counting theorem for the nonlinear sigma model in $D = 4$.

The polar part of the amplitudes involving at least one pion field is then completely determined by the invariants themselves upon projection on the relevant monomials. It depends on a finite number of parameters controlling the divergences of the ancestor amplitudes at any given order in the loop expansion, as a consequence of the weak power-counting theorem and of the

REFERENCES
1. R. Ferrari, "Endowing the nonlinear sigma model with a flat connection structure: A way to renormalization," JHEP **0508** (2005) 048 [arXiv:hep-th/0504023].
2. R. Ferrari e A. Quadri, "A weak power-counting theorem for the renormalization of the non-linear sigma model in four dimensions," arXiv:hep-th/0506220, to appear in International Journal of Theoretical Physics.

symmetric subtraction. As an example, we have given the complete set of counterterms at one loop level in terms of the coefficients of seven invariants. Moreover it turns out that the functional equation encodes a hierarchy among the amplitudes: once the ancestor amplitudes are known, all the remaining amplitudes can be obtained by functional differentiation of the functional equation itself.

We then show that the proposed subtraction procedure is symmetric, i.e. yields finite amplitudes fulfilling the defining functional equation.This has been checked at one-loop level in [1,2]. At higher orders in the loop expansion the bilinear term of the functional equation for the 1-PI generating functional yields non-trivial contributions depending on lower-order 1-PI Green functions. By using Quantum Action Principle arguments we have checked up to two loop level [3] that the subtraction procedure yields indeed finite amplitudes satisfying the functional equation (but the recursive method can be applied to all orders).

After having established the consistency of the subtraction procedure, the theory looks promising and one can think of possible phenomenological applications. The relation between the large mass limit (at fixed coupling constant) of the linear sigma model and the nonlinear sigma model in the proposed subtraction scheme is currently under investigation. The extension of the subtraction procedure to the Stueckelberg model for non-abelian massive gauge bosons will also be investigated.

REFERENCES
3. R. Ferrari e A. Quadri, "Renormalization of the non-linear sigma model in four dimensions: A two-loop example," JHEP **0601** (2006) 003 [arXiv:hep-th/0511032].

Generating functions for trees, forests and unicyclics on finite geometries

A. Sportiello[1], S. Caracciolo[1], and A.D. Sokal[2]

1 Dipartimento di Fisica, Università degli Studi di Milano
2 Department of Physics, New York University

A new method for proving Kirchhoff Matrix-Tree theorem, involving combinatorics of Grassmann variables, is developed. The theorem allows to evaluate the partition function of spanning trees on a given weighted graph, which emerges both in a limit of Potts Model, and of a free scalar fermion. The method generalizes to other counting problems beyond spanning trees: forests, hyper-trees and hyper-forests, and collections of unicyclic graphs, whose counterparts are more general cases of the related physical models. In particular, spanning forests correspond on Potts to consider the whole series in q, instead of a limit $q = 0$, while on the free-fermion theory correspond to a OSP(1|2) theory with variables on a supersphere of radius $1/q$, instead of its linearized limit of infinite radius. Ward identities for OSP(1|2) symmetry correspond to combinatorial identities for connectivity patterns among vertices on the forest. For periodic graphs in 2 dimensions special features emerge. A Renormalization-group analysis suggests that the Spanning Tree theory is a fixed point, w.r.t. parameter q, marginally unstable in the $q > 0$ physical region, thus showing Asymptotic Freedom, the crucial ingredient of QCD confinement, in a specially simpler template model.

The fixed point of spanning trees is a CFT with $c = -2$, and, on a domain with suitable boundary conditions, leads to the SLE_8 of Uniform Spanning Trees, where the stochastic curve is the contour of the tree on the medial lattice. This curve arises as well, in cylindric geometry, in the Temperley-Lieb transfer-matrix formulation of the problem. Interestingly enough, this algebra is also crucial in the recently-developed fields of Razumov-Stroganov conjectures for O(n) loop models, while our original OSP(1|2) model can be put in relation to an analytic continuation of O(n) to $n = -1$, through Parisi-Sourlas correspondence. For the Spanning Tree and Unicyclics partition functions on rectangular geometries, interesting features of quasi-modularity emerge, involving Eisenstein Series, in a way similar to what has been observed by Kleban and Zagier for the $q = 1$ percolation problem.

Introduction

Given a finite graph G, with arbitrary weights on the edges, the multivariate Tutte polynomial is the generating function for spanning subgraphs, with weight given by the product of the weights for the edges in the subgraph, times a factor q per connected component (beyond the first one), and a factor q' per independent loop.

This polynomial coincides with the Potts partition function on the given graph, expressed in Fortuin- Kasteleyn representation, and encodes all the information on the graph which could be deduced by Tutte's deletion/contraction procedure. The evaluation of the polynomial for an arbitrary graph is known to be a NP-complete problem almost everywhere in the (q,q') plane (Tutte plane), after a theorem of Vertigan and Welsh. Only a few exceptional points are allowed to have polynomial complexity, among which the limit $(q,q') = (0,0)$, corresponding to Spanning Trees [1]. This specific case is known to be solved by an analytic procedure, namely the calculation of a determinant of the so-called "Laplacian Matrix" of the graph, after a theorem of Kirchhoff of 1847.

Fig. 1
In order: a configuration of Potts model for $q = 3$, a configuration in the Fortuin-Kasteleyn decomposition, a spanning forest and a spanning tree, on a portion of the square lattice.

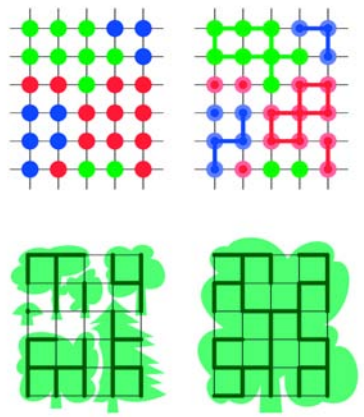

REFERENCES
1. A.D. Sokal, "The multivariate Tutte polynomial (alias Potts model) for graphs and matroids", Surveys in Combinatorics 2005, ed. by B.S. Webb, Cambridge University Press (2005)
arXiv: math.CO/0503607

Despite the first comprehension of these topics dates back to more than 150 years ago, many new things can still be learned, also in connection with recent developments, including Asymptotic Freedom in lattice models, quasi-modularity of CFTs in finite geometries, SLE_8 of Uniform Spanning Trees, and Temperley-Lieb Algebra in O(n) loop models.

1. Spanning trees and forests on generic graphs and hypergraphs

Our work started from a result of Liu and Chow, who described an algorithmic procedure for calculating the generating function for Spanning Forests, i.e., on (q,q') plane, a point with q'= 0, and arbitrary $q > 0$. We remarked how, rephrasing the determinant in Kirchhoff theorem as a fermionic Gaussian integral, a generalization of the involved combinatorics was possible, and a specific interacting part, added to the bare Laplacian term, is the exact counterpart of Liu and Chow procedure [2]. With similar techniques, we developed various other extensions, among which spanning collections of unicyclics on a graph, and hyper-trees and hyper-forests on a hyper-graph.

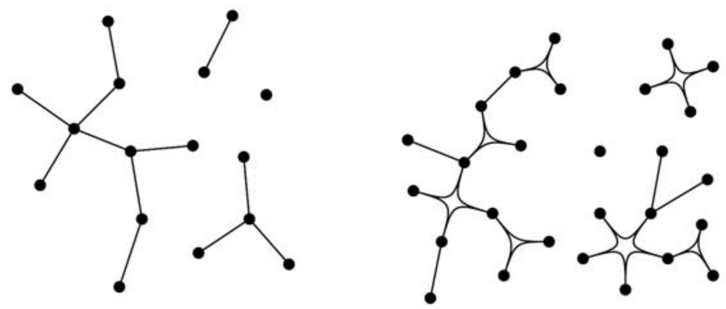

Fig. 2
A forest (left), and a hyper-forest (right)

Remarkably, the action of the physical model, written in terms of the Grassmann variables, has a perturbative connection with the OSP(1|2) vector model, i.e. a model of variables constrained on a supersphere with one bosonic and two fermionic degrees of freedom [2]. All the generalizations of the combinatorial technique have a counterpart on, and are indeed motivated by, their physical interpretation. The parameter q counting the components, beyond appearing as the Potts parameter, is related to the inverse radius of the supersphere (and indeed, a limit of infinite radius linearizes the constraint and makes the model exactly solvable - i.e. Kirchhoff theorem again). Then, the extension to hyper-trees and forests corresponds to higher-order terms in the OSP(1|2) original action, while the case of unicyclics corresponds to the introduction of a static gauge field, the weight for the cycles in unicyclic components being related to the circuitation of the gauge field.

In the generic framework of O(n) theories, or more generally of OSP(n|$2m$) theories, under perturbative analysis (which thus eliminates one bosonic degree of freedom), the fermionic nature of the remaining d.o.f. in OSP(1|2) accounts for a more rigorous control of the theory. Nilpotency gives a cut on the highest possible order in the interaction, and the most general interaction Hamiltonian in the OSP(1|2) formulation corresponds to a certain generating function for interacting hyper-forests, and surprisingly never involves different classes of subgraphs (for comparison, we recall that the covariant coupling to a gauge vector field produces an expansion over unicyclic subgraphs). So, at fixed dimensionality of the parameters, we have control on the general-Hamiltonian theory. Then, by Parisi-Sourlas correspondence, it is expected that the OSP(n|$2m$) theory has the same behaviour of the O(n-$2m$) theory. A comparison is in order with the Nienhuis loop-gas O(n) model, which gives a generic-n approach to the problem, but at fixed graph and specific choice of Hamiltonian (the graph must have coordination 3, and the Hamiltonian being exactly of the form $\ln(1 + n_i n_j)$. These two complementary approaches raise questions of universality for the classes of vector models with O(n) invariance.

As a side remark, we notice how the dense phase of O(n) loop model on the square lattice has gained renewed attention in recent times, in the framework of integrable systems, in connection to Razumov-Stroganov conjectures, involving the crucial emergence of Temperley-Lieb algebras as a natural transfer-matrix action for the configurations.

For a generic spanning-forest (or hyper-forest) model, trivial combinatorial relations can be stated, e.g. the probability that two vertices are in the same component, plus the probability that they are in different components, sum up to 1. Surprisingly enough, all these relations also come out as a result of Ward identities on the corresponding OSP(1|2) model, w.r.t. the symmetry generators which mix bosonic and fermionic degrees of freedom.

REFERENCES
2. S. Caracciolo, J.L. Jacobsen, H. Saleur, A.D. Sokal, A. Sportiello, "Fermionic field theory for trees and forests," *Phys. Rev. Lett.* 93 080601 (2004) arXiv: cond-mat/0403271

2. Specialities of 2-dimensional periodic lattices

When specialized to a planar periodic lattice, the results above are complemented by informations that can be extracted from the homogeneity of the problem. In particular, a Renormalization-group analysis of the OSP(1|2) model in D dimensions allows to determine that the model at $D = 2$ shows asymptotic freedom, around the fixed point of spanning trees, with marginal instability in the physical region $q > 0$ for the parameter q counting the components, where it flows towards the infinite-q limit of all isolated vertices. These results are in accord with the Baxter exact informations on Potts phase diagram for the square-lattice model, in (q,v) plane, in proximity of the $q = v = 0$ point.

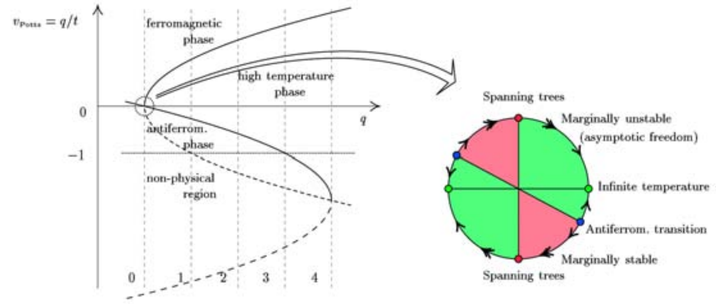

Fig. 3
Potts phase diagram on the square lattice (left), and a magnification of the limit $q = v = 0$, with $t = q/v$ fixed. The point $t = 0$ corresponds to spanning trees, and for t positive the RG flows is marginally unstable towards the infinite-t limit of all isolated vertices. In the unphysical region of negative t, the critical value $t = -1/4$ corresponds to the antiferromagnetic transition in Potts model.

The fixed point of Spanning Trees is a logarithmic CFT with central charge $c = –2$. We identified the family of operators with conformal weight $h = 1$ with combinatorial observables for edge-occupation, and conjectured a relation of the non-unitary family $h = –1/8$, with a twist operator on the boundary that exchanges the lattice with the dual lattice, and thus the spanning tree with the dual spanning tree on the complementary set of edges.

The model of Spanning Trees on the square lattice (oriented on 45 degrees) is related to the action of Temperley-Lieb algebra on a chain of even length, with loop parameter $t = 0$: a loop would correspond either to a cycle or an isolated component on the subgraph, and thus annihilates the wavefunction. A unique generalization to site-dependent loop parameters is compatible with the rules of the algebra, namely a "chequered" prescription, which distinguish among even and odd plaquettes, and leads to two parameters t and t', separately for cycles and isolated components, corresponding to the q and q' on Tutte's plane. The spanning-forest model is the special case $t' = 0$, $t > 0$. The Temperley-Lieb algebra, acting inside a transfer matrix, makes its second appearence, after the mysterious connection with Razumov-Stroganov conjectures and O(n) loop model.

Less on speculative basis, for the spanning-tree model on a D-dimensional cubic lattice, we made original calculations concerning the expectation values of a family of local observables: edge occupation correlation functions and probabilities of vertices to have given coordination. Because of a specific feature of the model, the former are obtained without need of subtractions. Their continuum limit is in accord with the CFT prediction for a primary field of dimension $h = 1$. On the other side, the probabilities for vertex coordination are stated in terms of lattice integrals. For $D = 2$, in the infinite-size limit, the two relevant integrals are 1/2 and $4/\pi$, and this is the reason why, curiously, the probabilities are integer-coefficient polynomials in $1/\pi$ (cfr. Table 1). The finite-size corrections, for the model on a rectangle, can be calculated systematically using [3], and involve Eisenstein series, a family of modular forms (i.e. functions with special properties under SL(2,**C**) transformations: they are like modular functions, up to a power of a pure Jacobian). Such a quasi-modular-invariance in a rectangular geometry, for a model in which the relative angle between the mesh and the geometry directions is expected to affect physical quantities also in the continuum limit, is unexpected in principle, but appears already in percolation theory (i.e. the point (q,q') = (1,1) in Tutte's plane), as pointed out by Kleban and Zagier.

Table 1
Probabilities for vertex coordination for spanning trees on a square lattice.

p(1)	$\pi^{-3}\, 8\, (\pi-2)$	0.295
p(2)	$\pi^{-3}\, 4\, (2\pi^2-9\pi+12)$	0.447
p(3)	$\pi^{-3}\, 2\, (\pi-2)\, (\pi^2-6\pi+12)$	0.222
p(4)	$\pi^{-3}\, (\pi-2)^2\, (4-\pi)$	0.036

REFERENCES
3. S. Caracciolo, A. Pelissetto, "Corrections to finite-size scaling in the lattice N-vector model for $N = \infty$," *Phys. Rev. D* 58 105007 (1998) arXiv: hep-lat/980400

Open quantum system theory: from microsystems to macrosystems

B. Vacchini[1] and L. Lanz[1]

1 Dipartimento di Fisica, Università degli Studi di Milano
INFN, Sezione di Milano

The description of open systems inside quantum mechanics has recently gained in interest both at the level of theory and applications, putting to work the full-fledged modern formulation of quantum mechanics, which displays most deep and fruitful connections with probability theory. The field is deeply connected to fundamental research e.g. through the theoretical description of experiments testing the borderline between classical and quantum world, such as most recent quantitative experiments on decoherence. A short overview of work recently done at the University of Milan on the subject will be given.

In recent times the word decoherence[1, 2] has become quite fashionable in order to describe a range of utterly different physical situations, which however all exhibit a common qualitative feature: a quantum system, due to its unavoidably imperfect isolation from the surrounding environment, shows in its dynamical evolution the suppression of typical quantum coherence properties, such as interference capability.

The basic ideas are actually very old and as it was recently stressed in[3] can be essentially traced back to the first studies on the measurement problem in quantum mechanics in the 50's (for a reference see [4, 5]). These studies, in which the main concepts related to decoherence already appeared, has led by now to relevant improvements in the formulation of quantum mechanics, going beyond Dirac's presentation and leading to the new concept of effect, positive operator valued measure, operation and instrument, also revealing most fruitful and interesting connections with the theory of stochastic processes; it appears indeed that many useful clues in studying the theory of quantum systems can be obtained from classical probability theory. In this report we will focus on recent work [6] showing how the characteristic function of a classical Lévy process, i.e. the Fourier transform of its probability density, is the natural quantity in order to describe loss of coherence in interferometry experiments with massive particles. These more advanced and flexible tools in the description of quantum systems are by now extensively used in quantum information and communication theory (for a reference see [7, 8]).

The aforementioned studies on the foundations of quantum mechanics also give a natural setting for the understanding of decoherence. Following Ludwig's approach to quantum mechanics microsystems only appear anchored to an objectively given macroscopic reality. The very concept of microsystem described inside one-particle quantum mechanics then appears as a highly schematized description of a typical non equilibrium system, where a *source part* affects in a stochastic way a *detecting part*. There is a field theoretical description of non equilibrium systems, due to Zubarev [9], where dynamics is given through classical state parameters, that we reformulated[10] in order to provide an objective background for microsystems inside quantum mechanics. We suggested [11] that just the breakdown of a deterministic dynamics of state parameters can be linked with a stochastic behaviour giving evidence of a microsystem. The macroscopic background in which these microsystems emerge indicates that decoherence might naturally occur and methods of open system theory come in the foreground.

We now focus on the issue of decoherence of the centre of mass degrees of freedom of massive test particles, an object of recent and very accurate quantitative experimental investigations [12, 13, 14], showing how these different situations can be addressed within a unified theoretical approach which puts into evidence how the loss of coherence in the off-diagonal position matrix elements of the statistical operator is generally described by the characteristic function of a Lévy process. The common feature of the abovementioned experiments is the fact that, provided dissipative effects which take place on a much longer time scale are neglected, the interaction causing decoherence can be characterized through momentum transfer events. In the Markovian case a common description of such dynamics can be obtained referring to the general structure of translation-covariant quantum-dynamical semigroups obtained by Holevo [15], relying on a quantum generalization of the Lévy-Khintchine formula. This mathematical result essentially gives the most general structure of an irreversible semigroup

REFERENCES
1. E. Joos et al., Decoherence and the Appearance of a Classical World in Quantum Theory 2nd ed. (Springer, Berlin, 2003).
2. H. P. Breuer and F. Petruccione, The Theory of Open Quantum Systems (Oxford University Press, Oxford, 2002).
3. M. Dubé and P. C. E. Stamp, Chem. Phys. **268**, 257 (2001).
4. G. Ludwig, Foundations of Quantum Mechanics (Springer, Berlin,1983).
5. A. S. Holevo, Probabilistic and Statistical Aspects of Quantum Theory (North-Holland, Amsterdam, 1982)
6. B. Vacchini, Phys. Rev. Lett. **95**, 230402 (2005).
7. G. Alber et al., Quantum Information, (Springer, Berlin, 2001).
8. A. S. Holevo, Statistical Structure of Quantum Theory, (Springer, Berlin, 2001).
9. D. N. Zubarev, V. Morozov, and G. Roepke, Statistical mechanics of non-equilibrium processes (Akademie-Verlag, Berlin, 1996).
10. L. Lanz, O. Melsheimer and B. Vacchini, Rep. Math. Phys. **46**, 191 (2000).
11. L. Lanz, B. Vacchini and O. Melsheimer, Quant. Inf. Comput. **4**, 513 (2004).
12. D. A. Kokorowski et al., Phys. Rev. Lett. **86**, 2191 (2001).
13. K. Hornberger et al., Phys. Rev. Lett. **90**, 160401 (2003).
14. L. Hackermüller et al., Nature **427**, 711 (2004).
15. A. S. Holevo, Izv. Math. **59**, 427 (1995); J. Math. Phys. 37, 1812 (1996).

dynamics compatible with translation invariance, and provides a quantum counterpart of classical results on Markov processes which are both space and time homogeneous, i.e. Lévy processes. Lévy processes are a class of processes, including Gaussian ones, which despite obeying the Chapman-Kolmogorov equation characterizing Markov processes not necessarily have finite variance, so that the central limit theorem does not always apply. Such processes were in fact found looking for generalizations of such theorem, and are both space and time homogeneous, thus naturally arising when considering space translation invariance. The general structure of the characteristic function of such processes is given by the famous Lévy-Khintchine formula (for a most compact presentation see [2] and references therein). The relevance of Lévy process in physics is growing [16], since they allow to cope with situations not encompassed by the central limit theorem.

If the dynamics causing decoherence is Markovian and described in terms of momentum transfers, so that in the absence of an external potential one has translation invariance, according to the aforementioned results by Holevo [15] the master-equation for the dynamics of the centre of mass degrees of freedom takes a peculiar form so that as shown in [6] one can write the general solution for the matrix elements of the statistical operator in the position representation. These matrix elements at a given time t are simply obtained by multiplying the matrix elements of the initial statistical operator by a function of time and difference in the two position labels, let us call it $\Phi(t, x-y)$, which turns out to be the characteristic function of a Lévy process, a quantity actually fully characterized by the Lévy-Khintchine formula. The fact that $\Phi(t, x-y)$ is a characteristic function (i.e. the Fourier transform of a probability density) automatically entails that its modulus is less than one and the value one for $\mathbf{x} - \mathbf{y}$ tending to zero, i.e. the natural properties in order to predict the reduction of the off-diagonal position matrix elements of the statistical operator due to decoherence. This suppression of coherence however happens with a variety of behaviours going far beyond the quadratic common lore corresponding to Gaussian statistics, depending on the process characterizing the physical interaction.

We now briefly mention a microphysical model giving a specific realization of the aforementioned general result, which as it turns out actually encompasses all known models of decoherence for the centre of mass degrees of freedom [1]. Let us consider the motion of a massive test particle interacting through collisions with a background gas, developed in detail in [17], where also dissipative effects have been taken into account, relying on a kinetic approach. Neglecting free motion and dissipation the master-equation is of the general form predicted by Holevo, and its structure depends on the background gas density, the Fourier transform of the interaction potential between test particle and gas particles, and a two-point correlation function characterizing the gas known as dynamic structure factor, which is a function of both momentum and energy transfer. For a finite macroscopic scattering cross-section one can introduce a scattering rate and a suitably normalized probability density $P(\boldsymbol{q})$ of scattering events corresponding to a momentum transfer $\boldsymbol{q}$. The solution of this master-equation leads to the appearance of the characteristic function of a class of Lévy processes known as compound Poisson processes, each characterized by a certain probability density $P(\boldsymbol{q})$ [18]. The physical picture behind them is the following: the dynamics is driven by collisions, the probability of having a definite number of collisions in a time t being given by a Poisson distribution with given intensity and mean, each collision however is not characterized by a fixed, deterministic value of the transferred momentum $\boldsymbol{q}$, but rather by a certain probability density $P(\boldsymbol{q})$, depending in the case under consideration on the two-body interaction potential and a suitable correlation function. This result generally applies to a situation in which one has a collection of momentum transfer events each characterized by a certain probability density, to be obtained or introduced by means of some microscopic or phenomenological model. It has been used for the theoretical analysis of decoherence experiments with fullerenes, both in the case of collisional decoherence [13] and of decoherence due to thermal emission of radiation [14]. Both situations correspond to compound Poisson processes, where the relevant probability density is obtained in terms of the collisional cross-section and the spectral photon emission rate respectively. According to a detailed theoretical analysis the final visibility is obtained by an average of the characteristic exponent over the possible scattering positions in the interferometer [19].

REFERENCES
16. Lévy Flights and Related Topics in Physics, M. F. Shlesinger et al. Eds., (Springer, Berlin, 1995).
17. B. Vacchini, Phys. Rev. Lett. **84**, 1374 (2000); J. Math. Phys. **42**, 4291 (2001); F. Petruccione and B. Vacchini, Phys. Rev. E 71, 046134 (2005).
18. W. Feller, An Introduction to Probability Theory and Its Applications 2nd ed. (Wiley, New York, 1971).
19. K. Hornberger et al., Phys. Rev. A **70**, 053608 (2004).

Effective field theories of QCD

A. Vairo[1]

1 Dipartimento di Fisica, Università degli Studi di Milano

In some physical systems, it is possible to exploit a hierarchy of scales to construct Effective Field Theories, which are simpler than, but equivalent to, QCD order by order in the ratio of the scales. Examples are Chiral Effective Theory, Heavy Quark Effective Theory, Non-Relativistic QCD, Soft-Collinear Effective Theory, ... We report about recent progress made in the construction of such Effective Field Theories and in their use to extract fundamental parameters of QCD from heavy quarkonia. Emphasis will be put on the research activity pursued in this area at the Physics Department of the University of Milano.

The Standard Model is the fundamental theory that describes, up to now completely successfully, all the phenomena occurring in particle physics. The sector of the theory that describes the strong interaction, i.e. the interaction of quarks and gluons, is called QCD. Differently from the other parts of the theory the low energy region of QCD cannot be studied by expanding in a small coupling constant, i.e. in perturbation theory. The non-perturbative nature of the QCD vacuum is a major difficulty that affects the determination of several observables in particle physics and some of the parameters of the Standard Model.

Heavy quarkonia [1] (bound states of two heavy quarks: bbar, ccbar, ...) are an ideal tool to study the non-perturbative dynamics of QCD. This because they are non-relativistic (NR) bound states and, therefore, characterized by at least three hierarchically ordered energy scales: m, mv and mv^2. We can say that these scales probe the QCD vacuum at different depths. The quantity m is the heavy-quark mass and v^2 « 1 the heavy-quark relative velocity. The mass m of the heavy quark is large enough to be treated perturbatively; the other scales may and may not lie in the perturbative regime in dependence of the specific system and process under examination. In any case, non-perturbative contributions can be factorized in well defined operator matrix elements. They may be fixed phenomenologically on some data set, used to make predictions on some other data set or calculated on the lattice.

Fig. 1

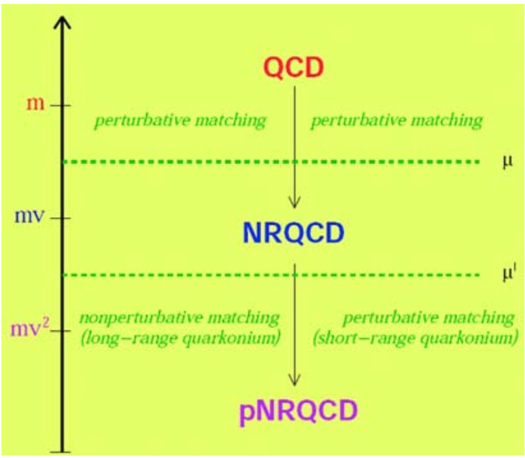

An Effective Field Theory (EFT) is a field theory that makes factorization among contributions coming from different scales explicit at the Lagrangian level. To be more precise, let us call H a system described by a fundamental Lagrangian L and suppose it characterized by 2 scales: K » k. The EFT Lagrangian, LEFT, suitable to describe H at scales lower than K, is characterized by a cut off K » l » k and some degrees of freedom that exist at scales lower than l. The Lagrangian LEFT is then made of all operators that may be built from the effective degrees of freedom and are consistent with the symmetries of the original Lagrangian L. Once the scale l has been run down to k, the power counting is homogeneous, so that the EFT is, indeed, organized as an expansion in k/K. Despite the EFT not being renormalizable in the traditional sense, it is renormalizable order by order in k/K. Each renormalized operator of the EFT is accompanied by a Wilson coefficient $c(K/l)$ that encodes the non-analytic behavior in K. The Wilson coefficients are calculated by imposing that LEFT and L describe the same physics at any finite order in the expansion. The procedure is called matching. Finally, we note that if K is much greater than the typical

REFERENCES
1. N. Brambilla et al., CERN-2005-005, (CERN, Geneva, 2005) [arXiv:hep-ph/0412158].
2. N. Brambilla, A. Pineda, J. Soto and A. Vairo, Rev. Mod. Phys. 77, 1423 (2005) [arXiv:hep-ph/0410047].

hadronic scale $c(K/l)$ may be calculated in perturbation theory, if not, the matching must rely on non-perturbative methods.

Several effective field theories for heavy quarkonium that take full advantage of the non-relativistic hierarchy of scales have been developed and used over the last decade. For a recent review we refer to [2]. NRQCD is the EFT that exploits the hierarchy $K = m$ » $k = mv$. Since m is much larger than the typical hadronic scale, the matching coefficients of NRQCD may be calculated in perturbation theory. pNRQCD is the EFT that exploits the hierarchy $K = mv$ » $k = mv^2$. If mv^2 is of the order of the typical hadronic scale, then the matching to pNRQCD may be still done in perturbation theory. We call weak coupling this regime, which may be suited to describe ground-state quarkonium. If not, then the matching to pNRQCD is non-perturbative. We call strong coupling this regime, which may be suited to describe excited quarkonium states.

In the following, I list some heavy quarkonium observables, where our understanding has significantly improved over the last years also through the work of the group at the University of Milano.

1. The energy between two static sources has been computed at three loop leading log accuracy (NNLL). This is not directly a heavy quarkonium observable, but provides the heavy quarkonium static potential and therefore enters crucially in the calculation of most heavy quarkonium observables. Of this quantity accurate lattice data exist that are, indeed, sensitive to that accuracy (see the following Figure: the dots stand for the lattice data of S. Necco and R. Sommer).

Fig. 2

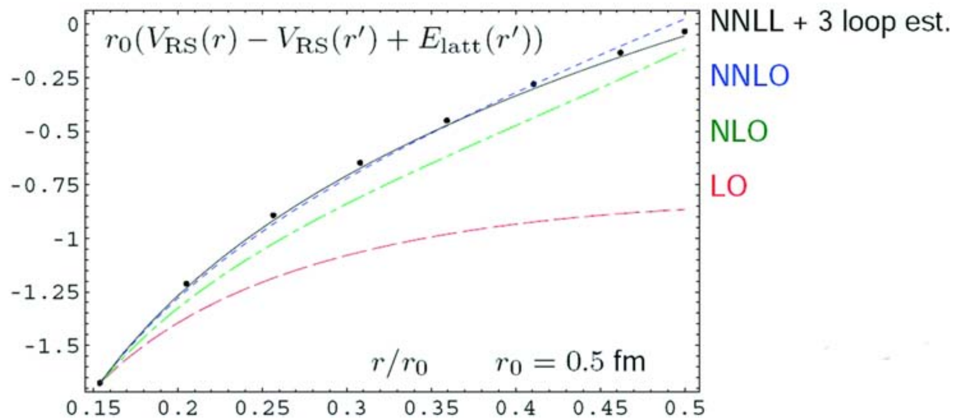

2. The accurate knowledge of the quarkonium potential makes it possible to extract the heavy quark masses from the masses of the heavy quarkonia ground states. Indeed, this is one of the most competitive sources of these fundamental parameters of the Standard Model. We list in the following table some recent determinations by different groups of the b and c masses in the MSbar scheme at NNLO and NNNLO accuracy. In one case, studied by our group, also the effect of the charm quark mass in charm quark loops has been taken into account. A full list of references may be found in [2].

Fig. 3

order	$\overline{m}_b(\overline{m}_b)$ (GeV)
NNLO**	4.24 ± 0.09
NNLO	4.21 ± 0.09
NNNLO*	$4.210 \pm 0.090 \pm 0.025$
NNLO +charm	$4.190 \pm 0.020 \pm 0.025$
NNNLO*	4.349 ± 0.070
NNNLO*	4.20 ± 0.04
NNNLO*	4.241 ± 0.070
order	**$\overline{m}_c(\overline{m}_c)$ (GeV)**
NNLO	1.24 ± 0.020

3. A powerful application of EFTs is the resummation of large logs, which steam from the different scales, by means of the Renormalization Group equations. A recent application of

this method has been the calculation of the ratio of the electromagnetic widths of the Upsilon (1S) and its pseudoscalar partner at NNLL accuracy. The last one has been the object of an intense search at the Tevatron and CLEO without success so far. In the following plot, the yellow band shows how stable the NNLL result is over a wide range of the factorization scale. The band shows the uncertainty in the strong coupling constant. Once the pseudoscalar partner of the Upsilon (1S) has been found, the measure of its electromagnet width may provide the most accurate source of the strong coupling constant at the bottom mass scale.

Fig. 4

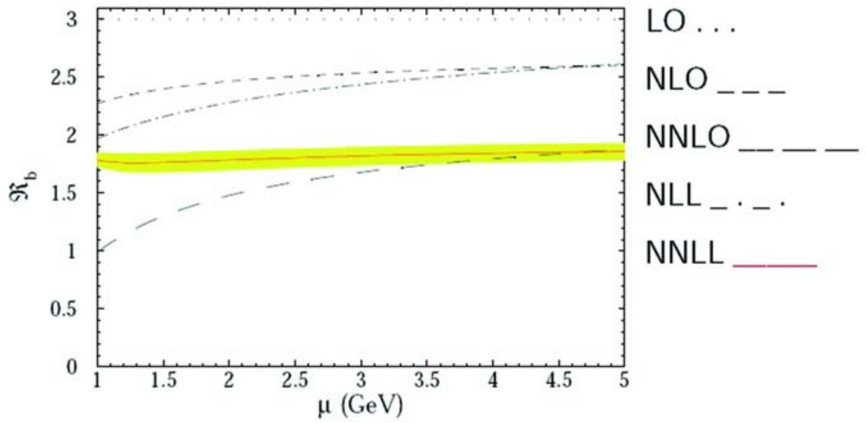

$$\frac{1}{\mathcal{R}_b} = \frac{\Gamma(^1S_0 \to \gamma\gamma)}{\Gamma(^3S_1 \to e^+e^-)} = 0.502 \pm 0.068 \pm 0.014$$

4. EFTs have also been successful to predict observables in the non-perturbative regime, like hadronic decay widths of higher quarkonium resonances. In the following plot, we show the prediction at LO and NLO of the ratio of the J = 0 and J = 1 P - wave bottomonium hadronic widths. The bands steam from the experimental uncertainties in the P - wave charmonium decay widths (for more details we refer to [2] and references therein).
This value has to be compared with the (later) measure by CLEOIII: 19.3(9.8).

Fig. 5

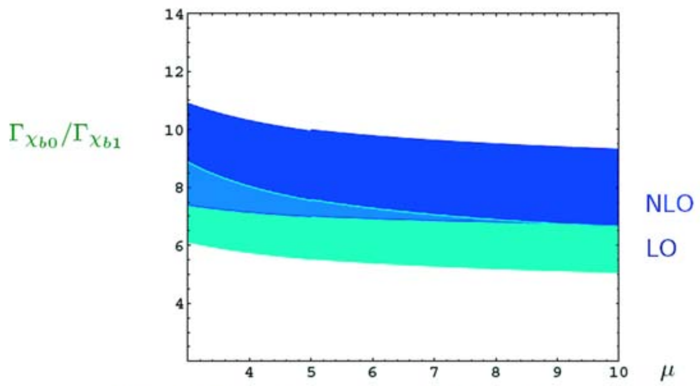

$$\frac{\Gamma(\chi_{b0}(1P) \to \mathrm{LH})}{\Gamma(\chi_{b1}(1P) \to \mathrm{LH})} = \frac{\Gamma(\chi_{b0}(2P) \to \mathrm{LH})}{\Gamma(\chi_{b1}(2P) \to \mathrm{LH})} = 8.0 \pm 1.3$$

In conclusion, Effective Field Theories provide a systematic tool to investigate a wide range of heavy quarkonium observables in the realm of QCD. This is most welcome if we want to take full advantage of the many new data that B-factories, CLEO and BES are providing in these years. EFTs also shed some light on the nature of the QCD potential and on the quantum mechanics of non-relativistic systems in a non-Abelian field theory. Finally, they provide a powerful tool to study the rather elusive low-energy dynamics of QCD in a controlled and systematic framework.

Precision tests of the standard model at the LHC

A. Vicini[1]

1 Dipartimento di Fisica, Università degli Studi di Milano

At the Large Hadron Collider (LHC), a proton-proton collider with a center of mass energy of 14 TeV under completion at the Geneva CERN, a detailed plan of searches aiming at discovering, if it exists, the Standard Model (SM) Higgs boson and, possibly, new physics signals, as described in several extensions of the SM. The experiments will develop systematic and accurate studies of standard physics, making more accurate and complete our description of the proton in terms of its elementary constituents, quarks and gluons, and measuring some fundamental parameters of the electroweak (EW) SM like for instance the mass of the W boson. In this paper we will briefly describe the method used to measure at an hadronic collider the mass of the W boson and how this value helps us in putting indirect limits on the mass of the Higgs boson.

The natural process for this kind of studies is the charged current Drell-Yan reaction, like e.g. $pp \to l + \nu_l$, namely the production of a high transverse momentum lepton pair, sufficiently isolated from the hadronic activity due to the disintegration of the incoming protons. This process is interpreted, at the partonic level, at lowest order in perturbation theory, as the subprocess $q_i\, \bar{q}_j \to W^+ \to l + \nu_l$. The reaction can be described as the production of a W boson via annihilation of the incoming quark-antiquark pair, and the corresponding cross-section has a resonance at the value of the W boson mass. The resonance can be observed from the distributions of the final state leptons. The natural observable in this case would be the invariant mass distribution, but, being the final state neutrino undetected, one has to resort to the transverse mass distribution, defined in terms of the transverse components of the lepton momenta, which can be measured with good accuracy. The transverse mass distributions has a jacobian peak at the W mass value, and therefore allows its determination. The experimental data of the transverse mass distribution are compared with theoretical predictions having the W mass as a free parameter. The result of the fit is interpreted as the measure of the mass of the W boson.

This schematic description is significantly modified by the presence of electromagnetic and weak radiative corrections: the final state leptons are dressed with additional photons which distort the W transverse mass distribution. From the operative point of view, it is necessary to decide: first, whether a photon has to be included in the computation of the final state transverse mass and, second, how to recombine the additional photons around the final state charged lepton, which can not be resolved with sufficient accuracy. A realistic description of the process can be obtained with an event generator, namely with a Montecarlo simulator which generates events, i.e. final state phase space configurations, with the corresponding weight given by the squared matrix element of the process. With such a tool, the computation of the cross section can easily include all the experimental cuts requested by the experimental setup.

The event generator HORACE has been developed in collaboration between Milano and Pavia [1] and includes at present, beyon the tree-level amplitude, the complete set of O(α) electroweak corrections and the leading-log description of higher orders QED radiation, in a parton shower approach. The O(α) real radiation, in leading log approximation, modifies the result of the fit of the experimental data by approximately 110 MeV (muon channel) with respect to the tree-level approximation. These effects have been already taken into account in the evaluation of the W mass at the Tevatron; the world average for the W mass is $m_W = 80.410 \pm 0.032$GeV. The central value of the fit is further modified when one uses the exact O(a) matrix element by -10 MeV. The order of magnitude of the mass shift induced by higher-order leading-log QED effects is of about + 10 MeV. The relevance of all these contributions should be understood in view of the experimental accuracy foreseen at the LHC in the measurement of the W mass of approximately 15 MeV.

An accurate measurement of the W mass can be used in the SM, in the framework of the global fit of all the EW precision data, to put indirect limits on the mass of the Higgs boson. If we choose α, G_μ, m_Z, respectively the fine structure constant, the Fermi constant and the

REFERENCES
1. C.M. Carloni Calame, G. Montagna, O. Nicrosini, M. Treccani, *Phys. Rev.* D69: 037301, (2004)
C.M. Carloni Calame, G. Montagna, O. Nicrosini, A. Vicini, JHEP 0612: 016, (2006).

mass of the Z boson, as input of the gauge sector of the SM lagrangian, then the value of the W mass is a prediction of the model. The latter can be derived by studying the muon-decay amplitude. The radiative corrections to this process, summarized by the parameter Δr, are sensitive, through virtual loops, to the value of the masses of all the particles of the model, in particular to those of the top quark and of the Higgs boson.

The very high experimental accuracy for many EW observables has required theoretical calculations at the second order in the perturbative expansion: in particular the 2-loop corrections to the muon-decay amplitude due to the top quark [2] modify the theoretical SM prediction of the W mass of about 20 MeV and are comparable to the order of magnitude of the present experimental error. Since the W mass depends quadratically on the top quark mass, a precise experimental measurement of the former sets stringent indirect limits on the value of the latter. Unfortunately a similar pattern does not hold for the Higgs boson mass, whose dependence from the theoretical predictions of the W mass is only logarithmic. Nevertheless a global fit of all EW observables allows to set an indirect limit at the 95% C.L. for $m_H = 219$ GeV.

The indication that a perturbative SM Higgs boson should be relatively light has stimulated many phenomenological studies concerning the production and the decay of this boson at the LHC. The dominant production mechanism is given by the annihilation of two gluons via a top quark loop (gluon-fusion), whose amplitude is known at NNLO-QCD. Furthermore, for a value of the Higgs boson mass smaller than 150 GeV, one clean signature that will allow to study its decay is in the two photons final state. The importance of these two processes has motivated the calculation of the 2-loop NLO EW radiative corrections to the corresponding amplitudes [3]. The presence in the latter of new kinematical thresholds, due to a pair of intermediate W bosons, makes this contribution not negligible, being equal to 5-10% of the lowest order prediction and comparable with the NNLO-QCD effects. In conclusion, these processes are well under control from the diagrammatic point of view; the main source of uncertainty is due to our knowledge of the proton partonic densities.

REFERENCES
2. G. Degrassi, P. Gambino, A. Vicini, *Phys. Lett.* B383: 219-226, (1996)
3. U. Aglietti, R. Bonciani, G. Degrassi, A. Vicini, *Phys. Lett.* B595: 432-441, (2004) Phys. Lett. B600: 57-64, (2004)

Medical and Health Physics

Early and delayed biological effects of high energy, high linear energy transfer charged particles

1 Dipartimento di Fisica, Università degli Studi di Milano and INFN-Milano
2 Dipartimento di Biologia e Genetica, Università degli Studi di Milano
3 Dipartimento di Scienze Fisiche, Università Federico II, Napoli, and INFN-Napoli

D. Bettega[1], P. Calzolari[1], L. Doneda[2], M. Durante[3], L. Tallone[1]

Introduction

Predictions about the magnitude of the risks due to space radiation are subject to very large uncertainties (1-3) which are mainly due to poor knowledge of the induced biological effects. The components of space radiation that are of concern are high energy charged particles, expecially the high energy nuclei of heavier elements (HZE) which are a component of the galactic cosmic rays. Several reports in the literature concern the biological effects of high energy heavy ions, (4-5), but very few data regard the delayed effects of HZE particles. In this paper we report the results of a study on the relative biological effectiveness of Fe, Ti and Si-ion beams (energy range between 0.2 and 1 GeV/n) for inactivation of the proliferative capacity of human cells and of their progeny (delayed reproductive death). Reference radiation was ^{60}Co gamma rays.

Materials and methods

Inactivation of the proliferative capacity of the directly irradiated cells and of their progeny were measured in AG1522 human fibroblast cells exposed to Fe-ion beams of energies between 0.2 and 1 GeV/n, 0.97 GeV/n Ti-ion and 0.49 GeV/n Si-ion beams and, for comparison, to ^{60} Co gamma rays. The cells were maintained in α MEM medium supplemented with 20% foetal calf serum at 37 °C in 95 % air: 5% CO_2 atmosphere. In these conditions the plating efficiency was 25% and the doubling time was 24 ± 2 h. The cells were tested for mycoplasma contamination before use. Three days before irradiation 2 10^5 cells were seeded into 25 cm^2 flasks (one or two flasks for each dose). The cells were irradiated in plateau phase. After exposure the cells were harvested by trypsinization, counted, diluted and plated into 25 cm^2 flasks (five samples for each dose) at suitable numbers for colony forming assay and incubated at 37 °C. After 14 days of incubation, four flasks for each dose were fixed and stained with 10% Giemsa solution for evaluation of inactivation of the proliferative capacity (survival). At the same time one flask for each dose was trypsinized, the cells diluted and seeded at low density into five further flasks and incubated again for 14 days for the delayed reproductive assay (cloning efficiency). For both the irradiated cells and their progeny, colonies with more than 50 cells were scored as survivors and the survival linear-quadratic model was fitted to the data.

Irradiations have been performed at the Heavy Ion Medical Accelerator Center (HIMAC) of the National Institute for Radiological Sciences (NIRS) in Chiba-Japan, with 0.2 and 0.5 GeV/n Fe-ion and 0.49 GeV/n Si-ion beams, and at the NASA Space Radiation Laboratory (NSRL) in Brookhaven, with 1 GeV/n Fe-ion and 0.97 GeV/n Ti-ion beams. LET values on target were 442, 200 and 147 keV / μm for 0.2, 0.5 and 1GeV/n Fe-ion beams, 106 and 56 keV/ μm for Ti and Si–ion beams respectively. Dose rate at the sample position was around 0.25 Gy/min and 1 Gy/min at HIMAC and NSRL respectively. Cells were irradiated with various doses in the dose-range between 0.25 and 2 Gy. Irradiation with γ rays was carried out at the ^{60}Co source at the Radiotherapy Unit, Istituto Nazionale dei Tumori, Milano. Dose rate was 1.5 Gy/min and dose-range was 0.5-4 Gy.

Results and discussion

Figures 1 and 2 show surviving fraction versus dose and cloning efficiency of the progeny of the irradiated cells versus the dose given to their progenitors for all the ion- beams studied. Data with γ-rays are shown for comparison in the figures. Two to three experiments were performed with the iron ion beams and with the gamma rays. Si and Ti-ion beams data are preliminary as they were obtained by only one experiment. The curves are the best fit to the data with a linear-quadratic equation. As can be seen from Fig.1 all the heavy ion beams induce inactivation more effectively than gamma rays with the exception of the lowest energy/highest LET, 0.2 GeV/n iron ion beam, which shows at low doses the lowest effectiveness. A possible reason for this low effectiveness could be that for this LET, the mean number of particles/cell nucleus in AG1522 cells is less than 1.5 for doses up to 0.5 Gy. At low doses therefore the fraction of cells which are not traversed by any ion is not negligibile i.e. it is about 50% at 0.25 Gy. Fig.2 shows that there is a dose dependent reduction of the cloning efficiency of the progeny of the irradiated cells compared with their controls with all types of radiations. The effect is higher with all the heavy ion beams compared to gamma rays, with the 1 GeV/n Fe-ion beam being the most effective. The effect is large, indeed 14 days after the delivery of 1 Gy with the 1 GeV/n iron ion beam, the cloning efficiency relative to controls reduced to about 30%. The phenomenon of the reduction in clonogenic potential of the progeny of cells that survive radiation exposure, termed as delayed reproductive death, has been studied extensively in the literature with low LET radiations (X or gamma rays). It is generally thought that this effect, transmissible over many generations, could be due to induced genomic instability in the cell population (6-9). The results of this experiment show that, compared with gamma rays, all the heavy ion beams are highly effective in inducing delayed reproductive death i.e. the dose giving 50% delayed reproductive death is similar to that giving 50% survival in the case of 1 GeV/n Fe-ion beam, whereas the two dose values differ by a factor of about two in the case of γ-rays.

REFERENCES
1. Cucinotta, F.A., Schimmerling, W., Wilson, J.W., Peterson, L.E., Badhwar, G.D., Saganti, P.B., and Dicello, J.F., Space Radiation Cancer risks and uncertainties for Mars missions. *Radiat. Res.* 156, 682 (2001).
2. Wilson, J., Shinn, J.L., Tripathi, R.K., Singleterry, R.C., Cloudsley, M.S., Thibeault, S.A., Cheatwood, F.M., Schimmerling, W., Cucinotta, F.A., Badhwar, G.D., Noor, A.K., Kim, M.Y., Badavi, F.F., Heinbockel, J.H., Miller, J., Zeitlin, C., Heilbronn, L. Issues in deep space radiation protection. *Acta astronautica*, 49, 289 (2001)
3. Schimmerling, W., Cucinotta, F. and Wilson J.W. Radiation risk and human space exploration. Adv. Space Res. 31, 27 (2003).
4. Blakely, E. and Kronenberg, A. Heavy-Ion radiobiology: new approaches to delineate mechanisms underlying enhanced biological effectiveness. Radiat. Res. 150, S12 (1998).
5. Durante, M. Radiation protection in space. *Rivista del Nuovo Cimento* 25, 1 (2002).

Fig.1
Surviving fraction versus Dose

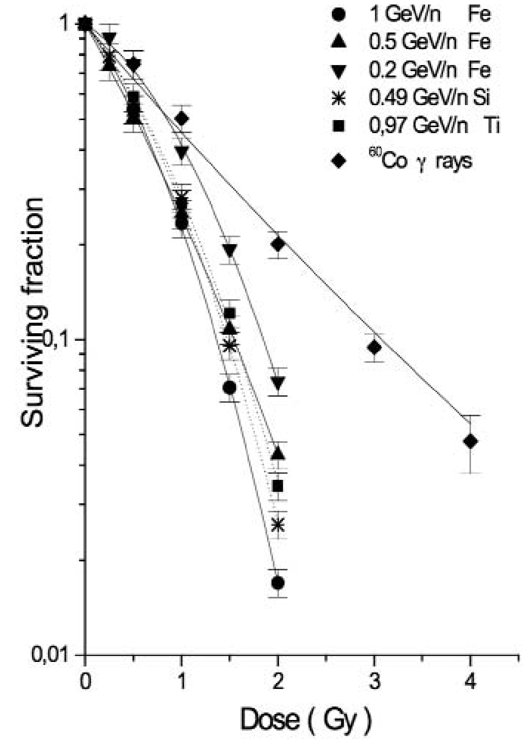

Fig.2
Cloning Efficiency of the Progeny of the irradiated cells versus dose given to the progenitors

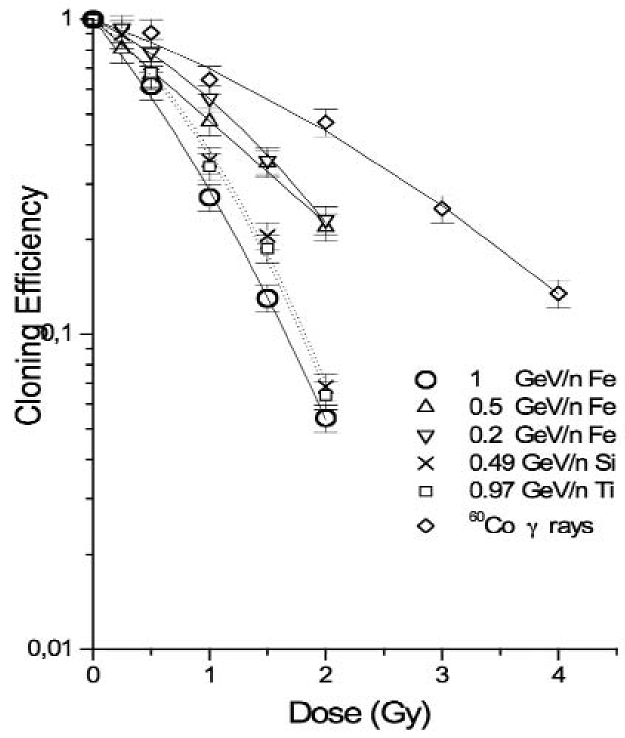

REFERENCES
6. Little, J.B. Radiation induced genomic instability. *Int. J. Radiat. Biol.* 74, 663 (1998)
7. Mendonca, M.S., Temples, T.M., Farrington, D.L. and Bloch, C. Evidence for a role of delayed death and genomic instability in radiation-induced neoplastic transformation of human hybrid cells. *Int. J. Radiat. Biol.* 74, 755 (1998).
8. Morgan, W.F., Day, J.P., Kaplan, M.I., McGhee, E.M. and Limoli, C.L. Genomic instability induced by ionizing radiation. *Radiat. Res.* 146, 247 (1996)
9. Seymour, C.B., Mothersill, C. and Alper, T. High yields of lethal mutations in somatic mammalian cells that survive ionizing radiation. *Int. J. Radiat. Biol.* 50, 167 (1986).

Relative Biological Effectiveness at low doses, RBE $_{\alpha}$, (RBE$_{\alpha}$ = α_{ion} /α_{γ}, α_{ion} and α_{γ} are the linear coefficients of the dose effect curves for the ion and the gamma rays), for survival and delayed reproductive death are reported in Fig.3. RBE$_{\alpha}$ higher than one is found for both effects with all the beams with exception of inactivation due to 0.2 GeV/n iron ion beam. RBE$_{\alpha}$ is maximum in the LET interval between 140-200 keV/mm with values of 1.6 ± 0.1 and 3.3 ± 0.6 for early and delayed reproductive death respectively. RBE$_{\alpha}$ of 0.6 ± 0.1 and 1.3 ± 0.2 is found for the 0.2 GeV/n iron ion beam with LET of 442 keV/ µm for survival and delayed reproductive death respectively.

The data were also analyzed on the basis of the particle fluence (Fig. 4 and 5). A different relationship is found: the 442 keV/µm Fe-ion beam, which was the least effective for both the effects, is the most effective based on fluence, whereas the 56 keV/µm Si-ion beam shows the lowest effectiveness, i.e. for an early or delayed inactivation level of 50%, the 442 ke V/µm Fe-ion beam is about 5 fold more effective than the Si-ion beam.

Fig. 3
RBE$_{\alpha}$ versus radiation LET

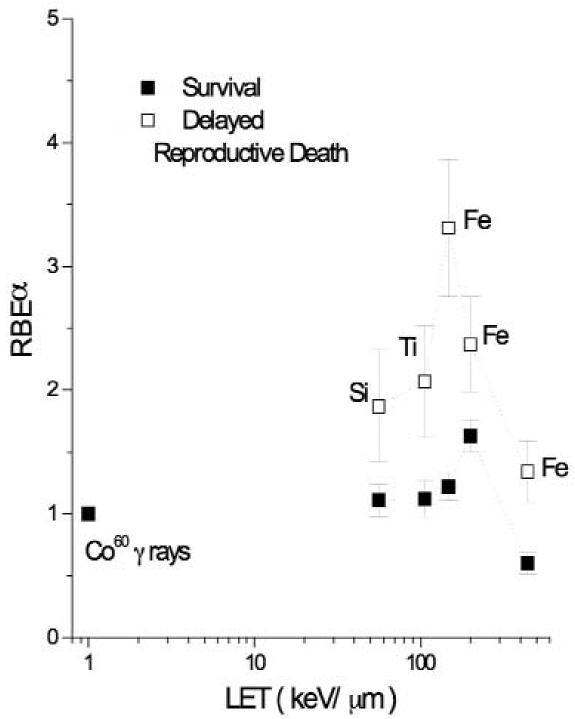

Fig. 4
Surviving fraction versus Fluence

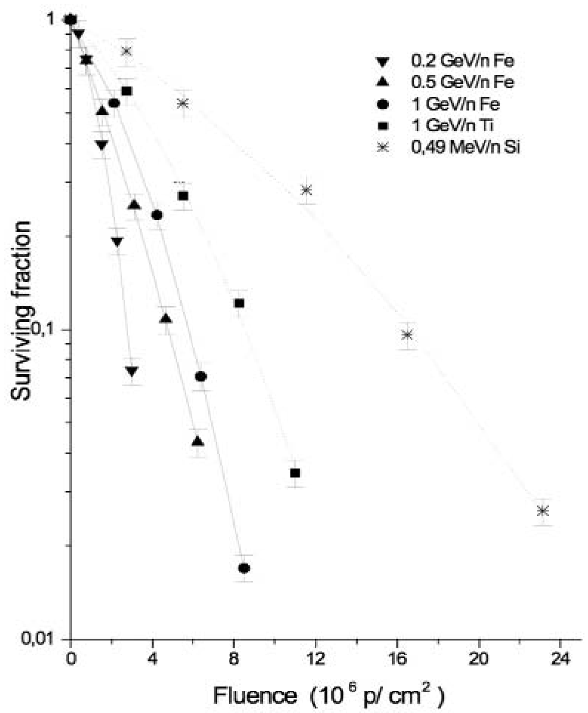

Fig. 5
Cloning Efficiency of the progeny of the irradiated cells versus Fluence given to the progenitors

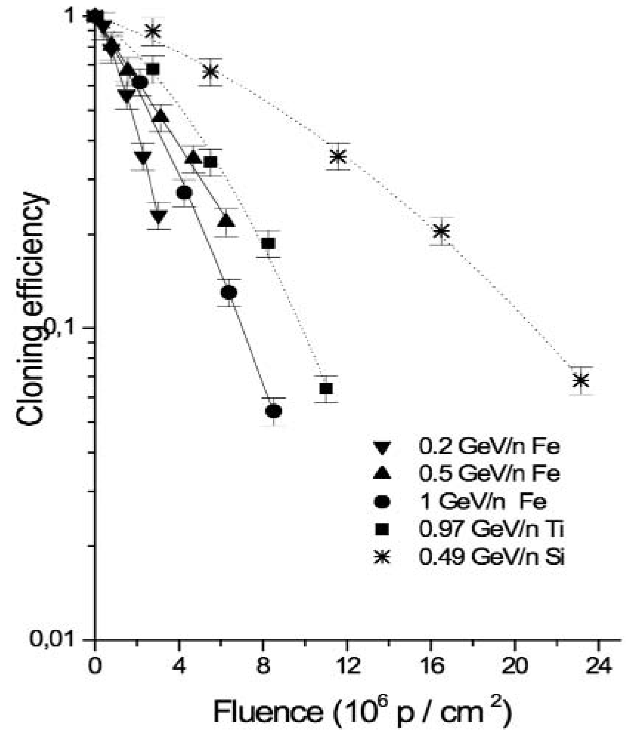

Conclusions

The results of this study show that exposure to high energy high LET ion beams induce delayed damage in the progeny of the irradiated cells in the form of reduced proliferative capacity which could indicate induced genomic instability. Compared with gamma rays, HZE particles show higher Relative Biological Effectiveness which is highest for LET values between 140-200 keV/µm and it is greater for delayed compared to early damage induction. Further studies on various delayed effects will be necessary to establish whether this result is a general phenomenon and to evaluate, if any, its consequences *in vivo*.

The results reported in this paper have been published in Advances in Space Research. 35(2):280-5, 2005.

Acknowledgements. This research project was funded by the Italian Space Agency (ASI) and by INFN

The contribution given by nuclear analytical techniques to the research in internal dosimetry

1 Dipartimento di Fisica, Sezione di Fisica Medica, Università degli Studi di Milano and INFN

M.C. Cantone[1], A. Giussani[1], and I. Veronese[1]

For a number of elements with radionuclides of significance in radiological protection, including Ru, Zr, Ce, Te and Mo, human data are poor or missing and biokinetic parameters are essentially extrapolated from data on animals. The use of stable isotopes is a publicly well acceptable and ethically justifiable method compared to the use of radioisotopes. Here is presented the developed methodology and the results obtained on volunteer subjects by using stable isotopes. The design of the investigation is taken from the standard procedure of the double tracer technique and consists in the simultaneous use of two tracers, one oral and one intravenous tracer. At different times blood samples are withdrawn, in some cases even urine is collected, and both isotopes are determined to obtain dynamical pictures of relevant processes such as intestinal absorption and the main excretion pathways. Techniques, based on activation analysis and mass spectrometry, were specifically optimised to discriminate and quantitate different isotopes of the same element in the complex matrices of the biological fluids in the order of ppb. New evidences were obtained from the direct observation on humans, which suggested modifications to be introduced in the current ICRP biokinetic models.

Introduction

The internal dose following the intake of radioactive materials cannot be measured directly and current approach adopted to provide internal dose estimates requires biokinetic models describing distribution and retention of radionuclides in selected organs and tissues. The internal dose estimates depends critically on the reliability of the biokinetic parameters used and for a number of elements with radionuclides of significance in radiological protection, including Ru, Zr, Ce, Te, and Mo, human data are poor or missing and biokinetic parameters are essentially extrapolated from data on animals. This work intends to present the contribution that basic nuclear analytical techniques, such as activation analysis and mass spectrometry, provide, presenting a well accepted and ethically justifiable approach, like the one based on the use of stable isotopes, as an alternative to the use of radioactive isotopes.

The design of biokinetic studies

The investigations on the biokinetics in humans here presented and conducted within a long dated cooperation with GSF in Munich, have been performed by using stable isotopes and by following a general design that is common in the case of radioactive isotopes. In particular the so called double tracer technique was used, that consists in the simultaneous administration of two tracers, one given orally and another intravenously, followed by the measurement of both tracer concentration in plasma and urine. At different times after the tracer administration, up to one day max, blood samples are withdrawn. Cumulated urine is collected within the first 48 h or within the first 330 h max. This approach permits to obtain dynamical pictures of relevant processes such as intestinal absorption and the main excretion pathways. Indeed, the time behaviour of the injected tracer represents the clearance from plasma, while the oral tracer concentration is the result of two competitive mechanisms: the passage to systemic circulation, that is the intestinal absorption, and the clearance itself [1]. For a better understanding of the process involved and of their significance in the absorption and distribution of the ingested elements of interest, the dependence of the absorption and of the biokinetic parameters on the chemical form, amount and composition of the ingestion was studied by using different intake conditions in volunteer subjects, according to the protocols approved by the Ethical Committee of Technical University of Munich for each of the elements investigated.

REFERENCES
1. Cantone M.C.,"Nuclear Techniques of Analysis in the Development of Biokinetic Models for Radiological Protection", *Long Range Plan, Town Meeting NUPECC, Darmstadt, Germany* (2003)

Analytical techniques

Nuclear analytical techniques, such as activation analysis and mass spectrometry, are well known methods for elemental analysis in biological samples, and both showed their ability to discriminate and quantitate different isotopes of the same element in the complex matrices of the biological fluids in the order of ppb (part per billion, µg/kg). In activation analysis nuclear

reactions are induced by bombarding the sample with projectiles of given type and energy, thus distinguishing the stable isotopes on the basis of the decay emissions of the radioactive reaction products. In mass spectrometry a series of electrical and/or magnetic fields is applied to the ionized sample, in order to discriminate between atoms or molecules with different mass to charge ratios (m/z values), thus distinguishing the stable isotopes on the basis of their nuclear mass. The widely used mass spectrometry versions (TIMS, ICP-MS) and the activation analysis by using photons, neutrons or charged particles (PAA, NAA, CPAA) have proved different performance, in relation to the matrix to be analysed and the isotopes and their amount to be determined, in terms of sensitivity and reliability. The data here reported relating to Ru, Zr and Mo investigation are obtained by using proton activation analysis in plasma sample and thermal ionization mass spectrometry in urine. In particular the stable isotopes ^{101}Ru and ^{99}Ru were used to study Ru biokinetics and the isotopes ^{96}Zr, ^{90}Zr and ^{96}Mo, ^{95}Mo respectively for Zr and Mo investigations. The procedure followed to prepare plasma samples for proton activation analysis is sketched in Fig. 1. Plasma was separated from whole blood by centrifugation and, after the addition of a known amount of an internal standard, the plasma samples are heated to dryness, powdered in an agate mortar and compressed to form a self supporting tablet. For urine sample preparation a procedure was purposely developed based on acid digestion by using a pressurized microwave decomposition. Activation of samples was performed with the proton beam of the Philips Cyclotron at the Paul Scherrer Institute in Villigen (Switzerland) up to 2002 and then with the proton beam of the Scanditronix MC 40 at the JRC in Ispra by using properly designed irradiation chambers. The used experimental conditions (energy, duration of irradiation, waiting time after EOB and counting time) are the result of a detailed optimization process [2] which is made for each one of the elements of interest to improve the minimum detectable quantity, thus to be able to maintain a reduced amount of the isotope to be ingested or injected in the investigations. The incoming proton beam energy of 19 MeV was chosen to induce predominantly the (p,n) nuclear reactions on ^{101,99}Ru, ^{96,95}Mo, ^{90}Zr and (p,2n) on ^{96}Zr, a beam intensity of 2 µA was used for a 6 sample sliding chamber and 10 µA for a 40 sample rotating chamber. After the irradiation, gamma spectrometry measurements were performed for each sample using HPGe detectors with PC based multichannel buffer cards. For instance detection limits, per gram of plasma, of 2 ng and of 1 ng for the isotopes ^{96}Zr and ^{90}Zr respectively were found for irradiation time: 40 h; cooling time: 24 h for ^{90}Zr and 30 days for ^{96}Zr; measuring time 10 h for ^{90}Zr and 3 days for ^{96}Zr and ^{90}Zr in the amount of 100 mg may be used for the injection and ^{96}Zr in the amount of 3-5 mg may be used for the ingestion.

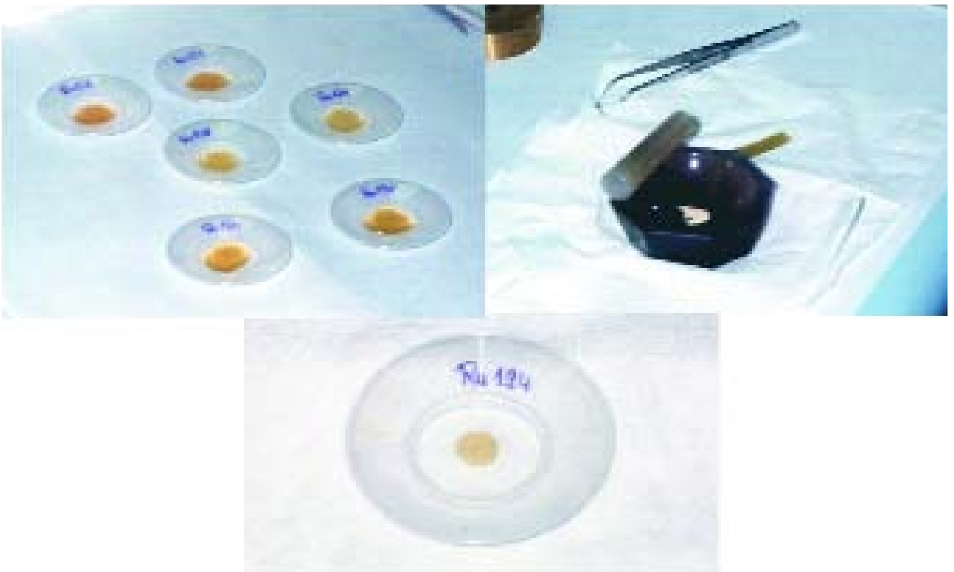

Fig. 1
Plasma preparation procedure for activation analysis.

REFERENCES
2. Veronese I., Cantone M.C., Giussani A., Maggioni T., Birattari C., Groppi F., Garlaschelli L., Werner E., Roth P., Hollriegl V., Louvat P., Felgenhauer N., Zilker Th., "Stable tracer investigations in humans for assessing the biokinetics of ruthenium and zirconium" *Radiation Protection Dosimetry* 105, 209 (2003)

Selected results and discussion

Figure 2 shows the time course in plasma of the ^{101}Ru isotope, that is the injected tracer used in Ru biokinetic investigations. The data obtained from 6 experiments performed in three volunteers, two repeated investigations for each subject, showed intraindividual similar Ru clearance. However, this behaviour is quite different from the single exponential course adopted in ICRP model for internal dose estimates and this discrepancy can be attributable to the fact that no data on Ru clearance in humans were available before these experiments with stable isotopes.

Figure 3 shows the results obtained in one of the three subjects investigated to study the influence of the chemical form on the plasma clearance of Ru in humans. In this investigation Ru was injected in form of citrate Ru complexes (organic) and in a second experiment, performed on the same subject, Ru was injected in inorganic form [3]. The time behaviour of Ru concentration in plasma in the two experiments, shows that organic form is cleared from the plasma very rapidly, while the inorganic Ru remains longer in the systemic circulation. These findings are also confirmed by the renal excretion patterns. Indeed, as shown in the upper part of the same figure, the urinary excretion for the organic Ru is high, more than 50 % in the first 24 h, while the inorganic Ru is excreted only about 25% in the 48 h.

Figure 4 shows, in one of the subjects investigated for Zr study, the time course of the percentage concentration for both the injected and ingested tracer and in particular the results of two independent investigations on the same subject are here reported [4]. The red curves represents the current predictions for Zr on the basis of ICRP models and the black curves are the result of fitting a modified model to the whole set of data. In comparison to ICRP predictions a faster absorption is found which is 4 times lower than the recommended value for members of the population. Differences in the value of intestinal absorption can have consequences on the calculation of dose and more significantly can be relevant when using the model for the interpretation of urine measurements after accidental incorporation to assess retrospectively intake and dose.

Fig. 2
Time courses of the injected Ru isotope. Two experiments for cach of the three subject investigated.

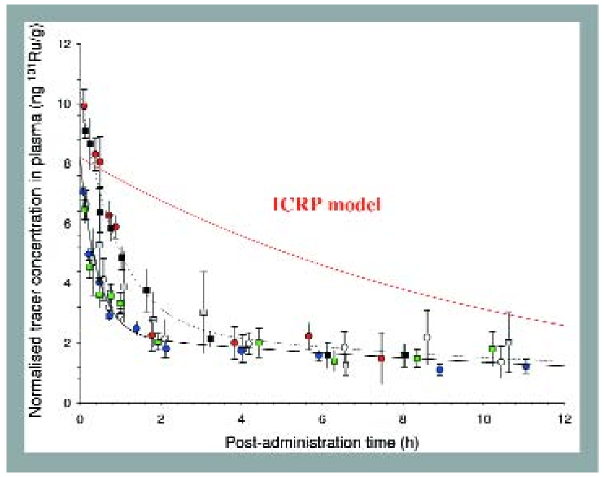

Fig. 3
Time behaviour in plasma and in urine of Ru injected tracer in two different chemical form (organic and inorganic).

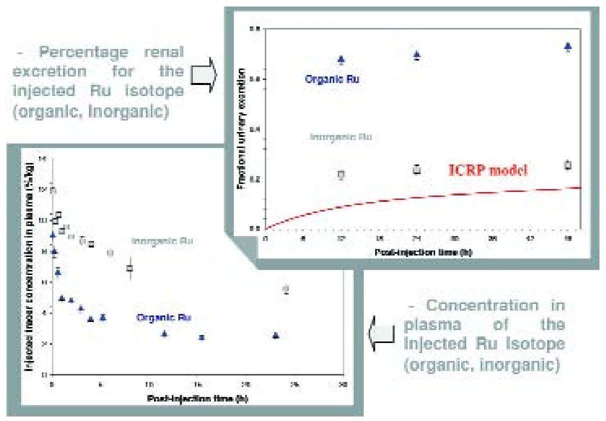

Fig. 4
Percentage concentration of ingested and injected Zr isotopes in one investigated subject.

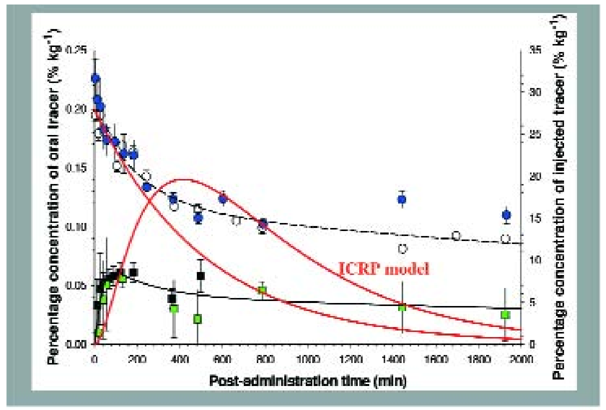

REFERENCES
3. Veronese I., Giussani A.,Cantone M.C., Birattari C., Bonardi M., Groppi F., Hollriegl V., Roth P., Werner E., "Influence of the chemical form on the plasma clearance of ruthenium in humans" *Applied Radiation and Isotopes* 60, 1, 7 (2004)
4. Veronese I., Giussani A., Cantone M.C., Maggioni T., Birattari C., Groppi F., Werner E., Roth P., Hollriegl V., "A re-evaluation of the biokinetics of zirconium in humans" *Applied Radiation and Isotopes* 58, 4, 431 (2003)

Figure 5 shows, as an example, the data of repeated investigations, on one subject, following different ingestion conditions. In the investigations the ingestion of different Mo amounts, in liquid and solid form, the use of intrinsic and extrinsic tag and the ingestion of black tea, as inhibitor of absorption, together with Mo, are included. These data are taken from a series of 63 studies on Mo biokinetics performed with 17 volunteers [5]. A number of considerations can be obtained from the different behaviours shown in the figure. It is evident that intestinal absorption is almost complete for aqueous solution, while decreases with increasing amount of ingestion and in the case of solid meal and this fact calls for definition of a separate set of parameters for liquid and solid ingestion. On the basis of the whole set of results the biokinetic model recommended by ICRP was upgraded and different sets of fractional transfer rates were proposed for liquid and solid ingestion. Dose per unit intake were calculated according to ICRP guidelines but using the revised model. Considerable deviations were observed for the dose to selected organs. For example, Fig. 6 shows the relative contribution of each organ/tissue to the committed dose after ingestion of ^{99}Mo (66 h half life) according to the ICRP models, where no distinction is taken between solid and liquid ingestion, and the relative contributions calculated by using the revised model based with separate parameters for liquid ingestion and for solid ingestion. For example, the dose per unit intake for colon, after ingestion of ^{99}Mo in solid form resulted about 7 times higher than the ICRP value, and consequently the relative contribution to the total dose is evidently different. This fact could be of importance with respect to deterministic effects to particularly radiosensitive organs.

Fig. 5
Percentage concentration of ingested Mo in one subject, under different ingestion conditions.

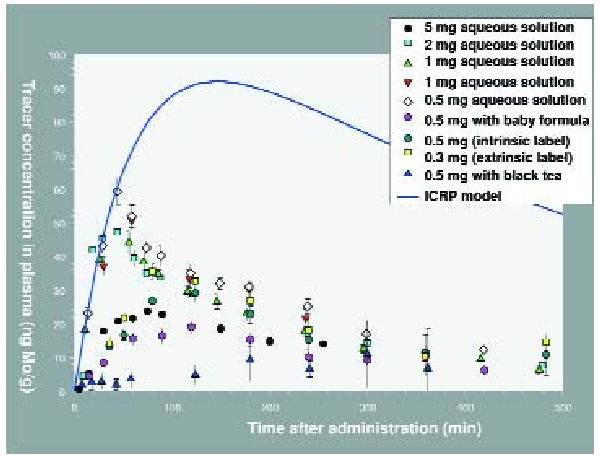

Fig. 6
Relative contributions of each target organ/tissue to the committed dose due to ^{99}Mo ingestion, as given by ICRP and as calculated by using the revised model with separate set of parameters fro liquid and solid ingestion.

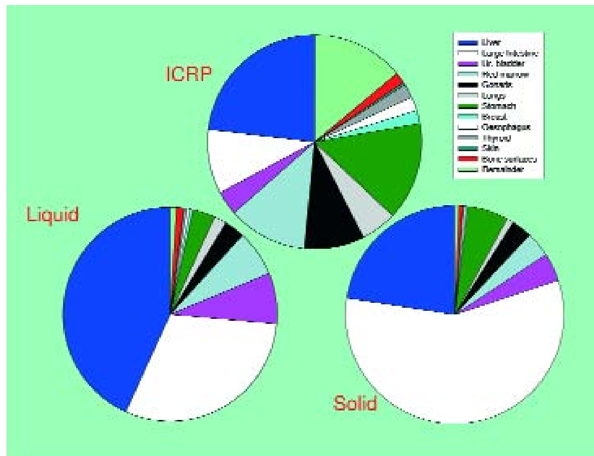

Conclusions

The use of stable isotopes as tracers, in combination with a suitable technique of analysis, such as activation with protons, has allowed obtaining biokinetic data for element of interest in radiological protection directly in healthy human subjects. The results of the tracer studies have filled a gap in the current knowledge proving information about kinetics of intestinal absorption and of blood plasma clearance that were previously not available or only based on experiments on animals. These new pieces of information have indicated a series of modifications that can be introduced in the current ICRP models towards a better confidence in internal dose estimates.

REFERENCES
5. Giussani A., Arogunjo A.M., Cantone M.C., Tavola F., Veronese I., "Rates of intestinal absorption of molybdenum in humans" *Applied Radiation and Isotopes* in press (2006)

Role of physics in a 'Trojan horse' method for radiotherapy

1 Dipartimento di Fisica, Università degli Studi di Milano and INFN

G. Gambarini[1]

1. Introduction

Slow neutrons have shown promising potentiality for treating diffuse or radio-resistant tumours. The energy delivered by slow-neutron interactions with tissue components is relatively low. On the opposite, if a drug containing suitable isotopes with high cross section for thermal neutrons can be concentrated in tumour tissue, then thermal neutron reactions release high energy in tumour tissue itself. This kind of radiotherapy was initially known as "Trojan horse" method. Boron neutron capture therapy (BNCT) takes advantage of the possibility of selectively accumulating the isotope ^{10}B in tumour cells and of the high cross section of the reaction with thermal neutrons

$$^{10}B(n,\alpha)^{7}Li\ (\sigma = 3837\ b).$$

The short range in tissue of the emitted α and ^{7}Li particles (<10 μm) allows localised energy release in tumour cells, saving the surrounding healthy tissue. Therefore, BNCT is of particular interest for diffused tumours, such as liver tumours. Moreover, owing to the high linear energy transfer (LET) and relative biological effectiveness (RBE) of α and ^{7}Li particles, BNCT is potentially effective for radio-resistant tumours, such as multiform glioblastoma and some kinds of melanomas. Very promising results have been obtained in trials on patients with glioblastoma or liver cancer. Interdisciplinary research is still carried out aimed at setting up suitable modalities for BNCT, in particular for achieving higher selectivity of the boron carrier (Chemistry and Biology), good quality of neutron fields (Nuclear Engineering and Physics) and reliable dosimetry methods (Physics).

2. Dosimetry for BNCT

As known, neutrons are not directly ionising particles. Then, during the exposure of a patient to thermal or epithermal neutrons, the absorbed dose in tissue is released by the various components of secondary radiation. For BNCT treatment planning, besides the radiotherapy dose in tumour tissue with accumulation of ^{10}B, it is necessary to evaluate the dose delivered by thermal and epithermal neutrons to healthy tissue too, because this information is necessary to establish the maximum neutron fluence admitted for the treatment. The reactions mainly responsible of the released energy in tissue or tissue-equivalent materials are:

$$^{1}H(n,\gamma)^{2}H\ \ (\sigma = 0.33\ b)$$

whose γ-rays (of 2.2 MeV) can travel many centimetres through tissue, and

$$^{14}N(n,p)^{14}C\ (\sigma = 1.81\ b)$$

whose emitted protons (of about 0.6 MeV) have short range in tissue and give local dose deposition. Moreover, epithermal and fast neutrons undergo elastic scattering (mainly with hydrogen) so that recoil nuclei also contribute to the absorbed dose. The spatial trends and the relative contributions to the total absorbed dose of such secondary components depend on neutron energy spectrum, on beam geometry and on the size and dimension of the irradiated volume. Owing to the different LET and RBE of the various kinds of secondary radiation, the various dose components have to be separately identified.

A method has been developed for imaging the various dose components in phantoms exposed in thermal or epithermal neutron fields suitable for BNCT. The method is based on optical imaging of suitably designed gel dosimeters, properly made up in the laboratory, that act as continuum dosimeters and allow achieving images of the absorbed dose. Dosimeter analysis consists in measurements of visible light transmission, imaged by means of a CCD camera. A gel dosimeter after irradiation in a BNCT phantom exposed in a reactor epithermal column is shown in Fig. 1. Gel dosimeters are particularly convenient for performing dose measurements in thermal or epithermal neutron fields. In fact, they have good tissue-equivalence for neutrons of whichever energy and also for the secondary radiation generated by neutron interactions. Moreover, it is possible to suitably design gel matrices with different elemental compositions so that the differential analysis of the responses of dosimeters with different isotopic content permits the various secondary-radiation components to be distinguished [1,2]. The method for separating the dose contributions, proposed and studied in the laboratory, consists in introducing, into the phantom of interest, coupled layers of gel dosimeters with a composition differing for the content of one isotope whose reaction with neutrons gives production of charged particles. The separation of dose contributions is obtained by pixel-to-pixel manipulations of the detected images, utilizing suitable procedures and algorithms. The images of thermal neutron fluence are obtainable too, by elaborating the images of the dose due to the charged particles emitted in the reactions of thermal neutrons with ^{10}B. Such particles, in fact, release their energy locally and then the thermal neutron fluence can be attained utilising kerma factors.

In order to study the reliability of the proposed method, experiments have been carried out at the fast research reactor Tapiro (ENEA, Casaccia, Rome), shown in Fig. 2, in the thermal and epithermal columns properly designed for BNCT research. In order to check the correctness of the obtained results, dose and fluence profiles have been extracted from images and their trend has been compared with the results obtained in a few positions by means of other dosimetry techniques. A suitable method for mapping gamma-dose and thermal neutron fluence with thermoluminescent dosimeters (TLD) has been developed in the laboratory [3]. Besides TLDs, also activation techniques and Monte Carlo calculations have been utilised for intercomparison of data. The consistency of the results obtained with the various methods has confirmed the reliability of the proposed procedure.

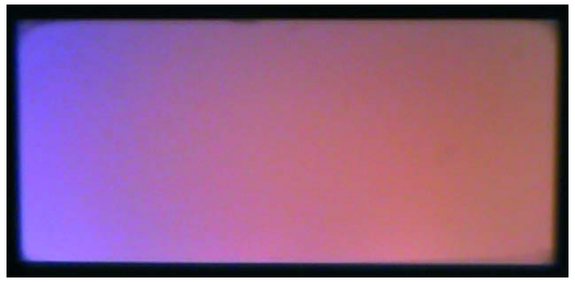

Fig. 1
Gel dosimeter after irradiation in a phantom exposed to a reactor epitermal neutron beam.

Fig. 2
Tapiro reactor of ENEA (Casaccia, Rome).

The method of gel dosimetry in neutron fields has encountered international interest, and experiments are now in development at nuclear reactors in other research centers where BNCT trials of patients have been performed. Besides Tapiro reactor, present experiments are mostly carried out at the TRIGA reactor of Pavia University, now recognized from the BNCT community in all the world owing to a successful treatment of human liver, at the HFR (high flux reactor) of the European Joint Research Center of Petten (Holland), that is the first European BNCT unit performing treatment of human patient, and at the LVR-15 reactor of Rez (Prague) where BNCT is studied and experimented from many years.

3. Some results

In Fig. 3, the total dose in the central plane of a phantom for BNCT experimentation is shown. The phantom was exposed in the epithermal column of TAPIRO reactor, up to a fluence of about 10^{13} cm^{-2} s^{-1}. The contributions to the total dose are from photons, from α and ^{7}Li charged particles emitted in ^{10}B reactions and from fast neutrons. In Fig. 4 the results of the separation of the therapy dose due to ^{10}B reactions and the photon plus fast neutron doses are reported. Photon and fast neutron doses have been separated too, with a method based on cou-

REFERENCES
1. Gambarini G., Birattari C., Colombi C., Pirola L. and Rosi G., "Fricke-Gel Dosimetry in Boron Neutron Capture Therapy", Radiation Protection Dosimetry 101, 419 (2002)
2. Gambarini G., Colli V., Gay S., Petrovich C., Pirola L., and Rosi G., "In-phantom imaging of all dose components in boron neutron capture therapy (BNCT) by means of gel dosimeters", Applied Radiation and Isotopes 61, 759 (2004)
3. Gambarini G., Klamert V., Agosteo S., Birattari C., Gay S., Rosi G., and Scolari L., "Study of a method based on TLD detectors for in-phantom dosimetry in BNCT", Radiation Protection Dosimetry 110, 631 (2004

ples of gel layers having the same composition but obtained one with water and the other with heavy water [4]. In Fig. 5, results of such separation are shown. Here depth dose profiles in the central axis of the phantom have been extracted from images, and compared with the results of TLD measurements and of Monte Carlo calculations. All dose profiles, extracted from dose images, are reported in Fig. 6.

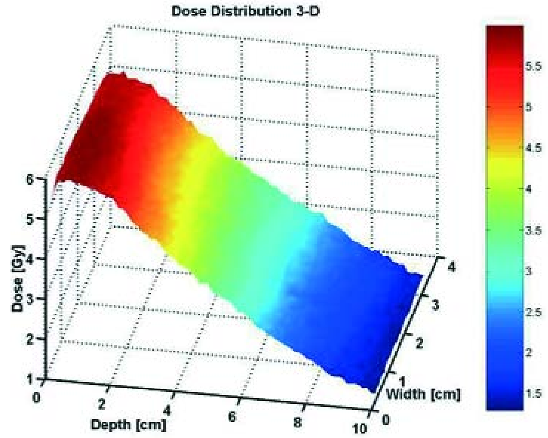

Fig. 3
Total dose in the central plane of a phantom for BNCT experiment, exposed to Tapiro epithermal beam.

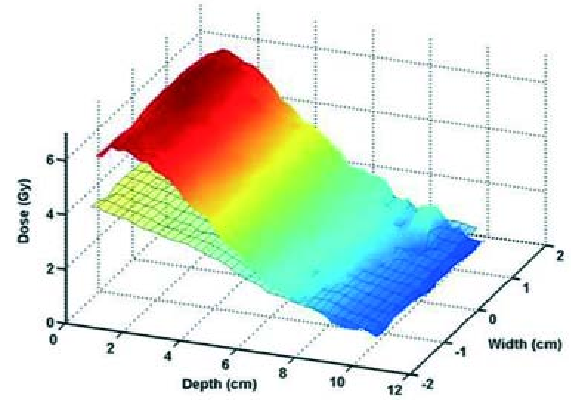

Fig. 4
Images of the therapy dose due to ^{10}B reactions and the photon plus fast-neutron doses.

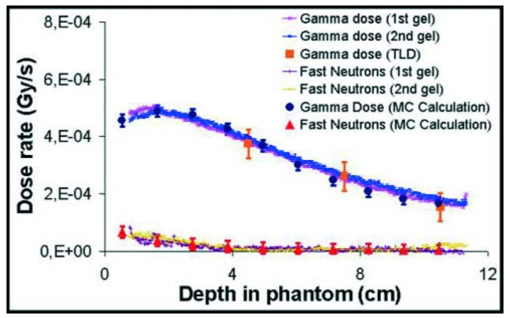

Fig. 5
Result of separation of photon and fast-neutron doses.

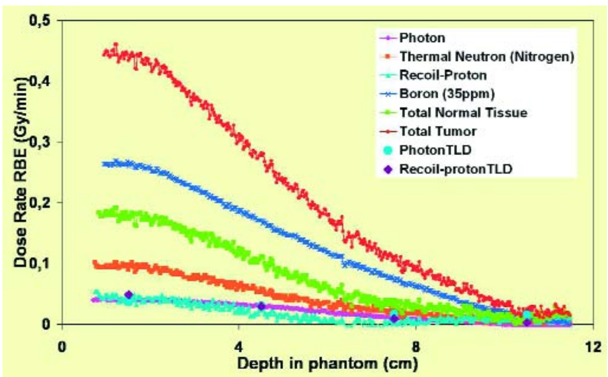

Fig. 6
Profiles of all the contributions to the absorbed dose along the central axis of the phantom exposed in the Tapiro epithermal column.

4. Final remarks

The proposed method has shown substantial potentialities. At present, no other method allows obtaining spatial images of all dose contributions in thermal or epithermal neutron fields.

REFERENCES
4. Gambarini, G., Agosteo, S., Danesi, U., Garbellini, F., Lietti, B., Mauri, M., Rosi, G., "Imaging and profiling of absorbed dose in neutron capture therapy", IEEE Trans. Nucl. Sci. 48, 780–784 (2001).

Production of non-conventional high specific activity radionuclides for biomedical, toxicological and environmental purposes

F. Groppi[1], M.L. Bonardi[2], S. Morzenti[3], E. Persico[4], L. Gini[5], E. Menapace[2], Z.B. Alfassi[3], B.L. Zhuikov[4], K. Abbas[5], and U. Holzwarth[5]

1 LASA, Dipartimento di Fisica, Università degli Studi di Milano and INFN
2 Divisione per le Tecnologie Fisiche Avanzate, ENEA, Bologna, Italy
3 Department of Nuclear Engineering, Ben Gurion University, Beer Sheva, Israel
4 Institute for Nuclear Research of Russian Academy of Sciences, Moscow, Russia
5 Institute for Health and Consumer Protection, Joint Research Centre, EC, Ispra (Va), Italy

Low- and medium-energy accelerators and sometimes thermal nuclear reactor, allow production of very high specific activity radionuclides (HSARNs) for biomedical, environmental, toxicological and occupational investigations. Specific Activities of the order of GBq·µg^{-1} are achieved; this means that the experiments can be carried out in the sub-nanogram range (nanochemistry). The HSARNs allow labeling increasing amounts of different chemical forms of toxicological or pharmacological interest, with the possibility to obtain dose vs. effect relationships on both cell cultures and laboratory animals. In nuclear medicine, "very high" A_S - in No Carrier Added radiopharmaceuticals - are normally required to avoid undesirable effects due to high chemical concentration of labeled species. Some labeled species are sparingly soluble in body fluids, organs and barrier membranes; some others present toxic or adverse effects onto humans; a low A_S(NCA) means a high molar concentration and could interfere into normal human metabolism, by inducing undesired pharmacological effects. High-resolution HPGe χ-spectrometry and β-spectrometry by liquid scintillation counting allow determination of radionuclidic and radiochemical purities of the tracer and determination of radiochemical yield of processing procedures. Chemical purity determination is carried out by a range of analytical and radioanalytical techniques. Radionuclide production for biomedical applications has been brought up in the years, at LASA, particularly in co-operation with JRC-Ispra of EC and LENA-Pavia.

Introduction

Specific Activity, Activity Concentration and Isotopic Dilution Factor: Specific Activity (A_S) of a radionuclide (RN), is defined as the ratio between the activity of the stated RN to the mass of "isotopic carrier" present in the sample, i.e. in the SI units this quantity is given in Bq.kg^{-1}, or in most practical cases GBq·µg^{-1}. With the term "isotopic carrier", we mean the total amount of both stable and radioactive atoms of same Z present in the sample. A_S must not be confused with the "activity concentration" C_A, that is the activity of a stated RN to the mass or (volume) of substrate where the RN is diluted in; in the SI, C_A has the same units of A_S. The A_S of a RN, if no other RNs of the same Z are present, is named Carrier Free, A_S (CF). This quantity is an *intensive parameter* that depends on the physical properties of RN only, in accordance to the definition: $A_S(CF) = N_{Av}\cdot\lambda\cdot M^{-1}$ where: N_{Av} is the Avogadro's constant and M is the atomic mass of the RN. This parameter is a physical constant, not depending on either decay time or chemical or physical environment. The higher is M the lower is A_S(CF); conversely, the shorter is the half-life of the RN, the higher is A_S. Actually, the atomic mass of different RNs of Periodic Table from medium to high Z varies of less of one order of magnitude, while the half-life is the parameter that determines the order of magnitude of A_S(CF). In practice, the Carrier Free condition can be achieved in a few selected cases.

It is useful to derive a further non-dimensional quantity (always > 1), the Isotopic Dilution Factor (IDF), defined as: IDF = (mass of isotopic carrier)/(mass of RN) = $A_S(CF)\cdot A_S^{-1}$. In order to optimize radionuclidic purity increasing at the same time A_S of light ion produced radionuclides, two main approaches must be considered. A. An accurate knowledge of "experimental" excitation functions of nuclear reactions involved, as a function of projectile energy, as well as the knowledge of the excitation functions of both "stable" and radioactive nuclides produced by side reactions, that are isotopic with the RN of interest; B. the optimization of very selective radiochemical separations of radionuclide produced, without "intentional" addition of either isotopic or even isomorphous/iso-dimorphous carrier. The radionuclides and labeled compounds obtained in this way are named No Carrier Added (NCA). Figure 1 reports the different definitions of A_S. Even without "intentional" addition of "isotopic carrier", the contamination by isotopic carrier is unavoidable and it is due to chemical impurities present in both target materials, target holders, chemicals used during radiochemical processing and even by contact of a HSARN with the polluted environment. Whenever the radiotrac-

REFERENCES
1. Bonardi M., Groppi F., and Mainardi H.S., "High Specific Activity Radioactive Tracers: a powerful tool for studying very Low Level and Long Term Exposure to different Chemical Forms of both Essential and Toxic Elements", *Microchemical Journal*, 73 (2002) 153.
2. Menapace E., Birattari C., Bonardi M.L., and Groppi F., "Experimental results and model calculation of excitation functions relevant to the production of specific radioisotopes for metabolic radiotherapy and for PET", *Radiation Physics and Chemistry*, 71 (2004) 493.
3. Bonardi M.L., Groppi F., Mainardi H.S., Kokhanyuk V.M., Lapshina E.V., Mebel M.V., and Zhuikov B.L., "Cross section studies on Cu-64 with zinc target in the proton energy range from 141 down to 31 MeV", *Journal of Radioanaytical Nucear Chemistry*, 264 (2005) 101.

er is used to label any chemical compound or radiopharmaceutical, the "isotopic carrier" is easily introduced into the sample by the labeling procedure. Finally, if in order to administer a radiopharmaceutical or labeled compound, use is made of a physiological medium or metallic injection needles, the sample is contaminated in principle by any element present in the Periodic Table, excluded a few "artificial" ones. A complete scheme showing the different steps that must be followed for reaching these results and achieve very high purity radionuclides and labeled compounds is reported in Fig. 2. In Fig. 3 are reported the main uses of HSARNs.

Fig. 1
Different definitions of specific activity S_A(NCA) for radionuclides and labeled compounds. The concept of isotopic dilution factor IDF is related to the definition of S_A(t), while the activity concentration C_A(t) has a completely different meaning.

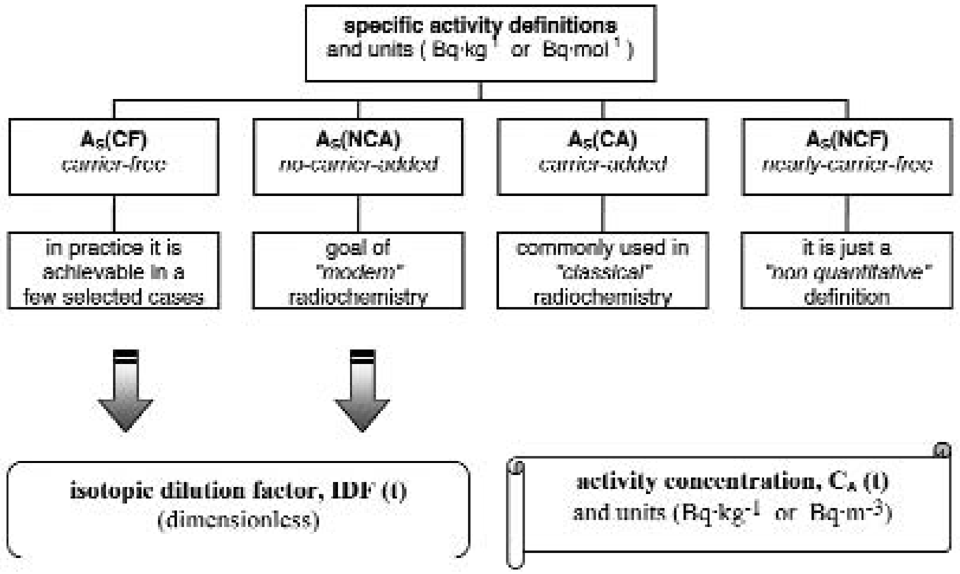

Fig. 2
Mains steps in cyclotron and nuclear reactor production of HSARNs and labelled compounds. Collaboration with international organisations is mandatory: IAEA, International Atomic Energy Agency, Nuclear Data Section, NDS, Vienna, Austria and ANS, American Nuclear Society, La Grange Park, Illinois, USA.

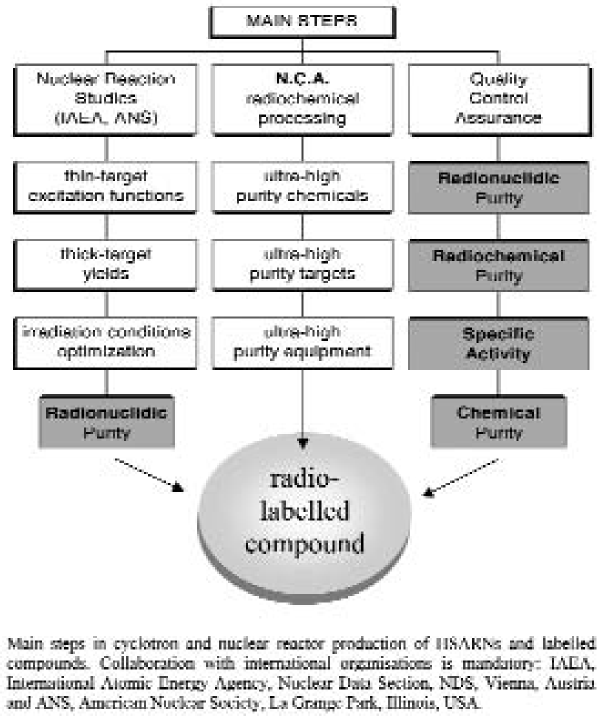

Fig. 3
Main modern applications of High Specific Activity Radionuclides in No Carrier Added form.

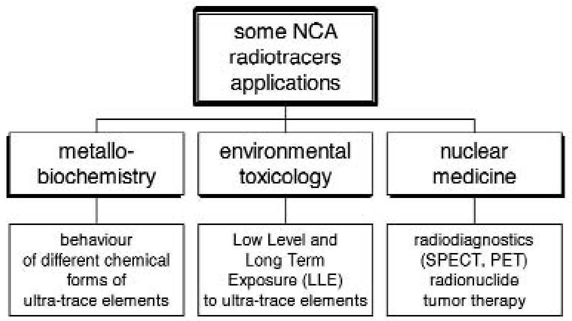

Experimental activity

Since the beginning of the 70's, a large range of HSARNs, have been produced at former Cyclotron Laboratory of the UNIMI. Several nuclear data for radionuclide production, measured in our Laboratory, are presently recommended by the Nuclear Data Section of IAEA, Vienna. More recently, use is made of the Cyclotron of JRC-Ispra, and the research Nuclear Reactor of the University and CNR of Pavia. Several International institutions are involved (Canada, Hungary, Israel, Russia, USA).

The Isotopic Carrier has two origins:

1. it is introduced into the sample by isotopic impurities present in both target materials, environment and chemicals used for radiochemical processing of the RN;
2. it is produced by side nuclear reactions and decay chains leading to both stable and radioactive isotopes of the same element (same compound). Thus, the nuclear reaction route and radiochemical processing procedure chosen are fundamental steps to gain HSARNs.

Reagents and chemical equipment

High purity water of Type I was produced with Millipore equipment supplied with deionised water obtained from a mixed-bed twin ion-exchange column. A total oxidable carbon (TOC) value of 10 ppb is achieved. All equipment are made by Teflon-PFA, for operations at temperature up to 200 °C. At higher temperature use is made of quartz-ware of nuclear grade. All the acids and organic chemicals are analysed for metal impurities by graphite-furnace atomic absorption spectrometry (GF-AAS), inductively coupled plasma optical-emission spectrometry (ICP-OES), instrumental neutron activation analysis (INAA) and by high-resolution γ spectrometry. Concentrated metal standard solutions are diluted as required for the standard additions and for method evaluation, by both GF-AAS, ICP-OES and INAA. All ion exchange resins used are of analytical grade purity. Suitable portions of resins are preconditioned by swelling either in high purity water, buffer or acidic solution and then filled into polypropylene columns and repeatedly washed, up to reach a constant pH value of the eluate. For some chemical separation and quality control, use is made of inorganic ion exchangers. All chromatographic fractions are collected in disposable plastic vials for both γ and β spectrometry.

Nuclear data traceability and isotope nomenclature

All nuclear data are treated in accordance with the IAEA recommendations. Whenever it is possible, the official IUPAC nomenclature and the SI are adopted.

Instrumentation

Nuclear activations are carried out at the compact cyclotron of JRC-Ispra of EC, as well as at the TRIGA thermal nuclear reactor of University and CNR Pavia. The accelerator (K=38) gains proton and alpha beams, with energy variable up to 38 MeV, as well as deuteron beams of energy up to 19 MeV. The nuclear reactor is a 250 kW research reactor, with 30 % enriched ^{235}U fuel rods. A thermal nuclear flux density varying from 10^{16} to 9 10^{16} $n{\cdot}m^{-2}{\cdot}s^{-1}$ is used in different cases (INAA and isotope production). The epithermal component of neutron spectrum was experimentally measured by Cd shielding and is less than 10%.

High-resolution gamma spectrometry is performed by four 50 cm^3 coaxial HPGe detectors, with intrinsic efficiency of 15%, with a peak to Compton ratio of 30 to 1 at 1 333 keV, FWHM 2.3 keV, connected to spectroscopy amplifiers and A/D 2 x 4096 MCAs. The spectroscopy amplifiers are set to gain a channel/energy conversion factor 2:1. Gamma spectra in the energy range up to 2 000 keV were acquired and analyzed by advanced s/w packages. The efficiency data, obtained by certified point sources of ^{152}Eu, ^{226}Ra and ^{133}Ba, are fitted by advanced s/w packages.

Beta spectrometry by liquid scintillation counting (LSC), is performed by a 1k MCA Liquid Scintillation Counter, with: three energy window, random coincidence monitor and Horrocks Number quenching correction capabilities. Large activities were measured by a well type ionisation chamber dose calibrator.

Metal determinations are performed with GF-AAS, ICP-OES, for most elements. Moreover, for some particular metals we use INAA, even if this technique could determine at least 35 trace elements simultaneously. Some irradiated targets are mineralized by a microwave digestion system. Some trace metal determinations are performed by anodic and cathodic stripping voltammetry too. For most elements an inter-comparison between the different analytical techniques is carrier out.

Specific activity determination

In most cases, in order to determine the experimental value of NCA Specific Activity, we use radiometric techniques, like γ and β spectrometry hyphenated with elemental analysis techniques, like GF-AAS, ICP-OES, NAA and ASV.

Nuclear reaction choice, energy threshold, Coulomb barriers

The choice of more suitable nuclear reaction for production of each specific RN is based on a preliminary study. Q values, energy thresholds for a charged particle on a target and Incoming particle Coulomb Barrier are calculated by the mass defects with kinematics in the laboratory system.

In a few selected cases, use is made of neutron-induced nuclear reactions in thermal nuclear reactor. This method leads to HSARNs only when the RN produced decays on the RN of interest by negatron decay: in this case the RN can be radiochemically separated from irradiated target. Otherwise, NAA is used for elemental chemical analysis of RN produced.

Conclusions

Medium energy cyclotron and sometimes nuclear reactors, allow production of HSARNs for biomedical, environmental, toxicological and occupational studies about long-term exposure to low doses of ultra-trace elements present in the ecosystems. Specific activities of the order of $GBq \cdot \mu g^{-1}$ are achieved, so the experiments can be carried out in the sub-nanogram concentration range.

HPGe γ spectrometry, allows both qualitative and quantitative analytical and radioanalytical investigations on activated targets and radiochemical fractions. Conversely, β spectrometry by LSC is intrinsically characterised by low-resolution capability, due to continuous spectra of beta emitters, but presents a very high counting sensitivity. After the End Of Chemical Processing of target itself, β spectrometry can be used effectively to follow either β or electron decay of pure RN. Elemental analysis techniques like AAS, ICP-OES, INAA, RNAA, ASV, allow the determination of No Carrier Added Specific Activity and the chemical purity of the radiotracer itself. As expected, the real specific activity is lower than the theoretical carrier free one; nevertheless, in most cases, the NCA HSARNs obtained are suitable for purposes envisaged. The use of extra-pure chemicals, targets and equipment allows reaching IDF values in the range from some tens to a few hundreds in some selected cases. Much lower IDF values were obtained with very rare elements.

A method for 3D imaging of absorbed dose in conformal radiotherapy

1 Dipartimento di Fisica, Università degli Studi di Milano
2 INFN

M. Carrara[1], G. Gambarini [1,2], S. Gay[1,2], L. Pirola[1], and M. Valente[1,2]

1. Introduction

In the last decade, technological radiotherapy (RT) improvements have been significant and consequently the use and importance of RT in cancer treatment have greatly increased. A fundamental advance has been the development of external beam techniques aimed at dose deliveries that are highly localised on the tumour volume, sparing at the same time most of the surrounding healthy tissues. These techniques include conformal RT as well as intensity modulated RT (IMRT). However, these methodological improvements require corresponding improvements in the dosimetry methods, in order to ensure that the values calculated with computer treatment planning systems (TPS), adopted in the clinical praxis, agree with the delivered dose distributions. Considering that traditional dosimeters are not well suited to this task, an alternative technique for 3D rendering of in-phantom absorbed dose has been studied and set up.

2. Materials and Methods

In a tissue-equivalent gel matrix, a ferrous sulphate solution and the metal-ion indicator Xylenol Orange (XO) are infused to assess the chemical continuum dosimeter (*gel-dosimeter*). Ionising radiation causes a conversion of ferrous ions Fe^{2+} into ferric ions Fe^{3+}. The complex of XO with Fe^{3+} produces visible light absorption around 585nm, with yield proportional to the absorbed dose. For the analysis, gel dosimeters are placed on a plane light source and transmittance images at 585nm are detected with a CCD camera, before and after their irradiation. Suitable software has been developed, able to carry out all the manipulations necessary to get the interactive rendering of dose profiles, surfaces and volumes, as well as of the isodose curves, starting from a set of acquired transmittance images.

3. Results

After having optimised the protocol for dosimeter preparation and the modality of detecting and manipulating optical images, the method's reliability has been verified. The obtained dose distributions have been compared with those measured by means of a cylindrical ionisation chamber or calculated with Monte Carlo simulations, adopting field geometries in which the last are reliable. After having assured reliability, many experimental configurations in conformal radiotherapy have been verified. As an example, following are reported isodose curves (Fig. 1) and 3D isodose distributions (Fig. 2) obtained in a special configuration of arc therapy. As a qualitative comparison, treatment planning system (TPS) (Prowess 3D) calculations are reported in Fig. 1, as well.

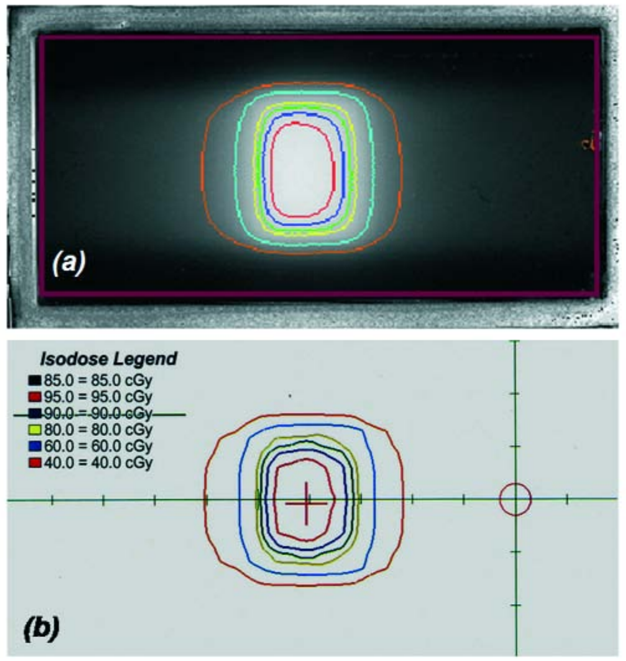

Fig. 1
Relative isodose curves obtained with a single gel-layer (a) and TPS (b) (95% red, 90% blue, 85% green, 80% yellow, 60% light blue, 40% orange)

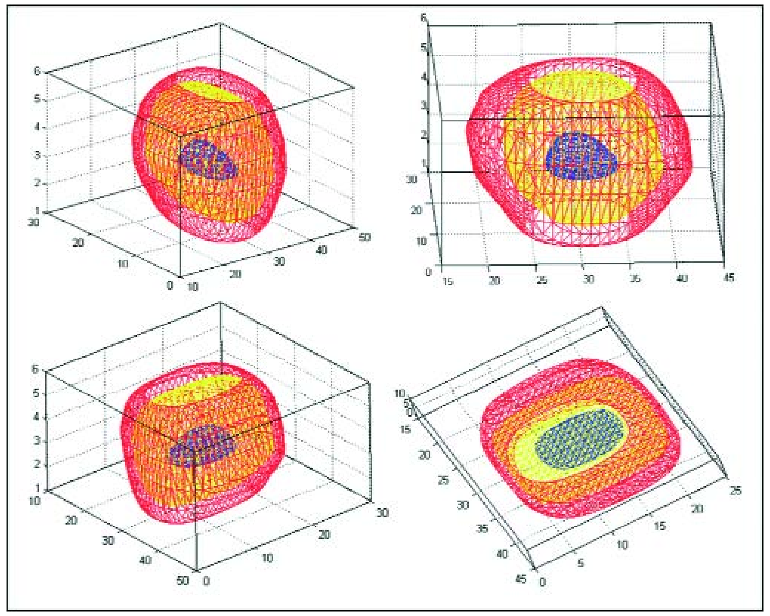

Fig. 2
3D distribution of relative isodoses
(95% blue, 80% yellow, 40% red)

4. Conclusions

The proposed method allows 3D imaging of absorbed dose with high reliability and good spatial resolution.

Development of biokinetic and dosimetric models for incorporation of radionuclides

1 Dipartimento di Fisica, Università degli Studi di Milano and INFN

A. Giussani[1], I. Veronese[1], and M.C. Cantone[1]

The assessment of the internal dose after incorporation of radioactive material requires reliable knowledge of its biokinetics in the human body. The International Commission of Radiological Protection (ICRP) presents, in its Publications, a selection of compartmental models describing absorption into the systemic circulation, transfer between organs and tissues, and excretion for a number of radionuclides and of radioactive compounds. For many substances of radiological relevance, however, lack of sufficiently robust experimental evidence prevents from defining detailed models with specifically determined parameter values. Consequently, the derived dosimetric estimates are of questionable value.

Recent studies with stable tracers conducted by our group have permitted to collect new experimental evidence regarding the biokinetics of elements of radiological relevance. Compartmental analysis approach has been used for interpreting the new pieces of information. In particular, the biokinetic model for radionuclides of molybdenum has been revised on the basis of data collected in a total of more than 50 investigations, and the consequences of this revision on the internal dose estimates have been evaluated [1-5].

Figure 1 shows the structure of the revised model; the new or revised features are indicated in green. Different sets of parameters are recommended in dependence of the chemical form of administration. Non linear kinetics had to be introduced in order to describe the variation of the observed features with mass and modality of administration.

Fig.1
Structure of the revised model for molybdenum

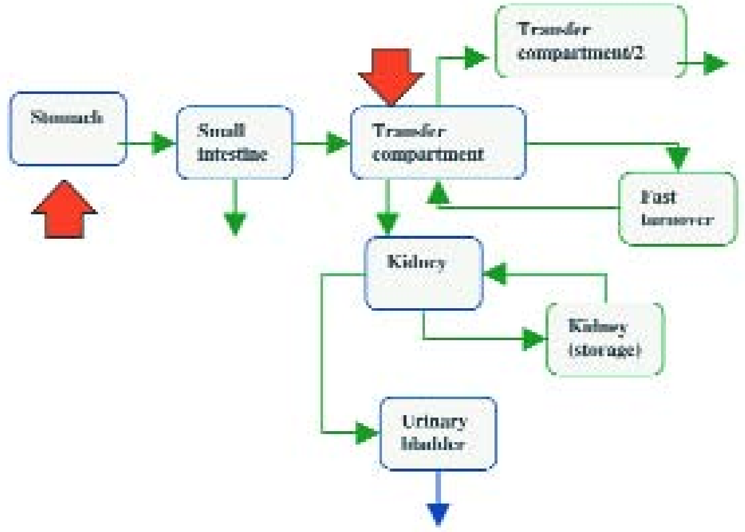

Figure 2 shows typical time patterns of the oral tracer, administered in two different forms to the same volunteer and the predictions of the revised model, obtained using specific parameters.

The revised model has also been used for the interpretation of bioassay data from a series of workers who were accidentally exposed to an aerosol containing ^{99}Mo and ^{99m}Tc [6]. Data from experiments with stable tracers have also been used for the validation of the models for radionuclides of ruthenium and zirconium.

Similarly, the compartmental analysis approach was used for the definition of specific pharmacokinetic models for radiopharmaceuticals employed in therapeutic nuclear medicine [7], specifically for ^{131}I as used in the treatment of patients with autonomous functioning thyroid nodule ([8], study conducted in association with Ospedale Maggiore Policlinico, Milano) and for ^{186}Re-HEDP employed for the pain palliation in patients with bone metastases ([9], study conducted in association with Ospedali Riuniti di Bergamo).

REFERENCES
1. Giussani A. et al.: “A biokinetic model for molybdenum radionuclides: new experimental results” *Radiat. Prot. Dosim.* 79**,** 367-70 (1998).
2. Giussani A. et al.: “A revised model of molybdenum biokinetics in humans for application in radiation protection” *Health Phys.* 75, 479-86 (1998).
3. Giussani A., et al.: “Dosimetry after ingestion of ^{99}Mo radionuclides”. *IV Congreso de Protección Radiológica de Países Europeos del Mediterráneo Occidental*, Barcelona, 27-29 May 1998.
4. Giussani A. et al.: “Internal dose for ingestion of molybdenum radionuclides based on a revised biokinetic model” *Health Phys.*, 78, 46 (2000)
5. Luciani A., et al.: “Sensitivity analysis techniques applied to a revised model of molybdenum biokinetics” *Radiat. Prot. Dosim.* 105, 239 (2003)

Fig. 2
Typical time patterns of the oral tracer and predictions of the revised model.

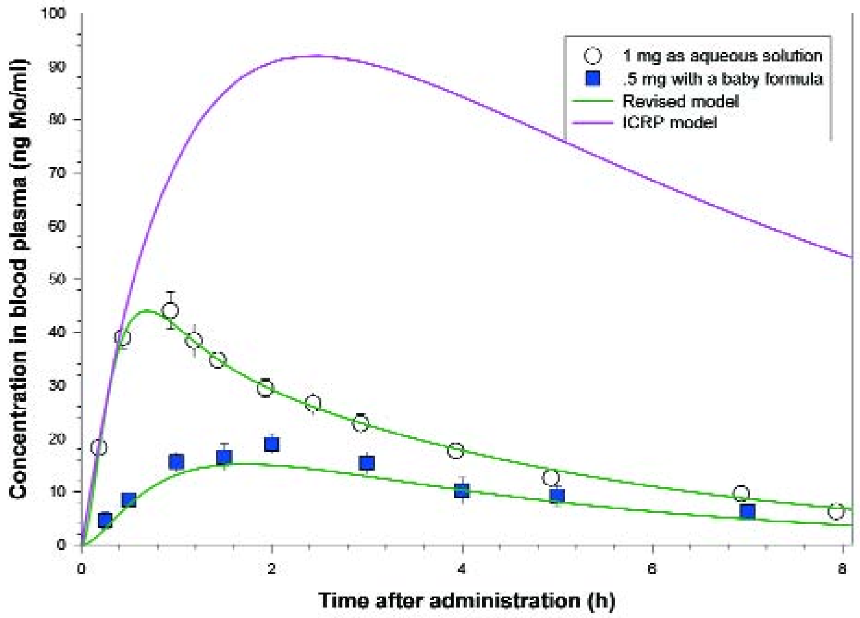

REFERENCES

6. Giussani A. et al.: “Validation of the revised model for the biokinetics of molybdenum with data from a real accidental case” 11th *International Congress of IRPA*, Madrid, 23-28 May 2004.

7. Giussani A. et al.: “Biokinetic assumptions and internal dose estimation in nuclear medicine” 10th *International Congress of the International Radiation Protection Association IRPA-10*, Hiroshima, 14-19 May 2000.

8. Giussani A. et al.: “A compartmental model of the biokinetics of radioiodine in patients suffering from the autonomous thyroid nodule (ATN) syndrome” *European Association of Nuclear Medicine Annual Congress*, Amsterdam, 23-27 August 2003.

9. Giussani A. et al.: “Modelling rhenium distribution and excretion after administration of [^{186}Re]-HEDP for bone pain palliation” *Workshop on Internal Dosimetry of Radionuclides*, Oxford, 9-12 September 2002.

The thermoluminescence peaks of quartz at intermediate temperatures and their use in dating and dose reconstruction

I. Veronese[1], A. Giussani[1], and M.C. Cantone[1]

1 Dipartimento di Fisica, Università degli Studi di Milano and INFN

Introduction

Among the luminescence materials, quartz is one of the most investigated specimens. Generally three main regions can be distinguished in the glow curve: the first consists in only one peak at low temperature, known as “110°C” peak. It was investigated by several authors because of its peculiarity of changing the sensitivity following thermal activation. A second region occurs at temperature higher than 300°C. The glow peaks of this region are known to be thermally stable and are mostly used in TL dating of archaeological manufactures [1]. Between these two regions, quartz exhibits other TL peaks. The sensitivity of these peaks is higher than those occurring at higher temperature, and therefore they are very promising in the assessment of relatively low dose values using samples of recent manufacture. Nevertheless, their employment for dose reconstruction applications requires prior investigations of their luminescent and dosimetric properties, as well as the assessment of the minimum anthropogenic dose detectable using these peaks [2, 3].

The TL peaks of quartz at intermediate temperatures

Figure 1 shows the spectral emission of pure quartz in the temperature range of interest measured using a high sensitive TL spectrometer [4]. Two main peaks (peak I and peak II) occur at temperature of 135°C and 185°C (heating rate 1°C/s) respectively. For both of them the emission band is centred at approximately 380 nm, suggesting the presence of a common recombination centre. The trap parameters of peak I and II were estimated using two different methods of analysis: peak shift (PS) and isothermal decay (ID) [5]. Some results of these analyses are summarised in Table 1.

Fig. 1
Spectral emission of pure quartz (3D vision and contour plot)

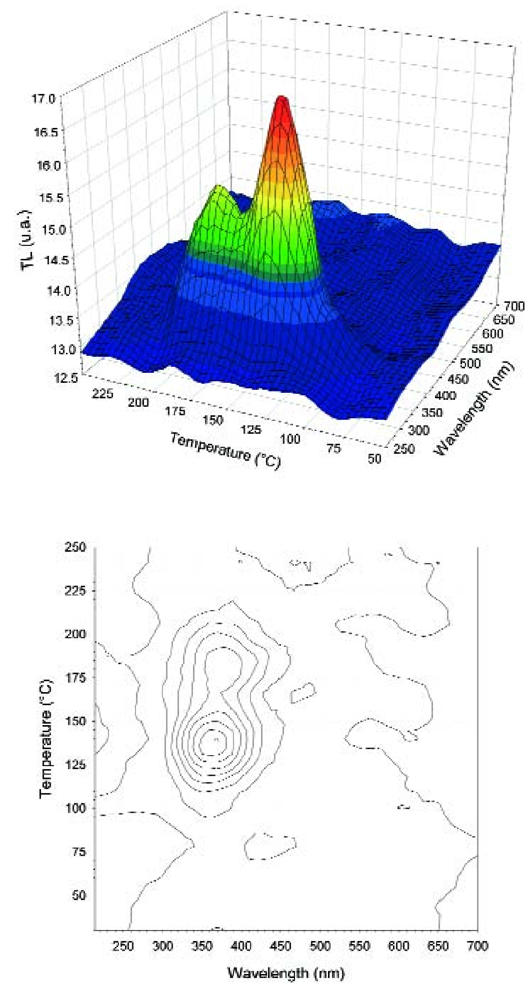

REFERENCES

1. Aitken M.J., *Thermoluminescence dating.* Academic Press, 1985

2. Veronese I., Giussani A., Göksu, H.Y., Martini M., *The trap parameters of electrons in intermediate energy levels in quartz.* Radiat. Meas. 38, 743-6, 2004

3. Veronese I., Giussani A., Göksu, H.Y., Martini M., *Isothermal decay studies of intermediate energy levels in quartz.* Radiat. Environ. Biophys. 43, 51-7, 2004

4. Martini M., Paravisi S. and Liguori C., *A new high sensitivity spectrometer for 3-D thermoluminescence analysis.* Radiat. Prot. Dosim. 66, 447-50, 1996

5. Chen R. and McKeever S.W.S., *Therory of Thermoluminescence and Related Phenomena.* World Scientific, 1997

Limits of thermoluminescence dosimetry

In thermoluminescence dosimetry, the accidental dose Dx can be assessed as the difference between the total accrued dose D_{TL} and the dose due to the natural sources of radiation (alpha, beta, gamma and cosmic rays) absorbed by the sample during its age A:

$$D_x = D_{TL} - A\cdot(N_\alpha + N_\beta + N_\gamma + N_C)$$

Accurate measurements of the terms contributing to Dx and of the uncertainties related to each of them were performed using quartz extracted from one brick and two tiles (50-80 years range) collected from an urban settlement. Independent methods like alpha-counting, beta dosimetry, gamma spectrometry and flame photometry were used for the annual dose assessment. Two approaches were employed for the evaluation of the total accrued dose: regenerative dose and additive dose [1]. The former enables to assess accidental doses as low as approximately 12 mGy by using 10 year old samples, but it can be applied only when sample sensitisation does not occur. The latter can be applied to any sample, however the related uncertainty is higher and minimum detectable anthropogenic dose in young samples amounts to 20 mGy [6].

Table 1
The trap parameters of peak I and II

Peak	Activation energy (eV)	Frequency factor (s^{-1})	Lifetime (at 15°C)	Method of analysis
I	1.13±0.03	$(3.35\pm2.99)\cdot10^{12}$	-	PS
I	1.22±0.02	$(3.39\pm1.46)\cdot10^{13}$	720±70 d	ID
II	1.46±0.06	$(7.79\pm10.91)\cdot10^{14}$	-	PS
II	1.36±0.02	$(2.23\pm0.75)\cdot10^{13}$	580±70 y	ID

REFERENCES
6. Veronese I., Giussani A., Göksu, H.Y., *Limits of thermoluminescence dosimetry using quartz extracted from recent building materials in urban settlements.* J. Env. Rad. 84, 319-39, 2006

History of Science and Physics Education

Difficoltà pluridecennali nei rapporti tra ricerca e politica

E. Bellone[1]

1 Dipartimento di Fisica, Università degli Studi di Milano

Non è trascorso molto tempo da quando Antonio Ruberti ricordava al paese, e non solo agli scienziati, la tenacia con cui, per decenni, una parte cospicua della politica aveva frainteso il valore della libera ricerca fondamentale. Ruberti aveva effettivamente vissuto nella cornice delle difficoltà causate da quel fraintendimento, sia nella sua qualità di Rettore della "Sapienza" di Roma, sia come ministro, sia nelle sue funzioni in incarichi europei. A suo avviso, la difficoltà più robusta stava nella popolarità del punto di vista secondo cui la scienza non è cultura vera e propria, ma è una forma della tecnica da valutare in termini di utilità o dannosità. Nella cultura diffusa nel paese questa svalutazione della scienza suscitava consensi, e molti responsabili in sede politica agivano appunto in tale sfera consensuale.

Ancora oggi è abbastanza popolare il punto di vista secondo cui la scienza non è cultura: la ricerca di base sarebbe allora da intendere come una mera tecnica. Ma le forme della tecnica possono generare anche cose pericolose. La libertà di espressione, che in genere si concede ai prodotti della cultura, non deve invece essere concessa a pratiche tecniche che sono potenzialmente dannose, e che debbono quindi essere soggette a controlli esterni alla comunità scientifica.

Questo atteggiamento non è alimentato da idee nuove o originali, ma da opinioni che risalgono ad epoche lontane. Le troviamo, per esempio, nelle pagine del "Dialogo" di Galilei. Ne è portavoce il filosofo Simplicio, il quale diffida delle dimostrazioni scientifiche ed esalta invece il sapere dei saggi, i quali si occupano solo di ciò che è "universale". Una persona veramente colta, quindi, lascia certe sottigliezze e certi "tritumi", che sarebbero soltanto da classificare sotto la voce "curiosità", ai matematici e ai vili meccanici.

Va tuttavia notato che il punto di vista di Simplicio è, nelle pagine galileiane, messo alla berlina: oggi, invece, sembra essere maggioritario, soprattutto fra coloro – intellettuali e politici – che riducono la scienza a mera *techne*. Se si accetta questa riduzione, allora si ammette anche che la tecnica può produrre forme *pratiche* di benessere o forme *pratiche* di danni.

Se così stanno le cose, allora va fatto quel passo ulteriore di cui già ho fatto cenno: controllare, dall'esterno della comunità scientifica, gli sviluppi della ricerca, così da impedire evoluzioni pericolose.

Essendo così impostato il problema, si tratta di trovarne qualche giustificazione. Un compito abbastanza facile, questo: basta pescare nelle acque delle ideologie. Se la scienza può essere una serva delle multinazionali, allora la libertà di ricerca va soppesata, caso per caso, in sede politica. Se la scienza può deturpare l'ambiente, allora la scienza libera è una utopia da demolire in sede politica e giuridica. Se la scienza può costituire un attentato allo spirito o alla dignità della persona, allora la libera ricerca deve sottostare a leggi che ne limitino la crescita.

Nei regimi democratici, operazioni di tale natura hanno ovviamente bisogno del consenso popolare. E una via maestra per formare il consenso è ben nota e ben praticata. È sufficiente diffondere tra i cittadini la paura.

Chi decide, però, quali siano i rischi che sarebbero connessi alla ricerca libera, e quali siano le leggi di controllo? Negli anni galileiani, per esempio, il rischio era stato individuato nel modello copernicano, e le leggi di controllo avevano stabilito sia la falsità del modello stesso, sia la necessità di impedire, anche con metodi spicci, le ricerche di un Giordano Bruno o di un Galileo Galilei.

Dobbiamo allora chiederci, con la necessaria franchezza, se quei metodi sono stati definitivamente respinti. La mia risposta è negativa.

Agli inizi degli anni Sessanta, in Italia, era in discussione la necessità di dotare il paese di centrali elettronucleari, così da liberare la nostra economia dalla dipendenza dalle fonti fossili e, in particolare, dal petrolio. Una discussione anche aspra, soprattutto perché la questione vera poggiava, ovviamente, su interessi economici enormi. Specifiche istituzioni politiche e specifici mezzi di informazione di massa seppero costruire il consenso attorno all'idea di bloccare la costruzione di impianti elettronucleari, presentandoli come dannosi per l'economia nazionale e pericolosi per la salute dei cittadini. E, nello stesso tempo, si ricorse a metodi decisamente spicci nei confronti di chi invece difendeva la necessità di innovare le nostre capacità energetiche: Enrico Mattei fu assassinato sul finire del 1961, e contro Felice Ippolito fu emessa, pochi mesi dopo, una sentenza di condanna a undici anni di galera.

Fatti da ricordare. Anche perché il rigetto delle centrali non fu il risultato di un referendum successivo al disastro di Chernobyl, ma l'esito di ciò che fu fatto accadere all'inizio degli anni Sessanta.

Ci si potrebbe a questo punto chiedere come mai la negazione della libera scienza abbia, nel nostro paese, un peso così rilevante nei rapporti tra politica e ricerca. La domanda è legittima: anche in Francia o in Inghilterra esistono resistenze alla modernizzazione e alla realizzazione di quella società della conoscenza che appunto si basa sulla forza della cultura scientifica, ma quelle resistenze non generano leggi contro le decine di impianti nucleari francesi o contro l'esplorazione in biologia molecolare e ingegneria genetica.

Il caso italiano è effettivamente un caso, nel senso che la paura verso la scienza ha da noi trovato un referente forte in molti intellettuali che hanno codificato la necessità di un rigetto della scienza come cultura.

Basti allora citare, per sommi capi, alcune fasi della battaglia culturale che fu condotta da un grande studioso come Benedetto Croce e che incise profondamente nelle opinioni maggiormente diffuse nella società civile. Nel 1911 Croce sconfisse, in un dibattito aspro, il tentativo che il matematico Federigo Enriquez stava elaborando per presentare la scienza come intrisa di valori culturali. La tesi crociana fu assai semplice. Essa sosteneva che solo le menti profonde o universali possono accedere alla cultura, essendo quest'ultima centrata su grandi questioni di metafisica o storia. Ma l'umanità conteneva anche menti "minute": a queste ultime era allora concesso di interessarsi di botanica o aritmetica. L'ironia e il sarcasmo si mescolavano così al disprezzo per quelle attività che già erano state bollate dal Simplicio di galileiana memoria. La miscela, nel 1911, vinse.

Parole ancora più severe furono usate da Croce, nel 1939, per liquidare le ricerche biologiche che si rifacevano al modello elaborato da Charles Darwin. Quelle ricerche, a parere del filosofo, suggerivano l'esistenza di "origini animalesche e meccaniche dell'umanità", e dovevano pertanto essere respinte poiché suscitavano solo "vergogna". Esse, infatti, negavano la presenza di una "favilla divina" nell'essere umano. Più tardi, in scritti che esercitarono una spiccata influenza in molti altri studiosi di vario orientamento filosofico e politico, Croce liquidò l'intero scenario scientifico, negandogli totalmente una qualsiasi rilevanza nel mondo dei valori e lasciandogli soltanto l'etichetta secondo cui una scienza è un elenco di ricette pratiche.

Dall'interno della comunità scientifica furono poche le voci che si alzarono per contrastare questa critica radicale di Croce, che si traduceva in banalizzazioni popolari di ampio successo sia nei mezzi di comunicazione di massa, sia nei programmi del sistema educativo nazionale.

Una maggioranza di scienziati ritenne opportuno fingere di poter vivere in qualche torre d'avorio. Una minoranza, invece, tentò di replicare, ma fu sconfitta con argomenti non diversi da quelli che già avevano bloccato il progetto di Enriquez. Non a caso spettò a un filosofo come Banfi, che davvero tentava di capire l'evoluzione della scienza , il compito di esprimere un giudizio decisamente negativo su quanto la filosofia italiana aveva fatto contro la cultura scientifica. Attorno alla metà del Novecento, infatti, Banfi scrisse con amarezza che gli scienziati italiani furono messi a tacere con gli strumenti della "ciarlataneria filosofica".

Un caso italiano, dunque, e solo italiano. Mentre il filosofo Banfi constatava il rigetto culturale della scienza in Italia, negli Stati Uniti il filosofo Schilpp curava un volume che nel

1949 sarebbe stato stampato con il titolo “Albert Einstein: Philosopher-Scientist”. Il volume era una raccolta di saggi, appositamente scritti da scienziati e da filosofi, che mettevano in luce, sotto angolature diverse, il grandioso impatto culturale del pensiero einsteniano.

Che fare, allora? Personalmente ritengo che sia accettabile l’opinione di uno storico della cultura come Paolo Rossi, secondo il quale una persona è colta se, oltre ad apprezzare Shakespeare, sa anche cogliere il significato di una legge fisica.

C’è molto da fare, qualora si accetti davvero questa regola. E, soprattutto per i giovani, c’è da rivendicare con orgoglio l’eredità di Galilei ed Einstein. Galilei pretendeva per sé il titolo di filosofo, ed Einstein amava dire che la scienza senza filosofia è arida, e che la filosofia senza scienza è vuota. La ricerca di base è cultura in quanto è guidata dalla curiosità, e la curiosità per i fenomeni osservabili è la matrice non della tecnica, ma di quella che in età galileiana si chiamava “filosofia naturale”, e che oggi può prosperare solo nella libertà.

Environmental Physics

The role of Ion Beam Analysis in environmental studies

R. Vecchi[1], G. Marcazzan[1], G. Valli[1], F. Lucarelli[2], S. Nava[2], M. Chiari[2], P. Prati[3], A. D'Alessandro[3], and F. Mazzei[3]

1 Istituto di Fisica Generale Applicata, Università degli Studi di Milano& INFN-Milano
2 Dipartimento di Fisica, Università di Firenze & INFN-Firenze
3 Dipartimento di Fisica, Università di Genova e &INFN-Genova

Ion Beam Analyses (IBA) – such as PIXE (Particle Induced X-ray Emission), PIGE (Particle Induced Gamma-ray Emission) and PESA (Particle Elastic Scattering Analysis) – have been applied to many different fields due to their high sensitivity, multi-elemental capabilities and non-destructive character. One of the many research fields that made use of IBA as an analytical technique was related to environmental studies, and in particular to atmospheric aerosols. Atmospheric aerosols play an important role in the physics of the atmosphere; they act as clouds condensation nuclei, are responsible for visibility reduction, contribute to global change and carry on a number of toxic metals inducing adverse health effects. Moreover, atmospheric particles contribute to the damage of cultural heritage.

In the frame of the aerosol research, the most interesting property of PIXE is that it provides quantitative analysis of elements which are markers for specific components or sources of particulate matter such as marine aerosol (Na, Cl), mineral dust (Al, Si, Ca, Ti, Sr), sulphates (S), biomass burning products or biogenic emissions (K, Zn, Rb), heavy oil combustion (V, Ni), incinerator emissions (K, Zn, Pb), traffic and industrial emissions (Mn, Ni, Cu, Zn, Pb). The knowledge of suitable markers for each emission source is very helpful in the application of statistical multivariate analysis such as receptor models (PCA, APCA, PMF,…) that lead to the identification and quantification of the contribution due to different emission sources.

The complementary use of PIXE and other IBA techniques such as PESA (for the determination of H, C, N, O), PIGE (for light element analysis) as well as chemical analysis (for the speciation of carbon compounds and for the quantification of the ionic content) allow a complete aerosol characterization and the possibility of a mass closure [1]. A typical aerosol sample consists of a thin layer of particles deposited on a filter support, its total thickness ranges from a few hundreds of $\mu g/cm^2$ up to 1 mg/cm^2 and it can therefore be considered as a thin target for energetic proton beams of a few MeV.

The yields of X-rays, gamma-rays and scattered particles after a few minutes of irradiation by some tens of nA of 2-4 MeV protons are generally sufficient to provide elemental concentrations for almost all the elements of interest for atmospheric aerosol studies. PIXE and complementary ion beam analytical techniques were implemented in the past by the authors for atmospheric aerosol studies at the INFN external beam facility in Florence, based on a KN3000 Van de Graaf accelerator [2] and, recently, at the new INFN-LABEC facility based on a Tandetron accelerator. PIXE analysis allowed the determination of elements with Z >10 which are generally detected in aerosol samples by routine analysis with Minimum Detection Limits (MDL) of the order of few (1–10) ng m^{-3} for most elements.

A problem with PIXE analysis is the X-ray self-absorption in the particulate matter deposit or in the single particle. The self-absorption effect influences especially the quantitative analysis of low atomic number elements (i.e. Na, Mg, Al, Si) and needs the introduction of correction factors generally calculated theoretically. Advantages of PIGE and PIXE contemporary application are – apart from the low Z elements detection to reach a complete mass balance – the possibility of determining experimentally the self-absorption correction factors which are essential to provide correct PIXE concentrations.

The application of PIXE/PIGE is mandatory when high-time resolution samples or size-segregated samples are of interest as they give the possibility of having an ion beam of reduced size and a good sensitivity also with small quantities of matter. High time-resolved and size-segregated samplings give insights into physical-chemical processes involving aerosols (production, transformation, transport, removal) and allow a direct comparison with gaseous pollutants and meteorological parameters, which are often monitored on an hourly basis. Time-series of hourly elemental concentrations have been obtained by our research group during previous monitoring campaigns at locations with different characteristics (urban, industrial,...) [3].

REFERENCES
1. Chiari M., Lucarelli F., Mazzei F., Nava S., Paperetti L., Prati P., Valli G. and R. Vecchi "Airborne particulate matter characterization in an industrial district near Florence, by PIXE and PESA". *X-Ray Spectrometry* 34, 323 (2005)
2. Del Carmine P., Lucarelli F., Mandò P.A., Moscheni G., Pecchioli A. and J.D. MacArthur. "PIXE measurement of air particulate elemental composition in the urban area of Florence, Italy". *Nuclear Instruments and Methods in Physics Research B* 45, 341 (1990)
3. D'Alessandro A., Lucarelli F., Mandò P.A., Marcazzan G., Nava S., Prati P., Valli G., Vecchi R., and A. Zucchiatti, "Hourly elemental composition and sources identification of fine and coarse PM10 particulate matter in four Italian towns", *Journal of Aerosol Science* 34, 243 (2003)

The experimental set-up for PIXE/PIGE analysis is shown in Fig. 1. Since X-ray production cross sections ranges over 3 order of magnitude, to obtain an efficient simultaneous detection of all the elements it is necessary to balance the counting rates of the different X-rays. The adopted solution is the use of a quite high beam current (5-15 nA) and two Si(Li) detectors (Si1 and Si2 in the Fig. 1), optimised respectively for low and medium-high X-ray energies. Moreover, helium gas flows into the volume in front of the detectors to reduce the possible attenuation of low energy X-rays by the air. A HPGe detector is used to collect the γ rays for PIGE analysis. For aerosol samples the total thickness (aerosol deposit + substrate) is small enough to let the beam pass through; as a consequence the charge can be measured simply integrating the beam charge on a graphite Faraday cup (FC) placed behind the sample.

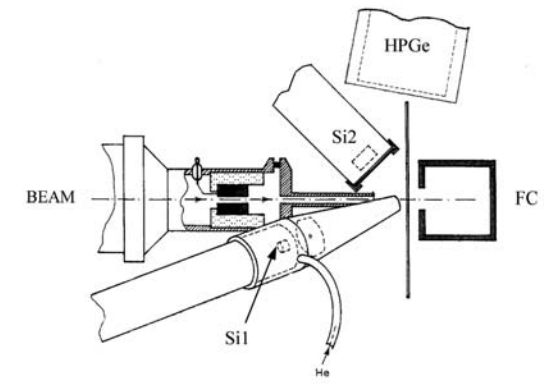

Fig. 1
KN3000 external PIXE-PIGE set-up at the INFN Van de Graaff accelerator of the INFN in Florence

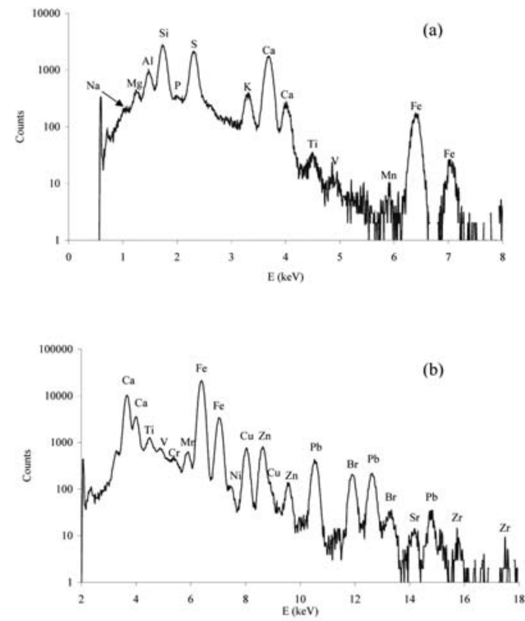

Fig. 2
PIXE spectra from a sample of aerosol, recorded simultaneously by Si1 (a) and Si2 (b).

A 2.990 MeV proton beam has been used so that the cross section for the Na(p;p'γ)Na (E = 440 keV) reaction, which is exploited for PIGE determination of Na [4], remains sufficiently constant even considering the moderate proton energy loss in the sample. Moreover, the beam energy is high enough to provide good sensitivity for PIXE. PIXE and PIGE analyses are now routinely and simultaneously performed by our group both on 1-hour resolution fine and coarse aerosol samples and on standard 24-h particulate matter deposits.

In order to allow a complete reconstruction of the aerosol mass, we implemented the light element (H, N, O and C) detection by means of in-vacuum Particle Elastic Scattering Analysis (PESA) with 3 MeV protons on particulate matter collected on Teflon filters. For the PESA measurements we used two fully depleted surface-barrier detectors arranged at forward and backward angles in a vacuum chamber. The detector used to measure the H content was placed at a scattering angle 30° while the other detector, used for the C, N and O concentration determination, was placed at 150° and the sample was placed in a vertical plane orthogonal to the beam. The beam current was integrated, after the sample, by a Faraday cup, kept at a positive voltage of about 70 V to avoid secondary electrons escape. [5]

Since mass resolution improves at higher beam energies, we selected the working ener-

REFERENCES
4. Boni, C., Caridi, A., Cereda, E. and G. M. Braga Marcazzan. A PIXE-PIGE setup for the analysis of thin samples. *Nuclear Instruments and Methods in Physics Research* B47, 133 (1990)
5. Chiari M, Del Carmine P., Lucarelli F., Marcazzan G., Nava S., Paperetti L., Prati P., Valli G., Vecchi R., and A. Zucchiatti, "Atmospheric aerosol characterisation by Ion Beam Analysis Techniques: recent improvements at the Van de Graaff laboratory in Florence", *Nuclear Instruments and Methods in Physics Research* B 219-220, 166 (2004)

gy in the highest proton energy range available at our Van de Graaff accelerator. To obtain quantitative results by direct comparison with thin standards, we worked at an energy of 3 MeV, where the proton elastic scattering cross sections on H, C, N and O are quite constant (better than 10%) over the range of proton energy loss in aerosol samples (≤ 100 keV). The calibration was achieved using a thin Upilex-S foil containing known areal density of H, C, N and O; the energy loss for 3 MeV protons in this foil is 120 keV. Preliminary test measurements were also carried out to identify the best aerosol filter for these analyses and Teflon membranes resulted to be the only substratum appropriate for PESA analysis. Using Teflon filters PIXE and PESA analyses are both possible on the same sample, but at the moment they are performed separately.

The coupling of the PIXE/PIGE and PESA techniques allows the 'mass closure', i.e. the measurement of the concentrations of all the elemental constituents of atmospheric aerosol. An example of their application for mass closure purposes, is shown in Fig. 4; it concerns a first aerosol characterisation of the atmospheric aerosol in the industrial area of Montelupo Fiorentino [1]. The assessment of the detailed elemental composition on a wide data-set allowed also the application of receptor models and led to the identification of main emission sources and their contribution.

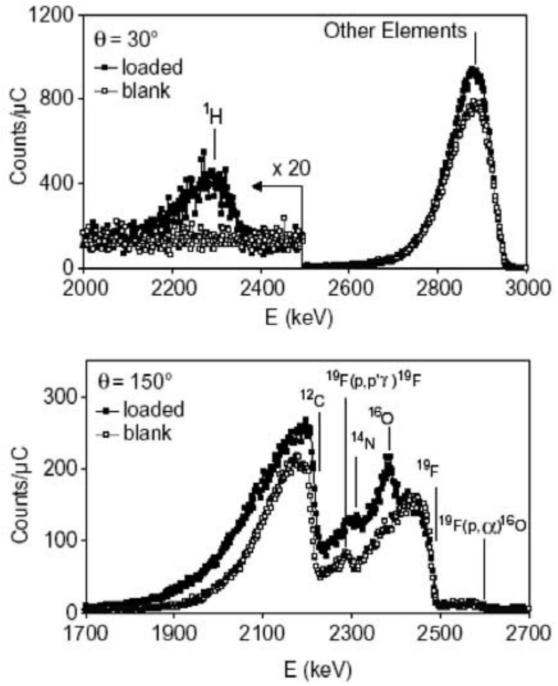

Fig. 3
Proton scattering spectra on blank and loaded Teflon filters, detected at an angle of 30° (above) and 150° (below).

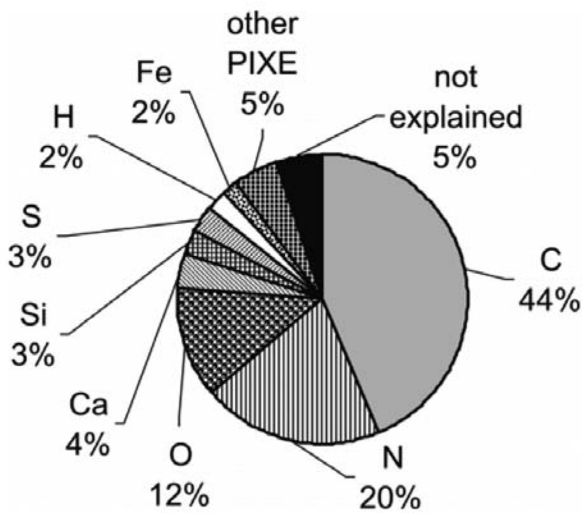

Fig. 4
Average contributions (in percentage) of the eight most abundant detected elements to the total PM10 mass.

Climate change and variability in Italy in the last two centuries

M. Brunetti[1], L. Buffoni[2], G. Lentini[3], F. Mangianti[4], M. Maugeri[3], F. Monti[3], T. Nanni[1], and R. Pastorelli[3]

1 ISAC-CNR - Via Gobetti 101, I-40129 Bologna, Italy
2 Osservatorio Astronomico di Brera Via Brera 28, I-20121 Milan, Italy
3 Istituto di Fisica Generale Applicata Via Brera 28, I-20121 Milan, Italy
4 Ufficio Centrale di Ecologia Agraria Via del Caravita 7A, I-00186 Rome, Italy

The Italian monthly temperature (mean, maximum and minimum) and precipitation secular data-set was updated and completely revised. Station density and metadata availability were greatly improved and the series were subjected to a detailed quality control and homogenisation procedure. The errors affecting original data were quantified by studying the temporal evolution of the mean adjustments applied to the series, and examined in the light of the station history. The results stress the importance of homogenisation in climate change studies. The final data set was clustered into climatically homogeneous regions by means of a Principal Component Analysis. Yearly and seasonal trend analysis were performed both on regional average series and on the mean Italian series (ITA). The results highlight a positive trend, for mean temperature, of about 1 K per century all over Italy: it is generally higher for minimum temperature than for the maximum one. The progressive application of trend analysis shows that this behavior is opposite in the last 50 years, the maximum temperature trend being stronger than that of the minimum temperature. This has led to a negative trend in the daily temperature range that, for the last 50 years, has become positive. Precipitation shows a decreasing tendency, even if low and rarely significant, the negative trend being only 5% per century on a yearly basis. A complete discussion of the data, the methods and the results is presented in [1]. Figures 1 and 2 display the ITA yearly temperature and precipitation records.

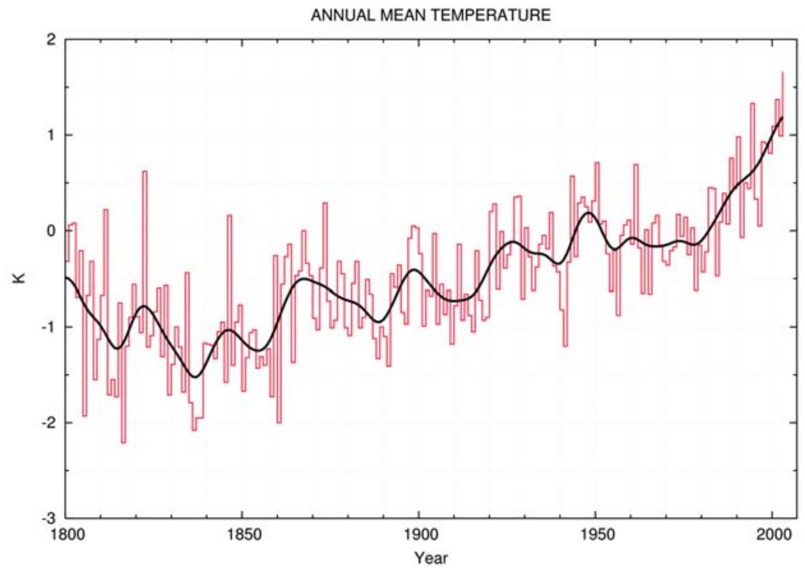

Fig. 1
Average Italian national series for mean temperature (1800–2003). The series is displayed together with an 11-year window 3-year σ Gaussian low-pass filter.

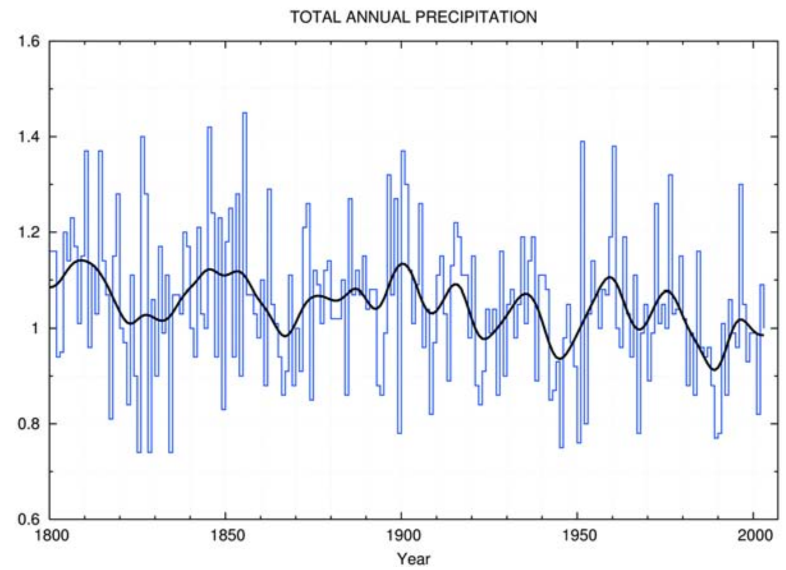

Fig. 2
Average Italian national series for precipitation (1800–2003). The series is displayed together with an 11-year window 3-year σ Gaussian low-pass filter.

REFERENCES
1. Brunetti, M., Maugeri, M., Monti, F., Nanni T., 2006 "Temperature and precipitation variability in Italy in the last two centuries from homogenised instrumental time series" International Journal of Climatology, 26, 345-381 (2006)

Natural radionuclides in the rocks of Valle del Cervo Pluton

U. Facchini[1], L. De Capitani[2], and M. Carnevale[1]

1 Istituto di Fisica Generale Applicata, Università degli Studi di Milano
2 Dipartimento di Scienze della Terra "A. Desio", Università degli Studi di Milano

The radionuclides from ^{238}U and ^{232}Th series represent, with ^{40}K, the main source of gamma radiation in the continental crust. The specific levels are related to the rock types. Highest radiation levels are mainly associated with felsic rocks, due to the geochemical behaviour of U, Th and K. These elements are more abundant in the continental crust than in the earth mantle and prefer the liquid phase during a process of crustal anatexis (partial melting) and subsequent fractional crystallization. Valle del Cervo Pluton is a composite body consisting of Monzonitic, Syenitic and Granitic Complexes formed by strongly K-enriched rocks. The areas, where these rocks crop out, are characterized by high natural radiation background. Gamma spectroscopy at high resolution, with HPGe, is the most used technique for quantitative analysis of gamma emitters radionuclides. The following hypothesis has been made: 1- Isotopic ratio between ^{235}U and ^{238}U is 7,2‰. 2- ^{238}U and ^{226}Ra are in secular equilibrium. 3- The exhalation rate of radon gas has been determined to be less than 1% of the total radon contained inside sample's volume. This rate is not relevant for examination of radon's daughters. For all the analysed rocks the U concentrations are lower than the Th ones.The rocks of the Granitic Complex show the lowest contents in elemental Th, whereas the elemental U values are similar to those of the Syenitic and Monzonitic Complexes. The specific activity related to syenite PM 26 is particularly interesting: 764 Bq/kg for ^{238}U and 478 Bq/kg for ^{232}Th. This rock is the most active. Moreover, the syenite LB 99, collected at the *La Balma quarry*, shows specific activities of 468 Bq/kg for ^{238}U and 381 Bq/kg for ^{232}Th, respectively. These values are relevant compared with those of other granitoids used as building stones.

Concentration, composition and sources of PM1 (particulate matter with d<1 μm) in Italian urban sites

R. Vecchi[1], G. Valli[1], M. Ceriani[1], F. Silvani[1], F. Lucarelli[2], S. Nava[2], M. Chiari[2], L. Paperetti[2], P. Prati[3], A. D'Alessandro[3], F. Mazzei[3], P. Fermo[4], A. Piazzalunga[4], and I. Garcia-Orellana[5]

1 Istituto di Fisica Generale Applicata, Università degli Studi di Milano & INFN-Milano
2 Dipartimento di Fisica, Università di Firenze & INFN-Firenze
3 Dipartimento di Fisica, Università di Genova & INFN-Genova
4 Dipartimento di Chimica Inorganica, Metallorganica e Analitica, Università degli Studi di Milano
5 Università di Siviglia (Spagna) & INFN-Firenze

In the frame of a national research project in 2004 we planned a monitoring campaign with the aim of characterising PM1 in three major Italian towns. This study completed previous researches on the PM10-PM2.5 characterisation performed by the authors in Milan, Genoa and Florence [1, 2]. The measurement campaigns were carried out in Milan, Genoa, and Florence using the same experimental methodology for sampling and elemental analysis (i.e. sequential samplers and ED-XRF spectrometry). Contributions from ionic components as well as elemental and organic carbon were also evaluated (by means of Ionic Chromatography and Thermal Gravimetric Analyzer/Fourier Transformed Infrared Spectroscopy, respectively). Gaseous pollutants concentrations and meteorological parameters were also available from the regional air quality network. In Milan, additional ^{222}Rn hourly measurements were performed to account for the stability/dispersion conditions of the atmosphere [3]. The PM1 mass concentration values were very high in Milan (wintertime median: 44.5 μg/m^3, summertime median: 19.1 μg/m^3), enhancing concern for possible health effects and problems in attaining the PM10 EU-limit. PM1 was about 40-60% of PM10 at the three investigated urban sites during both seasons. Aerosols of secondary origin (i.e. organics, nitrates and sulphates) dominated the PM1 mass at all sites accounting on the whole for about 80% of the mass. The application of receptor models allowed the identification of the emission sources and the quantification of their contribution to the particulate matter mass.

REFERENCES
1. Ariola V., Campajola L., D'Alessandro A., Del Carmine P., Gagliardi F., Lucarelli F., Mandò P.A., Marcazzan G., Moro R., Nava S., Prati P., Valli G., Vecchi R., and Zucchiatti A., "Aerosol characterisation in Italian towns by IBA techniques", *Nuclear Instruments and Methods in Physics Research* B 190, 471 (2002)
2. D'Alessandro A., Lucarelli, F. , Marcazzan, G., Nava, S., Prati, P., Valli, G., Vecchi, R., and Zucchiatti A., "A summertime investigation on urban PM fine and coarse fractions using hourly elemental concentration data series", *Il Nuovo Cimento*, 27C, 1, 17 (2004)
3. Vecchi R., Marcazzan G., Valli G., Ceriani M. and Antoniazzi C., "The role of atmospheric dispersion in the seasonal variation of PM1 and PM2.5 concentration and composition in the urban area of Milan (Italy)", *Atmospheric Environment*, 38, 4437-4446(2004).

The role of physical non destructive analyses in the studies of cultural heritage

M. Milazzo[1], D. Bertani[2], L. Bonizzoni[1], L. Consolandi[1], M. Gargano[1], N. Ludwig[3], and G. Poldi[1]

1 Istituto di Fisica Generale Applicata, Università degli Studi di Milano.
2 Istituto Nazionale di Ottica Applicata-CNR
3 Dipartimento di Fisica, Università degli Studi di Milano

Looking in general at the scientific methods of analysis, i.e. the methods of traditional sciences as chemistry, biology, informatics, geology, etc in their applications to Art and Archaeology there is no doubt that the primary role recognized to them by common awareness is in the conservation and restoration activities. It corresponds to the old latin sentence *primum vivere, deinde philosophare*, if we attribute also to studying and enjoying the testimonies of past civilization and art the role of a philosophical activity. On the contrary, there is a less diffuse awareness of the importance of the scientific analyses in the studies pertaining to Art and Archaeology, namely in a context which leaves conservation or restoring intents out of consideration.

The analyses which are considered non destructive, or non invasive, are by full right *physical* analyses, meaning by this term, as opposed to *chemical*, that the employed methods, going for instance from X-ray radiography to neutron activation, pertain by tradition to Physics. They do not require sampling or any preparation of the objects to be examined and for this reason are especially suited to be applied to Cultural Heritage. Physics (optical methods, for instance) plays a central role, also for the possibility of setting up portable instrumentations. We use the term *Archaeometry* for denoting the area of scientific disciplines, including Physics, dealing with measurements applied to *old* objects. Datations, in particular but not exclusively.

As already noted, the scope of applications of scientific analyses to cultural heritage should, in general, not be only considered as directed to tutelage, conservation, restoration, which are evidently of paramount importance, they, in fact, accomplish as well the task of supplying data for the *materic* characterization, which implement the ones of historical or stylistic pertinence, leaving conservation and restoration out of consideration.

In this contribution we show how several Physical methods can be applied in the field of *Archaeometry*, in particular we deal with infrared optical examinations of painting, which proved to be the best way to reveal the preparatory drawing, and XRF analysis. The latter is by far the most widespread technique in archaeometric applications. However, concerning quantitative analyses, several problem depending on the specific conditions of the measurements as, for instance, the irregular shape of a metallic object or the unknown composition of glass matrix must be solved. The methods pertaining to physics must be non destructive by definition; under this aspect several atomic physics methods are important (Ion beam analysis, for instance) and almost in their generality nuclear Physics methods. We can trace - for Italy at least - the origin of the application of nuclear Physics to Cultural Heritage back to the international conference held at Accademia Nazionale dei Lincei *Applicazione dei metodi nucleari nel campo delle opere d'Arte.* (Rome-Venice, may 24-29 1973). We cite after it the *International* workshop on I*on beam analysis in the arts and archaeology* (Pont-à-Mousson. France 1986) and finally, as the most recent, the 52nd annual Denver X-Ray conference where the plenary Session was devoted to *X-Ray Studies of Art and Archaeological Objects* (4-8 August 2003).

Ion beam analyses

In Fig. 1 we show several non destructive analyses in principle applicable to the examination of an ancient coin, for instance. They are grouped according to their probing depth. Not all of them are classifiable as *nuclear* analyses (SEM analysis, for instance). Nevertheless there is a logical criterion in associating them since the peculiarity of being non destructive is based on involving, in all cases, transitions of internal constituents of atoms: of course, nuclei in nuclear analyses, internal shell electrons in atomic analyses.

In Ion Beam Analyses (IBA) light ions, like protons, deuterons or helium ions, are used to bombard with a few Mev energy the sample under examination. The main advantage, compared to electrons, is that an ion beam can be employed in air and no sample preparation is implied. These are both evident advantages in examining art objects like paintings or statues. The analyses are

based either on atomic (PIXE or RBS) or nuclear (PIGE or PAA) interactions.

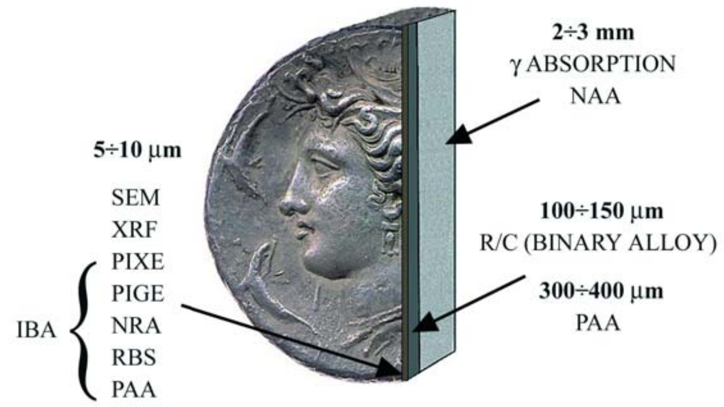

Fig. 1
Non-invasive analyses. SEM Scanning Electron Microscope, XRF X-Ray Fluorescence, PIXE Particle Induced X Emission, PIGE Particle Induced X Emission, NRA Nuclear Reaction Analyses, RBS Rutherford Back Scattering, PAA Proton Activation Analyses

PIXE is based on the analysis of characteristic X-Ray Fluorescence spectra excited by particle bombardment and it does not apply neither to the lightest elements nor to the heaviest ones. In the former case, in fact, XRF emission is disfavored compared with Auger electron emission, and the detection efficiency of solid state detectors, used for the so called Energy - Dispersive Spectroscopy as opposed to the traditional Wave Dispersive Spectroscopy, become very low at the lowest energies of X-Rays emitted by the lightest elements. For very heavy elements, on the other hand, K-shell ionization atomic cross sections becomes very small. PIXE analysis can also be performed quantitatively; the main difficulty for quantitative analysis depends on the progressive lowering, of the energy of ion traveling thorough the examined layer, due to the material stopping power, which in turn decreases the atom ionization cross sections. The stopping power effect depends on chemical composition which is evidently directly connected to XRF line intensities. So the algorithm relating Characteristic X-Ray intensity and concentration for each detected element is rather complicated.

XRF analysis, by definition, is the analysis where X-Rays are employed to excite characteristic X-Ray emission. Comparison between PIXE and XRF, has been already treated under several aspects. Sensitivities of the two analyses are on practice equivalent. The obvious advantage of XRF is that it requires much simpler and less expensive instrumentation than the ion accelerator and it is easily performed with portable instruments. Also quantitative analysis is comparatively easier for XRF than for PIXE, more over, the examined layer is thicker. Superior PIXE characteristics consists in the possibility of focusing very narrow proton probe so producing very good lateral definition. We note, however, that the most recent developments in X-Ray focusing exploiting glass capillary techniques allow X-Ray probes with lateral definition of a few microns to be manufactured.

Quantitative XRF analysis for cultural heritage

On the basis of the multiannual activity of our lab in the field of non destructive analyses applied to cultural heritage we will illustrate the typical problems found to obtain quantitative XRF analysis in case of paintings, metals, glasses and ceramics. We will deal only with XRF analyses performable with portable instruments which represent the most important task provided we are mostly concerned with *in loco* analyses.

Quantitative XRF analysis can in general be obtained at the following conditions.

1. Homogeneous composition of the sample on microscopic scale.
2. Secondary or negligible presence of non detectable light elements in the sample matrix for glasses and ceramics.
3. Regular shape or at least the existence of a flat zone on the irradiated surface for metallic samples.
4. Constant angles for exciting and emitted X-Ray directions all over the examined surface.

We see at first glance that such conditions are in general not all fulfilled in the objects pertaining to cultural heritage. There is, in fact, not at all or insufficient homogeneity in the painting brushes; presence of light elements, non detectable with solid state detectors, can be dominant or at least non negligible in glasses and ceramics; most of metallic objects, like coins for instance, have, non flat or irregular surfaces or, even worse, either natural or artificial patina can have been formed on the surface.
The last of above conditions of constant angles for irradiation and detection directions can strictly be satisfied only in ideal experimental set-up. On reality it can only be considered valid

in first approximation. The error depending on this approximation is in general acceptable in archaeometric applications and we shall not mention it any more.

In the XRF analyses of paintings the detection of some chemical elements typical of pigment composition gives a direct indication of the chemical nature of color material. We already commented on the fact that the irregularity of brush stroke makes in general so inhomogeneous the composition as to prevent from obtaining quantitative analysis. For painting, however, a peculiar interest exists on getting information on the stratigraphy or painting layer sequence. It can be obtained with the invasive technique of micro sampling and examination of thin or thick sections with optical or electron microscope. We note, however, that in many instances, as for painting Venetian school, the association of optical reflectance analysis, which pertains to the most external pigment layer, and XRF analysis, pertaining to the entire painting layer, allows to discriminate by non invasive method between over painting and internal painting composition (Fig. 2).

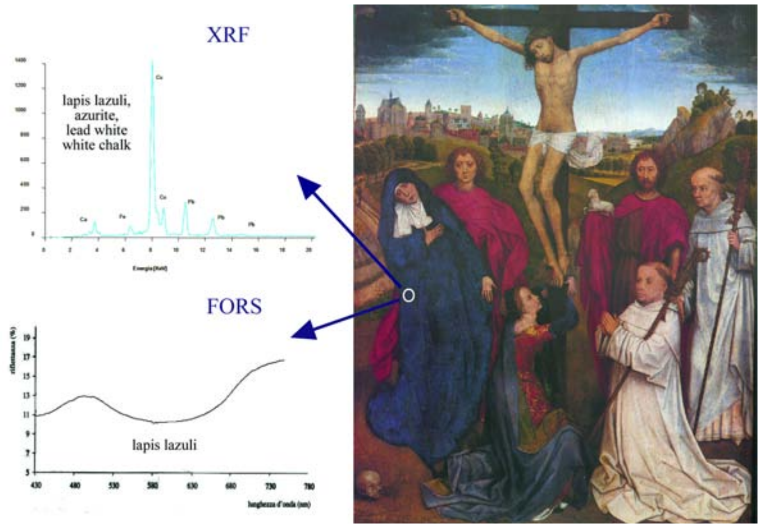

Fig. 2
Hans Memling, Crucifixion (1468-70)
Non invasive analysis based on reflectance spectroscopy, energy dispersive XRF, and Fiber Optical Reflectance Analysis

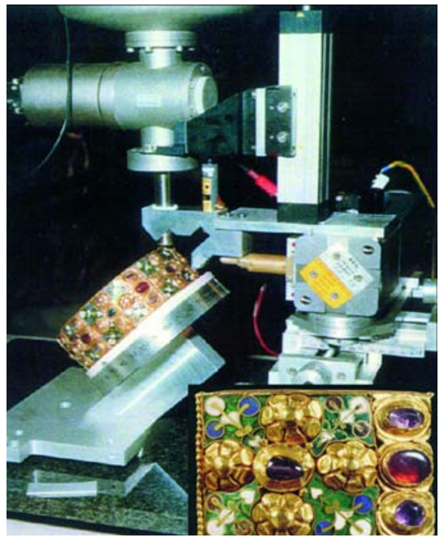

Fig. 3
Monza Iron Crown (bottom: detail).
Portable apparatus for XRF analyses of metals and glasses.

In the characterization of glasses and ceramics (Fig. 3), quantitative analyses are of fundamental importance. In general quantitative analyses rely on the possibility of evaluating autoabsorption corrections which depend on the sample composition. As already noted, light elements of the composition are not detected with the energy dispersive spectroscopy, so making the correction impossible. In this case we can exploit the peculiarity of light elements, in general, of having constant Compton mass absorption coefficient; so measuring the Compton scattering intensity of the exciting X-Rays we obtain a direct evaluation of the absorption coefficient of light matrix at the exciting energy and, by proper scaling laws, we can also evaluate the light matrix absorption effect for all involved X-Ray energies.

Recurring to scattering effect of the exciting X radiation is exploited to by pass the problem of the possible existence of an artificial or natural patina on metallic surface. In this case, we recur to both coherent, or Rayleigh (R), and incoerent, or Compton (C), scattering since

the ratio R/C is a critical function of the material atomic number. So, using X-Rays of energy high enough as to pass the patina thickness we can deduce, for instance, for the binary alloy of Ag-Cu coins the silver content which is the information of numismatic interest. The difficulty dependent on irregular form to obtain quantitative analysis of metallic specimens consists in the fact that unknown corrective shape factors must be included in the calculations which depends on both exciting and emitted characteristic X-Ray energies. Recurring to the expedient of measuring XRF line intensities as the average of different sample positions and using their relative values, it is however possible to obtain a few per cent errors in quantitative analysis of the alloys which are in general compatible with archaeometric requirements.

Infrared analyses of paintings

Optical analyses in general are the non-invasive physical analyses *pour excellence*. In particular, near infrared examination of paintings (IR reflectography) allows the detection of painting underdrawings. (Fig. 4) In cooperation with the national institute of applied optics (INOA) we gave origin to the “Centro Interdipartimentale di Riflettografia Infrarossa e di Diagnostica dei Beni Culturali” which is very active in supplying reflectographies of paintings of italian and foreign museums. In the “Laboratorio di Metrologia Ottica per i Beni Culturali” a prototype of a new infrared instrument was developed, based on the scanning of painting real imagine reduced on a minor scale, so offering the possibility of a substantial shortening of take time.

Fig. 4
Hans Memling, Crucifixion (1468-70) Top-left: visible inage detail.
Reflectographies obtained with different infrared detectors (Silicon, Lead sulfide, Mercury-Cadmiun Tellurium)

REFERENCES
1. J. Sherman, *Spectrochim. Acta*, 7, 283(1955)
2. J. W. Criss and L. S. Birks, *Anal. Chem*., 40, 1080 (1968)
3. R. M. Rousseau, *X-ray spectrom*., 13, 115 (1984)
4. L. Bonizzoni, A. Galli, M. Milazzo *X-ray spectrom*., 29, 443 (2000)
5. M. Milazzo and C. Cicardi, *X-ray Spectrom*., 26, 211 (1997)
6. Rindby et al., *X-ray spectom*.,22, (1989)
7. G. R. Lachance, F. Claisse *Quantitative X-ray Fluorescence Analysis* John Wiley and sons

Publications (2003-2006)

The list of publications for the year 2006 is highly incomplete, because the various divisions have supplied their publication list at different times during the editorial process.

Elementary Particle Physics

Articles

ABDALLAH J. et al. (including: ANDREAZZA A., VEGNI G., MERONI C., TRONCON C.) (2006).
Measurement and Interpretation of Fermion-Pair Production at LEP energies above the Z0 Resonance. EUROPEAN PHYSICAL JOURNAL C. vol. 45, pp. 589-632

ABDALLAH J. et al. (including: ANDREAZZA A., VEGNI G., MERONI C., TRONCON C.) (2006)
Determination of heavy quark non-perturbative parameters from spectral moments in semileptonic B decays. EUROPEAN PHYSICAL JOURNAL C. vol. 45, pp. 35-59

AUBERT B., et al. (including: BANFI D., CARMINATI L., CAVALLI D., CITTERIO M., COSTA G., DELMASTRO M., FANTI M., MANDELLI L., MAZZANTI M., TARTARELLI F.) (2006).
Construction, assembly and tests of the ATLAS electromagnetic barrel calorimeter. NUCL. INSTRUM. METH. A. vol. 558, pp. 388-418

AUBERT B., et al.(including: LAZZARO A., LOMBARDO V., PALOMBO F.) (2006).
Measurements of the absolute branching fractions of B+- —> K+- X(C anti-C). PHYS. REV. LETT. vol. 96, pp. 052002/1-052002/7

AUBERT B., et al. (including: LAZZARO A., LOMBARDO V., PALOMBO F.) (2006).
Measurement of branching fractions and resonance contributions for B0 —> ANTI-D0 K+ PI- and search for B0 —> D0 K+ PI- decays. PHYS. REV. LETT. vol. 96, pp. 011803/1-011803/7

AUBERT B., et al. (including: LAZZARO A., LOMBARDO V., PALOMBO F.) (2006).
Search for lepton flavor violation in the decay tau +- —> E+- gamma. PHYS. REV. LETT. vol. 96, pp. 041801/1-041801/7

AUBERT B., et al. (including: LAZZARO A., LOMBARDO V., PALOMBO F.) (2006).
Search for rare quark-annihilation decays, B- —> D(S)(*)- PHYS. REV. D. vol. 73, pp. 011103/1-011103/8

AUBERT B., et al. (including: LAZZARO A., LOMBARDO V., PALOMBO F.) (2006).
A study of E+ E- —> P anti-P using initial state radiation with BABAR. PHYS. REV. D. vol. 73, pp. 012005/1-012005/8

AUBERT B., et al. (including: LAZZARO A., LOMBARDO V., PALOMBO F.) (2006).
Measurement of the inclusive electron spectrum in charmless semileptonic B decays near the kinematic endpoint and determination of |V(UB)|. PHYS. REV. D. vol. 73, pp. 012006/1-012006/8

AUBERT B., et al. (including: LAZZARO A., LOMBARDO V., PALOMBO F.) (2006).
Measurement of the branching ratios gamma(D(S)*+ —> D(S)+ PI0) / gamma(D(S)*+ —> D(S)+ gamma) and gamma(D*0 —> D0 PI0) / gamma(D*0 —> D0 gamma). PHYS. REV. D. vol. 72, pp. 091101/1-091101/8

AUBERT B., et al. (including: LAZZARO A., LOMBARDO V., PALOMBO F.) (2006).
Measurement of neutral B decay branching fractions to K0(S) PI+ PI- final states and the charge asymmetry of B0 —> K*+ PI-. PHYS. REV. D. vol. 73, pp. 031101/1-031101/8

AUBERT B., et al. (including: LAZZARO A., LOMBARDO V., PALOMBO F.) (2006).
Measurements of the B —> X(S gamma) branching fraction and photon spectrum from a sum of exclusive final states. PHYS. REV. D. vol. 72, pp. 052004/1-052004/8

AUBERT B., et al. (including: LAZZARO A., LOMBARDO V., PALOMBO F.) (2006).
A study of B —> C and B —> U interference in the decay B- —> [K+ PI-](D) K*-. PHYS. REV. D. vol. 72, pp. 071104/1-071104/8

AUBERT B., et al. (including: LAZZARO A., LOMBARDO V., PALOMBO F.) (2006).
Measurement of the anti-B0 lifetime and the B0 anti-B0 oscillation frequency using partially reconstructed anti-B0 —> D*+ L- anti-NU(L) decays. PHYS. REV. D. vol. 73, pp. 012004/1-012004/8

ABDALLAH J. et al. (including: ANDREAZZA A., VEGNI G., MERONI C., TRONCON C.) (2005).
Bose-Einstein correlations in W+W- events at LEP2. EUROPEAN PHYSICAL JOURNAL C. vol. 44, pp. 161-174

ABDALLAH J. et al. (including: ANDREAZZA A., VEGNI G., MERONI C., TRONCON C.) (2005).
Determination of A(FB)(b) at the Z pole using inclusive charge reconstruction and lifetime tagging. EUROPEAN PHYSICAL JOURNAL C. vol. 40, pp. 1-25

ABDALLAH J. et al. (including: ANDREAZZA A., VEGNI G., MERONI C., TRONCON C.) (2005).
Coherent soft particle production in Z decays into three jets. PHYSICS LETTERS B. vol. 605, pp. 37-48

ABDALLAH J. et al. (including: ANDREAZZA A., VEGNI G., MERONI C., TRONCON C.) (2005).
Photon events with missing energy in e(+)e(-) collisions at root s=130 to 209 GeV. EUROPEAN PHYSICAL JOURNAL C. vol. 38, pp. 395-411

ABDALLAH J. et al. (including: ANDREAZZA A., VEGNI G., MERONI C., TRONCON C.) (2005).
Measurement of the energy dependence of hadronic jet rates and the strong coupling alpha(s) from the four-jet rate with the DELPHI detector at LEP. EUROPEAN PHYSICAL JOURNAL C. vol. 38, pp. 413-426

ABDALLAH J. et al. (including: ANDREAZZA A., VEGNI G., MERONI C., TRONCON C.) (2005).
Charged Particle Multiplicity in Three-Jet Events and Two-Gluon Systems. EUROPEAN PHYSICAL JOURNAL C. vol. 44, pp. 311-331

ABDALLAH J. et al. (including: ANDREAZZA A., VEGNI G., MERONI C., TRONCON C.) (2005).
Production of XI0(C) and XI(B) in Z decays and lifetime measurement of XI(B). EUROPEAN PHYSICAL JOURNAL C. vol. 44, pp. 299-309

AIROLDI A., ALIMONTI G., AMATI M., ANDREAZZA A., BULGHERONI A., CACCIA M., GIUGNI D., KUCEWICZ W., LARI T., MERONI C., RAGUSA F., TRONCON C., VEGNI G. (2005).
A chip removal facility for indium bump bonded pixel detectors. NUCLEAR INSTRUMENTS AND METHODS IN PHYSICS RESEARCH A. vol. 540, pp. 259-265

ALFIERI R., VACCAROSSA L. et al. (2005).
The INFN-Grid Testbed FUTURE GENERATION COMPUTER SYSTEMS. vol. 21, nr. 2, pp. 249-258

ANDREAZZA A. (2005).
Measurement of the tau lifetime with the DELPHI detector. NUCLEAR PHYSICS B. vol. 144, pp. 97-104

AUBERT B., et al. (including: BATTISTONI G., CARMINATI L., CAVALLI D., COSTA G., DELMASTRO M., FANTI M., MANDELLI L., MAZZANTI M., PERINI L., TARTARELLI F.) (2005).
Development and construction of large size signal electrodes for the ATLAS electromagnetic calorimeter. NUCL. INSTRUM. METH. A. vol. 539, pp. 558-594

AUBERT B., et al. (including: LAZZARO A., LOMBARDO V., PALOMBO F.) (2005).
Search for decays of B0 —> E+ E-, B0 —> MU+ MU-, B0 —> E+- MU-+. PHYS. REV. LETT. vol. 94, pp. 221803/1-221803-8

AUBERT B. et al. (including: LAZZARO A., LOMBARDO V., PALOMBO F.) (2005).
Evidence for B+ —> anti K0 K+ AND B0 —> K0 anti-K0, and meaurement of the branching fraction and search for direct CP violation B+ —> K0 PI+. PHYS. REV. LETT. vol. 95, pp. 221801/1-221801/7

AUBERT B. et al. (including: LAZZARO A., LOMBARDO V., PALOMBO F.) (2005).
Measurement of time-dependent CP asymmetries and the CP-ODD fraction in the decay B0 —> D*+ D*-. PHYS. REV. LETT. vol. 95, pp. 151804/1-151804/7

AUBERT B. et al. (including: LAZZARO A., LOMBARDO V., PALOMBO F.) (2005).
Observation of a broad structure in the PI+ PI- J / PSI mass spectrum around 4.26-GEV/C**2. PHYS. REV. LETT. vol. 95, pp. 142001/1-142001/7

AUBERT B. et al. (including: LAZZARO A., LOMBARDO V., PALOMBO F.) (2005).
Search for lepton-flavor and lepton-number violation in the decay tau- —> L-+ H+- H'-. PHYS. REV. LETT. vol. 95, pp. 191801/1-191801/7

AUBERT B. et al. (including: LAZZARO A., LOMBARDO V., PALOMBO F.) (2005).
Determination of |VUB| from measurements of the electron and neutrino momenta in inclusive semileptonic B decays. PHYS. REV. LETT. vol. 95, pp. 111801-1,111801/7

AUBERT B., et al. (including: LAZZARO A., LOMBARDO V., PALOMBO F.) (2005).
Measurement of time-dependent CP asymmetries in B0 —> D(*)D decays. PHYS. REV. LETT. vol. 95, pp. 131802/1-131802/7

AUBERT B. et al. (including: LAZZARO A., LOMBARDO V., PALOMBO F.) (2005).
Measurement of gamma IN B-+ —> D(*) K-+ decays with a dalitz analysis of D —> K0(S) PI- PI+. PHYS. REV. LETT. vol. 95, pp. 121802/1-121802/7

AUBERT B. et al. (including: LAZZARO A., LOMBARDO V., PALOMBO F.) (2005).
Production and decay of XI(C)0 at BABAR. PHYS. REV. LETT. vol. 95, pp. 142003/1-142003/7

AUBERT B. et al. (including: LAZZARO A., LOMBARDO V., PALOMBO F.) (2005).
Measurement of the branching fraction of upsilon (4S) —> B0 anti-B0. PHYS.REV.LETT. vol. 95, pp. 042001/1-042001/7

AUBERT B. et al. (including: LAZZARO A., LOMBARDO V., PALOMBO F.) (2005).
Improved measurement of the CKM angle alpha using B0(anti-B0) —> RHO+ RHO- decays. PHYS. REV. LETT. vol. 95, pp. 041805/1-041805/7

AUBERT B. et al. (including: LAZZARO A., LOMBARDO V., PALOMBO F.) (2005).
Measurement of branching fractions and charge asymmetries in B+ decays to eta PI+, eta K+, eta RHO+ and eta-prime PI+, and search for B0 decays to eta K0 and eta omega. PHYS. REV. LETT. vol. 95, pp. 131803/1-131803/7

AUBERT B. et al. (including: LAZZARO A., LOMBARDO V., PALOMBO F.) (2005).
Search for lepton flavor violation in the decay tau+- —> MU+- gamma. PHYS. REV. LETT. vol. 95, pp. 041802/1-041802/7

AUBERT B. et al. (including: LAZZARO A., LOMBARDO V., PALOMBO F.) (2005).
Measurement of branching fractions and time-dependent CP-violating asymmetries in B —> ETA-PRIME K decays. PHYS. REV. LETT. vol. 94, pp. 191802/1-191802/7

AUBERT B. et al. (including: LAZZARO A., LOMBARDO V., PALOMBO F.) (2005).
Branching fraction and CP asymmetries of B0 —> K0(S) K0(S) K0(S). PHYS. REV. LETT. vol. 95, pp. 011801/1-011801/7

AUBERT B. et al. (including: LAZZARO A., LOMBARDO V., PALOMBO F.) (2005).
Search for strange -pentaquark production in E+ E- annihilation AT S**(1/2) = 10.58-GEV and in upsilon (4S) decays. PHYS. REV. LETT. vol. 95, pp. 042002/1-042002/7

AUBERT B. et al. (including: LAZZARO A., LOMBARDO V., PALOMBO F.) (2005).
Improved measurements of CP-violating asymmetry amplitudes in B0 —> PI+ PI- decays. PHYS. REV. LETT. vol. 95, pp. 151803/1-151803/7

AUBERT B. et al. (including: LAZZARO A., LOMBARDO V., PALOMBO F.) (2005).
Search for factorization-suppressed B —> CHI(C) K(*) decays. PHYS. REV. LETT. vol. 94, pp. 171801/1-171801/7

AUBERT B. et al. (including: LAZZARO A., LOMBARDO V., PALOMBO F.) (2005).
Limit on the B0 —> RHO RHO0 branching fraction and implications for the CKM angle alpha. PHYS. REV. LETT. vol. 94, pp. 131801/1-131801/7

AUBERT B. et al. (including: LAZZARO A., LOMBARDO V., PALOMBO F.) (2005).
Measurement of branching fractions and charge asymmetries for exclusive B decays to charmonium. PHYS. REV. LETT. vol. 94, pp. 141801/1-141801/7

AUBERT B. et al. (including: LAZZARO A., LOMBARDO V., PALOMBO F.) (2005).
Measurement of branching fraction and dalitz distribution for B0 —> D(*)+- K0 PI+- decays. PHYS. REV. LETT. vol. 95, pp. 171802/1-171802/7

AUBERT B. et al. (including: LAZZARO A., LOMBARDO V., PALOMBO F.) (2005).
Branching fractions and CP asymmetries in B0 —> PI0 PI0, B+ —> PI+ PI0 AND B+ —> K+ PI0 decays isospin analysis of theB —> PI PI system. PHYS. REV. LETT. vol. 94, pp. 181802/1-181802/7

AUBERT B. et al. (including: LAZZARO A., LOMBARDO V., PALOMBO F.) (2005).
A search for the decay B+ —> K+ NU anti-NU. PHYS. REV. LETT. vol. 94, pp. 101801/1-101801/7

AUBERT B. et al. (including: LAZZARO A., LOMBARDO V., PALOMBO F.) (2005).
Measurements of the branching fraction and CP-violation asymmetries in B0 —> F(0)(980) K0(S). PHYS. REV. LETT. vol. 94, pp. 041802/1-041802/7

AUBERT B. et al. (including: LAZZARO A., LOMBARDO V., PALOMBO F.) (2005).
Search for the rare leptonic decay B- —> tau- anti-tau-neutrino. PHYS. REV. LETT. vol. 95, pp. 041804/1-041804/7

AUBERT B. et al. (including: LAZZARO A., LOMBARDO V., PALOMBO F.) (2005).
Improved measurement of CP asymmetries in B0 —> (C anti-C) KO* decays. PHYS. REV. LETT. vol. 94, pp. 161803/1-161803/7

AUBERT B. et al. (including: LAZZARO A., LOMBARDO V., PALOMBO F.) (2005).
Search for the radiative penguin decays B+ —> RHO+ gamma, B0 —> RHO0 gamma, and B0 —> omega gamma. PHYS. REV. LETT. vol. 94, pp. 011801/1-011801/7

AUBERT B. et al. (including: LAZZARO A., LOMBARDO V., PALOMBO F.) (2005).
Search for the W-exchange decays B0 —> D(S)(*)- D(S)(*)+. PHYS. REV. D. vol. 72, pp. 111101/1-111101/8

AUBERT B. et al. (including: LAZZARO A., LOMBARDO V., PALOMBO F.) (2005).
Measurement of the time-dependent CP-violating asymmetry in B0 —> K0(S) PI0 gamma decays. PHYS. REV. D. vol. 72, pp. 051103/1-051103/8

AUBERT B. et al. (including: LAZZARO A., LOMBARDO V., PALOMBO F.) (2005).
Dalitz plot analysis of D0 —> anti-K0 K+ K-. PHYS. REV. D. vol. 72, pp. 052008/1-052008/8

AUBERT B. et al. (including: LAZZARO A., LOMBARDO V., PALOMBO F.) (2005).
An amplitude analysis of the decay B+- —> PI+- PI+- PI-+. PHYS. REV. D. vol. 72, pp. 052005/1-052005/8

AUBERT B. et al. (including: LAZZARO A., LOMBARDO V., PALOMBO F.) (2005).
Measurement of the B+ —> P anti-P K+ branching fraction and study of the decay dynamics. PHYS. REV. D. vol. 72, pp. 051101/1-051101/8

AUBERT B. et al. (including: LAZZARO A., LOMBARDO V., PALOMBO F.) (2005).
A pprecision measurement of the lambda +(C) baryon mass. PHYS.REV.D vol.72, pp. 052006/1-052006/8.

AUBERT B. et al. (including: LAZZARO A., LOMBARDO V., PALOMBO F.) (2005).
Dalitz-plot analysis of the decays B+- —> K+- PI-+ PI+-. PHYS. REV. D. vol. 72, pp. 072003/1-072003/8

AUBERT B. et al. (including: LAZZARO A., LOMBARDO V., PALOMBO F.) (2005) .
Study of B —> PI L nu and B —> RHO L nu decays and determination of |V(UB)|. PHYS. REV. D. vol. 72, pp. 051102/1-051102-1

AUBERT B., et al. (including: LAZZARO A., LOMBARDO V., PALOMBO F.) (2005).
Measurement of CP observables for the decays B+- —> D0(CP) K*+-. PHYS. REV. D. vol. 72, pp. 071103/1-071103/8

AUBERT B. et al. (including: LAZZARO A., LOMBARDO V., PALOMBO F.) (2005).
Search for the rare decay anti-B0 —> D*0 gamma. PHYS. REV. D. vol. 72, pp.

051106/1-051106/8

AUBERT B. et al. (including: LAZZARO A., LOMBARDO V., PALOMBO F.) (2005).
Measurement of double charmonium production in E+ E- annihilations at S**(1/2) = 10.6-GEV. PHYS. REV. D. vol. 72, pp. 031101/1-031101/8
AUBERT B. et al. (including: LAZZARO A., LOMBARDO V., PALOMBO F.) (2005).
Search for the decay tau- to 4PI- 3PI+ (PI0) nu(TAU). PHYS. REV. D. vol. 72, pp. 012003/1-012003/8

AUBERT B. et al. (including: LAZZARO A., LOMBARDO V., PALOMBO F.) (2005).
Search for the rare decays B+ —> D(*)+ K0(S). PHYS. REV. D. vol. 72, pp. 011102/1-011102/8

AUBERT B. et al. (including: LAZZARO A., LOMBARDO V., PALOMBO F.) (2005).
Measurement of the branching fraction and decay rate asymmetry of B- —> D(PI+ PI= PI)) K-. PHYS. REV. D. vol. 72, pp. 071102/1-071102/8

AUBERT B. et al. (including: LAZZARO A., LOMBARDO V., PALOMBO F.) (2005).
Study of the tau- —> 3H- 2H+ tau-neutrino decay. PHYS. REV. D. vol. 72, pp. 072001/1-072001/8

AUBERT B. et al. (including: LAZZARO A., LOMBARDO V., PALOMBO F.) (2005).
Search for B —> U transitions in B- and D0 K- and B- —> D*0 K-. PHYS. REV. D. vol. 72, pp. 032004/1-032004/8

AUBERT B. et al. (including: LAZZARO A., LOMBARDO V., PALOMBO F.) (2005).
Measurement of time-dependent CP-violating asymmetries and constraints on sin (2beta + gamma) with partial reconstruction of B —> D*-+ PI+- decays. PHYS. REV. D. vol. 71, pp. 112003/1-112003/8

AUBERT B. et al. (including: LAZZARO A., LOMBARDO V., PALOMBO F.) (2005).
Evidence for the decay B+- —> K*+- PI0. PHYS. REV. D. vol. 71, pp. 111101/1-111101/8

AUBERT B. et al. (including: LAZZARO A., LOMBARDO V., PALOMBO F.) (2005).
Search for B —> J/PSI D DECAYS. PHYS. REV. D. vol. 71, pp. 091103/1-091103/8

AUBERT B. et al. (including: LAZZARO A., LOMBARDO V., PALOMBO F.) (2005).
Measurement of the branching fraction and the CP-violating asymmetry for the decay B0 —> K0(S) PI0. PHYS. REV. D. vol. 71, pp. 111102/1-111102/8

AUBERT B. et al. (including: LAZZARO A., LOMBARDO V., PALOMBO F.) (2005).
Measurement of the B0 —> D*- D(S)*+ AND D(S)+ —> PHI PI+ branching fractions. PHYS. REV. D. vol. 71, pp. 091104/1-091104/8

AUBERT B. et al. (including: LAZZARO A., LOMBARDO V., PALOMBO F.) (2005).
The E+ E- —> PI+ PI- PI+ PI-, K+ K- PI+ PI-, and K+ K- K+ K- cross sections at center-of.mass energies 0.5-GEV TO 4.5-GEV measured with initial-state radiation. PHYS. REV. D. vol. 71, pp. 052001/1-052001/8

AUBERT B. et al. (including: LAZZARO A., LOMBARDO V., PALOMBO F.) (2005).
Measurement of CP asymmetries in B0 —> PHI K0 and B0 -> K+ K- K0(S) DECAYS. PHYS. REV. D. vol. 71, pp. 091102/1-091102/8

AUBERT B. et al. (including: LAZZARO A., LOMBARDO V., PALOMBO F.) (2005).
A search for CP violation and a measurement of the relative branching fraction in D+ —> K- K+ PI+ decays. PHYS. REV. D. vol. 71, pp. 091101/1-091101/8

AUBERT B. et al. (including: LAZZARO A., LOMBARDO V., PALOMBO F.) (2005).
Search for the radiative decay B0 —> PHI gamma. PHYS. REV. D. vol. 72, pp. 091103/1-091103/8

AUBERT B. et al. (including: LAZZARO A., LOMBARDO V., PALOMBO F.) (2005).
Search for a charged partner of the X(3872) in the B meson decay B —> X-K,X- —> J/PSI PI- PI0. PHYS. REV. D. vol. 71, pp. 031501/1-031501/8

AUBERT B. et al. (including: LAZZARO A., LOMBARDO V., PALOMBO F.) (2005).
Measurement of the ratio B(B- —> D*0 K-) / B(B- —> D*0 PI-) and of theCP asymmetry of B- —> D*0(CP+) K- decays. PHYS.REV. D. vol. 71, pp. 031102/1-031102/8

AUBERT B. et al. (including: LAZZARO A., LOMBARDO V., PALOMBO F.) (2005).
Measurement of B meson decays to omega K* and omega RHO. PHYS. REV. D. vol. 71, pp. 031103/1-031103/8

AUBERT B. et al. (including: LAZZARO A., LOMBARDO V., PALOMBO F. (2005).
Ambiguity-free measurement of COS 2beta, time-integrated and time-dependent angular analyses of B —> J / PSI K PI. PHYS. REV. D. vol. 71, pp. 032005/1-032005/8

AUBERT B. et al. (including: LAZZARO A., LOMBARDO V., PALOMBO F.) (2005).
Measurement of the anti-B0 —> D*+ L- ANTI-nu-L decay rate and |V(CB)|. PHYS. REV. D. vol. 71, pp. 051502/1-051502/8

AUBERT B. et al. (including: LAZZARO A., LOMBARDO V., PALOMBO F.) (2005).
Study of the B- —> J/PSI K- PI+ PI- decay and measurement of the B- —> X(3872) K- branching fraction. PHYS. REV. D. vol. 71, pp. 071103/1-071103/8

AUBERT B. et al. (including: LAZZARO A., LOMBARDO V., PALOMBO F.) (2005).
A measurement of the total width, the electronic width, and the mass of the upsilon(10580) resonance. PHYS. REV. D. vol. 72, pp. 032005/1-032005/8

BRUZZI M. et al. (including: ANDREAZZA A., CITTERIO M., LARI T., MERONI C., RAGUSA F., TRONCON C.) (2005)
Radiation-hard semiconductor detectors for SuperLHC. NUCLEAR INSTRUMENTS AND METHODS IN PHYSICS RESEARCH A. vol. 541, pp. 189-201

COLAS J. et al. (including: BANFI D., CARMINATI L., CAVALLI D., COSTA G., DELMASTRO M., FANTI M., MANDELLI L., MAZZANTI M., TARTARELLI G.F.) (2005).
Position resolution and particle identification with the ATLAS EM calorimeter. NUCL. INSTRUM. METH. A. vol. 550, pp. 96-115

LARI T., OH A., WERMES N., KAGAN H., KEIL M., TRISCHUK W. (2005).
Characterization and modeling of non-uniform charge collection in CVD diamond pixel detector. NUCLEAR INSTRUMENTS AND METHODS IN PHYSICS RESEARCH A. vol. 537, pp. 581-593

MIRAMONTI L. (2005).
European underground facilities: an overview. AIP. vol. 785, pp. 3-11RE V. et al. (including: LAZZARO A., PALOMBO F.) (2005).
What can be learned from the BaBar silicon vertex tracker running experience. NUCLEAR INSTRUMENTS AND METHODS IN PHYSICS RESEARCH A. vol. 552, pp. 224-231

RE V. et al. (including: LAZZARO A., PALOMBO F.) (2005).
Radiation damage studies for the Babar silicon vertex tracker. NUCLEAR INSTRUMENTS AND METHODS IN PHYSICS RESEARCH A. vol. 549, pp. 11-15

SCHAEL S. et al. (including: RAGUSA F.) (2005).
Branching ratios and spectral functions of tau decays: Final ALEPH measurements and physics implications. PHYSICS REPORT - REVIEW SECTION OF PHYSICS LETTERS. vol. 421, pp. 191-284

SCHAEL S. et al. (including: RAGUSA F.) (2005).
Improved measurement of the triple gauge-boson couplings gamma WW and ZWW in e(+)e(-) collisions. PHYSICS LETTERS B. vol. 614, pp. 7-26

SCHAEL S. et al. (including: RAGUSA F.) (2005).
Two-particle correlations in pp, (p)over-bar(p)over-bar and (KSKS0)-K-0 pairs from hadronic Z decays. PHYSICS LETTERS B. vol. 611, pp. 66-80

SCHAEL S. et al. (including: RAGUSA F.) (2005).
Bose-Einstein correlations in W-pair decays with an event-mixing technique. PHYSICS LETTERS B. vol. 606, pp. 265-275

SCHAEL S. et al. (including: RAGUSA F.) (2005).
Single vector boson production in e(+)e(-) collisions at centre-of-mass energies from 183 to 209 GeV. PHYSICS LETTERS B. vol. 605, pp. 49-62

VEGNI G., BERGOMI N., CAZZANIGA L. (2005).
Computer methods in Physics, a course for future teachers. A five years experience. RECENT RESEARCH DEVELOPMENTS IN LEARNING

TECHNOLOGIES. vol. 1, pp. 390-394

ABDALLAH J. et al. (including: ANDREAZZA A., VEGNI G., MERONI C., TRONCON C.) (2004).
Searches for Neutral Higgs Bosons in Extended Models. EUROPEAN PHYSICAL JOURNAL C. vol. 38, pp. 1-28
ABDALLAH J. et al. (including: ANDREAZZA A., VEGNI G., MERONI C., TRONCON C.) (2004).
Determination of the e+e- —> gamma gamma (gamma) cross-section at Lep 2. EUROPEAN PHYSICAL JOURNAL C. vol. 37, pp. 405-419

ABDALLAH J. et al. (including: ANDREAZZA A., VEGNI G., MERONI C., TRONCON C.) (2004).
A precise measurement of the tau lifetime. EUROPEAN PHYSICAL JOURNAL C. vol. 36, pp. 283-296

ABDALLAH J. et al. (including: ANDREAZZA A., VEGNI G., MERONI C., TRONCON C.) (2004).
Search for fermiophobic Higgs bosons in final states with photons at LEP 2. EUROPEAN PHYSICAL JOURNAL C. vol. 35, pp. 313-324

ABDALLAH J. et al. (including: ANDREAZZA A., VEGNI G., MERONI C., TRONCON C.) (2004).
The measurement of alpha(s) from event shapes with the DELPHI detector at the highest Lep energies. EUROPEAN PHYSICAL JOURNAL C. vol. 37, pp. 1-23

ABDALLAH J. et al. (including: ANDREAZZA A., VEGNI G., MERONI C., TRONCON C.) (2004).
Study of tau-pair production in photon-photon collisions at Lep and limits on the anomalous electromagnetic moments of the tau lepton. EUROPEAN PHYSICAL JOURNAL C. vol. 35, pp. 159-170

ABDALLAH J. et al. (including: ANDREAZZA A., VEGNI G., MERONI C., TRONCON C.) (2004).
Search for supersymmetric particles assuming R-parity nonconservation in e+e-collisions at S**(1/2) = 192-GeV to 208-GeV. EUROPEAN PHYSICAL JOURNAL C. vol. 36, pp. 1-23

ABDALLAH J. et al. (including: ANDREAZZA A., VEGNI G., MERONI C., TRONCON C.) (2004).
Search for single top production via FCNC at LEP at sqrt(s) =189-208 GeV. PHYSICS LETTERS B. vol. 590, pp. 21-34

ABDALLAH J. et al. (including: ANDREAZZA A., VEGNI G., MERONI C., TRONCON C.) (2004).
Search for B0(s) - anti-B0(s) oscillations in DELPHI using high-pt leptons. EUROPEAN PHYSICAL JOURNAL C. vol. 35, pp. 35-52

ABDALLAH J. et al. (including: ANDREAZZA A., VEGNI G., MERONI C., TRONCON C.) (2004).
Search for charged Higgs bosons at Lep in general two Higgs doublet models. EUROPEAN PHYSICAL JOURNAL C. vol. 34, pp. 399-418

ABDALLAH J. et al. (including: ANDREAZZA A., VEGNI G., MERONI C., TRONCON C.) (2004).
Search for SUSY in the AMSB scenario with the DELPHI detector. EUROPEAN PHYSICAL JOURNAL C. vol. 34, pp. 145-156

ABDALLAH J. et al. (including: ANDREAZZA A., VEGNI G., MERONI C., TRONCON C.) (2004).
Measurement of the Forward Backward Asymmetries of e+e- —> Z —> b anti-b and e+e- —> Z -> c anti-c using prompt leptons. EUROPEAN PHYSICAL JOURNAL C. vol. 34, pp. 109-125

ABDALLAH J. et al. (including: ANDREAZZA A., VEGNI G., MERONI C., TRONCON C.) (2004).
Measurement of the lambda0(b) decay form-factor. PHYSICS LETTERS B. vol. 585, pp. 63-84

ABDALLAH J. et al. (including: ANDREAZZA A., VEGNI G., MERONI C., TRONCON C.) (2004).
A precise measurement of the B+, B0 and mean B hadron lifetime with the DELPHI detector at Lep 1. EUROPEAN PHYSICAL JOURNAL C. vol. 33, pp. 307-324

ABDALLAH J. et al. (including: ANDREAZZA A., VEGNI G., MERONI C., TRONCON C.) (2004).
Measurement of |V(CB)| using the semileptonic decay anti-B0(D) —> D*+ L-anti-nu(l). EUROPEAN PHYSICAL JOURNAL C. vol. 33, pp. 213-232

ABDALLAH J. et al. (including: ANDREAZZA A., VEGNI G., MERONI C., TRONCON C.) (2004).
Searches for invisibly decaying Higgs bosons with the DELPHI detector at LEP. EUROPEAN PHYSICAL JOURNAL C. vol. 32, pp. 475-492

ABDALLAH J. et al. (including: ANDREAZZA A., VEGNI G., MERONI C., TRONCON C.) (2004).
Measurement of the W-pair Production Cross-section and W Branching Ratios in e+e- Collisions at s**(1/2) = 161-209 GeV. EUROPEAN PHYSICAL JOURNAL C. vol. 34, pp. 127-144

ABDALLAH J. et al. (including: ANDREAZZA A., VEGNI G., MERONI C. TRONCON C.) (2004).
Final results from DELPHI on the searches for SM and MSSM Neutral Higgs bosons. EUROPEAN PHYSICAL JOURNAL C. vol. 32, pp. 145-183

ABDALLAH J. et al. (including: ANDREAZZA A., VEGNI G., MERONI C., TRONCON C.) (2004).
b-tagging in DELPHI at LEP. EUROPEAN PHYSICAL JOURNAL C. vol. 32, pp. 185-208

ABDALLAH J. et al. (including: ANDREAZZA A., VEGNI G., MERONI C., TRONCON C.) (2004).
Measurement of the W-pair Production Cross-section and W Branching Ratios in e+e- Collisions at S**(1/2)= 161-209 GeV. EUROPEAN PHYSICAL JOURNAL C. vol. 34, pp. 127-144

ANDREAZZA A. (2004).
Developments of the ATLAS PIXEL Detector. NUCLEAR INSTRUMENTS AND METHODS IN PHYSICS RESEARCH A. vol. 535, pp. 357-361

AUBERT B. et al. (including: LAZZARO A., LOMBARDO V., PALOMBO F.) (2004).
Measurement of the branching fraction for inclusive B- and anti-B0 decays to flavor-tagged D, D(S) and lambda(C). PHYS. REV. D. vol. 70, pp. 091106/1-091106/8

AUBERT B. et al. (including: LAZZARO A., LOMBARDO V., PALOMBO F.) (2004).
Search for D0 anti-D0mixing using semileptonic decays modes. PHYS. REV. D. vol. 70, pp. 091102/1-091102/8

AUBERT B. et al. (including: LAZZARO A., LOMBARDO V., PALOMBO F.) (2004).
Study of E+ E- —> PI+ PI- PI0 process using initial state radiation with Babar. PHYS. REV. D. vol. 70, pp. 072004/1-072004/8

AUBERT B. et al. (including: LAZZARO A., LOMBARDO V., PALOMBO F.) (2004).
Measurement of neutral B decay branching fraction to K0(S) PI+ PI- FINAL STATES. PHYS. REV. D. vol. 70, pp. 091103/1-091103/8

AUBERT B. et al. (including: LAZZARO A., LOMBARDO V., PALOMBO F.) (2004).
Search for the decay B0 —> J / PSI gamma. PHYS. REV. D. vol. 70, pp. 091104/1-091104/8

AUBERT B. et al. (including: LAZZARO A., LOMBARDO V., PALOMBO F.) (2004).
Search for B-meson decays to two-body final states with A0(980) MESONS. PHYS. REV. D. vol. 70, pp. 111102/1-111102/8

AUBERT B. et al. (including: LAZZARO A., LOMBARDO V., PALOMBO F.) (2004).
Measurement of branching fractions, and CP and isospin asymmetries, for B —> K* gamma. PHYS. REV. D. vol. 70, pp. 112006/1-112006/8

AUBERT B. et al. (including: LAZZARO A., LOMBARDO V., PALOMBO F.) (2004).
Study of B —> D(SJ)(*)+ anti-D(*)decays. PHYS. REV. LETT. vol. 93, pp. 181801/1-181801/7

AUBERT B. et al. (including: LAZZARO A., LOMBARDO V., PALOMBO F.) (2004).
Search for flavor-changing neutral current and lepton-flavor violating decays ofD0 —> L+ L-. PHYS. REV. LETT. vol. 93, pp. 191801/1-191801/7

AUBERT B. et al. (including: LAZZARO A., LOMBARDO V., PALOMBO F.) (2004).
Measurement of the B0 —> PHI K*0 decay amplitudes. PHYS.REV. LETT. vol. 93, pp. 231804/1-231804/7

AUBERT B. et al. (including: LAZZARO A., LOMBARDO V., PALOMBO F.) (2004).
Observation of direct CP violation in B0 —> K+ PI- decays. PHYS. REV. LETT. vol. 93, pp. 131801/1-131801/7

AUBERT B. et al. (including: LAZZARO A., LOMBARDO V., PALOMBO F.) (2004).
Branching fractions and CP asymmetries in B0 —> K+ K- K0(S) AND B+ —> K+ K0(S) K0(S). PHYS. REV. LETT. vol. 93, pp. 181805/1-181805/7

AUBERT B. et al. (including: LAZZARO A., LOMBARDO V., PALOMBO F.) (2004).
Measurement of time-dependent CP-violating asymmetries in B0 —> K*0 GAMMA (K*0 —> K0(S) PI0)decays. PHYS. REV. LETT. vol. 93, pp. 201801/1-201801/7

AUBERT B. et al. (including: LAZZARO A., LOMBARDO V., PALOMBO F.) (2004).
Search for B0 decays to invisible final states and to nu anti-nu gamma. PHYS. REV. LETT. vol. 93, pp. 091802/1-091802/7

AUBERT B. et al. (including: LAZZARO A., LOMBARDO V., PALOMBO F.) (2004).
Study of the decay B0(anti-B0) —> RHO+ RHO-, and constraint on the CKM angle alpha. PHYS. REV. LETT. vol. 93, pp. 231801/1-231801/7

AUBERT B. et al. (including: LAZZARO A., LOMBARDO V., PALOMBO F.) (2004).
Determination of the branching fraction for B —> X(C) L nu decays and of |V(CB)| from hadronic mass and lepton energy moments. PHYS. REV. LETT. vol. 93, pp. 011803/1-011803/7

AUBERT B. et al. (including: LAZZARO A., LOMBARDO V., PALOMBO F.) (2004).
Measurement of the direct CP asymmetry in B —> S gamma decays. PHYS. REV. LETT. vol. 93, pp. 021804/1-021804/7

AUBERT B. et al. (including: LAZZARO A., LOMBARDO V., PALOMBO F.) (2004).
Measurement of CP violating asymmetries in B0 —> K0(S) PI0 decays. PHYS. REV. LETT. vol. 93, pp. 131805/1-131805/7

AUBERT B. et al. (including: LAZZARO A., LOMBARDO V., PALOMBO F.) (2004).
Observation of the decay B —> J PSI eta K and search for X(3872) —> J / PSI eta. PHYS. REV. LETT. vol. 93, pp. 041801/1-041801/7

AUBERT B. et al. (including: LAZZARO A., LOMBARDO V., PALOMBO F.) (2004).
Search for B+- —> [K+- PI+-](D) K+- and upper limit on the—> U amplitude in B+- —> D K+-. PHYS. REV. LETT. vol. 93, pp. 131804/1-131804/7

AUBERT B. et al. (including: LAZZARO A., LOMBARDO V., PALOMBO F.) (2004).
Study of B+- —> J / PSI PI+- and B+- —> J / PSI K+- decays, measurement of the ratio of branching fractions and search for direct CP violation. PHYS. REV.LETT. vol. 92, pp. 241802/1-241802/7

AUBERT B. et al. (including: LAZZARO A., LOMBARDO V., PALOMBO F.) (2004).
Measurements of moments of the hadronic mass distribution in semileptonic B decays. PHYS. REV. D. vol. 69, pp. 111103/1-111103/8

AUBERT B. et al. (including: LAZZARO A., LOMBARDO V., PALOMBO F.) (2004).
Measurement of the electron energy spectrum and its moments in inclusive B —> X E nu decays. PHYS. REV. D. vol. 69, pp. 111104/1-111104/8

AUBERT B. et al. (including: LAZZARO A., LOMBARDO V., PALOMBO F.) (2004).
Limits on the decay rate difference of neutral B mesons and on CP, T, and CPT violation in B0 - anti-B0 oscillation. PHYS. REV. D. vol. 70, pp. 012007/1-012007/8

AUBERT B. et al. (including: LAZZARO A., LOMBARDO V., PALOMBO F.) (2004).
Measurement of the Inclusive Charmless Semileptonic Branching Ratio of B Mesons and Determination of $|V_{ub}|$. PHYS. REV. LETT. vol. 92, pp. 071802/1-071802/7

AUBERT B. et al. (including: LAZZARO A., LOMBARDO V., PALOMBO F.) (2004).
Observation of a Narrow Meson Decaying to $D^+_s pi^0 \gamma$ at a Mass of 2.458 GeV/c^2. PHYS. REV. LETT. vol. 92, pp. 031101/1-031101/7

AUBERT B. et al. (including: LAZZARO A., LOMBARDO V., PALOMBO F.) (2004).
Observation of $B^0 -> omega K^0, B^+ -> eta pi^+,and B^+ -> eta K^+ and Study of Related Decays PHYS. REV. LETT. vol. 92, pp. 061801/1-061801/7

AUBERT B. et al. (including: LAZZARO A., LOMBARDO V., PALOMBO F.) (2004).
Measurement of Branching Fractions and Charge Asymmetries in B^{+-} -> rho^{+-} pi^0 and B^{+-} -> rho^0 pi^{+-} and Search for B^0 -> rho^0 pi^0. PHYS. REV. LETT. vol. 92, pp. 101801/1-101801/7
AUBERT B. et al. (including: LAZZARO A., LOMBARDO V., PALOMBO F.) (2004).
Search for Lepton Flavor Violation in the Decay tau^- -> l^- l^+ l^-$. PHYS. REV. LETT. vol. 92, pp. 121801/1-121801/7

AUBERT B. et al. (including: LAZZARO A., LOMBARDO V., PALOMBO F.) (2004).
Search for the Rare Leptonic Decay B^+ -> mu^+ nu_{mu} PHYS. REV. LETT. vol. 92, pp. 221803/1-221803/7

AUBERT B. et al. (including: LAZZARO A., LOMBARDO V., PALOMBO F.) (2004).
Measurement of the B^+ /B^0 Production Ratio from the Upsilon(4S) Meson Using B^+ -> J/psi K^+ and B^0 -> J/psi K^0_S Decays. PHYS. REV. D. vol. 69, pp. 071101/1-071101/7

AUBERT B. et al. (including: LAZZARO A., LOMBARDO V., PALOMBO F.) (2004).
Study of B^{+-} \rightarrow J/\psi \pi^{+-}$ and $B^{+-} \rightarrow J/\psi K^{+-}$ Decays, Measurement of the Ratio of Branching Fractions and Search for Direct CP Violation. PHYS. REV. LETT. vol. 92, pp. 071802/1-071802/7

AUBERT B. et al. (including: LAZZARO A., LOMBARDO V., PALOMBO F.) (2004).
Limits on the Decay Rate Difference of Neutral B mesons and on CP, T, and CPT Violation in B^0 bar{B^0} Oscillations. PHYS. REV. LETT. vol. 92, pp. 181801/1-181801/7

AUBERT B. et al. (including: LAZZARO A., LOMBARDO V., PALOMBO F.) (2004).
Measurement of the Branching Fraction and Polarization for the Decay B^- -> D^{*0} K^{*-}. PHYS. REV. LETT. vol. 92, pp. 141801/1-141801/7

AUBERT B. et al. (including: LAZZARO A., LOMBARDO V., PALOMBO F.) (2004).
Measurement of the $B \rightarrow X_s l^+ l^-$ Branching Fraction with a Sum over Exclusive Modes. PHYS. REV. LETT. vol. 93, pp. 081802/1-081802/7

AUBERT B. et al. (including: LAZZARO A., LOMBARDO V., PALOMBO F.) (2004).
Measurement of the Ratio of Decay Amplitudes for bar{B} -> J/psi K^{*0} and B -> J/psi K^{*0}. PHYS. REV. LETT. vol. 93, pp. 081801/1-081801/7

AUBERT B. et al. (including: LAZZARO A., LOMBARDO V., PALOMBO F.) (2004).
Searches for B^0 Decays to Combinations of two Charmless Isoscalar Mesons. PHYS. REV. LETT. vol. 93, pp. 181806/1-181806/7

AUBERT B. et al. (including: LAZZARO A., LOMBARDO V., PALOMBO F.) (2004).
Study of B^{+-} -> J/psi pi^{+-} and B^{+-} -> J/psi K^{+-} Decays, Measurements of the Ratio of Branching Fractions and Search for Direct CP Violation. PHYS. REV. LETT. vol. 92, pp. 241822/1-241822/7

AUBERT B. et al. (including: LAZZARO A., LOMBARDO V., PALOMBO F.) (2004).
Measurements of Branching Fractions and CP Violating Asymmetries in B Meson Decays to Charmless Two Body States Containing a K^0. PHYS. REV. LETT. vol. 92, pp. 201802/1-201802/7

AUBERT B. et al. (including: LAZZARO A., LOMBARDO V., PALOMBO F.) (2004).
Measurement of Branching Fractions and Charge Asymmetries in B^{+-} -> rho^{+-} pi^0 and B^{+-} -> \rho^0 pi^{+-}. PHYS. REV. LETT. vol. 93, pp. 051802/1-051802/7

AUBERT B. et al. (including: LAZZARO A., LOMBARDO V., PALOMBO F.) (2004).
Measurement of the Time Dependent CP Asymmetry in the B^0 -> phi K^0 Decay. PHYS. REV. LETT. vol. 93, pp. 071801/1-071801/7

AUBERT B. et al. (including: LAZZARO A., LOMBARDO V., PALOMBO F.) (2004).
Study of High Momentum eta^{prime} Production in B -> eta^{prime} X_s. PHYS. REV. LETT. vol. 93, pp. 061801/1-061801/7

AUBERT B. et al. (including: LAZZARO A., LOMBARDO V., PALOMBO F.) (2004).

Measurement of the Branching Fractions and CP Asymmetry of B^- -> D^0_{CP} K^- Decays with the BaBar Detector. PHYS. REV. LETT. vol. 92, pp. 202002/1-202002/7

AUBERT B. et al. (including: LAZZARO A., LOMBARDO V., PALOMBO F.) (2004).
Measurement of Branching Fractions in B -> phi K and B -> phi pi and Search for Direct CP Violation in B^{+-} -> phi K^{+-}. PHYS. REV. D. vol. 69, pp. 011102/1-011102/8

AUBERT B. et al. (including: LAZZARO A., LOMBARDO V., PALOMBO F.) (2004).
J/psi Production via Initial State Radiation in e^+ e^- -> mu^+ mu^- gamma at an e^+ e^- Center of Mass Energy near 10.6 GeV. PHYS. REV. D. vol. 69, pp. 011103/1-011103/8

AUBERT B. et al. (including: LAZZARO A., LOMBARDO V., PALOMBO F.) (2004).
Measurement of the Branching fraction for B -> D^0 K^{*-}. PHYS. REV. D. vol. 92, pp. 051101/1-051101/8

AUBERT B. et al. (including: LAZZARO A., LOMBARDO V., PALOMBO F.) (2004).
Measurement of the Average ϕ Multiplicity in B meson Decay. PHYS. REV. D. vol. 69, pp. 052005/1-052005/8

AUBERT B. et al. (including: LAZZARO A., LOMBARDO V., PALOMBO F.) (2004).
Observation of a Narrow Meson Decaying to D^+_S pi^0 gamma at a Mass of 2.458 GeV/c^2. PHYS. REV. D. vol. 69, pp. 031102/1-031102/8

AUBERT B. et al. (including: LAZZARO A., LOMBARDO V., PALOMBO F.) (2004).
Measurement of Branching Fractions of Color Suppressed Decays of the \bar{B^0} meson to D^{*0} pi^0, D^{*0} eta, D^{*0} omega, and D^{*0} eta^{prime}. PHYS. REV. D. vol. 69, pp. 032004/1-032004/8

AUBERT B. et al. (including: LAZZARO A., LOMBARDO V., PALOMBO F.) (2004).
Measurement of the Branching Fraction for B^{+-} -> chi_{c0} K^{+-}. PHYS. REV. D. vol. 69, pp. 071103/1-071103/8

AUBERT B. et al. (including: LAZZARO A., LOMBARDO V., PALOMBO F.) (2004).
Measurement of sin^2 beta with Hadronic and Previously Unused Muonic J/psi Decays. PHYS. REV. D. vol. 69, pp. 052001/1-052001/8

AUBERT B. et al. (including: LAZZARO A., LOMBARDO V., PALOMBO F.) (2004).
Search for the Decay B^0 -> p bar{p}. PHYS. REV. D. vol. 69, pp. 091503/1-091503/8

AUBERT B. et al. (including: LAZZARO A., LOMBARDO V., PALOMBO F.) (2004).
B Meson Decays to eta^(prime) K^*, eta^(\prime) rho, eta^(prime) pi^0, omega pi^0, and phi pi^0. PHYS. REV. D. vol. 70, pp. 032006/1-032006/8

AUBERT B. et al. (including: LAZZARO A., LOMBARDO V., PALOMBO F.) (2004).
Branching Fraction Measurements of the Decays B -> eta_c K, where eta_c -> K bar{K} pi and eta_c -> 4\pi$. PHYS. REV. D. vol. 70, pp. 011101/1-011101/8

AVELLINO G. et al. (including:. Mezzadri M.,.Prelz F.). (2004).
The DataGrid Workload Management System: Challenges and Results. JOURNAL OF GRID COMPUTING. vol. 2, pp. 353-367

HEISTER A. et al. (inclusing: RAGUSA F.) (2004).
Measurement of W-pair production in e+e- collisions at centre-of-mass energies from 183 GeV to 209 GeV. EUROPEAN PHYSICAL JOURNAL C. vol. 38, pp. 147-160

HEISTER A. et al. (including: RAGUSA F.) (2004).
Constraints on anomalous QGC in e+e- interactions from 183 GeV to 209 GeV. PHYSICS LETTERS B. vol. 602, pp. 31-40

HEISTER A. et al. (including: RAGUSA F.) (2004).
Studies of QCD at e+e- centre-of-mass energies between 91 GeV and 209 GeV. EUROPEAN PHYSICAL JOURNAL C. vol. 35, pp. 457-486

HEISTER A. et al. (including: RAGUSA F.) (2004).
Two-dimensional analysis of Bose-Einstein correlations in Hadronic Z decays at Lep. EUROPEAN PHYSICAL JOURNAL C. vol. 36, pp. 147-159

HEISTER A. et al. (including: RAGUSA F.) (2004).

Absolute mass lower limit for the lightest neutralino of the MSSM from e+e- data at s**(1/2) up to 209 GeV. PHYSICS LETTERS B. vol. 583, pp. 247-263

RE V. et al. (including: BRENNA E., CITTERIO M., LANNI F., PALOMBO F.) (2004).
Radiation Hardness and Monitoring of the BaBar Vertex Tracker. NUCLEAR INSTRUMENTS AND METHODS IN PHYSICS RESEARCH A. vol. 518, pp. 290-294

RE V. et al. (including: BRENNA E., CITTERIO M., LANNI F., PALOMBO F.) (2004).
Sensor Performance of the BaBar Silicon Vertex Tracker after 4 Years of DataTaking. NUCLEAR INSTRUMENTS AND METHODS IN PHYSICS RESEARCH A. vol. 518, pp. 286-289

SCHAEL S. et al. (including: RAGUSA F.) (2004).
Search for pentaquark states in Z decays. PHYSICS LETTERS B. vol. 599, pp. 1-16

TRONCON C. (2004).
Radiation Hardness Performance of ATLAS Pixel Tracker. NUCLEAR INSTRUMENTS AND METHODS IN PHYSICS RESEARCH A. vol. 530, pp. 65/7

ABDALLAH J. et al. (including: ANDREAZZA A., VEGNI G., MERONI C., TRONCON C.) (2003)
The eta_c(2980) formation in two-photon collisions at LEP energies. EUROPEAN PHYSICAL JOURNAL C. vol. 31, pp. 481-489

ABDALLAH J. et al. (including: ANDREAZZA A., VEGNI G., MERONI C., TRONCON C.) (2003).
Searches for supersymmetric particles in e+e- collisions up to 208 GeV and interpretation of the results within the MSSM. EUROPEAN PHYSICAL JOURNAL C. vol. 31, pp. 421-479

ABDALLAH J. et al. (including: ANDREAZZA A., VEGNI G., MERONI C., TRONCON C.) (2003).
Search for an LSP gluino at LEP with the DELPHI detector. EUROPEAN PHYSICAL JOURNAL C. vol. 26, pp. 505-525

ABDALLAH J. et al. (including: ANDREAZZA A., VEGNI G., MERONI C., TRONCON C.) (2003).
Inclusive b Decays to Wrong Sign Charmed Mesons. PHYSICS LETTERS B. vol. 561, pp. 26-40

ABDALLAH J. et al. (including: ANDREAZZA A., VEGNI G., MERONI C., TRONCON C.) (2003).
A study of the energy evolution of event shape distributions and their means with the DELPHI detector at LEP. EUROPEAN PHYSICAL JOURNAL C. vol. 29, pp. 285-312

ABDALLAH J. et al. (including: ANDREAZZA A., VEGNI G., MERONI C., TRONCON C.) (2003).
Search for supersymmetric particles in light gravitino scenarios and sleptons NLSP. EUROPEAN PHYSICAL JOURNAL C. vol. 27, pp. 153-172

ABDALLAH J. et al. (including: ANDREAZZA A., VEGNI G., MERONI C., TRONCON C.) (2003).
Measurement of Inclusive f1 (1285) and f1 (1420) Production in Z Decays with the DELPHI Detector. PHYSICS LETTERS B. vol. 569, pp. 129-139

ABDALLAH J. et al. (including: ANDREAZZA A., VEGNI G., MERONI C., TRONCON C.) (2003).
Search for Doubly Charged Higgs Bosons at LEP2. PHYSICS LETTERS B. vol. 552, pp. 127-137

ABDALLAH J. et al. (including: ANDREAZZA A., VEGNI G., MERONI C., TRONCON C.) (2003).
Search for B0s - B0s oscillations and a measurement of B0d - B0d oscillations using events with an inclusively reconstructed vertex. EUROPEAN PHYSICAL JOURNAL C. vol. 28, pp. 155-173

ABDALLAH J. et al. (including: ANDREAZZA A., VEGNI G., MERONI C., TRONCON C.) (2003).
Study of Inclusive J/psi Production in Two-Photon Collisions at LEPII with the DELPHI Detector. PHYSICS LETTERS B. vol. 565, pp. 76-86

ABDALLAH J. et al. (including: ANDREAZZA A., VEGNI G., MERONI C., TRONCON C.) (2003).
ZZ production in e+ e- interactions at s**(1/2) = 183 - 209 GeV. EUROPEAN PHYSICAL JOURNAL C. vol. 30, pp. 447-466

ABDALLAH J. et al. (including: ANDREAZZA A., VEGNI G., MERONI C., TRONCON C.) (2003).

Search for resonant sneutrino production at s**(1/2) = 183 to 208 GeV. EUROPEAN PHYSICAL JOURNAL C. vol. 28, pp. 15-26

ABDALLAH J. et al. (including: ANDREAZZA A., VEGNI G., MERONI C., TRONCON C.) (2003).
Measurement of the e+e- -> W+W-gamma Cross-section and Limits on Anomalous Quartic Gauge Couplings with DELPHI. EUROPEAN PHYSICAL JOURNAL C. vol. 31, pp. 139-147

ABDALLAH J. et al. (including: ANDREAZZA A., VEGNI G., MERONI C., TRONCON C.) (2003).
A measurement of the branching fractions of the b-quark into charged and neutral b-hadrons. PHYSICS LETTERS B. vol. 576, pp. 29-42

ANDREAZZA A. (2003).
Performance of ATLAS PIXEL Detector Prototype Modules. NUCLEAR INSTRUMENTS AND METHODS IN PHYSICS RESEARCH A. vol. 513, pp. 103-106

AUBERT B., et al. (including: BATTISTONI G., CARMINATI L., COSTA G., DELMASTRO M., FANTI M., MANDELLI L., MAZZANTI M., TARTARELLI G. F.) (2003).
Performance of The ATLAS Electromagnetic Calorimeter End-cap Module 0. NUCL. INSTRUM. METH. A. vol. 500, pp. 178-201

AUBERT B., et al. (including: BATTTISTONI G., BONIVENTO W., CARMINATI L., CAVALLI D., COSTA G., DELMASTRO M., FANTI M., MANDELLI L., MAZZANTI M., PERINI L., RESCONI S., TARTARELLI G. F.) (2003).
Performance of The ATLAS Electromagnetic Calorimeter Barrel Module 0. NUCL. INSTRUM. METH. A. vol. 500, pp. 202-231 & Erratum-ibid. A517, pp. 399-402

AUBERT B. et al. (including LAZZARO A., LOMBARDO V., PALOMBO F.) (2003).
Measurement of the Branching Fraction for Inclusive Semileptonic B Meson Decays. PHYS. REV. D. vol. 67, pp. 031101/1-031101/8

AUBERT B. et al. (including LAZZARO A., LOMBARDO V., PALOMBO F.) (2003).
A Measurement of the B^0 -> jpsi pi^+ pi^- Branching Fraction. PHYS. REV. LETT. vol. 90, pp. 091801/1-091801/7

AUBERT B. et al. (including LAZZARO A., LOMBARDO V., PALOMBO F.) (2003).
Measurement of the CKM Matrix Element |V_{ub}| with B -> rho e nu Decays. PHYS. REV. LETT. vol. 90, pp. 181801/1-181801/7

AUBERT B. et al. (including LAZZARO A., LOMBARDO V., PALOMBO F.) (2003).
A Study of the Rare Decays B^0 -> D^{*+}_s pi^-$ and B^0 -> D^{*-}_s K^+. PHYS. REV. LETT. vol. 90, pp. 181803/1-181803/7

AUBERT B. et al. (including LAZZARO A., LOMBARDO V., PALOMBO F.) (2003).
Measurement of Branching Fraction and CP Violating Asymmetries in Neutral B Decays to D^{*+} D^{*-}. PHYS. REV. LETT. vol. 90, pp. 221801/1-221801/7

AUBERT B. et al. (including LAZZARO A., LOMBARDO V., PALOMBO F.) (2003).
Evidence for B^+ -> J/psi p bar{lambda} and Search for B^0 -> J/psi p bar{p}. PHYS. REV. LETT. vol. 90, pp. 231801/1-231801/7

AUBERT B. et al. (including LAZZARO A., LOMBARDO V., PALOMBO F.) (2003).
Observation of a Narrow Meson Decaying to D^+_s pi^0 at a mass of 2.32 GeV/c^2. PHYS. REV. LETT. vol. 90, pp. 242001/1-242001/7

AUBERT B. et al. (including LAZZARO A., LOMBARDO V., PALOMBO F.) (2003).
Study of the Time Dependent CP Asymmetry in Neutral B Decays to J/psi pi^0. PHYS. REV. LETT. vol. 91, pp. 061802/1-061802/7

AUBERT B. et al. (including LAZZARO A., LOMBARDO V., PALOMBO F.) (2003).
Observation of the Decay B^{+-} -> pi^{+-} pi^0, Study of B^{+-} -> K^{+-} pi^0, and Search for B^0 -> pi^0 pi^0. PHYS. REV. LETT. vol. 91, pp. 021801/1-021801/7

AUBERT B. et al. (including LAZZARO A., LOMBARDO V., PALOMBO F.) (2003).
Measurements of CP Violating Asymmetries and Branching Fractions in B Meson Decays to eta^{prime} K. PHYS. REV. LETT. vol. 91, pp. 161801/1-161801/7

AUBERT B. et al. (including LAZZARO A., LOMBARDO V., PALOMBO F.) (2003).
Measurements of the Branching Fractions and Charge Asymmetries of Charmless Three Body Charged B Decays. PHYS. REV. LETT. vol. 91, pp. 051801/1-051801/7

AUBERT B. et al. (including LAZZARO A., LOMBARDO V., PALOMBO F.) (2003).
Rare B Decays into States Containing a J/psi Meson and a Meson with s or \bar{s} Quark Content. PHYS. REV. LETT. vol. 91, pp. 071801/1-071801/7

AUBERT B. et al. (including LAZZARO A., LOMBARDO V., PALOMBO F.) (2003).
Search for D^0 bar{D^0} Mixing and a Measurement of the Doubly Cabibbo Suppressed Decay Rate in D^0 -> K pi Decays. PHYS. REV. LETT. vol. 91, pp. 171801/1-171801/7

AUBERT B. et al. (including LAZZARO A., LOMBARDO V., PALOMBO F.) (2003).
Limits on D^0 bar{D^0}Mixing and CP Violation from the Ratio of Lifetimes for Decays to K^- pi^+,K^-K^+ and pi^- pi^+. PHYS. REV. LETT. vol. 91, pp. 121801/1-121801/7

AUBERT B. et al. (including LAZZARO A., LOMBARDO V., PALOMBO F.) (2003).
Observation of a Significant Excess of pi^0 pi^0 Events in B Meson Decays. PHYS. REV. LETT. vol. 91, pp. 241801/1-241801/7

AUBERT B. et al. (including LAZZARO A., LOMBARDO V., PALOMBO F.) (2003).
Measurements of Branching Fractions and CP Violating Asymmetries in B^0 -> rho^{+-} h^{-+}. PHYS. REV. LETT. vol. 91, pp. 201802/1-201802/7

AUBERT B. et al. (including LAZZARO A., LOMBARDO V., PALOMBO F.) (2003).
Measurement of Time Dependent CP Asymmetries and the CP Odd Fraction in the Decay B^0 -> D^{*+} D^{*-}. PHYS. REV. LETT. vol. 91, pp. 131801/1-131801/7

AUBERT B. et al. (including LAZZARO A., LOMBARDO V., PALOMBO F.) (2003).
Rates, Polarizations, and Asymmetries in Charmless Vector Vectory B Meson Decays. PHYS. REV. LETT. vol. 91, pp. 171802/1-171802/7

AUBERT B. et al. (including LAZZARO A., LOMBARDO V., PALOMBO F.) (2003).
Evidence for the Rare Decay B -> K^* l^+ l^- and Measurement of the B -> K l^+ l^- Branching Fraction. PHYS. REV. LETT. vol. 91, pp. 221802/1-221802/7

AUBERT B. et al. (including LAZZARO A., LOMBARDO V., PALOMBO F.) (2003).
Study of Inclusive Production of Charmonium Mesons in B Decays. PHYS. REV. D. vol. 67, pp. 032002/1-032002/8

AUBERT B. et al. (including LAZZARO A., LOMBARDO V., PALOMBO F.) (2003).
Measurement of the B^0 Meson Lifetime with Partial Reconstruction of B^0 -> D^{*-} pi^+ and B^0 -> D^{*-} rho^+ Decays. PHYS. REV. D. vol. 67, pp. 091101/1-091101/8

AUBERT B. et al. (including LAZZARO A., LOMBARDO V., PALOMBO F.) (2003).
Simultaneous Measurement of the B^0 Meson Lifetime and Mixing Frequency with B^0 -> D^{*-} l^+ nu_l Decays. PHYS. REV. D. vol. 67, pp. 072002/1-072002/8

AUBERT B. et al. (including LAZZARO A., LOMBARDO V., PALOMBO F.) (2003).
Measurement of B^0 -> D^{*+} D^{*-} Branching Fractions and B^0 -> D^{*+}_s D^{*-} Polarization with a Partial Reconstruction Technique. PHYS. REV. D. vol. 67, pp. 092003/1-092003/8

AUBERT B. et al. (including LAZZARO A., LOMBARDO V., PALOMBO F.) (2003).
Measurement of the Branching Fractions for the Exclusive Decays of B^0 and B^+ to bar{D^*} D^* K. PHYS.REV. D. vol. 68, pp. 092001/1-092001/8

BARATE R. et al. (including: RAGUSA F., ANDREAZZA A., VEGNI G., MERONI C., TRONCON C.) (2003).
Search for the Standard Model Higgs Boson at LEP. PHYSICS LETTERS B. vol. 565, pp. 61-75

HEISTER A. et al. (including: RAGUSA F.) (2003).

Measurement of the hadronic photon structure function F2(gamma)(x,q**2) in two-photon collisions at Lep. EUROPEAN PHYSICAL JOURNAL C. vol. 30, pp. 145-158

HEISTER A. et al. (including: RAGUSA F.) (2003).
Exclusive production of pion and kaon meson pairs in two photon collisions at Lep. PHYSICS LETTERS B. vol. 569, pp. 140-150

HEISTER A. et al. (including: RAGUSA F.) (2003).
A measurement of the gluon splitting rate into c anti-c pairs in hadronic Z decays. PHYSICS LETTERS B. vol. 561, pp. 213-224

HEISTER A. et al. (including: RAGUSA F.) (2003).
Search for stable hadronizing squarks and gluinos in e+ e- collisions up to S**(1/2)=209 GeV. EUROPEAN PHYSICAL JOURNAL C. vol. 31, pp. 327-342

HEISTER A. et al. (including: RAGUSA F.) (2003).
Measurement of the inclusive D*+- production in gamma gamma collisions at LEP. EUROPEAN PHYSICAL JOURNAL C. vol. 28, pp. 437-449

RE V. et al. (including: BRENNA E., CITTERIO M., LANNI F., PALOMBO F.) (2003).
Status and Future Plans of the BaBar Silicon Vertex Tracker. NUCLEAR INSTRUMENTS AND METHODS IN PHYSICS RESEARCH A. vol. 511, pp. 1-5

Nuclear Physics

Books

BERTSCH R.A., BROGLIA R.A. (2005).
Oscillations in Finite quantum systems. 2nd Edition. pp. 212. CAMBRIDGE UNIVERSITY PRESS, CAMBRIDGE (UNITED KINGDOM).

BRINK D., BROGLIA R.A. (2005).
Superfluidity in nuclei: pairing in finite systems, pp. 378. CAMBRIDGE UNIVERSITY PRESS, CAMBRIDGE (UNITED KINGDOM).

BROGLIA R.A., WINTHER A. (2005).
Heavy Ion Reactions. 2nd Edition. pp. 504. WESTVIEW PRESS.

IORI I., BORTOLOTTI A. (2005).
XLIII International Meeting on Nuclear Physics. RICERCA SCIENTIFICA & EDUCAZIONE PERMANENTE. vol. 124, pp. 387

BROGLIA R.A., COLÒ G., ONIDA G., ROMAN H.E. (2004).
Solid state physics of finite systems: metal clusters, fullerenes, atomic wires. Advanced text in Physics, pp. 234.

SPRINGER-VERLAG, HEIDELBERG-NEW YORK.IORI I. (2004).
XLII International Meeting on Nuclear Physics. RICERCA SCIENTIFICA & EDUCAZIONE PERMANENTE. vol. 123, pp. 378

GADIOLI E. (2003).
Proceedings of the 10-th International conference on nuclear reaction mechanisms. RICERCA SCIENTIFICA ED EDUCAZIONE PERMANENTE, SUPPLEMENTO S122, Università degli Studi di Milano, 680 pp.

IORI I., MORONI A. (2003).
XLI International Meeting on Nuclear Physics. RICERCA SCIENTIFICA & EDUCAZIONE PERMANENTE. vol 120, pp. 388

Patents

BROGLIA R.A., TIANA G. (2005).
Methods for the identification of protein folding inhibitors. EUR 05015597.7. Università degli Studi di Milano.

BROGLIA R.A., TIANA G., PROVASI D. (2005).
A folding inhibitor of HIV-1 Protease as antiviral drug. USA 186924. Universita' degli Studi di Milano.

Articles

BROGLIA R.A., PROVASI D., VASILE F., OTTOLINA G., LONGHI R., TIANA G. (2006).
A folding inhibitor of the HIV-1 Protease. PROTEINS. vol. 62, p. 928

COLACINO S., TIANA G., BROGLIA R.A., COLOMBO G. (2006).
The Determinants of Stability in the Human Prion Protein: Insights into Folding and Misfolding from the Analysis of the Change in the Stabilization Energy Distribution in Different Conditions. PROTEINS. vol. 62, p. 698

DE FILIPPO E., AMORINI F., ANZALONE A., AUDITORE L., BARAN V., BERCEANU I., BLICHARSKA J., BRZYCHCZYK J., BORDERIE B., BOUGAULT R., BRUNO M., CARDELLA C., CAVALLARO S., CHATTERJEE M.B., CHBIHI A. et al. (2006).
Isoscaling in neck fragmentation. ACTA PHYSICA POLONICA. vol. B37, p. 199

GUILLOT J., GALES S., BEAUMEL D., FORTIER S., RICH E., VAN GIAI N., COLO' G., VAN DER BERG A.M., BRANDENBURG S., DAVIDS B., HARAKEH M.N., HUNYADI M., DE HUU M., VAN DER WERF S.Y. et al. (2006).
The (t,3He) reaction at 43 MeV/nucleon on 48Ca and 58Ni: Results and microscopic interpretation. PHYSICAL REVIEW C. vol. 73, p. 014616

PLANETA R., AMORINI F., ANZALONE A., AUDITORE K., BARAN V., BERCEANU I., BLICHARSKA J., BRZYCHCZYK J., BORDERIE B., BOUGAULT R., BRUNO M., CARDELLA C., CAVALLARO S., CHATTERJEE M.B., CHBIHI A. et al. (2006).
Isospin effects studied with the Chimera detector at 35MeV/nucleon. ACTA PHYSICA POLONICA. vol. B37, p. 1001

PODESTA A., TIANA G., MILANI P., MANNO M. (2006).
Early events in insulin fibrillization studied by time-lapse atomic force microscopy. BIOPHYSICAL JOURNAL. vol. 90, p. 589

PODOLYAK Z., GERL J., HELLSTROM M., BECKER F., GLANDINSKI K.A., GORSKA M., KELIC A., KOPATCH Y., MANDAL S., REGAN P.H., SCHMIDT K.H., WALKER P.M., WOLLERSHEIM H.J., BANU A., BENZONI G. et al. (2006).
High angular momentum states populated in fragmentation reactions. PHYSICS LETTERS B. vol. 632, pp. 203-206

PULLIA A., RIBOLDI S., FRANCHI G.M., ZOCCA F. (2006).
Digitized Preamplifiers: a Circuit Structure for Sliding-scale Optimization of the ADC Range. IEEE TRANSACTIONS NUCLEAR SCIENCE. vol. 53, nr. 1, pp. 1-6

AIGINGER H., ANDERSEN V., BALLERINI F., BATTISTONI G., CAMPANELLA M., CARBONI M., CERUTTI F., EMPL A., ENGHARDT W., FASSO A., FERRARI A., GADIOLI E., GARZELLI M.V., LEE K., OTTOLENGHI A. et al. (2005).
The Fluka code: new developments and application to 1 GeV/n iron beam. ADVANCES IN SPACE RESEARCH. vol. 35, pp. 214-222

AL-KHATIB A., SINGH A.K., HUBEL H., BRINGEL P., BURGER A., NEUSSER A., SCHONWASSER G., HAGEMANN C.B., HANSEN C.R., HERSKIND B., SLETTEN G., ALGORA A., DOMBRADI Z., GAL J., KALINKA G. et al. (2005).
High-spin states in 124Ba. ACTA PHYSICA POLONICA. vol. B36, pp. 1029-1032

ALDERIGHI M., AMORINI F., ANZALONE A., ARENA N., AUDITORE L., BASSINI R., BOIANO C., CARDELLA G., CAVALLARO S., CHATTERJEE M.B., D'ANDREA M., DEFILIPPO E., FICHERA F., GERACI E., GIUSTOLISI F. et al. (2005).
Particle identification via pulse shape analysis for large-area silicon detectors of the Chimera array. IEEE TRANSACTIONS NUCLEAR SCIENCE. vol. 52, p. 1624

ALDERIGHI M., AMORINI F., ANZALONE A., CARDELLA G., CAVALLARO S., DE FILIPPO E., GHILARDI D., GUAZZONI P., LA GUIDARA E., LANZANO G., LANZALONE G., MAIOLINO C., PAGANO A., PAPA M., PIRRONE S. et al. (2005).
PRESTO: a computational and storage unit for Chimera DAQ. IEEE TRANSACTIONS NUCLEAR SCIENCE. vol. 52, p. 1673

AMATORI A., TIANA G., SUTTO L., FERKINGHOFF-BORG J., TROVATO A., BROGLIA R.A. (2005).
Design of amino acid sequences to fold into C_alpha-model proteins. JOURNAL OF CHEMICAL PHYSICS. vol. 123, p. 54904

BARRANCO F., BORTIGNON P.F., BROGLIA R.A., COLO' G., SCHUCK P., VIGEZZI E., VINAS X. (2005).
Pairing matrix elements and pairing gaps with bare, effective and induced interactions. PHYSICAL REVIEW C. vol. 72, p. 054314

BECKER F., BANU A., BECK T., BEDNARCZYK P., DOORNENBAL P., GEISSEL H., GERL J., GORSKA M., GRAWE H., GREBOSZ J., HELLSTROM M., KOJOUHAROV I., KURZ N., LOZEVA R., MANDAL S. et al. (2005).
Status of the RISING project at GSI. THE EUROPEAN PHYSICAL JOURNAL A. vol. 25, Supplement 1, p. 719

BEDNARCZYK P., BANU A., BECK T., BECKER F., BENTLEY M.A., BENZONI G., BRACCO A., BURGER A., CAMERA F., DOORNENBAL P., FAHLANDER C., GEISSEL H., GERL J., GORSKA M., GRAWE H. et al. (2005).
Status of the rising project at relativistic energies. ACTA PHYSICA POLONICA B. vol. 36, pp. 1235-1244

BEMMERER D., CONFORTOLA F., LEMUT A., BONETTI R., BROGGINI C., CORVISIERO P., COSTANTINI H., CRUZ J., FORMICOLA A., FULOP Z., GERVINO G., GUGLIELMETTI A., GUSTAVINO G., GYURKY G., IMBRIANI G. et al. (2005).
Feasibility of low-energy radiative-capture experiments at the LUNA underground accelerator facility. EUR. PHYSICAL J. A. vol. 24, pp. 313-319

BENZONI G., BRACCO A., LEONI S., BLASI N., CAMERA F., GRASSI C., MILLION B., PALENI A., PIGNANELLI M., VIGEZZI E., WIELAND O., MATSUO M., DOSSING T., HERSKIND B., HAGEMANN G.B. et al. (2005).
Is the K-quantum number conserved in the order-to-chaos transition region? PHYSICS LETTER B. vol. 615, pp. 160-166

BRACCO A., BENZONI G., LEONI S., BLASI N., CAMERA F., GRASSI C., MILLION B., PALENI A., PIGNANELLI M., VIGEZZI E., WIELAND O., MATSUO M., DOSSING T., HERSKIND B., HAGEMANN G.B. et al. (2005).
Conservation of the K-quantum number in warm nuclei. NUCLEAR PHYSICS A. vol. 752, pp. 227c-230c

BROGLIA R.A. (2005).
Molecular clusters, in ENCYCLOPEDIA OF CONDENSED MATTER PHYSICS, Eds. F. Bassani, J. Liedl and P. Wyder, Elsevier Press, Amsterdam (The Netherlands), pp. 443-453

BROGLIA R.A. (2005).
Nuclear Models and Methods, in ENCYCLOPEDIA OF CONDENSED MATTER PHYSICS, Eds. F. Bassani, J. Liedl and P. Wyder, Elsevier Press, Amsterdam (The Netherlands), pp. 118-131

BROGLIA R.A. (2005).
Nuclei, in ENCYCLOPEDIA OF CONDENSED MATTER PHYSICS, Eds. F. Bassani, J. Liedl and P. Wyder, Elsevier Press, Amsterdam (The Netherlands), pp. 76-86

BROGLIA R.A. (2005).
Protein foldign and aggregation, in ENCYCLOPEDIA OF CONDENSED MATTER PHYSICS, Eds. F. Bassani, J. Liedl and P. Wyder, Elsevier Press, Amsterdam (The Netherlands), pp. 414-418

BROGLIA R.A., TIANA G., SUTTO L., PROVASI D., SIMONA F. (2005).
Design of HIV-1-PR inhibitors which do not create resistance: blocking the folding of single monomers. PROTEIN SCIENCE. vol. 14, p. 2668

BUERGER A., SAITO T., GRAWE H., HUEBEL H., REITER P., GERL J., GORSKA M., WOLLERSHEIM H.J., AL-KHATIB A., BANU A., BECK T., BECKER F., BEDNARCZYK P., BENZONI G., BRACCO A. et al. (2005).
Relativistic Coulomb Excitation of neutron-rich 54,56,58Cr: on the pathway of magicity from N=40 to N=32. PHYSICS LETTER B. vol. 622, p. 29

BURGER A., SAITO T., AL-KHATIB A., BANU A., BECK T., BECKER F., BEDNARCZYK P., BENZONI G., BRACCO A., BRINGEL P., CAMERA F., CLEMENT E., DOORNENBAL P., GEISSEL H., GERL J. et al. (2005).
Relativistic coulomb excitation of 54,56,58Cr. ACTA PHYSICA POLONICA B. vol. 36, pp. 1249-1252

BUTHELEZI E.Z., CERUTTI F., GADIOLI E., STEYN G.F., CONNELL S.H., COWLEY A.A. (2005).
Excitation functions of residues in the interaction of 12C with 103Rh up to an incident energy of 400 MeV. NUCLEAR PHYSICS. vol. A753, pp. 29-52

CAMERA F., KMIECIK M., WIELAND O., BENZONI G., BRACCO A., BRAMBILLA S., CRESPI F., MASON P., MORONI A., MILLION B., LEONI S., MAJ A., STYCZEN J., BREKIESZ M., MECZYNSKI W. et al. (2005).
GDR in hot nuclei: New measurements. ACTA PHYSICA POLONICA B. vol. 36, pp. 1145-1153

CERUTTI F., CLIVIO A., GADIOLI E. (2005).
A semiclassical formula for the reaction cross section of heavy ions. EUROPEAN PHYSICAL JOURNAL. vol. A25, pp. 413-418

DE FILIPPO E., PAGANO A., PIASECKI E., AMORINI F., ANZALONE A., AUDITORE L., BARAN V., BERCEANU I., BLICHARSKA J., BRZYCHCZYK J., BONASERA A., BORDERIE B., BOUGAULT R., BRUNO M., CARDELLA C. et al. (2005).
Dynamical fission in 124Sn+54Ni collision at 35AMeV. PHYSICAL REVIEW. vol. C71, p. 064604

DE FILIPPO E., PAGANO A., WILCZYINSKI J., AMORINI F., ANZALONE A., AUDITORE L., BARAN V., BERCEANU I., BLICHARSKA J., BRZYCHCZYK J., BONASERA A., BORDERIE B., BOUGAULT R., BRUNO M., CARDELLA C. et al. (2005).
Time sequence and time scale of intermediate mass fragment emission. PHYSICAL REVIEW. vol C71, p. 044602

DONATI P., GORI G., BARRANCO F., BROGLIA R.A., VIGEZZI E. (2005).
Effective pairing interaction induced by polarization effects in deformed nuclei. JOURNAL OF PHYSICS G. vol. 31, p. 295

FORTINI A., MAZZOLA M., MINA A., PROVASI D., COLO' G., ONIDA G., ROMAN H.E., BROGLIA R.A. (2005).
The role of quantal fluctuations in the optical response of small metal clusters. JOURNAL OF PHYSICS B. vol. 38, p. 1581

FRACASSO S., COLO' G. (2005).
Fully self-consistent charge-exchange quasiparticle random-phase approximation and its application to isobaric analog resonances. PHYSICAL REVIEW C. vol. 72, p. 064310

GADEA A., MARGINEAN N., CORRADI L., LENZI S.M., UR C.A., FARNEA E., DE ANGELIS G., FIORETTO E., NAPOLI D.R., STEFANINI A.M., SZILNER S., AXIOTIS M., BEHERA B.R., ATINA A.L., RUSU C. et al. (2005).
The CLARA-PRISMA setup installed at LNL: first results. JOURNAL OF PHYSICS G: NUCLEAR AND PARTICLE PHYSICS. vol. 31, p. S1443

GIORGETTI L., VIVERIT L., GORI G., BARRANCO F., VIGEZZI E., BROGLIA R.A. (2005).
Quasi-particle properties of trapped Fermi gases. JOURNAL OF PHYSICS B. vol. 38, p. 949

GORI G., RAMPONI F., BARRANCO F., BORTIGNON P.F., BROGLIA R.A., COLÒ G., VIGEZZI E. (2005).
Attractive and repulsive contributions of medium fluctuations to nuclear superfluidity. PHYSICAL REVIEW C. vol. 72, p. 11302

GRAMEGNA F., BARLINI S., KRAVCHUK V.L., LANCHAIS A.L., WIELAND O., BRACCO A., MORONI A., CASINI G., BENZONI G., BLASI N., BRAMBILLA S., BREKIESZ M., BRUNO M., CAMERA F., CHIARI M. et al. (2005).
Light charged particle emission and the giant dipole resonance in Ce nucleus. ACTA PHYSICA POLONICA B. vol. 36, pp. 1155-1160

GUAZZONI P., ZETTA L., COVELLO A., GARGANO A., GRAW G., HERTENBERGER R., WIRTH H.F., JASKOLA M. (2005).
120Sn homologous levels via the 123Sb(p,?)120Sn reaction: experimental evidence and microscopic calculations. PHYSICAL REVIEW. vol. C72, p. 044604

HADES Collaboration (including: IORI I., BORTOLOTTI A., TARANTOLA A., RIBOLDI S., PULLIA A., BASSINI R., BOIANO C., BRAMBILLA S., BASSI A.) (2005).
Di-electron measurements in C+C reaction at 2 A GeV with HADES. NUCLEAR PHYSICS A. vol. 752, pp. 433-438

HADES Collaboration (including: IORI I., BORTOLOTTI A., TARANTOLA A., RIBOLDI S., PULLIA A., BASSINI R., BOIANO C., BRAMBILLA S., BASSI A.) (2005).
Dilepton analysis in the HADES spectrometer for C+C at 2A GeV. JOURNAL OF PHYSICS G. vol. 31, pp. 231-237

HADES Collaboration (including: IORI I., BORTOLOTTI A., TARANTOLA A., RIBOLDI S., PULLIA A., BASSINI R., BOIANO C., BRAMBILLA S., BASSI A.) (2005).
Probing of in medium hadron structure with HADES. NUCLEAR PHYSICS A. vol. 749, pp. 150c-159c

HAMMOND G., BENTLEY M.A., BECKER F., GREBOSZ J., TAYLOR M.J., BANU A., BARTON C.J., BECK T., BEDNARCZYK P., BRACCO A., BRUCE A.M., BULLOCK L.C., BURGER A., CAMERA F., CHANDLER C. et al. (2005).Spectroscopy of T=3/2 mirror nuclei via two-step fragmentation using rising. ACTA PHYSICA POLONICA B. vol. 36, pp. 1253-1257

IMBRIANI G., COSTANTINI H., FORMICOLA A., VOMIERO A., ANGULO C., BEMMERER D., BONETTI R., BROGGINI C., CONFORTOLA F., CORVISIERO P., CRUZ J., DESCOUVMONT P., FULOP Z., GERVINO G., GUGLIELMETTI A. et al. (2005).
S-factor of N-14(p, gamma)O-15 at astrophysical energies. EUROPEAN PHYSICAL JOURNAL A. vol. 25, pp. 455-466

KMIECIK M., MAJ A., STYCZEN J., BEDNARCZYK P., BREKIESZ M., GREBOSZ J., LACH M., MECZYNSKI W., ZIEBLINSKI M., ZUBER K.,

BRACCO A., CAMERA F., BENZONI G., MILLION B., LEONI S. et al. (2005).
GDR feeding of the highly-deformed band in 42Ca. ACTA PHYSICA POLONICA B. vol. 36, pp. 1169-1174

KURASAWA H., SUZUKI T., BORTIGNON P.F. (2005).
Sum rules of the multiple giant resonance states. PROGRESS OF THEORETICAL PHYSICS. vol. 114, pp. 805-812

LACH M., STYCZEN J., MECZYNSKY W., BEDNARCZYK P., BRACCO A., GREBOSZ J., MAJ A., MERDINGER J.C., SCHULZ N., SMITH M.B., SPOHR K.M., ZIEBLINSKI M. (2005).
Unnatural-parity states in 44Sc. JOURNAL OF THE PHYSICAL SOCIETY OF JAPAN. vol. 25, p. 1

LEONI S., BENZONI G., BRACCO A., BLASI N., CAMERA F., GRASSI C., MASON P., MILLION B., PALENI A., PIGNANELLI M., VIGEZZI E., WIELAND O., MATSUO M., DOSSING T., HERSKIND B. et al. (2005).
Damping mechanisms and order-to-chaos transition in the warm rotating 163Er nucleus. PHYSICAL REVIEW C. vol. 72, p. 034307

LEONI S., BENZONI G., BRACCO A., BLASI N., CAMERA F., GRASSI C., MILLION B., PALENI A., PIGNANELLI M., VIGEZZI E., WIELAND O., MATSUO M., DOSSING T., HERSKIND B., HAGEMANN G.B. et al. (2005).
Warm rotating nuclei: Damping mechanisms and the order-to-chaos transition. ACTA PHYSICA POLONICA B. vol. 36, pp. 1121-1132

MASON P., BENZONI G., BRACCO A., CAMERA F., MILLION B., WIELAND O., LEONI S., SINGH A.K., AL-KHATIB A., HUBEL H., BURGER P., BRINGEL A., NEUSSER A., SCHONWASSER G., NYAKO B.M. et al. (2005).
Evidence for octupole correlations in 124,125Ba. PHYSICAL REVIEW C. vol. 72, p. 064315

MASON P., BENZONI G., BRACCO A., CAMERA F., MILLION B., WIELAND O., LEONI S., SINGH A.K., AL-KHATIB A., HUEBEL A., BRINGEL P., BUERGER A., NEUSSER A., SCHEONWASSER G., HAGEMANN G.B. et al. (2005).
Octupole signatures in 124,125Ba. JOURNAL OF PHYSICS G: NUCLEAR AND PARTICLE PHYSICS. vol. 31, pp. S1729-S1733

MILAZZO P.M., VANNINI G., AGODI C., ALBA R., BELLIA G., COLONNA N., CONIGLIONE R., DEL ZOPP A., FINOCCHIARO P., GRAMEGNA F., IORI I., MAIOLIN C., MARGAGLIOTTI G.V., MASTINU P.F., MIGNECO E. et al. (2005).
Size and asymmetry of the reaction entrance channel:Influence on the probabilityof neck production. NUCLEAR PHYSICS A. vol. 756, pp. 39-53

MUDAU L.J., CERUTTI F., GADIOLI E., MAIRANI A., FORTSCH S.V., BUTHELEZI E.Z., STEYN G.F., CONNELL S.H., LAWRIE J.J., NEVELING R., SMIT F.D., SIDERAS HADDAD E. (2005).
Production of 3He and 6He fragments in the interaction of 12C with 93Nb at 400 MeV. NUCLEAR PHYSICS. vol. A761, pp. 190-199

NYAKO B.M., PAPP F., GAL J., MOLNAR J., TIMAR J., ALGORA A., DOMBRADI Z., KALINKA G., ZOLNAI L., JUHASZ K., SINGH A.K., HUBEL H., AL-KHATIB A., BRINGEL P., BURGER A. et al. (2005).
Search for hyperdeformation in light Xe nuclei. ACTA PHYSICA POLONICA B. vol. 36, pp. 1033-1038

PERU S., BERGER J.F., BORTIGNON P.F. (2005).
Giant resonances in exotic spherical nuclei within the RPA approach with the Gogny force. EUROPEAN PHYSICAL JOURNAL A. vol. 26, pp. 25-32

PULLIA A., MAIOCCHI D., BERTUCCIO G., CACCIA S. (2005).
A compact VLSI dc restorer for multi-channel X-gamma ray detectors. IEEE TRANSACTIONS NUCLEAR SCIENCE. vol. 52, nr. 5, pp. 1643-1646

PULLIA A., ZOCCA F. (2005).
A low-noise preamplifier for gamma-ray sensors with add-on device for large-signal management. NUCLEAR INSTRUMENTS AND METHODS. sect. A, vol. 545, nr. 3, pp. 784-792

ROMOLI M., DI PIETRO M., VARDACI E., DE FRANCESCO A., MAZZOCCO M., BONETTI R., DE ROSA A., GLODARIU T., GUGLIELMETTI A., INGLIMA G., LA COMMARA M., MARTIN B., MASONE V., PARASCANDOLO D., PIERROUTSAKOU D. et al. (2005).
EXODET:
A new approach to detection systems for RIB nuclear physics based on ASIC chips developed for high-energy experiments. IEEE TRANSACTIONS ON NUCLEAR SCIENCE. vol. 52, pp. 1860-1864

STEYN G.F., FORTSCH S.V., LAWRIE J.J., BASSINI R., GADIOLI E., BIRATTARI C., CONNELL S.H. (2005).
Detection of single and resonant projectile fragments in 12C-induced reactions to the continuum. NUCLEAR INSTRUMENTS AND METHODS. vol. A538, pp. 559-573

TAYLOR M.J., HAMMOND G., BENTLEY M.A., BECKER F., GREBOSZ J., BANU A., BARTON C.J., BECK T., BEDNARCZYK P., BRACCO A., BRUCE A.M., BULLOCK L.C., BURGER A., CAMERA F., CHANDLER C. et al. (2005).
Spectroscopy of nuclei approaching the proton drip-line using a secondary-fragmentation technique with the RISING detector array. JOURNAL OF PHYSICS G: NUCLEAR AND PARTICLE PHYSICS. vol. 31, p. S1527

TIANA G., BROGLIA R.A., SUTTO L., PROVASI D. (2005).
Design of a folding inhibitor of the HIV-1 Protease. MOLECULAR SIMULATION. vol. 31, p. 765

TONEV D., DE ANGELIS G., PETKOV P., DEWALD A., GADEA A., PEJOVIC P., BALABANSKI D.L., BEDNARCZYK P., CAMERA F., FITZLER F., MOLLER P., MARGINEAN N., PALENI A., PETRACHE C., ZELL K.O. et al. (2005).
Check for chirality in real nuclei. THE EUROPEAN PHYSICAL JOURNAL A. vol. 25, supp. 1, pp. 447

TONEV T., DE ANGELIS G., PETKOV P.A., BRANT S., FRAUENDORF S., BALABANSKI D.L., PEJOVIC P., BAZZACCO D., BEDNARCZYK P., CAMERA F., FITZLER A., GADEA A., LENZI S., LUNARDI S. et al. (2005).
Transition Probabilities in 134Pr: A Test for Chirality in Nuclear Systems. PHYSICAL REVIEW LETTERS. vol. 96, p. 052501

WIELAND O., BARLINI S., KRAVCHUK V.L., BRACCO A., CAMERA F., GRAMEGNA F., MAJ A., BENZONI G., BLASI N., BRAMBILLA S., BREKIESZ M., BRUNO M., CASINI G., CHIARI M., GERACI E. et al. (2005).
The gamma-decay of the GDR in highly excited Ce nuclei. JOURNAL OF PHYSICS G: NUCLEAR AND PARTICLE PHYSICS. vol. 31, pp. S1973-S1977

WILCZYINSKI J., DE FILIPPO E., PAGANO A., AMORINI F., ANZALONE A., AUDITORE L., BARAN V., BERCEANU I., BLICHARSKA J., BRZYCHCZYK J., BONASERA A., BORDERIE B., BOUGAULT R., BRUNO M., CARDELLA C. et al. (2005).
How to calibrate the time scale of emission of intermediate mass fragments. INTERNATIONAL JOURNAL OF MODERN PHYSICS. vol. E14, p. 353

WOLLERSHEIM H.J., APPELBE D.E., BANU A., BASSINI R., BECK T., BECKER F., BEDNARCZYK P., BEHR K.H., BENTLEY M.A., BENZONI G., BOIANO C., BONNES U., BRACCO A., BRAMBILLA S., BRUNLE A. et al. (2005).
Rare ISotopes INvestigation at GSI (RISING) using gamma-ray spectroscopy at relativistic energies. NUCLEAR INSTRUMENTS AND METHODS A. vol. 537, pp. 637-657

ANDERSEN V., BALLARINI F., BATTISTONI G., CAMPANELLA M., CARBONI M., CERUTTI F., EMPL A., FASS A., FERRARI A., GADIOLI E., GARZELLI M.V., LEE K., OTTOLENGHI A., PELLICCIONI M., PINSKY L.S. et al. (2004).
The Fluka code for space applications: recent developments. ADVANCES IN SPACE RESEARCH. vol. 34, pp. 1302-1310

BARONI S., ARMATI M., BARRANCO F., BROGLIA R.A., COLO' G., GORI G., VIGEZZI E. (2004).
Correlation energy contribution to nuclear masses. JOURNAL OF PHYSICS G. vol. 30, p. 1353

BARRANCO F., BROGLIA R.A., COLO' G., GORI G., VIGEZZI E., BORTIGNON P.F. (2004).
Many-body effects in nuclear structure. EUROPEAN PHYSICAL JOURNAL A. vol. 21, p. 57

BATTISTONI G., CAVINATO M., CERUTTI F., CLIVIO A., FABRICI E., GADIOLI E., GADIOLI ERBA E., GARZELLI M.V., MAIRANI A., FERRARI A., BALLERINI F., OTTOLENGHI A., EMPL A., PINSKY L., FASS A. et al. (2004).
Heavy ion interactions from Coulomb barrier to some GeV/n: Boltzmann master equation theory and Fluka code performances. BRAZILIAN JOURNAL OF PHYSICS. vol. 34, pp. 897-900

BEDNARCZYK P., STYCZEN J., BRACCO A., CURIEN D., GREBOSZ J., LACH M., MAJ A., MERDINGER J.C., MECZYNSKI W., NOWACKI F., SMITH M.B., SPOHR K., VIVIEN J.P., ZEBLINSKI M. (2004).
Collectivity and single-particle degrees of freedom - Studies of light f(7/2) nuclei at EUROBALL IV and recoil filter detector. EUROPEAN PHYSICAL JOURNAL A. vol. 19, pp. 173-185

BOIANO C., BASSINI R., PULLIA A., PAGANO A. (2004).
Wide-dynamic-range fast preamplifier for pulse shape analysis of signals from high-capacitance detectors. IEEE TRANSACTIONS NUCLEAR SCIENCE. vol. 51, nr. 5, pp. 1931-1935

BROGLIA R.A., TIANA G., PROVASI D. (2004).
Simple model of protein folding and of non-conventional drug desig. JOURNAL OF PHYSICS-CONDENSED MATTER. vol. 16, p. R111

BUTHELEZI E.Z., AARDANEH K., STEYN G.F., GADIOLI E., COWLEY A.A., ALBERTINI F., CERUTTI F., NORTIER F.M., VAN DER WALT T.N., CONNELL S. (2004).
Isobaric yields and radiochemistry of near-target residues in the interaction of 12C and 16O with 103Rh at an incident energy of 400 MeV. JOURNAL OF RADIOANALYTICAL AND NUCLEAR CHEMISTRY. vol. 258, pp. 649-658

BUTHELEZI E.Z., GADIOLI E., STEYN G.F., ALBERINI F., BIRATTARI C., CABINATO M., CERUTTI F., CONNELL S.H., COWLEY A.A., FABRICI E., GADIOLI ERBA E. (2004).
Incomplete fusion of projectile fragments in the interaction of 12C with 133Rh up to 33 MeV / nucleon. NUCLEAR PHYSICS A. vol. 734C, pp. 553-556

CINAUSERO M., RIZZI V., VIESTI G., FABRIS D., LUNARDON M., MORETTO S., NEBBIA G., PESENTE S., BARBUI M., FIORETTO E., PRETE G., BRACCO A., CAMERA F., MILLION B., LEONI S. et al. (2004).
Double Giant Dipole Resonance in hot nuclei. NUCLEAR PHYSICS A. vol. 731, pp. 202-207

COLO' G., VAN GIAI N., MEYER J., BENNACEUR K., BONCHE P. (2004).
Microscopic determination of the nuclear incompressibility within the non-relativistic framework. PHYSICAL REVIEW C. vol. 70, p. 024307

DAIDONE I., SIMONA F., ROCCATANO D., BROGLIA R.A., TIANA G., COLOMBO G., DI NOLA A. (2004).
Beta-hairpin conformation of fibrillogenic peptides: structure and alpha-beta transition mechanism revealed by molecular dynamics simulations. PROTEINS. vol. 57, p. 198

FORMICOLA A., IMBRIANI G., COSTANTINI H., ANGULO C., BEMMERER D., BONETTI R., BROGGINI C., CORVISIERO P., CRUZ J., DESCOUVEMONT P., FULOP Z., GERVINO G., GUGLIELMETTI A., GUSTAVINO G., GYURKY G. et al. (2004).
Astrophysical S-factor of 14N(p, ?) 15O. PHYSICs LETTERS B. vol. 591, pp. 61-68

GADEA A., NAPOLI D.R., DE ANGELIS G., MENEGAZZO R., STEFANINI A.M., CORRADI L., AXIOTIS M., BERTI L., FIORETTO E., KROELL T., LATINA A., MARGINEAN N., MARON G., MARTINEZ T., ROSSO D., et al. [The EUROBALL and PRISMA-2 Collaboration] (2004).
Coupling a CLOVER detector array with the PRISMA magnetic spectrometer. EUROPEAN PHYSICAL JOURNAL A. vol. 20, pp. 193-197

GERACI E., ALDERIGHI M., ANZALONE A., AUDITORE L., BARAN V., BARNA R., BARTOLUCCI M., BERCEANU I., BLICHARSKA J., BONASERA A., BORDERIE B., BOUGAULT R., BRUNO M., BRZYCHCZYK J., CARDELLA C. et al. (2004).
Isotope correlations as a probe for freeze-out characterization: central 124Sn+64Ni, 112 Sn+58Ni collisions. NUCLEAR PHYSICS A. vol. 734, p. 524

GERACI E., BRUNO M., D'AGOSTINO M., DE FILIPPO E., PAGANO A., VANNINI G., ALDERIGHI M., ANZALONE A., AUDITORE L., BARAN V., BARNA R., BARTOLUCCI M., BERCEANU I., BLICHARSKA J., BONASERA A. et al. (2004).
Isoscaling in central 124Sn+64Ni, 112 Sn+58Ni collisions at 35 AMeV. NUCLEAR PHYSICS A. vol. 732, p. 173

GLADNISHKIA A., PODOLYAK K.A., REGAN Z.S., GERL P.H., HELLSTROM J., KOPATCH M., MANDAL Y., GORSKA S., PAGE M., WOLLERSHEIM R.D., BANU H.J., BENZONI A., BOARDMAN G., LA COMMARA H., EKMAN M. et al. (2004).
Angular momentum population in the projectile fragmentation of 238U at 750 MeV/nucleon. PHYSICAL REVIEW C. vol. 69, p. 24617

GORI G., BARRANCO F., VIGEZZI E., BROGLIA R.A. (2004).
Parity inversion and breakdown of shell closure in Be isotopes. PHYSICAL REVIEW C. vol. 69, p. 041302(R)GORINI G., PERELLI-CIPPO E., TARDOCCHI M., ANDREANI C., D'ANGELO A., PIETROPAOLO A., SENESI R., IMBERTI S., BRACCO A., PREVITALI E., PESSINA G., RHODES N.J., SCHOONEVELD E.M. (2004).
The resonant detector and its application to epithermal neutron spectroscopy. NUCLEAR INSTRUMENTS & METHODS. vol. 529, p. 293

GUAZZONI P., ZETTA L., COVELLO A., GARGANO A., GRAW G., HERTENBERGER R., WIRTH H.-F., JASKOLA M. (2004).
High resolution study of the the 116Sn(p,t) 114Sn reaction and shell model structure of 114Sn. PHYSICAL REVIEW C. vol. 69, p. 024619

HADES Colaboration (including: IORI I., BORTOLOTTI A., TARANTOLA A., RIBOLDI S., PULLIA A., BASSINI R., BOIANO C., BRAMBILLA S., BASSI A.) (2004).
Particle identification at HADES NUCLEAR. PHYSICS A. vol. 734, pp. 78-81

HADES Collaboration (including: IORI I., BORTOLOTTI A., TARANTOLA A., RIBOLDI S., PULLIA A., BASSINI R., BOIANO C., BRAMBILLA S., BASSI A.) (2004).
Charged hadrons and leptons identification at HADES. ACTA PHYSICA SLOVACA. vol. 54, pp. 375-384

HADES Collaboration (including: IORI I., BORTOLOTTI A., TARANTOLA A., RIBOLDI S., PULLIA A., BASSINI R., BOIANO C., BRAMBILLA S., BASSI A.) (2004).
Dielectron spectrometry with HADES. NUCLEAR PHYSICS NEWS. vol. 14, pp. 27-33

HADES Collaboration (including: IORI I., BORTOLOTTI A., TARANTOLA A., RIBOLDI S., PULLIA A., BASSINI R., BOIANO C., BRAMBILLA S., BASSI A.) (2004).
Study of e+,e- production in elementary and nuclear collisions near production threshold with HADES. PROGRESS IN PARTICLE AND NUCLEAR PHYSICS. vol. 53, pp. 49-58

HADES Collaboration (including: IORI I., BORTOLOTTI A., TARANTOLA A., RIBOLDI S., PULLIA A., BASSINI R., BOIANO C., BRAMBILLA S., BASSI A.) (2004).
Studying in-medium Hadron Properties with HADES. ACTA PHISICA POLONICA B. vol. 35, pp. 1119-1129

IMBRIANI G., COSTANTINI H., FORMICOLA A., BEMMERER D., BONETTI R., BROGGINI C., CORVISIERO P., CRUZ J., FULOP Z., GERVINO G., GUGLIELMETTI A., GUSTAVINO G., GYURKY G., JESUS A.P., JUNKER M. et al. (2004).
The bottleneck of CNO burning and the age of Globular Clusters. ASTRONOMY AND ASTROPHYSICS. vol. 420, pp. 625-629

JENSEN D.R., HAGEMANN G.B., HAMAMOTO I., HERSKIND B., SLETTEN G., WILSON J.N., ODEGARD S.W., SPOHR K.H., HUBEL H., BRINGEL P., NEUSSER A., SCHONWASSER G., SINGH A.K., MA W.C., AMRO H. et al. (2004).
Coexisting wobbling and quasiparticle excitations in the triaxial potential well of 163Lu. EUROPEAN PHYSICAL JOURNAL A. vol. 19, pp. 173-185

KMIECIK M., MAJ A., MILLION B., BREKIESZ M., KROLAS W., MECZYNSKI W., STYCZEN J., ZIEBLINSKI M., BRACCO A., CAMERA F., BENZONI G., LEONI S., WIELAND O., BRAMBILLA S., HERSKIND B. et al. (2004).
Probing Nuclear Shapes Close to the Fission Limit with the Giant Dipole Resonance in 216Rn. PHYSICAL REVIEW C. vol. 70, p. 064317

KROLL T.H., BAZZACCO D., VENTURELLI R., QUINTANA ARNES B., UR C.A., BELLATO M., ISOCRATE R., MANEA C.H., MENEGAZZO R., PAVAN P., ROSSI ALVAREZ C., FARNEA E., GADEA A. et al. (2004).
Gamma-ray tracking with the MARS detector. THE EUROPEAN PHYSICAL JOURNAL A. vol. 20, p. 205

LEONI S., MATSUO M., BRACCO A., BENZONI G., BLASI N., CAMERA F., GRASSI C., MILLION B., PALENI A., PIGNANELLI M., VIGEZZI E., WIELAND O., DSSING T., HERSKIND B., HAGEMANN A. et al. (2004).
Compound and rotational damping in warm deformed rare-Earth nuclei. PHYSICAL REVIEW LETTERS. vol. 93, p. 022501

MAJ A., KMIECIK M., BREKIESZ M., GREBOSZ J., MECZYNSKI W., STYCZEN J., ZIEBLINSKI M., ZUBER K., BRACCO A., CAMERA F., BENZONI G., MILLION B., BLASI N., BRAMBILLA S., LEONI S. et al. (2004).
Search for the Jacobi shape transition in light nuclei. EUROPEAN PHYSICAL JOURNAL A. vol. 20, pp. 165-166

MAJ A., KMIECIK M.,BRACCO A., CAMERA F., BEDNARCZYK P., HERSKIND B., BRAMBILLA S., BENZONI G., BREKIESZ M., CURIEN D., DE ANGELIS G., FARNEA E., GREBOSZ J., KICINSKA-HABIOR A. et al. (2004).
Evidence for the Jacobi shape transition in hot 48Ti. NUCLEAR PHYSICS A. vol. 731, pp. 319-326

MATSUO M., DOSSING T., BRACCO A., HAGEMANN G.B., HERSKIND B., LEONI S., VIGEZZI E. (2004).
Violation and persistence of the K-quantum number in warm rotating. NUCLEAR PHYSICS A. vol. 736, pp. 241-254

MILAZZO P.M., MARGAGLIOTTI G.V., RUI R., SISTO M., VANNINI G., BRUNO M., D'AGOSTINO M., AGODI C., ALBA R., BELLIA G., CONIGLIONE R., DEL ZOPPO A., FINOCCHIARO P., MAIOLINO C., MIGNECO E. et al. (2004).
The reaction entrance channel and isotopic composition of fragments in a dynamical and statistical multifragmentation regime. BRAZIL JOURNAL OF PHYSICS. vol. 34, pp. 929-932

MILLION B., BRACCO A., BENZONI G., LEONI S., CAMERA F., WIELAND O., MAJ A., KMIECIK M., GADEA A., HERSKIND B. (2004).
Study of thermally excited nuclei through E1 and E2 decay from collective modes. EUROPEAN PHYSICAL JOURNAL A. vol. 20, pp. 157-162

PAGANO A., ALDERIGHI M., AMORINI F., ANZALONE A., AUDITORE L., BARAN V., BARNA R., BARTOLUCCI M., BERCEANU I., BLICHARSKA J., BONASERA A., BORDERIE B., BOUGAULT R., BRUNO M., BRZYCHCZYK J. et al. (2004).
Fragmentation studies with the CHIMERA detector at LNS in Catania: recent progress. NUCLEAR PHYSICS A. vol. 734, p. 504

PULLIA A., BOIANO C., BASSINI R., PASCOVICI G. (2004).
Active reset of digitized preamplifiers for ionizing-radiation sensors. IEEE TRANSACTIONS NUCLEAR SCIENCE. vol. 51, nr. 3, pp. 831-835

PULLIA A., ISOCRATE R., VENTURELLI R., BAZZACCO D., BASSINI R., BOIANO C. (2004).
Characterization of HPGe-segmented detectors from noise measurements. IEEE TRANSACTIONS NUCLEAR SCIENCE. vol. 51, nr. 6, pp. 3086-3089

PULLIA A., RIBOLDI S. (2004).
Time-domain Simulation of electronic noises. IEEE TRANSACTIONS NUCLEAR SCIENCE. vol. 51, nr. 4, pp. 1817-1823

RAIOLA F., GANG L., BONOMO C., GYURKY G., ALIOTTA M., BECKER H.W., BONETTI R., BROGGINI C., CORVISIERO P., D'ONOFRIO A., FULOP Z., GERVINO G., GIALANELLA L., JUNKER M., PRATI P. et al. (2004).
Enhanced electron screening in d(d,p)t for deuterated metals. EUROPEAN PHYSICAL JOURNAL A. vol. 19, pp. 283-287

ROMOLI M., VARDACI E., DI PIETRO M., DE FRANCESCO A., DE ROSA A., INGLIMA G., LA COMMARA M., MARTIN B., PIERROUTSAKOU D., SANDOLI M., MAZZOCCO M., GLODARIU T., SCOPEL P., SIGNORINI C., BONETTI R. et al. (2004).
Measurements of 17F scattering by 208Pb with a new type of large solid angle detector array. PHYSICAL REVIEW C. vol. 69, pp. 064614-1-064614-8

ROSSE B., STEZOWSKI O., MEYER M., PREVOST A., REDON N., STYCZEN J., BREKIESZ M., GREBOSZ J., MAJ A., MECZYNSKI W., PAWLAT T., ZIEBLINSKI M., ZUBER K., BEDNARCZYK P., CURIEN D. et al. (2004).
Structure of polonium isotopes at high spin with RFD plus EUROBALL IV. INTERNATIONAL JOURNAL OF MODERN PHYSICS E NUCLEAR PHYSICS. vol. 13, p. 47

SAPIENZA P., CONIGLIONE R., COLONNA M., AGODI C., ALBA R., BELLIA G., DELZOPPO A., FINOCCHIARO P., GRECO V., LOUKACHINE K., MAIOLINO C., MIGNECO E., PIATTELLI P., SANTONOCITO D., COLONNA N. et al. (2004).
Energetic particle emission and nuclear dynamics around the Fermi energy. NUCLEAR PHYSICS A. vol. 734, pp. 601-604

SARCHI D., BORTIGNON P.F., COLO' G. (2004).Dipole states in stable and unstable nuclei. PHYSICS LETTERS B. vol. 601, p. 27

SCHONWASSER G., NENOFF N., HUBEL H., HAGEMANN G.B., BEDNARCZYK P., BENZONI G., BRACCO A., BRINGEL P., CHAPMAN R., CURIEN D., DOMSCHEIT J., HERSKIND B., JENSEN D.R., LEONI S., LO BIANCO G. et al. (2004).
Coexisting normal and triaxial superdeformed structures in 165Lu. NUCLEAR PHYSICS A. vol. 735, pp. 393-424

SIMONA F., TIANA G., BROGLIA R.A., COLOMBO G. (2004).
Modelling the alpha-helix to beta-hairpin transition mechanism and the formation of oligometric aggregates of the fibrillogenic peptide A-beta(12-28). JOURNAL OF MOLECULAR GRAPHICS & MODELLING. vol. 23, p. 263

STANOIU M., AZAIEZ F., DOMBRADI Z., SORLIN O., BROWN B.A., BELLEGUIC M., SOHLER D., SAINT LAURENT M.G., PENIONZHKEVICH Y., SLETTEN G., BORCEA C., BOURGEOIS C., BRACCO A., DAUGAS J.M., DLOUHY Z. et al. (2004).
N=14 and 16 shell gaps in neutron-rich oxygen isotopes. PHYSICAL REVIEW C. vol. 69, p. 034312

STANOIU M., AZAIEZ F., DOMBRADI Z., SORLIN O., BROWN B.A., BELLEGUIC M., SOHLER D., SAINT LAURENT M.G., PENIONZHKEVICH Y., SLETTEN G., BORCEA C., BOURGEOIS C., BRACCO A., DAUGAS J.M., DLOUHY Z. et al. (2004).
Study of neutron rich carbon and oxygen nuclei up to drip line. NUCLEAR PHYSICS A. vol. 746, p. 135c

TARDOCCHI M., PIETROPAOLO A., ANDREANI C., BRACCO A., D'ANGELO A., GORINI G., IMBERTI S., SENESI R., RHODES N.J., SCHOONEVELD E.M. (2004).
Cadmium-Zinc-Telluride photon detector for epithermal neutron spectroscopy-pulse height response. NUCLEAR INSTRUMENTS AND METHODS A. vol. 526, p. 477

TIANA G., COLOMBO M., PROVASI D., BROGLIA R.A. (2004).
Deriving amino acid contact potentials from their apparence frequencies in proteins: an inverse thermodynamical problem. JOURNAL OF PHYSICS-CONDENSED MATTER. vol. 16, p. 2551

TIANA G., DOKHOLYAN N.V., BROGLIA R.A., SHAKHNOVICH E.I. (2004).
The evolution dynamics of model proteins. JOURNAL OF CHEMICAL PHYSICS. vol. 121, p. 2381

TIANA G., SHAKHNOVICH B.E., DOKHOLYAN N., SHAKHNOVICH E.I. (2004).
Imprint of evolution on protein structures. PROCEEDINGS OF THE NATIONAL ACADEMY OF SCIENCES OF THE UNITED STATES OF AMERICA. vol. 101, p. 2846

TIANA G., SIMONA F., BROGLIA R.A., COLOMBO G. (2004).
Thermodynamics of beta-amyloid fibril formation. JOURNAL OF CHEMICAL PHYSICS. vol. 120, p. 8307

TIANA G., SIMONA F., DE MORI G.M.S., BROGLIA R.A., COLOMBO G. (2004).
Understanding the determinants of stability and folding of small globular proteins from their energetics. PROTEIN SCIENCE. vol. 13, p. 113

ANGELINI B., APICELLA M.L., APRUZZESE G., BARBATO E., BERTOCCHI A., BRACCO G., BRUSCHI A., BUCETI G., BURATTI P., CARDINALI A., CARRARO L., CASTALDO C., CENTIOLI C., CESARIO R., CIRANT S. et al. (2003).
Overview of the FTU results. NUCLEAR FUSION. vol. 43, p. 1632

BECKER B., ALBERTINI F., GADIOLI E., STEYN G.F., CAVINATO M., CONNELL S.H., COWLEY A.A., FABRICI E., FORTSCH S.V., GADIOLI ERBA E., LAWRIE J.J., SIDERAS HADDAD E. (2003).
Emission of Li, 7,9Be and B fragments in the interaction of 12C with 93Nb between 200 and 400 MeV. EUROPEAN PHYSICAL JOURNAL. vol. A18, pp. 639-644

BECKER B., ALBERTINI F., GADIOLI E., STEYN G.F., CAVINATO M., CONNELL S.H., COWLEY A.A., FABRICI E., FORTSCH S.V., GADIOLI ERBA E., LAWRIE J.J., SIDERAS HADDAD E. (2003).
Emission of Li, 7,9Be and B fragments in the interaction of 12C with 93Nb between 200 and 400 MeV. EUROPEAN PHYSICAL JOURNAL. vol. A18, pp. 639-644

BENZONI G., BRACCO A., CAMERA F., LEONI S., MILLION B., WIELAND O., BLASI N., PIGNANELLI M., MAJ A., KMIECIK M., HERSKIND B., HAGEMANN G.B., WILSON J., LO BIANCO G., PETRACHE C. et al. (2003).
Study of K selection rules in warm rotating nuclei. ACTA PHYSICA POLONICA B. vol. 34, p. 2221

BONNECAZE A., BRACCO A.D., DOUGHERTY S.T., NOCHEFRANCA L.R., SOLE P. (2003).
Cubic self-dual binary codes. IEEE TRANSACTIONS ON INFORMATION THEORY. vol. 49, p. 2253

BRACCO A. (2003).
Gamma decay from the GDR in highly rotating nuclei at low temperature. ACTA PHYSICA POLONICA B. vol. 34, p. 2163

BROGLIA R.A., TIANA G., BERERA R. (2003).
Resistance proof, folding-inhibitor drugs. JOURNAL OF CHEMICAL PHYSICS. vol. 118, p. 4754

CAMERA F., BRACCO A., NANAL V., CARPENTER M.P., DELLA VEDOVA F., LEONI S., MILLION B., MANTOVANI S., PIGNANELLI M., WIELAND O., BACK B.B., HEINZ A.M., JANSSENS R.V.F., JENKINS D., KHOO T.L. et al. (2003).

Radiative fusion from very symmetric reactions: the giant dipole resonance in the 197Au nucleus. PHYSICS LETTER B. vol. 560, p. 155

COLO' G., LENZI S.M., MAQUEDA E.E., VITTURI A. (2003).
Cross sections for the excitation of isovector charge-exchange resonances in 208Tl. PHYSICAL REVIEW C. vol. 67, p. 044306

D'AGOSTINO M., BRUNO M., GULMINELLI F., BOUGAULT R., CANNATA F., CHOMAZ P.H., GRAMEGNA F., IORI I., LE NEINDRE N., MARGAGLIOTTI G.V., MORONI A., VANNINI G., WIELECZKO J.P. (2003).
Critical-like behaviours in central and peripheral collisions: a comparative analysis. NUCLEAR PHYSICS A. vol.724, pp. 455-476

DE ANGELIS G., BRACCO A., CURIEN D. (2003).
The EUROBALL gamma ray detector array. EUROPHYSICS NEWS. vol. 34, p. 181

FARNEA E., DE ANGELIS G., GADEA A., BIZZETI P.G., DEWALD A., EBERTH G., COLO' G., GELLETLY W., KACI M.A., KINTZ N., KLUG T., KROLL T.H., LENZI S.M., LUNARDI S., MARGINEAN N. et al. (2003).
Isospin mixing in the 64Ge nucleus. PHYSICS LETTERS B. vol. 551, pp. 56-62

FORMICOLA A., IMBRIANI G., JUNKER M., BEMMERER D., BONETTI R., BROGGINI C., CASELLA C., CORVISIERO P., COSTANTINI H., GERVINO G., GUSTAVINO G., LEMUT A., PRATI P., ROCA V., ROLFS C. et al. (2003).
The LUNA II 400 kV accelerator. NUCLEAR INSTRUMENTS AND METHODS A. vol. 507, pp. 609-616

GADEA A., DE ANGELIS G., FARNEA E., MARGINEAN N., AXIOTIS M., MARTINEZ T., NAPOLI D.R., KROELL T.H., DE POLI M., SPOLAORE P., FIORETTO E., LENZI S.M., MAGLIONE E., UR C., LUNARDI S. et al. (2003).
Spectroscopy of Heavy N=Z Nuclei with GASP and EUROBALL. ACTA PHYSICA POLONICA B. vol. 34, p. 2429

GADIOLI E. (2003).
On the study of inclusive heavy ion reactions. FIZIKA. vol. B12, pp. 1-10

GADIOLI E., STEYN G. F., ALBERTINI F., BIRATTARI C., CAVINATO M., CONNELL S. H., COWLEY A. A., FABRICI E., FORTSCH S. V., GADIOLI ERBA E., LAWRIE J. J., PIGNI M., SELLSCHOP J. P. F., SIDERAS HADDAD E. et al. (2003).
Emission of intermediate mass fragments in the interaction of 16O with 59Co, 93Nb and 197Au. EUROPEAN PHYSICAL JOURNAL. vol. A17, pp. 195-212

GIAMBRONE G., SCHEIT S., BARRANCO F., BORTIGNON P.F., COLO' G., SARCHI D., VIGEZZI E. (2003).
Collective excitations in superfluid nuclei with finite-range interactions. NUCLEAR PHYSICS A. vol. 726, pp. 3-36

GLADNISHKI A., PODOLYAK Z.S., GERL J., HELLSTROM M., KOPATCH Y., MANDAL S., GORSKA M., REGAN P.H., WOLLERSHEIM H.J., BANU A., BENZONI G., BOARDMAN H., LA COMMARA M., EKMAN J., FAHLANDER C. et al. (2003).
Isomer spectroscopy in the neutron-deficient lead region following projectile fragmentation. ACTA PHYSICA POLONICA B. vol. 34, p. 2395

GRAMEGNA F., MASTINU P. F., VANNUCCI L., MORONI A., BRACCO A., CAMERA F., MILLION B., WIELAND O., BENZONI G., LEONI S., AIROLDI A., SACCHI A., GALBUSERA E., GIUSSANI A., OTTOLENGHI A. et al. (2003).
New perspectives for studies of reaction mechanisms at low-medium energies. ACTA PHYSICA POLONICA. vol. B34, pp. 2353-2362

GRAMEGNA F., MASTINU P.F., VANNUCCI L., BOSCOLO MARCHI E., CHERUBINI R., MORONI A., BRACCO A., CAMERA F., MILLION B., WIELAND O., BENZONI G., LEONI S., AIROLDI A., SACCHI R., GALBUSERA E. et al. (2003).
New perspectives for studies of reaction mechanisms at low-medium energies. ACTA PHYSICA POLONICA B. vol. 34, p. 2353

HADES Collaboration (including: IORI I., BORTOLOTTI A., TARANTOLA A., RIBOLDI S., PULLIA A.,BASSINI R., BOIANO C., BRAMBILLA S., BASSI A.) (2003).
Measurement of Po induced lepton with the HADES RICH detector. NUCLEAR INSTRUMENT & METHODS A. vol. 502, pp. 305-309

HERSKIND B., BENZONI G., WILSON J.N., DOSSING T., HAGEMANN G.B., SLETTEN G., RONN HANSEN C., JENSEN D.R., BRACCO A., CAMERA F., LEONI S., MASON P., WIELAND O., MAJ A., BREKIESZ M. et al. (2003).
Hunting grounds for Jacobi transitions and hyperdeformations. ACTA PHYSICA POLONICA B. vol. 34, p. 2467

JENSEN M.H., SNEPPEN K., TIANA G. (2003).
Sustained oscillations and time delays in gene expression of protein Hes1. FEBS LETTERS. vol. 541, p. 176

LACH M., STYCZEN J., MECZYNSKI W., BEDNARCZYK P., BRACCO A., GREBOSZ J., MAJ A., MERDINGER J.C., SCHULZ N., SMITH M.B., SPOHR K.M., VIVIEN J.P., ZIEBLINSKI M. (2003).
In-beam gamma-ray spectroscopy of 42Ca. EUROPEAN PHYSICAL JOURNAL A. vol. 16, p. 39

PULLIA A. (2003).
Additivity theorem for constrained optimum filters in the presence of colored noise. NUCLEAR INSTRUMENTS AND METHODS. sect. A, vol. 512, pp. 191-198

SCHONWASSER G., HUBEL H., HAGEMANN G.B., BEDNARCZYK P., BENZONI G., BRACCO A., BRINGEL P., CHAPMAN R., CURIEN D., DOMSCHEIT J., HERSKIND B., JENSEN D.R., LEONIE S., LO BIANCO G., MA W.C. et al. (2003).
One- and two-phonon wobbling excitations in triaxial 165Lu. PHYSICS LETTER B. vol. 552, pp. 9-16

TIANA G., PROVASI D., BROGLIA R.A. (2003).
Role of bulk and of interface contacts in the behaviour of model dimeric proteins. PHYSICAL REVIEW E, STATISTICAL, NONLINEAR, AND SOFT MATTER PHYSICS. vol. 67, p. 51909

WIELAND O., KROLL T.H., BAZZACCO D., VENTURELLI R., CAMERA F., MILLION B., MUSSO E., QUINTANA B., UR C.A., BELLATO M., ISOCRATE R., MANEA C., MENEGAZZO R., PAVAN P., ROSSI ALVAREZ C. et al. (2003).
Gamma-ray Tracking with Segmented HPGe Detectors. BRAZILIAN JOURNAL OF PHYSICS. vol. 33, p. 206

Accelerators and Related Technologies

Articles

ALFASSI Z.B., GROPPI F. (2005).
On the determination of the thermal neutron flux density by the measurement of the activity ratio 199Au/198Au. RAD. MEAS. vol. 39-5, pp. 561-563

ALFASSI Z.B., GROPPI F., BONARDI M.L., DE GOEIJ J.J.M. (2005).
On the "artificial" nature of Tc and the "carrier-free" nature of 99mTc from 99Mo/99mTc generators. APPL. RAD. ISOT. vol. 63-1, pp. 37-40

ARGINELLI D., MONTALTO M., BORTOLUZZI S., NOCENTE M., BONARDI M., GROPPI F. (2005).
Measurement of actinides in biological system; radioanalytical determination of americium in human urines by extraction cromatography and high resolution alpha spectrometry. J. RADIOANAL. NUCL. CHEM. vol. 263-2, pp. 275-279

BAGATTI D., CANTONE M.C., GIUSSANI A., RIDONE S., BIRATTARI C., BONARDI M.L., GROPPI F., MARTINOTTI A., MORZENTI S., GALLORINI M., RIZZIO E. (2005).
Analytical and radioanalytical quality control of purity and stability of radiopharmaceutical compound [186Re]HEDP for bone metastases pain palliation. J. RADIOANAL. NUCL. CHEM. vol. 263-2, pp. 515-520

BONARDI M.L. (2005).
Critical review of the "Handbook on Nuclear Chemistry": by A. Vertes, S. Nagy and Z. Klencs (Eds.) 5 Volumes, Kluwer Academic, The Netherlands. RAD. PHYS. CHEM. vol. 72, pp. 737-738

BONARDI M.L., DE GOEIJ J.J.M. (2005).
How do we ascertain specific activities in no-carrier-added radionuclide preparations? J. RADIOANAL. NUCL. CHEM. vol.263, pp. 87-92

BONARDI M.L., GROPPI F., MAINARDI H.S.C., KOKHANYUK V.M., LAPSHINA E.V., MEBEL M.V., ZHUIKOV B.L. (2005).
Cross-section studies on 64Cu with zinc target in the proton energy range from 141 down to 31 MeV. J. RADIOANAL. NUCL. CHEM. vol. 264-1, pp. 101-105

BONARDI M.L., RIZZIO E., GALLORINI M., GROPPI F., MAINARDI H.S. (2005).
Improved radiochemical separation of No-Carrier-Added vanadium-48 from proton irradiated titanium target. J. RADIOANAL. NUCL. CHEM. vol. 263-1, pp. 23-28

COMPTON C.C., GRIMM T.L., HARTUNG W., PODLECH H., YORK R.C., CIOVATI G., KNEISEL P., BARNI D., PAGANI C., PIERINI P. (2005).
Prototyping of a multicell superconducting cavity for acceleration of medium-

velocity beams. PHYSICAL REVIEW SPECIAL TOPICS - ACCELERATOR AND BEAMS. vol. 8, 042003, pp. 1-8

DE GOEIJ J.J.M., BONARDI M.L. (2005).
How do we define the concepts specific activity, radioactive concentration, carrier, carrier-free and no-carrier-added? J. RADIOANAL. NUCL. CHEM. vol. 263, pp. 13-18

GROPPI F., BONARDI M.L., BIRATTARI C., MENAPACE E., ABBAS K., HOLZWARTH U., ALFARANO A., MORZENTI S., ZONA C., ALFASSI Z.B. (2005).
Optimisation study of ?[ML3]-cyclotron production of At-211/Po-211g for high §[ML4]LET metabolic radiotherapy purposes. APPL. RAD. ISOT. vol. 63, pp. 621-631.

GROPPI F., LAVI N., ALFASSI Z.B., BONARDI M., BIRATTARI C. (2005).
On the high-resolution gamma-ray spectrometric measurement of 40K in natural and synthetic materials. RAD. PROT. DOS. vol. 115, pp. 441-444

GROPPI F., MAINARDI H.S., MARTINOTTI A., MORZENTI S., BONARDI M.L. (2005).
The use of liquid scintillation spectrometry as a very sensitive radioanalytical tool for the determination of alpha, beta and monochromatic electron emitting impurities in radiopharmaceutical compounds. J. RADIOANAL. NUCL. CHEM. vol. 263-2, pp. 521-525

BONARDI M.L., BIRATTARI C., GROPPI F., GINI L., MAINARDI C.H.S., MENAPACE E. (2004).
Determination of 125I impurities in [123I]-labelled radiopharmaceuticals, by liquid scintillation counting: sensitivity of the method. NUCL. INSTR. METH. B vol. 213C, pp. 348-350

BONARDI M.L., BIRATTARI C., GROPPI F., GINI L., MAINARDI H.S. (2004).
Cycloton production and quality control of "High Specific Activity" radionuclides in "No Carrier Added" form for radioanalytical applications in life sciences. J. RADIOANAL. NUCL. CHEM. vol. 259-3, pp. 415-419

GROPPI F., BONARDI M., BIRATTARI C., GINI L., MAINARDI C., MENAPACE E., ABBAS K., HOLZWARTH U., STROOSNIJDER R.M.F. (2004).
Thin-Target excitation functions and optimisation of N.C.A. 64Cu and 66Ga production by deuteron induced nuclear reactions on natural zinc target, for radiometabolic therapy and for PET. NUCL. INSTR. METH. B. vol. 213C, pp. 373-377

LAVI N., GROPPI F., ALFASSI Z.B. (2004).
On the measurement of 40K in natural and synthetic materials by the method of high-resolution gamma-ray spectrometry. RAD. MEAS. vol. 38-2, pp. 139-143

MENAPACE E., BIRATTARI C., BONARDI M.L., GROPPI F. (2004).
Experimental results and model calculations of excitation functions relevant to the production of specific radioisotopes for metabolic radiotherapy and for PET. RAD. PHYS. CHEM. vol. 71, pp. 943-945

RIDONE S., BIRATTARI C., BONARDI M., GROPPI F., MARTINOTTI A., MORZENTI S., CANTONE M.C. (2004).
Radioanalytical quality control on beta-emitting [186gRe]- and [153Sm]-radiopharmaceutical compounds for bone metastatses pain palliation. WORLD J. OF NUCL. MED. vol. 3-3, p. 241

ROSSI L., SORBI M., SPILLANTINI P. (2004).
A Superconducting Magnetic Lens for Solar Rays Protection in Manned Interplanetary Mission. IEEE TRANS. ON APPLIED SUPERCONDUCTIVITY. vol. 14, nr. 2, pp. 1696-1699

SEKUTOWICZ J., CASTRO P., GOSSEL A., KREPS G., LANGE R., MATHEISEN A., MOLLER W.-D., PETERS H.-B., PROCH D., SCHLARB H., SCHREIBER S., SIMROCK S., WENDT M., BABOI N., FERRARIO M. et al. (2004).
Test of two Nb superstructure prototypes. PHYSICAL REVIEW SPECIAL TOPICS - ACCELERATOR AND BEAMS. vol. 7, 012002, pp. 1-13

VERONESE I., GIUSSANI A., CANTONE M.C., BIRATTARI C., BONARDI M., GROPPI F., HOLLRIEGL V., ROTH P., WERNER E. (2004).
Influence of the chemical form on the plasma clearance of ruthenium in humans. APPL. RAD. ISOT. vol. 60-1, pp. 7-13

BAKKER R., HARTROTT M., JAESCHKE E., KRAMER D., CARNEIRO J.P., FLOTTMANN K., PIOT P., ROSSBACH J., SCHREIBER S., ABRAHAMYAN K., BAHR J., BOHNET I., DJORDJADZE V., GENSCH U., GRABOSCHI H.J. et al. (2003).
First beam measurements at the photo injector test facility at DESY Zeuthen. NUCLEAR INSTRUMENTS AND METHODS IN PHYSICS RESEARCH A. vol. 507, pp. 210-214

BIRATTARI C., BONARDI M.L., GROPPI F., GINI L., MAINARDI C., GHIONI A., BALLARINI G., MENAPACE E., ABBAS K., HOLZWARTH U., STROSNIJDER M.F. (2003).
Thin-target excitation functions and optimisation of simultaneous production of N.C.A. copper-64 and gallium-67 by deuteron induced nuclear reactions on natural zinc target. J. RADIOANAL. NUCL. CHEM. vol. 257, pp. 229-241

BONARDI M., BIRATTARI C., GROPPI F., GINI L., BALLARINI G., GHIONI A., MAINARDI H.S., GALLORINI M., RIZZIO E., SABBIONI E. (2003).
Preparation of High Specific Activity radiochemical forms of vanadium, manganese and thallium for metallo-toxicological studies. ANN. CHIM. vol. 9, pp. 363-372

BONARDI M.L., BIRATTARI C., GROPPI F., GINI L., MENAPACE E. (2003).
A rapid improved method for gamma spectrometry determination of thallium-202 impurities, in [thallium-201] labelled radiopharmaceuticals. J. LABELLED CPD. RADIOPHARM. vol. 46-1, p. S291

BONARDI M.L., BIRATTARI C., GROPPI F., MAINARDI C.H.S., MENAPACE E. (2003).
A competitive method for simultaneous deuteron-cyclotron production of No-Carrier-Added copper-64 and gallium-67,66 for application in PET radiodiagnostic and metabolic therapy of tumours. J. LABELLED CPD. RADIOPHARM. vol. 46-1, p. S289

BONARDI M.L., GROPPI F., BIRATTARI C., CANTONE M.C., GIUSSANI A., VERONESE I. (2003).
Analytical and radioanalytical quality control of purity and stability of radiopharmaceutical [186Re]HEDP for bone metastases pain palliation. J. LABELLED CPD. RADIOPHARM. vol. 46-1, p. S314

BONARDI M.L., GROPPI F., BIRATTARI C., MAINARDI C.H.S. (2003).
Thin-target excitation functions: a powerful tool for optimising yield, radionuclidic purity and specific activity of accelerator produced radionuclides. CZECHOSLOVAK J. PHYS. vol. 53, pp. A393-A403

BONARDI M.L., GROPPI F., RIZZIO E., GALLORINI M. (2003).
Radioanalytical Quality Controls by INAA and RNAA determination of Specific Activity, Chemical Purity and Isotopic Composition of labelled compounds. TRANSACTION OF THE ANS vol. 89, pp. 679-680

BONARDI M.L., GROPPI F., SABBIONI E. (2003).Production and radioanalytical quality control of high specific activity no-carrier-added radionuclides for environmental and biomedical purposes. TRANSACTION OF THE ANS. vol. 89, pp. 774-775

VERONESE I., CANTONE M.C., GIUSSANI A., BIRATTARI C., BONARDI M., GROPPI F., GARLASCHELLI L., MAGGIONI T., WERNER E., ROTH P., HOELLRIEGL V., LOUVAT P., FELGENHAUER N., ZILKER T. (2003).
Stable tracer investigations in humans for assessing the biokinetics of ruthenium and zirconium radionuclides. RAD. PROT. DOS. vol. 105, pp. 209-212

VERONESE I., GIUSSANI A., CANTONE M.C., MAGGIONI T., BIRATTARI C., GROPPI F., WERNER E., ROTH P., HOELLRIEGL V. (2003).
A re-evaluation of the biokinetics of zirconium in humans. APPL. RAD. ISOT. vol. 58/4, pp. 431-439

Electronics

Articles

BELLONI F., MARANESI P.G., RIVA M. (2005).
A new application of power electronics: the ion thruster HV drive. HAIT JOURNAL OF SCIENCE AND ENGINEERING B. vol. 2, nr. 5-6, pp. 762-775

MARANESI P.G., RIVA M. (2003).
Automatic modeling of PWM DC-DC converters. IEEE POWER ELECTRONICS LETTERS. vol. 1, nr. 4, pp. 97-100

Structure of Matter

Articles

BARBORINI E., BONGIORNO G., FORLEO A., FRANCIOSO L., MILANI P., KHOLMANOV I.N., PISERI P., SICILIANO P., TAURINO A.M., VINATI S. (2005).
Thermal annealing effect on nanostructured TiO2 microsensors by supersonic cluster beam depositions. SENSORS AND ACTUATORS. B, CHEMICAL. vol. 111-112, pp. 22-27

BARBORINI E., CONTI A.M., KHOLMANOV I., PISERI P., PODESTA A., MILANI P., CEPEK C., SAKHO O., MACOVEZ R., SANCROTTI M. (2005).
Nanostructured TiO2 films with 2 eV optical gap. ADVANCED MATERIALS. vol. 17, pp. 1842-1846

BONGIORNO G., BLOMQVIST M., PISERI P., MILANI P., LENARDI C., DUCATI C., CARUSO T., RUDOLF P., WACHTMEISTER S., CSILLAG S., CORONEL E. (2005).
Nanostructured CNx (0 < x < 0.2) films grown by supersonic cluster beam deposition. CARBON. vol. 43, pp. 1460-1469

BONGIORNO G., LENARDI C., DUCATI C., AGOSTINO R.G., CARUSO T., AMATI M., BLOMQVIST M., BARBORINI E., PISERI P., LA ROSA S., COLAVITA E., MILANI P. (2005).
Nanocrystalline metal/carbon composites produced by supersonic cluster beam deposition. JOURNAL OF NANOSCIENCE AND NANOTECHNOLOGY. vol. 5, pp. 1072-1080

CASARI C.S., LI BASSI A., BOTTANI C.E., LENARDI C., RAVAGNAN L., SIVIERO F., BARBORINI E., PISERI P., MILANI P. (2005).
Nanoscale and mesoscale properties of nanostructured carbon films. FULLERENES, NANOTUBES AND CARBON NANOSTRUCTURES. vol. 13, pp. 199-210

DEGOLI E., CANTELE G., OSSICINI S., MAGRI R., NINNO D., BISI O., PULCI O., ONIDA G., GATTI M., INCZE A., DEL SOLE R. (2005).
The electronic and optical properties of silicon nanoclusters: absorption and emission. OPTICAL MATERIALS. vol. 27, p. 1008

DUCATI C., BARBORINI E., BONGIORNO G., VINATI S., MILANI P., MIDGLEY P.A. (2005).
Titanium Fullerenoid Oxides. APPLIED PHYSICS LETTERS. vol. 87, p. 201906

FORTINI A., MAZZOLA M., MINA A., PROVASI D., COLO' G., ONIDA G., BROGLIA H.E., ROMAN R.A. (2005).
The role of quantal fluctuations in the optical response of small metal clusters. J. PHYS. B. vol. 38, p. 1581

GALLI D.E., ROSSI M., REATTO L. (2005).
Bose-Einstein condensation in solid 4He. PHYSICAL REVIEW. B, CONDENSED MATTER AND MATERIALS PHYSICS. vol. 71, pp. 140506/1-140506/4

GATTI M., ONIDA G. (2005).
Effects of local fields in time-dependent density functional theory shown in oxidized silicon clusters. PHYSICAL REVIEW B. vol. 72, p. 045442

INCZE A., ONIDA G., DEL SOLE R. (2005).
Ab initio study of reflectance anisotropy spectra of a submonolayer oxidized Si(100) surface. PHYS. REV. B. vol. 71, p. 035350

LENARDI C., MARINO M., BARBORINI E., PISERI P., MILANI P. (2005).
Evaluation of hydrogen chemisorption in nanostructured carbon films by near edge X-ray absorption spectroscopy. EUROPEAN PHYSICAL JOURNAL. B, CONDENSED MATTER PHYSICS. vol. 46, pp. 441-447

LI BASSI A., CATTANEO D., RUSSO V., BOTTANI C.E., BARBORINI E., MAZZA T., PISERI P., MILANI P., ERNST FO F., WEGNER K., PRATSINIS S.E. (2005).
Raman spectroscopy characterization of titania nanoparticles produced by flame pyrolysis: The influence of size and stoichiometry. JOURNAL OF APPLIED PHYSICS. vol. 98, pp. 074305/1-074305/9

LO VERSO F., PINI D., REATTO L. (2005).
Fluid-fluid and fluid-solid phase separation in non-additive asymmetric binary hard-sphere mixtures. JOURNAL OF PHYSICS-CONDENSED MATTER. vol. 17, pp. 771-796

MAZZA T., BARBORINI E., KHOLMANOV I.N., PISERI P., BONGIORNO G., VINATI S., MILANI P., DUCATI C., CATTANEO D., LI BASSI A., BOTTANI C.E., TAURINO A.M., SICILIANO P. (2005).
Libraries of cluster-assembled titania films for chemical sensing. APPLIED PHYSICS LETTERS. vol. 87, pp. 103108/1-103108/3

MIGLIO S., BRUZZI M., SCARINGELLA M., MENICHELLI D., LEANDRI E., BALDI A., BONGIORNO G., PISERI P., MILANI P. (2005).
Development of humidity sensors based on nanostructured carbon films. SENSORS AND ACTUATORS. B, CHEMICAL. vol. 111-112, pp. 140-144

MONTANARI B., BALLONE P., MAZZA T., MILANI P. (2005).
Vibrational properties of nanometric AB2 ionic clusters. JOURNAL OF PHYSICS: CONDENSED MATTER. vol. 17, p. 3787

MULAZZI E., PEREGO R., AARAB H. et al. (2005).
Optical properties of carbon nanotube-PPVcomposites: influence of the PPV conversion temperature and nanotube concentration. SYNTHETIC METALS. vol. 154, pp.221-224

PAROLA A., SALASNICH L., ROTA R., REATTO L. (2005).
Quantum phases of attractive matter waves in a toroidal trap. PHYSICAL REVIEW A. vol. 72, pp. 063612/1-063612/6

PODESTA' A., INDRIERI M., BROGIOLI D., MANNING G.S., MILANI P., GUERRA R., FINZI L., DUNLAP D. (2005).
Positively Charged Surfaces Increase the Flexibility of DNA. BIOPHYSICAL JOURNAL. vol. 89, p. 2558

PODESTA' A., RANUCCI E., MACCHI L., BONGIORNO G., FERRUTI P., MILANI P. (2005).
Micro-and nanoscale modification of PHEMA hydrogels by AFM lithography and nanoparticle incorporation. JOURNAL OF NANOSCIENCE AND NANOTECHNOLOGY. vol. 5, p. 429

PODESTA' A., TIANA G., MANNO M., MILANI P. (2005).
Early events in insulin fibrillization studied by time-lapse atomic force microscopy. BIOPHYSICAL JOURNAL. vol. 90, p. 589

POLLINI I. (2005).
Splitting of core-level lines in photoemission spectra of transition metal compounds, Philosophical Magazine, vol. 85, nr. 23, pp. 2641-2652

RAVAGNAN L., SIVIERO F., CASARI C.S., LI BASSI A., LENARDI C., BOTTANI C.E., MILANI P. (2005).
Photo-induced production of sp-hybridized carbon species from Ag-coated polytetrafluoroethylene (PTFE). CARBON. vol. 43, p. 1317

ROSSI M., GALLI D.E., REATTO L. (2005).
Layer by layer solidification of 4He in narrow porous media. PHYSICAL REVIEW. B, CONDENSED MATTER AND MATERIALS PHYSICS. vol. 72, pp. 064516/1-064516/12

SALASNICH L., PAROLA A., REATTO L. (2005).
Quasi-one-dimensional bosons in three-dimensional traps: From strong-coupling to weak-coupling regime. PHYSICAL REVIEW A. vol. 72, pp. 025602/1-025602/4X.

GONZE et al. (including G. ONIDA) (2005).
A Brief Introduction to the AbinitSoftware Package. ZEITSCHRIFT FUR KRISTALLOGRAPHIE. vol. 220, pp. 558-562

AGOSTINO R.G., CARUSO T., CHIARELLO G., FILOSA R., FORMOSO V., COLAVITA E., BARBORINI E., LENARDI C., PISERI P., MILANI P., LA ROSA S., BERTOLO M. (2004).
Spatially resolved valence band study of nanostructured carbon films containing transition metal nanocrystals. CARBON. vol. 42, pp. 923-929

BATANI D., STRATI F., STABILE H., TOMASINI M., LUCCHINI G., RAVASIO A., KOENIG M., BENUZZI-MOUNAIX A., NISHIMURA H., OCHI Y., ULLSCHMIED J., SKALA J., KRALIKOVA B., PFEIFER M., KADLEC C. et al. (2004).
Hugoniot data for carbon at megabar pressures. PHYSICAL REVIEW LETTERS. vol. 92, pp. 065503/1-065503/4

BENEDEK G., MILANI P. (2004).
Nanotecnologia e Nanotubi Enciclopedia del Novecento. Supplemento: Dal XX al XXI secolo: problemi e prospettive Istituto dell'Enciclopedia Italiana, Roma

BOTTI S., SOTTILE F., VAST N., OLEVANO V., REINING L., WEISSKER H.C., RUBIO A., ONIDA G., DEL SOLE R., GODBY R.W. (2004).
Long-range contribution to the exchange-correlation kernel of time-dependent density functional theory. PHYS. REV. B. vol. 69, p. 155112

BROGLIA R.A., COLO' G., ONIDA G., ROMAN H.E. (2004).
Monograph: Solid state physics of finite systems: Metal clusters, fullerenes, atomic wires. ADVANCED TEXTS IN PHYSICS SERIES. Springer, Berlin, pp. 234

BRUZZI M., MIGLIO S., SCARINGELLA M., BONGIORNO G., PISERI P., PODESTA' A., MILANI P. (2004).
First study of humidity sensors based on nanostructured carbon films produced by supersonic cluster beam deposition. SENSORS AND ACTUATORS. B, CHEMICAL. vol. 100, pp. 173-176

CARUSO T., AGOSTINO R.G., BONGIORNO G., BARBORINI E., PISERI P., MILANI P., LENARDI C., LA ROSA S., BERTOLO M. (2004).
Writing submicrometric metallic patterns by ultraviolet synchrotron irradiation of

nanostructured carbon and TiOx-carbon films. APPLIED PHYSICS LETTERS. vol. 84, pp. 3412-3414

CASARI C.S., BASSI A.L., RAVAGNAN L., SIVIERO F., LENARDI C., BARBORINI E., PISERI P., MILANI P., BOTTANI C.E. (2004).
Gas exposure and thermal stability of linear carbon chains in nanostructured carbon films investigated by in situ Raman spectroscopy. CARBON. vol. 42, pp. 1103-1106
CASARI C.S., BASSI A.L., RAVAGNAN L., SIVIERO F., LENARDI C., PISERI P., BONGIORNO G., BOTTANI C.E., MILANI P. (2004).
Chemical and thermal stability of carbyne-like structures in cluster-assembled carbon films. PHYSICAL REVIEW. B, CONDENSED MATTER AND MATERIALS PHYSICS. vol. 69, pp. 075422/1-075422/7

GALLI D.E., REATTO L. (2004).
Disorder phenomena in quantum solids with vacancies. JOURNAL OF LOW TEMPERATURE PHYSICS. vol. 134, pp. 121-131

GALLI D.E., REATTO L. (2004).
The shadow path integral ground state method: Study of confined solid 4He. JOURNAL OF LOW TEMPERATURE PHYSICS. vol. 136, pp. 343-358

HOGAN C., PAGET D., TERESHCHENKO O.E., REINING L., ONIDA G. (2004).
Optical anisotropy induced by cesium adsorption on the As-rich c(2x8) reconstruction of GaAs(001). PHYS. REV. B. vol. 69, p. 125332

IMPERIO A., REATTO L. (2004).
Bidimensional fluid system with competing interactions: Spontaneous and induced pattern formation. JOURNAL OF PHYSICS-CONDENSED MATTER. vol. 16, pp. S3769-S3789

LO VERSO F., REATTO L., FOFFI G., TARTAGLIA P., DAWSON K.A. (2004).
Star polymers: A study of the structural arrest in presence of attractive interactions. PHYSICAL REVIEW E, STATISTICAL, NONLINEAR, AND SOFT MATTER PHYSICS. vol. 70, pp. 061409/1-061409/13

MILANI A., PODESTA' A., BARBORINI E. (2004).
Cluster-assembled nanostructured carbon filmsThe Encyclopedia of Nanotechnology. AMERICAN SCIENTIFIC PUBLISHERS. vol. 2, pp. 1-26

MULAZZI E., BOTTA C., FACCHINETTI D. et al. (2004).
Evidence of conjugation length distributions in electroluminescent segmented PPV: absorption, photoluminescence and Raman scattering. SYNTHETIC METALS. vol. 142, pp. 85-92

MULAZZI E., PEREGO R., AARAB H. et al. (2004).
Photoconductivity and optical properties in composites of poly(paraphenylene vinylene) and single-walled carbon nanotubes. PHYSICAL REVIEW B. vol. 70, pp. 155206-155211

ORLANDI A., PAROLA A., REATTO L. (2004).
A microscopic approach to critical phenomena at interfaces: An application to complete wetting in the Ising model. PHYSICAL REVIEW E, STATISTICAL, NONLINEAR, AND SOFT MATTER PHYSICS. vol. 70, pp. 051611/1-051611/12

PISERI P., BARBORINI E., MARINO M., MILANI P., LENARDI C., ZOPPI L., COLOMBO L. (2004).
Hydrogen uptake in cluster-assembled carbon thin films: Experiment and computer simulation. JOURNAL OF PHYSICAL CHEMISTRY. B, CONDENSED MATTER, MATERIALS, SURFACES, INTERFACES & BIOPHYSICAL. vol. 108, pp. 5157-5160

PISERI P., TAFRESHI H.V., MILANI P. (2004).
Manipulation of nanoparticles in supersonic beams for the production of nanostructured materials. CURRENT OPINION IN SOLID STATE & MATERIALS SCIENCE. vol. 8, pp. 195-202

PODESTA' A., FANTONI G., MILANI P. (2004).
Quantitative nanofriction characterization of corrugated surfaces by Atomic Force Microscopy. REVIEW OF SCIENTIFIC INSTRUMENTS. vol. 75, p. 1228

PODESTA' A., IMPERADORI L., COLNAGHI W., FINZI L., MILANI P., DUNLAP D. (2004).
Atomic force microscopy study of DNA deposited on poly L-ornitine-coated mica. JOURNAL OF MICROSCOPY. vol. 215, p. 236

ROSSI M., VERONA M., GALLI D.E., REATTO L. (2004).
Alkali and alkali-earth ions in 4He systems. PHYSICAL REVIEW. B, CONDENSED MATTER AND MATERIALS PHYSICS. vol. 69, pp. 212510/1-212510/4

SALASNICH L., PAROLA A., REATTO L. (2004).
Dimensional reduction in Bose-condensed alkali-metal vapors. PHYSICAL REVIEW A. vol. 69, pp. 045601/1-045601/4

SALASNICH L., PAROLA A., REATTO L. (2004).
Transition from 3D to 1D in Bose gases at zero temperature. PHYSICAL REVIEW A. vol. 70, pp. 013606/1-013606/5
AGOSTINO R.G., CARUSO T., CHIARELLO G., CUPOLILLO A., PACILE D., FILOSA R., FORMOSO V., COLAVITA E., PAPAGNO L., DUCATI C., BARBORINI E., LENARDI C., BONGIORNO G., PISERI P., MILANI P. (2003).
Thermal annealing and hydrogen exposure effects on cluster-assembled nanostructured carbon films embedded with transition metal nanoparticles. PHYSICAL REVIEW. B, CONDENSED MATTER AND MATERIALS PHYSICS. vol. 68, pp. 035413/1-035413/12

AVERSA L., VERUCCHI R., BOSCHETTI A., PODESTA' A., MILANI P., IANNOTTA S. (2003).
Fullerene freejets-based synthesis of silicon carbide: heteroepitaxial growth on Si(111) at low temperatures. MATERIALS SCIENCE AND ENGINEERING B. vol. 101, p. 169

BALZAROTTI A., FANFONI M., PATELLA F., ARCIPRETE F., PLACIDI E., ONIDA G., DEL SOLE R. (2003).
The GaAs(001)c(4x4) surface: a new perspective from Energy Loss Spectra. SURFACE SCIENCE LETTERS. vol. 524, pp. L71-L76

BARBORINI E., KHOLMANOV I.N., CONTI A.M., PISERI P., VINATI S., MILANI P., DUCATI C. (2003).
Supersonic cluster beam deposition of nanostructured titania. EUROPEAN PHYSICAL JOURNAL D. vol. 24, pp. 277-282

BARBORINI E., LENARDI C., PISERI P., MILANI P., AGOSTINO R.G., CARUSO T., COLAVITA E., LA ROSA S., BERTOLO M., DUCATI C. (2003).
Morphology and electronic structure of nanostructured carbon films embedding transition metal nanoparticles. EUROPEAN PHYSICAL JOURNAL D. vol. 24, pp. 273-276

BENEDEK G., VAHEDI-TAFRESHI H., BARBORINI E., PISERI P., MILANI P., DUCATI C., ROBERTSON J. (2003).
The structure of negatively curved spongy carbon. DIAMOND AND RELATED MATERIALS. vol. 12, pp. 768-773

BOTTANI C.E., LI BASSI A., BEGHI M.G., PODESTA' A., MILANI P., BAUGHMAN R., ZAKHIDOV A., WALTERS D., SMALLEY R.E. (2003).
Dynamic light scattering from acoustic modes in single-walled carbon nanotubes. PHYSICAL REVIEW B. vol. 67, p. 155407

BRUZZI M., PISERI P., MIGLIO S., BONGIORNO G., BARBORINI E., DUCATI C., ROBERTSON J., MILANI P. (2003).
Electrical conduction in nanostructured carbon and carbon-metal films grown by supersonic cluster beam deposition. EUROPEAN PHYSICAL JOURNAL. B, CONDENSED MATTER PHYSICS. vol. 36, pp. 3-13

FOFFI G., SCIORTINO F., TARTAGLIA P., ZACCARELLI E., LO VERSO F., REATTO L., DAWSON K., LIKOS C.N. (2003).
Structural arrest in dense star polymer solutions. PHYSICAL REVIEW LETTERS. vol. 90, pp. 238301/1-238301/4

GALLI D.E., REATTO L. (2003).
Recent progress in simulation of the ground state of many Boson-systems. MOLECULAR PHYSICS. vol. 101, pp. 1697-1703

GALLI D.E., REATTO L. (2003).
Vacancy excitation spectrum in solid 4He and longitudinal phonons. PHYSICAL REVIEW LETTERS. vol. 90, pp. 175301/1-175301/4

HOGAN C., DEL SOLE R., ONIDA G. (2003).
Optical properties of real surfaces from microscopic calculations of the dielectric function of finite atomic slabs, PHYS. REV. B. vol. 68, p. 035405

HOGAN C., PAGET D., GARREAU Y., SAUVAGE M., ONIDA G., REINING L., CHIARADIA P., CORRADINI V. (2003).
Early stages of cesium adsorption on the As-rich c2x8 reconstruction of GaAs (001): Adsorption sites and Cs-induced chemical bonds. PHYS. REV. B. vol. 68, p. 205313

KHOLMANOV I.N., BARBORINI E., VINATI S., PISERI P., PODESTA A., DUCATI C., LENARDI C., MILANI P. (2003).
The influence of the precursor clusters on the structural and morphological evolution of nanostructured TiO2 under thermal annealing. NANOTECHNOLOGY. vol. 14, pp. 1168-1173

LI BASSI A., BEGHI M.G., CASARI C.S., BOTTANI C.E., PODESTA' A.,

MILANI P., ZAKHIDOV A., BAUGHMAN R., WALTERS D.A., SMALLEY R.E. (2003).
Inelastic light scattering from magnetically aligned single-walled carbon nanotubes and estimate of their two-dimensional Young's modulus. DIAMOND AND RELATED MATERIALS. vol. 12, p. 806

LO VERSO F., TAU M., REATTO L. (2003).
Star polymers: Study of fluid-fluid transitions in a system with a repulsive ultrasoft-core. JOURNAL OF PHYSICS-CONDENSED MATTER. vol. 15, pp. 1505-1520

MAGNANO E., CEPEK C., SANCROTTI M., SIVIERO F., VINATI S., LENARDI C., BARBORINI E., PISERI P., MILANI P. (2003).
Thermally induced changes in cluster-assembled carbon nanocluster films observed via photoelectron spectroscopy. APPLIED SURFACE SCIENCE. vol. 212, pp. 879-884

MAGNANO E., CEPEK C., SANCROTTI M., SIVIERO F., VINATI S., LENARDI C., PISERI P., BARBORINI E., MILANI P. (2003).
In situ growth and thermal treatment of nanostructured carbon produced by supersonic cluster beam deposition: An electron spectroscopy investigation. PHYSICAL REVIEW. B, CONDENSED MATTER AND MATERIALS PHYSICS. vol. 67, pp. 125414/1-125414/7

MAGNANO E., PADOVANI M., SPREAFICO V., SANCROTTI M., PODESTA' A., BARBORINI E., PISERI P., MILANI P. (2003).
Cluster beam microfabrication of SiC pattern on Si(100). SURFACE SCIENCE. vol. 544, pp. L709-L714

MICHELATO P., MONACO L., SERTORE D., POLLINI I. (2003).
Time- and angle-resolved photoelectron spectrometer based on a picosecond Nd: glass laser system. REVIEW OF SCIENTIFIC INSTRUMENTS. vol. 74, nr. 6, pp. 2977-2982

MULAZZI E., PEREGO R., BOTTA C. et al. (2003).
Radiative recombination studies on PPV and PPV SWNT composites. SYNTHETIC METALS. vol. 135, pp. 279-280

OSTROVSKAYA L., PODESTA' A., MILANI P., RALCHENKO V. (2003).
Influence of surface morphology on the wettability of cluster-assembled carbon films. EUROPHYSICS LETTERS. vol. 63, p. 401

OSTROVSKAYA L.YU., PEREVERTAILO V.M., MATVEEVA L.A., MILANI P., RALCHENKO V.G., SHPILEVSKY E.M. (2003).
Characterization of different carbon nanomaterials promising for biomedical and sensor applications by the wetting method. POWDER METALLURGY AND METAL CERAMICS. vol. 42, p. 1

PAGET D., TERESHCHENKO O.E., GORDEEVA A.B., BERKOVITS V.L., ONIDA G. (2003).
Origin of the broadening of surface optical transitions of As-rich and Ga-rich GaAs(001). SURFACE SCIENCE. vol. 529, nr. 1-2, pp. 204-214

PAROLA A., PINI D., REATTO L., TAU M. (2003).
Phase transitions in simple and not so simple binary fluids. JOURNAL OF PHYSICS-CONDENSED MATTER. vol., pp. 5381-5386

PINI D., TAU M., PAROLA A., REATTO L. (2003).
Phase diagram of symmetric binary mixtures at equimolar and non-equimolar concentrations: a systematic investigation. PHYSICAL REVIEW E. vol. 67, pp. 046116/1-046116/17

POLLINI I. (2003).
Electron correlation and hybridization in late-transition metal compounds. PHILOSOPHICAL MAGAZINE. vol. 83, nr. 6, pp. 775-787

POLLINI I. (2003).
Multiplet splitting of core-electron binding energies in chromium compounds. PHYSICAL REVIEW B. vol. 67, pp. 155111/1-155111/5

REATTO L., ORLANDI A., PAROLA A. (2003).
A bridge between the microscopic interaction potentials in a fluid and effective long-wavelength hamiltonians. MACROMOLECULAR THEORY AND SIMULATIONS. vol. 29, pp. 761-766

SALASNICH L., PAROLA A., REATTO L. (2003).
Modulation instability and complex dynamics of confined matter-wave solitons. PHYSICAL REVIEW LETTERS. vol. 91, pp. 080405/1-080405/4

WERY J., AARAB H., LEFRANT S., MULAZZI E. (2003).
Photoexcitations in composites of poly(paraphenylene vinylene) and single-walled carbon nanotubes. PHYSICAL REVIEW B. vol. 67, pp. 115202-115209

Quantum Optics, Coherent Phenomena, and Optoelectronics

Books

BONIFACIO R., CASAGRANDE F. (2005).
Optical bistability, in ENCYCLOPEDIA OF CONDENSED MATTER PHYSICS, G. Bassani, G. Liedl and P. Wyder eds. (Elsevier, Amsterdam, 2005). pp. 147-152

FERRARO A., OLIVARES S., PARIS M.G.A. (2005).
Gaussian states in Continuous variable Quantum Information (Bibliopolis, Napoli)

BENENTI G., CASATI G., STRINI G. (2004).
Principles of quantum computation and information. vol. 1: Basic concepts, World Scientific (SINGAPORE)

PARIS M. G. A., REHACEK J. (2004).
Quantum State Estimation. Lectures Notes in Physics 649 (SPRINGER, BERLIN, 2004)

Articles

BOTTIGLI U., GOLOSIO B., MASALA G.L., OLIVA P., STUMBO S., BRAVIN A., BACCI A., SERAFINI L., MAROLI C., PETRILLO V., FERRARIO M., VACCAREZZA C. (2006).
Effect of different spectral distributions to image a contarst detail phantom in the mammography energy range. IL NUOVO CIMENTO C. vol. 29, p. 1

CIALDI S., CASTELLI F., BOSCOLO I. (2006).
Rectangular pulse formation in a laser harmonic generation. APPL. PHYS. B. vol. 82, p. 383

D'AURIA V., DE LISIO C., PORZIO A., SOLIMENO A., PARIS M.G.A. (2006).
Transmittivity measurements by means of squeezed vacuum light. J. PHYS. B. vol. 39, p. 1187

GRAMEGNA M., GENOVESE M., BRIDA G., BONDANI M., ZAMBRA G., ANDREONI A., ROSSI A.R., PARIS M.G.A. (2006).
Measuring the photon distribution by ON/OFF photodectors. LASER. PHYS. vol. 16, p. 385

PETRILLO V., ALBERTI G., CELARDO L.G., CERUTTI F., FRANCHI S., MARIANI V. (2006).
Dynamics of two particles in a space-momentum entangled state interacting with a potential barrier. CENTRAL EUROPEAN PHYSICS JOURNAL. vol. 4, pp. 1-15

AGLIATI A., BONDANI M., ANDREONI A., DE CILLIS G., PARIS M.G.A. (2005).
Quantum and classical correlations of intense beams of light via joint photodetection. J. OPT. B. vol. 7, p. 652

BONIFACIO R., PIOVELLA N., ROBB G.R.M. (2005).
Quantum theory of SASE FEL. NUCLEAR INSTRUMENTS & METHODS IN PHYSICS RESEARCH. SECTION A, ACCELERATORS, SPECTROMETERS, DETECTORS AND ASSOCIATED EQUIPMENT. vol. 543, pp. 645-652

CASAGRANDE F., ENGLERT B.G., LOUGOVSKI P., LULLI A., SOLANO E., WALTHER H. (2005).
A Solvable Open Quantum System: The Strongly Driven Micromaser. OPTICS AND SPECTROSCOPY. vol. 99, pp. 301-306

CASAGRANDE F., LULLI A. (2005).
Generation and decoherence of mesoscopic superposition states in a strongly driven micromaser. EUROPEAN PHYSICAL JOURNAL D. vol. 36, pp. 123-128

CASAGRANDE F., LULLI A. (2005).
Atomic correlations and cavity field decoherence in a strongly driven micromaser. JOURNAL OF OPTICS B-QUANTUM AND SEMICLASSICAL OPTICS. vol. 7, pp. S437-S444

CIALDI S., BOSCOLO I. (2005).
A shaper for proving long laser waveforms. NUCL. INSTR. METH. PHYS. RES. A, vol. 538, pp. 1

COLA M.M., PARIS M.G.A. (2005).
Teleportation of bipartite states using a single entangled pair. PHYS. LETT A. vol. 337, p. 10

D'AURIA V., CHIUMMO A., DE LAURENTIS M., PORZIO A., SOLIMENO S., PARIS M.G.A. (2005).
Tomographic characterization of OPO sources close to threshold. OPT. EXPR. vol. 13, pp. 948-956

D'AURIA V., PORZIO A., SOLIMENO A., OLIVARES S., PARIS M.G.A. (2005).
Characterization of bipartite states using a single homodyne detector J. OPT. B. vol. 7, p. 750

FALLANI L., FORT C., PIOVELLA N., COLA M.M., CATALIOTTI F.S., BONIFACIO R., INGUSCIO M. (2005).
Collective atomic recoil in a moving Bose-Einstein condensate: From superradiance to Bragg scattering. PHYSICAL REVIEW A. vol. 71, pp. 0033612/1-0033612/8

FERRARO A., PARIS M.G.A. (2005).
Local vs Nonlocal cloning in a noisy environment. J. OPT. B. vol. 7, p. 532

FERRARO A., PARIS M.G.A. (2005).
Multimode entanglement and telecloning in a noisy environment. PHYS. REV A. vol. 72, p. 032312

FERRARO A., PARIS M.G.A. (2005).
Nonlocality of two- and three-mode continuous variable systems. J. OPT. B vol. 7, p. 174

GENONI M.G., PARIS M.G.A. (2005).
Optimal quantum repeaters for qubits and qudits. PHYS. REV. A. vol. 71, p. 052307

INVERNIZZI C., OLIVARES S., PARIS M.G.A., BANASZEK K. (2005).
Effect of noise and enhancement of nonlocality in on/off photodetection. PHYS. REV. A. vol. 72, p. 042105

OLIVARES S., PARIS M.G.A. (2005).
Photon subtracted states and enhancement of nonlocality in the presence of noise. J. OPT. B. vol. 7, p. 392

OLIVARES S., PARIS M.G.A. (2005).
Squeezed Fock state by inconclusive photon subtraction. J. OPT. B. vol. 7, p. 616

PARIS M.G.A. (2005).
Unitary local invariance. INT. J. QUANT. INF. vol. 3, p. 655

PETRILLO V., OLKHOVSKY V.S. (2005).
Tunnelling time of a Gaussian wave packetthrough two potential barriers. CENTRAL EUROPEAN PHYSICS JOURNAL. vol. 3, pp. 339-350

ROBB G.R.M., PIOVELLA N., BONIFACIO R. (2005).
The Classical and Quantum Regimes of Superradiant Light Scattering from a Bose-Einstein Condensate. JOURNAL OF OPTICS B - QUANTUM AND SEMICLASSICAL OPTICS. vol. 7, pp. 93-98

ROSSI A.R., PARIS M.G.A. (2005).
A two-step MaxLik-MaxEnt strategy to infer photon distribution from on/off... E. PHYS. JOUR. D. vol. 32, p. 223

SERAFINI A., PARIS M.G.A., ILLUMINATI F., DE SIENA S. (2005).
Quantifying decoherence of continuous variable systems. J. OPT. B. vol. 7, pp. R19-R36

ZAMBRA G., BONDANI M., ANDREONI A., GRAMEGNA M., GENOVESE M., BRIDA G., ROSSI A., PARIS M.G.A. (2005).
Experimental reconstruction of photon statistics without photon counting. PHYS. REV. LETT. vol. 95, p. 063602

ALESINI D. et al. (2004).
Status of the SPARC project. NUCL. INSTR. AND METH. A. vol. 528, p. 586

ALLEVI A., ANDREONI A., BONDANI M., FERRARO A., PARIS M. G. A., PUDDU E. (2004).
Quantum and classical properties of the fields generated by two interlinked. J. MOD. OPT. vol. 51, p. 1031

ALLEVI A., ANDREONI A., BONDANI M., PUDDU E., FERRARO A., PARIS M.G.A. (2004).
Properties of two interlinked chi2 interactions in non-collinear phase-matching. OPT. LETT. vol. 29, p. 180

BENZA V.G., CANALI C.M., STRINI G. (2004).
Landau-Zener quantum tunneling in disordered nanomagnets. PHYSICAL REVIEW B. vol. 70, pp. 1844261-69

BONIFACIO R., CATALIOTTI F.S., FALLANI L., FORT C., PIOVELLA N., INGUSCIO M. (2004).
Superradiant light scattering from a moving Bose-Einstein condensate. OPTICS COMMUNICATIONS. vol. 233, pp. 155-160

CASAGRANDE F., FERRARO A., LULLI A., BONIFACIO R., SOLANO E., WALTHER H. (2004).
How to measure the micromaser spectrum in the trapping state regime. JOURNAL OF MODERN OPTICS. vol. 51, pp. 973-977

CIALDI S., BOSCOLO I. (2004).
A laser pulse shaper for the low emittance radiofrequency SPARC electron gun. NUCL. INSTR.. METH. PHYS. RES. A. vol. 526, pp. 239-248

CIALDI S., BOSCOLO S., FLACCO A. (2004).
Features of a phase-only shaper relative to a long rectangular ultraviolet pulse. J. OPT. SOC. AM. B. vol. 21, p. 1693

COLA M.M., PARIS M.G.A., PIOVELLA N. (2004).
Robust generation of entanglement in Bose-Einstein condensates by collective atomic recoil. PHYS. REV. A. vol. 70, p. 043809

COLA M.M., PARIS M.G.A., PIOVELLA N., BONIFACIO R. (2004).
A condensate in a lossy cavity: collective atomic recoil and generation of entanglement. J. MOD. OPT. vol. 51, p. 1043

COLA M.M., PARIS M.G.A., PIOVELLA N., BONIFACIO R. (2004).
Entanglement in a Bose-Einstein condensate by collective atomic recoil. J. PHYS. B. vol. 37, p. 187

COLA M.M., PIOVELLA N. (2004).
Theory of collective Raman scattering from a Bose-Einstein condensate. PHYSICAL REVIEW A. vol. 70, pp. 045601/1-045601/4

FERRARO A., PARIS M.G.A., ALLEVI A., ANDREONI A., BONDANI M. (2004).
Three-mode entanglement by interlinked nonlinear interactions in optical chi2 media. J. OPT. SOC. AM. B. vol. 21, p. 1241

LOUGOVSKI P., CASAGRANDE F., LULLI A., ENGLERT B.G., SOLANO E., WALTHER H. (2004).
Solvable model of a strongly driven micromaser. PHYSICAL REVIEW A. vol. 69, pp. 023812/1-023812/9

OLIVARES S., PARIS M.G.A. (2004).
Binary communication in single-mode and entangled noisy channels. J. OPT. B. vol. 6, p. 69OLIVARES S., PARIS M.G.A. (2004).
Enhancement of nonlocality in phase space. PHYS. REV. A. vol. 70, p. 032112

OLKHOVSKY V.S., PETRILLO V., ZAICHENKO A.K. (2004).
Decrease of the tunneling time and violation of the Hartman effect for large barrier. PHYSICAL REVIEW A. vol. 70, p. 034103

PIOVELLA N., COLA M., BONIFACIO R. (2004).
Classical and quantum regimes in the collective atomic recoil laser from a Bose-Einstein condensate. JOURNAL OF MODERN OPTICS. vol. 51, pp. 1019-1023

PIOVELLA N., SALASNICH L., BONIFACIO R., ROBB G.R.M. (2004).
Atomicinteraction effects in the superradiant light scattering from a Bose-Einsteincondensate. LASER PHYSICS. vol. 14, pp. 278-283

PRATI F., BACHE M., CACCIA P., CASTELLI F. (2004).
Analysis of elliptically polarized states in vertical-cavity surface emitting lasers. PHYS. REV. A. vol. 69, p. 033810

ROBB G.R.M., PIOVELLA N., FERRARO A., BONIFACIO R., COURTEILLE PH.W., ZIMMERMANN C. (2004).
Collective atomic recoil lasing including friction and diffusion effects. PHYSICAL REVIEW A. vol. 69, pp. 041403/1-041403/4

ROSSI A.R., OLIVARES S., PARIS M.G.A. (2004).
Degradation of continuous variable entanglement in a phase-sensitive environment. J. MOD. OPT. vol. 51, p. 1057

ROSSI A.R., OLIVARES S., PARIS M.G.A. (2004).
Photon statistics without counting photons. PHYS. REV. A. vol. 70, p. 055801

ROSSI A.R., PARIS M.G.A. (2004).
About distillability of depolarized states. J. MOD. OPT. vol. 51, p. 1037

SERAFINI A., DE SIENA S., ILLUMINATI F., PARIS M.G.A. (2004).
Minimum decoherence cat-like states in Gaussian noisy channels. J. OPT. B. vol. 6, p. 591

SERAFINI A., ILLUMINATI F., PARIS M.G.A., DE SIENA S. (2004).
Entanglement and purity of two_mode Gaussian states in noisy channels. PHYS. REV. A. vol. 69, p. 023318

VON CUBE C., S. SLAMA, D. KRUSE, C. ZIMMERMANN, PH.W. COURTEILLE, G.R.M. ROBB, PIOVELLA N. (2004).
Self-synchronization and dissipation-induced threshold incollective atomic recoil lasing. PHYSICAL REVIEW LETTERS. vol. 93, pp. 083601/1-083601/4
ALESINI D. et al. (2003).
Conceptual design of a high-brightness linac for soft X ray SASE-FEL source. NUCL. INSTR. AND METH. A. vol. 507, p. 502

ALESINI D. et al. (2003).
The SPARC project: a high-brightness electron beam source at LNF to drive a SASE-FEL experiment NUCL. INSTR. AND METH. A. vol. 507, p. 345

BENZA V.G., STRINI G. (2003).
A single qubit Landau-Zener gate. FORTSCHR. PHYS. vol. 51, pp. 14-21

BOSCOLO I., CIALDI S., CATANI L., TAZZIOLI F., VICARIO C., ORLANDUCCI S., SESSA V., TERRANOVA M.L., ROSSI M. (2003).
Photo-emission from diamond films illuminated by intense Nd:YAG laser harmonics. APPL. PHYS. A. vol. 77, pp. 805-809

BOSCOLO I., CIALDI S., CATANI L., TAZZIOLI F., VICARIO C., ORLANDUCCI S., SESSA V., TERRANOVA M.L., ROSSI M. (2003).
Structural features of Diamond layers photo-emitting at sub-band gap energies. DIAMOND RELATED MAT. vol. 12, pp. 2186-2194

BOSCOLO I., CIALDI S., GAMMINO S., CIAVOLA G. (2003).
Operation of an electron-cyclotron-resonance ion source with supplemental electron injection. PHYS. REV. ST-AB. vol. 6, p. 073501

CASAGRANDE F., CASTELLI F., LULLI A. (2003).
Reply to comment on collective effects and trapping states by a quantum-trajectory treatment of micromaser dynamics. PHYSICAL REVIEW A. vol. 67, pp. 027802/1-027802/3

CASAGRANDE F., FERRARO A., LULLI A., BONIFACIO R., SOLANO E., WALTHER H. (2003).
How to measure the phase diffusion dynamics in the micromaser. PHYSICAL REVIEW LETTERS. vol. 90, pp. 183601/1-183601/4

CASAGRANDE F., FERRARO A., LULLI A., BONIFACIO R., SOLANO E., WALTHER H. (2003).
Micromaser spectrum and phase diffusion dynamics. JOURNAL OF OPTICS B-QUANTUM AND SEMICLASSICAL OPTICS. vol. 5, pp. S459-S466

OLIVARES S., PARIS M.G.A., BONIFACIO R. (2003).
Teleportation Improvement by Inconclusive Photon Subtraction. PHYSICAL REVIEW A. vol. 67, p. 032314

PARIS M.G.A., COLA M., PIOVELLA N., BONIFACIO R. (2003).
Radiation to atom quantum mapping by collective recoil in Bose-Einstein condensate. OPTICS COMMUNICATIONS. vol. 227, pp. 349-354

PARIS M.G.A., COLA M.M., BONIFACIO R. (2003).
Quantum state engineering assisted by entanglement. PHYS REV A. vol. 67, p. 042104

PARIS M.G.A., COLA M.M., BONIFACIO R. (2003).
Remote state preparation and teleportation in phase space J. OPT. B. vol. 5, p. 360

PETRILLO V., JANNER D. (2003).
Relativistic analysis of a wave packetinteracting with a quantum mechanical barrier PHYSICAL REVIEW A. vol. 67, p. 012110

PIOVELLA N. (2003).
Two-dimensional quantum theory of collective light scattering from Bose-Einstein condensates. LASER PHYSICS. vol. 13, pp. 1-8

PIOVELLA N., BERETTA V., ROBB G.R.M., BONIFACIO R. (2003).
Photon echo in the super-radiant light scattering from a Bose-Einstein condensate. PHYSICAL REVIEW A. vol. 68, pp. 021801/1-021801/4

PIOVELLA N., COLA M., BONIFACIO R. (2003).
Quantum fluctuations and entanglement in the collective atomic recoil laser using a Bose-Einstein condensate. PHYSICAL REVIEW A. vol. 67, p. 013817

Optics

Books

PIAZZA R., GIGLIO M. (2004).
The European Physical Journal E, Special Issue: Thermal Forces in Simple and Complex Fluids. vol. 15, 102 pp. LES ULIS: EDP Sciences (FRANCE)

Patents

GIGLIO M., POTENZA M.A.C. (2005).
A method for measuring properties of particels and corresponding apparatus. PCT/IB720057000362. Università degli Studi di Milano.

GIGLIO M., POTENZA M.A.C. (2005).
A method for measuring properties of particels by means of interference fringe analysis and corresponding apparatus. PCT/IB/2005/000411 - WO2005/083389. Università degli Studi di Milano.

POTENZA M.A.C., BROGIOLI D., GIGLIO M. (2003).
Descrizione di un procedimento per la misurazione di propriet‡ di materiali torbidi, e relativa apparecchiatura. TO2003A000830. CNR-INFM

Articles

ALAIMO M., MAGATTI D., FERRI F., POTENZA M.A.C. (2006).
Heterodyne speckles velocimetry. APPLIED PHYSICS LETTERS. vol. 88, p. 191101

CROCCOLO F., BROGIOLI D., VAILATI A., GIGLIO M., CANNELL D.S. (2006).
Use of dynamic Schlieren interferometry to study fluctuations during free diffusion. APPLIED OPTICS. vol. 45, p. 2166

POTENZA M.A.C., ALAIMO M., MAGATTI D., PESCINI D., FERRI F., GIGLIO M. (2006).
A new technique for fluid velocimetry. OPTICS AND LASERS IN ENGINEERING. vol. 44, pp. 722-731

VAILATI A., CERBINO R., MAZZONI S., GIGLIO M., NIKOLAENKO G., TAKACS C.J., CANNELL D.S., MEYER W.V., SMART A.E. (2006).
GRADFLEX, Fluctuations in Microgravity. APPLIED OPTICS. vol. 45, pp. 2155

CERBINO R., MAZZONI S., VAILATI A., GIGLIO M. (2005).
Scaling behavior for the onset of convection in a colloidal suspension. PHYSICAL REVIEW LETTERS. vol. 94, pp. 064501-064504

BROGIOLI D., VAILATI A., GIGLIO M., POTENZA M.A.C. (2004).
Near Field Scattering. PHYSICAL CHEMISTRY AND CHEMICAL PHYSICS. vol. 7, pp. 1547-1550

CARPINETI M., PIAZZA R. (2004).
Metastability and supersaturation limit for lysozyme crystallization. PHYSICAL CHEMISTRY CHEMICAL PHYSICS. vol. 6, pp. 1506-1511

FERRI F., MAGATTI D., POTENZA M.A.C., GIGLIO M. (2004).
Heterodyne near field scattering: a new technique for complex fluids. PHYSICAL REVIEW E. vol. 70, p. 041405

POTENZA M., BROGIOLI D., GIGLIO M. (2004).
Total Internal Reflection Scattering. APPLIED PHYSICS LETTERS. vol. 85, pp. 2730-2732

POTENZA M.A.C., MINARDI S., TRULL J., BLASI G., SALERNO D., VARANAVICIUS A., PISKARSKAS A., DI TRAPANI P. (2004).
Three dimensional imaging of short pulses. OPTICS COMMUNICATIONS. vol. 229, pp. 381-390

MAZZONI S., CERBINO R., BROGIOLI D., VAILATI A., GIGLIO M. (2004).
Transient oscillations in Soret-driven convection in a colloidal suspension. EUROPEAN PHYSICAL JOURNAL E. vol. 15, pp. 305-309

BROGIOLI D., VAILATI A., GIGLIO M. (2003).
A schlieren method for ultra-low angle light scattering measurements. EUROPHYSICS LETTERS. vol. 63, pp. 220-225

CERBINO R., VAILATI A., GIGLIO M. (2003).Fast-onset Soret-driven convection in a colloidal suspension heated from above. PHILOSOPHICAL MAGAZINE. vol. 83, p. 2023

Plasma Physics and Astrophysics

Books

BERTIN G., FARINA D., POZZOLI R. (2004).
Plasmas in the Laboratory and in the Universe: new insights and new challenges. AIP Conference Proceedings, vol. 703, 465 pp. MELVILLE, NEW YORK: American Institute of Physics (UNITED STATES).

Articles

TRENTI M., BERTIN G. (2006).
Partial suppression of the radial orbit instability in stellar systems. ASTROPHYSICAL JOURNAL. vol. 637, pp. 717-724

BARBIERI C.V., FRATERNALI F., OOSTERLOO T., BERTIN G., BOOMSMA R., SANCISI R. (2005).
Extra-planar gas in the spiral galaxy NGC 4559. ASTRONOMY & ASTROPHYSICS. vol. 439, pp. 947-956

BETTEGA G., CAVALIERE F., CAVENAGO M., ILLIBERI A., POZZOLI R., ROME' M. (2005).
Experimental investigation of the ion resonance instability in a trapped electron plasma. PLASMA PHYSICS AND CONTROLLED FUSION. vol. 47, pp. 1697-1708

BRADAC M., ERBEN T., SCHNEIDER P., HILDEBRANDT H., LOMBARDI M., SCHIRMER M., MIRALLES J.M., CLOWE D., SCHINDLER S. (2005).
Strong and weak lensing united. ASTRONOMY & ASTROPHYSICS. vol. 437, pp. 49-60

BRADAC M., SCHNEIDER P., LOMBARDI M., ERBEN T. (2005).Strong and weak lensing united. ASTRONOMY & ASTROPHYSICS. vol. 437, pp. 39-48

CHILDERS J., BERSANELLI M., FIGUEIREDO N., GAIER T.C., HALEVI D., KANGAS M., LEVY A., LUBIN P.M., MALASPINA M., MANDOLESI N., MARVIL J., MEINHOLD P.R., MEJIA J., NATOLI P., O'NAILL H. et al. (2005).
The Background Emission Anisotropy Scanning Telescope (BEAST) Instrument. Description and Performances. THE ASTROPHYSICAL JOURNAL SUPPL. vol. 158, pp. 124-138

CIOTTI L., BERTIN G. (2005).
A simple method to construct exact density-potential pairs from a homeoidal expansion. ASTRONOMY & ASTROPHYSICS. vol. 437, pp. 419-427

FIGUEIREDO N., BERSANELLI M., CHILDERS J., D'ARCANGELO O., HALEVI D., JANSSEN M., KEDWARD K., LEMASTER N., LUBIN P.M., MANDOLESI N., MARVIL J., MEINHOLD P.R., MEJIA J., MENNELLA A., NATOLI P. et al. (2005).
The optical design of the Background Emission Anisotropy Scanning Telescope. THE ASTROPHYSICAL JOURNAL SUPPL. vol. 158, pp. 118-123

JACCHIA A., DE LUCA F., RYTER F., BRUSCHI A., LEUTERER F., NEU R., PEREVERZEV G., SUTTROP W., WAGNER D. AND ASDEX UPGRADE TEAM (2005).
Nonlinear perturbative electron heat transport study in the ASDEX Upgrade tokamak. NUCLEAR FUSION. vol. 45, pp. 40-47

KOTELNIKOV I.A., POZZOLI R., ROME' M. (2005).
Diocotron instability in non-neutral plasmas with a stationary point inthe rotation frequency profile. PHYSICS OF PLASMAS. vol. 12, pp. 092105/1-092105/8

LOMBARDI M. (2005).
Optimal column density measurements from multiband near-infrared observations. ASTRONOMY & ASTROPHYSICS. vol. 438, pp. 169-185

LOMBARDI M., ROSATI P., BLAKESLEE J.P., ETTORI S., DEMARCO R., FORD H.C., ILLINGWORTH G.D., CLAMPIN M., HARTIG G.F., BENTEZ N., BROADHURST T.J., FRANX M., JEE M.J., POSTMAN M., WHITE R.L. (2005).
Hubble Space Telescope ACS Weak-Lensing Analysis of the Galaxy Cluster RDCS 1252.9-2927 at z = 1.24. ASTROPHYSICAL JOURNAL. vol. 623, pp. 42-56

MAASSBERG H., ROME' M., ERCKMANN V., GEIGER J., LAQUA H.P., MARUSHCHENKO N.B., W-AS TEAM. (2005).
Electron Cyclotron Current Drive in the WENDELSTEIN-7-AS Stellarator. PLASMA PHYSICS AND CONTROLLED FUSION. vol. 47, pp. 1137-1163

MEINHOLD P.R., BERSANELLI M., CHILDERS J., FIGUEIREDO N., GAIER T.C., HALEVI D., LAWRENCE C.R., KANGAS M., LEVY A., LUBIN P.M., MALASPINA M., MANDOLESI N., MARVIL J., MEJIA J., NATOLI P. et al. (2005).
A Map of the Cosmic Microwave Background from the BEAST experiment. THE ASTROPHYSICAL JOURNAL SUPPL. vol. 158, pp. 124-138

MEJIA J., BERSANELLI M., BURIGANA C., CHILDERS J., FIGUEIREDO N., KANGAS M., LUBIN P.M., MAINO D., MANDOLESI N., MARVIL J., MEINHOLD P.R., O'DWYER I., O'NAILL H., PLATANIA P., SEIFFERT M. et al. (2005).
Galactic Foreground Contribution to the BEAST CMB Anisotropy Maps. THE ASTROPHYSICAL JOURNAL SUPPL. vol. 158, pp. 109-117

O'DWIER I., BERSANELLI M., CHILDERS J., FIGUEIREDO N., HALEVI D., HUEY G.G., LUBIN P.M., MAINO D., MANDOLESI N., MARVIL J., MEINHOLD P.R., MEJIA J., NATOLI P., O'NEILL H., PINA A., et al. (2005).
The CMB Power Spectrum from the Background Emission Anisotropy Scanning Telescope (BEAST) Experiment. THE ASTROPHYSICAL JOURNAL SUPPL. vol. 158, pp. 93-100

SCHNEIDER P., KILBINGER M., LOMBARDI M. (2005).
The three-point correlation function of cosmic shear. II. Relation to the bispectrum of the projected mass density and generalized third-order aperture measures. ASTRONOMY & ASTROPHYSICS. vol. 431, pp. 9-25

TRENTI M., BERTIN G. (2005).
A family of models of partially relaxed stellar systems I. Dynamical properties. ASTRONOMY & ASTROPHYSICS. vol. 429, pp. 161-172

TRENTI M., BERTIN G., VAN ALBADA T.S. (2005).
A family of models of partially relaxed stellar systems II. Comparison with the products of collisionless collapse. ASTRONOMY & ASTROPHYSICS. vol. 433, pp. 57-72

TSIDULKO YU., POZZOLI R., ROME' M. (2005).
MEP: a 3D PIC Code for the Simulation of the Dynamics of a Non-Neutral Plasma. JOURNAL OF COMPUTATIONAL PHYSICS. vol. 209, pp. 406-420

ALESINI D. et al. (including ALESSANDRIA F., BACCI A., BOSCOLO I., BROGGI F., CIALDI S., DE MARTINIS C., GIOVE D., MAROLI C., MAURI M., PETRILLO V., ROME' M., SERAFINI L.) (2004).
Status of the SPARC project. NUCLEAR INSTRUMENTS & METHODS IN PHYSICS RESEARCH. SECTION A, ACCELERATORS, SPECTROMETERS, DETECTORS AND ASSOCIATED EQUIPMENT. vol. 528, pp. 586-590

BACCIGALUPI C., PERROTTA F., DE ZOTTI G., SMOOT G.F., BURIGANA C., MAINO D., BEDINI L., SALERNO E. (2004).
Extracting cosmic microwave background polarisation from satellite astrophysical maps. MONTHLY NOTICES OF THE ROYAL ASTRONOMICAL SOCIETY. vol. 354, pp. 55-70

BETTEGA G., CAVALIERE F., ILLIBERI A., POZZOLI R., ROME' M., CAVENAGO M., TSIDULKO YU. (2004).
Experimental investigation of coherent structures in a low-energy electron beam. APPLIED PHYSICS LETTERS. vol. 84, pp. 3807-3809

BRADAC M., LOMBARDI M., SCHNEIDER P. (2004).
Mass-sheet degeneracy:Fundamental limit on the cluster mass reconstruction from statistical (weak) lensing. ASTRONOMY & ASTROPHYSICS. vol. 424, pp. 13-22

BRADAC M., SCHNEIDER P., LOMBARDI M., STEINMETZ M., KOOPMANS L.V.E., NAVARRO J.F. (2004).
The signature of substructure on gravitational lensing in the LambdaCDM cosmological model. ASTRONOMY & ASTROPHYSICS. vol. 423, pp. 797-809

BURIGANA C., SANDRI M., VILLA F., MAINO D., BACCIGALUPI C., BERSANELLI M., MANDOLESI N. (2004).
Trade-off between angular resolution and straylight contamination in CMB anisotropy experiments. II - Straylight evaluation. ASTRONOMY & ASTROPHYSICS. vol. 428, pp. 311-325

CUTTAIA F., VALENZIANO L., BERSANELLI M.M., BUTLER C., D'ARCANGELO O., KETTLE D., LEVIN S., MANDOLESI N., MENNELLA A., MOREGANTE G., MORIGI G., RODDIS N., SIMONETTO A., TERENZI L., TOMASI M. et al. (2004).
Analysis of the Radiometer - Reference Load System on board the Planck-LFI instrument. NUCLEAR INSTR. & METHODS IN PHYS. RES. A. vol. 520, pp. 396-401

DONATI P., PIZZOCHERO P. (2004).
Fully Consistent Semi-Classical Treatment of Vortex-Nucleus Interaction in Rotating Neutron Stars. NUCLEAR PHYSICS. vol. A742, pp. 363-379

ESPOSITO B., BURATTI P., CIRANT S., LEIGHEB M., BRACCO G.,

CARRARO L., COCILOVO V., GABELLIERI L., GANDINI F., GIOVANNOZZI E., GORMEZANO C., JACCHIA A., LAZZARO E., DE LUCA F., MARINUCCI M. et al. (2004).
Transport studies in the FTU. FUSION SCIENCE AND TECHNOLOGY. vol. 45, pp. 370-386

FARINA D., POZZOLI R. (2004).
Large-amplitude oscillations and chaos in a Hamiltonian plasma system with many degrees of freedom. PHYSICAL REVIEW E, STATISTICAL, NONLINEAR, AND SOFT MATTER PHYSICS. vol. 70, pp. 036407/1-036407/5

KEIHANEN E., KURKI-SUONIO H., POUTANEN T., MAINO D., BURIGANA C. (2004).
A maximum likelihood approach to the destriping technique. ASTRONOMY & ASTROPHYSICS. vol. 428, pp. 287-298

MARIS M., MAINO D., BURIGANA C., MENNELLA A., BERSANELLI M., PASIAN F. (2004).
The effect of signal digitisation in CMB experiments. ASTRONOMY & ASTROPHYSICS. vol. 414, pp. 777-789

MENNELLA A., BACCIGALUPI C., BALBI A., BERSANELLI M., BURIGANA C., BUTLER C., CAPPELLINI B., DE GASPERIS G., HANSEN F., MAINO D., MANDOLESI N., MARIS M., MOREGANTE G., NATOLI P., PASIAN F. et al. (2004).
Imaging the first light: experimental challenges and future perspectives in the observation of the Cosmic Microwave Background Anisotropy. RECENT RESEARCH DEVELOPMENTS IN ASTRONOMY AND ASTROPHYSICS. vol. 2, pp. 1-57

POUTANEN T., MAINO D., KURKI-SUONIO H., KEIHANEN E., HIVON E. (2004).
Cosmic microwave background power spectrum estimation with the destriping technique. MONTHLY NOTICES OF THE ROYAL ASTRONOMICAL SOCIETY. vol. 353, pp. 43-58

SANDRI M., VILLA F., BURIGANA C., BERSANELLI M., MANDOLESI N. (2004).
Trade-off between angular resolution and straylight contamination in CMB anisotropy experiments. I - Pattern simulations. ASTRONOMY & ASTROPHYSICS. vol. 428, pp. 299-310

TERENZI L., MENNELLA A., BERSANELLI M., MANDOLESI N., MOREGANTE G., PRINA M., TOMASI M., VALENZIANO L. (2004).
Thermal Stability in Precision Cosmology Experiments: The Planck LFI Case. NUCLEAR INSTR. & METHODS IN PHYS. RES. A. vol. 520, pp. 393-395

AMORETTI M., BETTEGA G., CAVALIERE F., CAVENAGO M., DE LUCA F., POZZOLI R., ROME' M. (2003).
Cylindrical Penning trap for the study of electron plasmas. REVIEW OF SCIENTIFIC INSTRUMENTS. vol. 74, pp. 3991-3997

ALESINI D. et al. (including ACERBI E., ALESSANDRIA F., BARNI D., BELLOMO G., BOSCOLO I., BROGGI F., CIALDI S., DE MARTINIS C., GIOVE D., MAROLI C., PETRILLO V., ROME' M., SERAFINI L.) (2003).
The SPARC project: a high-brightness electron beam source at LNF to drive a SASE-FEL experiment. NUCLEAR INSTRUMENTS & METHODS IN PHYSICS RESEARCH. SECTION A, ACCELERATORS, SPECTROMETERS, DETECTORS AND ASSOCIATED EQUIPMENT. vol. 507, pp. 345-349

BERTIN G., LISEIKINA T., PEGORARO F. (2003).
Slow evolution of elliptical galaxies induced by dynamical friction I. Capture of a system of satellites. ASTRONOMY & ASTROPHYSICS. vol. 405, pp. 73-88

BERTIN G., TRENTI M. (2003).
Thermodynamic description of a family of partially relaxed stellar systems. ASTROPHYSICAL JOURNAL. vol. 584, pp. 729-734

CAPPELLINI B., MAINO D., ALBETTI G., PLATANIA P., PALADINI R., MENNELLA A., BERSANELLI M. (2003).
Optimised in-flight absolute calibration for extended CMB surveys. ASTRONOMY & ASTROPHYSICS. vol. 409, pp. 375-385

CIRANT S., BRACCO G., BRUSCHI A., BURATTI P., DE LUCA F., ESPOSITO B., GANDINI F., GIOVANNOZZI E., GRANUCCI G., JACCHIA A., LAZZARO E., MINARDI E., NOWAK S., RAMPONI G., SOZZI C., TUDISCO O. AND FTU TEAM AND ECRH GROUP (2003).
Transport studies with the ECH system on FTU tokamak . NUCLEAR FUSION. vol. 43, pp. 1384-1395

D'ARCANGELO O., GARAVAGLIA S., SIMONETTO A., SOZZI C., BERSANELLI M., MENNELLA A., VILLA F. (2003).
Measurements of beam pattern perturbation in corrugated feed horn arrays for CMB observations. EXPERIMENTAL ASTRONOMY. vol. 16, pp. 165-187

DONATI P., PIZZOCHERO P. (2003).
Is There Nuclear Pinning of Vortices in Superfluid Pulsars? PHYSICAL REVIEW LETTERS. vol. 90, p. 211101ETTORI S., LOMBARDI M. (2003).X-ray and weak lensing measurements of the mass profile of MS1008.1-1224: Chandra and VLT data. ASTRONOMY & ASTROPHYSICS. vol. 398, pp. L5-L9

FOSBURY R.A.E., VILLAR-MARTN M., HUMPHREY A., LOMBARDI M., ROSATI P., STERN D., HOOK R.N., HOLDEN B.P., STANFORD S.A., SQUIRES G.K., RAUCH M., SARGENT W.L.W. (2003).
Massive Star Formation in a Gravitationally Lensed H II Galaxy at z = 3.357. ASTROPHYSICAL JOURNAL. vol. 596, pp. 797-809
HEBER B., FERRANDO P., RAVIART A., PAIZIS C., SARRI G., POSNER A., WIBBERENZ G., MUELLER-MELLIN R., KUNOW H., POTGIETER M.S., FERREIRA S.E.S, BURGER R.A., FICHTER H. (2003).
Quiet time MeV electron increases at Solar maximum. Ulysses COSPIN/KET observations. ADVANCES IN SPACE RESEARCH. vol. 32, pp. 663-668

HEBER B., SARRI G., WIBBERENZ G., PAIZIS C., FERRANDO P., RAVIART A., POSNER A., MUELLER-MELLIN R., KUNOW H. (2003).
The Ulysses fast latitude scans: COSPIN/KET results. ANNALES GEOPHYSICAE. vol. 21, pp. 1275-1288

LODATO G., BERTIN G. (2003).
Non-Keplerian rotation in the nucleus of NGC 1068: evidence for a massive accretion disk? ASTRONOMY & ASTROPHYSICS. vol. 398, pp. 517-524

LODATO G., BERTIN G. (2003).
Probing the rotation curve of the outer accretion disk in FU Orionis objects with long-wavelength spectroscopy. ASTRONOMY & ASTROPHYSICS. vol. 408, pp. 1015-1028

LOMBARDI M., SCHNEIDER P. (2003).
Smooth maps from clumpy data: Generalizations. ASTRONOMY & ASTROPHYSICS. vol. 407, pp. 385-392

MAINO D., BANDAY A.J., BACCIGALUPI C., PERROTTA F., GORSKI K.M. (2003).
Astrophysical component separation of COBE-DMR 4-yr data with FastICA. MONTHLY NOTICES OF THE ROYAL ASTRONOMICAL SOCIETY. vol. 344, pp. 544-552

MAINO D., BURIGANA D., PASIAN F. (2003).
On the loss of telemetry data in full-sky surveys from space. NEW ASTRONOMY. vol. 8, pp. 711-718

MENNELLA A., BERSANELLI M., SEIFFERT M., KETTLE D., RODDIS N., WILKINSON A. (2003).
Offset balancing in pseudo-correlation receivers for CMB measurements. ASTRONOMY & ASTROPHYSICS. vol. 410, pp. 1089-1100

PALADINI R., BURIGANA C., DAVIES R.D., MAINO D., BERSANELLI M., CAPPELLINI B., PLATANIA P., SMOOT G.F. (2003).
A radio catalog of Galactic HII regions for application from decimeter to millimeter wavelenghts. ASTRONOMY & ASTROPHYSICS. vol. 397, pp. 213-226

PLATANIA P., BURIGANA C., MAINO D., CASERINI E., BERSANELLI M., CAPPELLINI B., MENNELLA A. (2003).
Full sky study of diffuse Galactic emission at decimeter wavelenghts. ASTRONOMY & ASTROPHYSICS. vol. 410, pp. 847-856ROME' M., ERCKMANN V., LAQUA H.P., MAASSBERG H., MARUSHCHENKO N.B. (2003).
Comparison of high-field-side and low-field-side launch ECCD in the W7-AS Stellarator. PLASMA PHYSICS AND CONTROLLED FUSION. vol. 45, pp. 783-792

RYTER F., TARDINI G., DE LUCA F., FAHRBACH H.-U., IMBEAUX F., JACCHIA A., KIROV K.K., LEUTERER F., MANTICA P., PEETERS A.G., PEREVERZEV G., SUTTROP W. AND ASDEX UPGRADE TEAM (2003).
Electron heat transport in ASDEX Upgrade: experiment and modelling. NUCLEAR FUSION. vol. 43, pp. 1396-1404

SCHNEIDER P., LOMBARDI M. (2003).
The three-point correlation function of cosmic shear. I. The natural components. ASTRONOMY & ASTROPHYSICS. vol. 397, pp. 809-818

Theoretical Physics

Books

COSENTINO LAGOMARSINO M., JONA P., BASSETTI B. (2006).
Randomization and Feedback Properties of Directed Graphs Inspired to Gene Networks. In: LECTURE NOTES IN BIOINFORMATICS (SPRINGER)

CARACCIOLO S. (2005).
Quantum Mechanics: Critical phenomena. In: BASSANI F., LIEDL J., WYDERP. ENCYCLOPEDIA OF CONDENSED MATTER PHYSICS (ELSEVIER, OXFORD). pp. 39-44

Articles

ALTARELLI G., BALL R.D., FORTE S. (2006).
Perturbatively stable resummed small x evolution kernels. NUCLEAR PHYSICS B. vol. 742, pp. 1-40BALL R.D., FORTE S. (2006).
All order running coupling BFKL evolution from GLAP (and vice-versa). NUCLEAR PHYSICS B. vol. 742, pp. 158-175

BARCHIELLI A., LUPIERI G. (2006).
Quantum measurements and entropic bounds on information transmission. QUANTUM INFORMATION & COMPUTATION. vol. 6, pp. 016-045

CARACCIOLO S., MOGNETTI B.M., PELISSETTO A. (2006).
Large-N(F) chiral transition in the Yukawa model. NUCLEAR PHYSICS B. vol. 741, pp. 421-440

CARACCIOLO S., MOGNETTI B.M., PELISSETTO A. (2006).
Polymer size in dilute solutions in the good-solvent regime. JOURNAL OF CHEMICAL PHYSICS. vol. 125, p. 094904

CARACCIOLO S., MOGNETTI B.M., PELISSETTO A. (2006).
Virial coefficients and osmotic pressure in polymer solutions in good-solvent conditions. JOURNAL OF CHEMICAL PHYSICS. vol. 125, p. 094903

CARLONI CALAME C.M., MONTAGNA G., NICROSINI O., VICINI A. (2006).
Precision electroweak calculation of the charged current Drell-Yan process. JOURNAL OF HIGH ENERGY PHYSICS. v. 0612, p. 016

FERRARI R., QUADRI A. (2006).
A Weak Power-Counting Theorem for the Renormalization of the Non-Linear Sigma Model in Four Dimensions. INTERNATIONAL JOURNAL OF THEORETICAL PHYSICS. vol. 45, pp. 2497-2515

FERRARI R., QUADRI A. (2006).
Renormalization of the Non-Linear Sigma Model in Four Dimensions: a two-loop example. JOURNAL OF HIGH ENERGY PHYSICS. vol. 0601:003, pp. 1-15

FORTE S., RIDOLFI G., ROJO J., UBIALI M. (2006).
Borel resummation of soft gluon radiation and higher twists. PHYSICS LETTERS SECTION B. vol. 635, pp. 313-319

MAURI A., PENATI S., PIRRONE M., SANTAMBROGIO A., ZANON D. (2006).
On the perturbative chiral ring for marginally deformed N=4 SYM theories. JOURNAL OF HIGH ENERGY PHYSICS. vol. 0608, p. 72

QUADRI A. (2006).
The Abelian embedding formulation of the Stuckelberg model and its power-counting renormalizable extension. PHYSICAL REVIEW D. vol. 73, p. 065024

ZECCA A. (2006).
Comoving self gravitating scalar field in the Newman Penrose formalism. INTERNATIONAL JOURNAL OF THEORETICAL PHYSICS. vol. 45, pp. 385-393

ZECCA A. (2006).
Massive field equations of arbitrary spin in Schwarzschild geometry: separation induced by spin-3/2 case. INTERNATIONAL JOURNAL OF THEORETICAL PHYSICS. vol. 45, pp. 2241-2247

ZECCA A. (2006).
Normal modes for massive spin 1 equation in Robertson-Walker space-time. INTERNATIONAL JOURNAL OF THEORETICAL PHYSICS. vol. 45, pp. 1981-1987

ZECCA A. (2006).
Proca fields interpretation of spin 1 equation in Robertson-Walker space-time. GENERAL RELATIVITY AND GRAVITATION. vol. 38, pp. 837-843

ZECCA A. (2006).
Separation of massive field equation of arbitrary spin in Robertson-Walker space-time. IL NUOVO CIMENTO B. vol. 121, pp. 167-173ZECCA A. (2006).
Solution of the Dirac equation in expanding universes. INTERNATIONAL JOURNAL OF THEORETICAL PHYSICS. vol. 45, pp. 44-52

ABBATE R., FORTE S. (2005).
Re-evaluation of the Gottfried sum using neural networks. PHYSICAL REVIEW D. vol. 72, p. 117503

BARCHIELLI A., LUPIERI G. (2005).
Instruments and channels in quantum information theory. OPTICS AND SPECTROSCOPY. vol. 99, pp. 425-432

BASSI A., IPPOLITI E., VACCHINI B. (2005).
On the energy increase in space-collapse models. JOURNAL OF PHYSICS A: MATHEMATICAL AND GENERAL. vol. 38, pp. 8017-8038

BOLZONI P., FORTE S., RIDOLFI G. (2005).Renormalization group approach to Sudakov resummation in prompt photon production. NUCLEAR PHYSICS B. vol. B731, pp. 85-108

CARACCIOLO S., GAMBASSI A., GUBINELLI M., PELISSETTO A. (2005).
Critical Behavior of the Two-Dimensional Randomly Driven Lattice Gas. PHYSICAL REVIEW E, STATISTICAL, NONLINEAR, AND SOFT MATTER PHYSICS. vol. 72, p. 056111

CARACCIOLO S., GUTTMANN A., JENSEN I., PELISSETTO A., ROGERS A., SOKAL A. (2005).
Correction-to-Scaling Exponents for Two-Dimensional Self-Avoiding Walks. JOURNAL OF STATISTICAL PHYSICS. vol. 120, pp. 1037-1100

CARACCIOLO S., MOGNETTI B.M., PELISSETTO A. (2005).
Large Nf behaviour of the Yukawa model: analytic results. POS PROCEEDINGS OF SCIENCE. vol. LAT2005, p. 187

CARACCIOLO S., MOGNETTI B.M., PELISSETTO A. (2005).
Two-Dimensional Heisenberg Model with Nonlinear Interactions: 1/N Corrections. NUCLEAR PHYSICS B. vol. B707, pp. 458-492

CARACCIOLO S., SPORTIELLO A. (2005).
O(n) vector model at n=-1, -2 on random planar lattices: a direct combinatorial derivation. JOURNAL OF STATISTICAL MECHANICS: THEORY AND EXPERIMENT. p. L02002

COSENTINO LAGOMARSINO M., JONA P., BASSETTI B. (2005).
The Logic Backbone of a Transciption Network. PHYSICAL REVIEW LETTERS. vol. 7, p. 95

DEL DEBBIO L., FORTE S., JOSE I., PICCIONE A., ROJO J. (2005).
Unbiased determination of the proton structure function F(2)**p with faithful uncertainty estimation. JOURNAL OF HIGH ENERGY PHYSICS. vol. 0503, p. 080

ELMETTI F., SANTAMBROGIO A., ZANON D. (2005).
On N=1 exact superpotentials from U(N) matrix models. JOURNAL OF HIGH ENERGY PHYSICS. vol. 0510, p. 104

FERRARI R. (2005).
Endowing the nonlinear sigma model with a flat connection structure: a way to renormalization. JOURNAL OF HIGH ENERGY PHYSICS. vol. 08, pp. 48-61

FERRARI R., PICARIELLO M., QUADRI A. (2005).
Some Conjectures on the Limit of Infinite Higgs Mass. PHYSICS LETTERS, SECTION B. vol. B611, pp. 215-221

GIUDICI M., MELES G.A., PONZINI G., PARRAVICINI G. (2005).
Identification of hydraulic transmissivity of a confined aquifer with the Differential system method: a tomographic appproach. GEOPHYSICAL RESEARCH ABSTRACTS. vol. 7, p. 02660

GLIOZZI F., LOTTINI S., PANERO M., RAGO A. (2005).
Random percolation as a gauge theory. NUCLEAR PHYSICS B. vol. 719, p. 255

GLIOZZI F., RAGO A. (2005).
Overlap of the Wilson loop with the broken-string state. NUCLEAR PHYSICS B. vol. 714, p. 91

MAURI A., PENATI S., SANTAMBROGIO A., ZANON D. (2005).
Exact results in planar N=1 superconformal Yang-Mills theory. JOURNAL OF HIGH ENERGY PHYSICS. vol. 0511, p. 024

PENATI S., SANTAMBROGIO A., ZANON D. (2005).

Two-point correlators in the beta-deformed N=4 SYM at the next-to-leading order. JOURNAL OF HIGH ENERGY PHYSICS. vol. 0510, p. 23

PETRUCCIONE F., VACCHINI B. (2005).
Quantum description of Einstein's Brownian motion. PHYSICAL REVIEW E. vol. 71, p. 046134

QUADRI A. (2005).
Slavnov-Taylor parameterization of Yang-Mills theory with massive fermions in the presence of singlet axial-vector currents. JOURNAL HIGH ENERGY PHYSICS. vol. 0506, p. 068

VACCHINI B. (2005).
Master-equations for the study of decoherence. INTERNATIONAL JOURNAL OF THEORETICAL PHYSICS. vol. 44, pp. 1011-1021

VACCHINI B. (2005).Theory of decoherence due to scattering events and Le'vy processes. PHYSICAL REVIEW LETTERS. vol. 95, p. 230402

ZECCA A. (2005).
Comoving Einstein-Maxwell equation in the Newman-Penrose formulation. IL NUOVO CIMENTO B. vol. 120, pp. 99-109

ZECCA A. (2005).
Massive Spin 1 Equation in Schwarzschild Geometry. IL NUOVO CIMENTO B. vol. 120, pp. 1017-1020

ZECCA A. (2005).
Solution of the Massive spin 1 Equation in Expanding Universe. IL NUOVO CIMENTO B. vol. 120, pp. 513-520

AGLIETTI U., BONCIANI R., DEGRASSI G., VICINI A. (2004).
Master integrals for the two-loop light fermion contributions to gg —-> H and H —-> gamma gamma. PHYSICS LETTERS B. vol. 600, pp. 57-64

AGLIETTI U., BONCIANI R., DEGRASSI G., VICINI A. (2004).
Two loop light fermion contribution to Higgs production and decays. PHYSICS LETTERS B. vol. 595, pp. 432-441

ALIANI P., ANTONELLI V., PICARIELLO M., TORRENTE-LUJAN E. (2004).
Neutrino mass parameters from KamLAND, SNO and other solar evidence. PHYSICAL REVIEW D. vol. 69, pp. 013005/1-013005/7

BARCHIELLI A., LUPIERI G. (2004).
Instrumental processes, entropies, information in quantum continual measurements. QUANTUM INFORMATION & COMPUTATION. vol. 4, pp. 437-449

BELGIORNO F., MARTELLINI M. (2004).
Black holes and the third law of thermodynamics. INTERNATIONAL JOURNAL OF MODERN PHYSICS D. vol. 13, pp. 739-770

CARACCIOLO S., GAMBASSI A., GUBINELLI M., PELISSETTO A. (2004).
Comment on "Dynamic behavior of anisotropic non-equilibrium driving lattice gases". PHYSICAL REVIEW LETTERS. vol. 92, p. 029601

CARACCIOLO S., GAMBASSI A., GUBINELLI M., PELISSETTO A. (2004).
Finite-Size Scaling in the Driven Lattice Gas. JOURNAL OF STATISTICAL PHYSICS. vol. 115, pp. 281-322

CARACCIOLO S., GAMBASSI A., GUBINELLI M., PELISSETTO A. (2004).
Reply to 'Comments to the letter "Transverse fluctuations in the driven lattice gas"'. JOURNAL OF PHYSICS A, MATHEMATICAL AND GENERAL. vol. 37, pp. 8193-8195

CARACCIOLO S., JACOBSEN J.L., SALEUR H., SOKAL A., SPORTELLO A. (2004).Fermionic field theory for trees and forests. PHYSICAL REVIEW LETTERS. vol. 93, p. 080601

CARACCIOLO S., SPORTIELLO A. (2004).
General duality for abelian-group-valued statistical-mechanics models. JOURNAL OF PHYSICS A, MATHEMATICAL AND GENERAL. vol. 37, pp. 7407-7432

CARMELI C., CASSINELLI G., DEVITO E., TOIGO A., VACCHINI B. (2004).
A complete characterization of phase space measurements. JOURNAL OF PHYSICS A: MATHEMATICAL AND GENERAL. vol. 37, pp. 5057-5066

CASELLE M., GRINZA P., RAGO A. (2004).
Amplitude ratios for the mass spectrum of the 2d Ising model in the high-T, H not equal 0 phase. JOURNAL OF STATISTICAL MECHANICS: THEORY AND EXPERIMENT. vol. 0410, p. P009

CASELLE M., PEPE M., RAGO A. (2004).
Static quark potential and effective string corrections in the (2+1)-d SU(2) Yang-Mills theory. JOURNAL OF HIGH ENERGY PHYSICS. vol. 0410, p. 005

DEGRASSI G., VICINI A. (2004).
Two loop renormalization of the electric charge in the standard model. PHYSICAL REVIEW D. vol. 69, p. 073007

DIJKGRAAF R., GRISARU M.T., LAM C.S., VAFA C., ZANON D. (2004).
Planar gravitational corrections for supersymmetric gauge theories. JOURNAL OF HIGH ENERGY PHYSICS. vol. 0404, pp. 28-34

FERRARI R., QUADRI A. (2004).
Physical Unitarity for Massive Non-abelian Gauge Theories in the Landau Gauge: Stueckelberg and Higgs. JOURNAL OF HIGH ENERGY PHYSICS. vol. 0411, pp. 19-38

GRINZA P., RAGO A. (2004).Finite temperature results on the 2d Ising model with mixed perturbation. JOURNAL OF PHYSICS A: MATHEMATICAL AND GENERAL. vol. 37, p. 4701

LANZ L., VACCHINI B., MELSHEIMER O. (2004).
On consistency of quantum theory and macroscopic objectivity. QUANTUM INFORMATION AND COMPUTATION. vol. 4, pp. 513-522

MAGHINI S., SANTAMBROGIO A., ZANON D. (2004).
Two-point functions for n=4 Konishi-like operators. JOURNAL OF HIGH ENERGY PHYSICS. vol. 0411, pp. 56-62

VACCHINI B. (2004).
Dissipative systems and objective description: quantum Brownian motion as an example. INTERNATIONAL JOURNAL OF THEORETICAL PHYSICS. vol. 43, pp. 1515-1525

VACCHINI B. (2004).
Quantum and classical features in the explanation of collisional decoherence. JOURNAL OF MODERN OPTICS. vol. 51, pp. 1025-1029

VACCHINI B., VIALE A., VICARI M., ZANGHI N. (2004).
Testing decoherence in interference experiments with macromolecules: the theoretical background. JOURNAL OF MODERN OPTICS. vol. 51, pp. 1071-1072

ZECCA A. (2004).
Normal modes and separable scalar field equation in spherically symmetric space-time. IL NUOVO CIMENTO B. vol. 119, pp. 411-417

ZECCA A. (2004).
Single Slit Diffraction Pattern for Particle Interacting with the Wall. IL NUOVO CIMENTO B. vol. 119, pp. 197-205

ZECCA A. (2004).
Static massless and time dependent massive self-gravitating scalar field in spherically symmetric comoving system. IL NUOVO CIMENTO B. vol. 119, pp. 521-529

ZECCA A. (2004).
Superposition, Entropy and Schmidt Decomposition of States. INTERNATIONAL JOURNAL OF THEORETICAL PHYSICS. vol. 43, pp. 1849-1856

ALIANI P., ANTONELLI V., PICARIELLO M., TORRENTE-LUJAN E. (2003).
KamLAND potentiality on the determination of neutrino mixing parameters in the post SNO-NC era. NEW JOURNAL OF PHYSICS. vol. 5., pp. 2/1-2/5

ALIANI P., ANTONELLI V., PICARIELLO M., TORRENTE-LUJAN E. (2003).
KamLAND, solar anti-neutrinos and their magnetic moment. JOURNAL OF HIGH ENERGY PHYSICS. vol. 0302, p. 025

ALIANI P., ANTONELLI V., R. FERRARI, PICARIELLO M., TORRENTE-LUJAN E. (2003).
Determination of neutrino mixing parameters after SNO oscillation evidence. PHYSICAL REVIEW D. vol. 67, pp. 013006/1-013006/5

ALTARELLI G., FORTE S., BALL R.D. (2003).An anomalous dimension for small x evolution. NUCLEAR PHYSICS B. vol. B674, pp. 459-483

BELGIORNO F. (2003).
Black hole thermodynamics in Caratheodory's approach. PHYSICS LETTERS A. vol. 312, pp. 324-330BELGIORNO F. (2003).
Notes on the third law of thermodynamics (I). JOURNAL OF PHYSICS A:

MATHEMATICAL AND GENERAL. vol. 36, pp. 8165-8193

BELGIORNO F. (2003).
Notes on the third law of thermodynamics (II). JOURNAL OF PHYSICS A: MATHEMATICAL AND GENERAL. vol. 36, pp. 8195-8221
BELGIORNO F. (2003).Quasi-homogeneous thermodynamics and black holes. JOURNAL OF MATHEMATICAL PHYSICS. vol. 44, pp. 1089-1128

BERRINO G., CACCIATORI S.L., CELI A., MARTUCCI L., VICINI A. (2003).
Noncommutative electrodynamics. PHYSICAL REVIEW D. vol. 67, p. 065021

CARACCIOLO S., GAMBASSI A., GUBINELLI M., PELISSETTO A. (2003).
Shape dependence of the finite-size scaling limit in a strongly anisotropic O(infty) model. EUROPEAN PHYSICAL JOURNAL B, CONDENSED MATTER PHYSICS. vol. 34, pp. 205-217

CARACCIOLO S., GAMBASSI A., GUBINELLI M., PELISSETTO A. (2003).
Transverse Fluctuations in the Driven Lattice Gas. JOURNAL OF PHYSICS. A, MATHEMATICAL AND GENERAL. vol. 36, pp. L315-L320

CARDELLA M.A., ZANON D. (2003).
Noncommutative deformation of four-dimensional Einstein gravity. CLASSICAL AND QUANTUM GRAVITY. vol. 20, pp. L95-L104

DIJKGRAAF R., GRISARU M.T., LAM C.S., VAFA C., ZANON D. (2003).
Perturbative computation of glueball superpotentials. PHYSICS LETTERS, SECTION B. vol. B573, pp. 138-146

DUDAL D., VERSCHELDE H., LEMES V.E.R., SARANDY M.S., SORELLA S.P., PICARIELLO M., VICINI A., GRACEY J.A. (2003).
More on ghost condensation in Yang-Mills theory: BCS versus Overhauser effect and the breakdown of the Nakanishi-Ojima annex SL(2,R) symmetry. JOURNAL OF HIGH ENERGY PHYSICS. vol. 0306, p. 003

FORTE S., RIDOLFI G. (2003).
Renormalization group approach to soft gluon resummation. NUCLEAR PHYSICS B. vol. B650, pp. 229-270

ONARINI A., FERRARI R., JAUHO A.P., MOLINARI L. (2003).
Virtual photon contribution to frictional drag in double - layer devices. PHYSICS LETTERS A. vol. 312, p. 123

ZECCA A. (2003).
Elementary solutions of Dirac equation with torsion in flat-space-time. IL NUOVO CIMENTO B. vol. 118, pp. 65-70

ZECCA A. (2003).
Gravitational and scalar field interacting through torsion. IL NUOVO CIMENTO B. vol. 118, pp. 191-196

ZECCA A. (2003).
Interacting Gravitational and Dirac Fields with Torsion. INTERNATIONAL JOURNAL OF THEORETICAL PHYSICS. vol. 42, pp. 2905-2911

ZECCA A. (2003).
Neutrino oscillations in Robertson-Walker space-time with torsion. IL NUOVO CIMENTO B. vol. 119, pp. 81-87

ZECCA A. (2003)
Self gravitating scalar field in spherically symmetric comoving system: solutions depending on one variable. IL NUOVO CIMENTO B. vol. 118, pp. 953-961

ZECCA A. (2003).
Superposition, Entanglement and Product of States. INTERNATIONAL JOURNAL OF THEORETICAL PHYSICS. vol. 42, pp. 1611-1618

ZECCA A. (2003).
The Scalar Wave Equation in the General Schwarzschild metric. IL NUOVO CIMENTO B. vol. 118, pp. 469-474

ZECCA A. (2003).The spin connection, the Dirac and the Einstein-Dirac equation in the Robertson-Walker space-time. IL NUOVO CIMENTO B. vol. 118, pp. 693-697

Medical and Health Physics

Books

ALLEVI P., ANASTASIA L., CANTONE M.C., MALCOVATI M., PAGANONI A.M., POLI M., TENCHINI M.L. (2005).
Volume: ESERCIZI - Prove d'esame ufficiali con soluzione e commento, per la preparazione agli esami di ammissione di Medicina, Odontoiatria, Veterinaria. Ed. Edises

ALLEVI P., ANASTASIA L., CANTONE M.C., MALCOVATI M., PAGANONI A.M., POLI M., TENCHINI M.L. (2005).
Volume : TEORIA - Per la preparazione agli esami di ammissione in Medicina, Odontoiatria, Veterinaria. Ed. Edises

ALLEVI P., ANASTASIA L., CANTONE M.C., MALCOVATI M., PAGANONI A.M., POLI M., TENCHINI M.L. (2005).
Volume : ESERCIZI - Per la preparazione agli esami di ammissione di Professioni Sanitarie e Scienze Motorie. Ed. Edises

ALLEVI P., ANASTASIA L., CANTONE M.C., MALCOVATI M., PAGANONI A.M., POLI M., TENCHINI M.L. (2005).
Volume : TEORIA - Per la preparazione agli esami di ammissione in Professioni Sanitarie e Scienze Motorie. Ed. Edises

ALLEVI P., ANASTASIA L., CANTONE M.C., MALCOVATI M., PAGANONI A.M., POLI M., TENCHINI M.L. (2005).
Volume : ESERCIZI - Per la preparazione agli esami di ammissione e orientamento dei corsi di laurea di Area Scientifica. Ed. Edises

ALLEVI P., ANASTASIA L., CANTONE M.C., MALCOVATI M., PAGANONI A.M., POLI M., TENCHINI M.L. (2005).
Volume : TEORIA - Per la preparazione agli esami di ammissione e orientamento dei corsi di laurea di Area Scientifica. Ed. Edises

Articles

MORONI A., BRUNO M., BARDELLI L., BARLINI S., BRAMBILLA S., CASINI G., CAVALETTI R., CHIARI M., CORTESI A., D'AGOSTINO M., DE SANCTIS J., GERACI E., GIORDANO G., GIUSSANI A., GRAMEGNA F. et al. (2006).
The Ring Counter (RCo): a high resolution IC-Si-CsI(Tl) device for heavy ion reaction studies at 10-30 MeV/A. NUCLEAR INSTRUMENTATION AND METHODS A. vol. 556, pp. 516-526

VERONESE I., GIUSSANI A., GOKSU H.Y. (2006).
Limits of thermoluminescence dosimetry using quartz extracted from recent building materials in urban settlements. JOURNAL OF ENVIRONMENTAL RADIOACTIVITY. vol. 86, pp. 319-336

BAGATTI D., CANTONE M.C., GIUSSANI A., RIDONE S., BIRATTARI C., BONARDI M.L., GROPPI F., MARTINOTTI A., MORZENTI S., GALLORINI M., RIZZIO E. (2005).
Analytical and radioanalytrical quality control of purity and stability of radiopharmaceutical compound [186gRe]ReHEDP for bone metastases pain palliation. JOURNAL OF RADIOANALITYCAL AND NUCLEAR CHEMISTRY. vol. 263, pp. 515-520

BETTEGA D., CALZOLARI P., DONEDA L., DURANTE M., TALLONE L. (2005).
Early and Delayed Reproductive Death in Human Cells Exposed to High Energy Iron Ion Beams. Advances in Space Research. vol. 35(2), pp. 280-285

COLIVA A., ZACCHETTI A., LUISON E., TOMASSETTI A., BONGARZONE I., SEREGNI E., BOMBARDIERI E., MARTIN F., GIUSSANI A., FIGINI M., CANEVARI S. (2005).
90Y labeling of monoclonal antibody MOv18 and preclinical validation for radioimmunotherapy of human ovarian carcinomas. CANCER IMMUNOLOGY AND IMMUNOTHERAPY. vol. 54, pp. 1200-1213

GAMBARINI G., CARRARA M., CORTESI M., DANESI U., GAY S., LUALDI M., MARCHESINI R., PIROLA L., TOMATIS S. (2005).
In-phantom Imaging of Absorbed dose: Intercomparison of Gel-Dosimeter, Gafchromic and Radiographyc Film Reliability. PHYSICA SCRIPTA. vol. T118, pp. 31-34

MANCOSU P., RIPAMONTI D., VERONESE I., CANTONE M.C., GIUSSANI A., TOSI G. (2005).
Angular dependence of the TL reading of thin alfa-Al2O3:C dosemeters exposed to different beta spectra. RADIATION PROTECTION AND DOSIMETRY. vol. 113, pp. 359-365

WIELAND O., BARLINI S., KRAVCHUK V.L., BRACCO A., CAMERA F., GRAMEGNA F., MAJ A., BENZONI G., BLASI N., BRAMBILLA S., BREKIESZ M., BRUNO M., CASINI G., CHIARI M., GERACI E. et al. (2005).
The gamma-decay of the GDR in highly excited Ce nuclei. JOURNAL OF PHYSICS G: NUCLEAR AND PARTICLE PHYSICS. vol. 31, pp. S1973-S1977

BACCARO S., CEMMI A., COLOMBI C., FIOCCA M., FIORANI O., GAMBARINI G., LIETTI B., PERRONE A., ROSI G. (2004).

n-phantom dose mapping in neutron capture therapy by means of solid state detectors. NUCLEAR INSTRUMENTS & METHODS IN PHYSICS RESEARCH. SECTION A, ACCELERATORS, SPECTROMETERS, DETECTORS AND ASSOCIATED EQUIPMENT. vol. B 213, pp. 666-669

BETTEGA D. (2004).
Cell transformation by light particles : Review of available data. RADIOTHERAPY & ONCOLOGY. vol. 73 (Suppl 2), pp. S155-S157

BURN K.W., COLLI V., CURZIO G., D'ERRICO F., GAMBARINI G., ROSI G., SCOLARI L. (2004).
Characterization of the TAPIRO BNCT Epithermal Facility. RADIATION PROTECTION DOSIMETRY. vol. 110, pp. 645-649

CECILIA A., BACCARO S., CEMMI A., COLLI V., FIORANI O., GAMBARINI G., PERRONE A., ROSI G., SCOLARI L. (2004).
Alanine and TLD Coupled Detectors for Fast Neutron Dose Measurements in Neutron Capyture Therapy. RADIATION PROTECTION DOSIMETRY. vol. 110, pp. 637-640

GAMBARINI G., BIRATTARI C., MARIANI M., MARCHESINI R., PIROLA L., PRESTINI P., SELLA M., TOMATIS S. (2004).
Study of light transmittance from layers of Fricke-xylenol-orange-gel dosimeters having different composition and analysed with various modalities. NUCLEAR INSTRUMENTS & METHODS IN PHYSICS RESEARCH. SECTION A, ACCELERATORS, SPECTROMETERS, DETECTORS AND ASSOCIATED EQUIPMENT. vol. B 213, pp. 321-324

GAMBARINI G., CARRARA M., COLLI V., GAY S., TOMATIS S. (2004).
Further developments and applications of layer gel dosimetry. JOURNAL OF PHYSICS: CONFERENCE SERIES. vol. 3, pp. 213-216

GAMBARINI G., COLLI V., GAY S., PETROVICH C., PIROLA L., ROSI G. (2004).
In-phantom imaging of all dose components in boron neutron capture therapy by means of gel dosimeters. APPLIED RADIATION AND ISOTOPES. vol. 61/5, pp. 759-763GAMBARINI G., KLAMERT V., AGOSTEO S., BIRATTARI C., FIOCCA M., GAY S., ROSI G., SCOLARI L. (2004).
Study of a Method Based on TLDs for in-Phantom Dosimetry in BNCT. RADIATION PROTECTION DOSIMETRY. vol. 110, pp. 631-636

ROSI G., GAMBARINI G., COLLI V., GAY S., SCOLARI L., FIORANI O., PERRONE A., NAVA E., FASOLO F., VISCA L., ZANINI A. (2004).
Characterization of the TAPIRO BNCT Thermal Facility. RADIATION PROTECTION DOSIMETRY. vol. 110, pp. 651-654

VERONESE I., GIUSSANI A., CANTONE M.C., BIRATTARI C., BONARDI M., GROPPI F., HOELLRIEGL V., ROTH P., WERNER E. (2004).
Influence of the chemical form on the plasma clearance of ruthenium in humans. APPLIED RADIATION AND ISOTOPES. vol. 60, pp. 7-13

VERONESE I., GIUSSANI A., GOHSU H.Y., MARTINI M. (2004).
Isothermal decay studies of intermediate energy levels in quartz. RADIATION AND ENVIRONMENTAL BIOPHYSICS. vol. 43, pp. 51-57

VERONESE I., GIUSSANI A., GOKSU H.Y., MARTINI M. (2004).
The trap parameters of electrons in intermediate energy levels in quartz. RADIATION MEASUREMENTS. vol. 38, pp. 743-746

BAGATTI D., CANTONE M.C., GIUSSANI A., VERONESE I., ROTH P., WERNER E., HOLLRIEGL V. (2003).
Regional dependence of urinary uranium baseline levels in non-exposed subjects with particular reference to volunteers from northern Italy. JOURNAL OF ENVIRONMENTAL RADIOACTIVITY. vol. 65, pp. 357-364

BETTEGA D., CALZOLARI P., DONEDA L., BELLONI F., TALLONE L., REDPATH J.L. (2003).
Differential effectiveness of solar UVB components in causing cell death, oncogenic transformation and micronucleus induction in human hybrid cells. INT.J. RADIAT. BIOL. vol. 79, pp. 211-216

GRAMEGNA F., MASTINU P.F., VANNUCCI L., BOSCOLO MARCHI E., CHERUBINI R., MORONI A., BRACCO A., CAMERA F., MILLION B., WIELAND O., BENZONI E., LEONI S., AIROLDI A., SACCHI L., GALBUSERA E. et al. (2003).
New perspectives for studies of reaction mechanisms at low-medium energies. ACTA PHYSICA POLONICA B. vol. 34, pp. 2353-2362

LUCIANI A., GIUSSANI A., CANTONE M.C., CASTELLANI C.M. (2003).
Sensitivity analysis techniques applied to a revised model of molybdenum biokinetics. RADIATION PROTECTION AND DOSIMETRY. vol. 105, pp. 239-242

VERONESE I., CANTONE M.C., GIUSSANI A., MAGGIONI T., BIRATTARI C., BONARDI M., GROPPI F., GARLASCHELLI L., WERNER E., ROTH P., HOLLRIEGL V., LOUVAT P., FELGENHAUER N., ZILKER Th. (2003).
Stable tracer investigations in humans for assessing the biokinetics of ruthenium and zirconium radionuclides. RADIATION PROTECTION AND DOSIMETRY. vol. 105, pp. 209-212

VERONESE I., GIUSSANI A., CANTONE M.C., MAGGIONI T., BIRATTARI C., GROPPI F., WERNER E., ROTH P., HOLLRIEGL V. (2003).
A re-evaluation of the biokinetics of zirconium in humans. APPLIED RADIATION AND ISOTOPES. vol. 58, pp. 431-439

History of Science and Physics Education

Books

BELLONE E. (2005).
La scienza negata. Il caso italiano, Codice, Torino, 2005

BELLONE E. (2005).
Le radici classiche della cultura scientifica contemporanea, Levi Lecture, San Raffaele, 20 giugno 2005, in Kos, 242

BELLONE E. (2005).
Progetto e direzione editoriale dei 17 volumi di La Scienza, Utet-La Repubblica, 2005

BELLONE E. (2004).
Albert Einstein. Opere scelte, ed. riveduta e corretta, Bollati-Boringhieri, Torino

BELLONE E. (2004).
Caos e armonia. Storia della fisica, nuova edizione, Utet, Torino

BELLONE E. (2003).
La stella nuova. L'evoluzione e il caso Galilei, Einaudi, Torino